

TAGUNGSBAND / PROCEEDINGS

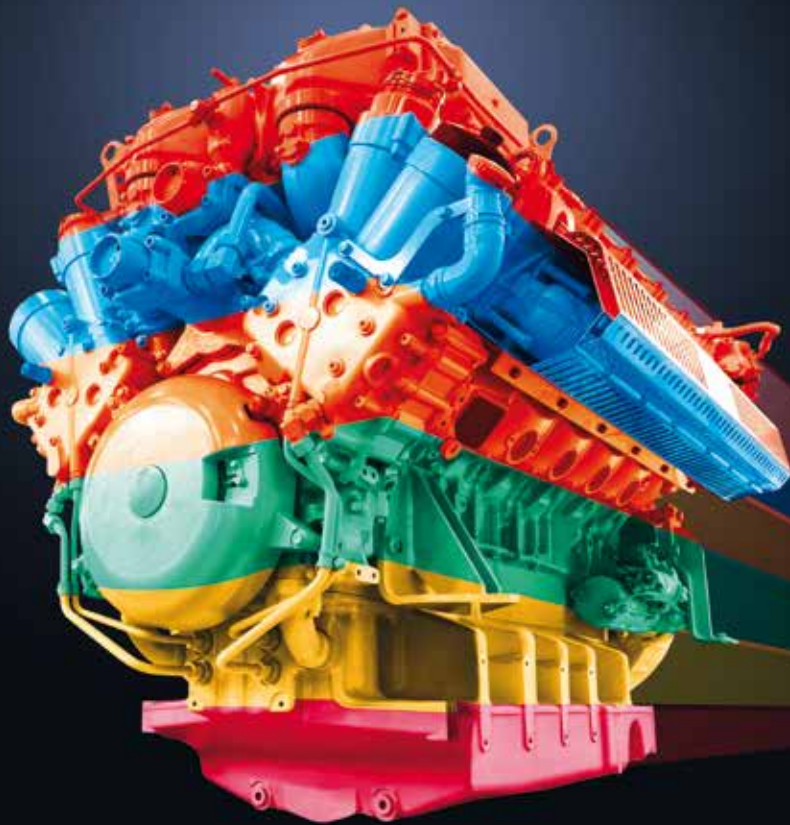
13. Dessauer Gasmotoren-Konferenz

15. /16. Mai 2024, Dessau-Roßlau, Sachsen-Anhalt

13th Dessau Gas Engine Conference

May 15-16, 2024, Dessau-Roßlau, Saxony-Anhalt

Der Veranstalter / The Organizer: WTZ Roßlau gmbH



13. Dessauer Gasmotoren-Konferenz **13th Dessau Gas Engine Conference**

15. /16. Mai 2024, Dessau-Roßlau, Sachsen-Anhalt
May 15-16, 2024, Dessau-Roßlau, Saxony-Anhalt



Der Veranstalter: WTZ Roßlau gGmbH
The Organizer: WTZ Roßlau gGmbH

Tagungsort/Conference Venue

Veranstaltungszentrum Golfpark Dessau
Junkersstraße 52
06847 Dessau-Roßlau, Germany
www.veranstaltungszentrum-dessau.de

Konferenzsprachen/Conference Languages

Die Konferenzsprachen sind Deutsch und Englisch.
Eine Simultanübersetzung wird angeboten.
Conference languages will be German and English.
Simultaneous interpretation will be arranged.

Konferenzdinner im Technikmuseum „Hugo Junkers“ **Conference Dinner in Technikmuseum „Hugo Junkers“**

Kühnauer Straße 161a
06846 Dessau-Roßlau
<https://technikmuseum-dessau.org>



Weitere Informationen
www.wtz.de/gasmotorenkonferenz



Further information
www.wtz.de/gasmotorenkonferenz/en/



Der Gasmotor wird bunt!

Dual Fuel
 # Fuel Share
 # H₂-Readiness
 # Wasserstoff
 # Ammoniak
 # H₂-Beimischung
 # Retrofit
 # ...und welche Rolle wird Methanol beim Gasmotor der Zukunft spielen?

Der Wasserstoffmotor kommt. Aufgrund der aufwendigen Speicherung von Wasserstoff stellt sich jedoch die Frage nach anderen Kraftstoffen, welche aktuell in Form von Methanol und Ammoniak als synthetische Alternativen diskutiert werden.

Je nach Kraftstoff bestehen vielfältige Fragestellungen zu den verschiedenen Brennverfahren. In Kombination mit der Frage nach der „richtigen“ Applikation, ob Off-Road, On-Road, Marine oder Power, entsteht ein bunter Blumenstrauß an Lösungsmöglichkeiten. Die genannten Konzepte lassen sich noch kombinieren, wenn zukünftig Fuel-Share, Dual-Fuel und Retrofit gefordert sind.

Dabei darf nicht vergessen werden, dass die bisherigen Kraftstoffe wie Erdgas und Biogas noch auf absehbare Zeit eine wichtige Rolle im Energiemix spielen.

Diesen bunten Mix an spannenden Fragestellungen rund um den Gasmotor möchten wir gern gemeinsam mit Ihnen auf der kommenden Gasmotoren-Konferenz diskutieren, aktuelle Trends erörtern sowie die erkennbaren Lösungsansätze präsentieren.

Hierzu lädt Sie das Team des WTZ Roßlau ganz herzlich zur 13. Dessauer Gasmotoren-Konferenz vom 15. bis 16. Mai 2024 nach Dessau-Roßlau ein. Wir freuen uns sehr auf Ihren Besuch!

New Gas engines are like a rainbow - multicoloured!

Dual Fuel
 # Fuel Share
 # H₂ -Readiness
 # Hydrogen
 # Ammonia
 # H₂ admixture
 # Retrofit
 # ...and what role will methanol play in the gas engine of the future?

The hydrogen engine is on its way. However, the complex storage of hydrogen leads to the question of other fuels, which are currently being discussed as synthetic alternatives in the form of methanol and ammonia.

The questions surrounding the different combustion processes differ depending on the fuel. In combination with the question of the „right“ application, whether off-road, on-road, marine or power, a colourful bouquet of possible solutions arises.

The above concepts can also be combined if Fuel Share, Dual Fuel and retrofit are requested in the future.

In this context, it is important to remember that current fuels such as natural gas and biogas will continue to have a significant influence on the energy mix in the foreseeable future.

At the 13th Dessau Gas Engine Conference, we would like to discuss with you this colourful mix of exciting questions concerning the gas engine, explore current trends and present the possible solutions.

For this purpose, the team of WTZ Roßlau would like to invite you to the 13th Dessau Gas Engine Conference from 15 to 16 May 2024 in Dessau-Roßlau, Germany.



Dr.-Ing. Christian Reiser
 WTZ Roßlau gGmbH



Karsten Stenzel
 WTZ Roßlau gGmbH

K1	Defossilierung von Hochleistungs-Anwendungen mit nachhaltigen Kraftstoffen Defossilization of high-power applications with sustainable fuels <i>Dr. D. Chatterjee*, Simon Hettig, Martin Miller ■ Rolls-Royce Power Systems AG</i>	→ 13
S1	Neue Motoren und Entwicklungstrends/New engines and development trends <i>Moderation: Prof. Ulrich Walther ■ Westsächsische Hochschule Zwickau</i>	→ 17
01	MAN ES - Die 49/60-Motorenfamilie - eine vielseitige Motorenplattform für höchste Leistung und Flexibilität MAN ES - The 49/60 engine family - a versatile engine platform for maximum performance and flexibility <i>Stefan Terbeck*, Michael Baldermann, Dr. Stefan Blodig, Paul Hagl, Michael Werner ■ MAN Energy Solutions SE</i>	→ 18
02	Die Verwendung von Holzgas zur CO₂-neutralen Energiegewinnung - Verbesserungen an einem Sondergasmotor Using Wood Gas for CO ₂ Neutral Power Generation - Performance Improvements of a Special Gas Engine <i>Mario Frischmann*, Dr. Robert Böwing, Stefan Schiestl ■ INNIO Jenbacher GmbH & Co. OG</i>	→ 36
S2	Wasserstoff - Stromerzeugung/Hydrogen - Power generation <i>Moderation: Prof. Thomas Koch ■ Karlsruher Institut für Technologie</i>	→ 51
03	Zertifizierung der H₂-Readiness von Gasmotorenkraftwerken H ₂ -Readiness certification of gas engine power plants <i>Dominik Voggenreiter*, Pierre Huck, Dr.-Ing. Thomas Gallinger ■ TÜV SÜD Industrie Service GmbH</i>	→ 52
04	ZG Wasserstoff-BHKW in der Praxis und die Entwicklung zum leistungsstarken Serienprodukt ZG hydrogen CHP in practice and the development into a high-performance series product <i>Frank Grewe* ■ ZG Energy AG; Dr. Sven Annas ■ ZG Energietechnik GmbH Rudolf HöB ■ Ostbayerische Technische Hochschule Amberg-Weiden</i>	→ 62
05	Auf dem Weg zum zuverlässigen Betrieb von Gasmotorenaggregaten mit reinem Wasserstoff Towards reliable genset operation with pure hydrogen <i>Dr. Marco Schultze*, Dr. Sebastian Ohler, Darshit Shah ■ Caterpillar Energy Solution GmbH Tom Krüger*, Manuel Cech, Carsten Tietze ■ WTZ Roßlau gGmbH</i>	→ 86
S3	Ammoniak - Schiffsanwendungen/Ammonia - Marine applications <i>Moderation: Prof. Andreas Wimmer ■ LEC Graz GmbH, Technische Universität Graz</i>	→ 101
06	Auslegung eines Ammoniak-Retrofit-Konzeptes für maritime Antriebseinheiten kleiner 400 kW Design of an ammonia retrofit concept for maritime propulsion units smaller than 400 kW <i>Dr.-Ing. Martin Theile*, Antje Hoppe ■ FVTR GmbH; Dr.-Ing. Sascha Prehn, Till Mante ■ Universität Rostock; Dr.-Ing. Lars Seidel, G. Mwathi ■ LOGE Deutschland GmbH</i>	→ 102
07	Entwicklung eines mittelschnelllaufenden Ammoniakmotors für die Schifffahrt Development of Medium Speed Ammonia Engine for Marine Application <i>Sadao Nakayama*, Shunsuke Kazama, Hiroki Naruse, Yutaka Masuda, Yutaka Mashima ■ IHI Power Systems Co., Ltd. Kenta Miyauchi, Koki Aiba, Takayuki Hirose ■ IHI Corporation</i>	→ 120
08	Entwicklung einer Ammoniak-betriebenen Cracker-Motor-Einheit als Antriebssystem für Binnenschiffe Development of an Ammonia-fueled Cracker-Engine-Unit as Propulsion System for Inland Waterway Vessels <i>Annalena Braun*, Dr.-Ing. Sören Bernhardt, Dr.-Ing. Heiko Kubach ■ Karlsruher Institut für Technologie; Torsten Baufeld ■ Liebherr; Prof. Dr.-Ing. Bert Buchholz, Dr.-Ing. Sascha Prehn ■ Universität Rostock Dr. Lena Engelmeier ■ Zentrum für Brennstoffzellentechnik; Prof. Dr.-Ing. Hinrich Mohr ■ GasKraft Engineering</i>	→ 132
S4	Grundlagenuntersuchungen/Fundamental studies <i>Moderation: Prof. Friedrich Wirz ■ Technische Universität Hamburg</i>	→ 153
09	Gleitlager-Performance in Anwendungen unter Verwendung alternativer Treibstoffe Plain Bearing Performance in Applications Utilizing Alternative Fuels <i>A. Zunhammer*, S. Kirchhamer, E. Bakk ■ Miba Gleitlager Austria GmbH, Laakirchen</i>	→ 154
10	Potenziale und Grenzen von unterschiedlichen Wasserstoffverbrennungskonzepten für Power Generation Applikationen Potential and limitations of different hydrogen combustion concepts for power generation applications <i>Dr. Nicole Wermuth*, Prof. Dr. Andreas Wimmer, Dr. Gernot Kammel ■ TLEC GmbH Dr. Nikolaus Spyra, Dr. Michael Url ■ INNIO Jenbacher</i>	→ 164
11	Abgasnachbehandlung für Methanol Dual-Fuel-Motoren Exhaust gas aftertreatment for methanol dual fuel engines <i>Dr. Daniel Peitz*, Dr.-Ing. Enno Eßer ■ HUG Engineering AG</i>	→ 176

K2	Analyse der globalen Wasserstoffversorgungsketten - Transportmöglichkeiten, Kosten und Anwendungen Global Hydrogen Supply Chain Analysis - Transport options, Costs and Applications <i>Robert Szolak</i> ■ Fraunhofer Institute for Solar Energy Systems ISE	→ 191
S5	Wasserstoff - Mobile Anwendungen/Hydrogen - Mobile applications Moderation: <i>Prof. Hermann Rottengruber</i> ■ Otto-von-Guericke-Universität Magdeburg	→ 199
12	Moderne H ₂ -Verbrennung am MAN H4576/State-of-the-art H ₂ combustion at the MAN H4576 <i>Peter Albrecht*</i> , <i>Dominik Hyna</i> , <i>Maximilian Weidner</i> , <i>Thomas Malischewski</i> , <i>Florian Lindner</i> ■ MAN Truck & Bus	→ 200
13	Leistungssteigerung von direkteinspritzenden H ₂ -Motoren mit flachem Brennraumdach Performance improvement of direct injection H ₂ ICE with flat cylinder heads <i>Dr.-Ing. Arne Güdden*</i> , <i>Dr.-Ing. Björn Franzke</i> , <i>Aleksandar Boberic</i> ■ FEV Europe GmbH; <i>Pascal Zimmer</i> , <i>Prof. Dr. Stefan Pischinger</i> ■ RWTH Aachen University	→ 212
S6	Methanol-Schiffsanwendung/Methanol - Marine applications Moderation: <i>Prof. Peter Eilts</i> ■ Technische Universität Braunschweig	→ 227
14	Methanol Retrofits für eine schnelle Netto-CO ₂ -Emissionsreduzierung im maritimen Markt Methanol Retrofits for a fast net-CO ₂ reduction in the Marine Market <i>Christian Kunkel*</i> , <i>Paul Hagl</i> , <i>Dr. Bhuvaneshwaran Manickam</i> , <i>Dr. Christopher Gross</i> , <i>Florian Eppler</i> ■ MAN Energy Solutions SE	→ 228
15	ABCs Methanol Zukunft/ABC's methanol future <i>Luc Mattheeuws*</i> , <i>Andreas van Gijzeghem</i> , <i>Rik de Graeve</i> , <i>Dr. Roel Verschaeren</i> ■ Anglo Belgian Corporation	→ 248
16	Entwicklung eines schnelllaufenden Methanol-Marinemotors im Projekt „meOHmare“ Development of a high speed methanol marine engine within the project „meOHmare“ <i>Dr. Patrick Moll*</i> , <i>Dr. Johannes Kech</i> , <i>Steffen Theiß</i> ■ Rolls-Royce Solutions GmbH	→ 260
S7	Gemischbildungskomponenten/Injection components Moderation: <i>Karsten Stenzel</i> ■ WTZ Roßlau gGmbH	→ 273
17	Wasserstoff-Verbrennungsergebnisse unter Niederdruck-Direkteinspritzung für Motoren mit 130 mm Bohrungsdurchmesser Hydrogen combustion results with low-pressure direct injection for 130 mm bore size engines <i>Patrick Send*</i> , <i>Dr. János Csató</i> , <i>Richard Pirkl</i> , <i>Günther Neuhaus</i> ■ Liebherr-Components Deggendorf GmbH <i>Francois Masson</i> ■ Liebherr Machines Bulle SA	→ 274
18	Neue Aspekte zur Gemischaufbereitung bei direkteinspritzenden Wasserstoffverbrennungsmotoren New Mixture Formation Processes in H ₂ Engines <i>Dr.-Ing. Olaf Weber*</i> , <i>Jan Leberwurst</i> , <i>Dr. rer. nat. Jochen Broz</i> , <i>Sebastian Sulzer</i> , <i>Dr. rer. nat. Oliver Hahn</i> ■ Schaeffler Technologies AG & Co. KG	→ 288
19	Herausforderungen für den Umstieg auf erneuerbare Energieträger aus Komponentensicht mit Fokus auf MPI Ventile für das LE-Motoren Segment Challenges for the transition to renewable fuels from component perspective with focus on MPI valves for Large Engines <i>Claudia Hengstberger*</i> , <i>Dr. Peter Christiner</i> , <i>Dr. Jens Olaf Stein</i> , <i>Michael Köhler</i> , <i>Dr. René Schimon</i> ■ Robert Bosch AG	→ 300
S8	Zündtechnologien/Ignition technologies Moderation: <i>Prof. Bert Buchholz</i> ■ Universität Rostock	→ 321
20	Entwicklung intelligenter Zündspulen für H ₂ ICE Anwendungen Smart Ignition Coil Development for H ₂ ICE Application <i>Dr. Stefano Papi*</i> , <i>Dr. Massimo Dal Re</i> , <i>Dr. John Burrows</i> , <i>Simone Daniele</i> ■ Tenneco Powertrain <i>Federico Ricci</i> , <i>Carlo Nazareno Grimaldi</i> ■ University of Perugia	→ 322
21	Zyklusweise Funkensteuerung: Die Zukunft bei Wasserstoffmotoren Same Cycle Spark Control: The Future of Hydrogen Engines <i>Emmanuella Sotiropoulou*</i> , <i>Dr. Luigi Tozzi</i> , <i>Supreeth Narasimhamurthy</i> ■ Prometheus Applied Technologies, LLC; <i>Luc Mattheeuws</i> , <i>Rik De Graeve</i> ■ Anglo Belgian Corporation NV <i>David Lepley</i> ■ Altronic LLC; <i>Bernhard Zemann</i> ; ■ Hoerbiger Wien GmbH	→ 336
	Liste der Autoren/List of the authors	→ 350
	Impressum/Notes	→ 356

Mittwoch, 15.05.2024/Wednesday May 15, 2024

- 08:00 Registrierung/Registration
08:30 Begrüßung/Welcome
Dr.-Ing. Christian Reiser ■ Geschäftsführer WTZ Roßlau gGmbH
- 08:35 Grußwort/Short welcoming speech
*Stefanie Pöttsch ■ Staatssekretärin im Ministerium für
Wirtschaft, Tourismus, Landwirtschaft und Forsten des Landes Sachsen-Anhalt*

Keynote

- 08:45 Defossilierung von Hochleistungs-Anwendungen mit nachhaltigen Kraftstoffen
K1 Defossilization of high-power applications with sustainable fuels
Dr. D. Chatterjee, Simon Hettig, Martin Miller ■ Rolls-Royce Power Systems AG*

Session 1 Neue Motoren und Entwicklungstrends/New engines and development trends
Moderation: Prof. Ulrich Walther ■ Westsächsische Hochschule Zwickau

- 09:00 MAN ES - Die 49/60-Motorenfamilie - eine vielseitige Motorenplattform für höchste Leistung und Flexibilität
01 MAN ES - The 49/60 engine family - a versatile engine platform for maximum performance and flexibility
Stefan Terbeck, Michael Baldermann, Dr. Stefan Blodig, Paul Hagl, Michael Werner ■ MAN Energy Solutions SE*
- 09:30 Die Verwendung von Holzgas zur CO₂-neutralen Energiegewinnung - Verbesserungen an einem Sondergasmotor
02 Using Wood Gas for CO₂ Neutral Power Generation - Performance Improvements of a Special Gas Engine
Mario Frischmann, Dr. Robert Böwing, Stefan Schiestl ■ INNIO Jenbacher GmbH & Co. OG*

- 10:00 Kaffeepause/Coffeebreak

Session 2 Wasserstoff - Stromerzeugung/Hydrogen - Power generation
Moderation: Prof. Thomas Koch ■ Karlsruher Institut für Technologie

- 10:30 Zertifizierung der H₂-Readiness von Gasmotorenkraftwerken
03 H₂-Readiness certification of gas engine power plants
Dominik Voggenreiter, Pierre Huck, Dr.-Ing. Thomas Gallinger ■ TÜV SÜD Industrie Service GmbH*
- 11:00 2G Wasserstoff-BHKW in der Praxis und die Entwicklung zum leistungsstarken Serienprodukt
04 2G hydrogen CHP in practice and the development into a high-performance series product
Frank Grewe ■ 2G Energy AG; Dr. Sven Annas ■ 2G Energietechnik GmbH;
Rudolf Höß ■ Ostbayerische Technische Hochschule Amberg-Weiden*
- 11:30 Auf dem Weg zum zuverlässigen Betrieb von Gasmotorenaggregaten mit reinem Wasserstoff
05 Towards reliable genset operation with pure hydrogen
Dr. Marco Schultze, Dr. Sebastian Ohler, Darshit Shah ■ Caterpillar Energy Solution GmbH
Tom Krüger*, Manuel Cech, Carsten Tietze ■ WTZ Roßlau gGmbH*

- 12:00 Mittagessen/Lunch

Mittwoch, 15.05.2024/Wednesday May 15, 2024**Session 3** Ammoniak - Schiffsanwendungen/Ammonia - Marine applications

Moderation: Prof. Andreas Wimmer ■ LEC Graz GmbH, Technische Universität Graz

13:30

06

Auslegung eines Ammoniak-Retrofit-Konzeptes für maritime Antriebseinheiten kleiner 400 kW
Design of an ammonia retrofit concept for maritime propulsion units smaller than 400 kW

Dr.-Ing. Martin Theile*, Antje Hoppe ■ FVTR GmbH

Dr.-Ing. Sascha Prehn, Till Mante ■ Universität Rostock

Dr.-Ing. Lars Seidel, G. Mwathi ■ LOGE Deutschland GmbH

14:00

07

Entwicklung eines mittelschnelllaufenden Ammoniakmotors für die Schifffahrt
Development of Medium Speed Ammonia Engine for Marine Application

Sadao Nakayama*, Shunsuke Kazama, Hiroki Naruse, Yutaka Masuda, Yutaka Mashima

■ IHI Power Systems Co., Ltd.

Kenta Miyauchi, Koki Aiba, Takayuki Hirose ■ IHI Corporation

14:30

08

Entwicklung einer Ammoniak-betriebenen Cracker-Motor-Einheit als Antriebssystem für Binnenschiffe
Development of an ammonia-fueled Cracker-Engine-Unit as Propulsion System for Inland Waterway Vessels

Annalena Braun*, Dr.-Ing. Sören Bernhardt, Dr.-Ing. Heiko Kubach ■ Karlsruher Institut für Technologie

Torsten Baufeld ■ Liebherr

Prof. Dr.-Ing. Bert Buchholz, Dr.-Ing. Sascha Prehn ■ Universität Rostock

Dr. Lena Engelmeier ■ Zentrum für Brennstoffzellentechnik

Prof. Dr.-Ing. Hinrich Mohr ■ GasKraft Engineering

15:00

Kaffeepause/Coffeebreak

Session 4 Grundlagenuntersuchungen/Fundamental studies

Moderation: Prof. Friedrich Wirz ■ Technische Universität Hamburg

15:30

09

Gleitlager-Performance in Anwendungen unter Verwendung alternativer Treibstoffe
Plain Bearing Performance in Applications Utilizing Alternative Fuels

A. Zunghammer*, S. Kirchhamer, E. Bakk

■ Miba Gleitlager Austria GmbH, Laakirchen

16:00

10

Potenziale und Grenzen von unterschiedlichen Wasserstoffverbrennungskonzepten für Power Generation Applikationen

Potential and limitations of different hydrogen combustion concepts for power generation applications

Dr. Nicole Wermuth*, Prof. Dr. Andreas Wimmer, Dr. Gernot Kammel ■ LEC GmbH

Dr. Nikolaus Spyra, Dr. Michael Uri ■ INNIO Jenbacher

16:30

11

Abgasnachbehandlung für Methanol Dual-Fuel-Motoren
Exhaust gas aftertreatment for methanol dual fuel engines

Dr. Daniel Peitz*, Dr.-Ing. Enno Eßer ■ HUG Engineering AG

17:00

Rückfahrt der Busse zu den Hotels/Return to the hotels

18:30

Abfahrt der Busse zur Abendveranstaltung/Departure of the busses to the Evening Event

Abendveranstaltung/Evening Event

19:00

Konferenzdinner im Technikmuseum „Hugo Junkers“, Kühnauer Str. 161a, 06846 Dessau-Roßlau
Conference Dinner in Technik Museum „Hugo Junkers“, Kühnauer Str. 161a, 06846 Dessau-Roßlau

Donnerstag, 16.05.2024/Thursday May 16, 2024

Keynote

08:45 **K2** Analyse der globalen Wasserstoffversorgungsketten - Transportmöglichkeiten, Kosten und Anwendungen
Global Hydrogen Supply Chain Analysis - Transport options, Costs and Applications
Robert Szolak ■ Fraunhofer Institute for Solar Energy Systems ISE

Session 5

Wasserstoff - Mobile Anwendungen/Hydrogen - Mobile applications
Moderation: *Prof. Hermann Rottengruber* ■ Otto-von-Guericke-Universität Magdeburg

09:00 **12** Moderne H₂-Verbrennung am MAN H4576
State-of-the-art H₂ combustion at the MAN H4576
*Peter Albrecht**, *Dominik Hyna*, *Maximilian Weidner*, *Thomas Malischewski*, *Florian Lindner* ■ MAN Truck & Bus

09:30 **13** Leistungssteigerung von direkteinspritzenden H₂-Motoren mit flachem Brennraumdach
Performance improvement of direct injection H₂ ICE with flat cylinder heads
*Dr.-Ing. Arne Güdden**, *Dr.-Ing. Björn Franzke*, *Aleksandar Boberic* ■ FEV Europe GmbH
Pascal Zimmer, *Prof. Dr. Stefan Pischinger* ■ RWTH Aachen University

10:00 Kaffeepause/Coffeebreak

Session 6

Methanol-Schiffsanwendung/Methanol - Marine applications
Moderation: *Prof. Peter Eilts* ■ Technische Universität Braunschweig

10:30 **14** Methanol Retrofits für eine schnelle Netto-CO₂-Emissionsreduzierung im maritimen Markt
Methanol Retrofits for a fast net-CO₂ reduction in the Marine Market
*Christian Kunkel**, *Paul Hagl*, *Dr. Bhuvaneshwar Manickam*, *Dr. Christopher Gross*, *Florian Eppler*
■ MAN Energy Solutions SE

11:00 **15** ABCs Methanol Zukunft
ABC's methanol future
*Luc Mattheeuws**, *Andreas van Gijzeghem*, *Rik de Graeve*, *Dr. Roel Verschaeren* ■ Anglo Belgian Corporation

11:30 **16** Entwicklung eines schnelllaufenden Methanol-Marinemotors im Projekt „meOHmare“
Development of a high speed methanol marine engine within the project „meOHmare“
*Dr. Patrick Moll**, *Dr. Johannes Kech*, *Steffen Theiß* ■ Rolls-Royce Solutions GmbH

12:00 Mittagessen/Lunch

Donnerstag, 16.05.2024/Thursday May 16, 2024

Session 7 Gemischbildungskomponenten/Injection components

Moderation: Karsten Stenzel ■ WTZ RoBlau gGmbH

13:30 **17** Wasserstoff-Verbrennungsergebnisse unter Niederdruck-Direkteinspritzung für Motoren mit 130 mm Bohrungsdurchmesser
Hydrogen combustion results with low-pressure direct injection for 130 mm bore size engines
Patrick Send*, Dr. János Csató, Richard Pirkl, Günther Neuhaus ■ Liebherr-Components Deggendorf GmbH
Francois Masson ■ Liebherr Machines Bulle SA

14:00 **18** Neue Aspekte zur Gemischaufbereitung bei direkteinspritzenden Wasserstoffverbrennungsmotoren
New Mixture Formation Processes in H₂ Engines
Dr.-Ing. Olaf Weber*, Jan Leberwurst, Dr. rer. nat. Jochen Broz, Sebastian Sulzer, Dr. rer. nat. Oliver Hahn
■ Schaeffler Technologies AG & Co. KG

14:30 **19** Herausforderungen für den Umstieg auf erneuerbare Energieträger aus Komponentensicht mit Fokus auf MPI Ventile für das LE-Motoren Segment
Challenges for the transition to renewable fuels from component perspective with focus on MPI valves for Large Engines
Claudia Hengstberger*, Dr. Peter Christiner, Dr. Jens Olaf Stein, Michael Köhler, Dr. René Schimon
■ Robert Bosch AG

15:00 Kaffeepause/Coffeebreak

Session 8 Zündtechnologien/Ignition technologies

Moderation: Prof. Bert Buchholz ■ Universität Rostock

15:30 **20** Entwicklung intelligenter Zündspulen für H₂ ICE Anwendungen
Smart Ignition Coil Development for H₂ ICE Application
Dr. Stefano Papi*, Dr. Massimo Dal Re, Dr. John Burrows, Simone Daniele
■ Tenneco Powertrain
Federico Ricci, Carlo Nazareno Grimaldi ■ University of Perugia

16:00 **21** Zyklusweise Funkensteuerung: Die Zukunft bei Wasserstoffmotoren
Same Cycle Spark Control: The Future of Hydrogen Engines
Emmanuella Sotiropoulou*, Dr. Luigi Tozzi, Supreeth Narasimhamurthy ■ Prometheus Applied Technologies, LLC
Luc Mattheeuws, Rik De Graeve ■ Anglo Belgian Corporation NV
David Lepley ■ Altronic LLC
Bernhard Zemann ■ Hoerbiger Wien GmbH

16:45 **Schlusswort/Closing Remarks**
Dr.-Ing. Christian Reiser;
Geschäftsführer WTZ RoBlau gGmbH

WTZ

INNOVATIVE
SCIENCE & RESEARCH

Was treibt uns in Zukunft an?

Methanol
Wasserstoff
Ammoniak

DME

HVO

FAME

OME

synthetisches
Methan

LOHC

SOFC

FT-Diesel



wtz.de

Keynote 1

**Defossilierung von Hochleistungs-Anwendungen
mit nachhaltigen Kraftstoffen**
Defossilation of high-power applications with sustainable fuels

Dr. D. Chatterjee*, Simon Hettig, Martin Miller · Rolls-Royce Power Systems AG

Defossilisation of high-power applications with sustainable fuels

Defossilierung von Hochleistungs-Anwendungen mit nachhaltigen Kraftstoffen

Dr. Daniel Chatterjee*, Simon Hettig, Martin Miller;
Rolls-Royce Power Systems AG

Abstract

To achieve a renewable energy supply for high power applications like aviation, mining and several marine applications, chemical energy carriers are essential to ensure the energy and propulsion demands in remote locations. Those applications are hard to electrify and hydrogen as well as hydrogen derivatives like methanol, ammonia and synthetic hydrocarbons (e-fuels) offers great potential for the defossilization. However, e-fuels are not an economically viable option yet, a market ramp-up is expected after 2030, evoked by ambitious CO₂ reduction targets and decreasing prices due to scale-up of production capacities. Furthermore, the storage of excess wind and solar electric power is a key element for a successful shift to a reliable climate-neutral energy supply, due to its fluctuating nature. Instead of storing electric energy directly in batteries, the conversion of electrical to chemical energy enables economically viable storage solutions.

For both, high power applications and storage of renewable excess electric power, hydrogen and derivatives produced by electrolysis with or without downstreamed fuel synthesis are the most prominent energy carrier in that respect. The advantages of easy transportation over long distances with reduced losses and long-term storage in large quantities enables a temporal and spatial decoupling of energy generation and demand-based energy supply.

Within this Keynote we would like to give an overview of the Ecosystem and showcase promising alternative fuels including their advantages and challenges for adopting them widely like CO₂ footprint (well-to-wheel / well-to-wake), the production costs and mid-term availability.

Kurzfassung

Um eine erneuerbare Energieversorgung für Hochleistungsanwendungen wie Luftfahrt, Bergbau und verschiedene Schiffsanwendungen zu erreichen, sind chemische Energieträger unerlässlich, um den Energie- und Antriebsbedarf an abgelegenen Orten zu decken. Diese Anwendungen sind schwer zu elektrifizieren und Wasserstoff sowie Wasserstoffderivate wie Methanol, Ammoniak und synthetische Kohlenwasserstoffe (E-Fuels) bieten ein großes Potenzial für die Defossilisierung. E-Fuels sind jedoch noch keine wirtschaftlich tragfähige Option, ein Markthochlauf wird nach 2030 erwartet, ausgelöst durch ehrgeizige CO₂-Reduktionsziele und sinkende Preise aufgrund des Ausbaus der Produktionskapazitäten. Darüber hinaus ist die Speicherung von überschüssigem Wind- und Solarstrom ein Schlüsselement für einen erfolgreichen Übergang zu einer zuverlässigen klimaneutralen Energieversorgung, da deren Stromerzeugung Schwankungen unterworfen ist. Anstatt elektrische Energie direkt in Batterien zu speichern, ermöglicht die Umwandlung von elektrischer in chemische Energie wirtschaftlich tragfähige Speicherlösungen.

Sowohl für Hochleistungsanwendungen an abgelegenen Orten als auch für die Speicherung von überschüssigem Strom aus erneuerbaren Energiequellen sind Wasserstoff und seine Derivate, die durch Elektrolyse mit oder ohne nachgeschaltete Brennstoffsynthese hergestellt werden, der wichtigste Energieträger. Die Vorteile des einfachen Transports über große Entfernungen mit geringen Verlusten und der langfristigen Speicherung in großen Mengen ermöglichen eine zeitliche und räumliche Entkopplung von Energieerzeugung und bedarfsgerechter Energieversorgung.

Im Rahmen dieser grundlegenden Bemerkung (Keynote) möchten wir einen Überblick über das H₂-Ökosystem geben und vielversprechende alternative Kraftstoffe mit ihren für den breiten Einsatz vorhandenen Vorteilen und Herausforderungen, wie CO₂-Fußabdruck (well-to-wheel / well-to-wake), die Produktionskosten und die mittelfristige Verfügbarkeit, vorstellen.

* Speaker/Referent

A series of horizontal lines for writing notes, spanning most of the page width.

Session 1

Neue Motoren und Entwicklungstrends New engines and development trends

**Moderation: Prof. Ulrich Walther
Westfälische Hochschule Zwickau**

MAN ES – The 49/60 engine family a versatile engine platform for maximum performance and flexibility

MAN ES – Die 49/60-Motorenfamilie Eine vielseitige Motorenplattform für höchste Leistung und Flexibilität

S. Terbeck*, M. Baldermann, Dr. S. Blodig, P. Hagl, M. Werner
MAN Energy Solutions, Augsburg, Germany

Abstract

In 2022, MAN Energy Solutions presented the Dual fuel variant as the next member of the new engine family 49/60 which includes also the pure gas (SI) and DF-M (Methanol) derivatives.

The most recent and innovative MAN-ES four-stroke technologies such as two-stage turbocharging, second-generation common rail injection and the new SaCoS5000 automation system are key elements of the engine family's architecture. Based on these genes, the 49/60 variants will set benchmarks in their respective market arenas in terms of performance, fuel efficiency, emissions and fuel flexibility. Due to their modular structure, all variants of the individual motor types can be manufactured with a minimum of variant parts.

Basis for all family derivatives is the standard 49/60 core engine. The modular construction kits of the core engine and the combustion-dependent components are optimized with regard to the multi-dimensional requirements of variant and configuration management as well as constraints for efficient logistic and production processes.

The 49' family portfolio covers stationary applications with V-type engines in the power range up to 26 MW, in the maritime sector L- & V-type engines up to 18.2 MW are available. This next generation of multi-fuel-engine foresees the ability to run on future fuels and is prepared for upcoming emission legislations.

With the new MAN-ES own developed automation system the 49/60 engine family is prepared for the digital future. Cyber security, Software-as-a-Service and service support based on augmented reality are key pillars of the MAN-ES digital presence and the digital future strategy.

This paper presents the results and experiences of the DF- and G- engine development and describes the implementation of the family concept.

Kurzfassung

Im Jahr 2022 stellte MAN Energy Solutions die Dual-Fuel-Variante als nächstes Mitglied der neuen Motorenfamilie 49/60 vor, die auch die Gas (SI) und DF-M (Methanol) Derivate umfasst.

Die neuesten und innovativsten MAN-ES-Viertakttechnologien wie die zweistufige Turboaufladung, die Common-Rail-Einspritzung der zweiten Generation und das neue

* Speaker/Referent

Automatisierungssystem SaCoS 5000 sind Schlüsselemente der Architektur der Motorenfamilie. Basierend auf diesen Genen setzen die 49/60-Varianten in ihren jeweiligen Marktsegmenten Maßstäbe hinsichtlich Leistung, Kraftstoffeffizienz, Emissionen und Kraftstoffflexibilität. Aufgrund ihres modularen Aufbaus können alle Varianten der einzelnen Motortypen mit einem Minimum an Variantenteilen gefertigt werden.

Basis für alle Familienderivate ist der serienmäßige 49/60-Kernmotor. Die modularen Baukästen des Kernmotors und der verbrennungsabhängigen Komponenten sind hinsichtlich der mehrdimensionalen Anforderungen des Varianten- und Konfigurationsmanagements sowie Randbedingungen für effiziente Logistik- und Produktionsprozesse optimiert.

Das Portfolio der 49'-Familie deckt stationäre Anwendungen mit V-Motoren im Leistungsbereich bis 26 MW ab, im maritimen Bereich stehen L- und V-Motoren bis 18,2 MW zur Verfügung. Diese nächste Generation von Mehrstoffmotoren ermöglicht den Betrieb mit künftigen Kraftstoffen und ist auf kommende Emissionsgesetze vorbereitet.

Mit dem neuen, von MAN-ES entwickelten Automatisierungssystem ist die 49/60-Motorenfamilie für die digitale Zukunft gerüstet. Cybersicherheit, Software-as-a-Service und Serviceunterstützung auf Basis von Augmented Reality sind wesentliche Säulen des digitalen Auftritts von MAN-ES und der digitalen Zukunftsstrategie.

Dieser Beitrag präsentiert die Ergebnisse und Erfahrungen der DF- und G-Motorentwicklung und beschreibt die Umsetzung des Familienkonzepts.

1. Einleitung

Die Anforderungen an einen neuen Verbrennungsmotor sind vielfältig und umfassen Aspekte wie zukünftige Kraftstoffe, Emissionsgrenzwerte und Märkte wie Schiffe und Kraftwerke in verschiedensten Applikationen (Abbildung 1).

Zukünftige Kraftstoffe müssen umweltfreundlich und nachhaltig sein, um die Emissionen von Treibhausgasen zu reduzieren und die Luftqualität zu verbessern. Synthetische Kraftstoffe wie eFuels, SNG und H₂ sind vielversprechende Alternativen, die in der Lage sind, den Kraftstoffbedarf in Logistik, Schiffs- und Luftverkehr in höherem Maße klimaneutral zu gestalten.

Die Emissionsgrenzwerte für Stickoxide, Kohlenmonoxid, Kohlenwasserstoffe und Feinstaub werden immer strenger, um die Umweltbelastung durch Verbrennungsmotoren zu reduzieren. Die Märkte für Schiffe und Kraftwerke erfordern Motoren, die sowohl mit Diesel als auch mit Erd- und Biogas betrieben werden können.

Die MAN ES 49/60-Motorenfamilie ist eine vielseitige Motorenplattform, die höchste Leistung und Flexibilität bietet und für eine Vielzahl von Anwendungen und Brennstoffen ausgelegt ist.

Die Plattform führt neue Technologien wie das MAN Common Rail 2.2-Einspritzsystem und die zweistufige Turboaufladung ein. Mit der neuesten Motorautomatisierung wird die Motorenfamilie 49/60 sehr hohen Anforderungen an die Cybersicherheit gerecht.

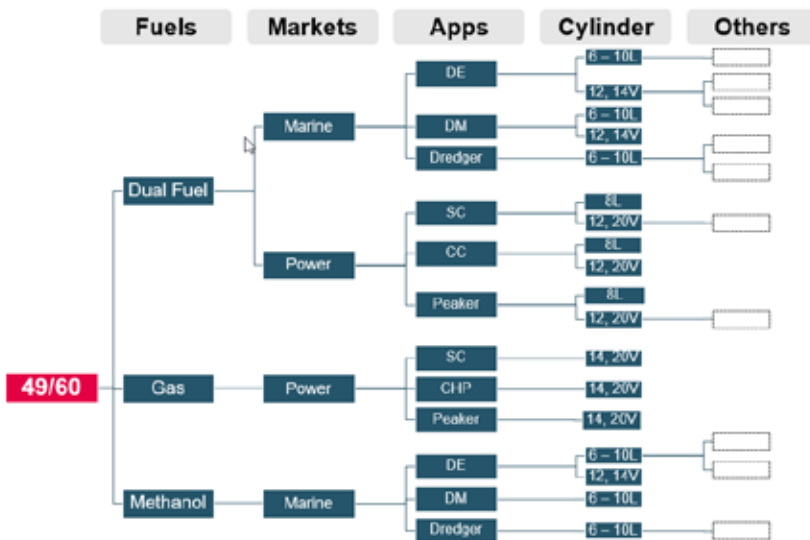


Abbildung 1: Variantenbaum 49/60 Motorenfamilie (Ausschnitt)

Eine große Produktvielfalt jedoch verursacht durch die Variantenzahl steigende Komplexitätskosten. Die Randbedingungen für effiziente Einkaufs-, Logistik- und Produktionsprozesse setzen Grenzen im Hinblick auf die Anzahl der Unterschiedsteile. Aus Kostengründen gilt es größtmögliche Skaleneffekte zu erzielen. Auch das Variantenmanagement in der späteren Serienabwicklung ist zu beachten.

Die Ziele für Herstell- und Variantenkosten wurden konkret zu Beginn der Entwicklung gleichrangig mit den typischen Kenngrößen wie Leistung, Effizienz und Emissionen festgelegt. Die Variantenplanung wurde somit nicht nur aus den Marktanforderungen abgeleitet, sondern auch auf die Anwendung eines stringenten Produktbaukastens ausgerichtet.

2. Produktbaukasten

Basierend auf der initial im Projekt erstellten Marktprognose und der daraus resultierenden Marktvarianz der notwendigen Vertriebsvarianten wurden in der Konzeptphase des Motorprojekts bereits die Weichen für eine modulare Motorenfamilie 49/60 gestellt. Mit Hilfe von Tools beziehungsweise Methoden wie dem Scheibenmodell und dem Merkmalsbaum (Abbildung 2) konnten die Anforderungen geordnet und strukturiert werden. Überflüssige Varianten wurden aussortiert und ähnliche Varianten wurden vereinheitlicht. Zusätzlich wurden die notwendige Funktionen für einzelne Gewerke sichtbar und konnten schon früh im Konzept mit eingeplant werden.

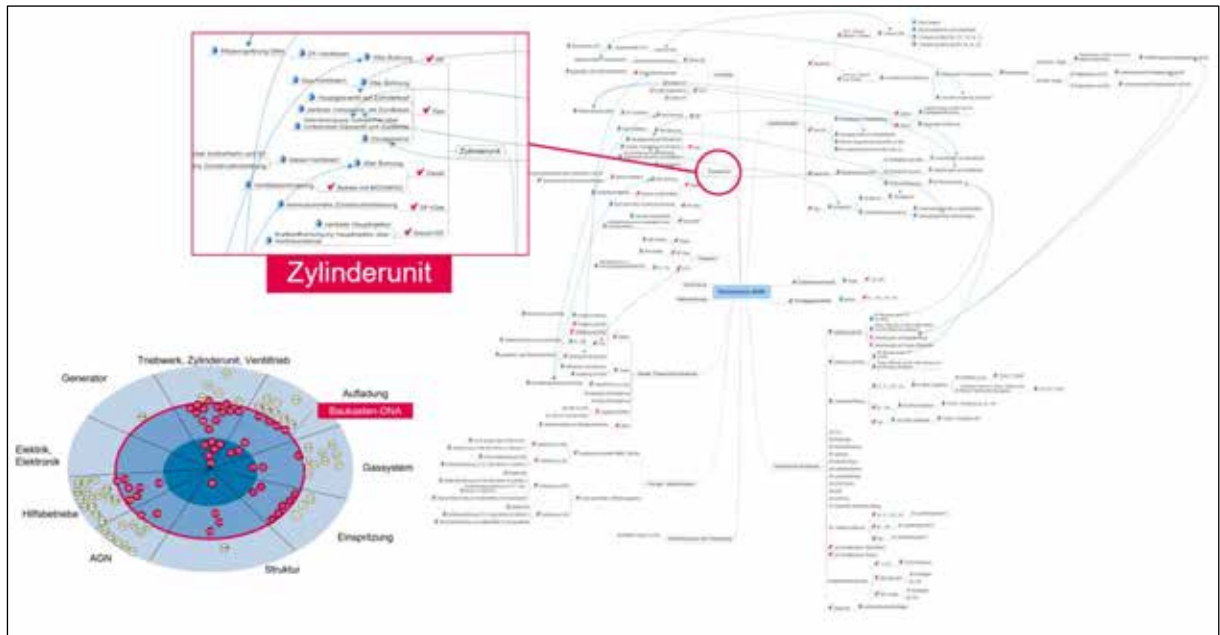


Abbildung 2: Konzeptioneller Baukastenaufbau 49/60

Baukasten Kraftstoffderivate

Aktuell sind im Portfolio des 49/60 die Kraftstoffvarianten Diesel, Dual Fuel und Gas verfügbar.

Für den modularen Aufbau der Familie wurden die beiden extremen Varianten Diesel und Dual Fuel als Basis verwendet. Die Diesel-Ausführung legt als minimale Ausstattungsvariante die Grundbasis auf der die anderen Varianten aufbauen. Die Dual Fuel-Ausführung bildet als komplexeste Ausstattungsvariante die Vollbestückung des Motors.

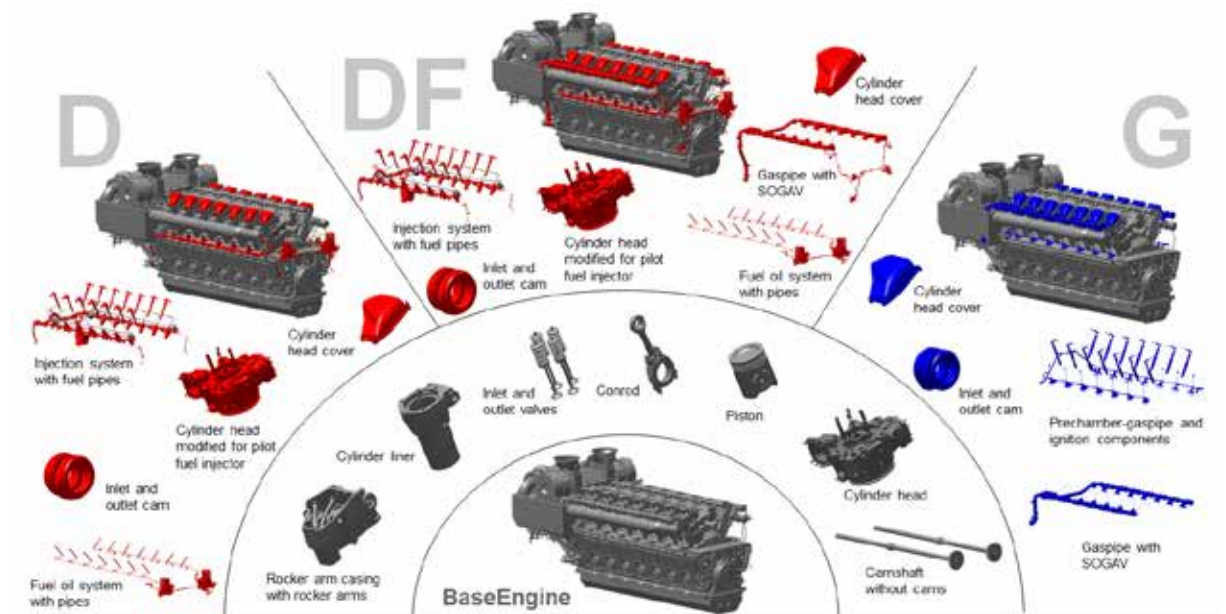


Abbildung 3: Motorenfamilie 49/60

Herauszustellen ist der Erfolg der Vereinheitlichung der brennraumführenden Bauteile. In den Kraftstoffderivaten Diesel, Dual Fuel und Gas können für die gleichen

brennraumbildenden Bauteile wie Zylinderkopf, Zylinderbuchse, Kolben inkl. Kolbenringe, Kipphebel und Ventile verwendet werden. Einzig der Zylinderkopf hat in der Variante Diesel und Dual Fuel eine zusätzliche Aufnahmebohrung für den Zündölinjektor des Zündölsystems. Dieser Unterschied in der mechanischen Bearbeitung gegenüber des G-Zylinderkopfs wird durch die Weiterentwicklung des Einspritzsystems zukünftig entfallen können.

Ermöglicht wurde dies durch die bestmögliche Optimierung der Bauteile sowie die Anpassung der Brennverfahren an die einheitliche Geometrie.

One fits all

Der Zylinderkopf hat als zentrale Brennraumkomponente eine wichtige Schnittstellenfunktion. Der Zylinderkopf des 49/60 wurde speziell für diese vielfältigen Anwendungen entwickelt. In Abbildung 4 werden die Möglichkeiten zur Aufnahme diverser kraftstoffspezifischer und auch regelungsabhängiger Komponenten dargestellt.

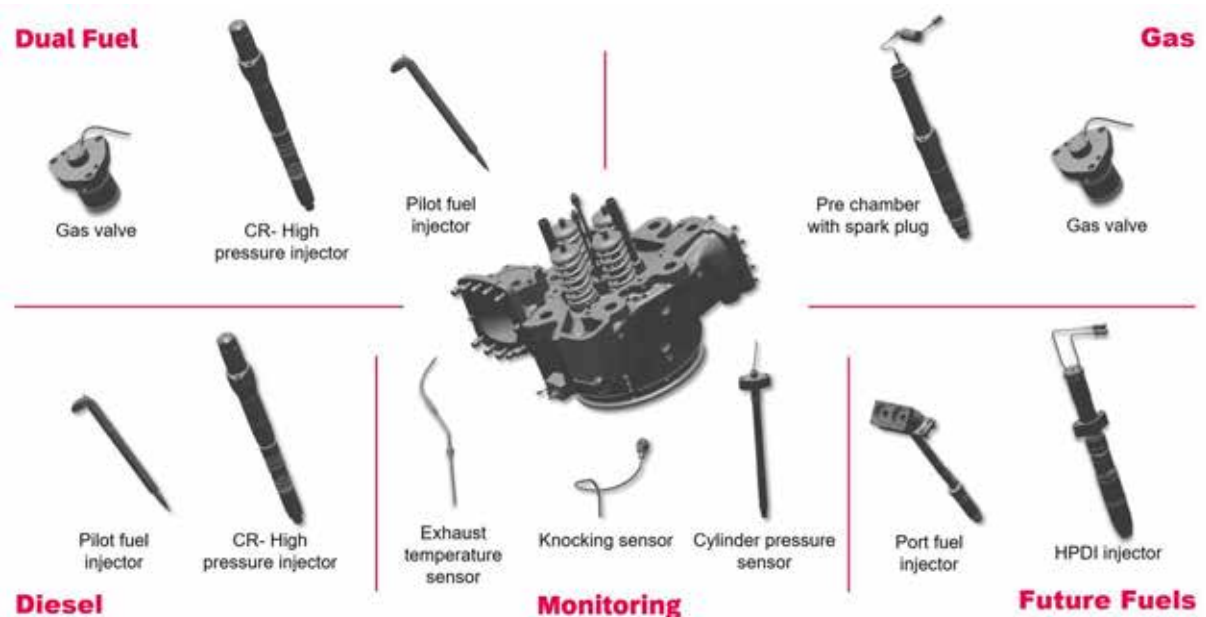


Abbildung 4: Zylinderkopf 49/60

Für Überwachungs- und Regelaufgaben steht dem 49/60 Zylinderkopf standardmäßig die Abgastemperaturmessung und die Zylinderdruckmessung zur Verfügung. Für gasspezifische Brennverfahren wird zusätzlich das Klopfsignal überwacht.

Der reine Dieselmotor wird mit dem Common Rail 2.2 – Hochdruckinjektor und dem Zündölinjektor ausgestattet. Für die zusätzliche Gasversorgung bei einem Dual Fuel Motor findet das Hauptgasventil seinen Platz auf dem Zylinderkopf mit Zugang zum Ladeluftkanal.

Bei der reinen Gasvariante des Motors wird der CR2.2 - Hochdruckinjektor durch die Gas-Vorkammer ersetzt. Ein Zündölinjektor wird hier nicht benötigt. Die Vorkammer ist mit einem Rückschlagventil und der elektrischen Zündeinrichtung inklusive Zündkerze ausgestattet. Das Gas bekommt die Vorkammer durch ein separates Vorkammergasventil.

Auch für zukünftige Kraftstoffe wie Methanol, Ammoniak oder auch Wasserstoff ist der Zylinderkopf ebenfalls hinsichtlich seiner möglichen Schnittstellen gerüstet. Hierzu kann der Zylinderkopf mit einem Port Fuel Injektor oder aber auch mit einem HPDI Injektor ausgestattet werden.

Flexibilität im Verdichtungsverhältnis

Aufgrund der Anforderungen der verschiedenen Brennverfahren und der Flexibilität der unterschiedlichen Kraftstoffe ergibt sich die Notwendigkeit eines Verdichtungsverhältnissbereichs.

Die konstruktive Darstellung soll möglichst einfach, kostengünstig und montagefreundlich dargestellt werden.

Dies ist beim 49/60-Motor mittels einer separaten Zwischenplatte in der Trennstelle des Pleuels gelöst. Mit der Dicke der Zwischenplatte kann die Gesamtlänge von Pleuelzapfen zu Pleuelbolzen eingestellt werden. Mit dieser Möglichkeit kann das Verdichtungsverhältnis von 11 – 20 variiert werden.

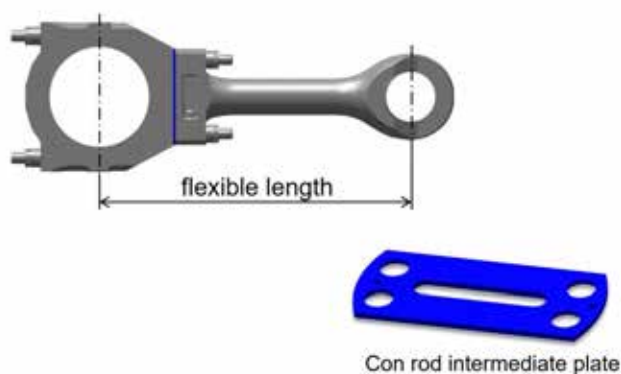


Abbildung 5: Flexibles Verdichtungsverhältnis

Ein Umbau der Zwischenplatte und somit ein Wechsel auf ein anderes Verdichtungsverhältnis kann im Bedarfsfall, zum Beispiel Retrofit, relativ einfach erfolgen. Ein Abbau von Powerunit-Komponenten ist nicht erforderlich. Der Wechsel kann komplett vom Triebraum aus erfolgen.

Vorteile eines stringenten Baukastens

Die Investition in einen modularen Aufbau macht sich in vielerlei Hinsicht wieder bezahlt. Die ersten Vorteile merkt man bereits in der konstruktiven Ausarbeitung beziehungsweise in der Pflege der Ausführungen. Als Beispiel ist der geringere Aufwand für Kollisionsprüfungen zu nennen.

Die weitaus mächtigeren Vorteile zeigen sich allerdings in der logistischen Abwicklung und im Beschaffungsprozess für Neubaumotoren:

- Größere Losgrößen in der Bauteilbeschaffung resultieren in niedrigeren Bauteilpreisen
- Bessere Bauteilverfügbarkeit durch „Purchase to stock“
- Reduzierte Endmontagezeit durch höheren Anteil an vormontierten Einheiten

Auch im weiteren Produktleben nach Auslieferung des Motors an den Kunden ist dieses modulare System vorteilhaft. Zum einen werden die Ersatzteilpreise und die Ersatzteilversorgung durch Gleichteile positiv beeinflusst aber auch ein potentieller Umbau auf ein anderes Kraftstoffdesign ist einfach umzusetzen. Im Beispiel Diesel zu Dual Fuel

müssen nur die gasspezifischen Bauteile nachgerüstet werden. Auch zukünftig werden die Kunden hiervon für ein potientiell Retrofit auf „Future Fuels“ Kraftstoffe profitieren.

3. Automation

Die 49/60 Motorfamilie ist mit der 5. Generation des MAN Energy Solution Automationssystems, SaCoS 5000, ausgestattet. Auch hier kommt ein Baukastenkonzept bzgl. Hard- und Software zum Einsatz, gleichzeitig wird insbesondere durch die Verbrennungsregelung die Plattformstrategie unterstützt und die Flexibilität der Brennverfahren erhöht.

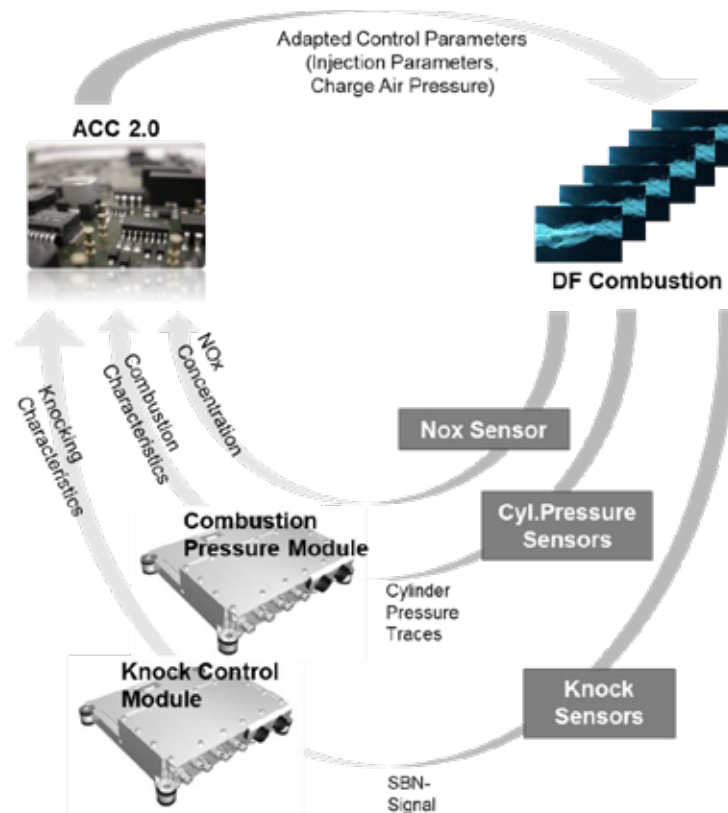


Abbildung 6: Verbrennungsregelung ACC 2.0

Die Verbrennungsregelung wurde für die 49/60-Baureihe grundlegend überarbeitet, und umfasst nun folgende Funktionen:

Balancing-Funktion: Beispielsweise durch Gasdynamik, aber auch durch Serienstreuung im Rahmen der zulässigen Toleranzen entstehen auch bei identischen Einstellparametern (Piloteinspritzung / Zündung) signifikante Unterschiede in der Verbrennung zwischen den einzelnen Zylindern. Die Varianz hängt wiederum von der Gesamt-Zylinderzahl ab, weshalb bislang teilweise bei bestimmten Zylinderzahlen konstruktive Maßnahmen getroffen wurden und / oder der Betriebsbereich eingeschränkt wurde. Durch die Verbrennungsregelung werden diese Unterschiede weitgehend ausgeglichen bzw. die Einstellparameter bestmöglich an die zylinderspezifischen Bedingungen angepasst. Einschränkungen im Betriebsbereich für einzelne besonders ungünstige Zylinderzahlen können damit vermieden werden.

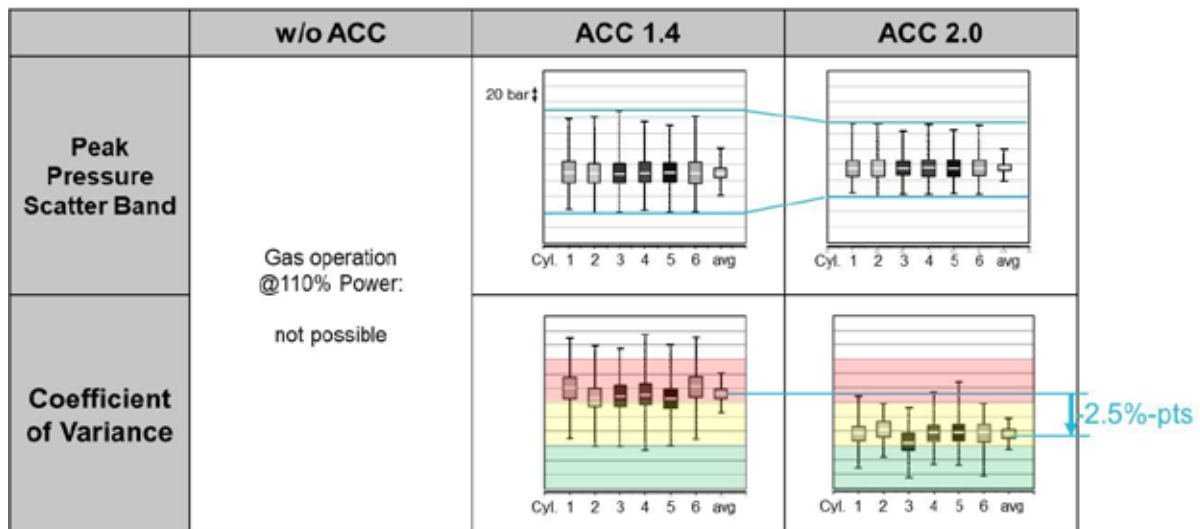


Abbildung 7: Laufstabilität bei 110 % Leistung im Gasbetrieb

Klopffregung: Auch die Klopfneigung bei den Gas- und DF-Brennverfahren unterscheidet sich zwischen den einzelnen Zylindern. Durch die Verbrennungsregelung werden insbesondere Zylinder mit erhöhter Klopfneigung effektiv entlastet. Damit ist ein stabiler Betrieb des Motors insgesamt näher an der Klopfgrenze möglich, womit einerseits höhere Wirkungsgrade erreicht werden und andererseits der Betriebsbereich bei kritischen Bedingungen (niedrige Methanzahl, hohe Ladelufttemperatur) erweitert werden kann. Wird dennoch die Klopfgrenze erreicht, beispielsweise bei deutlich reduzierter Methanzahl, so werden die Motoreinstellungen insgesamt adaptiert. Damit kann bestmöglich die verfügbare Leistung und der Wirkungsgrad aufrecht erhalten werden.

VVT: Gas- und DF-Brennverfahren reagieren sensibel auf die Verdichtungsendtemperatur und -druck, und damit insbesondere auf die Einlass-Schließt-Zeit bzw. den Miller-Faktor. Idealerweise würden die Steuerzeiten für verschiedene Brennverfahren und Lastbereiche individuell angepasst, um jeweils ideale Bedingungen für die Verbrennung zu schaffen. Stufenlos verstellbare VVT-Systeme sind allerdings kostenintensiv und fehleranfällig. Durch die Betriebspunktoptimierung der Verbrennungsregelung wird in gewissen Grenzen auch bei Baukasten bedingten, nicht-idealen Steuerzeiten, (z. B. CPP-Anwendung), eine hocheffiziente und schadstoffarme Verbrennung erreicht. Selbst der Schaltvorgang beim gestuften VVT-System, bei dem sich innerhalb sehr kurzer Zeit die Verdichtungsendbedingungen erheblich ändern, kann dynamisch ausgeregelt werden.

Der Einsatz der Verbrennungsregelung ermöglicht u. a. :

- Höchste Lastschaltfähigkeit
- Sehr große Betriebsbereiche mit später Leistungsreduzierung (MZ, LL-Temperatur)
- den kompletten Entfall der VVT beim G-Motor
- sowie den Einsatz der 3-stufigen VVT beim DF-Motor.
- und die Verwendung von Einheits-Nocken für G und DF

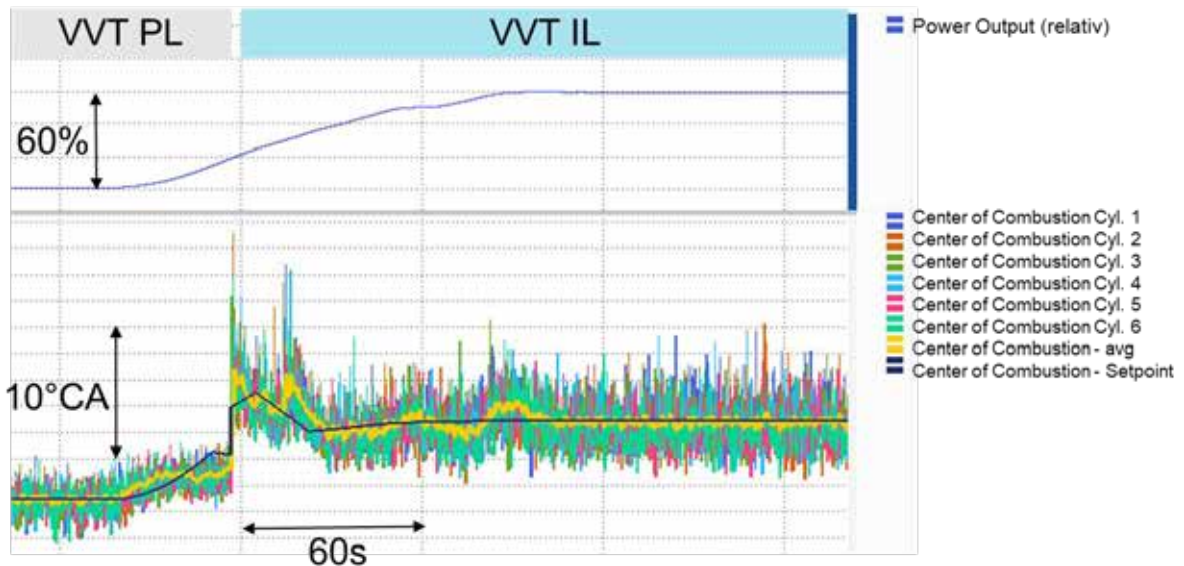


Abbildung 8: Verbrennungsschwerpunkte während einer Lastaufschaltung inkl. VVT-Schaltung (PL = part load; IL = intermediate load)

Schließlich werden durch die Verbrennungsregelung auch veränderte Umgebungsbedingungen, die auf den Motor insgesamt wirken, weitgehend ausgeglichen. Das können hohe Umgebungstemperaturen (\rightarrow erreichbare Ladelufttemperatur), unterschiedliche Luftfeuchte oder auch spezifische Kraftstoffeigenschaften wie z. B. Heizwert, Methan- und Cetanzahl sein (Abbildung 9).

Der Bedarf an konstruktiven Varianten für bestimmte Bedingungen wird damit reduziert bzw. der Einsatzbereich einzelner Varianten erweitert.

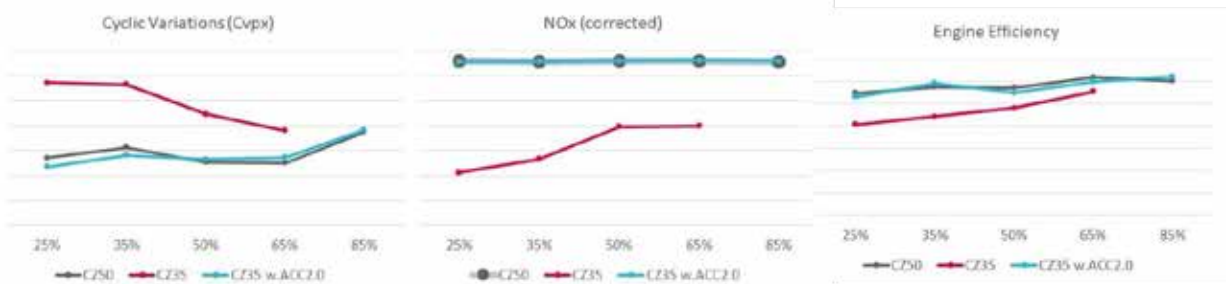


Abbildung 9: Einfluss von Pilotkraftstoffqualität (CZ); Kompensation mit Verbrennungsregelung

4. Ergebnisse

Während Entwicklung und Validierung des 49/60DF im Vollmotorenversuch durchgeführt wurden, lief zeitgleich die Brennverfahrensentwicklung des reinen Gasmotors (Vorkammer mit Zündkerze; G-Variante) im Einzylinderversuch.

Ausgestattet mit komplett identischen Bauteilen der DF-Variante kann mit dem G-Zündsystems die Zielleistung erreicht werden. Die geforderten HC Emissionen sowie der Zielwirkungsgrad für die G-Variante werden jedoch nicht erreicht (Abbildung 10 - rote Kurve). Durch eine gezielte Optimierung der Steuerzeiten und der Vorkammer können die G-spezifischen Ziele unter Beibehaltung aller anderen Bauteile realisiert werden.

Die Anforderungen der verschiedenen Brennverfahren an die Steuerzeiten erfordert hier einen Kompromiss im Gleichteilegedanken. Der HFO-Betrieb der DF-Variante macht eine bestimmte Ventilüberschneidung zur Einhaltung von Bauteil- und Abgasgrenztemperaturen notwendig. Für die G-Variante muss wegen der Einhaltung der geforderten HC Emissionen eine geringere Ventilüberschneidung angewendet werden (Abbildung 10 - blaue Kurve).

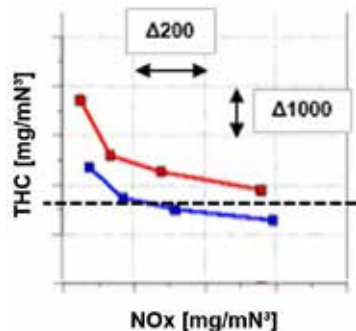


Abbildung 10: Vergleich: HC Emissionen im Gasbetrieb, Steuerzeiten DF (rot) und G-optimiert (blau)

Durch das stabile und robuste Zündverfahren der G-Variante kann zudem das System des variablen Einlassphasings (VVT) entfallen. Während die VVT essentiell für die Sicherstellung optimaler Pilot-Gas- und Dieselpbrennverfahren in einem Brennraum ist [1], kann die G-Variante mit festen Steuerzeiten höchste Leistungswerte bei niedrigsten Emissionen in Verbindung mit einer sehr guten Lastaufschaltfähigkeit bieten.

Abbildung 11 zeigt den Spitzendruck- und Brennverlauf der DF Variante im Dieselpbtrieb (innermotorisch TIERII - grün) und im Gasbetrieb (innermotorisch TIERIII - rot) sowie der G Variante (innermotorisch 800 mg/Nm³ HC – blau). Im Gasbetrieb kann bei beiden Varianten ein sehr ähnlicher Brennverlauf und somit eine nahezu vergleichbare Performance realisiert werden.

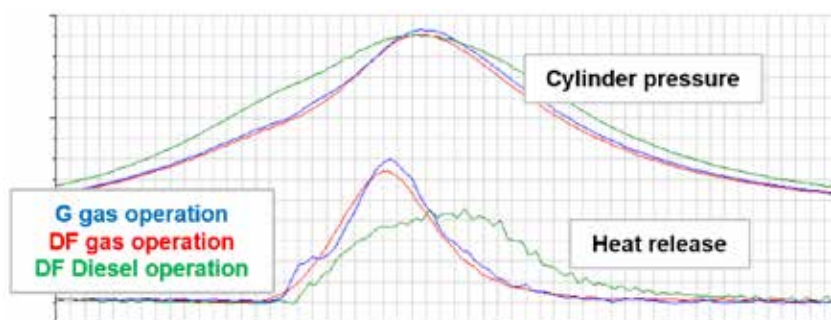


Abbildung 11: Zylinderdruckverlauf und Brennverlauf

49/60DF - Vollmotorversuch

Versuchsumfang und -inhalte

Hauptziele der Vollmotorerprobung sind sowohl die Validierung der mechanischen und thermodynamischen Motorauslegung als auch der Nachweis des Reifegrades der Motorapplikation. Ausgangspunkt bildeten hierbei die Ergebnisse der Brennverfahrensentwicklung und Vorvalidierung am Einzylindermotor. Als Vollmotor-Prototyp wurde ein Sechszylinder-Reihenmotor in Marinekonfiguration für Einmotoren-Antrieb ausgewählt. Der komplette Versuchsplan umfasst dabei etwa zweieinhalb Jahre inklusive zweier Hardware-Konfigurationen und einem Type-Approval-Test. Der Erststart des Motors

fand am 01.09.2021 statt, dem Termin der im Versuchsplan zwei Jahre zuvor festgelegt worden war.

Hauptmerkmale des 49/60DF Prototypmotors:

- 6-Zylinder Reihenmotor, 7800kW bei 600U/Min
- Betriebsdrehzahlbereich: 60 % der Nenndrehzahl für mechanische Antriebsanwendungen, 80 % für elektrische Gleitfrequenzanwendungen
- Schrägelastische Motorlagerung mit trockener Ölwanne
- Am Motor angebautes zweistufiges Auflademodul mit geregelter Ladelufttemperaturkühlung (Niederdruckstufe: TCT-40, Hochdruckstufe: TCX-21)
- Angebaute Medienpumpen für Schmieröl, HT- und LT-Kühlwasser
- Wastegate über beide Turbinenstufen zur Luftpfadregelung
- Ladeluft-Umblasen zum Steuern des Pumpgrenzabstands bei Betrieb mit variabler Drehzahl
- Ladeluft-Abblasen für arktische Umgebungsbedingungen
- 3-Punkt VVT auf Einlass-Seite
- Common Rail-Einspritzsystem der zweiten Generation mit separatem Pilot-Einspritzsystem
- Multi-Point-Hauptkammergaseindüsung

Kernergebnisse und Eckdaten der Prototyperprobung:

- 3000 Gesamtbetriebsstunden – davon 1700 im Gasbetrieb – mit über 3500 Betriebswertmessungen (Stand Februar 2024)
- Bestätigung einer hohen Auslegungs- und Übertragungsgüte der Vollmotordaten im Abgleich mit Einzylindermotor und thermodynamischer Auslegung
- Umfassende Bauteilmesskampagne zum Nachweis der Serientauglichkeit für alle Schlüsselkomponenten
- Nachweis der mechanischen Robustheit durch erfolgreich bestandenen 100h Extreme-Conditions Test (ECT)
- Validierung der Schweröлтаuglichkeit inklusive Startfähigkeit, Rußverhalten und direkter Umschaltung von HFO auf Gasbetrieb
- Kalibrierung und Validierung der neuen Verbrennungsregelung für Micro-Pilot Dual-Fuel-Brennverfahren
- Applikation und Optimierung des gesamten Betriebsbereichs für alle definierten Anwendungen:
 - o Validierte Hardware-Varianten: 3
 - o Validierte Applikations-Varianten: 5
- Ermittlung der Stabilitätsgrenzen und De-Rating-Punkte des Betriebskennfelds gemäß Lastenheft:
 - o Gas \geq Methanzahl 80 unter Marine-Tropenbedingungen und Weltbankbedingungen
 - o ISO-Bedingungen: Gas mit Methanzahl \geq 70 (wirkungsgradoptimierte Variante) / \geq 60 (betriebsbereichsoptimierte Variante)
 - o 10% Ausregelreserve [110 % maximum continuous rating (MCR)]
 - o maximal darstellbaren Lastrampen und Hochfahrzeiten mit umfassender Datenakquise
- Nachweis der Fähigkeit zur Kraftstoffumschaltung zwischen 10 % und 100 % MCR mit direkter Umschaltung von HFO- auf Gasbetrieb
- Erfolgreiche Zertifizierung des Reihenmotors im Zuge des Type Approval Test unter Beteiligung von sechs Marine-Klassen inklusive Anwendung für variable Drehzahl und Einmotorenantrieb.

		49/60DF	Δ zum 51/60DF HE
SFC 85% Marine	kJ/kWh	6990	-2,3 %
SFC 100% Stationär	kJ/kWh	6936	-1,6 %
SFOC 85% Marine	g/kWh	171	-2,9 %
SFOC 100% Stationär	g/kWh	171	-2,3 %
Zylinderleistung	kW/Zyl.	1300	+23,8 %
Eff. Mitteldruck	bar	23	+12 %

* Including pilot fuel oil, with attached pumps, E2/D2 IMO Cycle, ISO conditions, 50mbar exhaust back pressure, +5% tolerance, Gas Mode: Tier III, MN ≥ 80, pilot fuel DMA with CN ≥ 55; Diesel Mode: Tier II, DMA/DMB with NCV 42700kJ/kWh

Tabelle 1: Motor-Eckdaten

Parallel zur Prototypenprobung durchlief bereits im Spätsommer 2022 der erste Kundenmotor erfolgreich sein Werkabnahmeprogramm, im Verlauf des Jahres 2024 werden sieben weitere Motoren folgen und zahlreiche weitere befinden sich in der Projektierungsphase.

Sensitivität und Stabilität des Brennverfahrens mit optimierter Verbrennungsregelung

Ein modernes Dual-fuel-Brennverfahren das auf maximale Performance und Effizienz optimiert ist, reagiert sehr empfindlich auf jegliche Veränderungen in den Betriebsrandbedingungen. Die zunehmende Bandbreite an verfügbaren Pilot-Kraftstoff- und Brenngaszusammensetzungen verschärft diese Situation. Darum wurde die zuvor bereits beschriebene ACC-2.0 als erweitertes und robustes Verbrennungsregelungskonzept für den 49/60DF entwickelt um den Bedarfen der Micro-Pilot-gezündeten Dual-Fuel-Verbrennung gerecht zu werden. Während der gesamten Erprobungsphase hat die neue Verbrennungsregelung ihre Fähigkeit, die Kontrolle über das Brennverfahren zu behalten, eindrucksvoll unter Beweis gestellt, besonders in den Randbereichen des Betriebskennfeldes und im transienten Betrieb. Kernstück ist ein schneller und adaptiver Regelkreis für die Verbrennungsschwerpunktlage, der, in Verbindung mit der closed-loop NOx-Regelung, eine hohe Arbeitspunktstabilität und optimale Effizienz über einen weiten Betriebsbereich ermöglicht. Ergänzt wird die Regelung durch die bewährte Load-Balancing-Funktion, die eine permanente enge Gleichstellung aller Zylinder sicherstellt.

Variabler Einlassventiltrieb im Gasbetrieb

Da der ausgelegte Miller-Kreisprozess, der notwendig ist um die gesteckten Leistungs- und Wirkungsgradziele im Hochlastbereich zu erreichen, nicht geeignet ist um eine ausreichende Verbrennungsstabilität im Niedriglastbereich und bei Leerlauf sicherzustellen, wurde die weiter oben beschriebene Dreipunkt-VVT eingeführt (VVT). Während die Verwendung einer VVT im allgemeinen sehr gebräuchlich für Motoren von MAN Energy Solutions ist, stellte die Anwendung im Gasbetrieb ein Novum dar. Die Dyna-VVT arbeitet als Phasensteller mit drei diskreten Positionen und verfügt über einen patentierten Antrieb über Motor-Schmieröl, der weitere Aktuatoren und Steuerungen überflüssig macht (s. Abbildung 1).

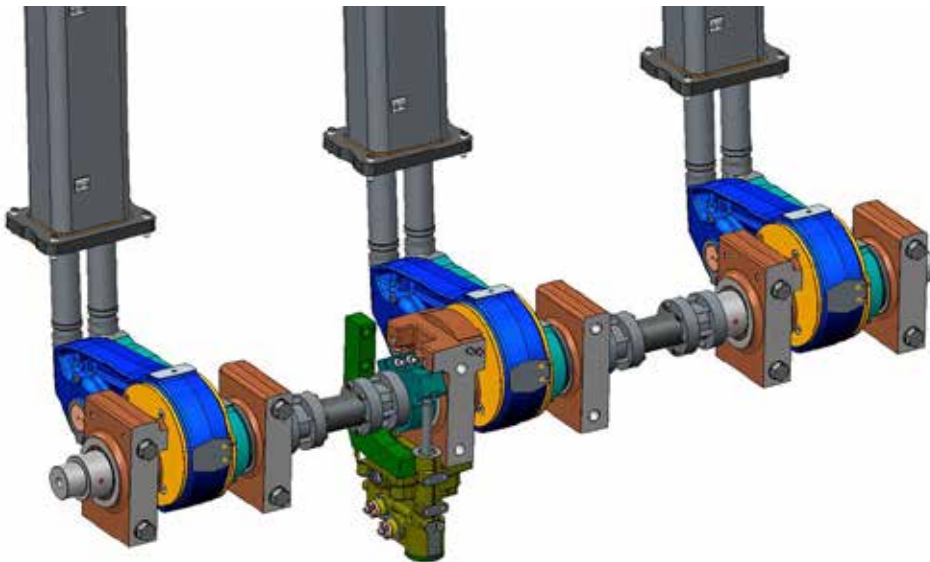


Abbildung 12: Dyna-VVT Antriebssegment

Neben der Betriebszuverlässigkeit und der mechanischen Haltbarkeit stand ein stabiles Motorverhalten während des VVT-Schaltvorgangs im Gasbetrieb im Fokus der Vollmotortests. Die schlagartige Änderung von Ladungswechsel und effektivem Verdichtungsverhältnis im Schaltvorgang stellen eine heftige Unstetigkeit für die Verbrennung dar. Eine Veränderung der Einlasssteuerzeiten erfordert signifikant unterschiedliche Motoreinstellungen um im gleichen Betriebspunkte ähnliche Verbrennungskennwerte zu erreichen. Um diese Unstetigkeit zu meistern bedarf es der Anwendung einer durchdachten Regelungsstrategie. Der 49/60DF zeigt, dass es möglich ist einen stoßfreien Übergang zwischen den unterschiedlichen VVT-Stellungen auch bei schnellen Lastrampen umzusetzen.

Vollmotorerfahrungen Common Rail System der zweiten Generation

Die 49/60 Motorenfamilie ist mit dem MAN Energy Solution Common Rail-Einspritzsystem der zweiten Generation ausgerüstet um:

- Auch im Flüssigkraftstoffbetrieb Best-In-Class Performance zu erreichen
- Eine solide Grundlage für zukünftige Weiterentwicklungen zu bieten
- Und nicht zuletzt den Weg für Future Fuel-Anwendungen mit MeOH und NH₃ zu ebnen

Die wesentlichste Innovation des Systems liegt darin, dass der Kraftstoffspeicherdruck bis an die Düse ansteht, was eine exzellente Gemischaufbereitung auch bei kleinen Einspritzmengen und die Fähigkeit zur Mehrfacheinspritzung ermöglicht. Das DF-Brennverfahren profitiert in mehrfacher Hinsicht von diesem Merkmal. So konnten das Rußverhalten im Teillastbetrieb und die Startfähigkeit mit HFO gegenüber dem 51/60DF deutlich verbessert werden (Abbildung 13:3). Das CR2.2-System erlaubt es dem 49/60DF trotz des niedrigen effektiven Verdichtungsverhältnisses mit HFO zu starten ohne dass dafür die Piloteinspritzung aktiv sein oder die Ladeluft vorgewärmt werden muss.

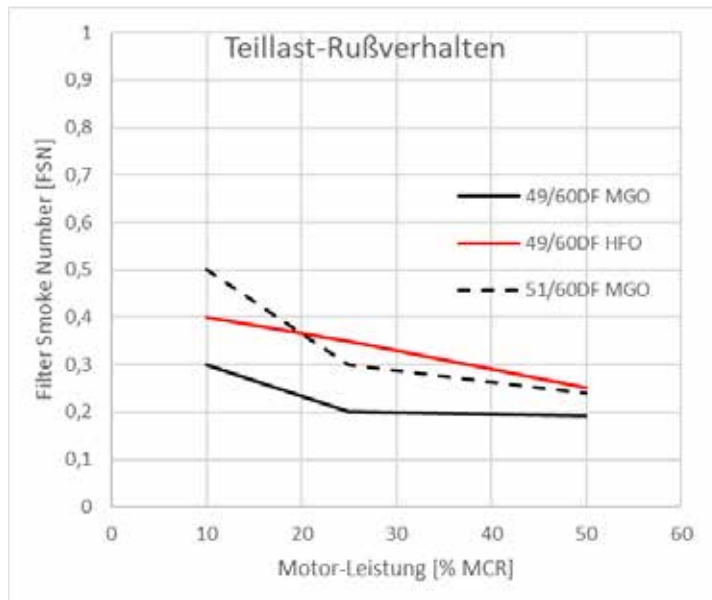


Abbildung 13: Teillast-Rußverhalten

Ergebnisse der Transientbetriebsvermessung

Starkes Millern und hoher Aufladegrad haben im Allgemeinen einen negativen Einfluss auf die dynamischen Fähigkeiten, weil dadurch die Phase des Luftmangels während der Lastaufnahme verlängert wird. Der 49/60DF nutzt eine Reihe gut aufeinander abgestimmter Maßnahmen und Schlüsseltechnologien welche diesen verzögernden Einfluss ausgleichen und in Summe eine herausragende transiente Motorperformance ermöglichen:

- Die VVT ermöglicht durch ein erhöhtes effektives Verdichtungsverhältnis bessere Ausgangsbedingungen für Lastaufschaltungen im Gasbetrieb. Auf diese Weise kann Klopfen während der Lasterhöhung unterdrückt werden, da der Motor mit niedrigerer Ladelufttemperatur betrieben werden kann als im Nennpunkt. Somit ist die VVT-Verstellstrategie im Einklang mit dem natürlichen Temperaturverlauf über der Ladedruckkurve. Ferner kann so das initiale Luft-Gas-Verhältnis magerer gewählt werden, wodurch zusätzlich Klopfabstand entsteht.
- Verglichen mit einem einstufigen Aufladesystem ermöglicht die zweistufige Aufladung einen schnelleren Ladedruckaufbau durch reduzierte drehende Massen. Zusätzlich zeichnet sich die Abgasführung des 49/60DF durch einen kompakten Aufbau mit geringen thermischen Verlusten aus, der den Ladedruckaufbau zusätzlich begünstigt.
- Die fortschrittliche Verbrennungsregelung des 49/60DF ist in der Lage das minimal fahrbare Luft-Gas-Verhältnis, das durch die Klopfgrenze bestimmt wird, kurzzeitig nach unten zu verschieben um Phasen des Luftmangels während der Turboladerbeschleunigung zu überbrücken.
- Die Lastaufschaltfähigkeit im Gasbetrieb kann durch die sogenannte „Fuel Oil Boost Injection Gas Mode“ nochmals erweitert werden in dem Gas durch Flüssigkraftstoff aus dem Haupteinspritzsystem ersetzt und so die Klopfgrenze durch ein abgemagertes Luft-Gas-Gemisch weiter verschoben wird.
- Im Flüssigkraftstoffbetrieb überkompensiert das CR 2.2 System mittels Einsatz der Boost Injection die negativen Effekte der starken Millersteuerzeiten durch kurze Ansprechzeiten und die überragenden Rauchgrenzabstand bei weitem.

Die Ergebnisse der Dynamikversuche am Prototypmotor waren überaus zufriedenstellend und markieren einen wichtigen Meilenstein in der Entwicklung des 49/60DF. Im direkten Vergleich mit dem 51/60DF zeigt der 49/60DF ein deutlich besseres Transientbetriebsverhalten (Abbildung 1414) obwohl gleichzeitig spezifische Leistung und

Wirkungsgrad gesteigert wurden (vgl. Tabelle 1). Die herausragenden dynamischen Fähigkeiten decken alle Standardsituationen des Motorbetriebs im reinen Gasbetrieb ab, auch Fälle wie Manövrierbetrieb und schnelles Hochfahren. Die „Fuel Oil Boost Injection“ wird im Gasbetrieb nur noch für außergewöhnliche Lastrampen benötigt.

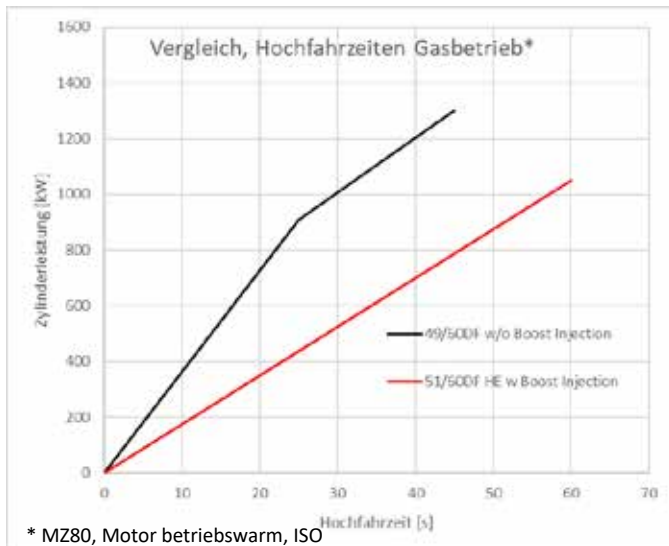


Abbildung 14: Hochfahrzeitenvergleich Gasbetrieb

Betrieb mit variabler Drehzahl im CPP-Kennfeld

Die wirkungsgradoptimierte Variante des 49/60DF deckt mit der Standard-Turbolader-Konfiguration ein breites Betriebskennfeld ab, das sich, neben elektrischen Antriebsanwendungen mit Konstantdrehzahl und Gleitfrequenz, sehr gut für mechanische Antriebsanwendungen mit hocheffizienten Verstellpropellersystemen eignet. Dabei liegt ein großer Teil des Dauerbetriebsbereichs auf der theoretischen Festpropellerkurve was einen optimalen Gesamtantriebswirkungsgrad ermöglicht (Abbildung 1515).

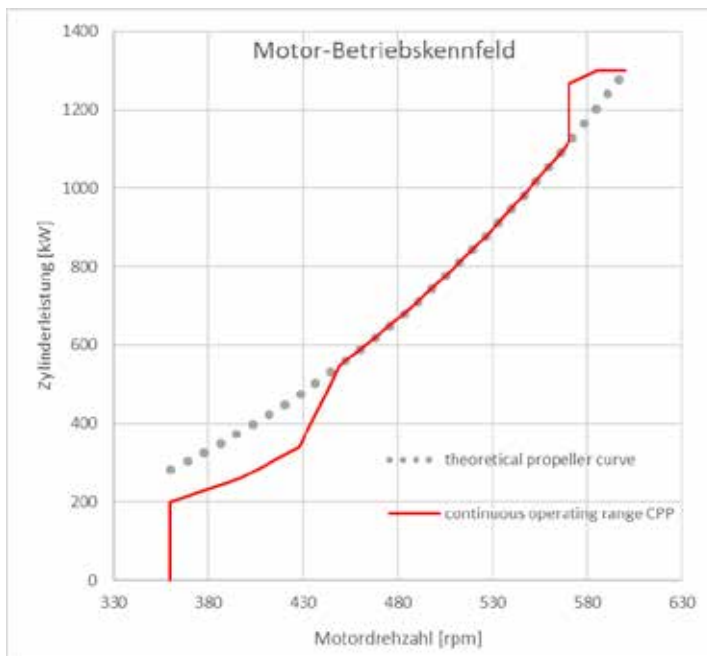


Abbildung 15: Motor-Betriebskennfeld Controllable pitch propeller (CPP)

Extreme Conditions Test und Type Approval Test:

Der Extreme Conditions Test (ECT) ist ein MAN Energy Solutions-spezifischer standardisierter Validierungs-Meilenstein den jede Motorbaureihe im Zuge der Prototypenprobung durchlaufen muss. Die veranschlagten 100 Betriebsstunden gliedern sich in drei Abschnitte:

- Der ECT selbst: fünf Stunden Betrieb bei 110 % Nennleistung mit Destillatkraftstoff. Schmieröldruck, Schmieröltemperatur und Kühlwassertemperatur werden dabei auf die festgelegten Grenzwerte für die Sicherheitsabschaltung eingestellt.
- Lastwechsellauf: Der Test umfasst insgesamt 19 Zyklen, angefangen mit acht Zyklen im HFO-Betrieb, einem Zwischenzyklus mit Destillatkraftstoff und zehn Zyklen im Gasbetrieb. Jeder Zyklus dauert fünf Stunden und stellt eine Sequenz mehrerer Laststufen von Leerlauf bis zur Maximalleistung dar (120 % MCR mit Flüssigkraftstoff / 110 % MCR mit Gas) und beinhaltet steile Lastrampen um die Motorstruktur hohem thermischen und mechanischen Stress auszusetzen.
- Full Torque Drückungstest: Betrieb des Motors für zweimal 30 Minuten bei minimaler Drehzahl mit Nennmoment um das tribologische System explizit zu beanspruchen. Als Abschluss dieses Abschnitts wird der Motor komplett entlastet und langsam mit der Drehzahl bis auf den Wert der Sicherheitsabschaltung beschleunigt.

Der ECT des 6L49/60DF Prototypmotors und die nachfolgende Inspektion aller wesentlichen belasteten Motorbauteile lieferten ein hervorragendes Ergebnis und liefern den Nachweis dafür, dass das Design den Belastungen des Feldbetriebs standhält.

Als neue Motortype muss der 49/60DF in Zuge eines Type Approval Tests zertifiziert werden um als Antriebsmotor auf Schiffen einsetzbar zu sein. Nach mehrwöchiger intensiver Vorbereitung konnten im März 2023 eine Woche lang im Beisein der Vertreter von sechs Schifffahrtsklassen alle notwendigen Tests erfolgreich vorgefahren werden. Dabei wurden neben einer intensiven Prüfung des Alarm- und Sicherheitssystems unter den verschärften Randbedingungen einer Einmotorenanwendung Lastpunkte auf der Konstantdrehzahllinie und der Propellerkurve bis auf 60 % Nenndrehzahl angefahren. Was für den Reihenmotor somit bereits abgeschlossen ist, steht für den V-Motor noch aus, da dieser von fast allen Schifffahrtsklassen als eigene Baureihe angesehen wird. Dieses Unterfangen ist jedoch bereits für Januar 2025 im Rahmen der Erprobung eines 12V-Kundenmotors eingeplant und wird den erfolgreichen Abschluss der 49/60DF Vollmotorerprobung bilden.

Weiterentwicklung von Brennverfahren und Methodik

Der Erkenntnisgewinn aus der bisherigen Brennverfahrensentwicklung ebenso wie der technologische Fortschritt im CFD-Umfeld ermöglichten es noch während der Vollmotorerprobung des 49/60DF eine Weiterentwicklung des Brennverfahrens anzustoßen. Neben dem Methanschlepp, der sowohl aus Marktsicht wie auch von regulatorischer Seite immer mehr in den Fokus rückt, bestand die Hauptmotivation zu diesem Schritt in der Schaffung einer robusten tribologischen Basis für zukünftige Kraftstoffe. Kernelemente bilden eine schadraumoptimierten Zylinderkopf-Buchsenkombination mit optimiertem Kraftfluss und eine verbesserte Gemischbildung im Einlasskanalbereich. Die Vollmotorerprobung im Anschluss an die Einzylinderentwicklung ab Mitte 2023 stand neben der Bauteilvalidierung im Zeichen der umfassenden Vermessung zum Aufbau eines DoE-Modells für alle projektierten Applikationen und Varianten. Dabei kam zum ersten Mal in vollem Umfang eine Strategie zum Einsatz bei der DoE-Modell, thermodynamisches Motor-Modell und Motorsteuerungs-Modell in einem virtuellen Motor zusammengeführt werden. Ziel ist, alle Zylinderzahlen und Varianten inklusive Auflade- und Ladungswechseleinflüssen an einem digitalen Zwilling des Motors im Vorfeld zu applizieren. Das umfasst sowohl die Optimierung der Kennfeldeinstellungen im Spannungsfeld von Wirkungsgrad und Emissionen wie auch Ermittlung von Steuerungs- und Regelungseinstellungen im stationären und dynamischen Motorbetrieb. Damit bietet das Werkzeug das Potential in erheblichem Umfang

Motorbetriebszeit und Entwicklungskosten einzusparen (ca. 20 % weniger Betriebswertemessungen für technische Verkaufsunterlagen und 50 % reduzierter Zeitbedarf bei der Applikationsoptimierung). Im Vorgriff auf die zukünftige Vollmotorerprobung des 49/60G wird dieses Vorgehen bereits auf Basis von Einzylinder-Daten angewandt, dadurch sind Betriebswerte zur Bedienung von Kundenprojektanfragen deutlich früher verfügbar und der Zeitbedarf am Vollmotor kann nochmals reduziert werden.

5. Zusammenfassung und Ausblick

Mit den aktuellen Derivaten 49/60, 49/60DF und 49/60G stehen nun Motoren mit höchster Leistung und Effizienz zur Verfügung. Im Vergleich zu den Vorgängermotoren wurde die Zylinderleistung um 23 % auf 1300kW/Zyl. angehoben.

Mit einem effektiven Wirkungsgrad bis zu 52,3 % im Gasbetrieb wird das Entwicklungsziel erreicht und der Vorgängermotor deutlich übertroffen. Hinzu kommt ein vergrößertes Betriebsfenster im Hinblick auf Umgebungsbedingungen und Methanzahlbedarf.

Im Gasbetrieb werden die Grenzwerte für Stickoxide nach IMO-Tier 3 bzw. nach Weltbank innermotorisch eingehalten werden. Gleichzeitig sind die HC-Emissionen gegenüber den Vorgängermotoren um mehr als 50 % reduziert.

Durch den modularen Baukasten ist es gelungen, trotz zahlreicher Anwendungsvarianten ein Höchstmaß an Gleichteilen zu verwirklichen. Insbesondere die standardisierte Power Unit lässt sich auch durch die Vormontage logistisch- und kostenoptimal herstellen.

Die Architektur der 49/60 Motorfamilie ermöglicht die vereinfachte Anpassung sowohl der Hard- als auch der Software der Brennverfahren für zukünftige Kraftstoffe wie Methanol, Ammoniak oder Wasserstoff als PFI oder auch HPDI.

.....

References

- [1] I. Wilke et al., CIMAC 2023, paper 146, "MAN ES 49/60DF - Maximum performance from the modular system"

Using Wood Gas for CO₂ Neutral Power Generation – Performance Improvements of a Special Gas Engine

Die Verwendung von Holzgas zur CO₂-neutralen Energiegewinnung – Verbesserungen an einem Sondergasmotor

Mario Frischmann*, **Stefan Schiestl**, **Robert Böwing**

INNIO Jenbacher GmbH & Co. OG, A

Abstract

Sustainably produced wood gas is a valid and proven fuel for CO₂-neutral and best-case CO₂-negative heat and power generation. However, the operation of large gas engines with wood gas comes with some challenges. Fuel gas characteristics such as low supply pressure, low calorific value and fluctuating composition lead to challenges regarding gas supply and gas mixing system. Furthermore, the high variety and variability of different species in the gas composition like CO, H₂, CH₄, N₂ and CO₂ make in-house investigations on development test benches difficult and expensive. Despite all these challenges, high power output, high efficiency and maximum engine uptime are required to meet customer expectations.

Various product development activities were conducted to further enhance customer benefits. These activities included investigations on multiple field test engines operating on wood gas with different hardware configurations. Various hardware and software changes were carried out to improve power output and engine uptime: The gas mixing system was redesigned to handle high gas volume flows at low gas supply pressures. Camshaft, piston and cylinder head, were optimized to achieve higher power output and higher efficiency. New engine oil formulations and piston ring packs were investigated to minimize abnormal combustion events and increase lubricant lifetime. Undesired engine responses to fast changes in gas quality were resolved by a newly developed software function. In addition, a new humidity control strategy to handle the condensation risks downstream of the intercooler was successfully implemented.

The stated development activities, which were supported by long-term field engine investigations, resulted in improved and even more robust wood gas engine performance with a power output of 1050 kW_{el} (about 14 bar BMEP) and an electrical efficiency of more than 40 %. This corresponds to an improvement of about 10 % in power output and about 1 %pt in electrical efficiency versus the previous engine version.

* Speaker/Referent

Kurzfassung

Nachhaltig erzeugtes Holzgas ist ein bekannter und bewährter Energieträger für die CO₂-neutrale bzw. im Optimalfall CO₂-negative Strom- und Wärmeerzeugung. Großgasmotoren damit zu betreiben ist jedoch mit einigen Herausforderungen verbunden. Die besonderen Gaseigenschaften wie niedriger Versorgungsdruck, niedriger Heizwert und schwankende Zusammensetzung sind Herausforderungen für die Gaszuführung und das Gasmischsystem. Außerdem machen die große Vielfalt und Variabilität der verschiedenen Bestandteile in der Gaszusammensetzung wie CO, H₂, CH₄, N₂ und CO₂ Untersuchungen an Entwicklungsprüfständen schwierig und teuer. Trotz dieser Herausforderungen sind eine hohe elektrische Leistung, ein hoher Wirkungsgrad und eine maximale Verfügbarkeit des Motors erforderlich, um die Erwartungen der Kunden zu erfüllen.

Um den Kundennutzen weiter zu erhöhen, wurden diverse Entwicklungsaktivitäten an mehreren holzgasbetriebenen Pilotmotoren durchgeführt, die mit unterschiedlichen Hardwarekonfigurationen ausgestattet waren. Eine Reihe von Hardware- und Software-Änderungen wurden vorgenommen, um die Leistungsfähigkeit und Verfügbarkeit des Motors weiter zu verbessern: Das Gasmischsystem wurde neu konzipiert, um den hohen Gasvolumenstrom bei niedrigem Gasversorgungsdruck zu bewältigen. Nockenwellen, Kolben und Zylinderkopf wurden optimiert, um die Motorleistung und den Wirkungsgrad zu steigern. Neue Ölformulierungen und Kloben-Ringpakete wurden eingeführt, um Verbrennungsanomalien zu verringern und die Schmierstofflebensdauer zu verlängern. Unerwünschte Reaktionen des Motors auf schnelle Änderungen der Gasqualität wurden durch eine neu entwickelte Softwarefunktion behoben. Eine neue Feuchtigkeits-Regelungsstrategie zur Verringerung des Kondensationsrisikos stromab des Ladeluftkühlers wurde erfolgreich implementiert.

Die genannten Entwicklungsaktivitäten, die durch Langzeitbeobachtungen unterstützt wurden, ergaben, dass die Pilotmotoren eine Leistung von 1050 kW_{el} (etwa 14 bar BMEP) mit einem elektrischen Wirkungsgrad von mehr als 40 % robust erreichen. Dies entspricht einer Verbesserung von ca. 10 % in der Motorleistung und ca. 1 %pkt im elektrischen Wirkungsgrad gegenüber der Vorgänger-Motorversion.

1. Introduction

The INNIO Group is a leading provider of energy solutions and services with its headquarter in Jenbach (Austria) and further main production sites in Waukesha (Wisconsin, USA) and Welland (Ontario, Canada). Using the brand names Jenbacher and Waukesha as well as the digital platform name myPlant, INNIO offers innovative systems for decentral power generation and gas compression. The Jenbacher gas engine gen-sets provide combined heat and power for a wide range of applications in a reliable and efficient manner covering an electrical power range from 250 kW_{el} to 10,6 MW_{el} at or near the point of use.

1.1 Jenbacher Type 4 Gen-Set

The Jenbacher Type 4 gen-sets were introduced in 2001 and cover an electrical power range from 900 kW_{el} to 1,6 MW_{el} today. About 5300 gen-sets have been delivered so far having gathered more than 100 million operating hours in total. Table 1 shows the main engine data.

Table 1: Jenbacher Type 4 engine data for natural gas operation with MN_{min} 75

Bore / stroke	mm	145 / 185
Cylinder displacement	dm ³	3.055
BMEP	bar	≤ 21
Rated speed	rpm	1500 (50 Hz), 1200 & 1800 (60 Hz)
Cylinder numbers	-	12, 16, 20
Electrical power	kW _{el}	935, 1250, 1560
Electrical efficiency ¹	%	≤ 44.0
Total efficiency ²	%	≤ 92.1

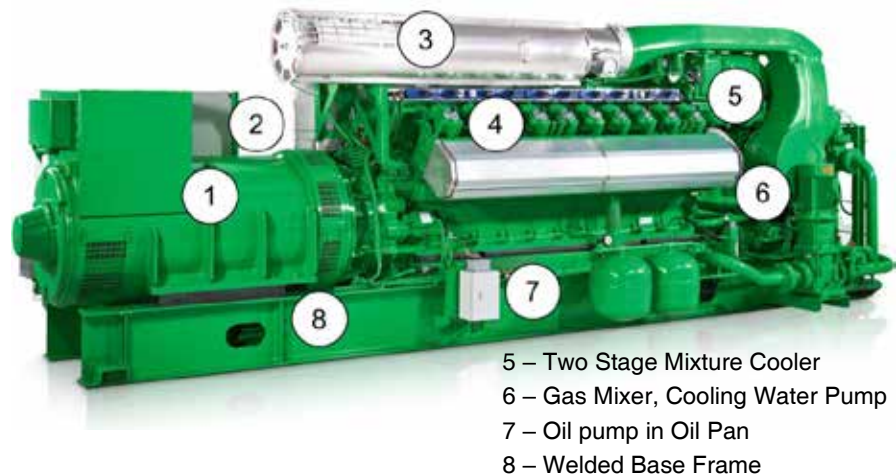
1. NO_x = 500 mg/Nm³ @ 5 % O₂ in the exhaust gas, 50 Hz operation
2. Electrical and thermal efficiency, 70°C cooling water return temperature, 120°C exhaust gas temperature downstream heat exchanger

The combustion system of this lean burn gas engine with direct ignition is based on a four valve cylinder head with high swirl intake ports, a Miller camshaft with late intake valve closing and a piston with a deep asymmetric bowl and distinct squish faces. The lean air-fuel mixture gets ignited by means of a shielded spark plug and a special ignition system.

Mixture preparation is being realized with a gas mixer and a gas control valve on the low-pressure side of the turbocharger compressor. Knock sensors are applied on each cylinder for combustion monitoring and engine protection. The engine power is controlled by means of a throttle flap and a compressor bypass valve.

The described engine concept enables high electrical and thermal efficiencies as well as low exhaust gas emissions. It also facilitates a large number of fuel gas applications covering a wide heating value range from 1 kWh/Nm³ (coal mine gas) to 26 kWh/Nm³ (propane) and a wide methane number range from 0 (hydrogen) to 150 (landfill gas). Figure 1 shows a J420 gen-set consisting of engine, generator and base frame.

- 1 – Generator
- 2 – Blow-By Filter
- 3 – Air-Filter
- 4 – Cylinder Heads



- 5 – Two Stage Mixture Cooler
- 6 – Gas Mixer, Cooling Water Pump
- 7 – Oil pump in Oil Pan
- 8 – Welded Base Frame

Figure 1: Jenbacher J420 gas engine gen-set

1.2 Wood Gas

The fossil fuel age seems to be coming to an end and bioenergy is increasingly in the focus of future-oriented business. In the heat and power generation of tomorrow, wood will play a particularly important role. With wood gas power plants, the renewable raw material can be utilised optimally, and the positive impact on climate relevant emissions has been confirmed. In contrast to wind and solar energy, bioenergy is a renewable energy that can be switched on and off when needed. Forest residues from sustainable managed resources are the input material for the wood gas production process. Three main steps are common for this process: Pyrolysis, gasification and preparation (filtration, cooling, washing). The gasification is performed in an oxygen-limited environment. Taking the biochar produced in the gasification step into account the gas production has a negative carbon dioxide footprint. This statement is valid if the biochar is not burned afterwards. Therefore, the biochar acts as a CO₂ sink. The chemical energy contained in the wood gas is the energy source for the internal combustion engine. Table 2 lists the gas composition and properties of a standard wood gas.

Table 2: Wood gas composition and properties

Main Component	Unit	Reference	Range
Methane CH ₄	Vol %	5	0 - 15
Longer chain hydrocarbons	Vol %	0	0 - 3
Carbon monoxide CO	Vol %	18	15 - 22
Hydrogen H ₂	Vol %	16	15 - 30
Nitrogen N ₂	Vol %	47	0 - 51
Carbon dioxide CO ₂	Vol %	14	0 - 25
Lower Heating Value	kWh / Nm ³	1.6 ¹	1,5 – 1,8
Laminar Flame Speed	cm / sec	30	16 – 65 ²
L _{min}	l air / l gas	1.35 ³	-

1. - 84 % compared to NG 2. + 71 % compared to NG 3. - 87 % compared to NG

2. Challenges and Customer Expectations

The INNIO Jenbacher engine platform Type 4 was introduced to the market in 2001. Next to engine operation with Natural Gas as energy source, INNIO Jenbacher have also been developing versions of the Type 4 engine for operation on non-natural gases since its release. In the beginning, the fuels landfill gas, biogas and coalmine gas were covered. As a second step engine operation with special gases like wood gas was realized. Back then wood gas production plants generated gas of low quality in respect to gas cleanliness. In 2018, a Type 4 wood gas engine was installed in Italy. The plant used a new and innovative gas production process. The purity of the gas was outstanding. The gas composition showed very low quantities of primary, secondary and tertiary tars, Sulphur, Ammonia and dust. The site has been producing 950 kW of electrical power and the same output of thermal heat with the help of the Jenbacher J420 engine. Over thousands of operating hours various engine operational characteristics like reliability, availability and wear status of components were observed in detail. Today about 45 % of the INNIO Jenbacher engines in Europe run on pipeline gas and 55 % on Non-Natural Gases. In this segment approximately 40 wood gas fueled INNIO Jenbacher engines are in operation. Pilot engine activities at five customer sites guarantee the further development of this version. The following observations can be shared:

Engine operation highlights:

1. High start success rate
2. High reliability and availability at an early stage
3. Constant efficiency over lifetime
4. Low NOx emissions
5. Low maintenance costs (including emission aftertreatment)
6. Low wear on components
7. High lifetime of spark plugs and engine oil

Gas production and engine operation challenges:

1. Low gas supply pressure, low gas calorific value and fluctuating gas compositions
2. Occurrence of combustion abnormalities
3. Maximum gas mixer capacity touched due to gas pressure changes
4. Control instabilities triggered by gas quality changes

Customer expectations for future improvements:

1. Higher engine power output, higher engine efficiency and higher engine uptime

At early operation hours engine reliability and availability were usually high. After thousands of operating hours on the system engine shutdowns increased and engine reliability decreased. Combustion abnormalities were one driver of this change. Field measurement campaigns with the goal to understand the root cause were initiated. The data acquisition during these campaigns helped to understand the underlying mechanism in detail. In a next step the robustness of the system was improved. Mechanical investigation efforts resulted in increased knowledge about combustion chamber deposit built up as well as the condition and wear rate of the engine parts.

3. Product Development

The development of large internal combustion engines that utilize wood gas as an alternative fuel is a complex process, requiring a detailed integration of software and hardware elements. This chapter will look closely at these two crucial elements, explaining how they work together

and synergize to build a functional, efficient, and reliable system. The focus will be placed on the unique challenges and customer expectations associated with wood gas as outlined in chapter 2. The methodology used for the product development involved the review of internal knowledge, documentation and field experience, as well as the understanding of customer needs. All were required to identify components on the existing baseline wood gas engine version (B) which could be improved to overcome the challenges and meet customer expectations. This initial improvement step is then followed by long-term investigations of pilot engines at customer sites, which was a crucial step to finalize the product development process.

3.1 Hardware

In comparison to the existing baseline engine version (B), the new engine version (D) utilizes several newly developed or adapted hardware components. Some of these components are described in the following chapters.

3.1.1 Gas Mixing Concept

To handle low gas supply pressure paired with high volume flow the gas mixing layout was optimized to minimize pressure losses and ensure sufficient mixing quality. With this step also the complexity of the system could be reduced and therefore the design process could be simplified. Figure 2 shows the gas mixing layout for the existing baseline engine version (B) and figure 3 shows the gas mixing layout for the newly developed engine version (D).

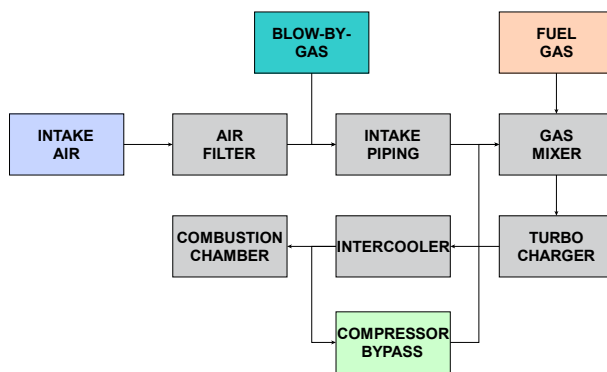


Figure 2: Gas mixing layout for the existing baseline engine version (B)

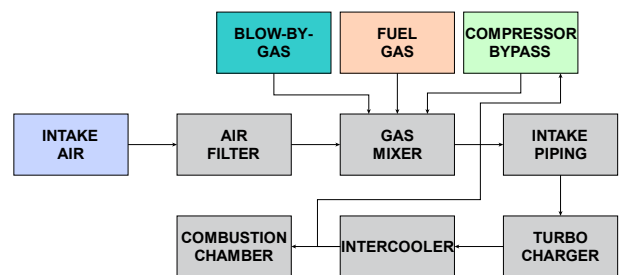


Figure 3: Gas mixing layout for the newly developed engine version (D)

The three media flows “blow-by gas”, “fuel gas” and “compressor bypass gas” are directed into separate chambers of the new three-chamber gas mixer. The three-chamber gas mixer consists of individual chambers in one housing being connected via bores to a venturi ring insert.

To make the design process easier, more accurate and more repeatable a 0D calculation tool based on Bernoulli’s law was developed to design the three-chamber gas mixer for special gas applications. The tool requires engine and gas mixer parameters as input and delivers various pressure and flow parameters as outputs. The following parameters are being used:

- **Input:** Venturi diameters, total areas of bores (number of bores, diameter of bores)
- **Output:** Suction pressure for blow-by-gas, pressure loss for fuel gas, air-fuel mass ratio

The accuracy of the calculated pressure losses is a measure for the quality of the calculation tool. The homogeneity of the air-fuel mixture is a measure for the quality of the gas mixer layout. To validate both the calculation tool and the gas mixer layout, additional pressure sensors were installed in the three chambers of the gas mixer at a pilot engine on customer site. Figure 4 shows the difference between the measured and the calculated values for the pressure loss over the fuel gas path and the throat pressure of the venturi insert. The throat pressure corre-

sponds to the pressure level at the smallest diameter of the venturi insert. At full load, the calculation differs by a maximum of -5 mbar for the fuel gas pressure loss and by a maximum of -22 mbar for the throat pressure. Calculations were performed using Bernoulli's law, which exclusively considers ideal, laminar and incompressible flows. Also, interactions between all three flows cannot be considered by simply using Bernoulli's law. Differences between calculation and measurements can thus be attributed to those circumstances. To validate the mixing quality of the gas mixer layout for wood gas, the individual exhaust gas temperatures downstream of the cylinder heads were measured and compared to the ones of a natural gas engine with similar hardware. Figure 5 shows that the spread between coldest and warmest cylinder exhaust gas temperature (as a measure for the mixing quality) is lower for the wood gas engine than for the natural gas engine. That can be related to the design of the venturi ring and the lower air fuel mass ratio compared to natural gas.

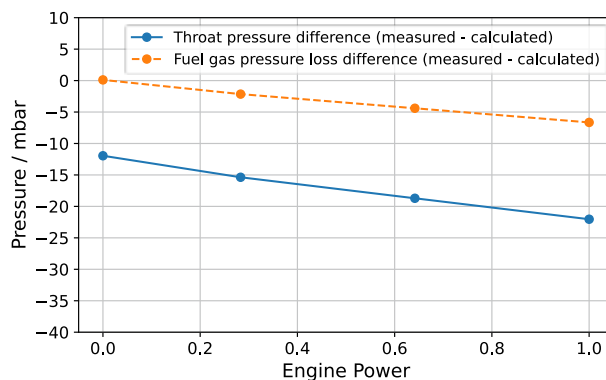


Figure 4: Differences between measured and calculated pressure values

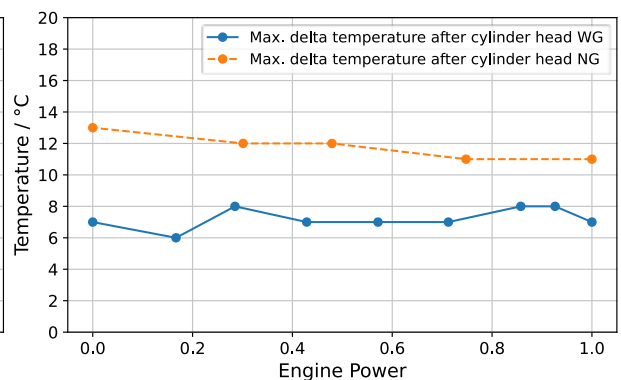


Figure 5: Spread between coldest and warmest cylinder exhaust gas temperature

With these results the changes to the gas mixing system (implementing a three-chamber concept) are validated and approved. Future calculations will benefit from the empirically determined offset (blue line in figure 4) that is applied to the throat pressure. The calculation tool can now be used straightforwardly to design venturi inserts for other special gas applications as well.

3.1.2 Combustion Concept

To improve the engine performance, camshaft, piston and cylinder head were upgraded with the new engine version (D). The camshaft layout was changed from filling optimized timing to late intake valve closing to make use of the Miller effect and increase the knock margin, see figure 6. In addition, the exhaust valve lift was increased to reduce the related flow losses.

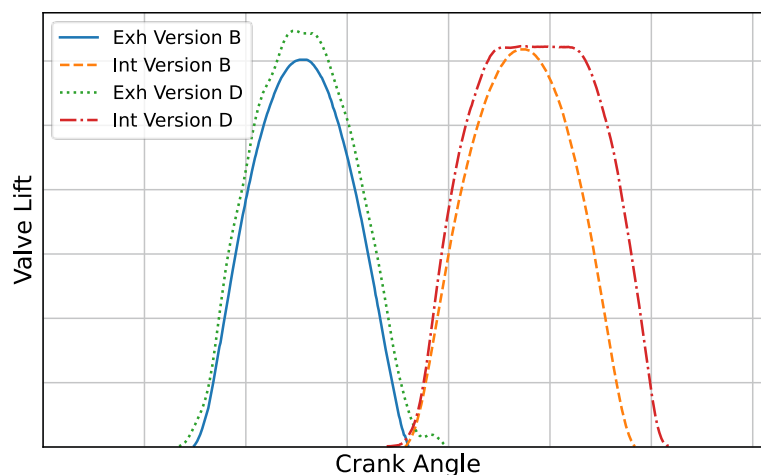


Figure 6: New camshaft with adapted dynamic valve lifts

The increased knock margin was used to apply an aluminum piston with higher compression ratio, see figure 7. Furthermore, a new cylinder head, with improved inlet and exhaust port flow characteristics and an optimized cooling was employed, see figure 8.



Figure 7: New aluminum piston with increased compression ratio

- 1 - Optimized intake port, valves & valve seat rings
- 2 - Optimized exhaust port, valves & valve seat rings
- 3 - Optimized flame deck machining
- 4 - New rocker arm bracket and rocker arm
- 5 - Improved cooling

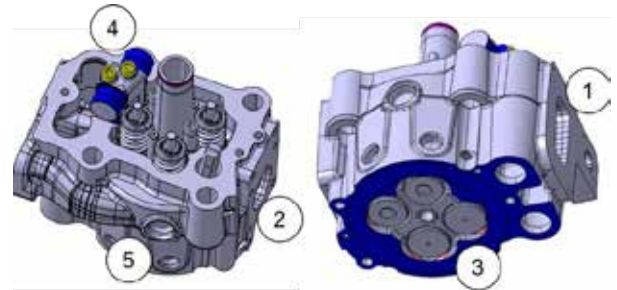


Figure 8: New cylinder head with improved flow characteristics and optimized cooling

The motivation to modify and adjust the combustion concept was to increase engine power and efficiency while maintaining a robust and reliable system. The various development steps including the stated changes in camshaft, piston and cylinder head are shown in figure 9. An overall increase in break mean-effective pressure of 10 % and in mechanical engine efficiency of 1 %pt. could be realized (from B to D).

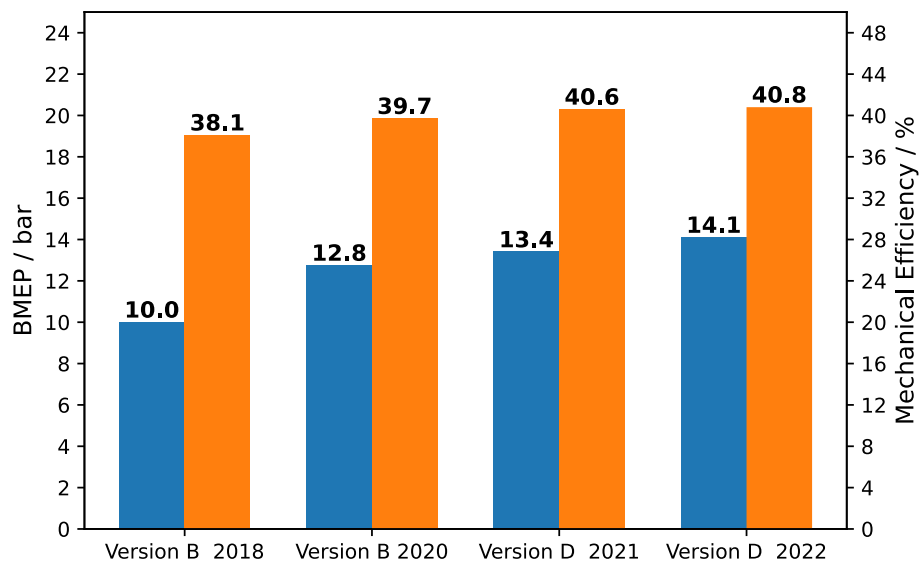


Figure 9: Long term investigation results for Version (B) and Version (D)

3.1.3 Lubrication Concept

It was observed that the likelihood of uncontrolled combustion events increases during long run engine operation. Three major phenomena were noticed: Combustion knocking (auto-ignition in unburnt end-gas), spontaneous pre-ignition (auto-ignition by additional energy sources like oil-droplets) and glow ignition (auto-ignition at hot surfaces). It was also observed that combustion chamber deposits on piston, cylinder-head and spark plug increase the number of these events. A chemical analysis of the deposits showed that oil ash is the main residual. Oil

formulation and consumption are thus levers to reduce deposits and consequently abnormal combustion. Based on these findings two improvement steps were defined.

Oil formulation:

Various investigations were carried out to develop a high performing engine oil for Wood Gas applications. The goal was to provide a commercially attractive product to the customer with low deposit forming characteristics enabling a stable combustion performance over lifetime.

To achieve these goals, development activities on single cylinder engines and proof of performance activities on multi cylinder engines in the field were conducted. The testing at the single cylinder engine was done to grasp the number of abnormal combustion events for different oil types at various engine BMEP levels, see figure 10. This measurement campaign was recorded with Hydrogen as a fuel. The testing at customer site was done to assess oil lifetime, deposit build up and specific lubrication costs.

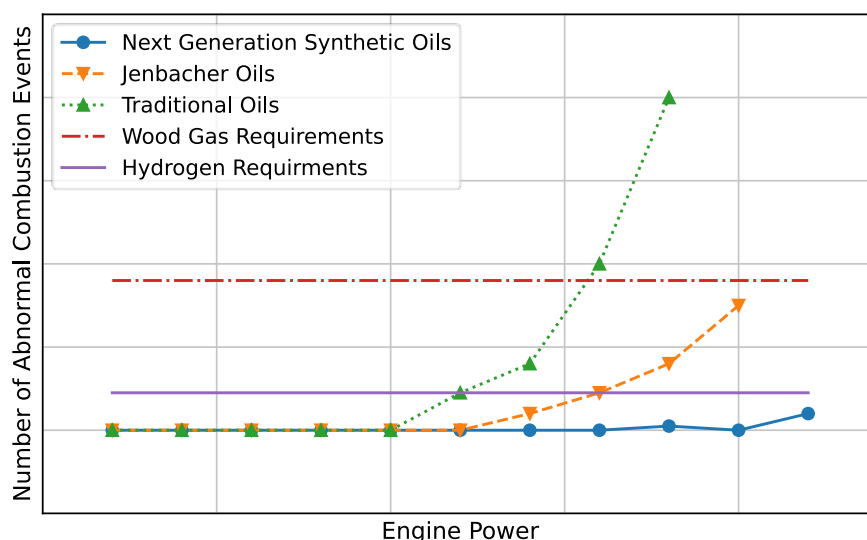


Figure 10: Impact of oil formulation on abnormal combustion events

Various oil types were assessed including group 1 and higher group classes. Significantly reduced abnormal combustion events and thus noticeably higher engine reliability numbers were achieved with Jenbacher N oil and Jenbacher S oil. Both oil types meet the defined requirements and thus fulfill wood gas specifications. The change to a more suitable lubricant enables an oil lifetime extension by 245 % and thus a significant operating cost reduction for the customer.

Oil consumption:

The oil control ring of the piston was modified to improve the radial force pressing the ring against the liner. The ring tension was adapted to increase the contact pressure by $\approx 50\%$. This led to a reduction in oil consumption. Based on this positive result achieved in special gas operation it was decided to serialize the improved ring for most of the type 4 engine versions.

3.2 Software

The existing baseline engine software has been improved by adding two new functions.

3.2.1 Fast-Gas-Quality-Change Function

Fast changes in wood gas quality can happen periodically due to nitrogen purging in the gas production process. They can lead to undesired engine responses like power overshoots. This problem could be solved by developing a Fast-Gas-Quality-Change function. The normalized engine response for the existing baseline version can be seen in figure 11. To handle undesired power overshoots, parameterized time frames, lambda offset and time delay were introduced. The periodical start of the software function is triggered by a customer signal. By freezing actuators, deactivating software functionalities and forcing settings to defined parameterized values, power overshoots could be totally eliminated, see figure 12 and table 3. The settling time for power oscillations after an unpreventable power undershoot could be reduced to just ten seconds.

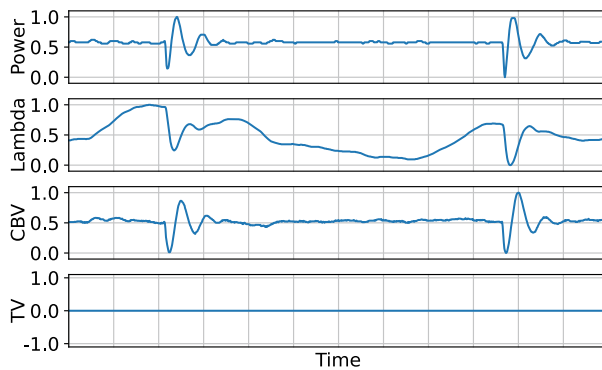


Figure 11: Normalized engine response, baseline engine version (B)

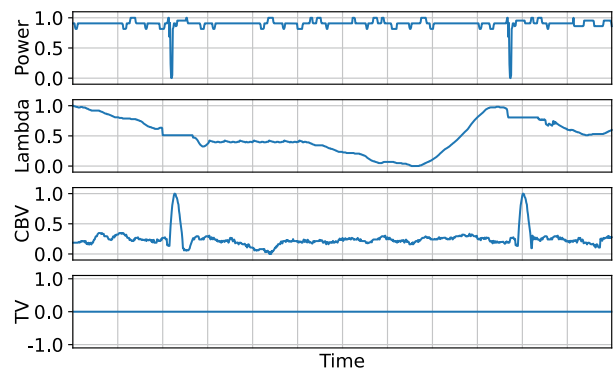


Figure 12: Normalized engine response, new engine version (D)

Table 3: Engine response parameters before and after the software implementation

Response parameter	Before software implementation	After software implementation
Power overshoot	~ 10 %	0 %
Power undershoot	~ 10 %	~ 10 %
Settling time for power oscillation	~ 45 s	~ 10 s
Misfire, knocking, etc.	none	none

3.2.2 Improved-Humidity-Compensation Function

The Improved-Humidity-Compensation function was developed as a control strategy to avoid condensation downstream of the intercooler, at times of high water content in the air-fuel mixture. Figure 13 shows a schematic overview including main signals and calculations. This improved function considers the humidity content in the air and in the fuel gas.

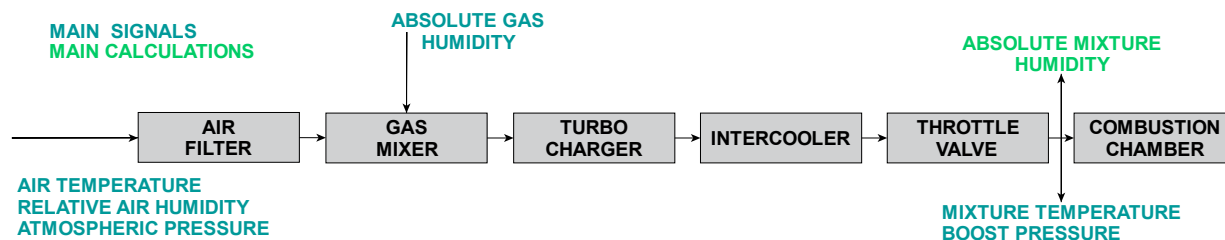


Figure 13: Improved-Humidity-Compensation function, schematic overview

If during steady state engine operation, the absolute mixture humidity increases, the theoretical pressure at which condensation will form reduces. Therefore, the maximum allowed boost pressure is decreased when absolute mixture humidity increases. If the actual boost pressure reaches the boost pressure limit based on absolute mixture humidity, this is the point at which there is a risk of condensation after the intercooler, see line **A** in figure 14.

The first countermeasure is to increase the mixture temperature to a parameterized maximum value (which increases the maximum boost pressure for a given absolute mixture humidity), see timeframe from line **A** to line **B**. If the actual boost pressure is still higher than the maximum allowed boost pressure the power is decreased until the actual boost pressure is lower than the maximum allowed boost pressure, see line **C**.

For validation purposes the value of the absolute gas humidity was manipulated. The artificial increase in absolute mixture humidity correctly triggered a decrease in the maximum allowed boost pressure and subsequently also an increase in mixture temperature to the maximum parameterized value. After reaching the maximum allowed mixture temperature engine power was correctly reduced as well, see figure 14

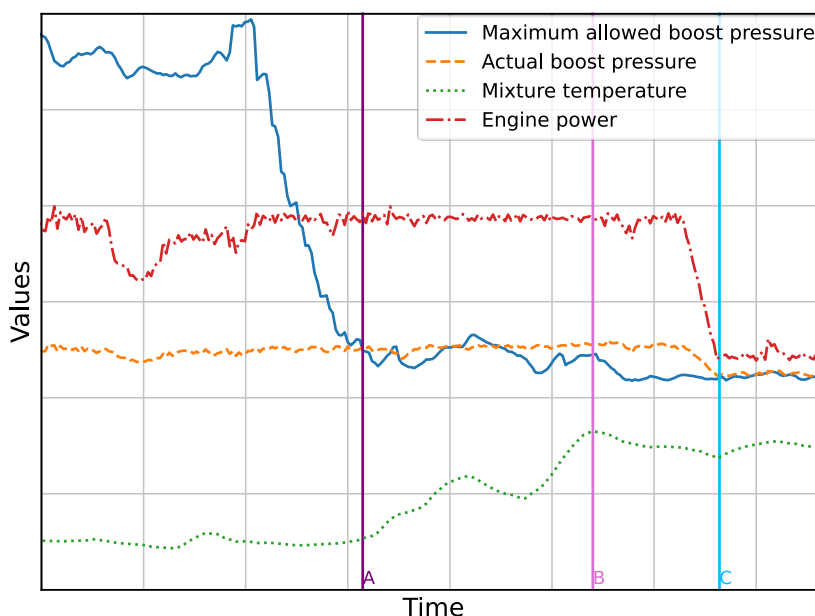


Figure 14: Validation results for the improved-humidity-compensation function

4. Summary and Outlook

Sustainably produced wood gas is a valid and proven fuel for CO₂-neutral and best-case CO₂-negative heat and power generation. However, the operation of large gas engines with wood gas comes with some challenges. Various hardware and software changes were carried out to improve power output and engine uptime: The gas mixing system was redesigned to handle high gas volume flows at low gas supply pressures. Camshaft, piston and cylinder head, were optimized to achieve higher power output and higher efficiency. New engine oil formulations and piston ring packages were investigated to minimize abnormal combustion events and increase lubricant lifetime. Undesired engine responses to fast changes in gas quality were resolved by a new software function. In addition, a new humidity control strategy was successfully implemented.

The stated development activities, supported by long-term field engine investigations, resulted in improved and more robust wood gas engine performance with a power output of 1050 kW_e (about 14 bar BMEP) and an electrical efficiency of more than 40 %. This corresponds to an improvement of about 10 % in power output and about 1 %pt in electrical efficiency versus the previous engine version. Table 4 gives an overview of the achieved improvements.

Table 4: New wood gas engine version performance

Hardware & Software Changes	Achieved Product Characteristics						
	Low supply pressure	Low calorific value	Fast gas quality changes	High engine power	High engine efficiency	High engine uptime	Low operating costs
Gas Mixer Concept	≥ 50 mbar(g)	≥ 1.6 kWh/Nm ³					
Combustion Concept				+10 %	+1 %pt		
Lubrication Concept						> 8000 oph/year	+245 % lifetime
Fast-Gas-Quality-Change-Function		10 %/s std. is ≤ 4 %/min	3 MN/s std. is ≤ 10 MN/min			> 8000 oph/year	
Humidity-Compensation-Function						> 8000 oph/year	

1. MN = Methane Number

Proven technology for natural gas operation and additional developments for special gas applications could further improve the system performance in future. Steel piston technology for example would reduce pollutant emissions, increase efficiency and lower engine operating costs.

Using wood gas instead of natural gas decreases the heating value of the air-fuel mixture by about 21 %. This means that a higher boost pressure is required for a comparable power level. High-pressure turbocharger technology would enable further engine power increase and lower specific engine costs.

References

- [1] Martin Schneider: „Technischer Stand der Holzvergasung und Anwendung in KWK-Anlagen aus der Sicht eines Gasmotorherstellers“; 12. Internationalen Anwenderkonferenz Biomassevergasung, 2023, Innsbruck, Tyrol
- [2] Zita Baumann: „Machen Sie sich bereit für eine Zukunft mit Wasserstoff“, 12th Dessau Gas Engine Conference, 2022, Dessau-Roßlau, Saxony-Anhalt
- [3] Clément Leroux, Robert Böwing, Bernadet Hochfilzer, Alexander Zuschnig and Manuel Behr: “Hydrogen in the Gas Network – Challenges and Solutions for High Performing Engines for Power Generation”, International MTZ Conference, Heavy-Duty, On- and Off-Highway Engines, 2022
- [4] Andreas Kunz: “Gas Engines: Renewable Power with Operational Flexibility”, Key-Note, 9th AVL Large Engines TechDays, 2021, Fully Digital
- [5] Stephan Laiminger et al.: “Hydrogen as Future Fuel for Gas Engines”, CIMAC Vancouver, 2019
- [6] Jochen Fuchs, Robert Böwing, Josef Schlag and Christoph Hollaus: „The next Generation of Jenbacher Type 4 Gas Engine from INNIO“; 11th Dessau Gas Engine Conference, 2019, Dessau-Roßlau, Saxony-Anhalt
- [7] Stefan Prankl, Robert Böwing, Herbert Schaumberger, Rob Wilson, Dietmar Heintschel and Thomas Eisenbruch: „Improving fuel flexibility: New Jenbacher gas engine versions with high power density for gases with high carbon dioxide content“, 13th Intern. MTZ Conference, Heavy-Duty, On- and Off-Highway Engines, 2018, Cologne
- [8] Robert Böwing: “Use of Special Gases in Power Plant Engines” in chapter “Off-Highway-Gas Engines” in “Natural Gas and Renewable Methane for Powertrains”, ISBN: 978-3-319-23225-6, 2016
- [9] Jochen Fuchs, Alissa Gebhardt, Alexander Leitner, Josef Thalhauser, Georg Tinschmann, Christian Trapp: “Technology Blocks for High Performance Direct Ignition Gas Engines”, 7th International MTZ Conference, Heavy-Duty, On- and Off-Highway Engines, 2012, Nuremberg
- [10] Homepage Syncraft: www.syncraft.at
- [11] Elena Käßler: “Lebenszyklusanalyse der Strom- und Wärmeerzeugung einer Holzvergasungsanlage inklusive Nahwärmenetz“, Masterarbeit zur Erlangung des akademischen Grades, 2017, Dornbirn, Vorarlberg

Abbreviations

BMEP	–	Brake mean effective pressure
MN	–	Methane number
WG	–	Wood gas
NG	–	Natural gas
CBV	–	Compressor bypass valve
TV	–	Throttle valve

Session 2

**Wasserstoff - Stromerzeugung
Hydrogen - Power generation**

**Moderation: Prof. Thomas Koch
Karlsruher Institut für Technologie**

H₂-Readiness certification of gas engine power plants

Zertifizierung der H₂-Readiness von Gasmotorenkraftwerken

Dominik Voggenreiter*, Pierre Huck, Dr. Thomas Gallinger
TÜV SÜD Industrie Service GmbH, Munich, Germany

Abstract

Hydrogen will play an important role in the energy system of the future and the suitability of gas engine power plants for hydrogen is becoming increasingly important. Together with partners, TÜV SÜD has developed a guideline for assessing the hydrogen-readiness of gas engine power plants. This serves as a basis for the certification of concepts of original equipment manufacturers and engineering, procurement and construction companies as well as for specific projects. The aim of this presentation is to give an overview of the latest developments, experiences, and challenges in this field.

Kurzfassung

Wasserstoff wird im Energiesystem der Zukunft eine wichtige Rolle einnehmen und die Eignung von Gasmotorenkraftwerken für Wasserstoff gewinnt zunehmend an Bedeutung. TÜV SÜD hat zusammen mit Partnern eine Guideline zur Bewertung der Wasserstofftauglichkeit von Gasmotorenkraftwerken entwickelt. Diese dient als Grundlage für die Zertifizierung von Konzepten von Erstausrüstern und Engineering-, Beschaffungs- und Bauunternehmen sowie für spezifische Projekte. Ziel dieses Vortrags ist es, einen Überblick über die neuesten Entwicklungen, Erfahrungen und Herausforderungen auf diesem Gebiet zu geben.

1. Introduction

Hydrogen will play an important role to decarbonize the energy production in the future. This also concern gas engine power plants. Original equipment manufacturers (OEM) and engineering, procurement and construction (EPC) companies are developing concepts to make sure that their plant can be operated with hydrogen when it will be available in sufficient quantities. However, there is currently not a single, transparent definition of the terminology of hydrogen-readiness. Therefore, operators, investors or insurance companies have difficulties in checking the claim made by OEM or EPC companies.

2. Guideline structure and content

A first guideline was developed by TÜV SÜD to provide a definition of the hydrogen-readiness of a gas turbine combined cycle power plant. Based on the interest of the industry, it was decided to extend the applicability range to gas engine plants. To make sure that the guideline is appropriate and applicable from the start, the development was supported by the inputs and peer-reviews of market players. The guideline is structured in four main parts, as shown in Figure 1.

* Speaker/Referent



Figure 1: Structure of the guideline

In the first part, the covered plant configurations are described. However, the guideline and the related certification scheme were built modularly to make sure that different plant configurations or even (main) systems or components only can be covered by applying the relevant sections only.

In the second part, the boundary conditions, which need to be explicitly stated as part of a hydrogen-readiness assessment, are described. For example, the operating time with natural gas until the transition to a given mixing ratio of hydrogen shall be known. The configuration of the gas supply after the transition shall also be clear. In addition, a few evaluation schemes are defined, as they are particularly important to evaluate the hydrogen-readiness of a power plant. For example, it shall be understood if a given component is originally built as being capable for the use in hydrogen environment when it will become available, or if a retrofit or a replacement would be necessary. Another important aspect is the Technology Readiness Level (TRL) of the proposed technical solutions. The OEMs are currently working on the development of mature solutions for the safe and stable combustion of high hydrogen concentrations. These development programs are not yet fully completed and this needs to be clearly understood when speaking about the hydrogen-readiness of a plant concept.

In the third part of the guideline, the influences of switching from natural gas to hydrogen on all the relevant main components, systems and overarching topics are described. From those influences the technical requirements for a hydrogen-readiness concept are derived. A key element in the development of the guideline was to define a meaningful split of a gas engine plant in different subtopics, ensuring to cover all the potentially relevant effects of switching

from natural gas to hydrogen in a power plant. The important aspects to be considered in the case of a gas engine power plant are summarized in Table 1.

In the fourth and final part, the certification scheme derived from the technical considerations in the first three parts is described. It is a scheme with three different levels, which will be explained further in the following section.

Table 1: Key points to be considered when assessing the hydrogen-readiness of a gas engine power plant

Relevant Systems/ Components and Themes	Key points to be considered regarding H ₂ -Readiness
Plant-Related Fuel Gas Supply	Classification of components and systems in the categories "H ₂ -capable", "Retrofitting required", "Replacement required" or "Obsolescence" requires detailed consideration of materials, avoidance of hydrogen embrittlement and tightness .
Gas Engine	Development work is still ongoing, especially regarding combustion, given the different combustion characteristics of hydrogen. Therefore, a TRL must be assigned to each component in a specific gas engine when assessing its H ₂ -Readiness.
Plant-Related Exhaust Gas System	Due to variations in the physical properties of the exhaust gas (e. g. volume flow, temperature, pollutant concentrations), the design and operating conditions of plant-related exhaust gas system components, such as heat recovery, after-treatment and condensation systems or silencers , may be subject to changes in pressure drop, noise emission or sizing (exhaust gas heat exchanger or SCR).
Auxiliaries	The use of hydrogen may lead to changes in the requirements for auxiliary systems, such as the engine cooling system (change in temperature level) or civil works components. Explosion protection requirements for electrical devices in these auxiliary systems may also be affected.
Building	Precautions to avoid H ₂ accumulation should be considered early in the design (e. g. avoid zones with stagnating air exchange rate or consider roof openings). Space for additional systems such as mixing skirts should be considered as well.
HVAC	Ventilation concepts against the formation of explosive atmospheres must be adapted due to the potentially higher risk of explosion when using hydrogen.
Plant-Related Instrumentation & Control	Changes to sensor systems and their interfaces to software as well as to control and protection concepts are possible and should be investigated. Additional space should be provided in the initial plant design to accommodate for potentially more sensor signals, higher required processor capacity or additional control cabinets when introducing hydrogen.
Overall Plant Performance	Gas engine power plants can only be optimised for a certain H₂ blending ratio range . Therefore, the plant operator should ideally communicate as early as possible a roadmap of realistic H₂ mixing ratios during the lifetime of the plant. In this way, the plant can be accordingly optimised from the start of operation using natural gas and the extent of required changes or their potential impact on efficiency, power output or emissions can be limited . This is also true in the case of a retrofit , but given the lesser possibilities of adaptation, potential losses in performance cannot be completely excluded.
Explosion Protection Concept	None of the explosion relevant characteristics is affected significantly by the addition of up to 10 mol% hydrogen and the mixtures remain in explosion Group IIA, as for pure natural gas. For mixtures with more than 10 mol% hydrogen , a change of explosion group is possible. Up to a hydrogen content of 25 % H ₂ Group IIA is sufficient; otherwise explosion Group IIC / IIB+H ₂ is appropriate.
Fire Protection Concept	The principle of plant fire protection, including early fire detection, remains fundamentally unchanged when hydrogen is used. Updating of the fire protection concept may be required, e. g. sensitivity of detectors. If additional explosion protection measures are required, they may influence fire protection .
Hazard and Risk Analysis	Revision of the hazard and risk analyses for all plant systems or components is probably not needed . A revision, either complete or limited to a modification of the analyses with natural gas, is expected for the plant-related fuel gas supply system, the gas engine and the plant-related exhaust gas system .
Conformity	New systems or components required for the use of hydrogen shall be delivered with the relevant conformity declarations. For existing systems or components , the need for a reassessment will arise from e. g. the relevant or non-relevant nature of the changes resulting from the use of hydrogen.
Permits	Introduction of hydrogen may affect the validity of permits. The distinction between a minor change , with the obligation to notify, and a substantial change , with the obligation to submit a new application, will be crucial.

3. Certification scheme

There are three levels to make sure that all market players can use the guideline and to have a follow-up effect of projects.

The first level in the certification scheme is called the Concept Certificate. From the point of view of the lifecycle of a power plant it is relevant in the bidding phase, when a conceptual design of the plant is available, including e.g., the plant configuration, the specifications of the main systems and components with, amongst others, the material classes, which are planned to be used, as well as the operational and safety concepts. The goal of the Concept Certification is to confirm that the hydrogen-readiness concept of the OEM and/or EPC covers all necessary topics and is technically realizable given the selected boundary conditions. From a process perspective it is also checked that the hydrogen-readiness concept is integrated in the bidding process. Hence, the Concept Certificate is not focused on a specific project but rather focuses on the bidding process of a plant. However, as part of the certification, an exemplary project-specific application of the hydrogen-readiness concept is investigated. This first level of certification is mostly relevant for OEM and/or EPC, which want to show to their customers, that a third-party independently checked the relevance of their hydrogen-readiness concept.

The second level in the certification scheme is called the Project Certificate. Compared to the first level of certification, it is relevant later in the lifecycle of a power plant, namely in the planning and/or construction phase of the power plant, in most of the cases for the initial use of natural gas. At this stage detailed specifications and designs of the main systems and components are available, suppliers should be selected or at least short-listed and the construction or even commissioning phase of the power plant might already have started. As the name of the certificate indicates it is project-specific, in contrary to the first level of certification. The goal of the certification process is to confirm that the plant will be or is being built according to the hydrogen-readiness concept proposed in the bidding phase and according to the specific boundary conditions of the project. The Project Certificate is mostly relevant for the operator of the power plant, but the process requires inputs from the OEM and EPC.

The third level in the certification scheme is called the Transition Certificate. From a timeline perspective it is relevant when the transition from the use of natural gas to hydrogen is about to happen. The plant has been operating for a certain time with natural gas but the hydrogen supply is now available and the necessary retrofit measures conceptually defined in the hydrogen-readiness concept are now detailed and about to be implemented. There is also a detailed understanding of the impact of switching from natural gas to hydrogen on the plant performance and safety concept. As for the second level of certification, the Transition Certificate is project-specific and is typically relevant for the plant operator, who wants to obtain an independent confirmation of the implementation of the relevant retrofit measures and of the impact of the transition on plant performance and safety.

The main features of the above described three levels of certification are summarized in Table 2 below.

Table 2: Three levels in the certification scheme

Level	1	2	3
Certificate Name	H ₂ -Readiness Concept Certificate	H ₂ -Readiness Project Certificate	H ₂ -Readiness Transition Certificate
Relevant Project Phase	Bidding	Planning/construction with natural gas firing	Actual implementation of retrofit measures to use H ₂
Main Focus	Generic concept followed to ensure H ₂ -Readiness	Implementation of the H ₂ -Readiness concept for a specific plant	Impact of the implemented retrofit measures on plant operability, safety and performance
Potential Certificate Holder	Plant manufacturer, EPC, OEM	Plant owner, plant manufacturer, EPC	
Project-Specific	No	Yes	

It was chosen to introduce these three levels for two main reasons. On the one hand, it allows having a system, which is relevant for all parties involved in a power plant project from the OEM through the EPC to the operator. On the other hand, it also ensures a “follow-up” effect from the early design phase to the actual use of hydrogen in the power plant, as there might be years between those two points in time, during which the state-of-the-art as well as the TRL of the technical solutions implemented might evolve.

4. Experience during pilot certifications

The certification schemes of both guidelines (gas turbines and engines) were already used for several certifications, with a few examples listed below:

- Concept Certifications are completed for Type 4 and Type 6 engine series of INNIO Jenbacher (new build and retrofit), the SGT-800 and SGT-9000HL gas turbine series of Siemens Energy (new build) and heat recovery steam generators (HRSG) and waste heat recovery units (WHRU) of NEM Energy (new build).
- For the second level (Project Certificate), one certification was completed for the 120 MW_{el} and 160 MW_{th} combined heat and power plant “Heizkraftwerk Süd” of the utility company “Leipziger Stadtwerke”, which uses two SGT-800 gas turbines supplied by Siemens Energy.
- So far, no Transition Certificate was issued. This step is expected to become relevant once enough hydrogen is available to be used in large-scale power plant projects.

Within these certification projects, a number of observations have been made which can be grouped into the following categories and which it is worth commenting on in greater detail, as they are representative of the points deserving particular attention in the field of hydrogen-readiness certification:

- Deviations in TRL level definition
- Scope/Responsibilities when only certifying parts of the guideline
- End-user information
- Purchased parts
- Tightness and explosion protection
- Collecting all necessary information

4.1 Deviations in TRL level

There are standards available covering the definition of the TRL level, such as ISO 16290. Nevertheless, these standards and the included definitions are either quite high level or branch specific and are not covering gas turbine or engine power plants. To create consistent assessment factors, TRL levels from 1 to 9 were defined within the guideline, which are more specific and explained by examples. This was performed together with the industry partners. As a minimum requirement for certification, TRL 5 must be achieved for each item, as the chances of a successful development are relatively high above this threshold.

Since the TRL levels in the standards available are quite high level, every company has its own definition. During the pilot certifications it was realized that the differences between the TRL levels in the companies and the guidelines may lead to discussions, especially with personnel or management that is not deeply involved within the certification process. Fortunately, this challenge could always be solved by clear communication and explanation of the background. As a lesson learned, this topic is now addressed at the very beginning of the certification process to ensure that all participants in the certification project understand the purpose of the TRL scale as introduced by the guideline.

4.2 Scope/Responsibilities when only certifying parts of the guideline

It is essential to define the certification scope unambiguously for each project. In addition, defining what is out of scope can help to better understand the scope. As mentioned above, the guidelines are modular, so that (main) systems or components of gas turbine or engine power plants can also be certified. Therefore, the modules which must be covered as well as the included requirements to be fulfilled must be chosen individually from one certification to another.

This has led to intense discussions during the first certifications, especially as the company's responsibilities can vary from project to project. Therefore, a clear communication and/or discussion was necessary to define the relevant scope. Interestingly, the discussions partly went in different directions: some responsibilities were not fully known to the certified companies. On the other hand, some responsibilities (perceived as such) were already covered, when they should be the responsibility of a supplier or the customer. Hence, there was also a learning process for the certified companies during certification.

4.3 End-user information

End-user information e.g., installation, operation, or maintenance manuals, working material instructions, etc., are relevant parts of every machine or plant. They are also in part the result of the hazard and risk analysis and should ensure a safe and efficient operation over the whole lifetime. If a component or facility is intended to be used with hydrogen, this must also be mentioned within the end-user information. If a component/facility is first operated with natural gas and later transferred to hydrogen operation, the end-user information must also indicate which parts/components have to be adapted or changed. Hence, the end use is generally covered within the certification scheme of the guidelines.

Based on TÜV SÜD experience (not only from hydrogen projects), end-user information are sometimes not considered with the fully adequate level of effort. Since end-user information include a shift of responsibility from the supplier to the integrator and further to the operator,

the end-user information should be prepared in a proper way. For supply parts, the end-user information of the supplier should also be checked.

4.4 Purchased parts

There are two possible ways of proving the suitability of supply parts for hydrogen operation:

1. Get a conformity statement from the supplier
2. Perform own tests

Getting conformity statements from suppliers can be time-consuming, particularly from suppliers of small (bulk) parts like sensors, small armatures etc. Hence, it is preferable to contact the supplier quite early in the certification process to avoid or at least reduce any delay due to missing information.

As already noted in the previous chapter, the end-user information of the supplier should cover or at least have some information regarding hydrogen operation.

4.5 Tightness and explosion protection

From a safety perspective, one of the most important differences between natural gas and hydrogen are the tightness requirements, since hydrogen is much more fugitive and is not odorized. In a typical hydrogen supply line, there are screwed connections, houses, couplings and/or flanges included for various reasons, which may be susceptible to hydrogen emission.

In addition, the combustion chamber of a hydrogen engine is not tight towards other areas of the engine. This leads to the occurrence of hydrogen within not only the combustion system but almost the whole engine (Figure 2). Nevertheless, there are different areas with different concentrations of hydrogen, for example the gas supply with pure hydrogen and pressures up to tens of bar (after gas train depending on the engine setup). In the crank case, there is a hydrogen air mixture with oil mist at very low pressures that may form an explosive atmosphere. In the exhaust system hydrogen is only present after special events like misfiring or during startup, which need a proper explosion protection evaluation. In addition, there are usually some hydrogen emissions towards the outside of the engine, which are relevant for the explosion concept of the operator.

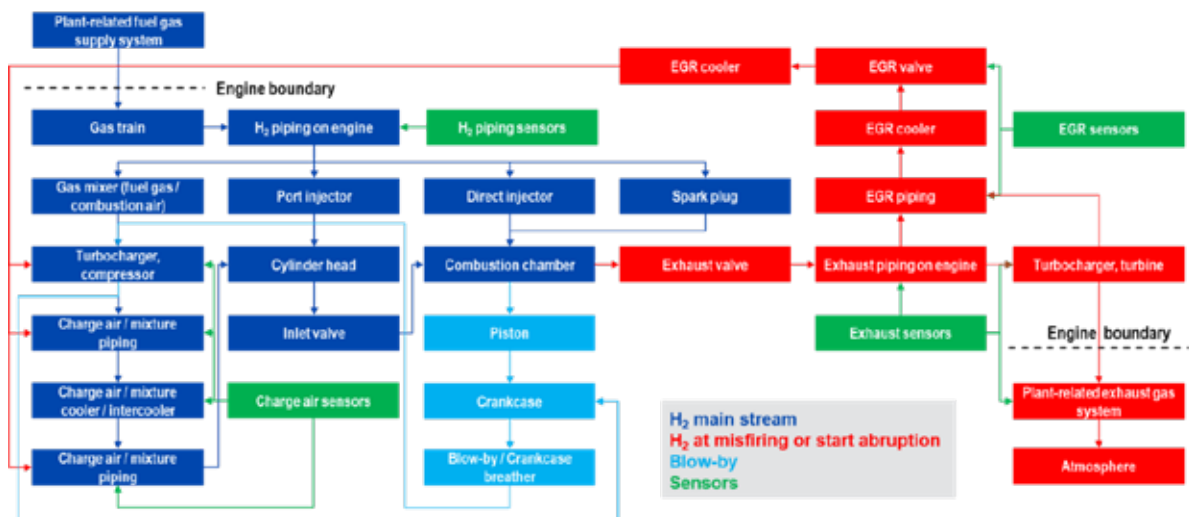


Figure 2: Hydrogen flows within a gas reciprocating engine. This flow diagram covers

different engine design approaches, hence not all flow paths may be applicable in a certain engine design.

One experience of the pilot certifications was, that the manufacturers of components and systems need to be aware that, especially with hydrogen, there is in many cases no such thing as “perfectly tight”, but only “tight enough covering operators and regulatory requirements”. This leads to the necessity of providing additional (end-user) information to the operator e.g., for his explosion protection concept, like hydrogen leakage rates of connections and of the engine itself.

4.6 Collecting all necessary information

Collecting information takes time. Hence one experience from the certification was, that information collection is the most time-consuming part of the certification. Therefore, information was not submitted to the certifying party at once, but within several packages, optionally combined with a short online meeting if some documents needed further explanation. Using this approach, the certifying party was able to check the submitted documents, while the company certified worked in parallel on the remaining documents or questions raised. This saved time and ensured a constant flow of information, so that all certification partners always had a common understanding of the progresses of certification.

5. Summary and next steps

A certification guideline on the hydrogen-readiness of gas engine power plants was developed with input and peer reviews from relevant market players, such as OEMs, EPCs, operators or insurance companies and investment banks. The derived certification system has been validated by the completed pilot certifications. The experiences made during the pilot certifications are constantly implemented in the certification concept. The first revisions of the guideline were already published based on the experience gained from the certification projects and the progress made in the state of the art. The guideline is intended to be a living document, and further revisions are planned on a regular basis, e.g., since new standards on hydrogen vessels and piping may become available in the future.

Certification based on the guidelines is currently a voluntary exercise for OEMs, EPCs and operators, who wish to reduce their uncertainties related to the use of hydrogen but also to demonstrate to others that their concepts have been independently confirmed by a third party. However, legislation on the specific subject of hydrogen-readiness is developing rapidly in countries such as Germany and the UK. For example, the forthcoming "Kraftwerksstrategie" (power plant strategy) in Germany aims to organize tenders for the construction of new hydrogen-ready power plants with a total capacity of up to 4 times 2.5 GW. In this context, the hydrogen-readiness of candidate projects may need to be verified and validated by an independent third party. With the experience gained in this field since 2021, TÜV SÜD is ready to further support this development towards the use of hydrogen in electricity and heat generation.

References

- [1] H₂-Readiness of Gas Engine Power Plants; Public Abstract; Version 2023; TÜV SÜD Industrie Service GmbH
- [2] H₂-Readiness of Combined Cycle Power Plants; Public Abstract; Version 2023; TÜV SÜD Industrie Service GmbH

2G hydrogen CHP in practice and the development into a high-performance series product

2G Wasserstoff- BHKW in der Praxis und die Entwicklung zum leistungsstarken Serienprodukt

Frank Grewe* – 2G Energy AG

Dr.-Ing. Sven Annas – 2G Energietechnik GmbH

Rudolf Höß – Ostbayerische Technische Hochschule Amberg-Weiden

Kurzfassung

Die 2G Wasserstofftechnologie blickt auf eine fast 15-jährige Entwicklungsgeschichte zurück. Die erste Maschine für reinen Wasserstoff ging im Jahr 2012 in den Probetrieb, am Berliner Hauptstadtflughafen BER. Seither hat diese Technologie eine steigende Dynamik erfahren. Im Jahr 2018 ging das zweite Wasserstoff BHKW von 2G in Betrieb, beim Stadtwerk Haßfurt. In etwa zu dieser Zeit findet Wasserstoff mehr und mehr Einzug in die politische Debatte um unser Energiesystem der Zukunft - nicht nur in Deutschland, sondern weltweit. So wurde das Wasserstoff BHKW in Haßfurt mit mehreren Preisen prämiert, unter anderem mit dem renommierten Handelsblatt Energy Award. Im Zeitraum 2018 bis 2020 setzte 2G sieben Wasserstoff BHKW ab, in den Jahren 2021 und 2022 folgten jeweils sieben weitere Maschinen und im Jahr 2023 waren es zehn an der Zahl. Diese positive Dynamik setzt sich weiter fort. Waren die ersten Projekte häufig in geförderte Forschungsvorhaben gebettet und sind damit auch kaum in einen regulären Dauerbetrieb übergegangen, so finden sich derzeit mehr und mehr Anwendungen, in denen der Wasserstoff kommerziell zur Strom- und Wärmeproduktion durch ein 2G BHKW genutzt wird.

Im Vortrag werden die Erfahrungen aus mehr als 30 realisierten Wasserstoffprojekten beleuchtet: Anwendungsfälle, allgemeine Erfahrungen im Umgang mit dem Medium Wasserstoff, landesspezifische Regularien, die Umrüstung eines Erdgas BHKW auf Wasserstoff im Feld bei einer Kundenanlage und nicht zuletzt die allgemeinen Betriebserfahrungen der BHKW aus der Praxis.

Zudem werden der aktuelle Stand der 2G Wasserstofftechnologie und die laufende Weiterentwicklung gezeigt. Dabei liegt der Schwerpunkt auf der Leistungssteigerung auf Erdgasniveau durch Betrachtung unterschiedlicher Gemischbildungsverfahren und der Untersuchung von Schmierölrührentzündung.

Abstract

Hydrogen technology by 2G can look back on almost 15 years of continuous development. The first machine intended to operate exclusively on hydrogen took up service at the BER, the airport of Berlin, in 2012. Since then, the technology increasingly gained momentum.

In 2018, 2G commissioned a second hydrogen CHP at the public utilities of Haßfurt. It was around the same time that hydrogen increasingly entered into the political debates on the future of our energy system - not only in Germany, but worldwide. The hydrogen CHP in Haßfurt

* Speaker/Referent

subsequently received multiple distinctions including the renowned Handelsblatt Energy Award. Between 2018 and 2020, 2G distributed seven hydrogen CHP, in 2021 and 2022 it was a further seven respectively and in 2023 the number rose to ten systems. And the positive momentum carries on.

While the initial projects were often integrated into subsidized research projects which rarely saw them operate in regular continuous operation, the more recent projects increasingly see hydrogen CHP by 2G used in commercial heat and electricity production applications.

The lecture will shine a light on experience gained across over 30 realized hydrogen projects: applications, general experience in handling hydrogen as a material, country-specific regulations, retrofitting a natural gas CHP in the field to run on hydrogen and, last but not least, our practical experience of operating hydrogen CHP.

Additionally, it shows the current state of the 2G hydrogen technology and its ongoing development. The focus lies on the performance upgrade of hydrogen units to the specific power output of the natural gas portfolio by analyzing different mixture formation processes and the investigation of lube oil pre ignition.

1. Introduction

The construction of the first, exclusively hydrogen-fueled 2G CHP in 2012 laid the foundation for a growing area of business of the 2G Energy AG. At the time, hydrogen was not a factor in the political debate in Germany. Instead, an "All Electric" strategy was favored. Over the years, reality sank in and since 2018, 2G realized more than 30 hydrogen projects and the trend is still rising. Besides Germany, Japan and Canada gained the most momentum. Overall, hydrogen technology by 2G is represented in nine countries across four continents.

Two factors play a particular role in this growth:

- The system's ability to operate on other gases besides hydrogen, especially natural gas.
- The possibility to process impure waste hydrogen from industrial processes.

Figure 1 provides an overview of projects realized until now.

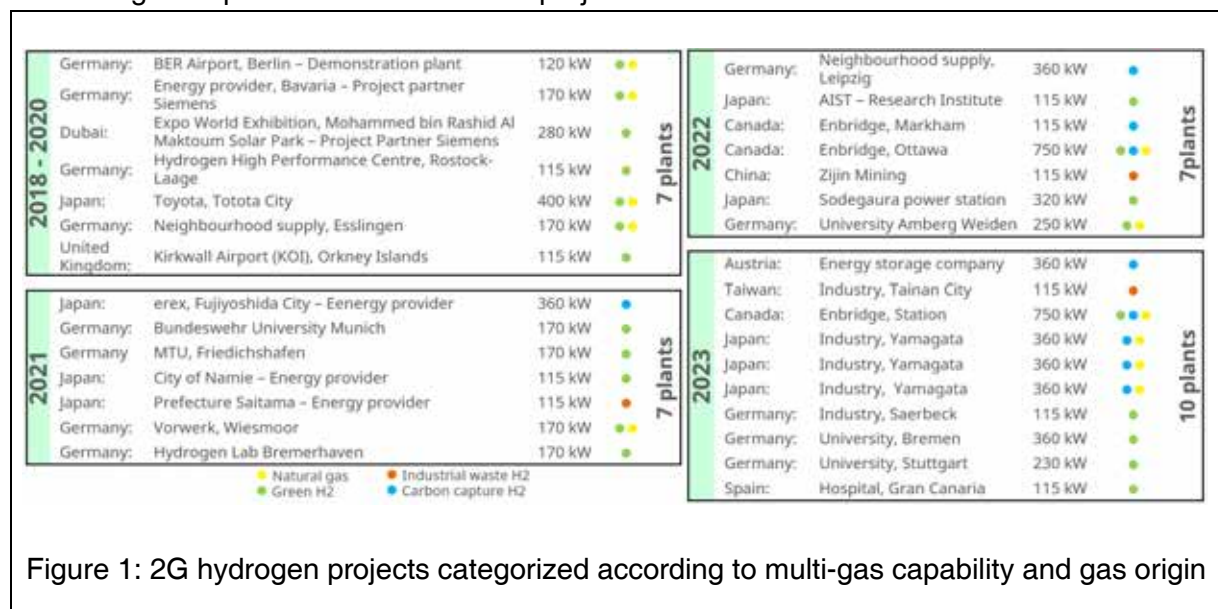
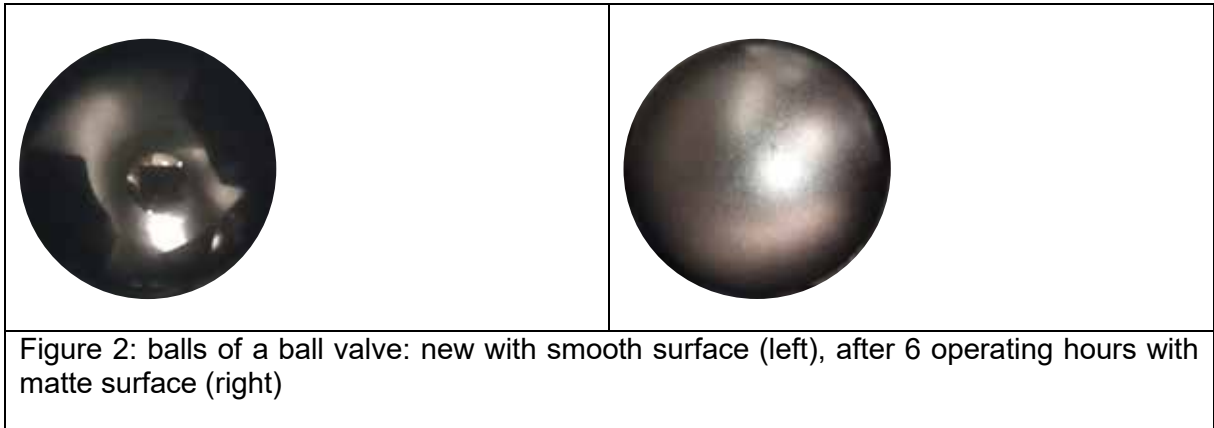


Figure 1: 2G hydrogen projects categorized according to multi-gas capability and gas origin

2. Lessons Learned

Years of experience in handling special gas mixtures were transferable to the hydrogen sector. A factor that accelerated development. That applies to selecting the right materials as well as the hydrogen utilization by the engine. And still a mistake happened:

Hydrogen has a significant impact on the properties of the materials used in the system. Consequently, the selection of an inappropriate material for a ball valve led to wear and leakages within no more than six operating hours, which is an astonishingly short time span (Figure 2).



Although handling hydrogen requires a certain degree of diligence, it still is a combustible gas like natural gas. Against this background, the implementation of hydrogen and natural gas projects is very similar. Therefore, the general rule book for projects with combustible gases provides safe guidelines for hydrogen that especially come into effect when there are no country-specific regulations.

Beyond that, 2G created extensive documentation on the installation of hydrogen products. It contains tools to facilitate the selection of the appropriate materials, for explosion prevention and for general risk assessments. The international 2G Partner network can access the documentation via my.2-g.com.

3. 2G hydrogen products

The product portfolio (Figure 3) contains six different engine series, from four to 20 cylinders, approved for mean effective pressures of up to 14 bar. Depending on the series, the cylinder volume is between 2 and 2.2 liters. Increasing the mean effective pressure is a critical component of further development.



The current decision for a lower mean pressure is less of a technical necessity than a strategic decision. Individual projects with greater output than depicted in the diagram under "today" were already green-lit.

4. Projects

4.1. Retrofitting in the field – OTH Amberg-Weiden

As part of the energy transition and the uncertainties it entails, 2G can retrofit natural gas engines in the field to run on hydrogen which ensures an immense degree of flexibility. The agenerator 406 H2 at the Ostbayerische Technische Hochschule (OTH) Amberg-Weiden - a technical university - exemplifies this. For the first time, 2G converted a natural gas CHP in the field to run purely on hydrogen. The retrofitting turned into an event that even attracted political attention (Figure 4).



Figure 4: Bavarian Minister President Markus Söder (left) in conversation with Raphael Lechner (right) from OTH Amberg-Weiden about the 2G hydrogen CHP [1].

An agenitor 406 NG that left the factory in April 2019 was converted.

Figure 5 shows the efficiency curve for the specific output of the natural gas module before the retrofitting as well as the curve for the hydrogen CHP after the retrofitting for hydrogen and natural gas operation at up to 18 bar BMEP.

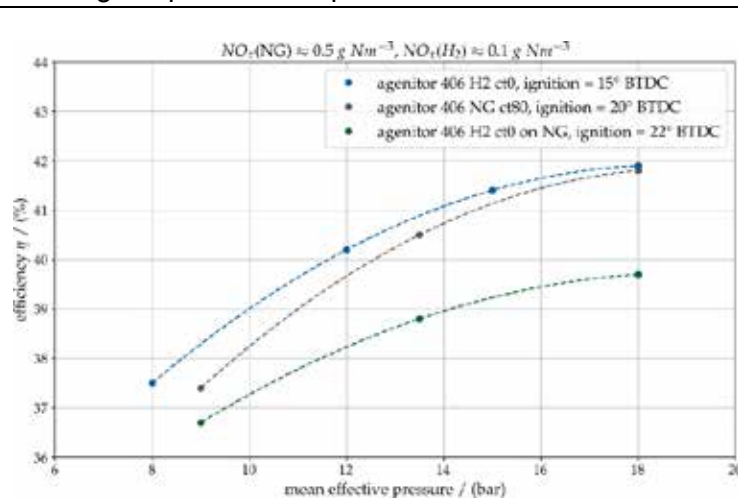


Figure 5: efficiency curve for varying fuel and engine configurations

Key components replaced as part of such a retrofitting:

- Turbocharging components
- Wastegate
- Pistons incl. bushings
- Hydrogen gas train
- Hydrogen injectors (incl. distributor rail and injection device)
- Injector control device
- Software adjustment
- Safety features (gas sensors, shut-off valves etc.)

Figure 6 provides an overview of the retrofitted system.

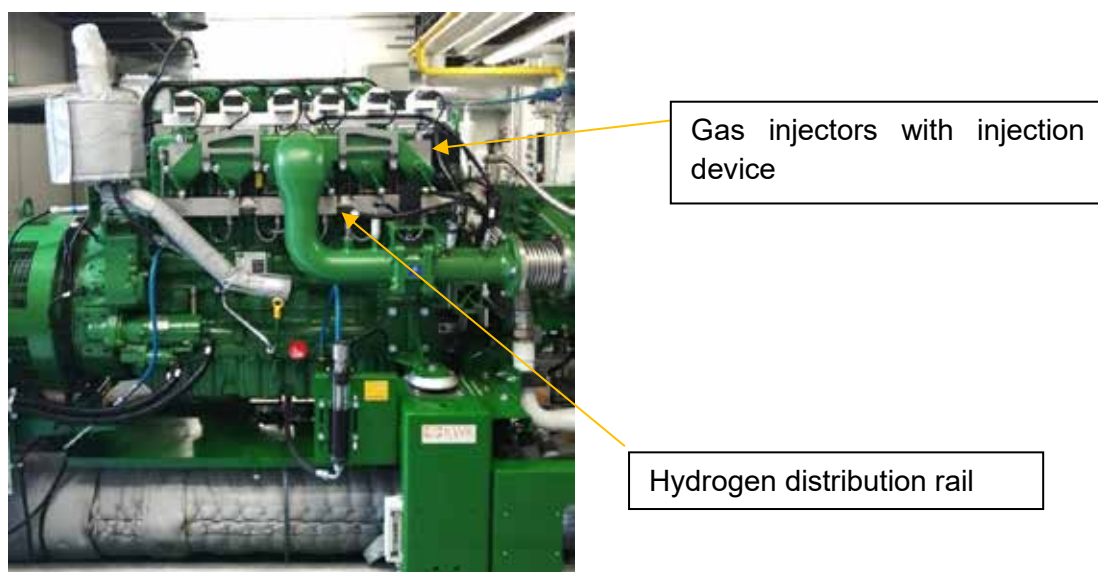


Figure 6: OTH plant converted to hydrogen

The retrofitting cost amounted to approximately 25% of the original order value and the work was realized in only 66 man-hours. However, it must be taken into account that the retrofitting was not performed as part of a scheduled inspection where the pistons, for example, would have been replaced regularly and where such items would not add any cost. Thanks to the gathered experience and the continued development of the technology to reduce costs, such activities will be offered at a significantly reduced price in the series process. The promise to offer hydrogen retrofitting for no more than 15% of the initial sum invested can be fulfilled in series.

4.2. Blue and green hydrogen for peak load coverage - Project Enbridge

This system in Enbridge, Canada, is another example for successful hydrogen strategy implementation. Enbridge operates the world's largest pipeline system for crude oil and liquids. The pipelines extend over 13,500 kilometers through Canada and the US. As a first step towards reducing the company's CO₂ emissions, Enbridge started operating a wind farm and a solar park with a combined output of 340 MW in 2007. Additionally, Enbridge has a 49.9% stake in the offshore wind farm project "Hohe See" located in the North Sea. To clean up the energy mix with regards to gas in addition to electricity, green and blue hydrogen are mixed into the natural gas network.

An agenitor 404 H₂ (115 kW_{el.}) integrated into the Enbridge Technology Operations Center in Markham is the first hydrogen CHP by 2G in North America. The hydrogen used to fuel the system is produced by an electrolyzer on site.

The follow-up project, two agenitor 420 H₂ (750 kW_{el.}), produces green energy for peak load coverage.

All three cogeneration systems can be operated on a mixture containing from 25 to 100 % hydrogen and natural gas. This variety of mixtures is possible because the systems are each equipped with a multi-point injection system (MPI) and a single-point injection system (SPI) as well as a conventional gas blending system. The control-related tasks are performed by the 2G CHP control system. The share of hydrogen in the mix is supposed to steadily increase over the duration of the project until it eventually reaches 100%. Figure 7 provides a schematic representation of the concept.

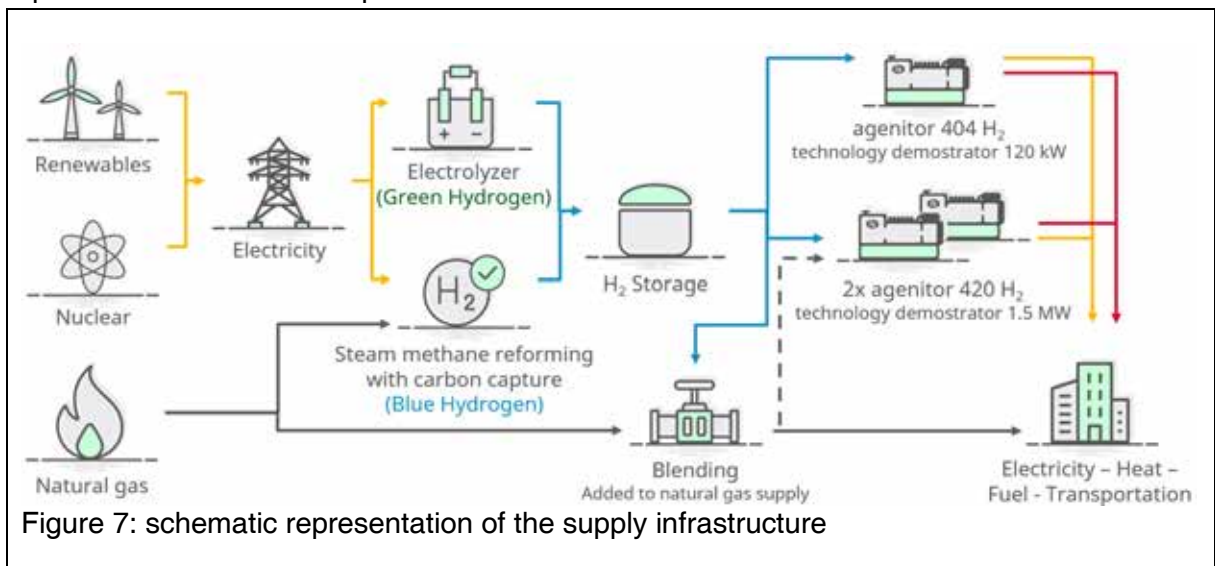


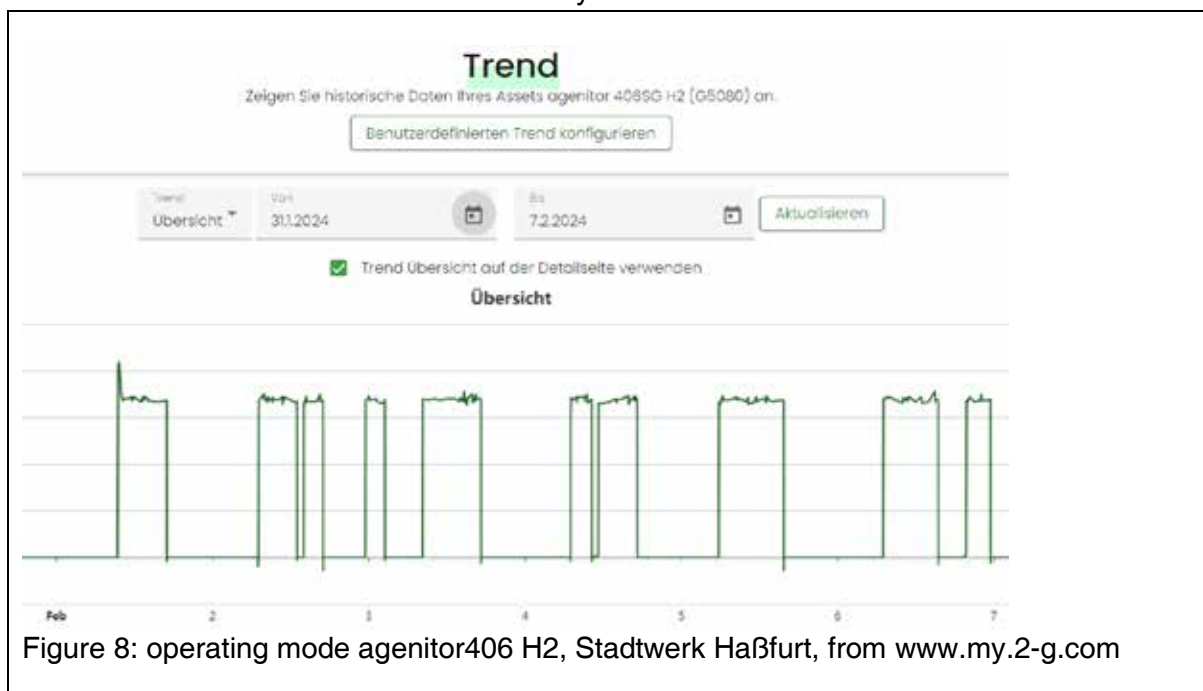
Figure 7: schematic representation of the supply infrastructure

Hydrogen generated from natural gas is often not entirely purified and still contains trace amounts of hydrocarbons. The processes to increase the quality include membrane technology, for example. However, the added processing is not necessary to operate 2G hydrogen CHP systems. The systems can run on impure hydrogen which can be a significant cost benefit.

4.3. Green hydrogen - Project Stadtwerk Haßfurt

Stadtwerk Haßfurt is probably the most renowned 2G hydrogen project. The system won the prestigious Handelsblatt Energy Award in 2019 and somewhat paved the way for the technology's growing success.

The trend visualization on my.2-g.com (Figure 8) shows the system's mode of operation throughout the selected period. The system's integration into the electricity market is clearly visible. The heat is sensibly used in a nearby school.



The system built in 2018 is the first hydrogen unit by 2G that is used for economic purposes. Overall it already produced more than 1 TWh of electrical energy. In combination with the electrolyzer and a hydrogen tank, the overall system is a symbol for successful, bidirectional sector integration.

5. Future development

Natural gas today, hydrogen tomorrow - that is the perspective for CHP technology. Attaining the output density of current natural gas CHP technology must be the minimum development goal. However, the emissions must be reduced to a fraction of what they are today, especially with regards to nitrogen oxide emissions (NO_x). 2G is taking three fundamental measures based on the gathered experiences:

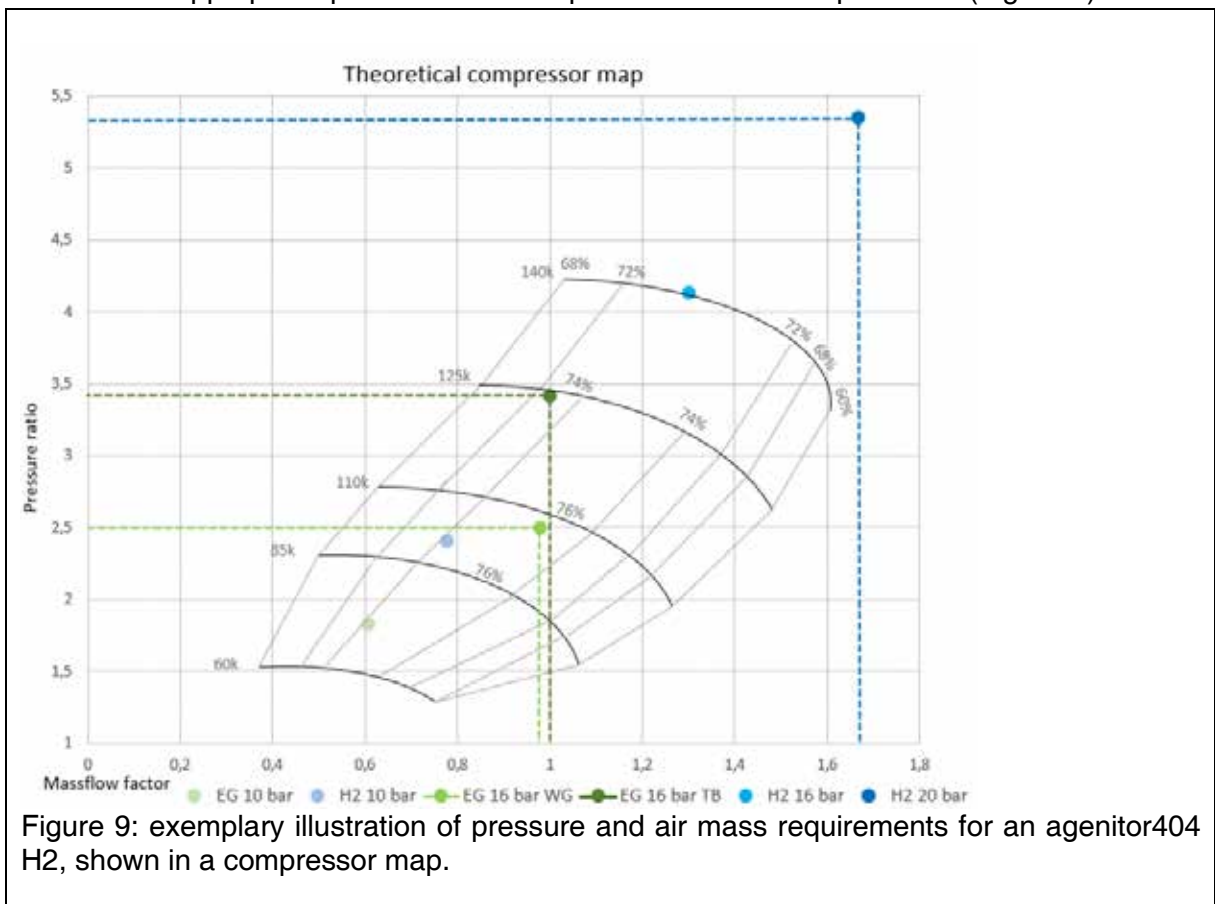
1. Optimization of the turbocharging unit to meet the elevated air consumption of extremely lean mixtures.

2. Homogenization of the mixture to prevent inhomogeneous zones within the combustion chamber.
3. Prevention of lube oil pre ignition prevent knocking occurrences.

Beyond that, further steps are being taken to ensure elevated specific outputs under safe operating conditions.

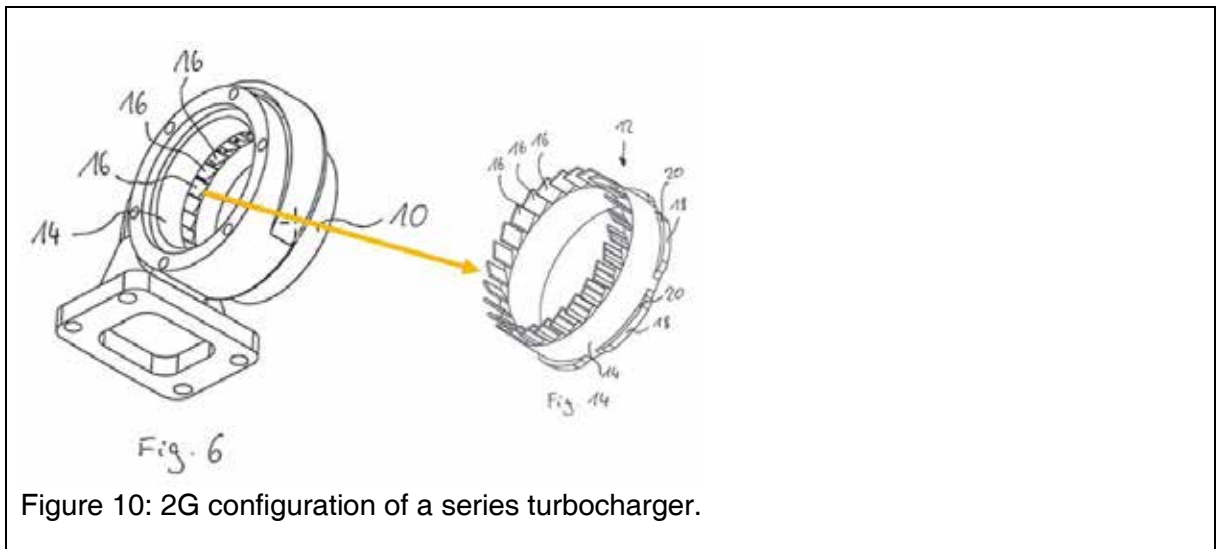
5.1. Turbocharging system

The lean operation of hydrogen engines at low nitrogen oxide emission levels requires a significant air mass, given the air ratio of $\lambda \approx 3$. Therefore, the turbocharger must be capable to deliver an appropriate pressure level despite low exhaust temperatures (Figure 9).

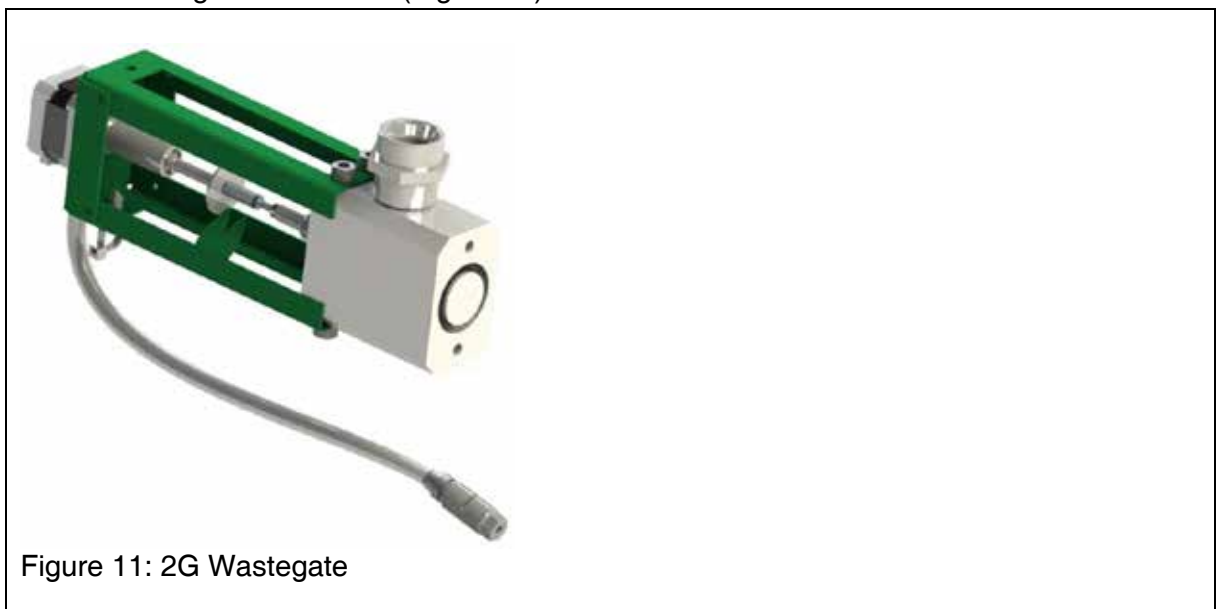


There is a variety of well developed turbochargers in the output range above 500 kW_{el.} that can be flexibly adapted using the nozzle rings and diffusers.

For lower output ranges, the automotive sector is the only recourse. Configuring these turbochargers for higher pressure ranges presents a challenge. For one, information on their characteristics is often insufficient and secondly, these turbochargers are not meant for modification. 2G has developed a patented solution for the retrofitting of series turbochargers. Although the compressor map of the turbocharger remains limited, it can be adjusted to the conditions via the turbine (Figure 10). This creates a minimum of configuration options and engines of lower power ranges can also be prepared for hydrogen.

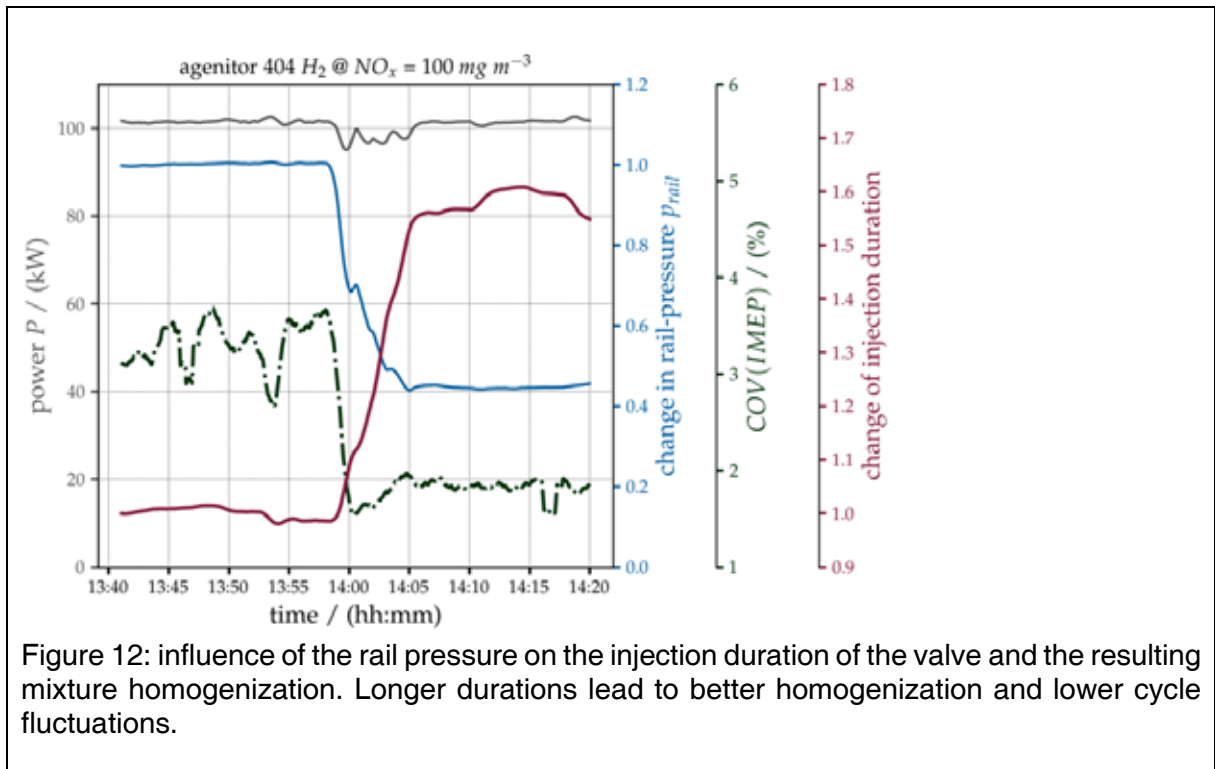


At the point of full-load operation, the exhaust temperature of a hydrogen engine, operated with natural gas is about 120 K higher than during hydrogen operation. This exhaust gas energy hits a turbocharger configured for extremely lean mixtures and cold exhaust temperatures (cf. map in Figure 9). To be able to operate engines on more than one gas type in one configuration, the adjustability of turbochargers is a key factor. 2G primarily uses an exhaust wastegate to this end (Figure 11).



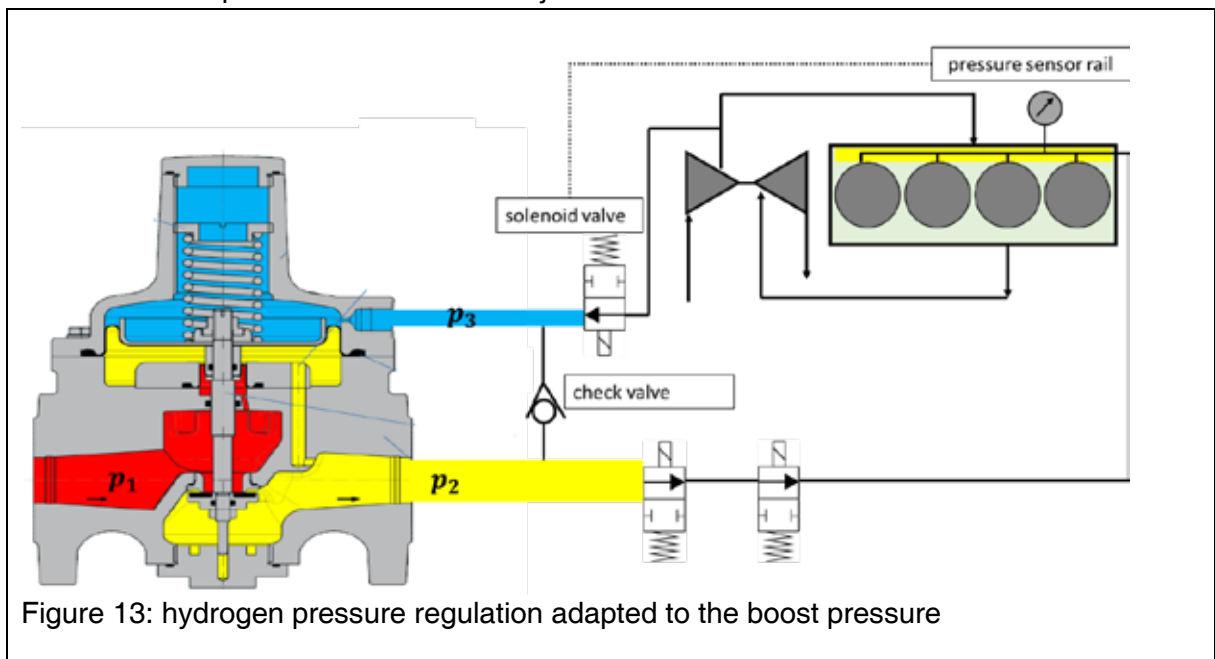
5.2. Mixture injection, homogenization and uniform distribution among cylinders

The first gas injectors that were subjected to testing showed an increased susceptibility to fluctuating injection durations, especially in case of elevated pressure differences between hydrogen and compressed air. That resulted in a proportionately elevated COV (Figure 12).

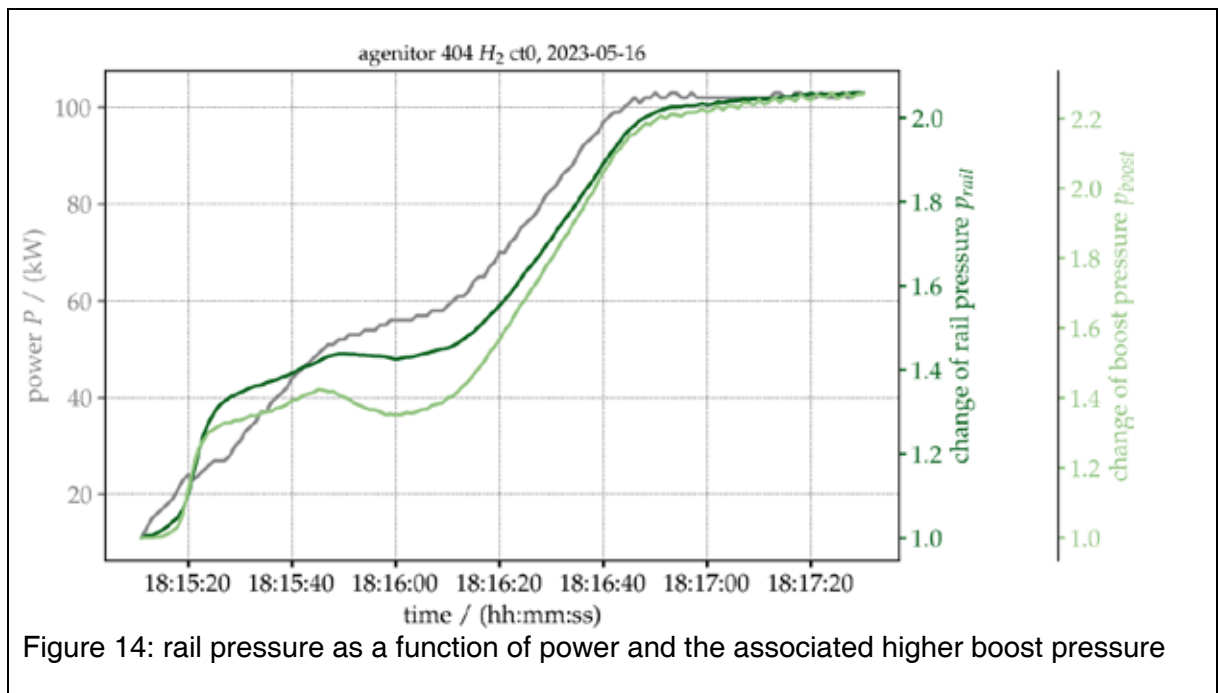


Lowering the pressure of the rail leads to prolonged injection durations, thus stabilizing the COV at a value slightly below 2%. By innovating the injector control devices and using adjusted injectors, the value was improved to below 1%. Consequently, the COV is about 0.5 percentage points lower than for natural gas applications.

A steady pressure gradient is required to ensure low cycle fluctuations even under partial load conditions. This was achieved by coupling rail and boost pressure (Figure 13). Furthermore, it ensures a lower pressure loss over the injection section.



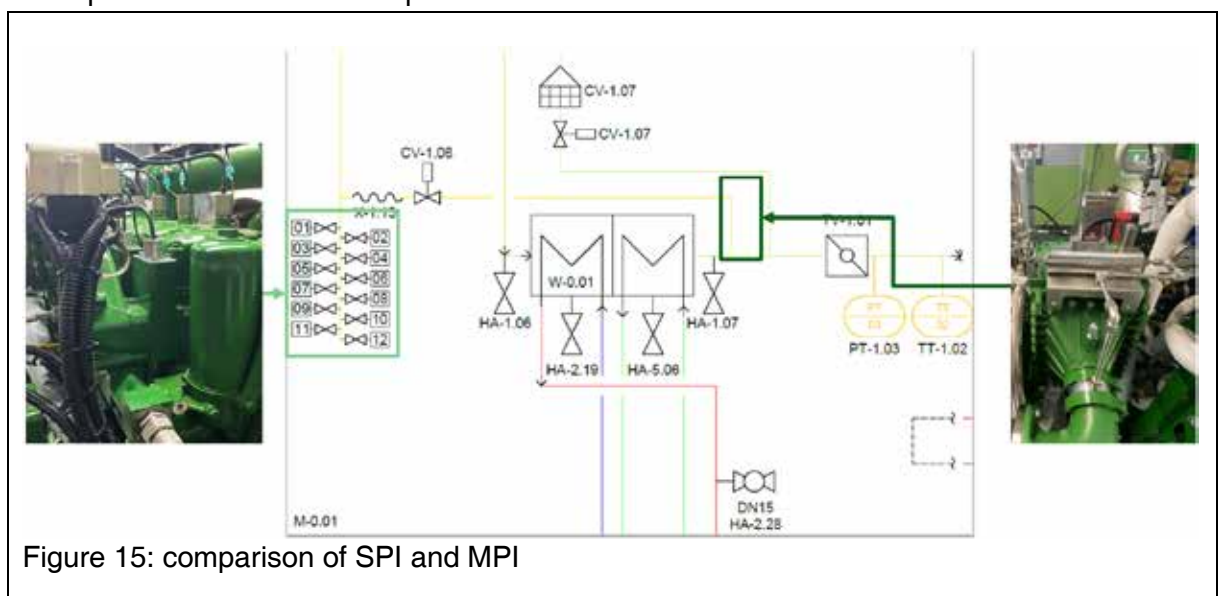
As a result, the pressure gradient Δp between boost and rail pressure remains steady.



A less significant pressure differential Δp has several positive effects at this point:

- Improved mixture homogenization due to more time for blending
- Improved precision of injector control due to extended time span
- Improved injector wear due to less forces impacting the valve inside the injector

Besides the multi-point injection (MPI), the single-point injection (SPI) is used for mixtures that contain other components than hydrogen. That is particularly necessary when the mass flow rate increases drastically. Chapter 6 provides more information on the topic. Figure 15: shows a comparison of the two concepts.



The SPI is used to inject a lean, ideally not yet flammable mass of gas. There were also tests where gas was injected via the SPI exclusively to determine the difference in mixture homogenization. At low mean effective pressures, hydrogen operation resulted in an expectedly minimal COV of below 1% (Figure 16).

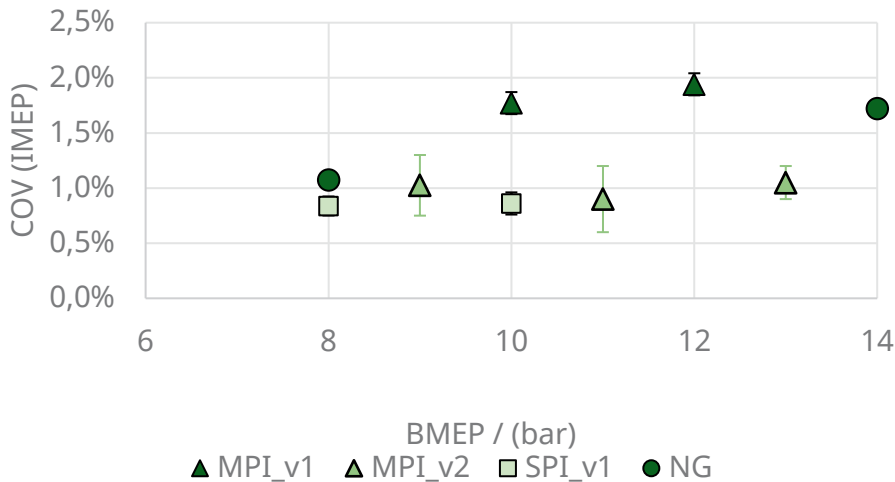


Figure 16: comparison of COV of MPI, SPI and natural gas via conventional mixture formation (all H₂ engine configuration)

To limit the zone inside the engine where a combustible mixture forms, 2G mostly relies on multi-point injection with an injection point as close to the inlet valve as possible (Figure 17).



Figure 17: gas intake via hydrogen injector (MPI)

Gas can only be supplied when the inlet valve is open. This concept ensures that no combustible gas-air mixture can remain outside the cylinder. However, this process leaves little time and space to form a homogeneous gas-air mixture.

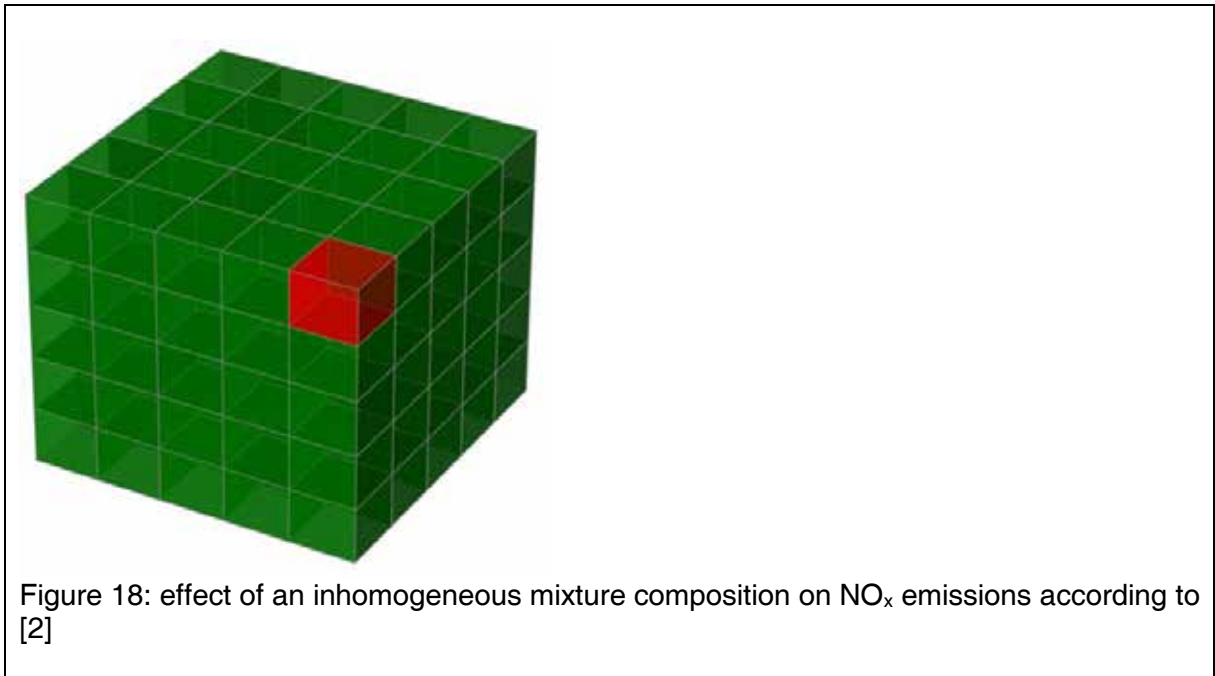
In order to operate the engine at extremely low NO_x emissions while sacrificing as little efficiency as possible, an extremely homogeneous hydrogen-air mixture must form during a brief injection phase. The impact of insufficient homogenization is made clear by the following depiction (Figure 18:).

Any volume with a 5 x 5 x 5 grid

124 cubes: $\lambda = 2.99 \rightarrow 49 \text{ mg Nm}^{-3} \text{ NO}_x$

1 cube: $\lambda = 2.05 \rightarrow 5,420 \text{ mg Nm}^{-3} \text{ NO}_x$

\rightarrow Combined **91.97 mg Nm⁻³ NO_x**



Generally speaking, the difference in molecule size between hydrogen and the components of air is beneficial for the mixture composition.

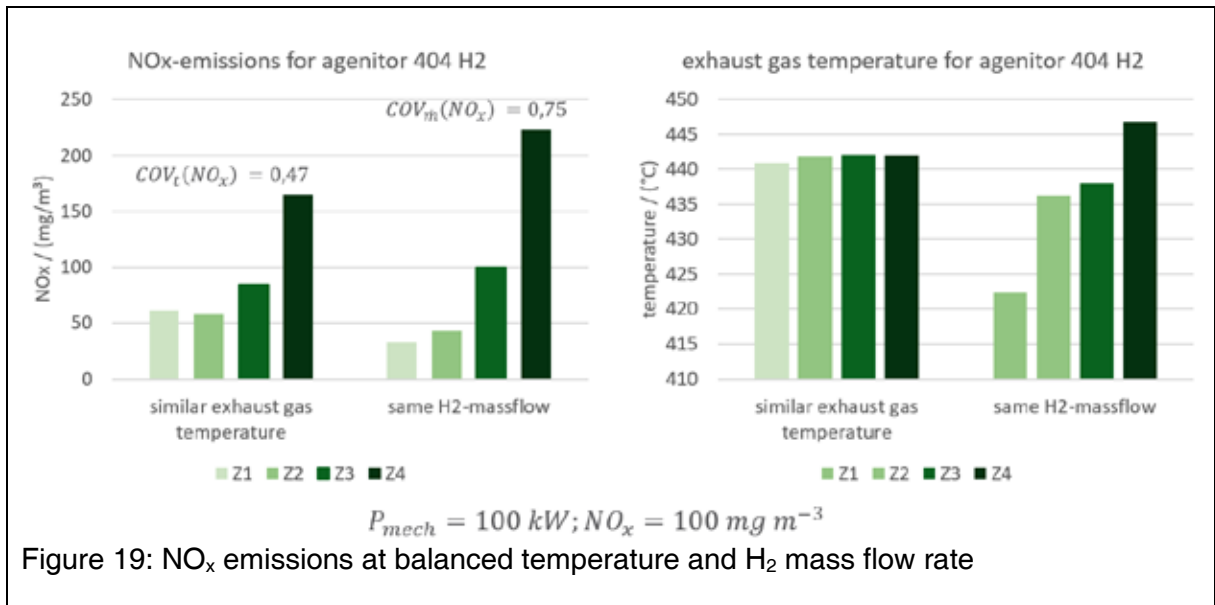
Axial injection was applied as a baseline to assess varying mixture composition procedures leading to the conclusion that while the pressure loss for hydrogen applications is minimal, the blending is insufficient. CFD simulations (Table 1) show that different nozzle layouts with radial outlets deliver very positive results while a central mixing star was found unsuitable for practical applications due to structural constraints.

Table 1: results of CFD calculation for mixture formation process: study was carried out by OTH Amberg-Weiden.

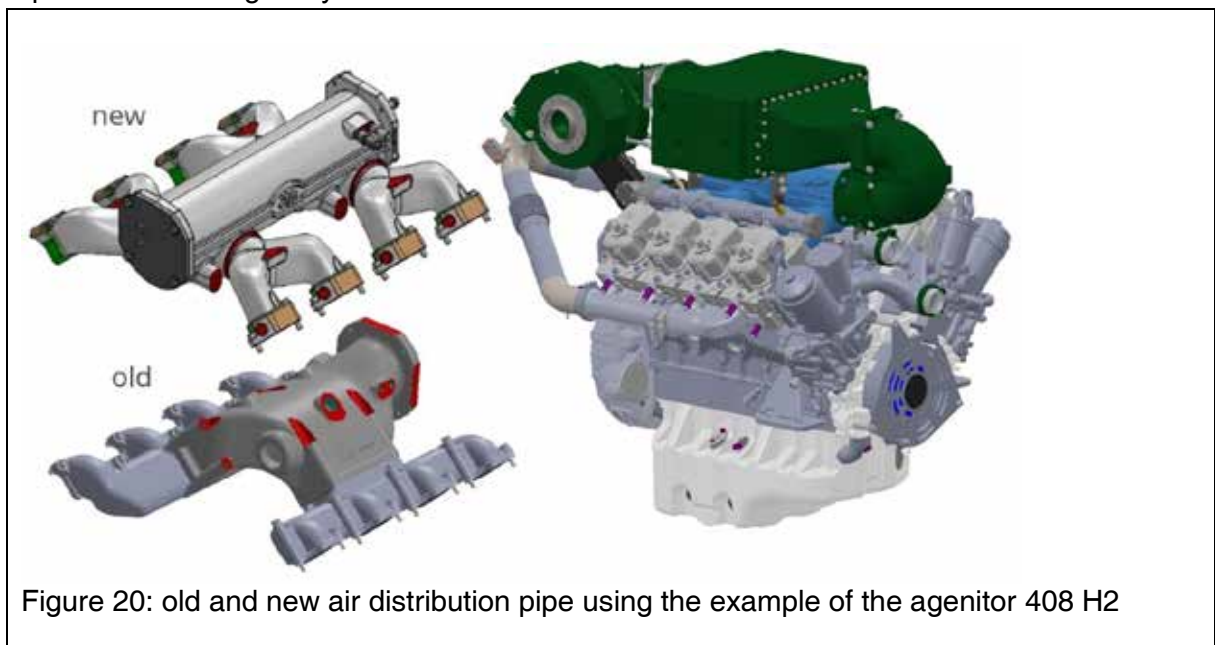
Geometry variants	Pressure loss (hydrogen-side)	Uniformity Index (phi)
Axial nozzle layout	0.01 – 0.02 bar	0.77
Radial nozzle layout V1	0.04 – 0.09 bar	0.85
Radial nozzle layout V2	0.16 – 0.36 bar	0.85
Mixing star	0.02 – 0.05 bar	0.88

In addition to the mixture composition, attention must be paid to a balanced cylinder charge. Tests with equal hydrogen injection times show that the cylinders exhibit extremely different NO_x emissions.

An equalization based on the individual exhaust gas temperature sensors is insufficient to reach an equalization among cylinders (Figure 19).



Until 2023, 2G used air distribution pipes from the diesel portfolio of the base engine supplier. A switch to optimized air distribution pipes able to hold the hydrogen injectors was part of the hydrogen technology development process (Figure 20). This measure ensures sufficient equalization among all cylinders.



5.3. Early Ignition, Lube Oil Pre ignition

Although at 600 °C the spontaneous ignition temperature of hydrogen is almost on the level of natural gas, it requires significantly less ignition energy while its flame spread is much faster. Obviously, the mixture composition (λ) and the mixture homogenization as described under 5.2 also play a role, but our observations have shown that even careful configuration leaves the possibility of uncontrolled combustion.

5.3.1.Reduction of oil entrainment

At < 0.1 g/kWh (full load operation), the oil consumption of 2G engines is minimal. To determine appropriate measures, operating states outside of full load operation, notably start-up and shutdown processes as well as the minimal load range, must be considered. In these load ranges, the combustion chambers experiences rather low pressures, even down to negative pressure. The piston ring package for the engines can be adjusted to this circumstance by using a three-part oil scraper ring, for example, that runs significantly more stable in negative pressure ranges. Valve stem sealing also has an impact. 2G uses stem caps with high initial tension instead of an O-ring (Figure 21, Figure 22).



Figure 21: three-part oil scraper ring



Figure 22: valve, guide with stem cap and seal-ring

Low combustion chamber temperatures could favour an increased build-up of oil carbon, as there is less burn-off. However, this effect has not yet been observed in 2G systems (Figure 23). The combustion chambers have proven to be mostly free of deposits, even after prolonged service times.



Figure 23: combustion chamber endoscopy of piston and firebox cover

5.3.2. Measures to prevent lube oil pre ignition

2G hydrogen engines employ a combustion concept based on the swirl-type intake of the mixture via the cylinder head, high turbulence due to omega-shaped combustion cavity and a specifically configured passive pre-chamber spark plug.

Optical combustion chamber assessments, published in 2013 [3], have shown that operation on hydrogen or gases with a significant hydrogen share can lead to lube oil pre ignition. In that case, the combustion was based on a tumble concept. The interesting part of this observation is that more pre ignitions occurred on the inlet side, meaning the relatively colder side of the combustion chamber. They concluded that the tumble carried droplets of lubricating oil from the cylinder liner to the center of the combustion chamber where it leads to the pre ignition of the mixture.

Therefore, the swirl concept seems to be superior in so far as the droplets stay on the cylinder wall due to the centrifugal effect of the swirl. However, the flame front of the spark plug only reaches them later. Consequently, the optimal system configuration remains a question of engine-individual alignment.

Lube oil pre ignition can happen in 2G units. Their criticality depends on frequency and the resulting pressure peak. Since these events do neither develop gradually nor exist across multiple engine cycles (Figure 24) it makes no sense to react to them via the knock control.

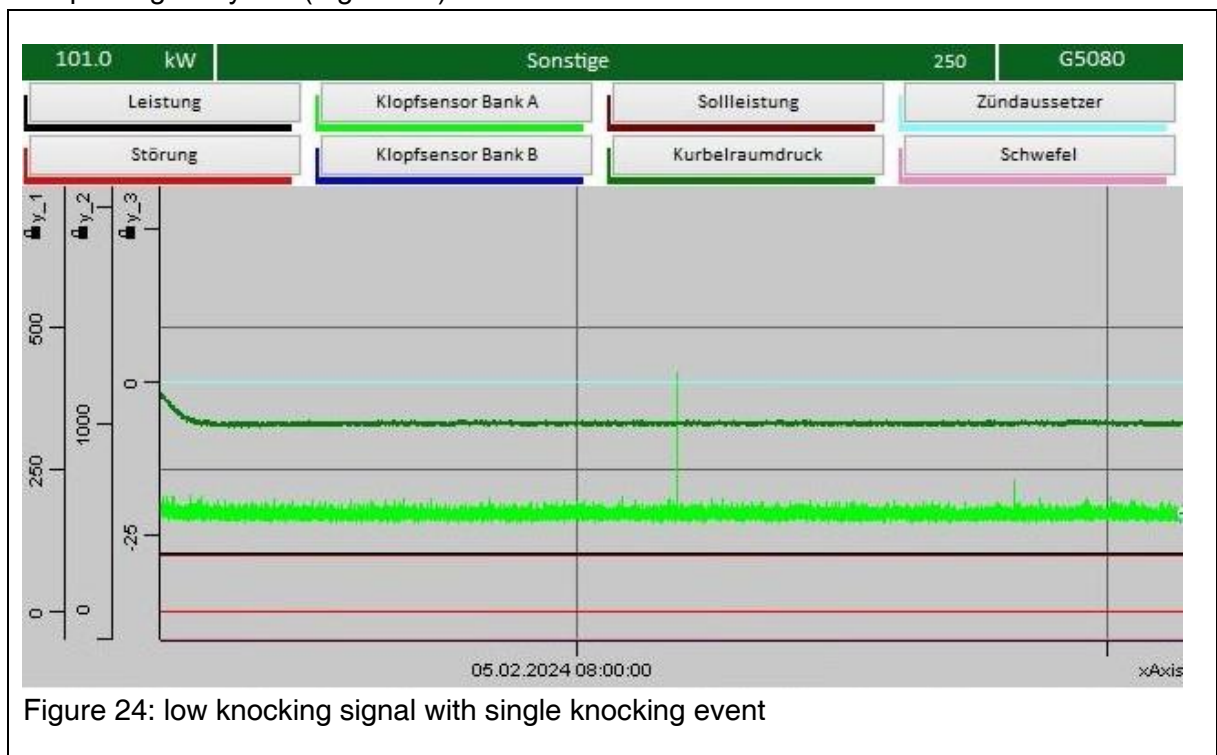


Figure 24: low knocking signal with single knocking event

The impact of the lubricating oil formula on the combustion was tested on the 2G engine test stand (Figure 25). Petro-Canada Lubricants provided various formulas for the tests.



Figure 25: hydrogen test bench

Knocking combustion was triggered by a richer operation. The engine displays significant differences with regards to knocking stability depending on the lubricating oil.

To research the premature ignitions, the ignition timing was delayed to make flame front overlaps easier to identify (Figure 26). Lube oil pre ignitions or rather early ignitions became evident. The choice of lubricating oil had an impact.

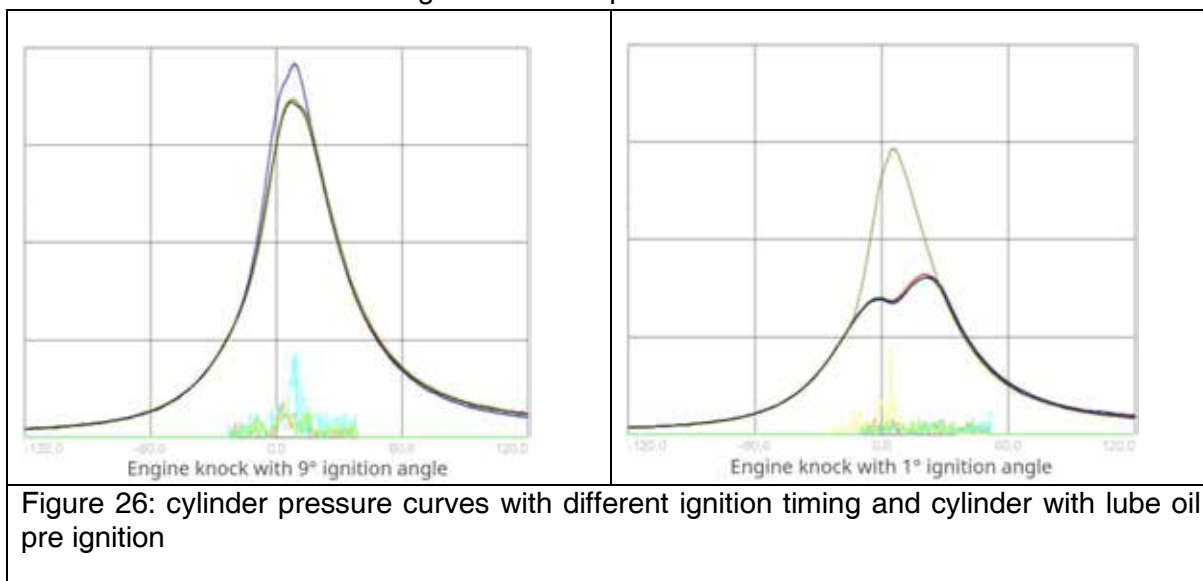
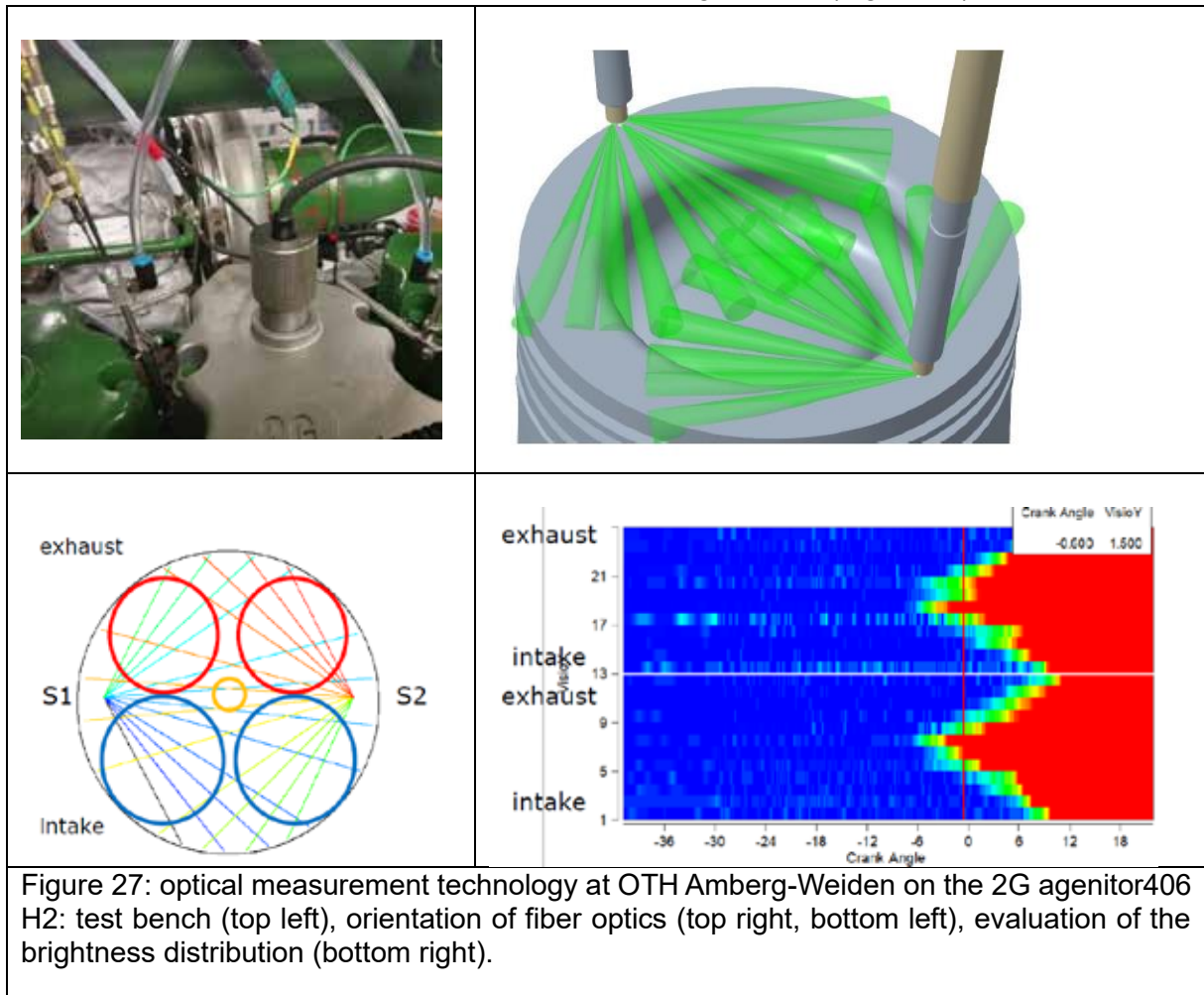


Figure 26: cylinder pressure curves with different ignition timing and cylinder with lube oil pre ignition

Consequently, using the lubricating oil with a formula adapted for hydrogen operation is sensible.

5.3.3. Optical assessment of lube oil pre ignitions

To further research the correlations, an agenitor 406 H2 is being subjected to optical combustion chamber assessments at the OTH Amberg-Weiden (Figure 27).



Two combustion chamber sensors with 12 light cones respectively observe especially the edge zone of the chamber to detect combustion anomalies. It is possible to allocate the observations in terms of location and time.

Furthermore, an endoscope with a UV camera is used to assess the flame spread and with a view especially on the spark plug (Figure 28).



Figure 28: UV camera with combustion chamber endoscope

During the first preemptive tests in low-load natural gas operation, it recorded flares from the pre-chamber spark plug and a glowing particle inside the combustion chamber (Figure 29).

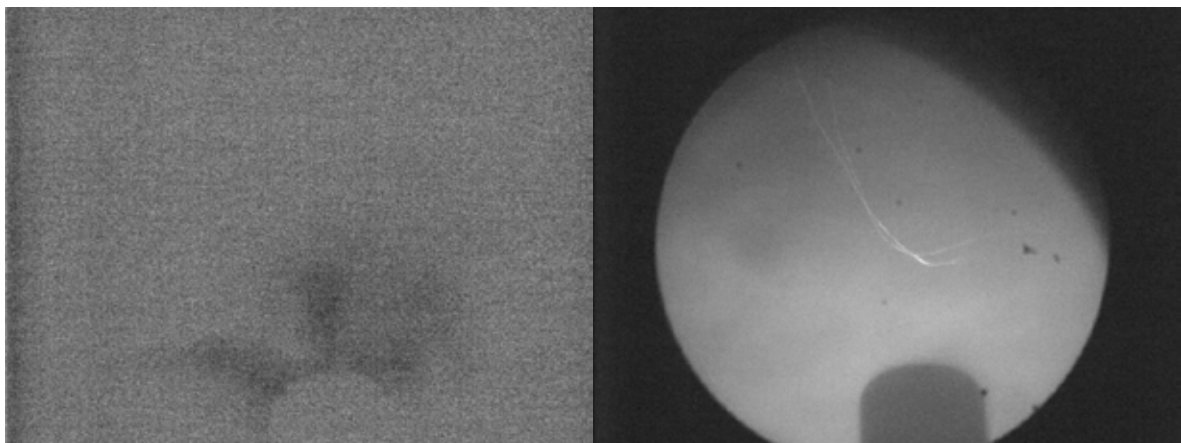


Figure 29: pre-chamber flares and glowing particles in the combustion chamber

The tests on lube oil pre ignition could not be performed before finalization of this manuscript. The findings on pre ignition effects in hydrogen operation will be used for further engine technology development.

5.3.4. Crankcase ventilation and blow-by

2G uses a highly efficient crankcase ventilation filter. In new condition, the degree of separation amounts to 99.95% and only decreases to 99.85% after 8,000 operating hours. Consequently, blow-by scarcely introduces oil particles.

The water content in the lubricating oil according to an analysis after 1,000 operating hours is depicted in Table 2.

Table 2: water content in blow by gas and in oil according to oil analysis

	Water content in blow-by gas	Water content in Oil after 1.000 ohp
Hydrogen ($\lambda \approx 2.8$)	3.8 Vol. %	350 ppm
Natural Gas ($\lambda \approx 1.7$)	2.1 Vol. %	100 – 350 ppm
Natural Gas ($\lambda \approx 1$)	6.2 Vol. %	500 – 1,000 ppm

The data pool being insufficient for now, the fluctuation margins for hydrogen operation can not be specified.

To prevent water condensation in the oil sump and the periphery, some 2G models for lambda-1 operation are equipped with crankcase ventilation (Figure 30). Should hydrogen engines prove to have similar challenges, the proven ventilation can be relied upon.



Figure 30: oil-water emulsion in refilling system

Measurements show that the blow-by gas has a hydrogen content of approx. 10%. This constitutes a combustible mixture, although with an extremely lean air-fuel ratio of approx. lambda 4. This finding can be disregarded since the energy required to ignite this mixture would be very high. Additionally, there is no ignition source. Combustible mixtures also occur in the crankcases of traditional natural gas applications and have never been a problem over decades of practical experience. The maximum possible explosion pressure is below the level of the natural gas mixture. Consequently, the mechanical stability of the crankcase is under less stress than in the case of natural gas ignition.

6. Waste hydrogen

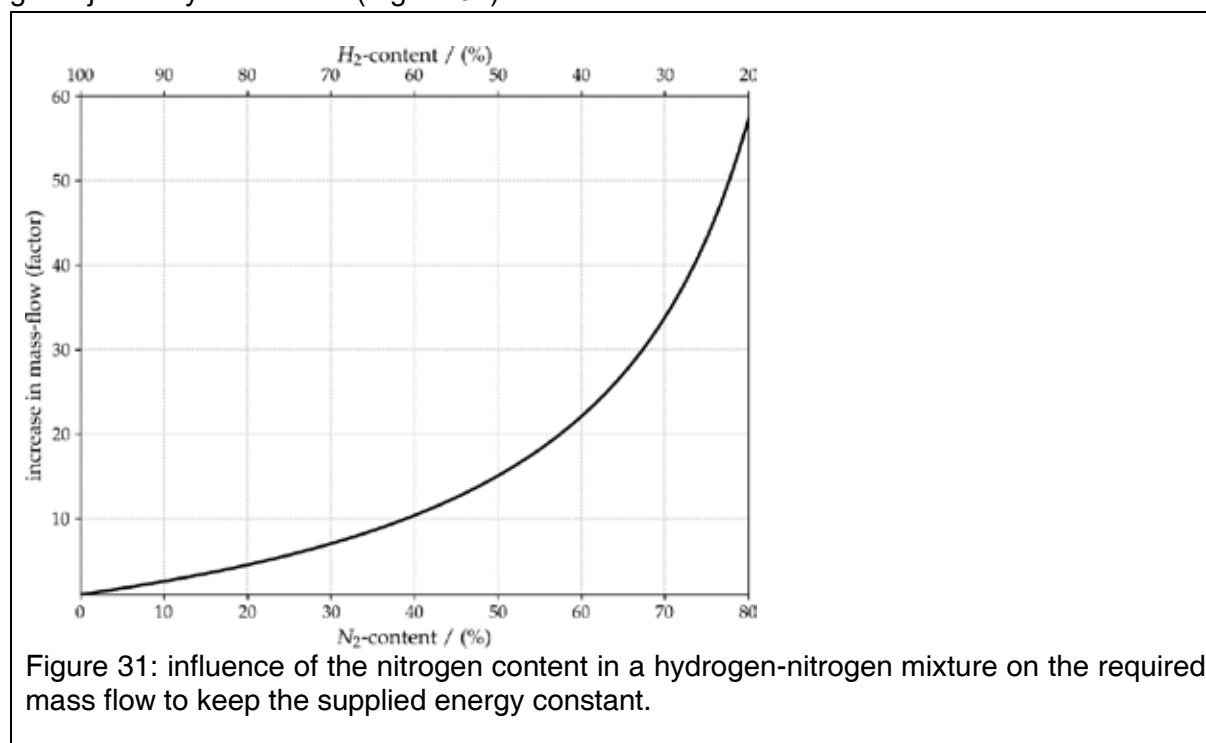
The recovery of hydrogen produced by industrial processes to produce energy is another possible area of application for the 2G hydrogen technology. An advantage of using combustion engines in this process is their imperviousness to concomitant substances in the hydrogen gas. Besides hydrogen, it mostly contains higher hydrocarbons or nitrogen.

Table 3 shows some of the gas compositions that 2G system run on.

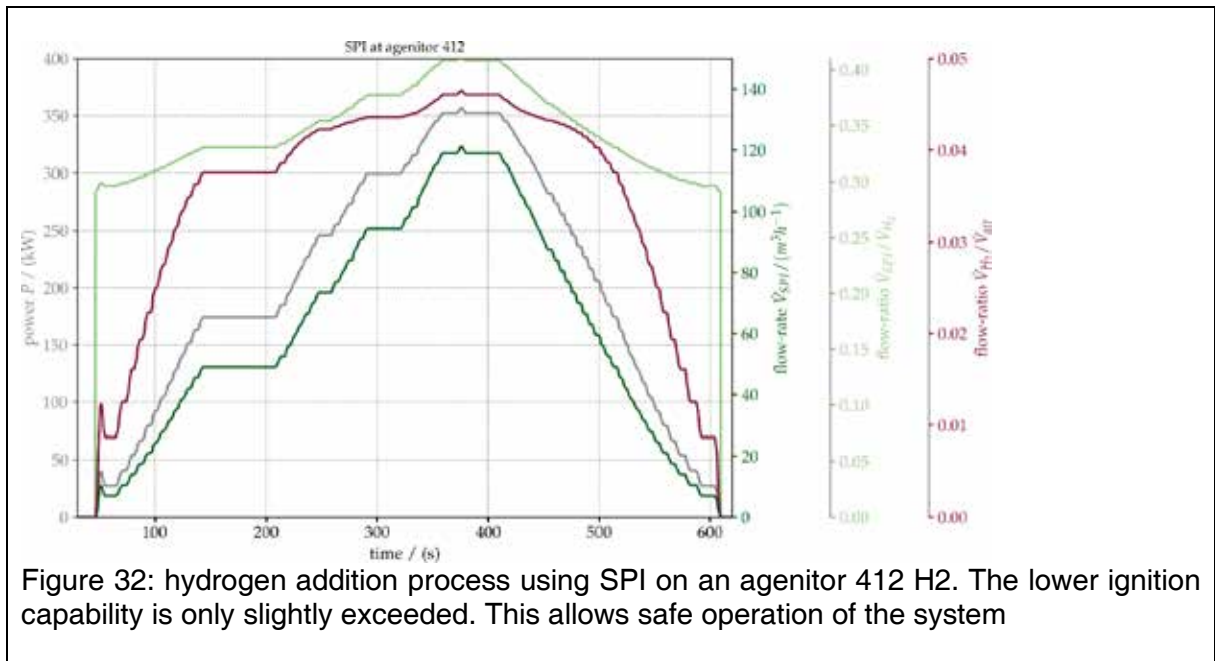
Table 3: accompanying substances for non-high-purity hydrogen

Data in %	unit	H ₂	CH ₄	CO	N ₂	Ar	H ₂ O
G6332	412	97.25	1	0.69	0.68	0.1	0.28
G6275	408	different mixtures / use for academic purpose					
G6244	404	90			10		
G6133	412	98	2				

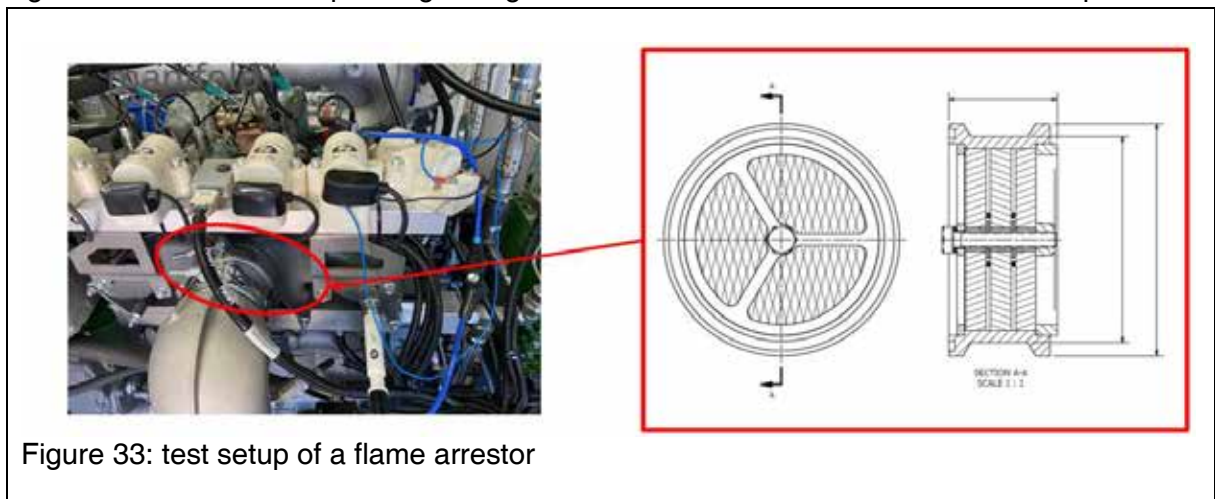
Gas injection via multi-point injection is already a challenge with these mixtures, because even small volumetric shares lead to a drastic increase in the overall mass. As an example: 1% nitrogen on 99% hydrogen suffices to increase the overall mass that must be taken in via the gas injector by about 14% (Figure 31).



New injector configurations tailored to the application would be required to enable the injection of such gases via MPI. Since that approach would be complicated and make for minimal quantities 2G decided to use additionally single-point injection (SPI) in such cases. The SPI serves as a mass injector that is supposed to introduce the leanest mixture possible, below the ignition limit, if possible. Figure 32 shows the gas admixture via SPI as a function of output. Tests on the agenitor 412 H₂ (cf. Table 3, G6332) show an H₂ concentration of 4.6% at full load which means the mixture is at the lower end of the ignition limit. The ignition energy required for such a mixture is higher than the energy required by a natural gas lambda-1 engine and therefore noncritical for this type of admixture.



Additionally, a flame arrestor (Figure 33) is being used. Ignition tests showed that it succeeds in extinguishing a lean mixture. The mixture volume, lambda and charge pressure play significant roles. A corresponding configuration of the flame arrestor ensures safe operation.



7. Conclusion

The adaption of highly developed gas engines for operation on hydrogen already underwent thorough testing and has been the subject of numerous publications. By applying this basic know-how, it is possible to operate steadily with mean effective pressures up to 15 bar.

For further performance increases, the specific base engine characteristics become increasingly important. They must be researched individually and solutions must be developed. The lecture went more into detail on the factors turbocharging, mixture composition and knocking prevention. 2G developed solutions for each of the categories that show promising results in practice. The long-term testing has not yet concluded.

After successful verification of the findings, lifting the performance levels to today's natural gas units will be possible. Further performance increases are being tested as part of research projects.

References

- [1] OTH, „Bilder im Rahmen des Besuchs des bayrischen Ministerpräsidenten Markus Söder,“ 2020.
- [2] R. Herdin, in 42. Internationales Wiener Motorensymposium , 2020.
- [3] H.-B. Snuis, „Method to quantify and visualize abnormal combustion of a SI engine,“ *INTERNATIONAL COUNCIL ON COMBUSTION ENGINES*, 2013.

Towards reliable genset operation with pure hydrogen

Auf dem Weg zum zuverlässigen Betrieb von Gasmotorenaggregaten mit reinem Wasserstoff

Dr. M. Schultze*, **D. Shah**, **Dr. S. Ohler**
Caterpillar Energy Solutions GmbH, Mannheim

T. Krüger*, **M. Cech**, **C. Tietze**
WTZ Roßlau gGmbH, Dessau-Roßlau

Supported by:



on the basis of a decision
by the German Bundestag

Abstract

In this article will be presented the achievements of a joint project of the WTZ with Caterpillar on gas engine operation with pure hydrogen, funded by PTJ/BMWK. The goal was to develop a highly efficient engine running on pure hydrogen from renewable sources to enable sustainable decentralized heat and power generation.

Engine operation with pure hydrogen imposes a few additional challenges compared to the operation with natural gas. In this article, we will be focusing on major changes to engine design and operation compared to conventional natural gas operation.

A major building block in the development of the hydrogen engine was the review and evaluation of different mixture formation strategies for pure hydrogen. The production natural gas engine that was used as a baseline for the hydrogen engine featured a fumigating system based on the Venturi principle. We performed an evaluation of the conventional mixing system with pure hydrogen. However, due to the higher risk of backfire events this option has been discarded in favor of a port injection system. The design approach and the control strategy of the port injection system will be discussed. Additional modifications e. g. optimizing the turbocharger specification to pure hydrogen operation have been applied but will not be reviewed in detail in this article.

After the commissioning and the validation of the new components and the hydrogen injection controls were completed successfully, the team focused on deploying a safe and reliable operating strategy. The primary goal was to demonstrate capability to run on pure hydrogen and to determine maximum power output within combustion limitations. The article will provide an overview of the demonstrated performance with 100% hydrogen and review the challenges the team encountered during the calibration optimization process.

* Speaker/Referent

Kurzfassung

In diesem Artikel werden die Ergebnisse eines vom PTJ/BMWK geförderten gemeinsamen Projekts des WTZ mit Caterpillar zum Betrieb von Gasmotoren mit reinem Wasserstoff vorgestellt. Ziel war es, einen hocheffizienten Motor zu entwickeln, der mit reinem Wasserstoff aus erneuerbaren Quellen betrieben wird, um eine nachhaltige dezentrale Wärme- und Stromerzeugung zu ermöglichen.

Der Betrieb von Motoren mit reinem Wasserstoff bringt im Vergleich zur Nutzung von Erdgas einige zusätzliche Herausforderungen mit sich. In diesem Artikel konzentrieren wir uns auf die wesentlichen Änderungen in der Motorkonstruktion und während des Betriebs im Vergleich zum herkömmlichen Erdgasbetrieb.

Ein wesentlicher Baustein bei der Entwicklung des Wasserstoffmotors war die Untersuchung und Bewertung verschiedener Gemischbildungsstrategien für reinen Wasserstoff. Der Serien-Erdgasmotor, der als Basis für den Wasserstoffmotor gedient hat, verfügt über einen Gasmischer, der mit dem Venturi-Prinzip arbeitet. Im Rahmen dieser Arbeit ist eine Bewertung des konventionellen Mischsystems für den Betrieb mit reinem Wasserstoff durchgeführt worden. Aufgrund des erhöhten Risikos von Rückzündungen wurde diese Option jedoch zugunsten eines Port-Fuel-Injection-Systems verworfen, dessen Konstruktionsansatz und die Regelstrategie diskutiert werden. Zusätzliche Modifikationen, wie z. B. die Optimierung der Turbolader-Spezifikation für den Betrieb mit reinem Wasserstoff, wurden vorgenommen, werden in diesem Artikel aber nicht im Detail behandelt.

Nach der erfolgreichen Inbetriebnahme und Validierung der neuen Komponenten sowie der Steuerung für die Wasserstoffeinblasung hat sich das Team auf die Entwicklung einer sicheren und zuverlässigen Betriebsstrategie konzentriert. Das Hauptziel bestand darin, die Fähigkeit zum Betrieb mit reinem Wasserstoff nachzuweisen und die maximale Leistungsabgabe innerhalb der Verbrennungsgrenzen zu bestimmen. Der Artikel gibt einen Überblick über die nachgewiesene Leistung mit 100% Wasserstoff und geht auf die Herausforderungen ein, die während der Kalibrierung aufgetreten sind.

1. Introduction

The successfully completed joint research and development project consistently follows the strategic goals of the 7th Energy Research Program [1] of the Federal Government of the Federal Republic of Germany and is derived directly from the global requirements for climate and environmental protection. Among other things, it provides for an increased use of alternative fuels to reduce carbon dioxide and methane emissions. The conversion of renewable electricity into chemical energy sources enables long-term storage of renewable energy, which increases security of supply. At this point, the gas engine can also contribute to sector coupling and help to increase the stability of the energy system and reduce the costs of the energy transition. In particular, the sectors for the efficient use of electricity from renewable energy sources in the areas of heating and cooling are being coupled with each other. The National Hydrogen Strategy [2] published by the Federal Government takes up this approach and intends to focus on the long-term orientation of decentralized energy and heat supply regarding the use of renewable energies.

This intention can be implemented using green hydrogen, which is produced from renewable energies, in the hydrogen engine in the CHP application. The requirements for CHP units powered by gas engines are very diverse and will continue to increase. Due to their high level of development, it is possible to meet these requirements. For example, the CHP units have high efficiencies for cost-effective plant operation and at the same time can be used flexibly to compensate for fluctuating energies from wind and photovoltaics. In this way, they support the power grid statically and, if necessary, dynamically. In addition, the use of hydrogen produced with surplus electricity contributes to the decarbonization of electricity generation in the CHP plant, so that the goals of the Paris Climate Agreement can be achieved. In addition, the reliability and durability of the products expected by the customer can be guaranteed.

The aspects described above, in particular the engine consequences of alternative fuels on the energy sector, were taken up in this joint project and investigated on a gas engine. As a result, it was possible to gain the expected fundamental knowledge for the development of novel gas engines for stationary applications in accordance with 44th BImSchV and 13th BImSchV and to incorporate them into the CO₂-neutral future programs for the reduction of exhaust emissions. Some of the findings of the project from the project partners WTZ Roßlau GmbH and Caterpillar Energy Solutions will be presented in more detail.

2. Project description

The overarching goal of the joint research and development project was to exploit the considerable potential of gas engines to reduce emissions for the energy sector using renewable fuels. The use of hydrogen in the energy sector requires a significant further development of gas engines available today, which are primarily powered by fossil natural gas. For example, the brake mean effective pressures of hydrogen engines previously demonstrated in laboratory operations are still well below the average pressures of natural gas series engines in comparable applications. The limitation of energy density results from the risk of compression-ignition phenomena (e.g. "knock"), which can put a lot of strain on engine components and even the entire engine.

The aim of the work carried out was therefore to extend the operating limits of the hydrogen engine. Existing studies have already shown that the use of hydrogen in near-series gas engines is not sufficient for the CHP application requirements. The planned investigations were therefore aimed at analyzing the influence of the combustion properties of the hydrogen on the combustion process, considering the operating conditions of a CHP. The in-depth clarification of these relationships was experimentally tested and precisely analyzed.

To secure the desired increase in the engine's performance, further optimization of the mixture formation and valve timing was required. In addition to the integration of the hydrogen components and the consideration of various safety aspects, the further development of the combustion process was also one of the major challenges of the planned project.

3. Development focus

A TCG 3016 V08 engine was used in this study, which was slightly adapted for operation with hydrogen as fuel gas. The standard natural gas variant of the test engine is equipped with a Venturi gas mixer, which is used to mix the fuel gas into the air flow upstream of the turbocharger compressor. Furthermore, the engine is operated with Otto timing and its mean effective pressure is 18.9 bar.

For the usage of pure hydrogen as fuel, the test engine was equipped with a Port Fuel Injection (PFI) system instead of the Venturi gas mixer. In addition, a modified, but close to production design, turbocharger was installed to meet the changed requirements of the air system due to the high volume flows at very lean engine operation and the comparatively low exhaust gas enthalpy. In the course of this study, the impact of a reduced compression ratio and Miller timing on the combustion recipe was also investigated. Due to the high boost pressure requirement of an engine with Miller timing, an external compressor was used to increase the turbocharger intake pressure, as the used turbocharger was not able to provide the required boost pressure on its own during hydrogen operation.

The PFI system provides some benefits, especially for hydrogen combustion. Since the fuel gas is injected close to the intake valves, the volume in the engine filled with a combustible air fuel mixture is reduced. Hence, the risk of a backfire induced flame propagation into the intake manifold is eliminated. From the performance point of view port fuel injection is beneficial since no low-density hydrogen has to be compressed by the turbo charger. Furthermore, since the fuel supply of each cylinder can be controlled individually for each cylinder, the implementation of advanced control concepts is possible.

The design and the diameter of the hydrogen supply rails was optimized using 1D simulations to minimize pressure fluctuations in the rails caused by the fuel injection process. Based on the simulation results the injection valves of each engine bank were supplied with hydrogen via a separate rail (Figure 1), which proved to be the most advantageous solution of the gas system.

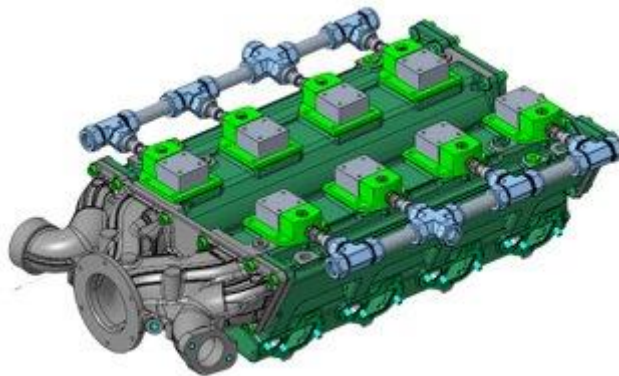


Figure 1: TCG 3016 V08 with installed fuel gas supply and PFI valves.

The flow characteristics of different potential injector tube designs (Figure 2) were investigated using CFD simulations. The best homogenization of air and fuel as well as the best capture rate of hydrogen in the cylinder was predicted with the design variant shown in Figure 2 c. Consequently, this variant was used for the engine tests. This design includes a long injection tube that is closed at its end. The hydrogen exits through lateral slits at the lower end of the tube towards the cylinder inlet channels.

The tube design for introducing the hydrogen has a significant influence on the engine behavior and the probability of anomalies, especially on the occurrence of backfire in the charge air

system. In the present case, it was found that equal utilization of the cylinder intake channels increases the trapped hydrogen mass in the cylinder. This injection strategy also improves the homogenization of the air/fuel mixture.

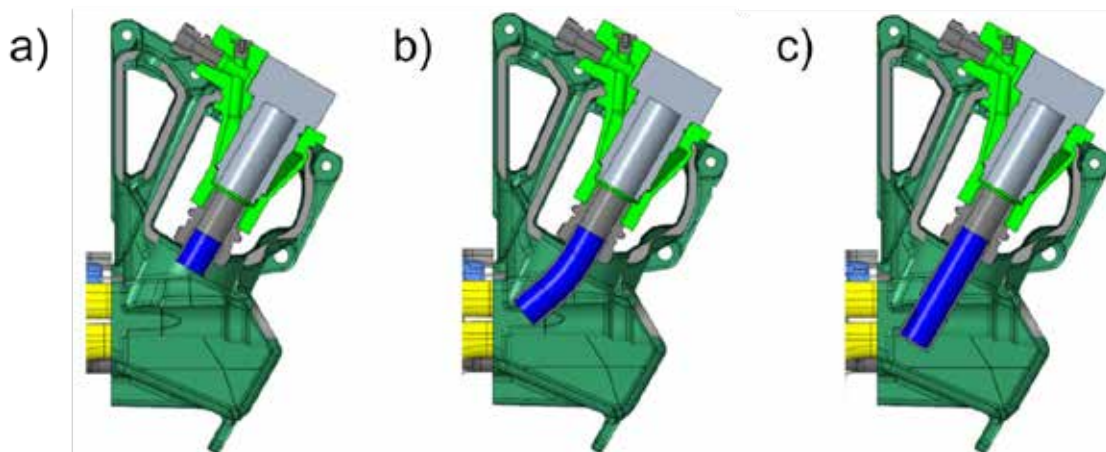


Figure 2: Investigated injector tube variants.

A hybrid controller configuration was developed to enable the engine operation with hydrogen as a fuel gas leveraging current engine electronic hardware configuration and software infrastructure, to assure robust engine operation with needed preliminary protection. Combining it with an additional controller, to integrate Port Fuel Injection along with advanced pressure sensing module to enable advanced engine protection. A combination of test cell automation and engine controls interface was leveraged to enable safe operation with needed tunability for parameters in focus.

A simplified schematic of the above-mentioned hybrid control system configuration is depicted in Figure 3.

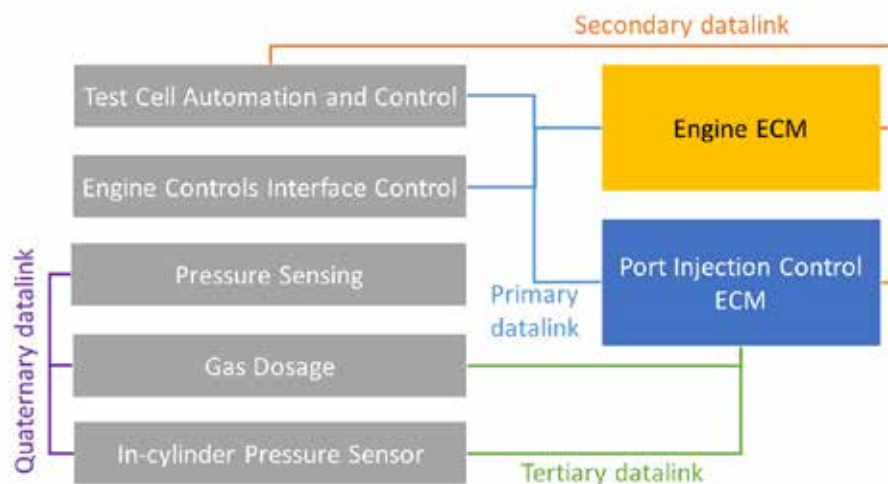


Figure 3: Schematic of the installed hybrid control system.

Such a set up offered flexibility to investigate multiple approaches for PFI integration and its control, allowing further exploration of engine monitoring and protection concepts for hydrogen operation. These advanced controls strategies were key enablers for a stable engine operation

and assured quick transitions of operating conditions while minimizing downtime during investigations.

Extensive measurement campaigns were recorded by varying engine parameters to assess and compare natural gas and hydrogen operation. The focus was primarily on load, ignition timing, and mixture variations. Testing also gained insight into the influence of hydrogen-typical combustion anomalies, knocking and the impact of fuel injection timing on combustion stability and engine performance. In addition, parameters such as valve timing, compression ratio, oil lubricating system and air system were modified to evaluate the impact of these building blocks on combustion stability and maximum load.

4. Operational challenges

Abnormal combustion is an important factor in the development process of gas engines. This includes mainly pre-ignition, backfire, and knocking. When using hydrogen as a fuel these phenomena must be considered even more than with other gaseous fuels due to the fuel's high reactivity, flammability, and low ignitability limits [3, 4]. In gas engines, pre-ignition can be caused by different effects. Potential ignition mechanisms are oil droplets or other hot particles in the cylinder and hot components such as the spark plug or the exhaust valves. Hydrogen also has high risk for autoignition, meaning that a hydrogen/air mixture can ignite spontaneously at sufficiently high temperatures without a dedicated ignition source [5]. Typically, the combustion stability will decrease at higher load since the elevated pressure and temperature will favor abnormal combustion events.

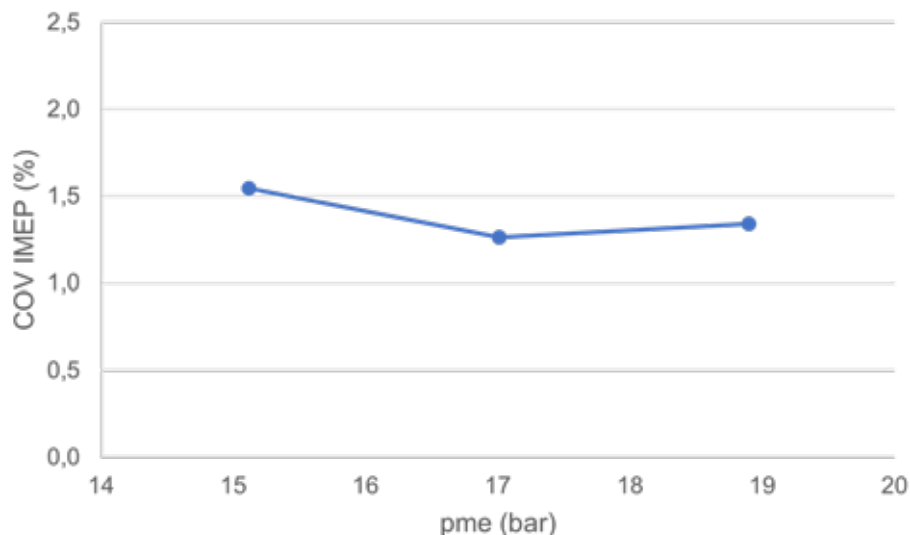


Figure 4: CoV of mean indicated pressure (IMEP) at different load points.

As shown in Figure 4 the coefficient of variation ($CoV = \frac{\text{standard deviation}}{\text{mean}}$) of the mean indicated pressure IMEP remains stable at a low level when approaching the design power output of the test engine. However, a working cycle based analysis of the cylinder pressure data shows that the frequency of pre-ignition events increases as the load increases (see Figure 5). At $p_{me} = 15.1$ bar the beginning of the combustion (CA10) is very uniform resulting in similar peak cylinder pressure values. At $p_{me} = 18.9$ bar there are several cycles which show a very early start of combustion due to pre-ignition. The peak cylinder pressure of these cycles is hence significantly increased (see cycles marked with arrows). The data also shows that pre-ignition does not change the combustion velocity as the duration until the center of heat release is

reached remains constant. As discussed later, the high peak cylinder pressures caused by pre-ignition must not necessarily be a result of knocking combustion.

When using hydrogen, it was possible to operate the engine very stable without abnormal combustion events at $p_{me} = 15.1$ bar (80% of the nominal natural gas power output of the test engine) with relatively low adaption effort. As shown later in this paper, pre-ignition can be controlled by different operational parameters, so we expect to mitigate abnormal combustion events by using a further adapted engine control strategy to achieve higher loads. Irrespective of this, other concepts for increasing engine performance, such as water injection or exhaust gas recirculation, are discussed in the literature but have not been considered in this study.

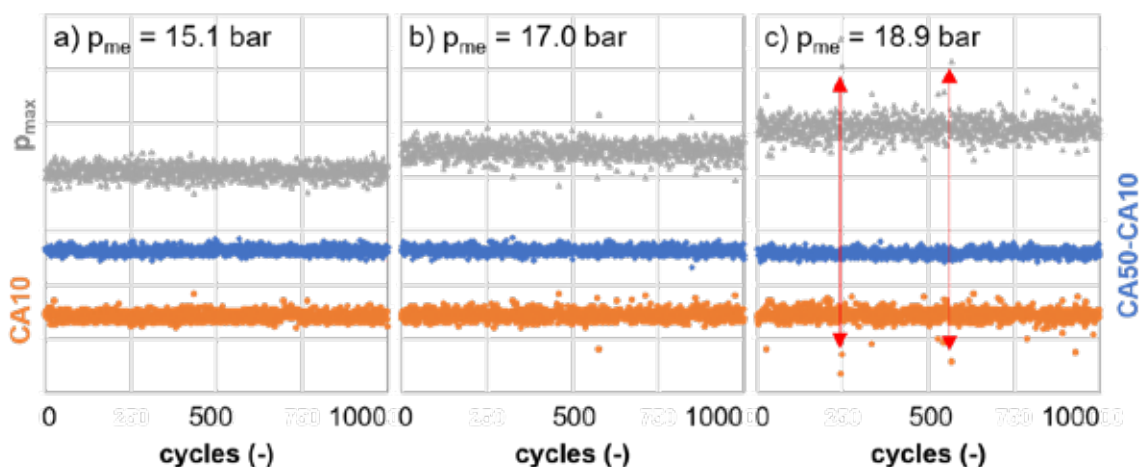


Figure 5: Start of combustion (CA10), duration until center of heat release is reached (CA50-CA10) and peak cylinder pressure at different load points.

In addition to pre-ignition knocking is another abnormal combustion mode which is of relevance in gas engine development when running towards higher efficiency and higher power density. Hence, investigations were conducted to understand this mode of abnormal combustion with 100% hydrogen, its detection possibilities, and the needed protection action to achieve maximum possible power in a stable manner. As a baseline, the production natural gas approach was referenced to analyze combustion knock detection accuracy and impact of hydrogen combustion on the key detection parameters.

Current baseline engine uses an indirect combustion knock detection approach which is based on vibration sensing. The raw vibration signal is processed in the signal processing unit to determine the knock intensity, based on which the protective action is defined. To analyze the impact of hydrogen as a fuel on knock detection, its impact on key detection parameters like signal processing window of interest, frequency filters and vibration threshold correlation was evaluated.

Theoretical analysis of the combustion chamber resonance frequency was conducted as mentioned in multiple literatures [6] as a first step for filter development. With increasing percentage of hydrogen in the fuel, the resonance frequency did increase for a given mode. As the shift is very marginal, a common filter can be developed and used to process signal for operation with either natural gas or hydrogen fuel and their blends. Table 1 provides details on the combustion chamber frequencies that were calculated for three different gas compositions.

Table 1: Combustion chamber resonance frequency analysis.

		100% CH ₄	25% H ₂ + 75% CH ₄	100% H ₂
Calculated speed of sound	(m/s)	907.77	915.19	955.07
Isentropic exponent of the air/fuel mixture	(-)	1.3947	1.3951	1.4018
Specific gas constant of the mixture	(J/kgK)	295.42	300.18	325.35
1. Circumferential mode	(kHz)	4.03	4.06	4.24
2. Circumferential mode		6.69	6.74	7.03
1. Radial mode		8.39	8.46	8.82
3. Circumferential mode		9.20	9.27	9.68
4. Circumferential mode		11.64	11.74	12.25
Combination of circumferential and radial mode		11.67	11.77	12.28

Note: Same gas temperature was assumed for all three gas compositions

Pressure traces of multiple normal and knocking combustion cycles were analyzed for natural gas, hydrogen, and a 25% H₂ / 75% natural gas blend to define the window of interest. A common signal processing window can be used as the point of occurrences of combustion knock are within a very comparable window for all the fuels in focus.

As shown in Figure 6, combustion knock events could be successfully detected for natural gas, pure hydrogen, and the 25% H₂ / 75% natural gas blend using common window of interest and filter calibration. Nevertheless, an application specific vibration threshold correlation would be essential to achieve needed knock detection accuracy for fuels in focus.

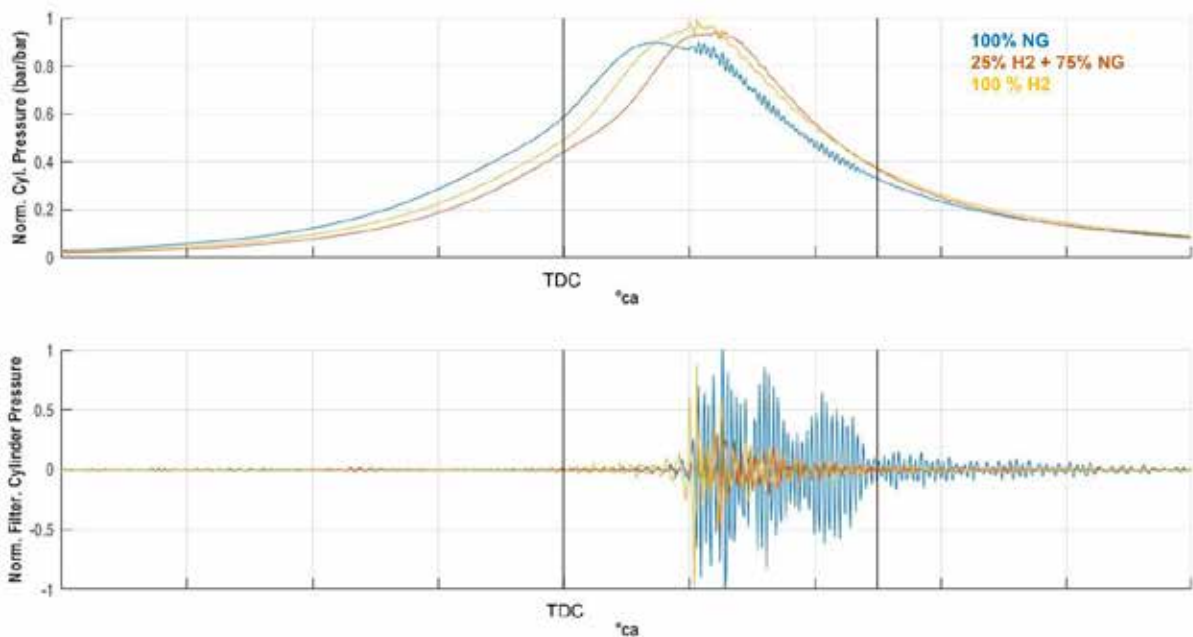


Figure 6: Knock events and knock analysis windows.

By using a separate control unit, various injection strategies with constant injection start and injection end were applied. Furthermore, this system allowed the implementation of different combustion anomaly reaction strategies. The need for this arose from the observations made during the test period with the high-pressure port fuel injection system.

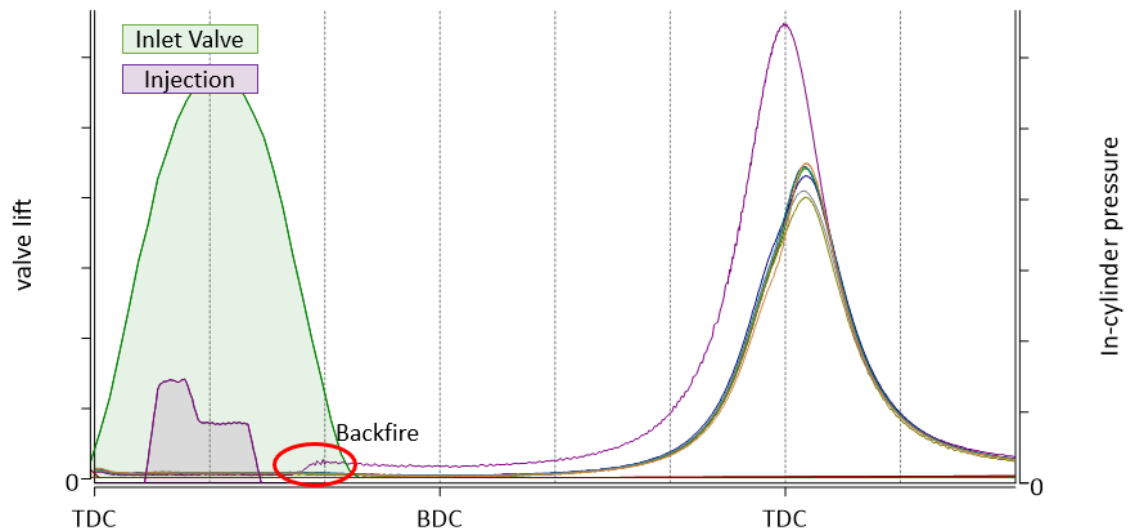


Figure 7: Backfire with high in-cylinder pressure.

At the limits of stable combustion, the frequency of abnormal combustion events such as pre-ignition, knocking and backfire is increased. The latter occur particularly frequently and without detectable prior indications. In the event of backfire, the injected hydrogen ignites locally within the intake channel when the intake valve is open (Figures 7 and 8).

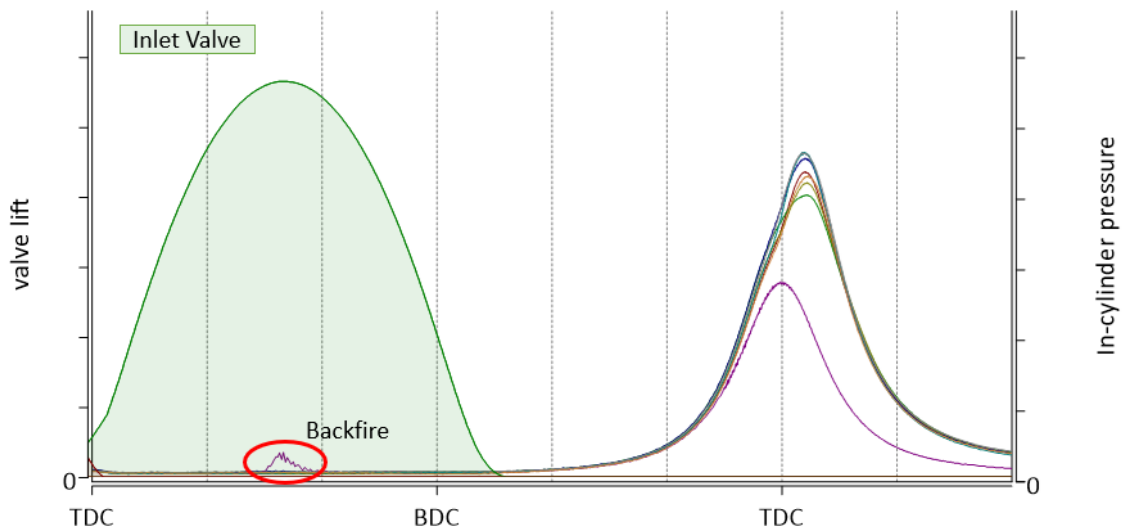


Figure 8: Backfire with compression curve.

While still burning, the mixture is compressed further, and the peak cylinder pressure exceeds the average value clearly (Figure 7) as the combustion of the remaining unburnt fuel is completed in the cylinder. If all hydrogen is already completely converted while the intake valve is still open, it can be observed that the intake mass is only compressed without performing any combustion work. The longer this state was maintained, the higher the measured temperature in the intake manifold rose. This suggests that the gas that continues to be injected ignites at the flame in the inlet duct or that the prevailing high temperatures lead to auto-ignition. Consequently, a quasi-steady flame is formed in the cylinder inlet channel.

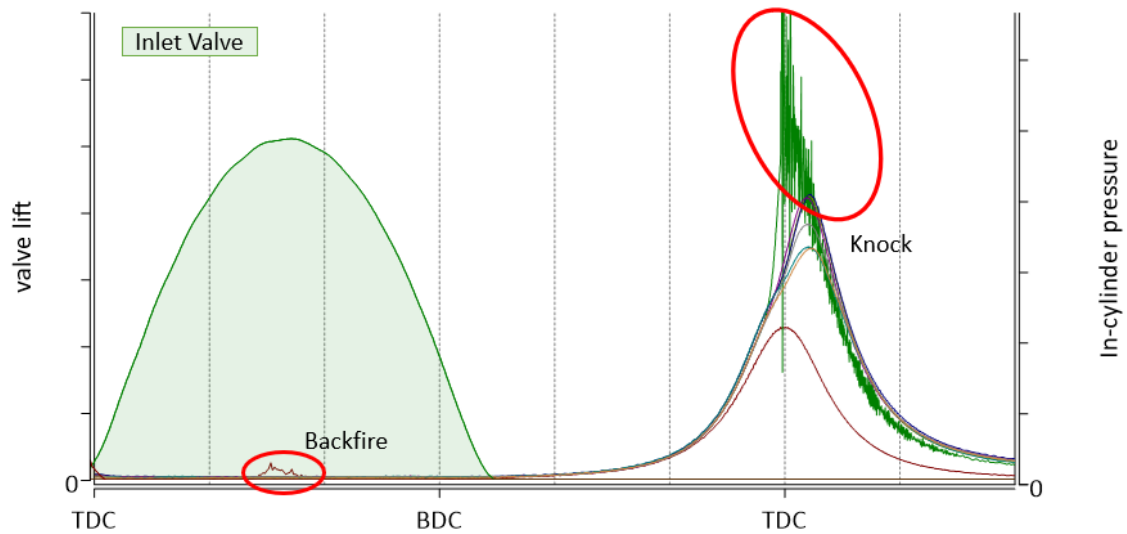


Figure 9: Critical knock event due to early combustion and richer gas mixture.

In addition to the lack of expansion work, the total exhaust gas enthalpy also decreases, which leads to reduced compressor work of the turbocharger. If unregulated, the resulting reduced boost pressure can lead to unintentional enrichment of the fuel-air mixture in other cylinders and thus to critical knock events (Figure 9). Another potential risk is the spread of the flame to other cylinders and injection valves, respectively. Ultimately, this behavior must lead to the engine being shut down, as a safe operating state can no longer be maintained.

To counteract this, a routine was implemented in the control system with the aim of interrupting the injection process at the corresponding cylinder. With the help of these measures, engine operation could be continued despite anomalies, as the flame is extinguished due to the absence of hydrogen. Continuing the engine tests without restarting the engine is essential for a targeted investigation of these abnormal combustion events.

The mixture formation upstream the cylinder has proven to be a particularly influential factor for the frequency of backfire events. Moving the injection window in relation to the opening of the intake valve (Figure 10) has been proven to be an important parameter for preventing backfires.

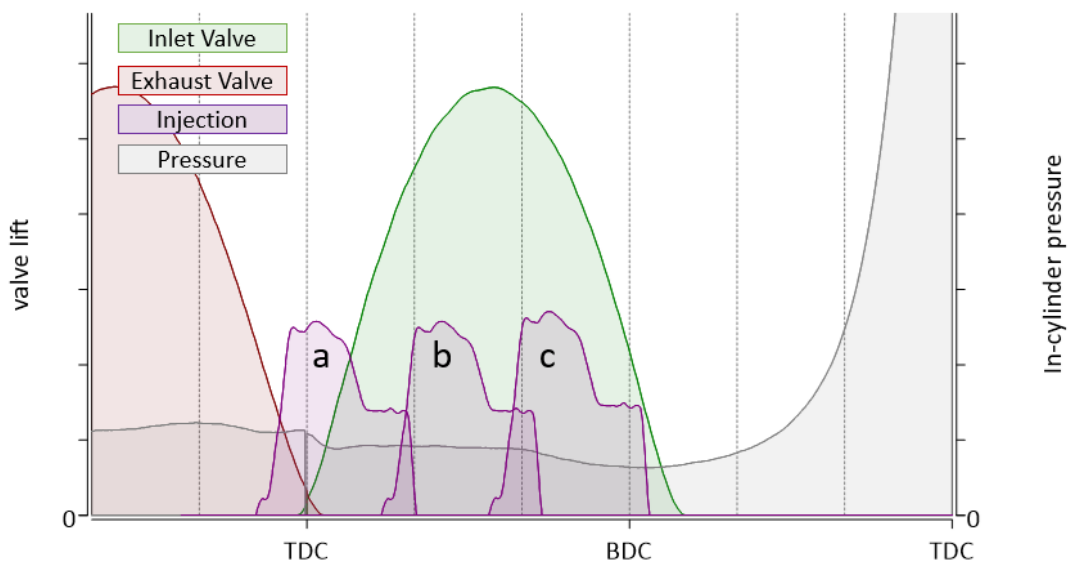


Figure 10: Injection timing overview.

The possible fuel injection window is limited by the inlet valve opening times. The latest time of injection (Figure 10 c) must be selected in a way that the maximum amount of injected fuel is trapped in the cylinder. The time offset between the end of the injector flow and the flow into the cylinder caused by the gas dynamics and flow duration must be considered. If the hydrogen is injected too late, residual hydrogen will remain in front of the inlet valve, as this closes during the inflow process. In the following cycle, remaining hydrogen can ignite on hot residual gases in the cylinder, which in turn can lead to ignition of the fresh hydrogen charge in the intake tract.

The other extreme, too early fuel injection (Figure 10 a) also leads to the phenomenon described since hydrogen can reach the intake valves before they start to open. Fuel injection as early as possible, while the intake valve is open and part of the fresh air has already passed the valve into the cylinder, proved to be the most favorable strategy (Figure 10 b).

The suspected ignition source, the remaining hot exhaust gas in the cylinder, could not be conclusively proven, but the influence of the combustion temperature on the frequency of events could. A particularly high combustion temperature, caused by the enrichment of the mixture, has been shown to increase the probability of anomalies. Based on this observation, the results achieved were mainly attainable with the aid of very lean gas mixtures with lower combustion temperatures, which, in addition to the high demands on the air system due to the lower exhaust gas enthalpy, also had to be considered.

A further limitation of the injection timing resulted from the increasing injection duration with the increase in the amount of gas to be injected to increase the engine output. If the injection duration is longer than the optimum injection window, anomalies are increasingly likely to occur. The selection of suitable injection valves with the appropriate flow rate and the shortest possible injection duration is crucial here.

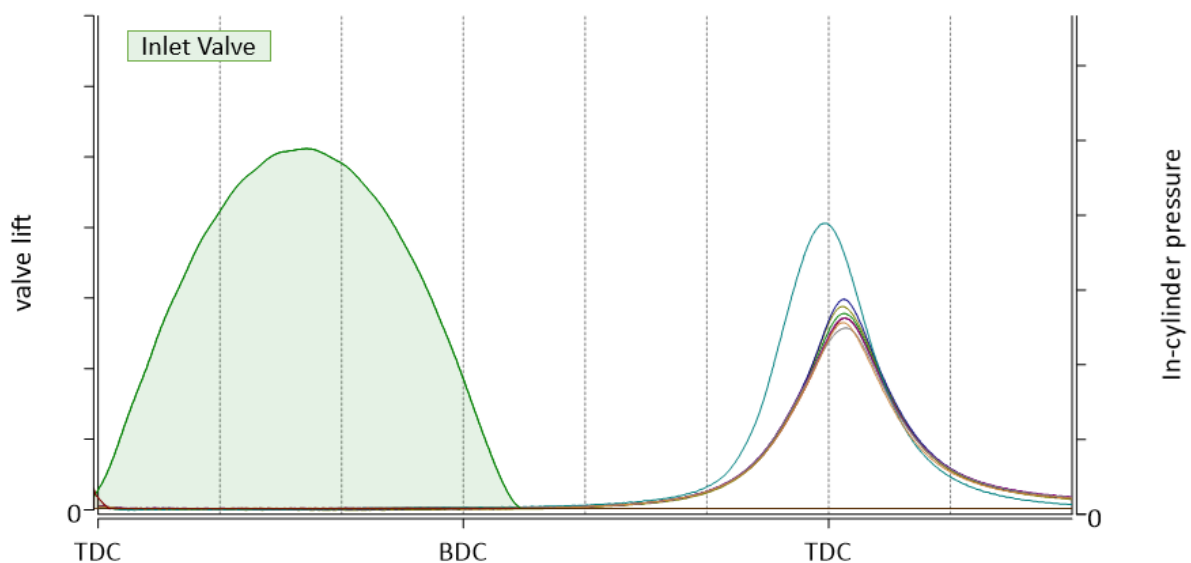


Figure 11: Pre-ignition.

The probability of occurrence of the abnormal combustion events discussed so far varies. While the probability of backfire is strongly correlated to the fuel injection and inlet valve opening timing, pre-ignition (Figure 11), i.e., the ignition of the mixture in the cylinder before the actual ignition, occurs typically less frequently and is triggered mainly by high cylinder pressures and temperatures.

These events can occur over a longer period due to a self-reinforcing effect caused by the increase in pressure and temperature levels from cycle to cycle. In the upper load range, this

phenomenon can lead to an overload of the mechanical components, which reduces the durability of the components and, in the worst case, can lead to immediate machine failure.

5. Conclusion

Within the project, the necessary measures, and adaptations from pure natural gas to pure hydrogen operation were investigated in detail. Particular attention was paid to the limits of engine combustion and internal engine measures to reduce anomalies in 100% hydrogen operation.

The adjustments to the engine and the injection strategy were tailored to achieve maximum specific output. At the same time, the modifications made to the standard natural gas engine were kept to a minimum. Furthermore, the measures were designed and tested regarding maximum efficiency. A necessary increase in boost pressure, which had already been determined as a necessity in advance of the investigations, also entails a higher component load on the charge air path. From a safety point of view, this aspect also had to be investigated and measures taken during the project.

The overall tasks have a special significance in the research project described here. The combustion engine itself had to be adapted to hydrogen operation in terms of safety. This applies to the charge air system, the hydrogen injection, the hydrogen periphery upstream of the injection, the exhaust tract, and some individual components. The test bed was upgraded in terms of safety for hydrogen operation.

Acknowledgement

The authors would like to thank the Federal Ministry for Economic Affairs and Climate Action on behalf of the H2VKM partners for funding the project as well as the Project Management Jülich for the excellent administrative project support.

References

- [1] Bundesministerium für Wirtschaft und Energie. 7. Energieforschungsprogramm – Innovation für die Energiewende. Berlin, 2018. (<https://www.bundesregierung.de/bregde/service/publikationen/7-energieforschungsprogramm-der-bundesregierung-1522080>)
- [2] Bundesministerium für Wirtschaft und Energie. Die Nationale Wasserstoffstrategie. Berlin, 2020. (<https://www.bmbf.de/bmbf/shareddocs/downloads/files/die-nationale-wasserstoffstrategie.pdf>)
- [3] F. Dryer, M. Chaos, Z. Zhao, J. Stein, J. Alpert, C. Homer. Spontaneous ignition of pressurized releases of hydrogen and natural gas into air. *Combustion Science and Technology* 179:4 (2007), 663-694
- [4] K. Koyanagi, M. Hiruma and S. Furuhashi. Study on Mechanism of Backfire in Hydrogen Engines. SAE Technical Paper 942035 (1994)
- [5] F. A. Williams. Detailed and reduced chemistry for hydrogen autoignition. *Journal of Loss Prevention in the Process Industries* Volume 21, Issue 2, (2008)
- [6] N. Adolph. Messung des Klopfens an Ottomotoren. RWTH Aachen, Dissertation (1983)

Galí complete Starting Solutions



we supply all our products in ATEX-IECEx version

Air Starter

Powerful high pressure starters to start Engines up to 7.000 kw and more.



Turning Mechanism

For engine build-up and service work.



Shut off Valve

Immediate emergency stop of the engine in case of safety reasons.



Hydraulic Starter

For special application and emergency sets (black start).



Galí | Technical Solutions
since 1951

SPAIN gali@galigrup.com
GERMANY info@gali.de
FRANCE comexp@gali-france.fr
ITALY gali@gali-italia.it
CHINA china@galigrup.com

www.galigrup.com

Session 3

Ammoniak - Schiffsanwendungen Ammonia - Marine applications

**Moderation: Moderation: Prof. Andreas Wimmer
LEC Graz GmbH, Technische Universität Graz**

Design of an ammonia retrofit concept for maritime propulsion units smaller than 400 kW

Auslegung eines Ammoniak-Retrofit-Konzeptes für maritime Antriebseinheiten kleiner 400 kW

Dr.-Ing. M. Theile^{*1}, A. Hoppe¹, T. Mante², Dr.-Ing. S. Prehn², G. Mwathi³, Dr.-Ing. L. Seidel³

¹Forschungszentrum für Verbrennungsmotoren und Thermodynamik Rostock GmbH, Rostock/Germany

²Chair of piston machines and internal combustion engines (LKV) of the University of Rostock, Rostock/Germany

³LOGE Deutschland GmbH, Cottbus/Germany

Abstract

The inland shipping sector in Germany emits around 1.6 million tons of CO₂ per year. To drive decarbonization forward, the existing fleet must be technically updated. In order to achieve a high CO₂ reduction at low investment costs, one approach is to retrofit the propulsion systems to make them capable of using alternative fuels.

Ammonia, as a nitrogen-based hydrogen carrier, offers an excellent alternative to the classic regenerative fuels, since neither soot nor CO₂ emissions are produced during internal combustion and, in perspective, regenerative production will be more energy-efficient than that for alternatives such as methanol. However, complex ignition characteristics as well as low flame speed of ammonia pose challenges for combustion process development.

In this study, results of a new developed dual-fuel ammonia-diesel combustion process are presented, which is considered as a retrofit option for inland shipping vessels. A GHG reduction of up to 70% was achieved by a suitable injection strategy of the pilot fuel. The pollutant emissions such as ammonia and nitrous oxide are at a very low level. With the use of an SCR catalyst and an assumed conversion rate of 90%, it is also possible to remain below the current IMO limit value for NO_x.

In addition to the results of the combustion process investigations, results from the development of simulation models are also presented. The modeling of this combustion process is challenging due to the interaction between the low temperature combustion of hydrocarbons and the ammonia amount. The developed models show good agreement with the experimental combustion and cylinder pressure curves.

Kurzfassung

Der Binnenschifffahrtssektor in Deutschland emittiert ca. 1,6 Mio. Tonnen CO₂ pro Jahr. Um die Dekarbonisierung voranzutreiben, muss die Bestandsflotte technisch umgerüstet werden. Einen Ansatz, der eine hohe CO₂-Reduktion bei geringen Investitionskosten erlaubt, stellt das Retrofit der Antriebsanlagen auf den Einsatz alternativer Kraftstoffe dar.

Ammoniak bietet als Wasserstoffträger auf Stickstoffbasis eine hervorragende Alternative zu den klassischen regenerativen Kraftstoffen, da bei der innermotorischen Verbrennung weder Ruß noch CO₂-Emissionen entstehen und die regenerative Produktion perspektivisch energieeffizienter gegenüber Alternativen wie Methanol sein wird. Die geringe Zündneigung von Ammoniak sowie dessen niedrige Flammgeschwindigkeit stellen die Brennverfahrensentwicklung jedoch vor Herausforderungen.

* Speaker/Referent

In dieser Studie werden Ergebnisse eines neu entwickelten Dual-Fuel Ammoniak-Diesel Brennverfahrens vorgestellt, welches als Retrofit-Option für die Binnenschifffahrt konzipiert wurde. Durch eine geeignete Einspritzstrategie des Zündbeschleunigers wurde eine GHG-Reduktion von bis zu 70 % erreicht. Die Schadstoffemissionen, wie Ammoniak und Lachgas, liegen dabei auf einem sehr niedrigen Niveau. Unter Einsatz eines SCR-Katalysators mit einer angenommenen Umsatzrate von 90 % ist es zudem möglich den aktuellen IMO-Grenzwert für NOx einzuhalten.

Neben den Ergebnissen der Brennverfahrensuntersuchungen werden auch Resultate aus der Entwicklung von Simulationsmodellen präsentiert. Die Modellierung dieses Dual-Fuel-Brennverfahrens ist durch die Wechselwirkung zwischen der Niedertemperaturverbrennung von Kohlenwasserstoffen und dem Ammoniakgehalt eine Herausforderung. Die entwickelten Modelle zeigen eine gute Übereinstimmung mit den experimentellen Druck- und Brennverläufen.

1. Introduction

Due to the global CO₂ emissions of maritime and inland shipping, decarbonization in this industry is necessary in order to achieve national, EU or global climate targets. Due to the long service life of ships - especially inland vessels, whose average age in Germany is around 48 years - the CO₂ emissions of the existing fleet must be reduced. One way to achieve this is to use climate-neutral fuels. Although complete climate neutrality is possible with classic regeneratively produced fuels (e.g. synthetic methane, e-methanol, synthetic paraffinic fuels, etc.), the availability of CO₂ for synthesis could become a challenge in the future. Here, ammonia (NH₃) offers a possible alternative as a hydrogen carrier on a nitrogen basis. It is one of the best-known chemical substances due to its use in agriculture and industrial processes. Despite challenging flame properties in terms of ignitability and flame speed, it is almost certain in the maritime industry that ammonia will be used as a future climate-neutral motor fuel.

By switching from carbon-based fuels to the nitrogen-based fuel ammonia, emissions of unburned hydrocarbons (including methane slip) and particulates can presumably be reduced to almost zero. There is thus the potential for a "zero-carbon emission" ship, whereby both local and global (e.g. CO₂ emissions) environmentally harmful effects can be reduced or avoided altogether.

The joint project "AmmoniaEngine" (German: "AmmoniakMotor") has set itself the goal of investigating the internal combustion of ammonia as a fuel in a real engine and developing corresponding simulation models in order to be able to develop future retrofit concepts for inland navigation.

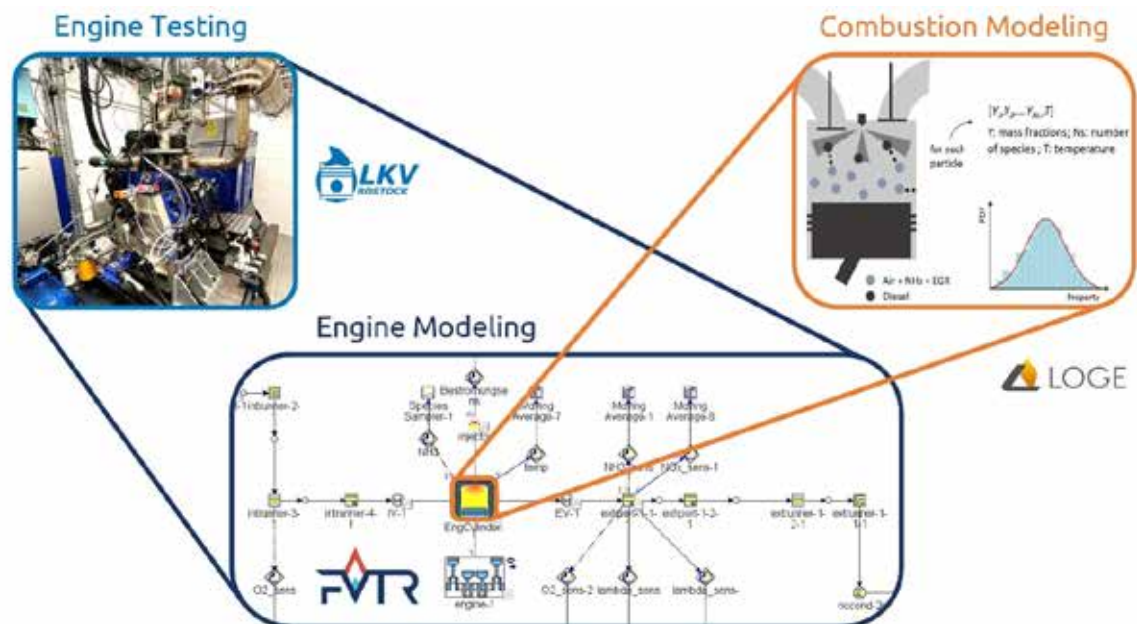


Figure 1: Interaction of the project partners in the joint project "AmmoniaEngine" for modeling the internal combustion of ammonia in engines

2. Ammonia as fuel

Ammonia can be used as a fuel in gaseous or liquid form and as direct or intake manifold injection in engines. It can be combined with diesel, gasoline or other alternative fuels such as hydrogen, biodiesel and synthetic diesel fuels. The engine test bench and the combustion process were developed and realized as a premixed ammonia-diesel dual-fuel concept and are highlighted and shown schematically in detail in Figure 2.

As in many studies already carried out (see [1,2,3]), a dual-fuel combustion process with diesel as ignition fuel is investigated, but in comparison to [3] in the context of intake manifold

injection, as a higher retrofit potential is assumed here. The number of publications on pure ammonia combustion as a diesel engine concept is low (see e.g. [4,5]), as high compression ratios of up to 35:1 are required for compression ignition. The usual approach is therefore to use a promotor with a high self-ignition tendency (e.g. diesel).

The biggest challenge when using ammonia as a fuel is its high toxicity and the associated safety requirements. This requires sensitive and precise safety technology, especially for the test bench systems used in this joint project. Rooms that could potentially be contaminated with ammonia must be equipped accordingly with gas detectors and a coupled permanent gas warning system. Adequate ventilation and appropriate personal protective equipment (e.g. gas mask and full-body suit) are essential when working with ammonia.

In terms of combustion behavior, ammonia has disadvantages compared to conventional fuels and therefore cannot be replaced 1:1. The most important combustion properties are listed below:

- Auto-ignition temperature: 630 °C [6] is significantly higher than diesel (180-320 °C)
- Laminar flame speed: 0.07 m/s [6] is significantly lower than gasoline (0.4 m/s) [7] or methane (0.37 m/s) [6] (all at standard conditions)
- Adiabatic flame temperature: 1800 °C [6] is lower than many other fuels (diesel: 2327 °C [7], gasoline: 2307 °C [7], methane: 1950 °C [6])

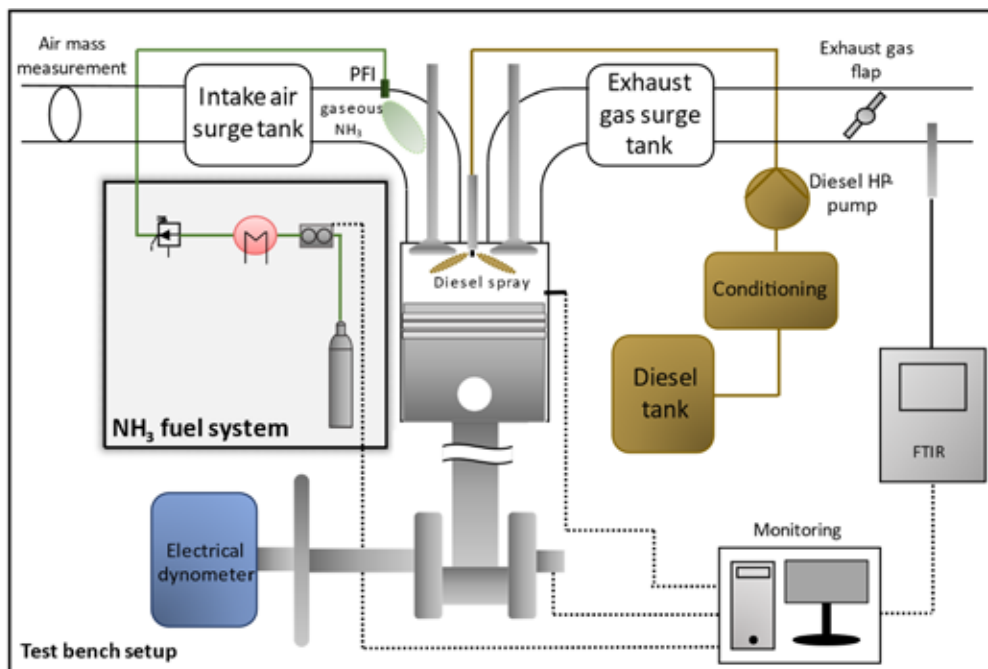


Figure 2: Schematic of the NH₃ research engine test rig used in the “AmmoniaEngine” joint project

A diesel-like combustion process with auto-ignition and diffusion-controlled combustion is not technically feasible using ammonia due to the auto-ignition temperature. The laminar flame speed in turn makes complete conversion more difficult with premixed (spark ignited) combustion, which significantly restricts classic lean-burn processes compared to today's natural gas engines, for example. Higher flame temperatures are therefore expected, so that thermal nitrogen oxide formation is more pronounced. High water content and possible ammonia slip pose new challenges for exhaust gas aftertreatment. The formation of nitrous oxide (N₂O) must be avoided due to the high greenhouse gas factor (~300).

Another important aspect of ammonia is its corrosiveness when interacting with copper-based metals or sealing materials (e.g. in pipes, valves, measuring systems, injection nozzles). To avoid leaks after a short time, the systems must be carefully planned. The corrosion behavior of ammonia against various materials used in engine construction has not yet been comprehensively researched.

3. NH₃ research engine test bench

3.1 Single cylinder engine

At the chair of piston machines and internal combustion engines (LKV) of the University of Rostock, a 1-cylinder research engine was converted to dual-fuel operation with ammonia and diesel. Figure 3 shows the test bench and test engine used. The relevant engine parameters of the 1-cylinder engine are listed in Table 1.

Validated diesel operation forms the basis for testing the dual-fuel concept. The test bench has a fully conditionable intake air system. This includes the combustion air supply by a compressor, a pressure control valve, a mass flow measurement system, an electric heater and a control valve on the exhaust side to realize the back pressure. The diesel fuel system can be varied in terms of fuel temperature and rail pressure. The temperatures of the cooling water and oil systems can also be adjusted. A very wide range of engine operating parameters (e.g. free variation of injection times and durations) can be realized with an openly accessible research engine control unit.

In addition to the internal combustion processes and emissions, wear and lubricant effects are also investigated. Oil samples are analyzed and evaluated in the LKV's associated lubricant laboratory, allowing signs of wear and changes in lubrication properties to be detected very quickly.

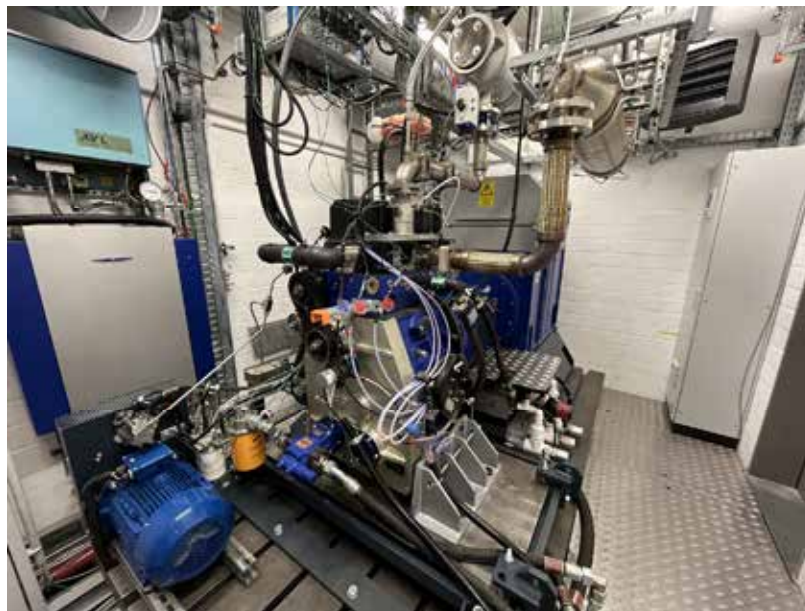


Figure 3: 1-cylinder NH₃ research engine at the LKV, University of Rostock

Table 1: Engine parameters

1-cylinder, 4-stroke diesel	
Rated speed	2300 rpm
Rated power	45 kW
Bore	110 mm
Stroke	136 mm
Displacement	1.29 l
Compression ratio	16.4:1
Charge pressure system	extern

3.2 Ammonia Fuel System

The ammonia fuel system (Figure 4) is also variable in terms of injection pressure, temperature and quantity. The ammonia is stored in a pressurized gas cylinder. To ensure safety, this is located in a permanently ventilated gas cylinder cabinet in the test bench room, in which the entire fuel system is also located, so that possible leaks do not contaminate the test bench room. A gas sensor in the exhaust air of the cabinet detects possible ammonia leaks. The safety technology also includes sufficiently strong ventilation of the test bench room, additional gas sensors, a gas warning control unit, gas masks, an emergency shower and an oxygen breathing apparatus for emergencies. The procedures for changing, opening and closing the gas cylinder or switching off the test bench at the end of the working day are strictly regulated so that the entire test bench is as safe as possible.

The safe handling of ammonia is a decisive criterion for its use as a fuel. The fuel system is shown schematically in Figure 4. The ammonia is extracted in liquid form, processed and vaporized after measuring the mass flow with a Coriolis measuring system. If required, the ammonia can also be transported into the engine in liquid form. After vaporization, a pressure reducer regulates the gaseous ammonia to the desired pressure and a proportional valve or special gas injection nozzles control the mass of ammonia that is mixed with the combustion air at the engine intake manifold. Several ball and solenoid valves, which are closed in the standard state, can interrupt the ammonia flow in an emergency. A safety valve and several flushing connections for nitrogen to flush the lines have been installed.

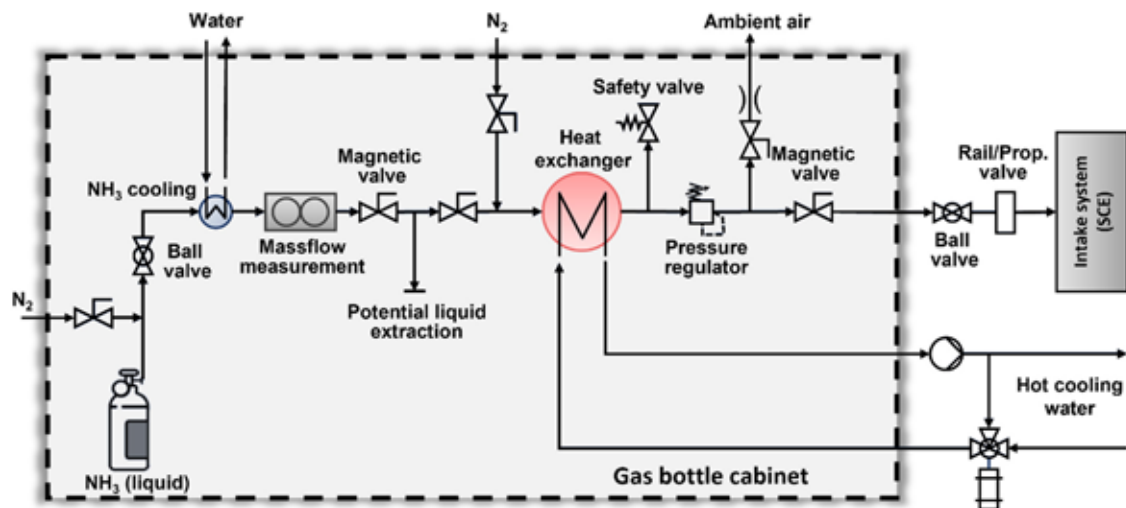


Figure 4: The "AmmoniaEngine", which was set up as part of the joint project

4. Simulation models

4.1 Stochastic Reactor Model (SRM)

The SRM is used in this study to model the combustion process. It takes into account turbulence and inhomogeneity effects during combustion. In the calculation, the homogeneity of the combustion chamber is represented by a statistical distribution and the physical variables are described by a probability density function (PDF) (see [8,9,10,11,12]). In the SRM, the mass in the reactor is stochastically divided into virtual packages, so-called particles. Each particle has its own chemical composition, temperature and mass and can mix with other particles and exchange heat with the walls [10].

In the transport equations, the piston work, convective heat transfer, chemical reactions, direct fuel injection and evaporation are modeled via source terms. Furthermore, molecular mixing due to turbulence is modeled via a term. To close the system of equations, a modified Euclidean Minimum Spanning Tree (EMST) mixing model is used (see [13,14]), which takes

into account the locality in the particle mixing process for the mixing fraction. As a result, only neighboring particles in the mixing fraction space can mix with each other.

The SRM contains a phenomenological turbulence model for calculating the scalar mixing based on various parameters for the charge movement in the combustion chamber (e.g. swirl, squish, etc.). The corresponding factors must be calibrated for the respective engine. The calibration was carried out using the LOGEngine expert system with the experimental pressure curve of the operating point with pure diesel as the target. A good agreement between the experimental pressure curve and the model prediction was achieved, as will be shown in a later section.

4.2 Chemical model

Within the project a new detailed and reduced reaction mechanism was developed.

The commercial diesel used in the experiment was modeled by a 3-component surrogate consisting of 17.2 vol% 1-methylnaphthalene for the aromatic fraction, 76.1 vol% n-decane for the n-alkane fraction and 6.7 vol% methyl decanoate to model the FAME content.

The chemical model for fuel oxidation and emission formation is based on the current LOGefuel reaction model. The model for n-decane and methyl decanoate was taken from [15,16] and updated to achieve better agreement with the experiments on ignition delay time and emission formation. A comparison of the predicted and measured ignition delay time for different fuel components and the speciation of ammonia / hydrogen mixture is shown in Figure 5. The partial models for ammonia oxidation and NO_x chemistry were taken from [17,18]. The detailed reaction mechanism consisted of 1307 species and was then reduced to 491 species using the technique described in [16,19] in order to shorten the calculation time for simulations with direct solution of the chemistry or generation of look up tables.

4.3 Pressure analysis tool

FVTR uses its own thermodynamic pressure curve analysis software for the 0D analysis of the combustion process. Based on the measured high-resolution cylinder pressure curve of the engine and other stationary measurement data (e.g. fuel and air mass flows, NH₃ content), time curves (e.g. combustion rate, temperature curve) as well as global parameters and mean values (e.g. ignition timing, ignition delay, combustion center of gravity, indexed mean pressure) are determined. A zero-dimensional one-zone model is used as the basis, in which the cylinder charge is considered as an ideally homogenized gas. For the closed process of the high-pressure phase, masses, species and energy are thermodynamically balanced according to the resolution of the pressure data in order to draw conclusions about the combustion process. The use of ammonia is taken into account both in the combustion equation and in the determination of the thermophysical properties. For combustion, a model fuel consisting of carbon, hydrogen, oxygen and nitrogen (C_vH_wO_xN_y) is calculated on the basis of the NH₃ content and a global equation for the stoichiometric conversion is formulated. The caloric properties are determined using NASA polynomials [19] in order to take into account the influence of the different fuel and exhaust gas compositions on the thermodynamic properties (e.g. specific heat capacity). This means that the properties of ammonia are taken into account in all modeled balances (mass, species and energy balance). The combustion curves created with this tool are used for comparison with the simulation curves predicted by LOGE.

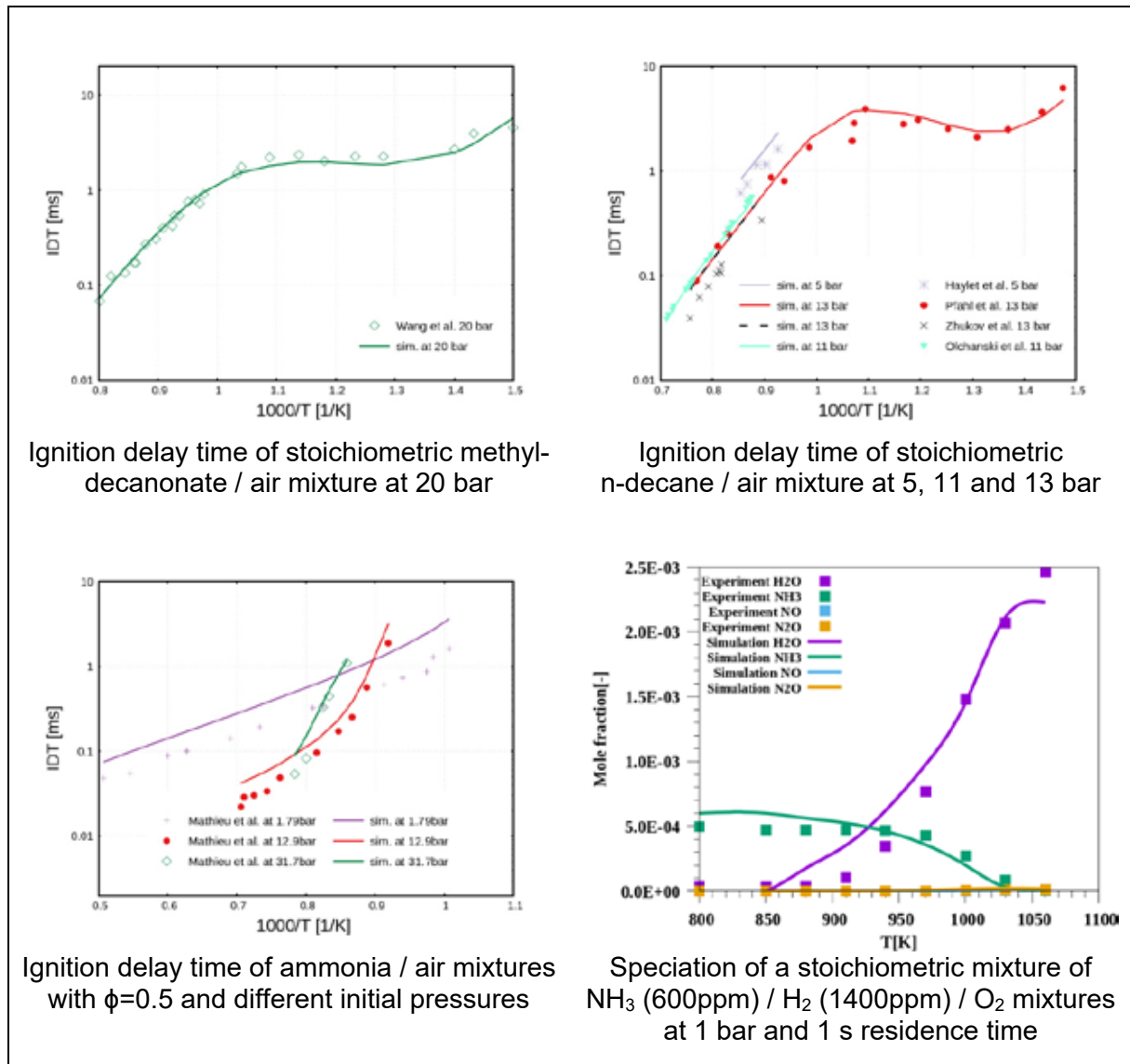


Figure 5: Comparison of the predicted and measured ignition delay times of different diesel and ammonia fuel mixtures in shock tubes at different pressures and speciation of NH_3 -mixtures

4.4 GT-Power model

As part of the project, a 0D/1D model of the NH_3 research engine was created using the commercial software GT-Power. In accordance with the engine test bench at the LKV, the intake and exhaust path, including the air and exhaust gas calming volume, was taken into account. Furthermore, ammonia injection was implemented in the air path upstream of the inlet valve. The model is shown in Figure 1.

As part of the project, the effects of different ammonia substitution rates were initially investigated using the dual-fuel combustion models already implemented. Diesel injection was modeled using the “DIPulse” model, while premixed ammonia combustion was modeled using the “SITurb” model, which calculates the turbulent combustion velocity based on the laminar flame velocity of the ammonia and the charge movement. Virtual sensors were also integrated to detect the ammonia slip.

In the course of the project, the ammonia-diesel SRM developed by LOGE was then coupled with the GT-Power model in order to be able to make predictive statements about engine behavior.

5. Simulation and experimental results

5.1 Preliminary investigations using GT-Power

As part of preliminary investigations, a model validation was first carried out using the GT-Power model based on various diesel reference points. As a result, the effects of substituting diesel with ammonia were investigated. The results are shown exemplary for a 50% load operating point in Figure 6. A very early pre-injection was used to create a reactive partially premixed atmosphere, followed by a main injection right before top dead center. In a pure diesel operating point (0% substitution rate), the diesel mass from the pre-injection ignites on its own in a 2-stage ignition. This complex ignition process cannot be seen in the GT-model, but the overall combustion regarding ignition delay, pre-combustion and main combustion event was modelled sufficiently. To model the effects of ammonia on the ignition delay, the ignition model itself had to be adapted using a functional correlation between the model constant "Ignition Delay Multiplier" and the ammonia substitution rate.

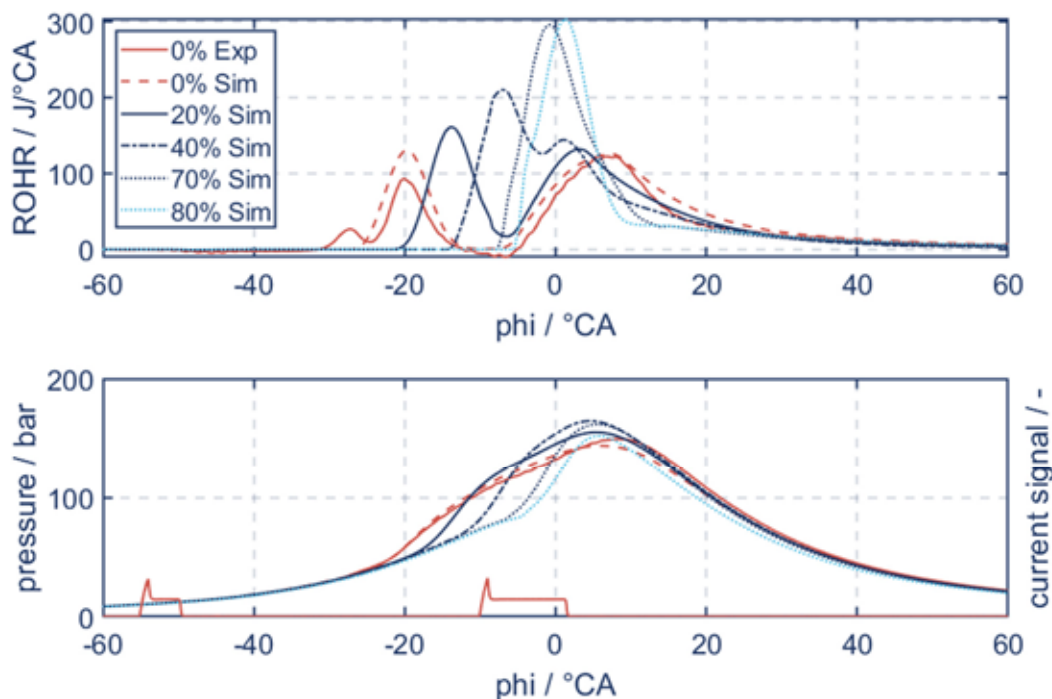


Figure 6: Exemplary experimental and simulated combustion processes as a result of substituting diesel with ammonia (0%, 20%, 40%, 70% and 80% energetic)

Analyzing the combustion behavior when substituting diesel with rather small amounts of ammonia, a strong increase in ignition delay can be seen directly. With higher substitution rates, the pre-ignition combustion event combines with the diffusion combustion event of the main injection. At 70% substitution rate (energetic), only one main combustion event could be identified.

Higher amounts of substitution rates could be modeled, but showed a different overall behavior compared to the experimental investigations (see Chapter 5.2). The main injection mass was set to zero, to achieve a substitution rate of 80%. This showed only minor changes in the ignition delay and combustion duration in contrast to the experimental data.

The preliminary studies carried out confirmed the need for coupling the GT-Power model with the developed SRM, due to the lack of predicting of the 2-stage ignition phase and the combustion behavior at higher substitution rates. Further detailed combustion analyses can then be carried out in a predictive manner.

5.2 Experimental investigations

Various series of measurements were carried out on the engine test bench in order to obtain a database for model development and a general understanding of internal ammonia-diesel dual-fuel combustion.

In the investigations presented in this paper the series of measurements always began with pure diesel operation as a reference. From this point onwards, ammonia was gradually added to the combustion process and less diesel fuel was injected at the same time. The total energy quantity of the two fuels was kept constant. In order to increase the substitution rate, the duration of the main diesel injection was gradually shortened.

Since detailed injection strategies for ammonia-diesel dual-fuel combustion methods were rather unknown a new approach based on known engine behavior of LNG dual-fuel engines was developed.

Figure 7 shows the pressure and heat release curves over the diesel substitution rates at middle engine load (50%). The pressure curve shows a steady increase in maximum pressure over the substitution rate. At 80% substitution, the maximum cylinder pressure decreases due to an unstable combustion caused by low ignition energy from the diesel to sufficiently ignite the ammonia-air mixture. Therefore, 80% of ammonia energy amount represent the limit of the substitution rate for the operation point with the presented boundary conditions.

Based on the pure diesel operation the combustion of the diesel pilot mass can be clearly recognized by the heat release curve of the pure diesel point. The combustion of the pre-injected diesel mass is split in two phases. The first peak can be identified as cool-flame combustion of diesel. With increasing combustion temperatures, the cool-flame combustion decreases and the full oxidation of the pre-injected diesel mass takes place [20]. The intensity of the pre-combustion here is just below the level of the main combustion. This is because of the high diesel mass in the pre-injection compared to the mass in the main injection, which helps to burn the ammonia in the whole combustion chamber. The cool-flame combustion of the diesel decreases by adding more ammonia and shifts towards top dead center (TDC). By increasing the substitution rate, a shift of the pre-combustion to a later state can be seen as well. Because the cool-flame combustion of diesel decreases and therefore more diesel remains, the full oxidation of the pre-injected diesel and ammonia increases. For high substitution rates, the pre-combustion merges with the main combustion and results in one intensive combustion event.

By increasing the substitution rate and therefore having more ammonia in the combustion chamber, the NH_3 -slip increases. The value for a substitution rate of 70% is at 383 ppm and the N_2O emissions are below 10 ppm (except for 80%). These values are on a very low level for this retrofit-concept combustion process. The CO_2 emissions decrease due to the substitution of the diesel fuel. Even the CO emissions decrease over substitution rate and stay on a low level (except for 80%).

Since the focus is on a constant total energy flow of the two fuels, the combustion air ratio (λ) and the efficiency vary slightly with substitution rate. Nevertheless, it can be seen that the efficiency does not decrease with higher substitution rates. The combustion duration decreases with higher substitution rates due to the changing combustion events (less/no more cool-flame combustion, merging of pre-injected oxidation into main injection combustion event).

Figure 8 shows an increase of the substitution rate for an engine load of 75%. The starting point is again a pure diesel point. Increasing the substitution rate above 50% requires an adoption of the main diesel injection to limit the cylinder pressure gradient. With the optimized injection parameters, the substitution advanced to 70%. For higher substitution rates, the diesel mass from the main injection was shifted into the pre-injected mass and the pre-injection timing was optimized to reach a stable combustion. With this configuration, a substitution rate of 80% could be achieved with a stable combustion and good emission results. A further increase of the ammonia energy amount was not possible for this operation conditions.

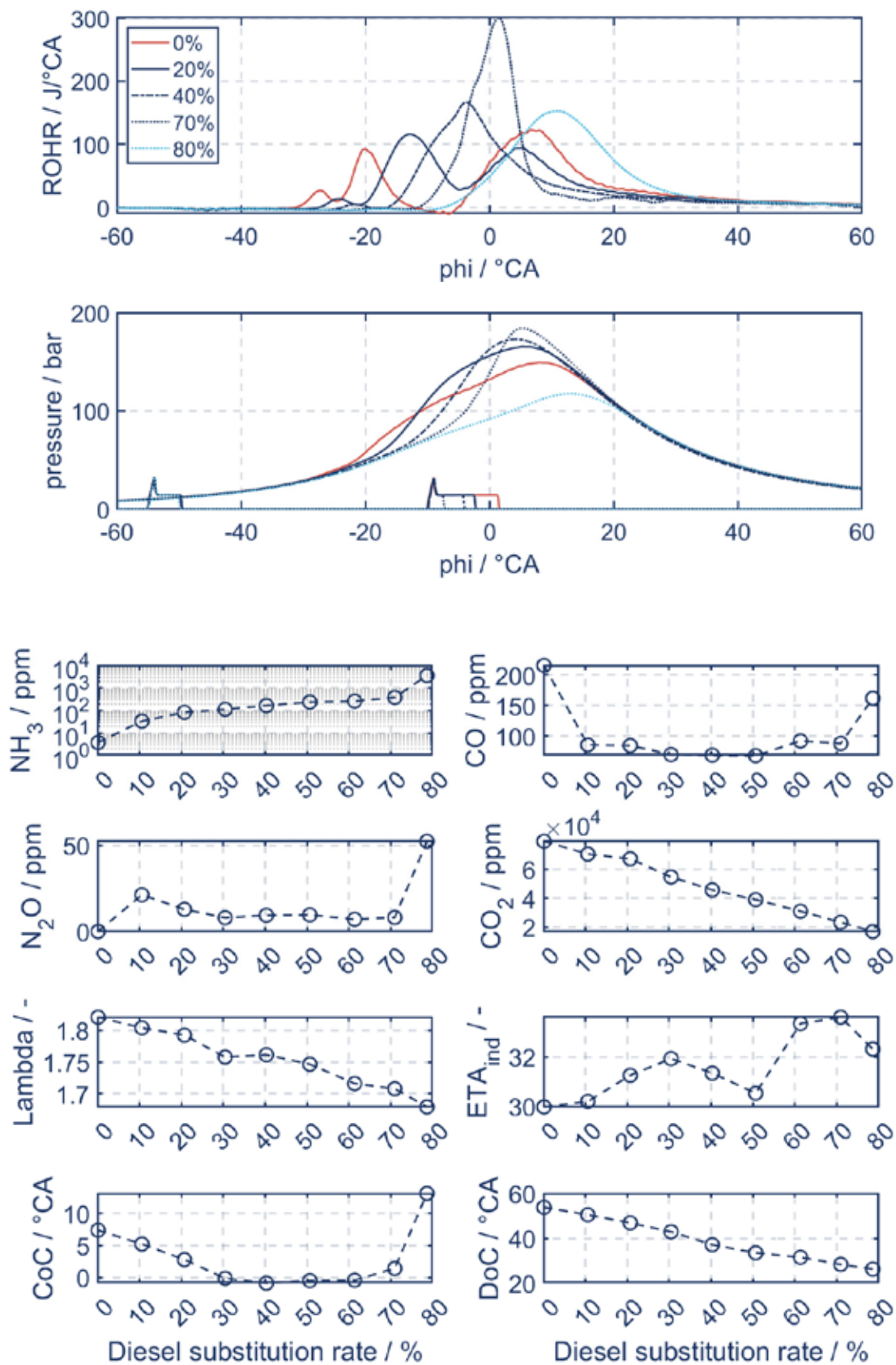


Figure 7: Pressure curves and heat release rates of the experimental data from the NH₃-engine at the University of Rostock for the substitution of diesel (shortening of the main injection period). Engine speed: 1500 rpm; engine load: 50%; total energy flux by fuel: 180 MJ/h; diesel injection pressure: 900 bar.

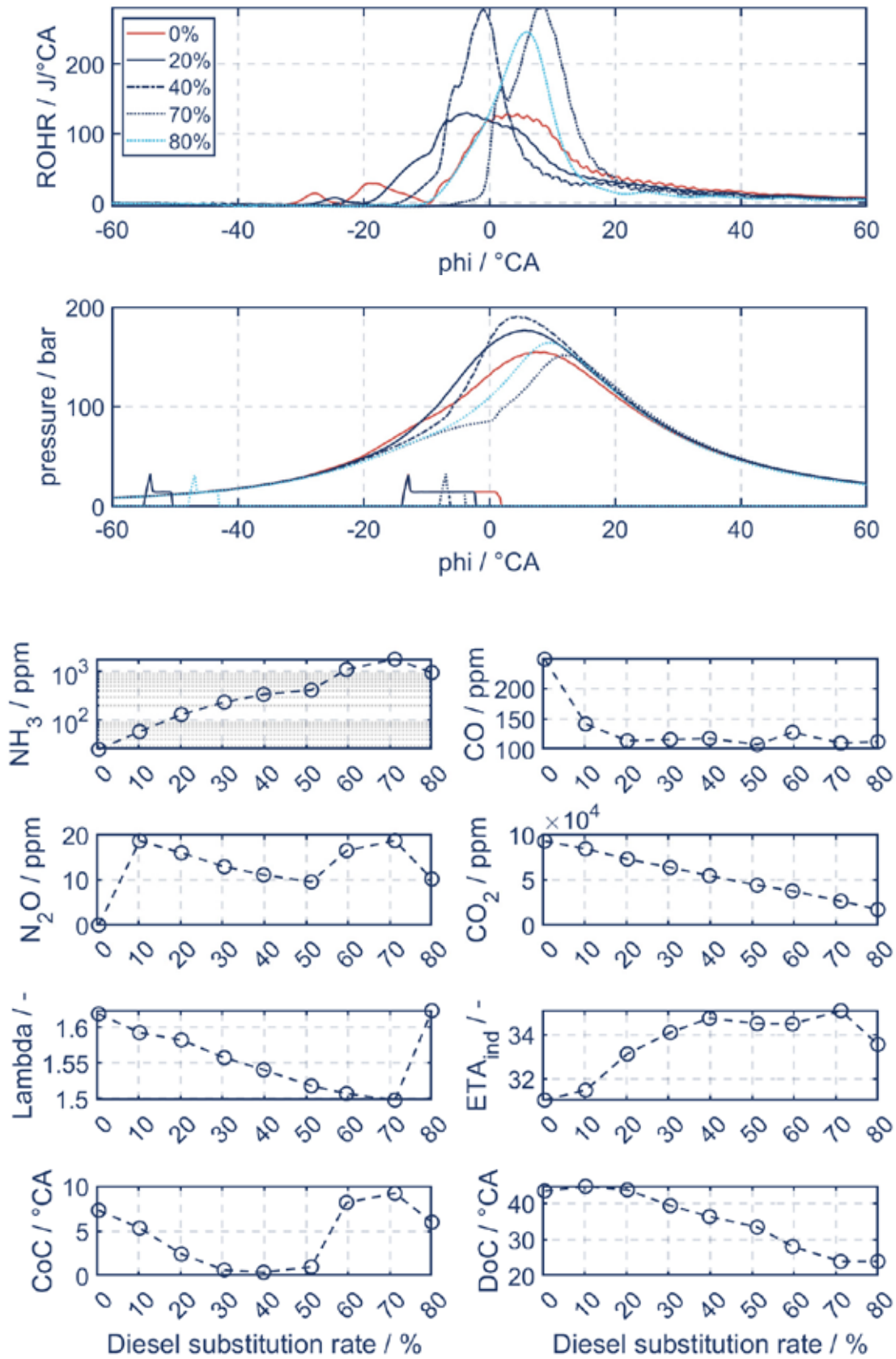


Figure 8: Pressure curves and heat release rates of the experimental data from the NH₃-engine at the University of Rostock for the substitution of diesel (shortening of the main injection period). Engine speed: 1500 rpm; engine load: 75%; total energy flux by fuel: 210 MJ/h; diesel injection pressure: 900 bar.

Based on the pure diesel case, the rate of heat release shows similar effects to the combustion at lower engine load (see Figure 7). For 75% load again, with increasing ammonia share, the cool-flame combustion of the diesel decreases and the whole pre-combustion shifts towards TDC. There is a significant difference between the 20% and 40% substitution rate, as with the higher substitution rate the entire combustion takes place in a single intensive heat release process. This shows the effect of the shifted oxidation of the pre-injected diesel mass. Therefore, the combustion duration decreases. The 70% substitution point has an optimized diesel main injection timing. Since the timing is closer to the TDC, the energy release is much later than e.g. at 40% substitution rate. This clearly can be seen regarding the center of combustion (CoC), which shifts from 1 °CAaTDC (40% substitution rate) to 9 °CAaTDC (70% substitution rate) and therefore shifts to the area of thermodynamic optimum. To ensure low nitrogen emissions at 80% substitution rate there is no diesel main injection and the diesel mass in the pre-injection was increased and shifted towards TDC.

The N₂O emissions are below 20 ppm in the measurements up to a substitution rate of 80%. The NH₃ concentration increases over the diesel substitution rate up to 1000 ppm. As expected, the CO₂-emissions decrease linearly. The CO emissions are constant from 20% to 80% substitution rate at 120 ppm. As said, the combustion duration (DoC) decreases with higher substitution rates because of the changing combustion process effects with increasing ammonia amount. The center of combustion (CoC) varies over the substitution rate due to the different optimization processes.

In conclusion, due to an innovative diesel injection strategy, the rate of diesel substitution could be increased up to 70% for 50% of engine load and up to 80% for 75% of engine load with a stable combustion process. The high substitution rates of diesel result in low carbon dioxide emissions. In order to consider the total greenhouse gas emissions, N₂O emissions must also be taken into account. Based on pure diesel combustion, the concentration rises to 10-20 ppm with increasing substitution levels. Due to the low N₂O concentration in the exhaust gas, the GHG reduction potential of ammonia as a fuel can be exploited very well (see Figure 9).

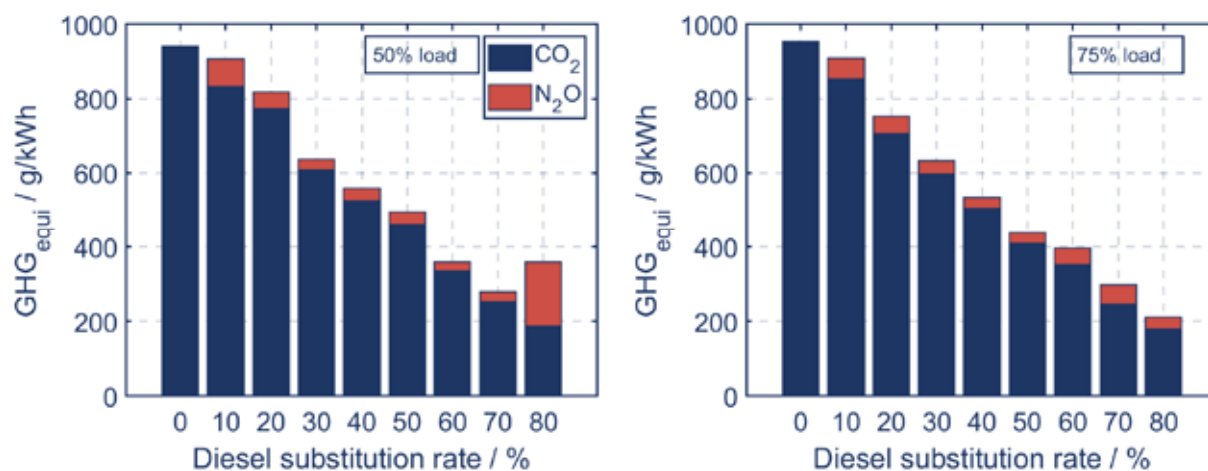


Figure 9: Greenhouse gas emissions (CO₂ and N₂O) as CO₂ equivalent over the substitution rate for 50% engine load (left) and 75% engine load (right) with engine speed of 1500 rpm

5.3 Simulation results

The modeling was carried out equivalent to a hypothetical real retrofit, where only information on pure diesel operation is available. This means that the parameters of the k-ε model were only trained to correspond to the measured pressure curve for pure diesel. The k-ε model is able to capture the effects of different injection times and durations on turbulence and mixing.

The emission and combustion predictions for operating points with ammonia are achieved without adjusting the parameters in the combustion model. The experiments were used to set up sensitive reactions for the ammonia-hydrocarbon interactions.

With the help of the detailed chemistry model, a detailed analysis of the combustion behavior was first carried out. Among other things, combustion-relevant species such as HO_2 , H_2O_2 , alkyl peroxide radicals, OH and nitrogen-containing intermediates were analyzed in order to identify the oxidation pathways, compare them with literature data and adjust the reaction constants of specific reaction pathways as part of a sensitivity analysis [20,21].

Figure 10 shows that the SRM model is able to predict the delay in the start of combustion when the amount of ammonia is increased. Good agreement is found in the pressure curve for most operating points. The number of combustion peaks and the disappearance of the main ignition event of the pilot injection for 70% ammonia are well predicted. However, phenomena relevant to combustion and thus emissions were discovered in the course of this joint project, which are complex (e.g. complex multiple injection strategies). This underlines that there are still many unknowns in the modeling of NH_3 /hydrocarbon combustion.

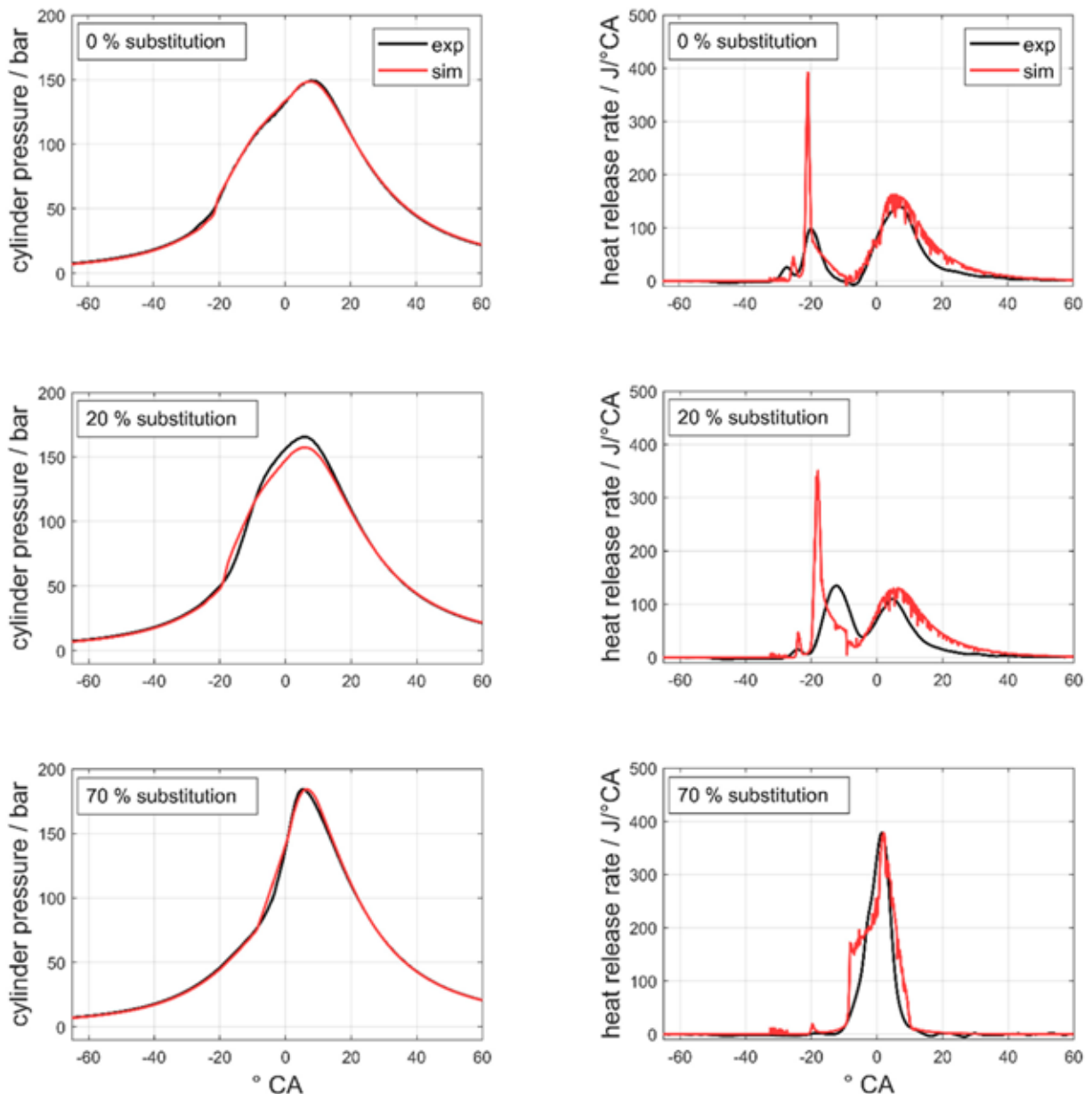


Figure 10: Comparison between experimental and simulation results with regard to pressure curves (left) and firing curves (right)

An overview of the measured and predicted exhaust gas emissions is shown in Figure 11. It can be seen that the predicted O_2 and CO_2 exhaust emissions are within the experimental uncertainty, which proves that the initial conditions and the composition of the substitute fuel are close to the experimental setup. The predicted NO emissions are close to the measured values for pure diesel and 70% ammonia, and the trend towards lower NO emissions at 30% and 40% substitution rate is predicted. The increase in N_2O for 0% to 10% ammonia content is well predicted. With increasing substitution rates, there are slight deviations, which are reduced by further parameterization of the models. Overall, the prediction quality is sufficient and will be further improved in the course of the project.

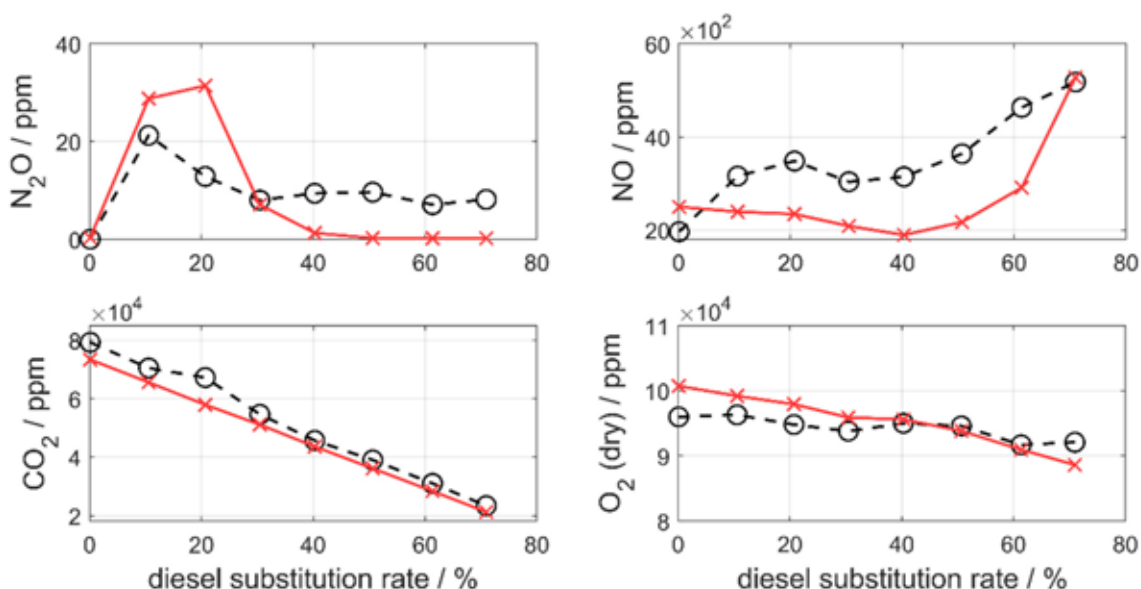


Figure 11: Comparison of measured and predicted emissions without taking valve overlap into account

6. Summary

This article presents and discusses the very successful development of an efficient ammonia/diesel dual-fuel combustion process with substitution rates of up to 80% and low ammonia slip as well as N_2O emissions. The total greenhouse gas emissions could be significantly reduced by 79%. This was largely achieved through the development of an innovative injection strategy, which clearly overcompensates for the challenging properties of the ammonia fuel. The combustion process developed has some complex combustion characteristics, such as a pronounced low-temperature combustion as a result of very early diesel pilot injection and the effect of increased premixed ammonia on the heat release rate of the pilot [20].

As part of the joint project, simulation models were developed that allow this complex internal engine combustion to be calculated and analyzed. Modeling this combustion process is a challenge due to the interaction between the low-temperature combustion of hydrocarbons and the ammonia content. The models developed show good agreement with the experimental combustion process and pressure curves.

The entire study only considers the raw emissions of the engine; potential exhaust gas aftertreatment systems are currently not part of the investigations. By developing special systems for this application, it will be possible to reduce emissions even further and thus also fall below the required limit values with regard to NOx emissions. With an assumed conversion rate of an SCR catalytic converter of 90%, the NOx emissions for a substitution rate of 70%, for example, would already correspond to the IMO TIER 3 limit values for shipping [18].

Furthermore, NH_3 and N_2O emissions can be further reduced with exhaust gas aftertreatment systems.

Together with a retrofit solution, ammonia as a fuel can bring great overall benefits for environmentally friendly shipping. In further investigations, an increase in the ammonia content with adapted injection parameters of the diesel fuel will be analyzed in order to be able to assess the potential of a retrofit combustion process more precisely. With more knowledge about the combustion process, it will be possible to develop further operating modes on the test bench. Even if the combustion process works well, it is not yet fully understood and should be researched further.

Acknowledgements

This research was funded by the German Federal Ministry for Economic Affairs and Climate Action on the basis of a decision by the German Bundestag (project no. 03SX549), which is gratefully acknowledged.



References

- [1] Førby, N., Thomsen, T., Cordtz, R., Bræstrup, F. and Schramm, J. 2023. Ignition and combustion study of premixed ammonia using GDI pilot injection in CI engine, *Fuel*, 331
- [2] Nadimi, E., Przybyła, G., Lewandowski, M. and Adamczyk, W. 2023. Effects of ammonia on combustion, emissions, and performance of the ammonia/diesel dual-fuel compression ignition engine, *Journal of the Energy Institute*, 107
- [3] Stenzel, K., Arndt, H., Thorau, P., Scharl, V. and Sattelmayer, T. 2022. AmmoniaMot – Experimental investigations of an ammonia dual-fuel combustion process for decarbonization of the maritime sector, 7th Rostock Large Engine Symposium, Rostock, Germany
- [4] Tornatore, C., Marchitto, L., Sabia, P. and De Joannon, M. 2022. Ammonia as Green Fuel in Internal Combustion Engines: State-of-the-Art and Future Perspectives, *Frontiers in Mechanical Engineering*, Vol. 8:944201
- [5] Gray, J., Dimitroff, E., Meckel, N. and Quillian, R. 1967. Ammonia Fuel-Engine Compatibility and Combustion, *SAE Trans*, 75, 785–807
- [6] Hideaki Kobayashi et al. “Science and technology of ammonia combustion”. In: *Proceedings of the Combustion Institute* 37.1 (2019), pp. 109–133. doi: 10.1016/j.proci.2018.09.029. url: <https://www.sciencedirect.com/science/article/pii/S1540748918306345> visited at February 23th, 2024.
- [7] Gupta B. 2008. Hydrogen fuel production, transport and storage, CRC Press
- [8] Pasternak, M. 2016. Simulation of the Diesel Engine Combustion Process Using the Stochastic Reactor Model, Brandenburg University of Technology Cottbus-Senftenberg
- [9] Kraft, M. 1998. Stochastic Modeling of Turbulent Reacting Flow in Chemical Engineering, VDI Verlag
- [10] Tuner, M. 2008. Stochastic Reactor Models for Engine Simulations, Lund
- [11] Pope, S. 1985. Pdf Methods for Turbulent Reactive Flows, *Progress in Energy and Combustion Science*, 11(2):119-192
- [12] Harworth, D. 2010. Progress in Probability Density Function Methods for Turbulent Reacting Flows, *Progress in Energy and Combustion Science*, 36(2):168-259
- [13] Franken, T., Sommerhoff, A., Willems, W., Matrisciano, A. et al. 2017. Advanced Predictive Diesel Combustion Simulation Using Turbulence Model and Stochastic Reactor Model, *SAE Technical Paper* 2017-01-0516, doi:10.4271/2017-01-0516
- [14] Bernard, G., Scaife, M., Bhave, A., Ooi, D. et al. 2016. Application of the SRM Engine Suite over the Entire Load Speed Operation of a U.S. EPA Tier 4 Capable IC Engine, *SAE Technical Paper*, 2016-01-0571
- [15] Xiaoxiao Wang. 2018. Kinetic mechanism of surrogates for biodiesel, Brandenburg University of Technology Cottbus

- [16] Matrisciano, A., Seidel, L., Mauss, F. 2022. An a priori thermodynamic data analysis based chemical lumping method for the reduction of large and multi-component chemical kinetic mechanisms, *International Journal of Chemical Kinetics*, 54:523-540
- [17] Shrestha, K., Giri, B., Elbaz, A., Issayev, G., Roberts, W., Seidel, L., Maus, F. 2022. A Detailed Chemical Insights into the Kinetics of Diethyl Ether Enhancing Ammonia Combustion and the Importance of NO_x Recycling Mechanism, *A Farooq Fuel Communications*, 10:100051
- [18] Manna, M., Sabia, P., Shrestha, K., Seidel, L., Raqucci, R., Mauss, F., de Joannon, M. 2022. NH₃-NO interaction at low-temperatures: An experimental and modelling study, *Proceedings of the Combustion Institute 2022*
- [19] Seidel, L., Netzer, C., Hilbig, M., Mauss, F., Klauer, C., Pasternak, M., Matrisciano, A. 2017. Systematic reduction of detailed chemical reaction mechanisms for engine applications, *J. Eng. Gas Turbines Power*, 139(9): 091701
- [20] Mante, Till; Prehn, Sascha; Seidel, Lars; Mestre, Laura; Theile, Martin; Hoppe, Antje et al. (2023): Numerical Study of NH₃-DieselCombustion in a Retrofit for Marine Engines using Detailed Kinetics. In: VDMA (Hg.): 30th CIMA World Congress 2023. 30th CIMAC World Congress 2023. Busan South Korea, June 12th-16th
- [21] Lamoureux, N., El Mehubi, H., Pillier, L., de Persis, S. and Desgroux, P. 2016. Modeling of NO formation in low pressure premixed flames, *Combustion and Flame*, 163 557-575

Development of Medium Speed Ammonia Engine for Marine Application

Entwicklung eines mittelschnelllaufenden Ammoniakmotors für die Schifffahrt

Sadao Nakayama*, IHI Power Systems Co., Ltd., Japan
Shunsuke Kazama, IHI Power Systems Co., Ltd., Japan
Hiroki Naruse, IHI Power Systems Co., Ltd., Japan
Yutaka Masuda, IHI Power Systems Co., Ltd., Japan
Yutaka Mashima, IHI Power Systems Co., Ltd., Japan
Kenta Miyauchi, IHI Corporation, Japan
Koki Aiba, IHI Corporation, Japan
Takayuki Hirose, IHI Corporation, Japan

Abstract

As well as hydrogen, methanol, synthetic methane and other liquid fuels like biofuels, ammonia is attention as one of the new alternative fuels in maritime industry to decrease Green House Gas (GHG) emission. However, ammonia is difficult to adapt in internal combustion engines due to low ignitability and low burning velocity. Therefore, a test was conducted with Rapid Compression Expansion Machine (RCEM) to investigate the combustion characteristics of ammonia/air pre-mixture. RCEM test was followed by Single Cylinder Engine (SCE) test to clarify optimum engine operating parameters for ammonia fuel operation. After the SCE test, various tests were carried out by adapting the operating conditions (compression temperature, equivalence ratio, etc.) with newly designed full-scale dual-fuel engine for ammonia use. As a result, stable operation with ammonia/air pre-mixture with a fuel mixture ratio of over 90% was achieved. Combining with catalyst, ammonia emission and N_2O in the exhaust gas after the catalyst were kept at very low level. GHG reduction ratio with including N_2O emission in ammonia mode compared to diesel mode was over 80% which satisfies with IMO GHG target for year 2040. Also, IMO NO_x Tier III emission regulation can be complied with ammonia mode by using the catalyst. This paper describes the development process and performance. This project is approved by NEDO as part of the Green Innovation Fund project. (NEDO: New Energy and Industrial Technology Development Organization)

Kurzfassung

Neben Wasserstoff, Methanol, synthetischem Methan und anderen flüssigen Kraftstoffen wie Biokraftstoffen gewinnt Ammoniak als einer der neuen alternativen Kraftstoffe in der maritimen Industrie an Beachtung, um den Ausstoß von Treibhausgasen (THG) zu verringern. Allerdings lässt sich Ammoniak in Verbrennungsmotoren aufgrund der geringeren Zündfähigkeit und der langsameren Verbrennungsgeschwindigkeit nicht einfach verwenden. Daher wurden Tests mit der Rapid Compression Expansion Machine (RCEM) durchgeführt, um die Verbrennungseigenschaften eines Ammoniak-Luft-Vorgemischs zu untersuchen. Auf den Einzylindermotor-Test (SCE) folgten RCEM-Tests, um die optimalen Motorbetriebsparameter usw. für den Betrieb mit Ammoniakkraftstoff zu klären. Nach dem SCE-Test wurden verschiedene Tests mit einem neu konstruierten Motor in Originalgröße durchgeführt, in denen

* Speaker/Referent

die Betriebsbedingungen (Verdichtungstemperatur, Äquivalenzverhältnis usw.) für den Ammoniak Einsatz angepasst wurden. Als Ergebnis wurde ein stabiler Betrieb mit Ammoniak-Luft-Vormischung mit einem Kraftstoffgemischverhältnis von über 90 % nachgewiesen. In Kombination mit einem nachgeschalteten Katalysator wurden Ammoniakemission sowie N_2O -Ausstoß aus dem Auspuffrohr nach dem Katalysator auf sehr niedrigem Niveau gehalten. Das THG-Reduktionsverhältnis unter Einbeziehung der N_2O -Emissionen im Ammoniakmodus im Vergleich zum Dieselmodus lag bei über 85 %, was dem IMO-THG-Ziel für das Jahr 2040 entspricht. Auch die IMO NO_x Tier III-Emissionsvorschriften können durch die Verwendung des Katalysators im Ammoniakmodus eingehalten werden. In dieser Arbeit werden Entwicklungsprozess und Leistung.

Dieses Projekt wurde vom Projekt des Grünen Innovationsfonds von NEDO genehmigt. (NEDO: Neue Organisation für die Entwicklung von Energie- und Industrietechnologien)

1. Introduction

Ammonia fuel is attention in the marine industry as an alternative fuel for reducing greenhouse gas (GHG) emissions. The International Maritime Organization (IMO) declared at the MEPC 80 meeting that its goal is to reduce GHG emissions by more than 20% within 2030, 70% by 2040 (compared to 2008 levels), and 100% by or around, i.e. close to 2050, compared to 2008 levels. Amid the introduction of such regulations, classification societies predict that 20% to 40% of ships will be running on ammonia fuel by 2050. As of the end of 2022, approximately 150 ammonia-ready vessels have been ordered ^[1]. Therefore, it is considered essential to develop marine engines that can use ammonia fuel.

On the other hand, ammonia fuel is considered difficult to apply to engines due to slow combustion speed and large amount of required ignition energy. Therefore, first, the ignition conditions and combustion characteristics of ammonia premixture with pilot liquid fuel were clarified using a rapid compression and expansion machine (RCEM). The combustion conditions of ammonia fuel obtained from the rapid compression machine were then reproduced in a single-cylinder engine (SCE), to clarify the possibility of engine operation with ammonia fuel. Furthermore, the performance with ammonia fuel in a full-scale engine were evaluated by reproducing the operating conditions obtained from the SCE test.

2. Fundamental Combustion Test

In order for ammonia to be used as an engine fuel, the ignition conditions and combustion characteristics must be clarified. An RCEM (Figure 1), that can simulate the temperature and pressure inside the combustion chamber of internal combustion engine was used to evaluate the ignition and combustion characteristics of the ammonia premixture using pilot fuel (Marine Diesel Oil: MDO). The specifications of the RCEM are shown in Table 1 and the test conditions are shown in Table 2.

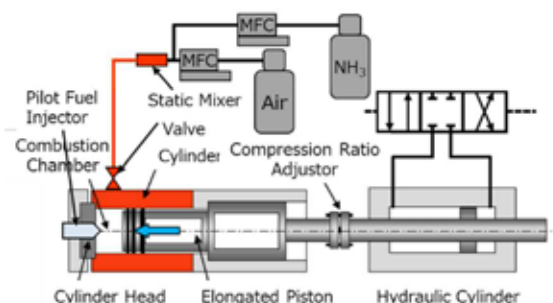


Figure 1. Schematic of Rapid Compression and Expansion Machine (RCEM)

Table1. Specification of RCEM

Bore	150 mm
Stroke	180 mm
Swept Vol.	3.18 L
Piston Speed	Equivalent to 750 min ⁻¹
Maximum Cylinder Pressure	20 MPa

Table2. Test Condition

Compression Pressure	2.6~13.3 MPa
Compression Temperature	750 K
Equivalence Ratio of NH ₃	0.1~1.0
Fuel Share Ratio	30~90 %
Pilot Fuel Injection Timing	Parameter
Pilot Fuel Injection Pressure	Parameter
Pilot Fuel Injection Quantity	Parameter

The RCEM can hydraulically stroke the piston from bottom dead center to top dead center in the time equivalent to 750 min⁻¹ of an actual engine. In order to achieve the target temperature and pressure at compression end, the intake pressure, the intake temperature before compression, and the compression ratio were adjusted. The mixture ratio of ammonia and air was adjusted by a mass flow controller, and the premixture was formed by a static mixer and supplied into the combustion chamber before compression.

The downstream of the static mixer and the wall surface of the RCEM combustion chamber were heated to a temperature equivalent to the intake temperature. The combustion characteristics of the premixture of ammonia and air were evaluated by injecting the pilot liquid fuel after the piston reaching the top dead center.

As a result of the preliminary test, it was found that a compression end temperature of 750 K or higher is required to ignite the ammonia premixture. Therefore, subsequent RCEM tests were conducted uniformly at 750 K. The fuel share ratio is the heat ratio of the pilot fuel and the ammonia fuel, as shown in Equation 1.

$$\text{Fuel Share Ratio} = \frac{Q_{NH_3}}{Q_{NH_3} + Q_{pilot}} \quad (1)$$

Where:

Q_{NH_3} = ammonia fuel injection quantity [kJ/cycle]

Q_{pilot} = pilot fuel injection quantity [kJ/cycle]

Figure 2 shows the combustion duration by the equivalence ratio and the fuel share ratio of the combined ammonia fuel and pilot fuel. As the ammonia premixture becomes lean, the combustion duration increases, and the combustion duration also increases with an increase in the fuel share ratio. From these results, combustion duration is determined by the equivalence ratio and the fuel share ratio of the ammonia premixture. Furthermore, combustion

duration equivalent to LNG with Ammonia fuel can be achieved by optimizing the fuel share ratio and the equivalence ratio in the ammonia premixture.

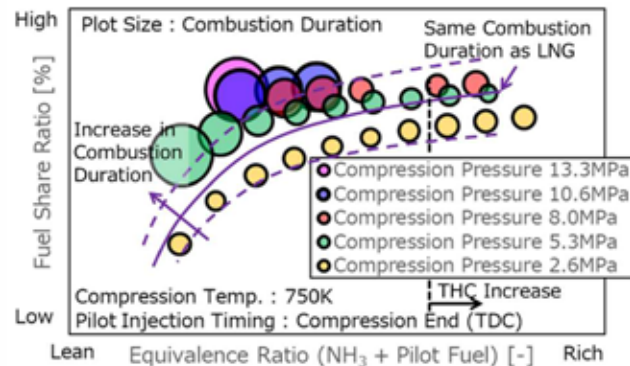


Figure 2. Combustion Duration by Equivalence Ratio and Fuel Share Ratio

3. Single Cylinder Engine (SCE) Test

The combustion conditions obtained in the RCEM test were reproduced in a SCE to evaluate the possibility of engine operation with ammonia fuel. Figure 3 shows a schematic, and Table 3 shows the specifications of the SCE. The SCE uses a side injector system, and pilot fuel is injected from two injectors in the combustion chamber. Ammonia is continuously supplied to the engine by a mass flow controller. Therefore, some ammonia will slip directly to the exhaust pipe during the valve overlap period. As a result, unburned ammonia above a certain level is always detected in the exhaust gas. The output shaft of the SCE is connected to a flex dynamometer, and the load and speed are controlled by the dynamometer.

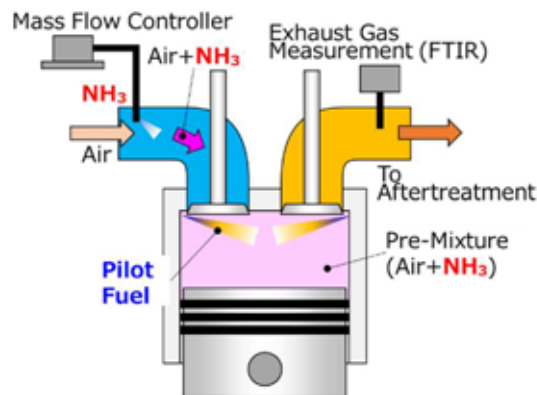


Figure 3. Schematic of Single Cylinder Engine (SCE)

Table 3. Specifications of SCE

Bore	180 mm
Stroke	200 mm
Displacement	5.1 L
Rated Power	57.3 kW
Rated Speed	750 min ⁻¹
BMEP	1.8 MPa
Number of Pilot Injector	2 (from each side)

The effects of compression end temperature and ammonia premixture equivalence ratio on combustion stability and exhaust emission performance were evaluated. Table 4 shows the test conditions.

Table 4. Test Conditions of Single Cylinder Engine

Equivalence Ratio (Pilot Fuel + NH ₃)	0.5~1.2
Equivalence Ratio of NH ₃	0.3~0.95

First, the effect of the compression end temperature on combustion stability and exhaust emission performance during engine operation was evaluated. As shown in Figure 4, as the compression end temperature decreases, the Coefficient of Variance (COV) of the indicated mean effective pressure (IMEP) increases, which indicates unstable combustion. On the other hand, no significant effect on COV of maximum combustion pressure (P_{max}) was observed in the tested temperature range. Focusing on exhaust emission performance, as shown in Figure 5, unburned ammonia and N₂O increased as the compression end temperature decreased, while NO_x decreases. This is assumed to be simply due to the decrease in combustion temperature caused by the decrease in the compression end temperature. From these results, it is considered that compression end temperature needs to be higher than a certain level for stable engine operation with ammonia fuel.

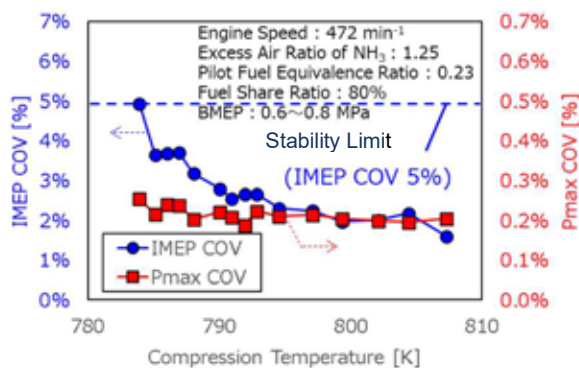


Figure 4 Combustion Stability vs Compression Temperature

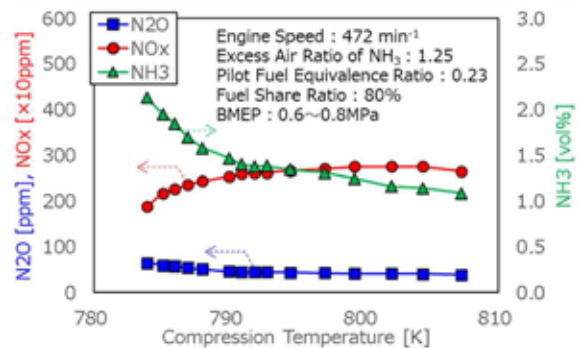


Figure 5 Exhaust Gas Emission vs Compression Temperature

Next, the effect of ammonia premixture equivalence ratio on engine operation was evaluated. As shown in Figure 6, the COV of IMEP increases as the ammonia premixture becomes lean. On the other hand, as the ammonia premixture becomes rich, the COV of P_{max} increases. This is due to the lack of air for the pilot fuel to ignite due to the rich ammonia premixture, resulting in unstable pilot ignition. Same can be mentioned by increase in CO as shown in Figure 7. The COV of P_{max} increased also due to the longer ignition delay. From these results, it is considered that there is appropriate range in equivalence ratio of the ammonia premixture for stable combustion in the engine.

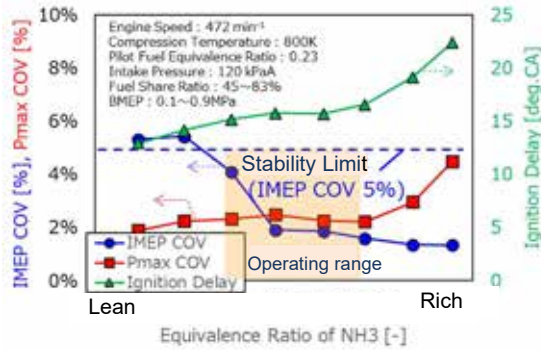


Figure 6 Combustion Stability vs Equivalence Ratio of NH₃

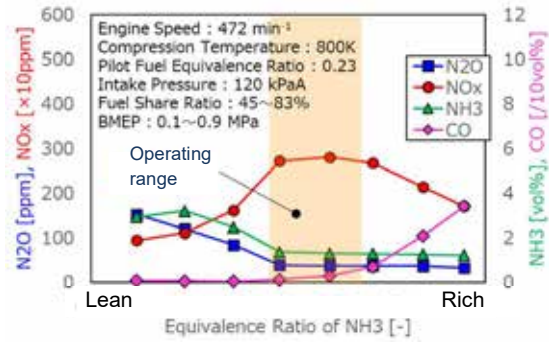


Figure 7 Exhaust Gas emission vs Equivalence Ratio of NH₃

Focusing on exhaust gas emission, as the ammonia premixture becomes lean, unburned ammonia and N₂O increase (Figure 7). On the other hand, a peak in NO_x emission can be observed. Unburned ammonia, N₂O, and CO became minimal within a specific range of equivalence ratio. Combined with combustion stability, there is an optimal range of equivalence ratio of the ammonia premixture, and this operation range was targeted for full-scale engine. Although the operating range will be within the NO_x emission peak, it can be reduced using after-treatment system such as SCR.

4. Full-scale Engine Test

4.1 Specification of full-scale engine

Based on the RCEM and SCE test results, an improved design for the 6-cylinder LNG dual-fuel engine (6L28AHX-DF) with a bore of 280 mm was implemented and named 6L28ADF. The improved design includes increasing the geometric compression ratio, optimizing the intake and exhaust systems, enlarging the fuel gas supply system, and enhancing the pilot fuel supply system. Figure 8 shows the main modifications to the full-scale engine, and the engine specifications are shown in Table 5.

Table 5. Full-Scale Engine Specification

Engine	6L28ADF
Number of Cylinder	6
Bore	280 mm
Stroke	390 mm
Rated Power	1618 kW
Rated Speed	750 min ⁻¹
BMEP	1.8 MPa

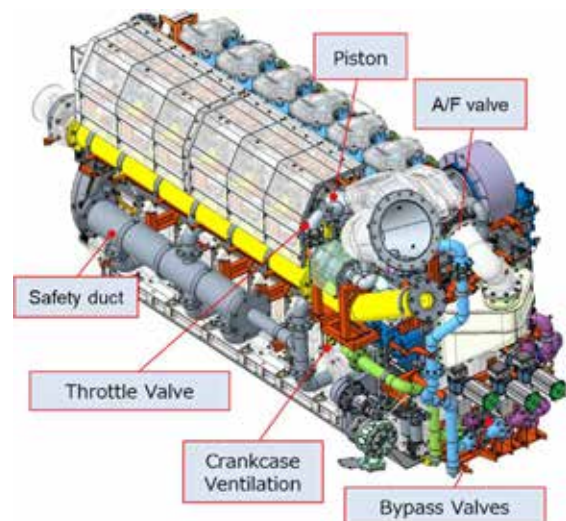


Figure 8 3D-Diagram of Full-Scale Engine

The intake and exhaust system were optimized to control the optimal amount of air for combustion of the ammonia premixture. The diameter of the air supply bypass valve has been increased and a bypass valve has been added. In the full-scale engine, gasified ammonia fuel is injected into the intake port at the appropriate timing, so ammonia slip can be reduced compared to the SCE. Unburned ammonia and NO_x contained in the exhaust gas were treated

by a catalyst installed in the exhaust pipe. Two FTIRs were installed to measure the exhaust gas concentration before and after the catalyst, respectively.

4.2 Specification of full-scale engine

The engine test bench consists of various auxiliary devices such as the fuel system (ammonia, MDO), coolers for the jacket water and lubrication oil, engine starting system, exhaust duct, water brake, measuring device, alarm device, and a control device (Figure 9) [3].

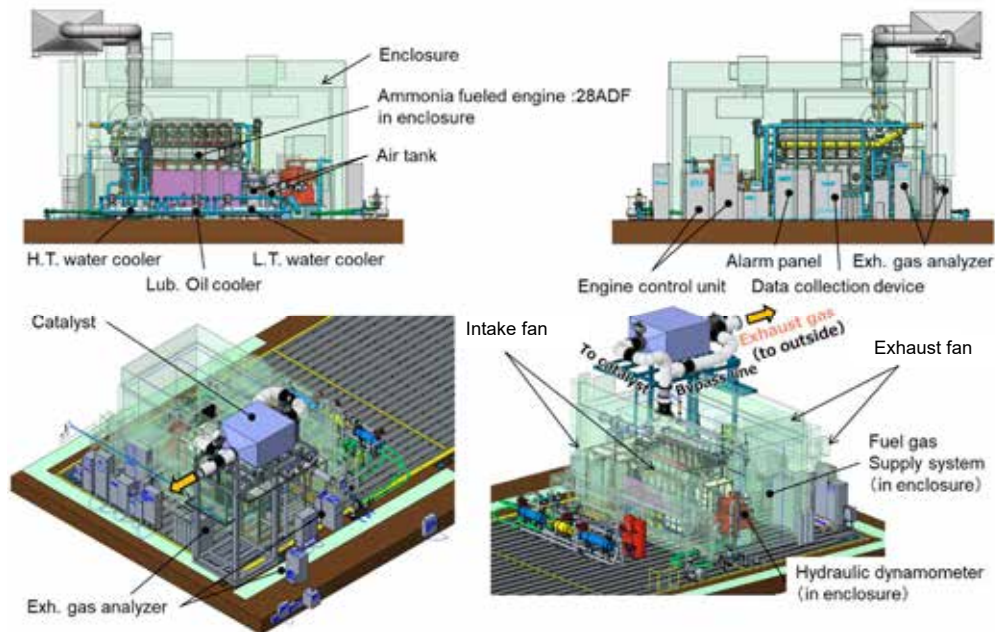


Figure 9 Schematic of Engine Test Bench

The full-scale engine has proactive measures to prevent ammonia leakage, such as double-walled gas piping and a mist separator with an exhaust fan. Additionally, an enclosure has been installed to enclose the engine and some of the operating equipment in case an unexpected leakage event occurs. The enclosure is equipped with an intake fan and an exhaust fan, and the operation of both fan is precisely controlled to keep the pressure inside the enclosure slightly below atmospheric pressure.

The fuel supply system has a role in controlling the flow rate and pressure of ammonia gas from the ammonia supply facility and distributing the gas to the test engine and the exhaust gas treatment catalyst. Also, the system is required to have the ability to supply gas in response to the change in engine operating load. Furthermore, it has a function to purge the piping with N_2 gas to remove ammonia in the engine piping during inspecting or replacing parts.

4.3 Performance

Firstly, Figure 10 shows the cylinder pressure and rate of heat release (ROHR) of the LNG dual fuel engine (6L28AHX-DF), in LNG mode (which is the base engine of 6L28ADF), and the ROHR of diesel mode and ammonia mode in 6L28ADF. The combustion performance such as ROHR and maximum combustion pressure of ammonia mode is equivalent to LNG mode by reproducing the ammonia premixture operating conditions obtained from the RCEM and single-cylinder engine test results. Furthermore, it was confirmed that the fuel mixture ratio in ammonia mode can be reached up to approximately 95%, which is comparable to the fuel share ratio in LNG.

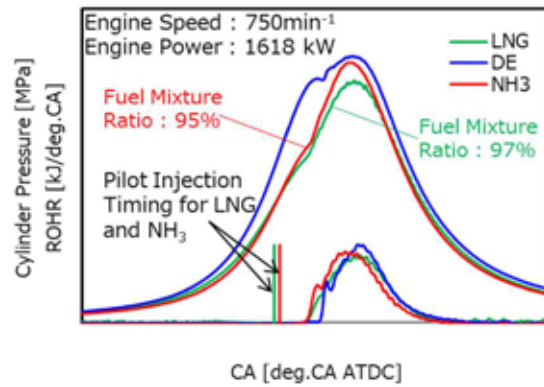


Figure 10 Cylinder Pressure and ROHR in LNG mode, Diesel Mode and NH₃ Mode

Next, the fuel share ratio and exhaust gas performance of ammonia mode in marine E3 mode are shown in Figure 11 to Figure 15. A fuel share ratio of over 90% was achieved at each load in E3 mode. Due to the necessity of certain amount of pilot fuel to ignite the ammonia premixture, the fuel share ratio decreases as the engine output decreases. As shown in Figure 12, by installing the catalyst in the exhaust pipe, the ammonia after the catalyst is less than 5 ppm, which fulfills the original target value of 25 ppm or less. Also, it is considered that the increase in unburned ammonia as engine output increases is due to the increase in the fuel share ratio. It is expected that unburned ammonia can be reduced by optimizing ammonia injection conditions and the spray of the pilot injector. As shown in Figure 13, this engine can meet the IMO Tier II NO_x regulation (9.6 g/kWh) in diesel mode, and the Tier III NO_x regulation (2.4 g/kWh) in ammonia mode by using a catalyst.

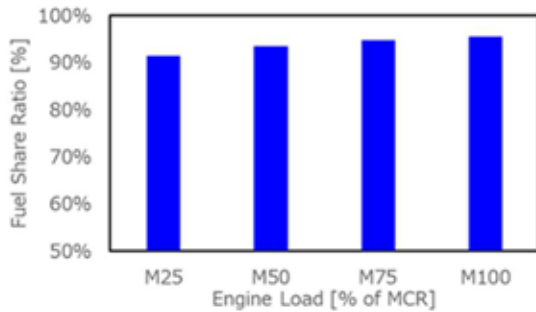


Figure 11 Fuel Share Ratio at E3 mode

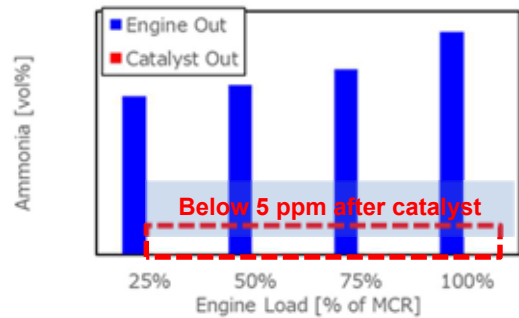


Figure 12 Ammonia Emission at E3 mode

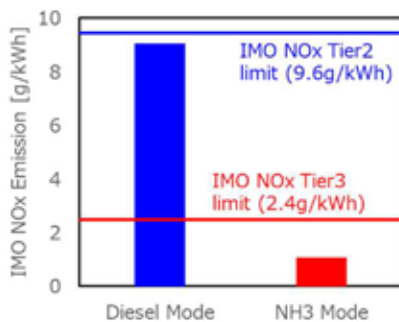


Figure 13 IMO NO_x Emission at E3 mode

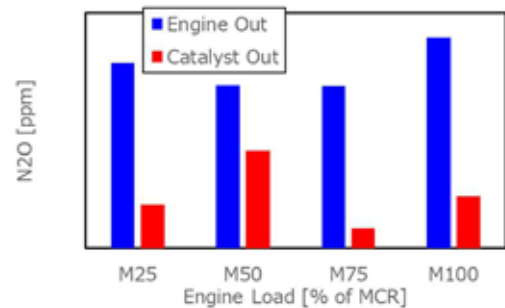


Figure 14 N₂O Emission at E3 mode

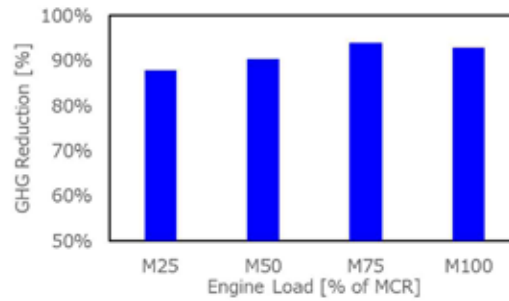


Figure 15 GHG Reduction at E3 mode

As shown in Figure 14, N_2O emission, which has 265 times the GHG effect compared to CO_2 , was decreased after the catalyst under all operating conditions. N_2O can be reduced by a catalyst, and further reduction in N_2O reduction can be expected by optimizing the exhaust gas conditions (temperature, exhaust gas components, etc.). The GHG reduction rate of the ammonia mode (considering the N_2O concentration at the catalyst outlet) against the diesel mode was calculated. The calculation was performed using Equation 2, and the CO_2 density conversion factor in ammonia mode was obtained according to ISO 8178-1. The exhaust gas air volume in each mode was calculated by adding the fuel flow rate to the intake air mass flow obtained from the bell mouth attached to the compressor inlet. As shown in Figure 15, GHG reduction rate of the ammonia mode compared to the diesel mode in E3 mode reaches over 90%.

$$GHG_{Reduction} = 1 - \frac{U_{gasNH_3} \times (CO_{2,gasNH_3} + 265 \times N_{2O,gasNH_3}) \times q_{mewNH_3}}{U_{gasDE} \times CO_{2,gasDE} \times q_{mewDE}} \quad (2)$$

Where:

U_{gasnh_3} = 0.001649 (CO_2 density conversion factor in NH_3 mode)

$CO_{2,gasnh_3}$ = CO_2 concentration in NH_3 mode (ppm)

$N_{2O,gasnh_3}$ = N_2O concentration in NH_3 mode (ppm)

q_{mewnh_3} = Exhaust gas flow in diesel mode (kg/h)

U_{gasDE} = 0.001517 (CO_2 density conversion factor in diesel mode)

$CO_{2,gasDE}$ = CO_2 concentration in diesel mode (ppm)

q_{mewDE} = Exhaust gas flow in diesel mode (kg/h)

4.4 Safety

Ammonia is toxic, and human can detect its odor even at low concentrations. Therefore, the ammonia fuelled engines need to be modified to prevent ammonia leakage. The fuel system that supplies ammonia fuel to the engine is designed with a double-wall pipe structure, similar to conventional dual fuel engines, to prevent leakage from pipe joints. In addition, leakage from the inner pipe of the double-wall pipe can be detected using a gas detector in the annular space of the pipe. In conventional reciprocating engines, blow-by gas that flow into the crankcase spreads throughout the entire engine. Thus, during engine operation, there is a possibility of small ammonia leakage from the shaft seals and various gaps in the engine due to the pressure difference with the engine room. In order to prevent ammonia from leaking to the engine room, a ventilation fan equipped with an oil mist separator was installed to maintain negative pressure inside the crankcase at all times.

The ammonia concentration in each area was measured while operating in ammonia mode (Figure 16). The ammonia concentration inside the crankcase was measured by FTIR installed downstream of the oil mist separator. The measurement results showed that there is ammonia

blow-by inside the crankcase. But the ammonia concentration around the engine measured by a gas detector was 0 ppm, and no odor of ammonia was detected.

The ammonia concentration inside the crankcase decreases to several thousand ppm after the engine is stopped. By operating the ventilation fan for the crankcase, no ammonia odor or ammonia was detected around the crankcase door even when the door was opened. Therefore, it is desirable to operate the ventilation fan also during maintenance.

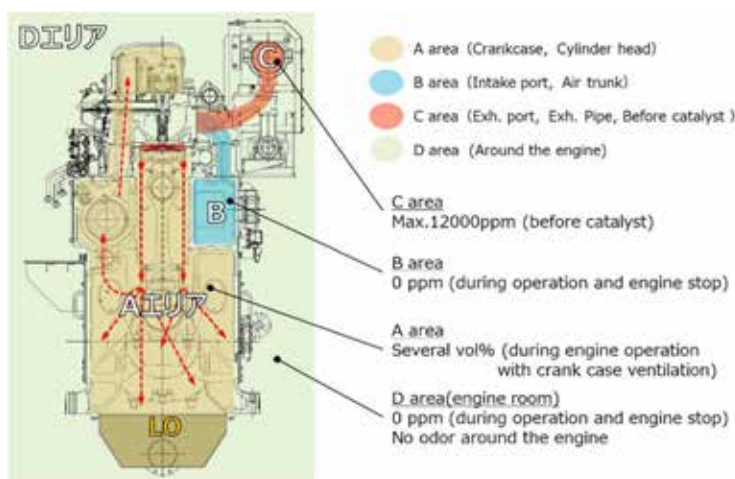


Fig.16 Ammonia Concentration and Odor around the Engine

5. Conclusion

The authors have developed ammonia fueled medium speed 4-stroke engine that contributes to reduce GHG emission from ships. Using RCEM, the ignition conditions and combustion characteristics of an ammonia premixture using pilot liquid fuel were clarified. By reproducing the results of RCEM test using a SCE, the possibility of operating the engine using ammonia fuel was confirmed. Based on these results, a full-scale engine was modified and demonstrated its performance. Through the development process, the following results were obtained.

- 1) Stable operation of the ammonia-fueled full-scale engine was achieved by optimizing the conditions of ammonia premixture (compression end temperature and pressure, equivalence ratio, etc.) and ignition (injection timing, quantity, etc.).
- 2) GHG reduction rate of over 85% was achieved in ammonia mode compared to diesel mode by using a catalyst.
- 3) Unburned ammonia and N_2O in the exhaust gas were kept at very low level at each load in marine E3 mode.
- 4) It was confirmed that the full-scale engine complies with IMO NO_x Tier III regulations in ammonia mode.
- 5) No ammonia odor or ammonia was detected around the engine by constantly maintaining negative pressure inside the crankcase, and the engine could be operated safely with ammonia fuel.

6. Acknowledgement

The research and development of the ammonia-fueled full-scale engine were carried out with the aid of a grant from the Green Innovation Fund of the New Energy and Industrial Technology Development Organization (NEDO). The authors would like to express their deep gratitude for this opportunity.

References

- [1] <https://www.iea.org/reports/net-zero-roadmap-a-global-pathway-to-keep-the-15-0c-goal-in-reach>
- [2] Y. Masuda, et al., "Development of Ammonia Fueled Engine for Medium Speed Marine Engine", The 34th Internal Combustion Engine Symposium, 2023, No. 20234655 (written in Japanese)
- [3] T. Tagai, "Development of marine 4-stroke ammonia fueled engine", Journal of the JIME, Vol. 58, No. 5 (2023) (written in Japanese)

Development of an Ammonia-fueled Cracker-Engine-Unit as Propulsion System for Inland Waterway Vessels

Entwicklung einer Ammoniak-betriebenen Cracker-Motor-Einheit als Antriebssystem für Binnenschiffe

A. Braun¹, H. Kubach¹, S. Braun¹, M. Reinbold¹, S. Bernhardt¹, N. Gierenz³, B. Buchholz³, L. Engelmeier⁴, L. Fehlemann⁴, J. Plass⁴, M. Steffen⁴, T. Baufeld², S. Prehn³, H. Mohr^{5*}

¹ Karlsruhe Institute of Technology, Karlsruhe/Germany

² Liebherr Machines Bulle SA, Bulle/Switzerland

³ University of Rostock, Rostock/Germany

⁴ The hydrogen and fuel cell center ZBT GmbH, Duisburg/Germany

⁵ GasKraft Engineering, Beckdorf/Germany

*Corresponding Author: hinrich.mohr@gaskraft-engineering.co

Abstract

Ships are an essential part of the global transport systems for goods and people. They represent the most efficient and climate-friendly transport method. However, a further reduction in emissions, especially CO₂, is necessary. Since pure electrification by using batteries as energy storage is not a solution in most cases due to the required operation range, the use of alternative fuels based on renewable energies is expedient. The CAMPFIRE partner alliance is therefore working intensively on the use of regeneratively produced ammonia as a maritime fuel and energy storage for regeneratively produced hydrogen. Due to the higher demand for hydrogen in the future, it will have to be imported and stored in ammonia for transportation. This will also increase the transport capacity required for inland shipping to distribute the energy from the seaports to the domestic market. Against this background, a project consortium of the CAMPFIRE partner alliance is developing and testing a propulsion system for inland vessels that runs exclusively on ammonia. The heart of this project is a cracker-engine-unit. During the work, the ammonia cracker is developed and built, the characteristics and challenges of ammonia combustion in the engine are systematically examined, the entire system is designed, the full engine unit with generator is containerized and finally tested holistically. In addition, the special safety aspects when using ammonia in the maritime environment are analyzed. The combination of the technologies used is intended to enable completely climate-neutral ship operations. The paper and presentation deal with an overview of the current work. This includes examples from the results of systematic combustion studies on the single-cylinder engine and the required injector technology. The various

* Speaker/Referent

configurations are evaluated for performance and emissions for a maritime application and then used as a basis for the full engine configuration. Furthermore, the development work on the cracker, which splits a partial stream of ammonia into hydrogen and nitrogen and thus supplies the ignition fuel for the engine, will be presented.

Kurzfassung

Schiffe sind ein wesentlicher Bestandteil der globalen Transportsysteme für Waren und Menschen. Sie stellen die effizienteste und klimafreundlichste Transportmethode dar. Dennoch ist eine weitere Reduzierung der Emissionen, insbesondere von CO₂, notwendig. Da eine reine Elektrifizierung durch den Einsatz von Batterien als Energiespeicher aufgrund der erforderlichen Reichweite in den meisten Fällen nicht in Frage kommt, ist der Einsatz von alternativen Kraftstoffen auf Basis erneuerbarer Energien sinnvoll. Die CAMPFIRE-Partnerallianz arbeitet daher intensiv an der Nutzung von regenerativ erzeugtem Ammoniak als maritimen Treibstoff und Energiespeicher von regenerativ erzeugtem Wasserstoff. Wegen der zukünftig größeren Nachfragen an Wasserstoff wird dieser importiert werden müssen und für den Transport in Ammoniak gespeichert werden. Damit wird u. a. auch die benötigte Transportkapazität in der Binnenschifffahrt steigen, um die Energie von den Seehäfen ins Landesinnere zu verteilen. Vor diesem Hintergrund entwickelt und erprobt ein Projektkonsortium ein Antriebssystem für Binnenschiffe, das ausschließlich mit Ammoniak betrieben wird. Das Herzstück dieses Projekts ist eine Cracker-Motor-Einheit. Im Rahmen der Arbeiten wird der Ammoniak-Cracker entwickelt und gebaut, die Eigenschaften und Herausforderungen der Ammoniakverbrennung im Motor systematisch untersucht, das Gesamtsystem ausgelegt, die komplette Motoreinheit mit Generator containerisiert und schließlich ganzheitlich getestet. Darüber hinaus werden die besonderen Sicherheitsaspekte beim Einsatz von Ammoniak in der maritimen Umgebung analysiert. Die Kombination der eingesetzten Technologien soll einen vollständig klimaneutralen Schiffsbetrieb ermöglichen. Das Manuskript gibt einen Überblick über die laufenden Arbeiten. Dazu gehören Beispiele aus den Ergebnissen systematischer Verbrennungsstudien zum Einzylindermotor und der erforderlichen Injektortechnologie. Die verschiedenen Konfigurationen werden hinsichtlich Leistung und Emissionen für eine maritime Anwendung bewertet und dann als Grundlage für die vollständige Motorkonfiguration verwendet. Außerdem werden die Entwicklungsarbeiten am Cracker vorgestellt, der einen Teilstrom von Ammoniak in Wasserstoff und Stickstoff aufspaltet und damit den Zündbrennstoff für den Motor liefert.

1. Introduction

Shipping is a major and irreplaceable means of transporting people and particularly goods worldwide. Ships provide the most efficient and therefore most climate friendly method of transport. However, further improvement of greenhouse gas emissions will be needed to cope with the requirements for a sustainable future. Potentially climate neutral mobility might be realized utilizing battery in road-based applications. For ships the energy densities of batteries are too low for most application scenarios [1]. In this respect alternative ways of providing stored renewable energies for ships are needed. Green hydrogen is a promising option for this task, but the energy density of elemental hydrogen (both, compressed or liquefied) is still too low. Conversion of hydrogen into a liquid fuel is therefore highly interesting. Classical hydrocarbons, that could be produced via e.g. the Fischer-Tropsch-process from hydrogen, seem attractive in this regard as conventional engines could be used. Of course, they require a concentrated carbon source e.g. from carbon capture and storage (CCS) plants, if no energy demanding and expensive direct air carbon capture is applied on a large scale. Consequently, the availability of CO₂ becomes a limiting factor for production capacities, which prohibits their wide-spread application [2]. In contrast, ammonia can be produced from hydrogen by conversion of hydrogen with abundantly available nitrogen [3]. So, ammonia has started drawing major attention by researchers as well as the maritime industry and authorities as a storage form for hydrogen and energy [4, 5]. Ammonia can be utilized directly in internal combustion engines as a fuel, but its combustion properties are not optimal for the engine process. Particularly its low ignitability and flame speed pose some challenges, especially for high-speed engines, as well as its potential corrosive attack [6]. Mixing with a certain amount of hydrogen as a pilot fuel can help to handle this issue [7]. The provision of this hydrogen could be facilitated by decomposition of a small share of the ammonia immediately before the engine in a cracker unit. To realize such a process in a reasonable manner, proper system integration is required. In this paper the application of ammonia as a fuel for inland water vessels is discussed by addressing the recent development topics.

2. System concept for inland water vessels

Inland shipping uses a large network of interconnected rivers, canals and lakes, primarily in Europe, North America and the Far East. The rather inconspicuous ships mostly transport dry and wet bulk goods as well as containers. Another expanding application is inland waterway transport with passengers. In addition to self-propelled monohull vessels, there are also push boats and tugs that move unpowered barges. Vessel sizes are often limited by the size of the lock basins, which allow the vessels a difference in height. These sizes are usually standardized in the respective regions. A typical size is the so-called European ship for European inland waters of class IV with a length of 85 m and a width of 9.5 m. The maximum transport capacity of this type of ship is 1350 tons. In 2020, the average age of German inland waterway vessels was 46.7 years [8].

Due to their smaller size and lower water resistance, the power requirement of inland waterway vessels is specifically lower than that of seagoing vessels, as the speeds are lower and there are almost no waves and winds to take into account. The highest power requirement is needed for upstream travel on rivers against the current. The so-called European ship type already mentioned has a typical power requirement of 600 kW. In the past, this was handled by a medium-speed engine that drove a single propeller with a fairly large diameter via a reduction gear. As river water levels have been low more frequently over the last decade due to low rainfall in Europe, new vessels are being designed with two or even three smaller diameter propellers to reduce the draft of the vessel. These smaller propellers are driven mechanically by high-speed engines via a Z-drive or electrically via a generator. Naturally, a lower water level greatly increases the power requirement for a European ship type (see Table 1). With the

same performance, the ship's speed is reduced to 50% if the water level is lowered from 5 m to 2.5 m and the draught is limited to 2 m.

Table 1: Influence of water level on ship speed @ constant engine power [9]

Engine Power / kW	Water Level / m	Ships Draught / m	Ship Speed/ km/h
600	5	2.5	17
600	2.5	2	8.5

In order to drive forward the decarbonization of shipping, the CAMPFIRE project CF08_2 is developing an ammonia-powered, containerized inland vessel propulsion system with 350 kW propulsion power and testing it "on land". Figure 1 shows a schematic overview of the propulsion system. To improve the ignition and efficient conversion of the ammonia in the engine, a low amount of hydrogen is required as ignition improver. For this purpose, an ammonia cracker is connected upstream of the engine, which decomposes a partial flow of the ammonia into hydrogen and nitrogen and feeds this mixture to the combustion engine.

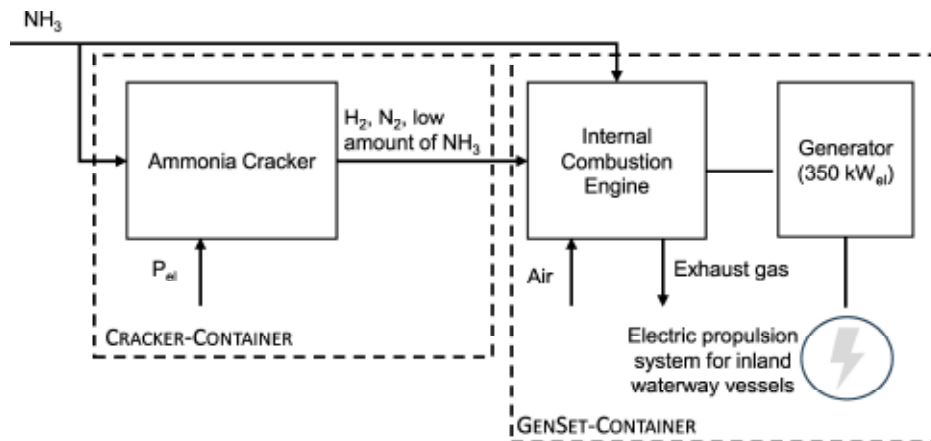


Figure 1: Scheme of the ammonia-powered propulsion system of an inland waterway vessel

3. Methodology of Development

3.1. Internal Combustion Engine

The development of a new combustion process involves uncertainties and, due to the novelty of ammonia as a fuel, a lack of both experience and validated tools. The development process therefore includes both expected and unexpected challenges. The expected challenges are mainly due to the chemical properties of ammonia. On the one hand, the rather poor combustion properties as described in the previous chapters, and on the other hand, the possible incompatibility of materials. Other known challenges include the lack of validated simulation tools that would allow rapid refinement and validation of new concepts. Examples of the lack of experience include atomization, evaporation and mixing behavior, combustion behavior, and heat release of ammonia. In the case of conventional fuels, there is a wealth of experience in terms of appropriate modeling. To achieve the ultimate goal of developing a combustion process for a multi-cylinder engine, the following strategy is used (Figure 2). A single-cylinder engine is used to test the basic concepts. The extensive instrumentation of this research engine allows the determination of the calibration quantities required for the essential 0D/1D simulations. The models validated on the single-cylinder engine are then used for the process development of the multi-cylinder engine. Certain quantities that cannot be measured directly are determined using detailed 3D flow simulations. These quantities are then fed into the 0D/1D tools. The final step is to apply the knowledge gained from the single-cylinder test bench and the validated 0D/1D models to the complete engine. The experimental work on combustion process development is carried out in Karlsruhe on a single-cylinder engine

derived from the Liebherr multi-cylinder diesel engine. The multi-cylinder engine tests will be carried out in Rostock by the University of Rostock.

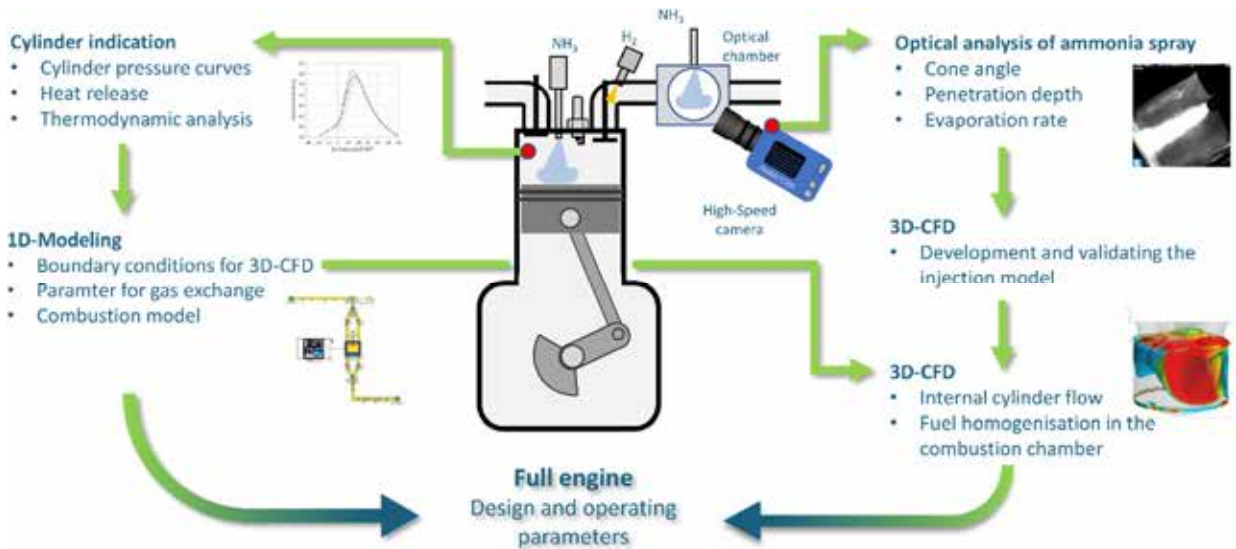


Figure 2: Development methodology for the combustion process

3.2. Cracker

In order to supply the required amount of hydrogen to the engine, a certain share of the ammonia feed has to be decomposed into hydrogen by the use of a suitable process. The decomposition into hydrogen and nitrogen is often referred to as ammonia cracking and is an endothermic process with a reaction enthalpy of about 46 kJ/mol. The reaction equation without intermediate steps can be seen in equation (1) [10].

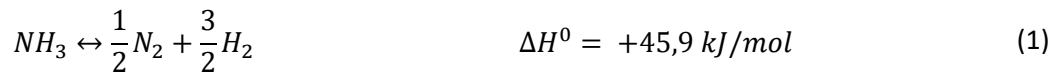


Figure 3 shows the equilibrium ammonia mole fraction as a function of temperature at pressures of 1 bara, 5 bara and 10 bara. In accordance with Le Chatelier's principle, the equilibrium shift can be achieved by increasing temperature or reducing pressure.

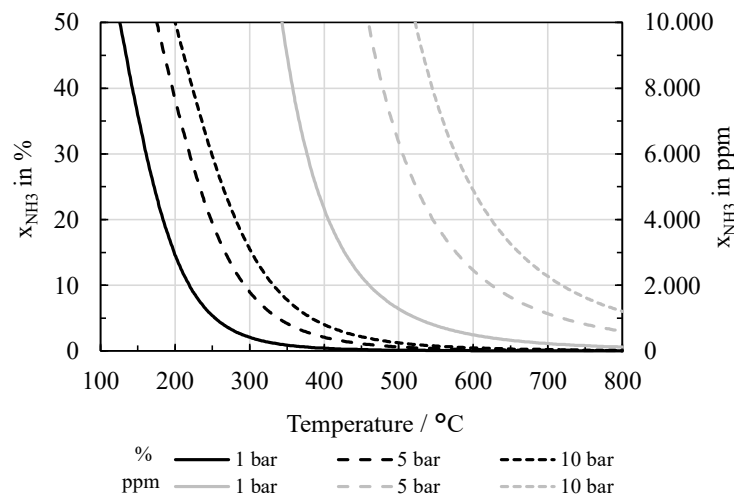


Figure 3: Simulated equilibrium ammonia mole fraction as a function of temperature at a pressure of 1 bara, 5 bara and 10 bara, simulated with Aspen Plus®

In practice, the chemical equilibrium shown in Figure 3 is not achieved due to kinetic limitations, especially at low temperatures. Thus, in order to provide hydrogen in a sufficient amount both a *catalyst* and *higher temperatures* (up to 900 °C) are required.

As such, the development of the ammonia cracker starts with the identification and selection of a suitable catalyst. For this purpose, various catalysts are procured and extensively tested with regard to their conversion as a function of temperature, gas hour space velocities and pressure as well as long-term stability. Focus lies on monolithic catalysts (ceramic and metallic), as these are particularly advantageous when vibrations in mobile applications cause abrasion in bulk catalysts [11].

Preliminary investigations have shown that the conditions in an ammonia cracker, characterized by the combination of high temperature and an ammonia-rich atmosphere, lead to considerable material damage due to nitridation. The next step is therefore the selection of an appropriate reactor material. Promising material candidates are thus identified in an extensive literature survey. Subsequently, long term exposure tests are carried out to verify the suitability of the selected materials.

Based on the properties of the carefully chosen catalyst and reactor material as well as according to the requirements set by the engine the ammonia cracker is developed, focusing on an optimized heat integration and thus high efficiency. Aspen Plus® is used to model and compare different possible process designs, as well as to determine energy and material flows, necessary for engineering the ammonia cracker components such as reactor, heat exchangers, burner, compressors etc. The detailed engineering of the single components is supported by multiphysics simulations (COMSOL Multiphysics®) as well as FEM simulations (Nastran, Autodesk Inventor). This is followed by the engineering and construction of the ammonia cracking plant, comprising the ammonia cracker, balance of plant components, rack, enclosure including an appropriate control system (SPS). The ammonia cracking plant is being put into operation at the ZBT and is extensively tested and optimized. The plant will then be containerized and transferred to Rostock to be coupled with the engine for extensive testing of the entire system. Both initial characterization at ZBT as well as subsequent tests in Rostock will be used for process optimization aided by dynamic process simulations in AVL Cruise™ M.

4. Results

4.1. Single-cylinder Engine

A single-cylinder research engine was built on a test bench at the Institute of Internal Combustion Engines at KIT. The engine is based on a Liebherr D966 diesel engine and was modified to meet the requirements of the new combustion process. The Diesel injector was replaced by an injector that can inject both hydrogen and ammonia in liquid and gaseous form. As ammonia has a very low calorific value of only 18.8 MJ/kg compared to diesel fuel, the injection system must be designed for comparatively large mass flows in order to achieve diesel-like mean pressures. As this combustion process is a spark-ignition principle, a spark plug must also be integrated into the cylinder head. In addition to the possibility of direct injection, both media can also be injected into the intake manifold. The test bench was equipped with a suitable fuel infrastructure for this purpose. While hydrogen is already available in cylinders at a pressure of 300 bar, the ammonia, which is also available in cylinders, is brought to the desired injection pressure of up to 30 bar via a compressor station. Dual-fuel operation with ammonia and hydrogen is necessary at most operating points, as ammonia is difficult or impossible to ignite with a conventional spark plug and has slow combustion rates [12]. Hydrogen supports the ignition process and ensures a higher burning rate. On the other hand, the high enthalpy of vaporization of ammonia can bring advantages. For example, the cooling effect could suppress knocking combustion and reduce nitrogen oxide emissions. The development goal is to operate the engine with as little hydrogen as possible while maximizing efficiency and reducing emissions. As the hydrogen is provided by the aforementioned cracker, it can then be built as small and cost-effective as possible and operated with low energy consumption. In this study, operating limits for the maximum and minimum hydrogen content are to be determined for the single-cylinder engine when the

ammonia is injected into the intake manifold in liquid form and the hydrogen in gaseous form. The main limiting factors are the occurrence of knocking combustion or pre-ignition, excessive variance in the mean pressure and exceeding the permissible exhaust gas temperature and permissible peak pressure.

Table 2: Engine parameters

Cylinder	1
Stroke	157 mm
Bore	135 mm
Compression ratio	14
Max. speed	1900 rpm
Operating principle	4-stroke
Displacement	2.24 l
Type	Modified Liebherr diesel engine

4.1.1. Injection timing

The homogenization of the cylinder charge can be significantly influenced by the injection timing. The hydrogen is injected at the start of injection at $\text{SOI} = 330^\circ\text{CA bTDCf}$ and is already in gaseous form. The ammonia must first evaporate and mix with the hydrogen and the air in the combustion chamber. The influence of the start of injection of ammonia is investigated in three steps by varying the ammonia/hydrogen ratio. Starting at $\text{SOI} = 130^\circ\text{CA bTDCf}$, the ammonia is injected shortly after IVC and thus has the maximum time span to evaporate before IVO. A significant proportion of the vaporization can thus already take place in the intake port. Due to the very high enthalpy of vaporization, there is significant icing on the outside of the intake manifold. In the second step, injection begins at $\text{SOI} = 265^\circ\text{CA bTDCf}$, synchronized with the intake at maximum open IV. In the last variant at $\text{SOI} = 360^\circ\text{CA bTDCf}$, injection begins shortly after IVO (403°CA bTDCf).

Figure 4 shows the coefficient of variation (COV) of the indicated mean effective pressure (IMEP) over the energetic ammonia content for the three injection timings mentioned. The series of measurements was carried out at $\text{IMEP} = 17$ bar, which corresponds to a power output of 44 kW. The upper limit value results from exceeding a COV of 3%. At $\text{SOI} = 360^\circ\text{CA bTDCf}$, this is the case with an energetic ammonia content of approx. 83%. If the ammonia content is increased further, the COV gradients for all SOI increase very sharply, so that stable engine operation is no longer possible. For this reason, no further increase was made.

In all three cases, the lower limit results from the occurrence of knocking combustion. Over the entire course, the IMEP shows the lowest cyclical fluctuations with intake-synchronous injection ($\text{SOI} = 265^\circ\text{CA bTDCf}$). Apparently, this injection start leads to the best mixture preparation and stabilization of combustion.

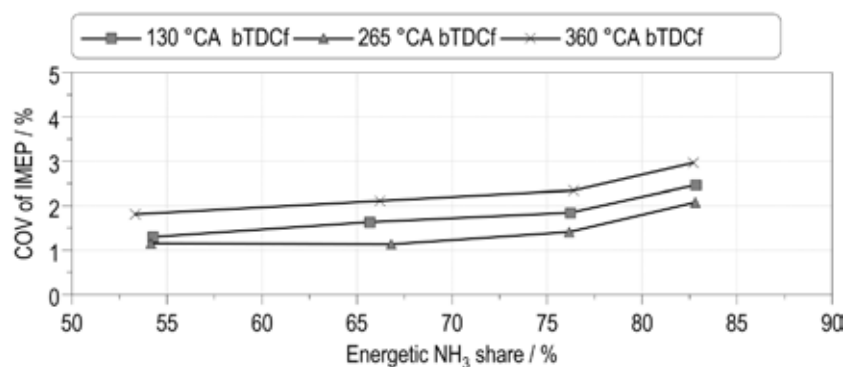


Figure 4: Influence of the ammonia start of injection timing on the COV of IMEP

4.1.2. Influence of the charge air temperature

In addition to the injection timing, the charge air temperature also has an influence on the mixture formation and thus the combustion stability, but also on the ignition behavior and thus on the occurrence of knocking events. To evaluate this influence, the charge air temperature was set to 40 °C, 60 °C and 80 °C. As in the previous chapter, the coefficient of variation of the indicated mean effective pressure over the energetic ammonia content up to approx. 83% is shown in Figure 5. A comparison of the two boundary values 40 °C and 80 °C shows the expected effect with high ammonia contents. The increased charge air temperature supports evaporation and mixture formation and stabilizes combustion, which is reflected in a reduced COV. The opposite effect occurs in the direction of lower energetic ammonia content. Here, the high temperature has a negative effect on knocking behavior. Increased knocking events worsen the COV here and lead to an interruption of operation with higher ammonia proportions and correspondingly less hydrogen. Since high hydrogen contents due to heavy knocking and pre-ignition represent the critical limit in terms of damage, especially at full load, the charge air temperature of 40 °C was initially selected for the further series of measurements for safety reasons.

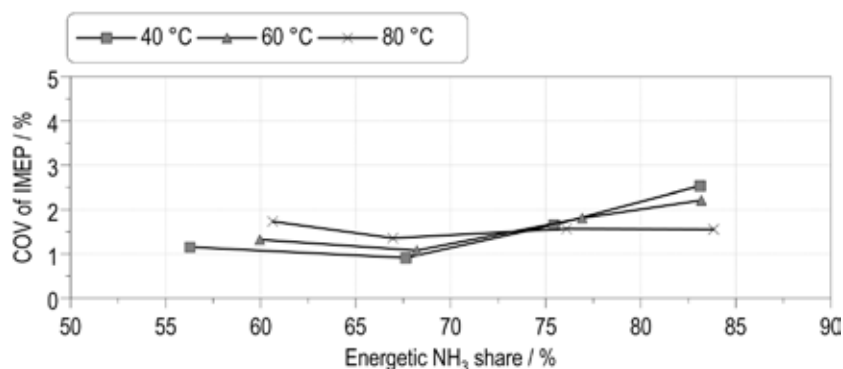


Figure 5: Influence of the charge air temperature on the COV of IMEP

4.1.3. Load Variation

The target speed of the final engine application is 1,500 rpm. The engine must be able to cover the entire load range. For this reason, a load sweep is analyzed at this speed with four steps in IMEP: 6.3 bar (25%), 11.5 bar (50%), 17 bar (75%) and 22 bar (100%). In this investigation the start of injection for ammonia is set to 130 °CA bTDCf and a charge air temperature of 40 °C is set. At this point, SOI = 130 °CA was chosen because optical investigations of the ammonia injection are also available here, which can be used for further interpretation of mixture formation effects. The initial focus is on the question of the range in which the energetic ammonia content can be varied depending on the load and what limits this range. Furthermore, it should be clarified how the emissions and efficiency depend on the selected ammonia proportion.

Figure 6 shows the IMEP, Lambda, the COV, as well as the center of combustion (AI50%) with the associated ignition timing for the different load levels. The maximum load corresponds to an effective output of 60 kW. This even slightly exceeds the desired target value of at least 57 kW. The load ranges 50% to 100% were run with a stoichiometric air/fuel ratio. As the engine does not have a throttle, the air ratio increases to Lambda=2.5 at 25% load. Since it is not trivial in test operation to keep the load exactly constant when changing the hydrogen/ammonia proportion and the associated change in the combustion process, small changes can be seen both in the load and in the air ratio (especially at 25% load, since the load is directly related to the air ratio here). The center of combustion was set to about 10 °CA aTDC as a compromise between the best possible efficiency and slightly reduced knocking tendency at high hydrogen percentages, since the engine has a high compression ratio for hydrogen operation with Epsilon = 14.

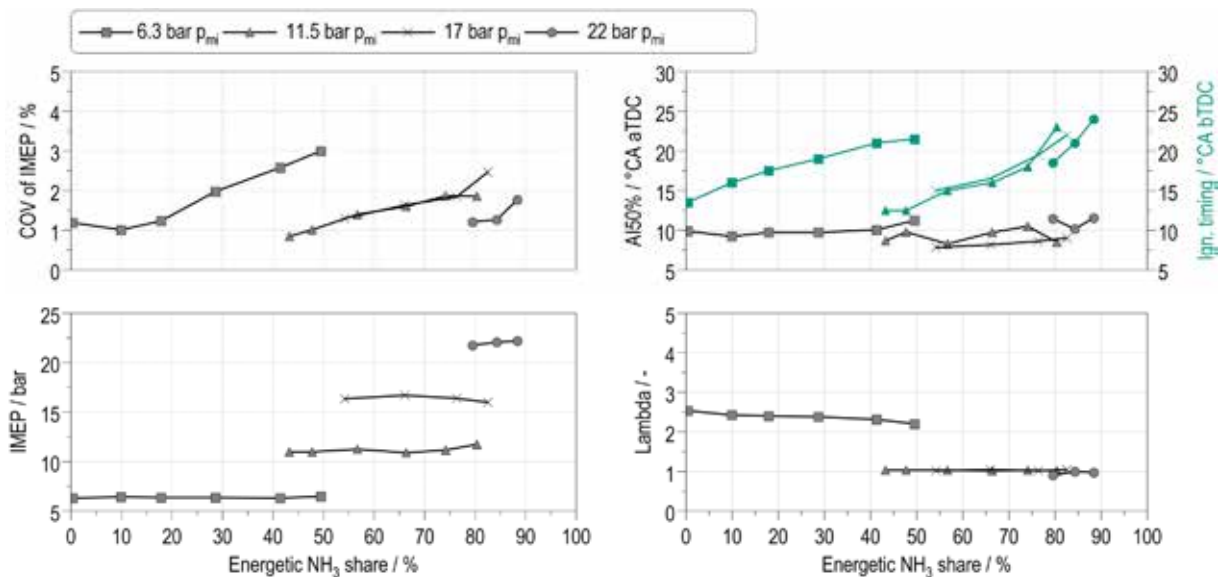


Figure 6: COV of IMEP, AI50, ignition timing, IMEP and Lambda at load variation

Pure hydrogen operation without combustion anomalies is possible with a low load and high air ratio. If the ammonia content is increased, the COV initially rises continuously up to an ammonia content of 50%. The gradient then increases significantly, and the cyclical fluctuations increase to such an extent that useful engine operation is no longer possible. At higher loads, no such sharp increase in running unsteadiness can be seen. However, if the ammonia content is increased further at loads above 25%, combustion misfires occur directly, so that engine operation is no longer possible. On the other hand, pure hydrogen operation is no longer possible at these loads. The lower limit of the ammonia content results here from a sharp increase in knocking combustion. If the ammonia content is lowered further, spontaneous pre-ignition occurs, resulting in extreme knocking and peak pressure overshoot. In Figure 7 left, 200 cylinder pressure curves for maximum hydrogen content (21% energetic) are shown for full load. In some cycles, very noticeable knocking already occurs. The maximum pressure amplitudes exceed 12 bar. If the hydrogen content is increased even slightly further, the knocking increases extremely and pre-ignition occurs. As a measured value recording takes approx. 30 seconds, this was not carried out for reasons of engine protection. Figure 7 on the right shows that individual cycles with very low peak pressures and very late combustion already occur at the upper limit of the ammonia content (88% energetic). With a further increase in the ammonia content, complete combustion misfires then occur, which no longer permit useful engine operation.

As mentioned in the introduction, the center of combustion was set to around 10 °CA aTDC. If the ammonia content is increased, this results in an increased spark advance requirement. This is plausible, as ammonia itself can hardly be ignited with a conventional spark plug as used here. Hydrogen is used for this purpose and to increase the flame speed. After ignition and with increasing temperature, ammonia decomposes into nitrogen and hydrogen, which further accelerates the flame speed and the heat release rate and thus the decomposition of ammonia [12]. After a longer ignition phase, a self-reinforcing acceleration effect of the flame speed can occur, so to speak.

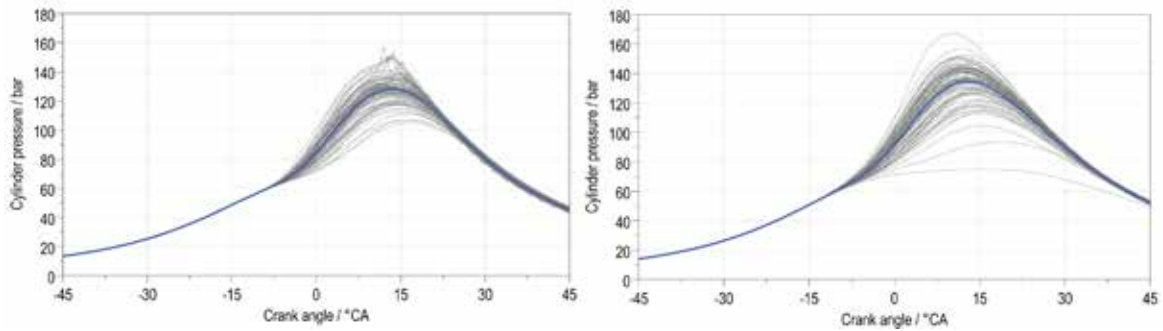


Figure 7: Cylinder pressure of a 100% load point with minimum (left) and maximum (right) amount of NH_3 , averaged cylinder pressure in blue

As can be seen in Figure 8, the efficiency increases noticeably with the load. At 22 bar, there is only one measuring point, as with a higher NH_3 content and correspondingly lower H_2 mass flow, the latter was below the measuring limit of the Coriolis flow meter. What was not initially expected is the fact that the efficiency also tends to increase with the ammonia content. However, this statement is also supported by the drop in exhaust gas temperature, which indicates an increase in efficiency at constant load. The detailed analysis of the combustion behavior and the resulting effects on efficiency and emissions is the subject of ongoing investigations. The exhaust gas temperature is already in the limit range from 50% load on. With regard to the thermal stability of the cylinder head, 650 °C must not be exceeded here. The maximum peak pressure, on the other hand, whose limit value is 220 bar, is not critical at any load point. However, if pre-ignition occurs when the hydrogen content is slightly too high, it may well be exceeded. Therefore, such combustion anomalies must be avoided in all cases by maintaining a suitable distance from the corresponding limit value for the critical hydrogen concentration.

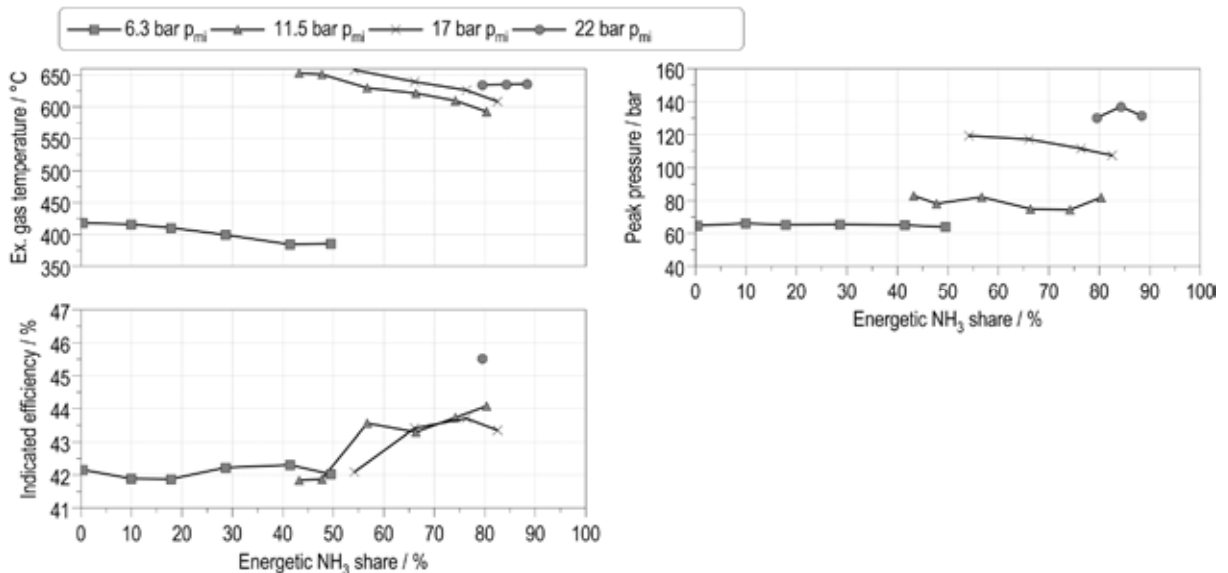


Figure 8: Exhaust gas temperature, peak pressure and indicated efficiency

In summary, the limits for the maximum ammonia content and the latter are shown in Figure 9. The following limits were set: Exhaust gas temperature = 650 °C, COV IMEP = 3%, maximum cylinder pressure = 220 bar. Only at a load of 25% does COV IMEP clearly reach an abort criterion. As already mentioned, the exhaust gas temperature is close to the limit value and the peak pressure is not critical. At loads higher than 25%, there is an abrupt transition from moderate COV IMEP below the limit value to operation that is no longer free of misfires and thus to termination.

The minimum ammonia content and thus the maximum hydrogen content always result from the occurrence of knocking and pre-ignition, apart from the 25% load point.

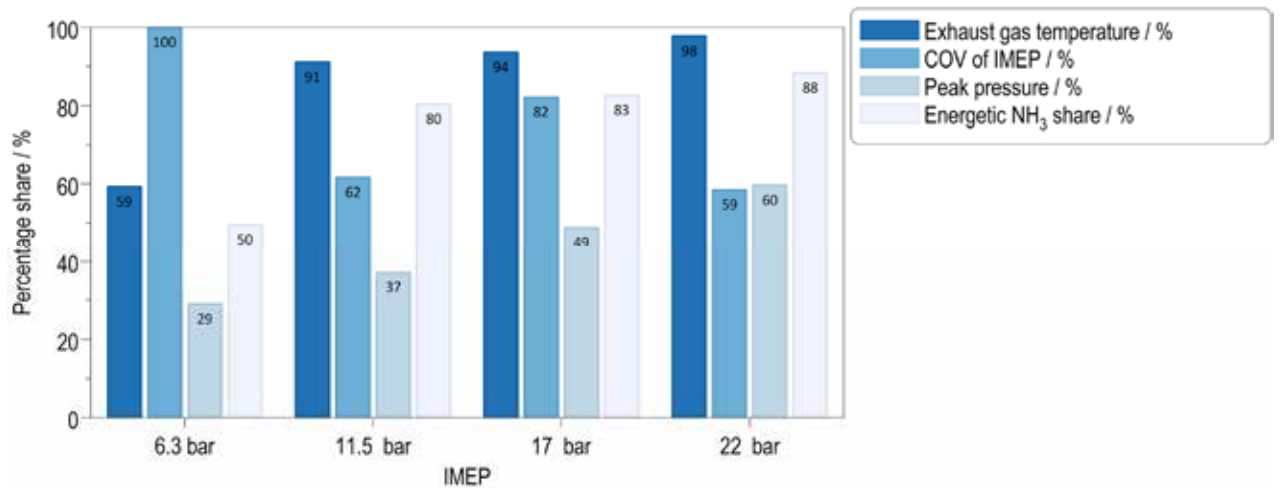


Figure 9: Termination criteria for the further substitution of ammonia for each load point

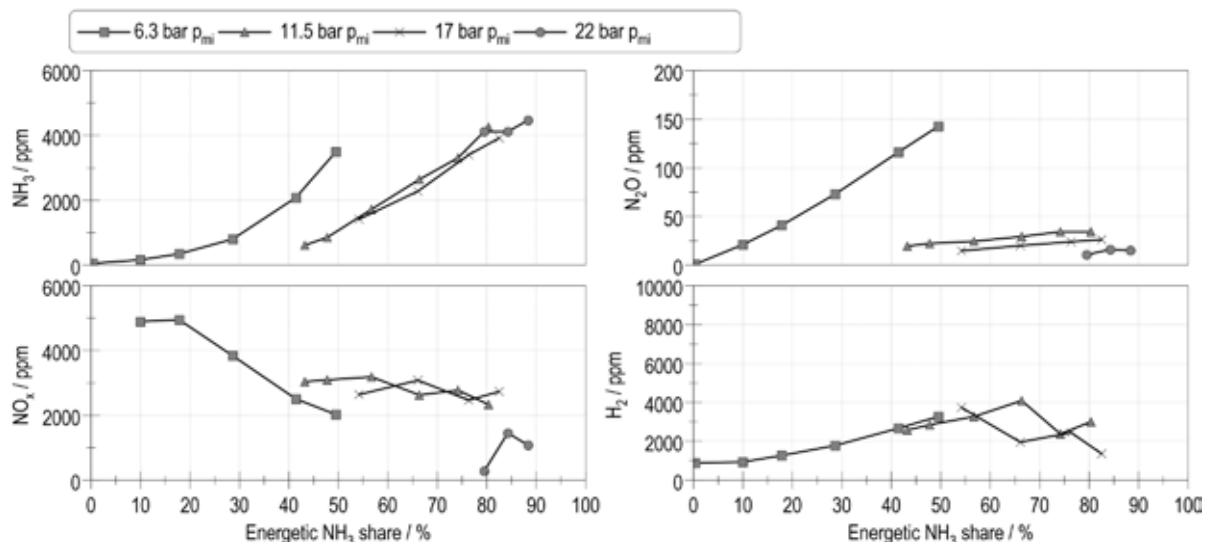


Figure 10: NO_x, NH₃, N₂O and H₂-Emissions of the ammonia-hydrogen-combustion process

Figure 10 shows the most important emissions. In $\lambda=1$ operation, NH₃ emissions increase almost linearly with the ammonia content. The peak values for the ammonia slip are between 4,000 and 4,500 ppm, irrespective of the load. At a load of 6.3 bar IMEP and lean operating mode, ammonia emissions even increase almost exponentially from zero and reach a maximum of approximately 3,800 ppm. This is also where the highest N₂O emissions occur at 150 ppm. At higher loads, the dependence on the NH₃ content is negligible and the values are in the lower two-digit ppm range. The NO_x reaches its peak value of 5,000 ppm at the lowest load and low ammonia content, respectively at high H₂ content. As the ammonia content increases further, the NO_x decreases to 2,000 ppm. At higher loads, no such dominant dependence of the NO_x concentration in the exhaust gas on the NH₃ content in the fuel is evident. In combustion engines with conventional fuels, nitrogen oxide formation is mainly caused by atmospheric nitrogen according to the Zeldovich mechanism. In this case, so-called fuel-NO can be formed at temperatures as low as 800 °C via the formation of intermediate products such as hydrocyanic acid (HCN) and hydrazine (NH_n), especially if hydrogen is present at the same time, and may explain the high nitrogen oxide emissions in the exhaust gas even at low load and high air ratio. The values for 11.5 and 17 bar IMEP are all between 2,000 and 3,200 ppm. The lowest values occur at maximum load and are well below 2,000 ppm. The hydrogen slip increases significantly and steadily with the ammonia content at the lowest load until the peak value of around 3,500 ppm is reached. At the two medium loads, no

continuous dependence is recognizable. At 50% load, the NO_x is between 2,000 and 4,000 ppm and tends to be constant at 3,000 ppm on average. At 75% load, a decrease can be seen with increasing ammonia content from 4,000 to below 2,000 ppm. It is possible that the relatively high hydrogen emissions result from flame quenching effects caused by the cooling due to the high enthalpy of vaporization of the ammonia.

4.2. ICE Simulation

The 0D/1D model is generated using the GT-Power software package from Gamma Technologies. This software tool is widely used in the automotive and engine industries.

In addition to modelling the engine parts and piping, various combustion models can be set to simulate NH₃/H₂ combustion. In the current investigation, the predictive SI-Turb model is used, which is preferred for spark-ignited engines. A key element of this two-zone model is the calculation of the combustion velocity by determining the flame front velocity. This flame front velocity is divided into a laminar and a turbulent velocity. For conventional fossil fuels, the laminar flame velocities can be obtained from a library. For blends of non-carbon fuels, however, further development was required. The basis for this data is adapted from [14].

The turbulent flame velocity formula consists of several multipliers that need to be calibrated using the previously collected measurements. Before this calibration process can begin, the engine model must be correctly constructed. A key aspect of the engine flow model is the correct modelling of the cylinder head. For example, the intake and exhaust ports cannot be represented by individual short pipes due to their complexity, so they are modelled using a discharge coefficient sub-model.

Reliable determination of discharge coefficients has a huge impact on the accuracy of 0D/1D simulations used in the engine design and optimization process. Based on these coefficients, the 1D model calculates the cylinder charge and the trapped mass after gas exchange. Traditionally, charge coefficients are determined by evaluating a large number of measurements using a stationary flow bench. Since it is not possible to subject the engine head to the experimental setup, a virtual version of the flow bench was developed using the commercial software CONVERGE and used for the investigation. TECPLOT 360 was used to analyze the results.

4.2.1. Virtual Flowbench Simulation with 3D-CFD

Theory

A discharge coefficient describes the ratio of the isentropic flow cross-section to the reference valve cross-section.

$$\alpha_V = \frac{A_{is}}{A_V} \quad (2)$$

Isentropic flow does not include friction or other hydrodynamic effects. In combination with the isentropic velocity and density (c_{is} and ρ_{is}) the mass flow can be derived.

$$\dot{m} = A_{is} \cdot c_{is} \cdot \rho_{is} \quad (3)$$

Isentropic velocity can be determined as follows.

$$c_{is} = \sqrt{\frac{2 \cdot \kappa}{\kappa - 1} \cdot R_{air} \cdot T_1 \cdot \left(1 - \left(\frac{p_2}{p_1}\right)^{\frac{\kappa-1}{\kappa}}\right)} \quad (4)$$

Where T_1 and p_1 are the temperature and pressure far upstream of the valves, p_2 is the cylinder pressure, R_{air} is the gas constant of air, and κ is the specific heat ratio of air.

Isentropic density can be derived with the density ρ_1 far upstream, the pressure ratio and specific heat κ .

$$\rho_{is} = \rho_1 \cdot \left(\frac{p_2}{p_1}\right)^{\frac{1}{\kappa}} \quad (5)$$

A more detailed description of the dependencies and assumptions can be found in [14].

The swirl and tumble generated during the intake stroke has critical effects on the cylinder charge and mixing behavior in the cylinder. To capture these effects in the 0D/1D model, additional swirl and tumble coefficients for the intake valves are required. Based on the software provider of the 0D/1D model, the following calculation method is used for the swirl coefficient, where M_S is the angular momentum flux in the swirl direction and B is the bore of the cylinder [15].

$$C_S = \frac{2 \cdot M_S}{\dot{m} \cdot u_{is} \cdot B} \quad (6)$$

The calculation of the tumble coefficient is similar to the angular momentum flux in tumble direction.

Model Setup and Results

The geometry of the virtual flow bench consists of the intake port, exhaust port, and cylinder of the engine, combined with relaxation zones to ensure numerical stabilization of the simulation. In order to study the intake valve flow from the inlet to the cylinder (defined as the downstream direction), the liner was enlarged to a length of 2 times bore. In addition, the piston was removed and replaced with a circular plane in all models. To study the backflow from the piston to the inlet (defined as the upstream direction), the inlet port was also extended with a relaxation vessel for a numerically stable simulation. The same methods were applied to the simulation models of the exhaust valve studies. As mentioned earlier, additional swirl and tumble coefficients are needed for the downstream simulations of the intake valve. For this, a region approximately 0.5 times bore vertical distance from the cylinder head is used to calculate the angular momentum flux. The four geometries for the numerical investigations are shown in Figure 11.

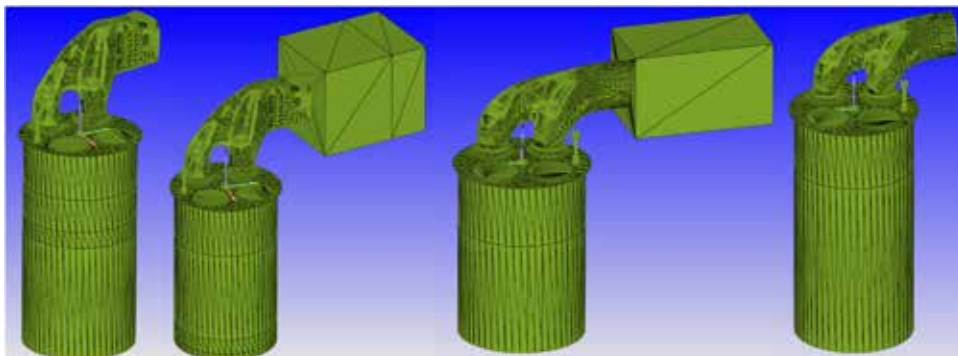


Figure 11: Geometries for the virtual flow bench

A steady-state solver with the PISO algorithm is used to compute the results. For turbulence modeling, the k-eps URANS is used. To ensure mesh independence of the numerical results, five different meshes were generated with base sizes ranging from 16 mm to 8 mm. All meshes generated include scale 2 refinements at the valves and valve seats to ensure that all flow phenomena are captured. In addition, the mesh around the surfaces is refined with fixed embeddings at scale 6. The intake and exhaust ports and the cylinder walls are refined at a scale of 4. Figure 12 shows the 16 mm and 8 mm meshes, both with a valve lift of 1.5 mm.

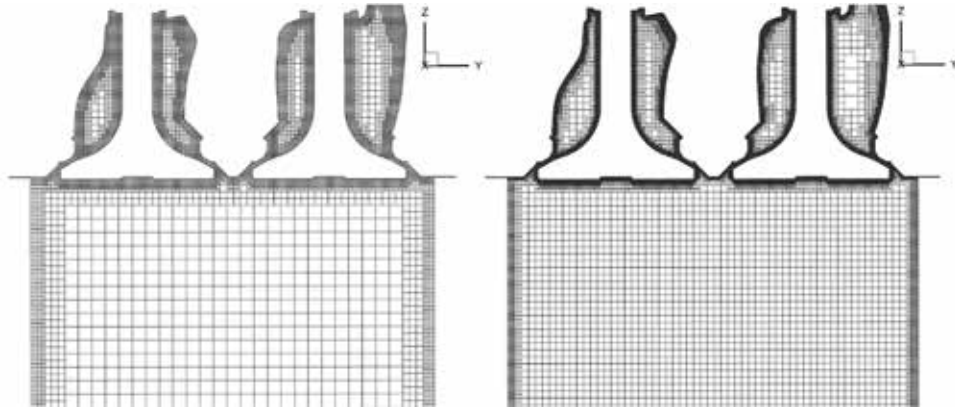


Figure 12: Lateral slices of the cylinders, coarsest (left) and finest mesh investigated

The mesh independence study simulations were all performed with 1.5 mm valve lift, as this is where the highest velocities and therefore the most complex flow phenomena occur. The following Table 3 lists the characteristics and results of the mesh independence study simulations.

Table 3 Values of mesh independence study

Base Size [mm]	Cell Count [mio.]	Mass Flow [g/s]	Deviation [%]
16	1.57	41.9942	-
14	2.08	41.2042	1.88
12	2.81	40.8229	0.93
10	4.21	40.8282	-0.01
8	6.64	40.9369	-0.27

As can be seen in Table 3, when using a 12 mm mesh, the deviation is already less than 1% compared to 14 mm. For further investigations, a base mesh size of 10 mm was chosen. To prove the pressure independence of the results, 1.5 mm lift simulations with 40 mbar to 90 mbar pressure drop between inlet and outlet boundary conditions were set up. Figure 13 shows the dependence of the flow coefficient on the pressure drop.

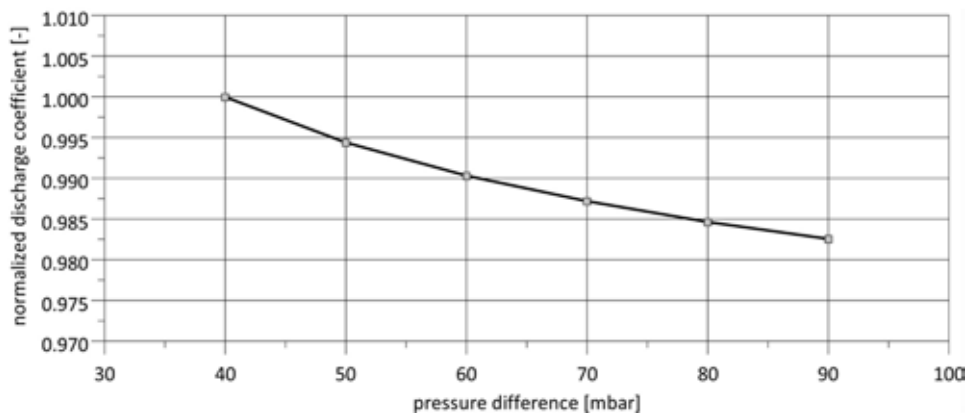


Figure 13: Normalized discharge coefficient over pressure difference

Figure 13 illustrates that as the pressure difference increases, the relative change in the discharge coefficient becomes smaller. Larger pressure differences result in higher velocities and higher computational costs. This is because smaller time steps are required during the calculation to reach the CFL criterion. Since the change in the discharge coefficient at 70 mbar compared to the 60 mbar version is -0.32% and the computational effort is still acceptable, 70 mbar pressure difference is used for the investigations. The independence of the results from the pressure difference is approximately confirmed.

Using a pressure difference of 70 mbar and 4.21 million cells, a simulation with a total wall clock time of 2 hours and 14 minutes was successfully completed. This performance was made possible by the parallel processing capability of 3 nodes with 76 cores each on a high-performance computing system.

4.2.2. 1D-Engine Modell

The relevant variables for the creation of the discharge coefficients were the valve lift, the mass flow through the cylinder ports, the upstream temperature and the physical properties of the used gas.

By applying the formulas (2-4) the following discharge coefficients can be calculated (see Figure 14).

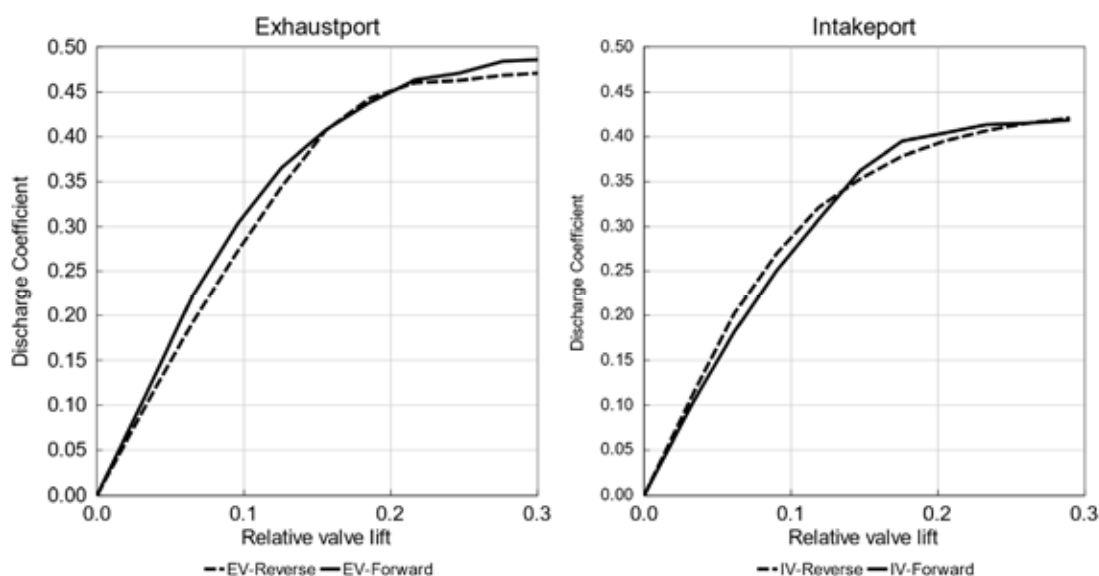


Figure 14: Calculated discharge coefficients for Intake (left) and exhaust ports (right)

Although the coefficients represent the flow well, there are still uncertainties regarding the heat transfer from the cylinder head to the charge air. This can be considered by a heat transfer model, which needs to be calibrated due to insufficient input data about the cooling flow around the intake and exhaust ports. The resulting heat transfer has a large impact on the volumetric efficiency of the engine. To calibrate this heat-transfer coefficient, a variety of motoring curves have been measured. Figure 15 shows the variation of engine speed and load respectively charge air pressure.

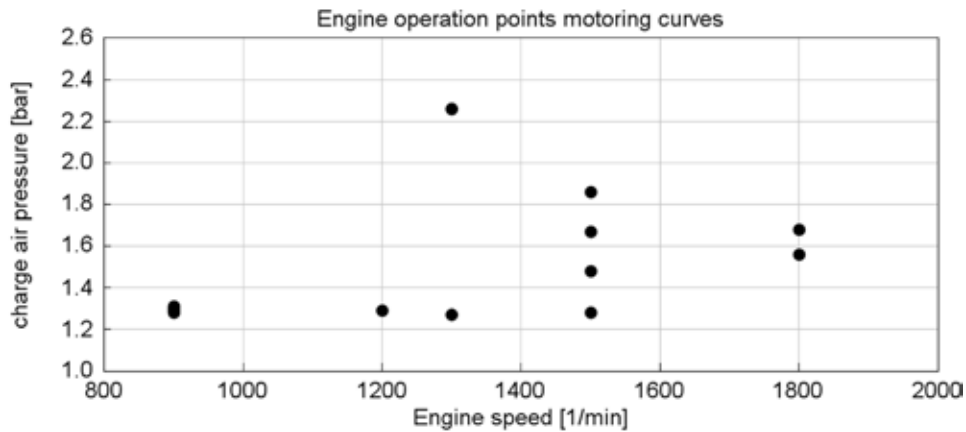


Figure 15: chosen engine operating points of the motoring curves

After the calibration has been conducted, a comparison between the measured and the simulated air masses in the cylinder is shown in Figure 16. It can be stated that the simulated air masses differ from the measurements within a 3% confidence band. The overall average error is -0.28% which is satisfying regarding the occurring normal measurement errors.

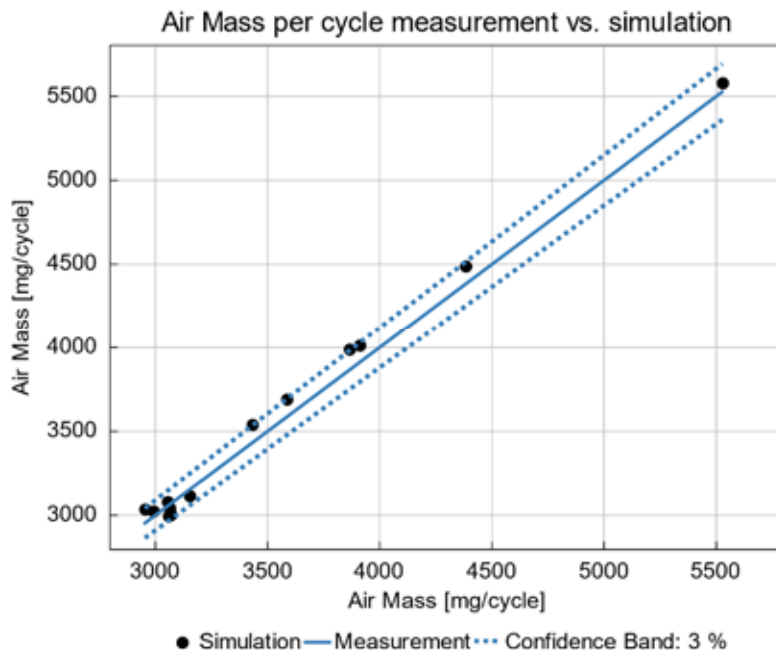


Figure 16: comparison of simulated and measured air masses per engine cycle

The resulting motoring pressure curve of a chosen operating point can be seen in Figure 17. It shows a good match between the simulation and the measurement data. With the correct cylinder head multipliers, the calibration of the combustion model can be carried out in a following step.

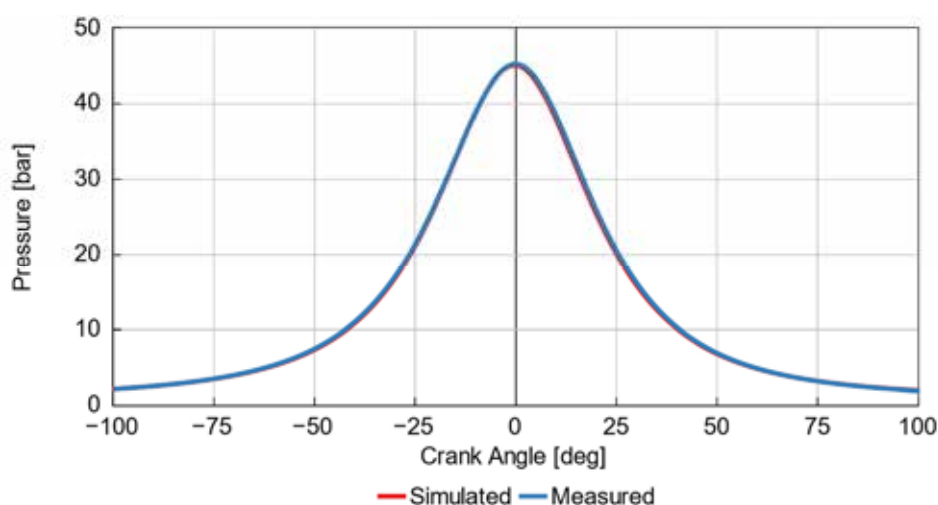


Figure 17: comparison of simulated and measured motoring curves at 1500 rpm and 1,3 bar charge air pressure

4.3. Cracker

Specifications

The cracker is developed under consideration of different boundary conditions. On the one hand, the catalyst sets a lower limit for the reaction temperature. Below this temperature, sufficient conversion is no longer achieved. The temperature has been determined in various catalyst tests. On the other hand, temperature limitations set by the material of the reactor wall are taken into account. Extensive literature research showed that the number of materials which meet the requirements set by temperature, pressure and the presence of ammonia and hydrogen is limited. However, one material could be identified that is certified for pressure applications (>500 mbar.g) and which shows promising results to withstand ammonia atmosphere up to 750 °C. This temperature limit is currently being verified by means of isothermal exposure tests in ammonia atmosphere at high temperature and high pressure including subsequent metallographic examinations. In addition to the temperature limits set by the catalyst and the reactor material the cracker has to fulfill the requirements set by the engine. The main requirements are summarized in Table 4. The Cracker has to provide a hydrogen power of 150 kW_{H₂} which corresponds to a hydrogen mass flow of 4.5 kg/h. The pressure of the product gas needs to be at least 8 bara. Moreover, it is desirable that the product temperature is below 60 °C and the residual ammonia content is less than 5 mol%. According to the requirements imposed by mobile application, a monolithic catalyst system is to be used.

Table 4: Boundary conditions for the development of the ammonia cracking plant

Description	Value
Hydrogen power of the cracker product gas	150 kW
Cracker product gas pressure	> 8 bara
Cracker product gas temperature	< 60 °C
Residual ammonia content of the cracker product gas	$x_{\text{NH}_3} < 5 \text{ mol\%}$ (corresponds to conversion > 90%)
Catalyst	Monolith

The heat required for the endothermic reaction is to be provided either by a) a hot gas generated by a gas burner or b) electrically, whereby the burner is to be operated with ammonia and a certain amount of the cracker product gas. Experiments at ZBT have shown that the combustion of a fuel with a composition of $x_{\text{NH}_3} = 40 \text{ mol\%}$, $x_{\text{N}_2} = 15 \text{ mol\%}$ and

$x_{H_2} = 45$ mol% has similar properties to the combustion of natural gas. Therefore, an ammonia content of 40 mol% is assumed.

Process development

A simplified flow diagram of the gas-heated process developed in Aspen Plus® is depicted in Figure 18. Ammonia is fed to the process as a gas (10 bar, 25 °C) and is preheated in a first heat exchanger (1) before being decomposed in the reactor (4). The product gas is then used to preheat the educt. A partial flow of the product gas is taken downstream of the first heat exchanger (1) and is fed to the burner (5) along with a second ammonia educt stream. In a second heat exchanger (2), the product gas is cooled to the required temperature of 60 °C, thereby preheating a secondary air stream. The temperature of the secondary air stream is further increased by the flue gas emitting the reactor in a third heat exchanger (3), thereby cooling down the exhaust gas. The preheated secondary air stream is used to control the flue gas temperature and, as the flue gas is used to heat the reactor, in the end to control the reaction temperature as well as the reactor wall temperature.

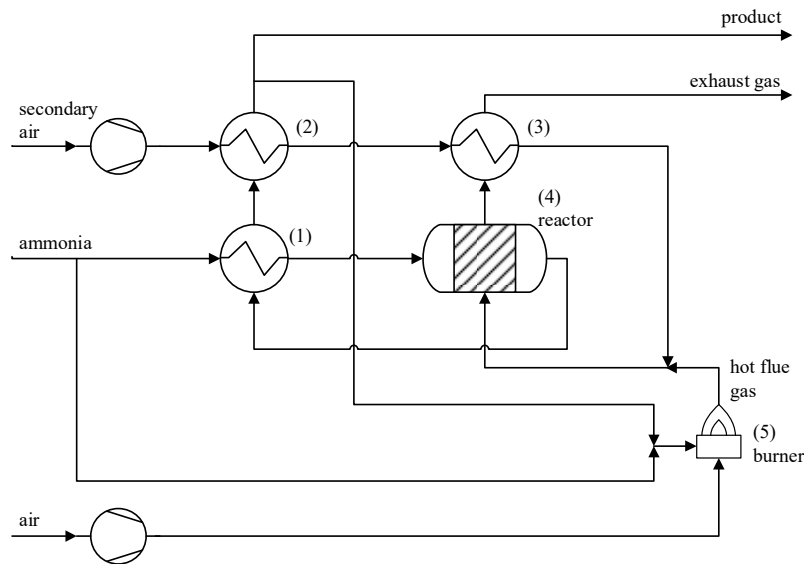


Figure 18: Simplified process flow diagram of the ammonia cracker

The amount of energy provided by the burner is 35 kW and the total amount of ammonia required is approximately 32 kg/h. The efficiency of the process is calculated according to equation (7) and is based on the lower heating value (H_L) and considers the energy required for compressors but neglects heat losses. In addition, since the system should be able to work autarkic on a ship, it is assumed that all electric energy consumed by the cracker system has to be produced by the GenSet with an efficiency of $\eta_E = 38\%$. The compressor efficiency is conservatively estimated at $\eta_C = 30\%$.

$$\eta_{Cr} = \frac{\dot{m}_{H_2} \cdot H_{LH_2} + \dot{m}_{NH_3} \cdot H_{LNH_3}}{(\dot{m}_{NH_3B} + \dot{m}_{NH_3C}) \cdot H_{LNH_3} + \frac{1}{\eta_C \cdot \eta_E} \cdot P_c} \quad (7)$$

For the given boundary conditions set by the engine, the wall material and the catalysts a maximum efficiency of 71% is achieved.

A simplified flow diagram of the electrically heated process is illustrated in Figure 19. Similar to the gas-heated process, ammonia is fed to the system at 25 °C and 10 bar and is preheated in a first heat exchanger (1). The preheated ammonia is decomposed in an electrically heated reactor (2). The hot product is used to preheat the ammonia feed. The product outlet temperature of 145 °C exceeds the limit of 60 °C so additional cooling is necessary. Since this system does not need a burner and a secondary air system it is much less complex. Also due

to the missing secondary air system no compressors are necessary which leads to an increased efficiency of up to 80%. Because of its lower complexity and higher efficiency compared to the gas heated process, the electrically heated system is being further developed. Based on the results of the process simulation, the components can be designed in detail in a following step.

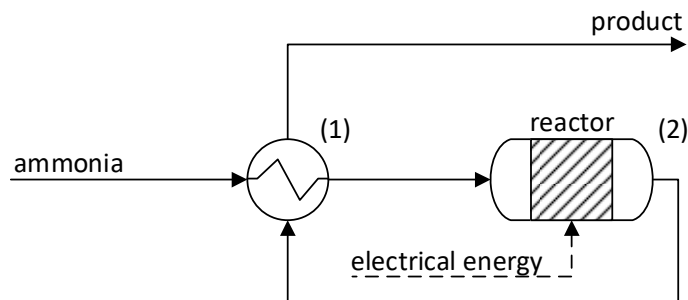


Figure 19: Simplified process flow diagram of the electrically heated ammonia cracker

5. Conclusion & Outlook

The pressing necessity of CO₂ emission reduction in all industries implies that solutions for the shipping branch must be developed as well with high priority. Beside others, green ammonia looks like a promising fuel for ships. Worldwide trading and handling of ammonia are already in place and ease the establishment of a respective marine fuel supply chain. Ammonia can act as an attractive hydrogen carrier because much less effort in transport and distribution in comparison to pure hydrogen is required. Production can happen at locations of renewable energy generation e.g. from solar, wind and hydropower.

In the presented project a maritime propulsion system is developed based on a new concept consisting of a pressurized ammonia cracker and a high-speed engine. The envisaged use case for this setup are vessels for inland water ways. Therefore, important topics are the system integration for future simple handling and the safety aspects to be considered on board. The technological aspects and challenges for establishing such a system were discussed in this paper. This includes especially the partly ammonia cracking towards hydrogen at engine boost pressure level as integral part of the combustion process as well as the impacts of ammonia on the engine setup and operation. By deepening the simulation tasks, fed by the results from systematic investigations on a single-cylinder engine, the complete process is optimized. This enables us to prepare the multi-cylinder engine by receiving the latest setup based on the final simulation and single-cylinder engine results.

As soon as the containerization of the multi-cylinder engine is finalized, the engine container is going to be tested at the CAMPFIRE Open Innovation Lab (COIL) near to Rostock/Germany. Later, this will be married with the ammonia cracker as completed system for initial and later endurance testing.

6. Acknowledgements

This work was carried out within the CAMPFIRE project of the Hydrogen Flagship Project TransHyDE and was funded by German Federal Ministry for Education and Research. Convergent Science provided CONVERGE licenses and technical support for this work. The authors acknowledge support by the state of Baden-Württemberg through bwHPC.

References

- [1] Nathan Gray et al. "Decarbonising ships, planes and trucks: An analysis of suitable low-carbon fuels for the maritime, aviation and haulage sectors". In: *Advances in Applied Energy* 1 (2021), p. 100008. ISSN: 26667924. DOI: 10.1016/j.adapen.2021.100008.
- [2] J. Walter, M. Borning, and A. Moser. "Analyzing the Potential Production Amount of Synthetic Fuels in Germany". In: *2021 IEEE Madrid PowerTech*. IEEE, 2021, pp. 1–6. ISBN: 978-1-6654-3597-0. DOI: 10.1109/PowerTech46648.2021.9494888.
- [3] Ghassan Chehade and Ibrahim Dincer. "Progress in green ammonia production as potential carbon-free fuel". In: *Fuel* 299 (2021), p. 120845. ISSN: 0016-2361. DOI: 10.1016/j.fuel.2021.120845.
- [4] Aaishi Ashirbad and Avinash Kumar Agarwal. "Scope and Limitations of Ammonia as Transport Fuel". In: *Greener and Scalable E-fuels for Decarbonization of Transport*. Ed. by Avinash Kumar Agarwal and Hardikk Valera. Energy, Environment, and Sustainability. Singapore: Springer, 2022, pp. 391–418. ISBN: 978-981-16-8343-5. DOI: 10.1007/978-981-16-8344-214.
- [5] Rachael H. Dolan, James E. Anderson, and Timothy J. Wallington. "Outlook for ammonia as a sustainable transportation fuel". In: *Sustainable Energy & Fuels* 5.19 (2021), pp. 4830–4841. DOI: 10.1039/D1SE00979F.
- [6] A. Feindt. *Ammoniak in der Schifffahrt*. Hamburg, 2023
- [7] Hinrich Mohr. *CAMPFIRE – Development of an Ammonia-fueled Cracker-Engine-Power Unit for Inland Waterway Shipping*. Hamburg, Sept. 6, 2022.
- [8] Sandra Tjaden. *Struktur der deutschen Binnenschiffsflotte*. Ed. by Wasserstraßen- und Schifffahrtsverwaltung des Bundes. Apr. 26, 2023. url: <https://www.forschungsinformationssystem.de/servlet/is/123471/> visted at June 13, 2023.
- [9] Volker Renner and Wolfgang Bialonski. "Technische und wirtschaftliche Konzepte für flußangepaßte Binnenschiffe". In: *Versuchsanstalt für Binnenschiffbau e.V., Duisburg 1701* (2004).
- [10] Cecil E. Vanderzee und Delbert L King „The enthalpies of solution and formation of ammonia” *The Journal of Chemical Thermodynamics* 4(5):675-683, 1972.
- [11] Jacob A. Mouljin et al. "Monolithic Catalysts and Reactors: High Precision with Low Energy Consumption" *Advances in Catalysis Volume 54, Chapter 5* (2011)
- [12] Zaev, I., Smirnov, S., and Gordeev, V., "Performance of the Mixture of Ammonia and Ammonia Decomposition Products as a Carbon-Free Fuel for Spark Ignition Engines," *SAE Technical Paper 2023-01-1638*, 2023, <https://doi.org/10.4271/2023-01-1638>. Peoples Friendship University of Russia
- [13] Pessina, V.; Berni, F.; Fontanesi, S.; Stagni, A.; Mehl, M. (2022): Laminar flame speed correlations of ammonia/hydrogen mixtures at high pressure and temperature for combustion modeling applications. In: *International Journal of Hydrogen Energy* 47 (61), S. 25780–25794. DOI: 10.1016/j.ijhydene.2022.06.007
- [14] Basshuysen, R. v.; Schäfer, F. (2015): *Handbuch Verbrennungsmotoren*. Wiesbaden, S.487 DOI: 10.1007/978-3-658-04678-1
- [15] *GAMMA TECHNOLOGIES: Engine Performance Application Manual: Version 2022*. S.20

Session 4

Grundlagenuntersuchungen Fundamental studies

**Moderation: Moderation: Prof. Friedrich Wirz
Technische Universität Hamburg**

Plain Bearing Performance in Applications Utilizing Alternative Fuels

Gleitlager-Performance in Anwendungen unter Verwendung alternativer Treibstoffe

A. Zunghammer*, S. Kirchhamer, E. Bakk

Miba Gleitlager Austria GmbH, Laakirchen

Abstract

The increasing demand for sustainable and eco-friendly transportation solutions has led to the development of alternative-fueled engines. These engines utilize non-conventional fuels such as methanol, hydrogen, and ammonia, which have the potential to reduce greenhouse gas emissions and mitigate the environmental impact of internal combustion engines.

This paper investigates the performance of plain bearings in alternative-fueled engines, focusing on the tribological behavior, material compatibility, and design considerations. A comparative analysis of plain bearing performance in engines using different alternative fuels is presented, highlighting the challenges and opportunities associated with each fuel type.

Furthermore, the paper examines the specific challenges faced by plain bearings in internal combustion engines fueled by ammonia, hydrogen, and methanol. These fuels, while offering significant environmental benefits, introduce unique operating conditions that can affect bearing performance and longevity. To address these new challenges, the paper explores the development of new test methods tailored to the unique requirements of engines using these alternative fuels. By optimizing bearing performance in ammonia, hydrogen, and methanol-fueled engines, this research aims to facilitate the widespread adoption of these fuels and support the transition towards more sustainable transportation systems.

The study also explores the influence of lubrication and surface engineering on bearing performance, emphasizing the need for advanced materials and coatings to ensure reliable operation under varying operating conditions. Finally, the paper proposes design guidelines and recommendations for optimizing plain bearing performance in alternative-fueled engines, paving the way for more efficient and environmentally friendly transportation systems.

Kurzfassung

Die steigende Nachfrage nach umweltverträglichen und nachhaltigen Verkehrslösungen hat zur Entstehung von Motoren mit alternativen Kraftstoffen geführt. Diese Motoren setzen auf unkonventionelle Treibstoffe wie Methanol, Wasserstoff und Ammoniak, die dazu beitragen können, die Emission von Treibhausgasen zu senken und die ökologischen Auswirkungen von Verbrennungsmotoren zu mindern.

In dieser Studie wird die Leistungsfähigkeit von Gleitlagern in Motoren mit alternativen Kraftstoffen untersucht, wobei der Fokus auf tribologischen Eigenschaften, Materialkompatibilität und konstruktiven Aspekten liegt. Eine vergleichende Analyse der Gleitlagerperformance in Motoren, die unterschiedliche alternative Kraftstoffe einsetzen, wird vorgestellt und zeigt die Herausforderungen und Möglichkeiten im Zusammenhang mit den verschiedenen Kraftstoffarten auf.

* Speaker/Referent

Zudem betrachtet die Arbeit die besonderen Schwierigkeiten, mit denen Gleitlager in Verbrennungsmotoren konfrontiert sind, die mit Ammoniak, Wasserstoff und Methanol betrieben werden. Obwohl diese Kraftstoffe erhebliche Umweltvorteile bieten, ergeben sich daraus spezielle Betriebsbedingungen, die die Leistung und Lebensdauer der Lager beeinträchtigen können. Um diesen neuen Herausforderungen entgegenzuwirken, behandelt die Studie die Entwicklung neuer Testverfahren, die speziell auf die Anforderungen von Motoren abgestimmt sind, die alternative Kraftstoffe nutzen. Durch die Verbesserung der Lagerleistung in Motoren, die mit Ammoniak, Wasserstoff und Methanol betrieben werden, soll diese Forschung die breite Akzeptanz dieser Kraftstoffe fördern und den Wandel hin zu nachhaltigeren Verkehrssystemen unterstützen.

Des Weiteren analysiert die Studie den Einfluss von Schmierstoffen und Oberflächenbehandlung auf die Lagerleistung und unterstreicht die Bedeutung von hochentwickelten Materialien und Beschichtungen, um einen zuverlässigen Betrieb unter variierenden Betriebsbedingungen sicherzustellen. Abschließend werden in der Arbeit Richtlinien und Empfehlungen für die Optimierung der Gleitlagerleistung in Motoren mit alternativen Kraftstoffen vorgeschlagen, um den Weg für effizientere und umweltschonendere Verkehrssysteme zu ebnen.

1. Introduction

In recent years, the necessity to reduce CO₂ emissions and combat climate change has led to an increasing interest in the decarbonization of the internal combustion engine. The development and implementation of sustainable engine applications are pivotal steps towards mitigating the environmental impact of the transportation industry. Within this context, the evaluation of plain bearing performance in sustainable engine applications becomes of great significance.

Decarbonizing the internal combustion engine is a central issue addressed in this context. New alternative fuels such as ammonia (NH₃), hydrogen (H₂), or methanol (MeOH) are being considered as potential solutions for reducing CO₂ emissions. The interactions of combustion products and fuel residues with plain bearing materials, as well as their reactions with oils, must also be examined to assess their impact on the performance of the plain bearings.

A key driver of the decarbonization of the internal combustion engine is various regulations, such as those set by the International Maritime Organization (IMO) for reducing CO₂ emissions in the marine segment. These regulations set ambitious targets for reducing greenhouse gas emissions and require the development and implementation of sustainable technologies and fuels in the shipping industry.



Figure 1: IMO GHG Strategy 2023 (DNV Maritime Forecast to 2050)

Another significant aspect is the growing demand for sustainable use of engine oils. The use of innovative, fully synthetic base oils, which do not originate from fossil sources, such as polyester and polyglycols, is gaining increasing popularity. This leads to new oil formulations and additives, which can play a crucial role in material compatibility within the engine. Additionally, these more sustainable oil formulations, as well as longer oil lifetimes and extended oil change intervals, contribute to more efficient resource use and a reduction in environmental impact.

All these potential changes in the combustion engine system make it necessary to adapt the performance of plain bearings to the new requirements arising from the use of alternative fuels such as methanol, hydrogen, and ammonia. Overall, the analysis of plain bearing performance in environmentally friendly engine applications provides a detailed insight into the various aspects and helps to expand the knowledge about the challenges and opportunities in this area.

In the upcoming chapters, we will thoroughly discuss the properties of alternative fuels in combustion engines and introduce the test strategies developed by Miba, which aim to comprehensively evaluate the new requirements for plain bearing materials.

2. Alternative Fuels

The use of alternative fuels has significant impacts on the combustion characteristics within the engine as well as on the performance of the plain bearings.

Table 1: Overview of the characteristics of alternative fuels¹:

Fuels	Energy density [MJ/L]	Wear	Corrosion	Cavitation	Storage
Hydrogen	8,0	+++ (knocking)	+	+++	Gas / Liquid
Methanol	15,7	++	+	++	Liquid
Ammonia	11,3	++	++	+++	Liquid
SAF ²	35	0	0	0	Liquid

While hydrogen as an alternative fuel in internal combustion engines offers several advantages, the rapid propagation of the flame front can also have negative impacts. An increased combustion speed can heighten the risk of knocking, particularly under high loads and rotational speeds. Knocking is caused by the spontaneous autoignition of the fuel, leading to inconsistent pressure rises within the combustion chamber, potentially damaging both the engine and the plain bearings. Moreover, local hot spots or oil and ash residues in contact with hydrogen can lead to uncontrolled ignition. To manage the negative effects of the rapid flame front propagation with hydrogen, new additive formulations in the engine oil can be utilized, among other things.

¹ Zhifeng, Z. 2023, Bearing testing and validation to optimize bearing design, CIMAC, 2023, Busan, 025

² SAF (Sustainable Aviation Fuel) – Nachhaltiger Luftfahrttreibstoff hergestellt aus H₂ und CO₂ als Kerosin-Ersatz. [<https://www.lufthansagroup.com/de/verantwortung/klima-umwelt/sustainable-aviation-fuel.html>]

In the case of ammonia, corrosion resistance is a crucial factor in the development of new engines. Due to the strong alkaline character of ammonia and its tendency to form copper complexes, the selection of materials used in an ammonia-powered engine is of paramount importance.

Furthermore, all alternative fuels, due to their high hydrogen content chemical structure, generate significantly more water during combustion compared to conventional diesel fuel. If the water content in the oil rises to a certain degree, the risk of cavitation and tribological problems at the plain bearings increases.

All engine adjustments for efficiency and new fuels affect the lifespan and stability of the engine components. New fuel tank systems and reformers, as well as new exhaust aftertreatment systems, are being developed, altering the engine design and the environment of their components. Since the crank mechanism, including the plain bearings, is one of the core components at the heart of the engine, investigations for safe long-term operation are necessary. To compensate for the negative influences of blow-by, a new development of lubricants may be required, affecting the plain bearing tribology and stability. Consequently, the development and testing of plain bearing types must be adjusted.

3. Bearing Performance

The testing and evaluation processes for types of sliding bearings encompass both laboratory trials, such as the assessment of corrosion resistance and long-term stability, as well as the exploration of tribological properties, including the formation of tribo-layers at the interfaces of the friction partners. Additionally, test stand tasks are conducted to simulate start/stop behaviour, hydrodynamic behaviour, or dirt compatibility.

The adjustment of the parameters to be tested (load, speed, oil temperatures, etc.) to the respective engine application is crucial in order to enable a precise simulation of the real operating conditions.

Table 2: Expected bearing performance in different applications:

Bearing test parameters	High Speed Engine	Medium Speed Engine
Load profile	< 95 MPa	< 49 MPa
Rotation speed	< 18 m/s 14 m/s average	< 15 m/s 11 m/s average
Max. lifetime	< 60.000 hours	< 60.000 hours
Start/Stop cycles	< 1.000 cycles	< 1.000 cycles
Dirt resistance	++	+++
Cavitation resistance	++	++
Corrosion resistance	+++	++

3.1. Oil Material Compatibility Tests

In light of the transition from conventional diesel engines to alternative fuel systems, it is crucial for Miba as a plain bearing manufacturer to consider the entire engine system, from combustion to the use of various engine oils.

The choice of the correct engine oil can significantly affect the longevity and performance of plain bearings. Incorrect additive packages and the associated oil aging in alternative fuels (also in connection with combustion products and blow-by of unburned fuel) can impair the bearing's life span. Therefore, it is of utmost importance to select the appropriate oil-material combinations for each application.

To identify and quantify potential chemical interactions between plain bearing materials and engine oils, both in their new and aged state, specialized test procedures based on static oil-material compatibility tests have been developed. These procedures are based on a combination of the ASTM D130³ und VDMA 24570⁴ standards. As part of the test process, material strips (pure metals and plain bearing material compounds) are immersed in new or aged oil at temperatures between 60°C and 180°C. The samples are weighed at regular intervals to assess weight loss and the visual appearance as an indicator of susceptibility to corrosion.

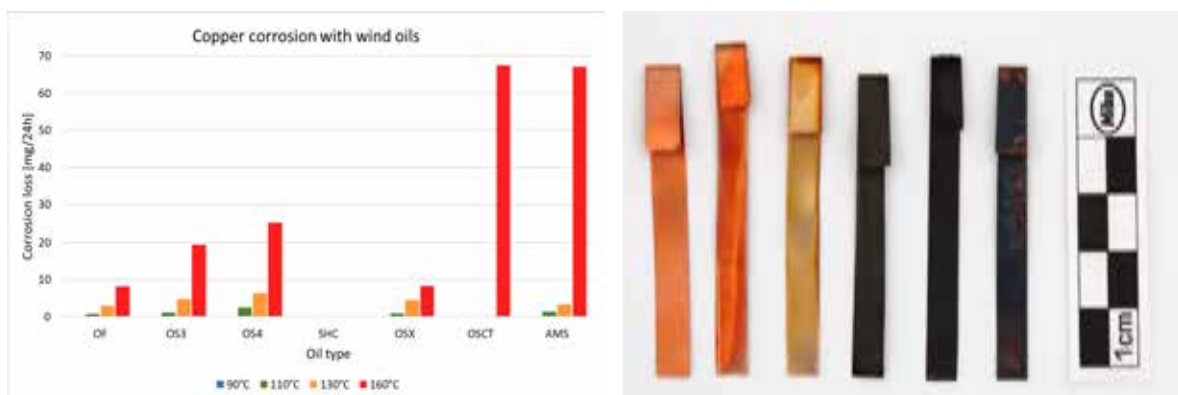


Figure 2: Oil Material Compatibility Tests for Copper Materials

Miba is currently developing a test setup for artificial oil aging (on a small scale for oil volumes < 200 mL) to better understand the processes of oil aging in the engine and their effects on the bearing material. For this purpose, oil samples are aged under the influence of various combustion products and alternative fuels. In combination with the previously described static oil-material compatibility tests and tribometer trials, the effects of different conditions and fuels on the bearing performance can be evaluated.

The primary objective of oil aging and oil-material compatibility tests is to reproduce field results at a laboratory scale and to integrate them into test rigs in collaboration with external partners and universities. This contributes to the development of new materials and technologies for future applications.

³ ASTM D130 – Standard Test Method for Corrosiveness to Copper from Petroleum Products by Copper Strip Test

⁴ VDMA 24570:1999-03 – Fluidtechnik - Biologisch schnell abbaubare Druckflüssigkeiten - Prüfung der Einwirkung auf Legierungen aus Buntmetallen



Figure 3: Laboratory scale artificial oil ageing.

3.2. Tribological Testing

To gain a deeper understanding of the tribological interactions between different material-oil combinations and thus be able to draw direct conclusions about bearing performance in engine applications, Miba conducts comprehensive tribological investigations. The insights gained from these experiments enable statements about the formation of tribofilms, the influence of aged engine oils (especially in connection with alternative fuels) and possible tribocorrosion phenomena in use. This information contributes to optimizing the performance and longevity of plain bearings under various operating conditions and to support future developments.

For the tribological investigations, Miba uses a ring-on-disc tribometer. Different bearing materials are tested with application-specific engine oils. In the tribological tests, both the coefficient of friction and the contact potential are measured. The measurement of the contact potential serves, among other things, as in-situ detection for the build-up of insulating, tribologically active boundary layers.

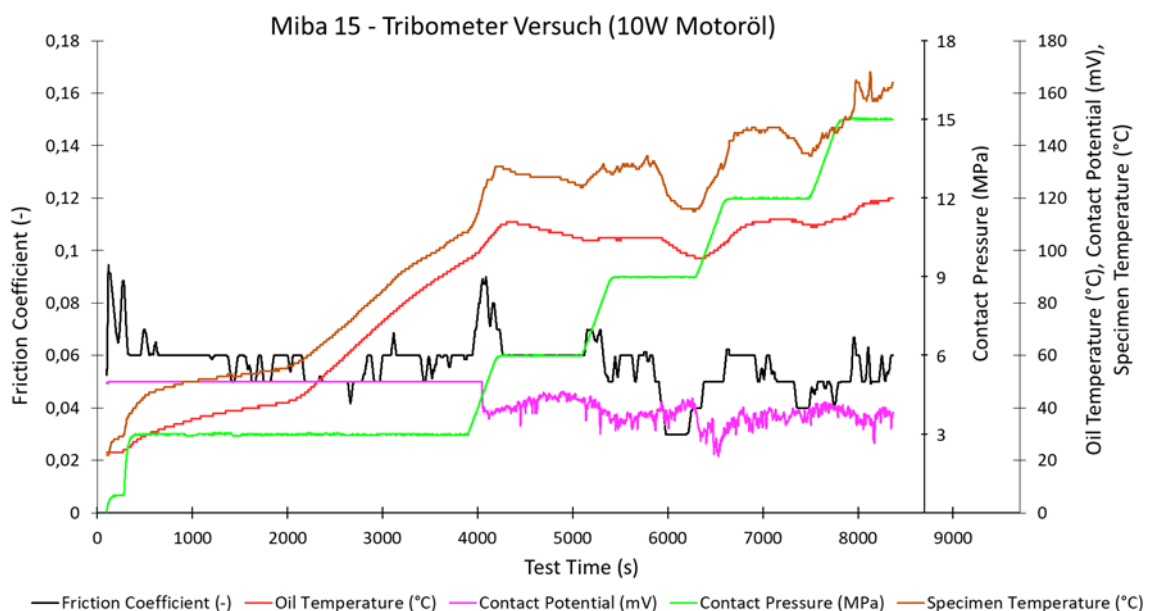


Figure 4: Tribometer-Test with Aluminium-Tin-Material (Miba 15)

Through the targeted examination of friction properties and wear behavior under controlled conditions, the tribometer enables the systematic analysis of the interactions between different sliding bearing materials and the additives or degradation products present in the lubricant. The insights gained can help to better understand the wear and friction mechanisms in the engine.

3.3. Investigations on the bearing test rigs

Bearing test bench analyses occupy a central position in assessing the wear resistance and load capacity of plain bearings. To achieve meaningful results, the bearings are examined under various load profiles and speeds, with test parameters such as load, sliding speed, and oil specifications meticulously selected. The results are determined through wear measurements and removal rates at the bearing edges and in the center of the main load area to provide a comprehensive picture of the bearing's performance.

In addition to the regular wear test program, long-term studies can be conducted to simulate and evaluate the wear resistance of the bearings over extended operating periods. During the test execution, the same conditions as in the previously described wear tests are maintained, but the test duration is extended to differentiate long-term wear from run-in wear, thus enabling a more precise assessment of the bearing's longevity.

Table 3: Miba test programs on the bearing test rigs:

Test program Application Test parameter	Test objectives	Test criteria
Load / Wear Medium speed 75 MPa, 12 m/s, 15 h	Wear resistance	Wall thickness [µm] Fatigue
Load / Wear Medium speed 75 MPa, 12 m/s, 70 h	Long-time wear resistance	Wall thickness [µm] Fatigue
Load / Wear High speed 75 MPa, 20 m/s, 15 h	Wear resistance	Wall thickness [µm] Fatigue
Seizure Test Step Load, 12 m/s	Seizure (Tribology)	Load capability [MPa]
Misalignment Medium & High Speed 75 MPa, 12 m/s, 15 h	Adaptability	Load distribution Seizure
Continuous dirt Medium & High Speed 75 MPa, 16 m/s	Dirt Resistance	Dirt contamination in the oil [shocks]

An essential aspect in the evaluation of plain bearings is the behavior of bearing materials under mixed friction or boundary lubrication conditions. Start-stop studies simulate the startup process of an engine through cyclic speed variations at constant load, confronting the bearings with changing friction situations.

Static and dynamic load tests complement the investigations by determining the load limits of the bearings and providing information about the seizure behavior under extreme conditions. The bearings are subjected to a successively increasing test load until failure occurs, to determine the resilience under extreme conditions.

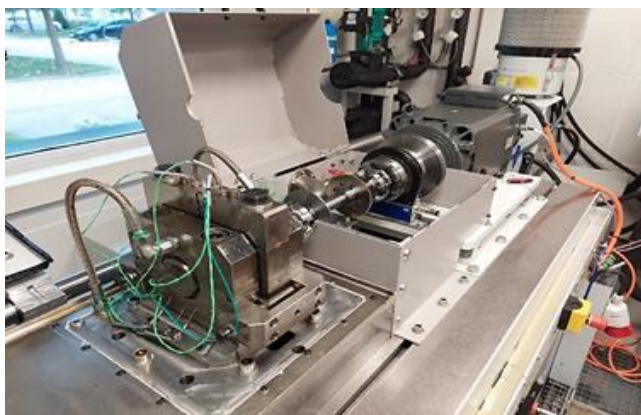


Figure 5: Miba test rig

Dirt resistance tests aim to assess the robustness of bearing materials against hard particles that can accumulate through contaminants or abrasion in the oil. In these tests, the bearings are operated under a defined load and sliding speed, while hard particles (e.g., silicate particles) are directly introduced into the oil supply line. This emulates conditions under which bearings must operate in contaminated environments.

Misalignment and adaptation tests examine the adaptability of the bearings under local overload and, in particular, the sensitivity to edge loading. These tests simulate local overloads that can be caused by improper installation of the bearings or irregularities in the crankcase. The bearings are operated under a defined load and sliding speed, while the drive shaft is slightly tilted to induce misloads, edge loads, and local overload of the plain bearings.

The bearing test benches provide the opportunity to thoroughly evaluate the properties of plain bearings under various conditions in the engine and thus make a decisive contribution to the development of efficient and sustainable technologies.

4. Summary

The impending transformations regarding performance improvements, fuel consumption minimization, and environmental regulations, such as alternative fuels, will also have implications for engine components and necessitate a continuous further development of bearing materials and types. Against this backdrop, it is indispensable for Miba to continuously expand internal testing capacities and develop innovative testing procedures in order to meet the challenges ahead in the coming years.

A comprehensive testing concept, based on several different levels (lab tests, tribometers, and bearing test benches), allows for future requirements of bearing materials to be estimated and the materials to be optimized accordingly. By expanding expertise in the investigation of plain bearing materials, such as the development of artificial oil aging concepts and cavitation tests on a laboratory scale, Miba is well-equipped to successfully meet the upcoming challenges brought about by new trends in engine development.

References

- [1] <https://www.lufthansagroup.com/de/verantwortung/klimaumwelt/sustainable-aviation-fuel.html>
- [2] Zhifeng, Z. 2023, Bearing testing and validation to optimize bearing design, CIMAC, 2023, Busan, 025
- [3] ASTM D130 – Standard Test Method for Corrosiveness to Copper from Petroleum Products by Copper Strip Test
- [4] VDMA 24570:1999-03 – Fluidtechnik - Biologisch schnell abbaubare Druckflüssigkeiten

Potential and limitations of different hydrogen combustion concepts for power generation applications

Potenziale und Grenzen unterschiedlicher Wasserstoffverbrennungskonzepte für Kraftwerksanwendungen

**Dr. N. Wermuth^{12*}, Dr. M. Lackner¹, Dr. G. Kammel¹, Dr. M. Malin¹,
Prof. Dr. A. Wimmer¹², Dr. M. Url³, Dr. N. Spyra³,**

¹LEC GmbH, Graz, Austria; ²Technical University Graz, Austria; ³INNIO Jenbacher GmbH & Co OG, Austria

Abstract

Global warming is one of the biggest challenges the world faces in the 21st century. The global carbon dioxide concentration in the atmosphere is continuously rising by 2 – 3 ppm per year and has already passed the 420 ppm-mark. Power and heat generation is responsible for about a quarter of greenhouse gas emissions globally. While the worldwide demand for electricity is projected to increase two to threefold until 2050, the European Union made a commitment to decrease greenhouse gas emissions in the same time to net-zero. The key element to achieving this ambitious goal is a global transition from a fossil fuel-based energy system to a system that is built on renewable energy sources. The fluctuating nature of renewables makes it necessary to deploy dispatchable power generation capability for grid balancing and peak shaving. Hydrogen can be produced easily from renewable energy sources via electrolysis during times with an oversupply of electricity and be used for power generation in an internal combustion engine when electricity demand exceeds the supply.

Dedicated hydrogen engines that are designed for hydrogen-specific requirements such as high charge dilution and high boost pressure have the potential to achieve similar power output as natural gas fueled power plants. This article describes various hydrogen combustion concepts and focusses on hydrogen direct injection. Based on the experimental evaluation of the different concepts on single cylinder research engines and computational fluid dynamics simulation the trade-offs in dilution, knocking and nitrogen oxide emissions are compared and the limiting factors and future research needs are identified.

Kurzfassung

Die globale Erwärmung ist eine der größten Herausforderungen, vor denen die Welt im 21. Jahrhundert steht. Die globale Kohlendioxidkonzentration in der Atmosphäre steigt kontinuierlich um 2 bis 3 ppm pro Jahr und hat bereits die 420-ppm-Marke überschritten. Die Strom- und Wärmezeugung ist für etwa ein Viertel der weltweiten Treibhausgasemissionen verantwortlich. Während die weltweite Stromnachfrage bis 2050 voraussichtlich um das Zwei- bis Dreifache ansteigen wird, hat sich die Europäische Union verpflichtet, die Treibhausgasemissionen in der gleichen Zeit auf null zu senken. Das Schlüsselement zur Erreichung dieses ehrgeizigen Ziels ist ein weltweiter Übergang von einem auf fossilen Brennstoffen basierenden Energiesystem zu einem System, das auf erneuerbaren Energiequellen beruht. Die fluktuierende Natur der erneuerbaren Energien macht es erforderlich, zusätzliche Kraftwerkskapazitäten zur Netzstabilisierung und zur Abdeckung von Spitzenlasten vorzuhalten. Wasserstoff kann in Zeiten eines Überangebots aus Strom erneuerbarer Energiequellen durch Elektrolyse hergestellt

* Speaker/Referent

und bei Bedarf zur Stromerzeugung in einem Verbrennungsmotor verwendet werden, wenn die Stromnachfrage das Angebot übersteigt.

Gasmotoren, die für wasserstoffspezifische Anforderungen wie hohe Ladungsverdünnung und hohe Ladedrücke ausgelegt sind, haben das Potenzial, gleiche Leistungsdichten zu erreichen wie heutige Erdgaskraftwerke. In diesem Beitrag werden verschiedene Wasserstoffverbrennungskonzepte beschrieben, wobei der Schwerpunkt auf der Wasserstoffdirekteinspritzung liegt. Auf der Grundlage experimenteller Untersuchungen an Einzylinder-Forschungsmotoren sowie anhand von Gemischbildungssimulationen werden die verschiedenen Konzepte verglichen, limitierende Faktoren identifiziert sowie der künftige Forschungsbedarf dargestellt.

1. Introduction

Internal combustion engines are not just used in automotive and other on-road applications but also in high-power systems such as power plants, locomotives, ships and mining equipment. These engines are well suited to serve as climate-neutral, zero environmental impact sources of mechanical energy if the transition from fossil to renewable fuels can be achieved. As the Intergovernmental Panel on Climate Change (IPCC) has indicated, drastic measures are needed to keep the global mean temperature increase well below 2 °C and if possible, limit it to not more than 1.5 °C compared to pre-industrial levels. In order to reduce anthropogenic carbon dioxide (CO₂) emissions to zero by 2050, the right path must be taken now and global CO₂ emissions must be reduced to 55 % of the 2010 level by 2030 [1]. Governments worldwide put forward ever more ambitious greenhouse gas (GHG) emission reduction targets. The 2030 Climate Target Plan of the European Commission proposes to reduce GHG emissions at least by 55 % of the 1990 levels by 2030 [2] and in February 2024 the European Commission recommended a 90 % net GHG emission reduction by 2040 [3] (Figure 1).

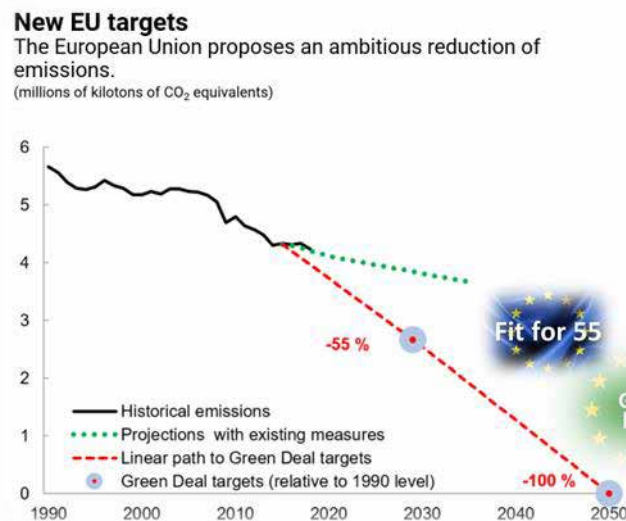


Figure 1: European Union Commission targets for greenhouse gas emission reduction

Today's use of fossil fuels is not sustainable but the use of carbon capture technologies might be used as an interim and transitional measure to mitigate the negative impact of continued use of fossil fuels. Biomass-derived liquid fuels are considered an alternative to fossil fuels, but widespread application is limited due to the scarcity of agricultural resources and only up to 30 % of the fuel demand for road transportation alone is predicted to be produced by 2060 [4]. Electricity generated from renewable energy sources such as photovoltaics, wind turbines and hydro-power is the most promising starting point for a sustainable path for green energy

and transportation systems (Figure 2). Electricity from photovoltaics and wind exhibits a high degree of volatility due to short-term and seasonal fluctuations. Thus, short- and long-term energy storage is necessary in conjunction with rapidly dispatchable power generation. Battery storage systems are characterized by fast charge and discharge cycles and offer high storage efficiency but a low storage density. Chemical storage in secondary energy carriers based on hydrogen from electrolysis has a lower storage efficiency but considerably higher storage density. These secondary energy carriers can be used as e-fuels in power plants and hard to abate applications such as aviation or shipping.



Figure 2: Pathway to green energy systems

In this article the use of hydrogen for high power density, high efficiency and low emission power plant applications is explored via 3D computational fluid dynamics (CFD) simulation and experimental investigations. Different hydrogen admission concepts, i.e., port fuel injection (PFI) and direct injection (DI), are investigated and key characteristics and performance metrics compared. Finally, the path forward to achieve reliable and robust hydrogen operation in a power plant matching today's natural gas power plant performance will be laid out.

2. Hydrogen power plants

The EU taxonomy provides the framework for green investments and therefore also for hydrogen power plants from 2035. "Hydrogen readiness" for power plants, however, is not defined in EU legislation. The association of engine power plant manufacturers has developed a common "Hydrogen readiness" definition for engine-driven gas-fired power plants based on the percentage of hydrogen used by the plant and the technical and financial effort required to achieve the desired hydrogen (H_2) readiness level in the future [5] (Figure 3).



Figure 3: Hydrogen readiness definition according to [5]

Today nearly all major large engine OEMs are developing hydrogen-fueled power plant solutions and several products are already commercially available. While some engines in the portfolio are currently designed for admixing of hydrogen only (mostly limited to 25 percent by volume) [6], others can operate on pure hydrogen [7][8][9]. The latter, however, operate at significantly lower rated power than their natural-gas fueled counterparts. The key target for future hydrogen power plants is to achieve the same or higher power output as state-of-the-art natural gas-fueled power plants.

Hydrogen combustion concepts

The design of hydrogen combustion concepts is driven by the chemical and physical properties of hydrogen. Key hydrogen properties for use in internal combustion engines are listed in Table 1 and compared to those of other e-fuels. Especially the high laminar flame speed in stoichiometric mixtures and the very low minimum ignition energy stand out in comparison to the other fuels. In order to mitigate the hydrogen combustion velocity and prevent unacceptable peak cylinder pressures and pressure rise rates the amount of charge dilution has to be increased compared to other fuels.

Table 1: Properties of hydrogen and other e-fuels

Fuel	Lower heating value (gravimetric) [MJ/kg]	Lower heating value (volumetric) [MJ/l]	Laminar flame speed (stoichiometric) [m/s]	Min. ignition energy [mJ]	Autoignition temperature [K]
Drop-in e-fuel (diesel-like)	43	36	0.87	0.23	483
e-methane	50	36	0.38	0.29	868
e-methanol	19	15	0.36	0.14	712
e-ammonia (liquid, -33 °C)	20	14	0.07	8.000	930
e-hydrogen (liquid, -253 °C)	120	9	3.50	0.017	858

The low ignition energy increases the risk of preignition. Preignition is one of several combustion anomalies that can occur with hydrogen fueling, together with backfiring or knocking. Figure 4 illustrates the types and differentiations of combustion anomalies.

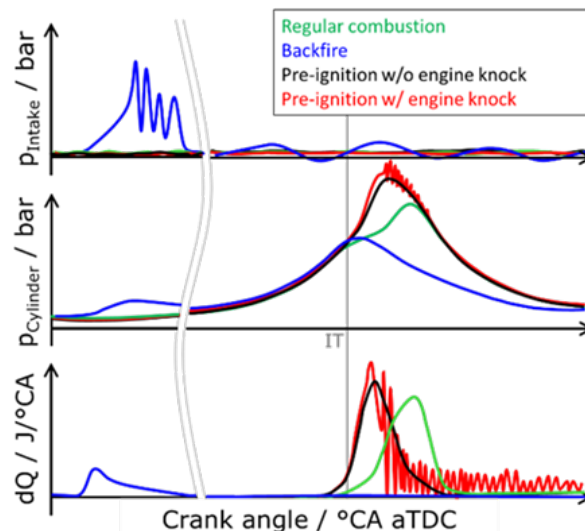


Figure 4: Illustration of typical cylinder and intake manifold pressure traces and heat release rates for regular combustion cycles and combustion anomalies

The regular combustion (green) exhibits the expected behavior with the cylinder pressure increase and heat release after the ignition timing. Combustion cycles in which pre-ignition occurred are shown in black and red. In both cycles the heat release starts during the compression stroke before the ignition timing and both cycles exhibit significantly higher peak cylinder pressures than for regular combustion. The potential root causes are numerous and include surface ignition on hot spots in the combustion chamber, residual gas from the previous combustion event, hot oil particles or residual charge in the ignition system. A backfiring cycle (shown in blue) might have the same root causes as a preignition but occurs earlier in the combustion cycle when the intake valves are still open such that the intake manifold pressure increases and bears the risk of severe damages of the intake system. Avoidance of hot spots in the combustion chamber and sufficient charge dilution are prerequisites to reduce the risk of preignition. Since the entering of lubricant into the combustion chamber cannot be fully avoided it is crucial to ensure that the lubricant formulation is suitable for hydrogen engines. Therefore, a test procedure was developed at the LEC GmbH to assess the impact of lubricant formulations on the occurrence of combustion anomalies in hydrogen-fired engines [10] and select suitable lubricants for hydrogen engine operation.

The autoignition temperature of hydrogen is in a similar range as that of methane and significantly higher than that of fuels typically used in diesel engines. Therefore, compression ignition engine concepts typically require a small amount of a high cetane number fuel to initiate combustion. In this article the focus lies on pure hydrogen combustion and only spark ignition concepts with different types of fuel admission are considered (Figure 5). From left to right the complexity but also the performance potential of the concepts increases. The concept with central mixture formation is well suited for fuel gas mixtures such as those found in flexible gas networks. The other two concepts are dedicated for pure hydrogen operation. For large cylinder displacement volumes both concepts are typically equipped with a precombustion chamber. Hydrogen direct injection, when taking place after intake valve closing, prevents the occurrence of backfiring into the intake manifold, has the potential for higher volumetric efficiency and is regarded as a key technology component for increasing power density. While in automotive application hydrogen injection pressures in the range of several hundred bar for direct injection are common, a medium-pressure range of 30 – 40 bar is typically used for large engine investigations. The lower hydrogen pressure was found to lower the technical barriers of the injector and to reduce the energy consumed for hydrogen compression, and system cost [11]. In the literature the different combustion concepts have also been combined with exhaust gas recirculation or water injection for suppression of hydrogen preignition and nitrogen oxide (NO_x) formation, the latter being associated with efficiency penalties [12]. The achievable compressor pressure ratio and turbocharger efficiency were found to set clear limits to the potentially feasible excess air ratio and power density of the engine [13].

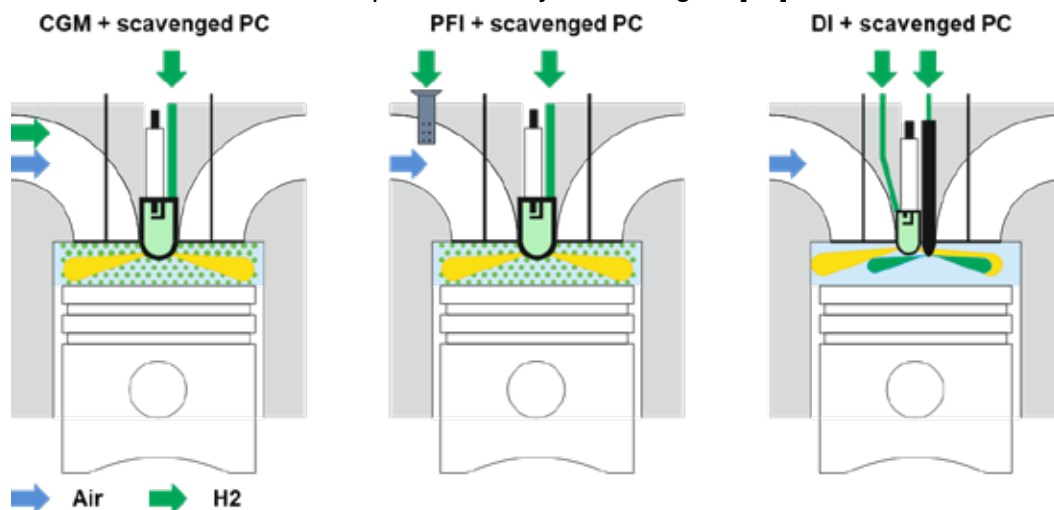


Figure 5: Hydrogen combustion concepts for spark ignition engines

3. Experimental and simulation results

The need for dedicated hydrogen engines becomes apparent when comparing the heat release rates for a given operating condition with pure natural gas fueling and with an admixture of as little as 25 percent by volume of hydrogen (Figure 6). The combustion is significantly accelerated and without any corrective measures the emission of nitric oxides is going to increase. With an appropriate control strategy, the impact of this hydrogen addition can be compensated, thus ensuring that no performance deviation occurs and emission limits are not exceeded.

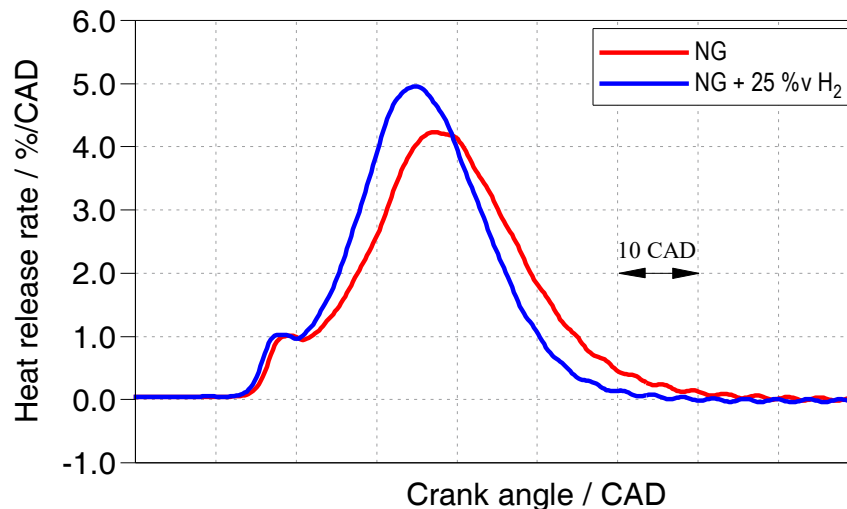


Figure 6: Heat release rate comparison for natural gas and admixing of 25 %v hydrogen

With pure hydrogen fueling control strategies alone are insufficient to ensure operation with high efficiency and low emissions and other concepts are required. Detailed investigations of a dedicated hydrogen combustion concept with direct injection were performed by LEC GmbH, INNIO Jenbacher GmbH & Co OG and Robert Bosch AG within the “H2Factory¹” project on a single cylinder research engine. The results are contrasted in this article with other hydrogen combustion concepts to highlight the benefits and improvement potential.

Hydrogen direct injection enables the application of different injection strategies. In this section the impact of various injection parameters on key performance indicators has been investigated. Figure 7 shows the measurement results for a variation of the injection timing (SOC – start of injector current) for an operating condition with fixed indicated mean effective pressure (IMEP) and fixed combustion phasing (CA50) and excess air ratio (EAR). Starting from an early injection timing when the intake valves are still open and successively retarding the injection results in a slight increase of the peak cylinder pressure and a significant increase in the (relative) knock intensity and the NO_x emissions. As expected, the volumetric efficiency is increasing because a larger portion of the gas exchange is taking place before the injection starts.

¹ The project „H2Factory“ received funding from the Austrian Climate and Energy Fund, NEFI.

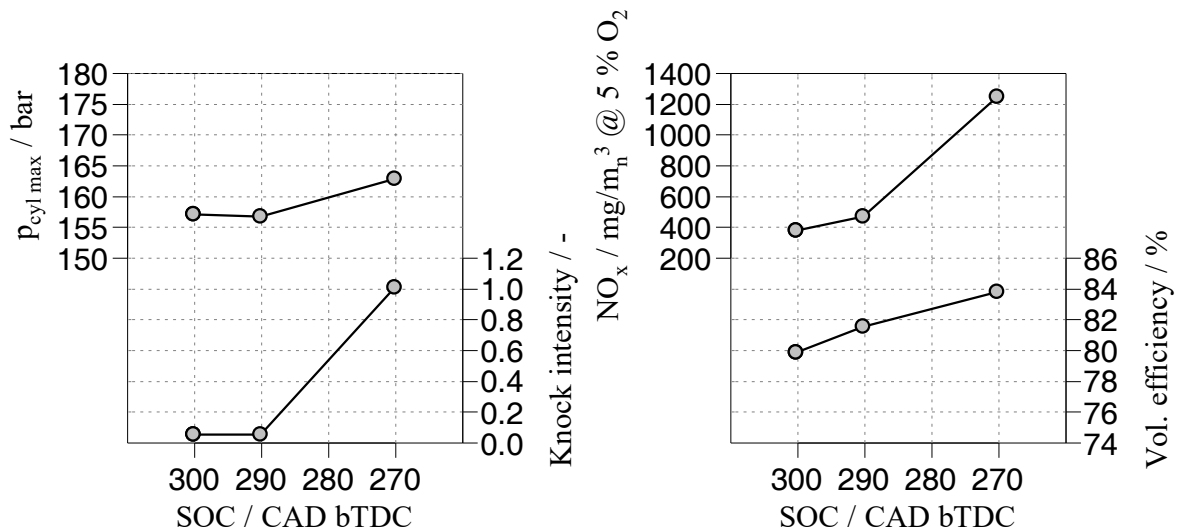


Figure 7: Selected measurement parameters for a variation of the hydrogen injection timing

A similar behavior was observed when the injection was split into two phases with constant SOC and an increasingly larger share of the second injection (Figure 8). With a larger share of the hydrogen injected after the intake valves were closed the knock intensity and the NO_x emissions increased significantly. Since the combustion phasing and the excess air ratio were maintained, it can be assumed that the mixture homogenization is insufficient and zones with a rich mixture exist that contribute disproportionately to the NO_x emission formation and are the source for the onset of knocking combustion.

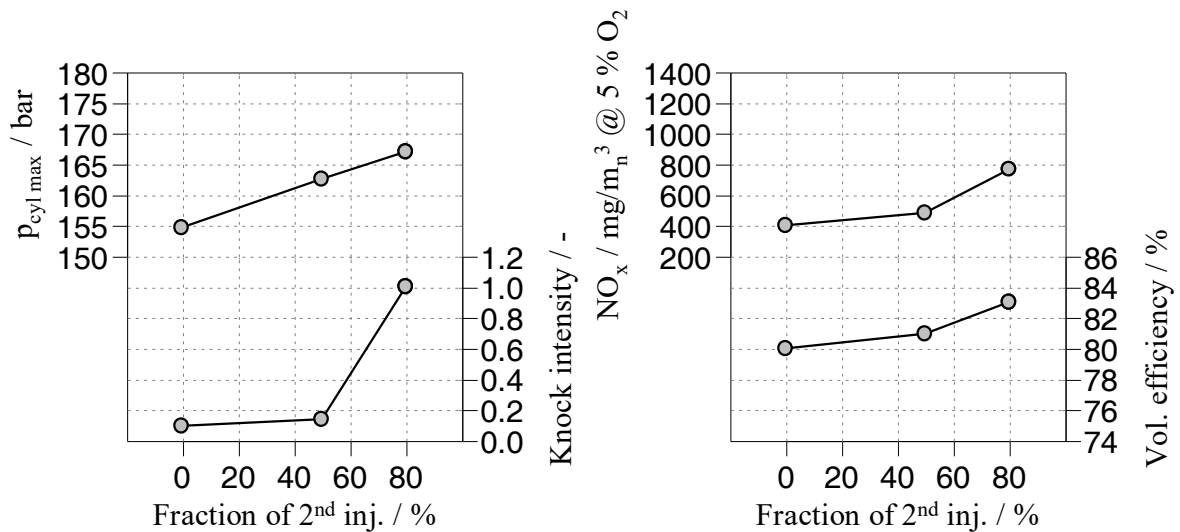


Figure 8: Selected measurement parameters for a variation of the hydrogen split ratio

The impact of the hydrogen supply pressure on this effect was studied in a separate measurement series. In this set of experiments the SOC was maintained while the injection pressure was increased (Figure 9). Starting from a supply pressure of 28 bar there was a decrease in emissions and knock intensity observed with increasing pressure but the curves flattened quickly and no significant improvement was achieved thereafter.

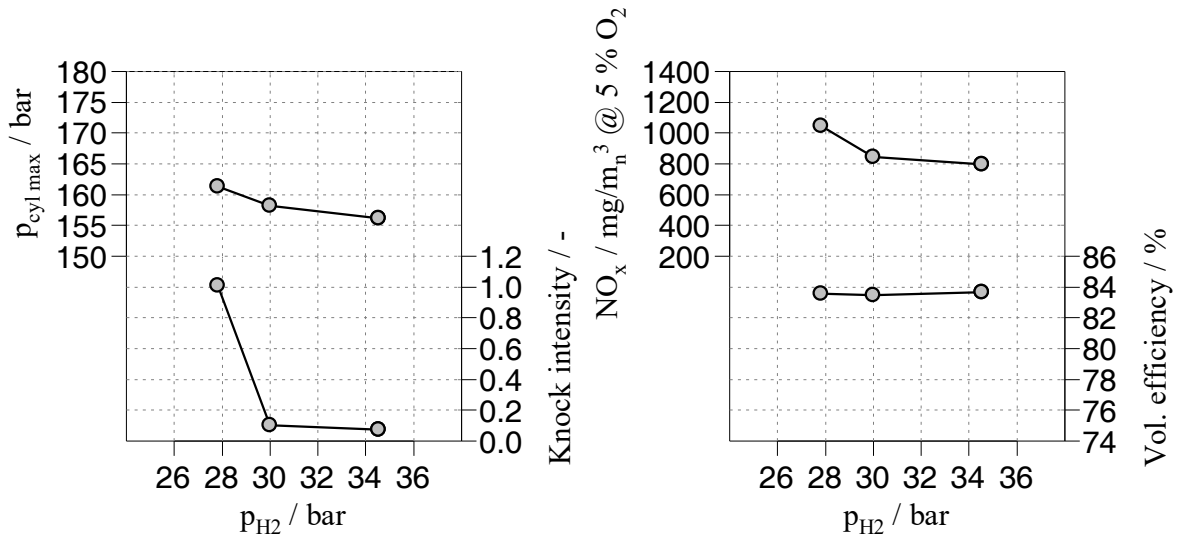


Figure 9: Selected measurement parameters for a variation of the hydrogen injection pressure

The investigation of the different injection strategies showed that there is a trade-off between the benefits of higher volumetry efficiency and the avoidance of backfiring on the one hand and the negative impact on knocking and emission formation on the other hand and that the injection strategy alone is insufficient to alleviate the shortcomings.

In order to assess the performance of the direct injection concept in comparison to a port fuel injection concept different operating points have been plotted on a NO_x emission vs. dilution map (Figure 10). The colors in the plots represent the boost pressure, coefficient of variation of the IMEP (COV_{IMEP}) and knock intensity, respectively. Even though the exact operating conditions cannot be matched between port fuel injection and direct injection points, it can be seen that with port fuel injection significantly lower NO_x emissions could be achieved with the same dilution rate. The boost pressure demand for a given dilution rate is lower for the direct injection due the hydrogen admission after the intake valves have been closed but the COV_{IMEP} and the knock intensity are higher than for the port fuel injection.

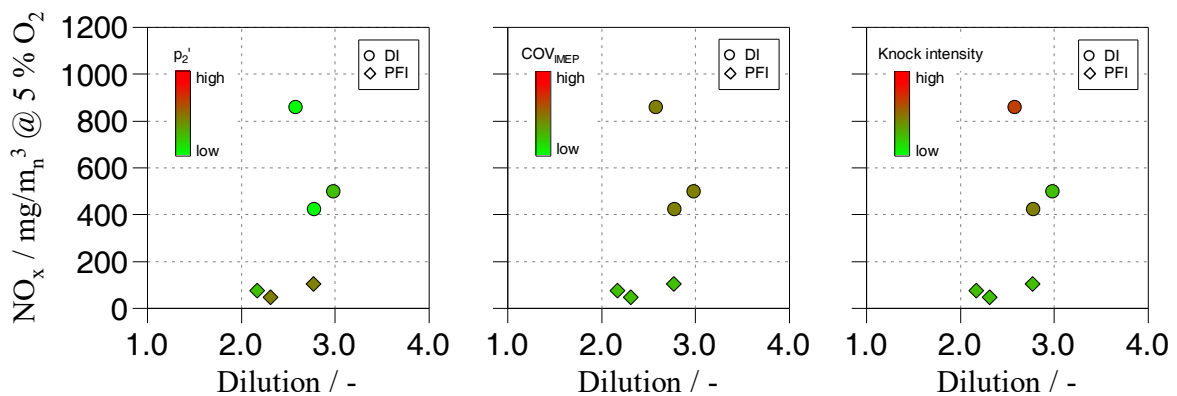


Figure 10: Comparison of various PFI and DI combustion concepts

For the direct injection concept sensitivity studies were performed for different hardware and operating parameters. The results of these variations are displayed in (Figure 11). A variation of the intake valve closing time achieved lower NO_x emissions, slightly reduced the knock intensity but increased the boost pressure demand significantly. While this increase can be accomplished easily in a single cylinder engine environment where the boost pressure is supplied by an electrically driven compressor, this increase might be challenging for an engine that is relying on the turbocharger to supply the boost pressure. An increase of the dilution

alone reduced the NO_x emissions and the knock intensity but of course also increased the boost pressure demand. Retarding the combustion phasing achieved a significant reduction of the NO_x emissions but did not impact the knock intensity significantly, indicating again that the observed behavior differs from the behavior of typical premixed combustion with homogenous fuel-air mixtures.

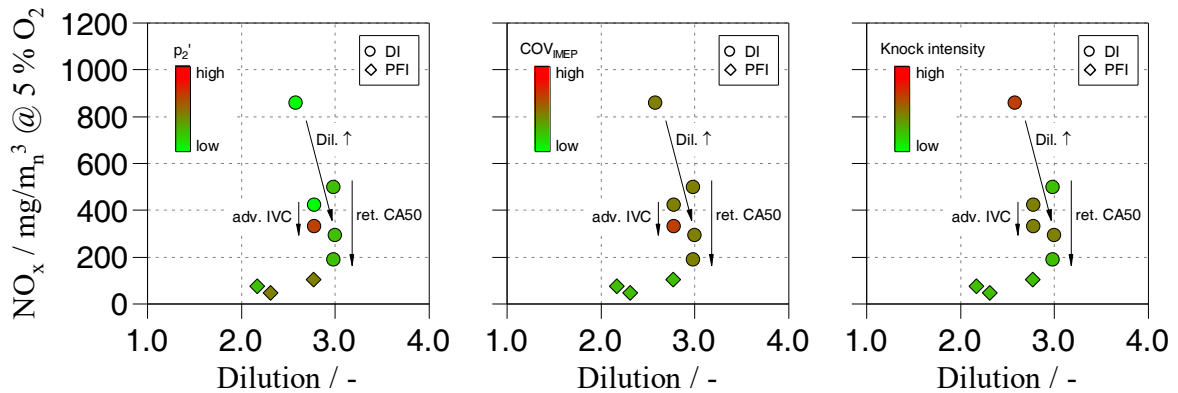


Figure 11: Impact of improvement measures on DI combustion concept performance

This hypothesis is also substantiated when comparing the heat release rates for a fixed IMEP and combustion phasing for port fuel injection and direct injection (Figure 12). Even though the global parameters and the shape of the curves are very similar, it can be seen that the initial heat release occurs more rapidly for the direct injection concept, inducing stronger pressure fluctuations.

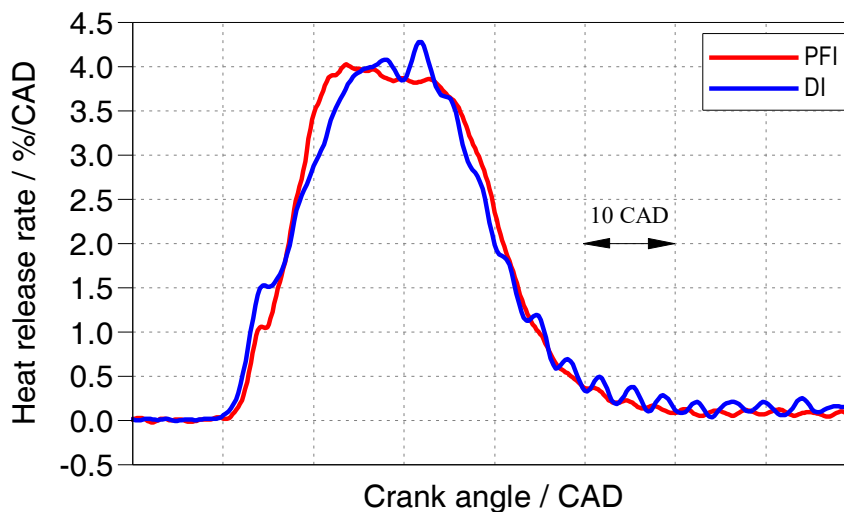


Figure 12: Comparison of heat release rates for PFI and DI operation

For an assessment of the mixture homogeneity 3D CFD simulations have been performed for port fuel injection and for direct injection with various geometry variants. The homogeneity was assessed based on the uniformity index (Figure 13, top). The uniformity index for the port fuel injection rapidly increases during the injection, aided by the high flow velocity and turbulence of the air mass flow, and continues to rise during the compression stroke, reaching values above 0.9 at the end of the compression stroke when the ignition takes place. A significantly different behavior was observed for the direct injection design variants. The increase of the uniformity index during the injection is significantly smaller and continues to increase at a relatively steady pace until the ignition takes place. At this time the high uniformity index of the

port fuel injection could not be achieved, corroborating the premise of insufficient mixture formation with the direct injection concept. The differences in the mixture homogeneity are also visible in the simulated hydrogen mass fraction distribution in a cross section of the cylinder at the time of ignition (Figure 13, bottom) where the PFI variant shows significantly lower variations.

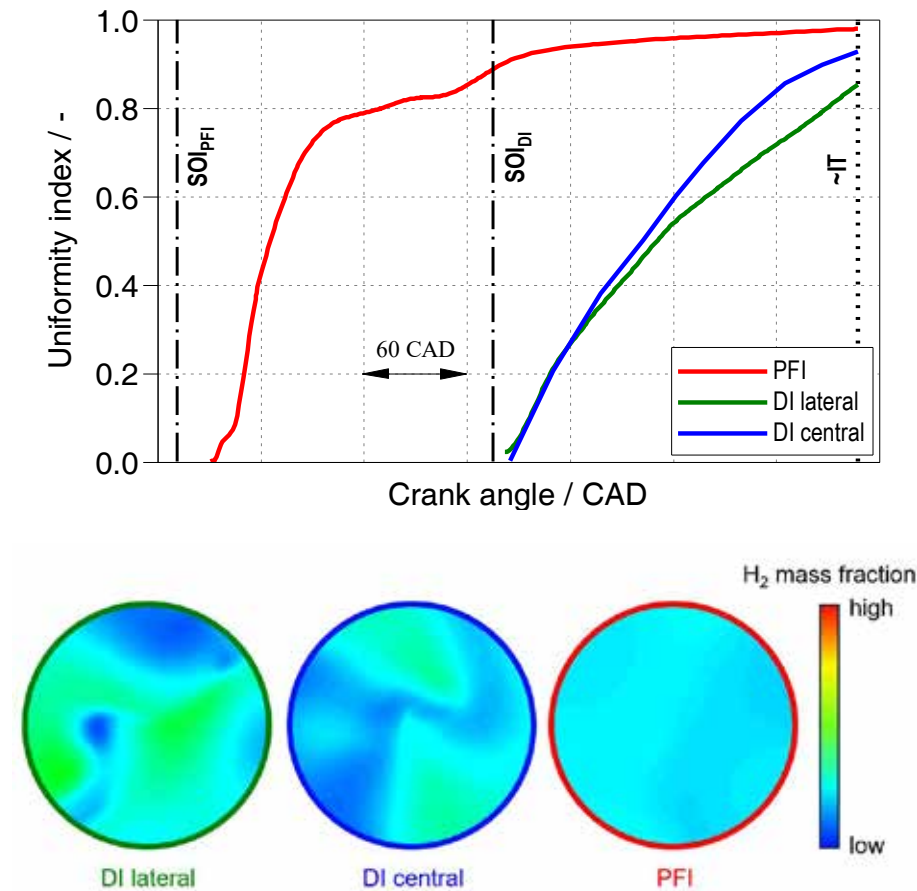


Figure 13: Temporal evolution of the in-cylinder mixture homogeneity for PFI and DI combustion concepts (top) and H_2 mass fraction distribution at ignition timing (bottom)

The simulation results substantiate the findings from the experimental investigations, namely the insufficient homogenization in the combustion chamber, as the root cause for the differences in the NO_x emissions and knock behavior between port fuel injection and direct injection.

4. Conclusions

Hydrogen will play a significant role in the decarbonization of various industries and particularly the power generation sector. Hydrogen has already shown the potential to replace carbon-based fuels in internal combustion engines. For a widespread use in power plants, it is crucial to achieve the same power densities with hydrogen fueling as with the fuels, typically natural gas, it is replacing. In the experiments on a single cylinder research engine conducted within this research a hydrogen combustion concept based on direct injection into the cylinder was validated for indicated mean effective pressures of more than 20 bar. The mixture formation and homogenization, however, was found to be more challenging with direct injection than with

port fuel injection. 3D CFD simulation of the injection and mixture formation was shown to be a useful tool to assess the processes in the combustion chamber and will be used in future research to further optimize the injector and combustion chamber in conjunction with the operating strategies in order to improve homogeneity, lower required dilution levels and thus enable even higher power densities.

In addition to further research on injection and combustion it will also be necessary to address other issues including hydrogen concentrations in the crank case and blow-by handling, lubricant performance and material compatibility and embrittlement of components in contact with high hydrogen concentrations.

References

- [1] IPCC: “Global warming of 1.5 °C. An IPCC Special Report on the impacts of global warming of 1.5°C above pre-industrial levels and related global greenhouse gas emission pathways, in the context of strengthening the global response to the threat of climate change, sustainable development, and efforts to eradicate poverty”, Masson-Delmotte, V., P. Zhai, H.-O. Pörtner, D. Roberts, J. Skea, P.R. Shukla, A. Pirani, W. Moufouma-Okia, C. Péan, R. Pidcock, S. Connors, J.B.R. Matthews, Y. Chen, X. Zhou, M.I. Gomis, E. Lonnoy, T. Maycock, M. Tignor, and T. Waterfield (eds.). <https://www.ipcc.ch/sr15/>, accessed on December 28th, 2020.
- [2] European Commission: “2030 Climate Target Plan”. https://ec.europa.eu/clima/policies/eu-climate-action/2030_ctp_en#:~:text=With%20the%202030%20Climate%20Target,target%20of%20at%20least%2040%25, accessed on January 28th, 2021.
- [3] European Commission: Recommendations for 2040 targets to reach climate neutrality by 2050, https://commission.europa.eu/news/recommendations-2040-targets-reach-climate-neutrality-2050-2024-02-06_en?prefLang=de, accessed on February 11, 2024.
- [4] Bacovsky, D.: “The Role of Renewable Transport Fuels in Decarbonizing Road Transport – Summary Report”, AMF Annex 58 / IEA Bioenergy Task 41 Project 10, A Report from the Advanced Motor Fuels TCP and IEA Bioenergy TCP, https://iea-amf.com/app/webroot/files/file/Annex%20Reports/AMF_Annex_58_Summary%20Report.pdf, accessed on December 30th, 2020.
- [5] Eugene, H2-Readiness, [Why H2-Readiness? | EUGINE](#), accessed on February 25, 2024.
- [6] Caterpillar, Renewable hydrogen and hydrogen blends, https://www.cat.com/en_US/by-industry/electric-power/electric-power-industries/hydrogen.html, accessed on February 25, 2024.
- [7] S. Laiminger, K. Payrhuber, A. Kunz, N. Wermuth, A. Wimmer, The role of gas engines in a future energy market with sustainable fuels, presented at 30th CIMAC World Congress 2023: Meeting the Future of Combustion Engines, Busan, June, 2023.
- [8] INNIO, Hydrogen, CO₂-neutral power generation solutions, <https://www.ienergy.com/en/energy-solutions/energy-sources/hydrogen>, accessed on February 25, 2024.
- [9] 2G, agenitor, [agenitor | 75-450 kW | Der globale Effizienzmaßstab : 2G Energy \(2-g.com\)](#), accessed on February 25, 2024.
- [10] W. Koch, L. Pearson, N. Wermuth et al., Development of lubricants for hydrogen fueled gas engine power plants, presented at 30th CIMAC World Congress 2023: Meeting the Future of Combustion Engines, Busan, June, 2023.
- [11] T. Tsujimura, Y. Suzuki, Development of a large-sized direct injection hydrogen engine for a stationary power generator, International Journal of Hydrogen Energy, Volume

44, Issue 22, 2019, Pages 11355-11369, ISSN 0360-3199,
<https://doi.org/10.1016/j.ijhydene.2018.09.178>.

- [12] Eicheldinger, S., Waligorski, D., Wachtmeister, G. et al. Leistungspotenzial von Wasserstoffverbrennungsmotoren für Industrieanwendungen. *MTZ Motortech Z* 83, 58–62 (2022). <https://doi.org/10.1007/s35146-022-0859-x>
- [13] R. Ryser, C. Bessonard, H. Martin, W. Fimml, N. Wermuth, A. Wimmer, Influence of CH₄/H₂ blend ratio on turbocharging & combustion in high-speed gas engines, presented at 30th CIMAC World Congress 2023: Meeting the Future of Combustion Engines, Busan, June, 2023.

Acknowledgements

The authors would like to acknowledge the financial support of the "COMET - Competence Centers for Excellent Technologies" Program of the Austrian Federal Ministry for Climate Action, Environment, Energy, Mobility, Innovation and Technology (BMK) and the Austrian Federal Ministry of Labor and Economy (BMAW) and the Provinces of Salzburg, Styria and Tyrol for the COMET Centre (K1) LEC GETS. The COMET Program is managed by the Austrian Research Promotion Agency (FFG).

Part of this research was carried out within the NEFI project H2Factory, which is funded by the Austrian Climate and Energy Fund as part of the Energy Showcase Region and the Federal Ministry for Climate Action, Environment, Energy, Mobility, Innovation and Technology (BMK).

Acronyms

CA50	Crank angle 50 % energy release
CFD	Computational fluid dynamics
CO ₂	Carbon dioxide
COV _{IMEP}	Coefficient of variation of IMEP
dQ	Energy release rate
DI	Direct injection
EAR	Excess air ratio
GHG	Greenhouse gas
H ₂	Hydrogen
IMEP	Indicated mean effective pressure
IT	Ignition timing
NG	Natural gas
NO _x	Nitrogen oxides
p _{cylinder}	Cylinder pressure
p _{hydrogen}	Hydrogen supply pressure
p _{intake}	Pressure in intake manifold
PFI	Port fuel injection
SI	Spark ignition
SOC	Start of injector current
SOI	Start of injection

Exhaust gas aftertreatment for methanol dual fuel engines

Abgasnachbehandlung für Dual-Fuel Methanol Motoren

Dr. Daniel Peitz, Dr.-Ing. Enno Eßer

HUG Engineering AG, Elsau, Switzerland

Abstract

Methanol as a combustion fuel is considered to be a promising option for reducing greenhouse gas emissions - provided the alcohol is produced with a low carbon footprint. Combustion in dual fuel engines may be achieved via different pathways, either in a diffusive or premix principle. Both routes come with specific challenges and opportunities, this contribution focuses on the emission aspects and consequences on the exhaust gas aftertreatment. Due to the different combustion modes different exhaust conditions and pollutant concentrations are observed, while emission targets and ambitions remain identical.

In terms of exhaust gas aftertreatment the different emissions compared to combustion of Diesel or natural gas require adaptations, depending on the specific deviations. Particularly in case of port fuel injection concepts with potentially higher concentrations of unburnt (CH_3OH) or partially burnt (e.g. HCHO) fuel components side reactions on the SCR catalyst used for NO_x reduction become significant. These side reactions not only impact the NO_x removal performance but also give rise to undesired secondary emissions. The relevant reactions are briefly introduced, pointing out at which exhaust conditions they may detrimentally impact current SCR system designs, but also providing guidance to how combustion concepts could be optimized to reduce requirements for additional aftertreatment. Additionally, exhaust gas aftertreatment system architectures designed for the various engine concepts are presented allowing a comparison of different engine combustion concepts regarding emissions.

Overall, achieving lower greenhouse impact by switching to alternative fuels such as methanol also requires careful consideration of the associated changes for exhaust gas aftertreatment. Close collaboration on this topic between engine development and exhaust gas aftertreatment ensures to meet legal pollutant requirements while maintaining low emissions of undesired non-regulated substances.

Kurzfassung

Methanol gilt als vielversprechende Kraftstoffoption zur Verringerung der Treibhausgasemissionen – vorausgesetzt, der Alkohol wird mit einem geringen CO_2 -Fußabdruck hergestellt. Die Verbrennung in Dual-Fuel Motoren kann sowohl diffusiv als auch vorgemischt erfolgen, wobei beide Wege spezifische Herausforderungen und Möglichkeiten mit sich bringen. Dieser Beitrag konzentriert sich auf Emissionen und die Auswirkungen auf die Abgasnachbehandlung. Aufgrund der verschiedenen Verbrennungsarten beobachtet man unterschiedliche Abgasbedingungen und Schadstoffkonzentrationen, während die Emissionsziele identisch bleiben.

Bezüglich Abgasnachbehandlung erfordern die Dual-Fuel Konzepte im Vergleich zur Verbrennung von Diesel oder Erdgas Anpassungen in Abhängigkeit der spezifischen Emissionen. Insbesondere bei Saugrohreinspritzkonzepten mit potenziell höheren Konzentrationen unverbrannter (CH_3OH) oder teilweise verbrannter (z.B. HCHO)

* Speaker/Referent

Kraftstoffkomponenten werden Nebenreaktionen an dem zur NO_x-Reduktion eingesetzten SCR-Katalysator bedeutsam. Diese Nebenreaktionen beeinträchtigen nicht nur die erzielten NO_x-Emissionen, sondern führen auch zu unerwünschten Sekundäremissionen. Die relevanten Reaktionen werden kurz vorgestellt und aufgezeigt, bei welchen Abgasbedingungen sich nachteilige Effekte auf die derzeit eingesetzten SCR-Systeme ergeben. Gleichzeitig werden auch Hinweise gegeben, wie Verbrennungskonzepte optimiert werden könnten, um den Bedarf an zusätzlicher Nachbehandlung zu verringern. Darüber hinaus werden für die verschiedenen Motorkonzepte konzipierte Abgasnachbehandlungs-Systemarchitekturen vorgestellt.

Insgesamt erfordert die Verringerung der Treibhausgasemissionen durch die Umstellung auf alternative Kraftstoffe wie Methanol auch eine spezifische Betrachtung der nachgelagerten Abgasnachbehandlung. Eine enge Zusammenarbeit zwischen Motorenentwicklung und Abgasnachbehandlung stellt dabei sicher, dass die gesetzlichen Schadstoffgrenzwerte erfüllt und gleichzeitig der Ausstoß von unerwünschten, nicht regulierten Abgaskomponenten minimiert wird.

1. Introduction

The reliable, flexible and cost-effective energy conversion by internal combustion engines is unquestioned, yet it's obvious the chemical energy carriers must change: Away from combustion of fossil fractions with full release of the resulting fossil CO₂, towards a lower CO₂ net emission future.

In terms of energy storage, the essential properties are storage density and required conditions for stable and safe storage. Compounds which can be stored as a liquid at (close to) ambient conditions are clearly preferable compared to more dilute gaseous energy carriers which require high pressures or cryogenic conditions for storage in reasonable dimensions. Consequently, methanol, the simplest alcohol possible, is considered as a future fuel for combustion engines. It can be produced by biological processes from biomass, but also via syngas derived from various sources, ultimately even from captured CO₂ and low CO₂ footprint H₂. Methanol is already a globally traded commodity handled at large scales, still largely produced from fossil resources, but biomass is becoming a more relevant feedstock.

In terms of engine technologies for methanol combustion, there are two fundamental options, one being diffusive combustion with direct injection, the other premix combustion without the requirement for methanol high pressure direct injection to be integrated. Both routes come with specific advantages and shortcomings, in the end there are good reasons to see both in the market. As the presented contribution is focusing on exhaust gas aftertreatment aspects, the difference of the combustion concepts in yielding different exhaust composition is highlighted: While the exhaust components are generally the same in both routes, the concentrations are not. In comparison to premix combustion, diffusive combustion typically yields a higher level of complete combustion of injected methanol, achieving lower amounts of unburnt or only partially burnt fuel components. Exhaust temperatures may also vary between the two engine concepts, but due to the many other factors which impact this parameter, it should not be discussed at this point but covered by presenting results over a wide temperature window. The ignition architecture considered in this contribution is limited to Diesel pilot dual fuel concepts, compression ignition of methanol as also investigated [1], is not considered.

Hug Engineering has demonstrated to be a reliable partner for exhaust gas aftertreatment systems in demanding applications of stationary [2] or mobile [3] engines. This contribution focusses to support the transition towards low CO₂ footprint fuels via methanol combustion engines with dedicated aftertreatment systems.

2. Challenges of standard SCR and SCR + Oxidation catalyst exhaust gas aftertreatment systems in methanol operation

In Diesel operation, unburnt fuel emissions consist mostly of hydrocarbon molecules like long-chain alkanes, alkenes and aromatic compounds which do not significantly inhibit the SCR reaction on common VWT (Vanadia-tungsten-titania) based SCR catalysts. However, in methanol operation with high shares of methanol substituting Diesel fuel, the hydrocarbon composition changes to be dominated by unburnt methanol (CH_3OH) and formaldehyde (HCHO) as incomplete combustion product from methanol.

Depending on the combustion concept, the absolute amount of incompletely and unburnt compounds in the exhaust varies, also engine designs affect the concentrations. As a general indication, air-fuel premix concepts in small bore engines running at higher rpm are prone to produce higher amounts of emissions. Hereby, unburnt hydrocarbon emissions can reach significantly more than 1'000 ppm, at these levels, the impact on the SCR performance is clearly noticed as shown in Figure 1. Here, the addition of 3'000 ppm methanol to synthetic exhaust gas (700 ppm NO_x , 5 vol.% H_2O , air balance) has significant impact on the NO_x conversion at otherwise identical conditions (NH_3 to NO_x ratio, $\alpha = 0.9$).

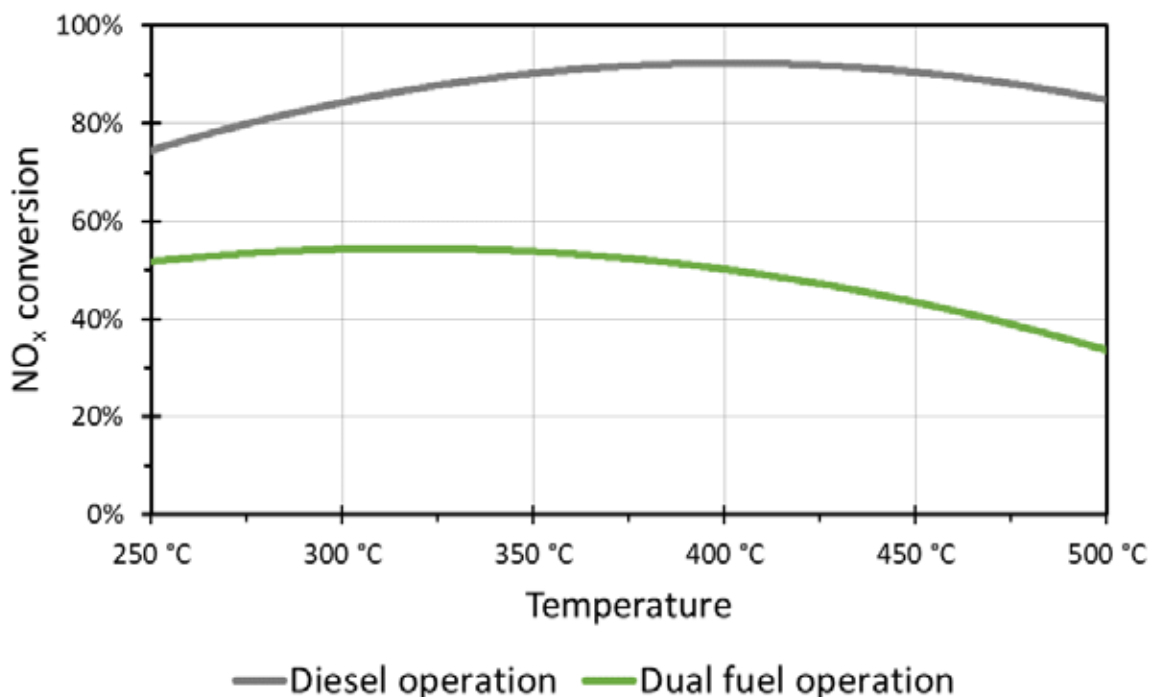
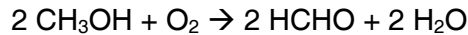
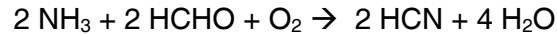


Figure 1: NO_x conversion in Diesel and Dual fuel methanol operation on a SCR catalyst. Reaction conditions: $c(\text{NO}_x) = 700$ ppm, $c(\text{NH}_3) = 630$ ppm, $c(\text{H}_2\text{O}) = 5$ vol.%, air balance + $c(\text{CH}_3\text{OH}) = 3'000$ ppm in methanol operation.

The impact on NO_x conversion depends on the exhaust gas temperature ranging from -21% at 250 – 400°C to -52% at 500°C thereby compromising achievable NO_x emission levels. The formation of HCN via the decomposition of methanol [R1] and consecutive reaction with NH_3 [R2] leads to the consumption of NH_3 , limiting the SCR reaction and causing toxic HCN concentrations. Depending on engine configuration, combustion principle, methanol fuel share, air-fuel-ratio and other parameters, the water content may differ strongly from the assumed concentration of 5 vol.%. Additional measurements (not presented in this contribution) have indicated a significant impact of water content in the exhaust gas on the catalyst's behavior making measurements dedicated to specific engine operation necessary for final assessment.



R1



R2

Under the assumed conditions, HCN concentrations above 350 ppm were detected (see Figure 2) which is more than 100 times above the allowed occupational threshold limit value of 0.8 ppm according to EU REACH regulation.

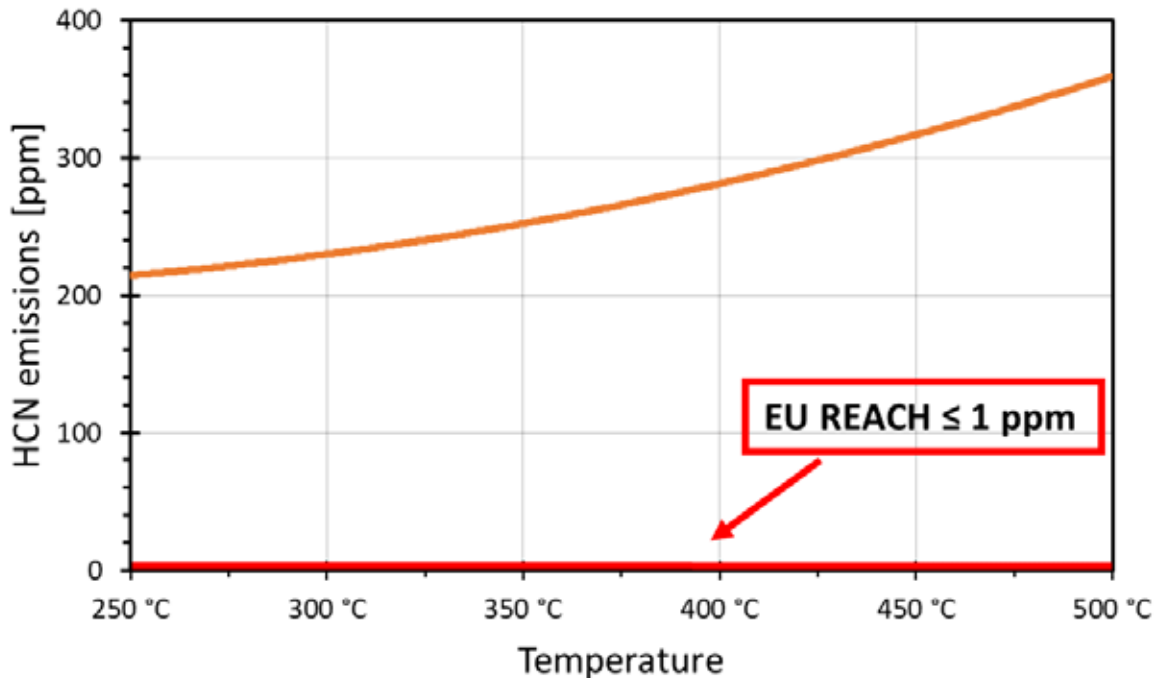
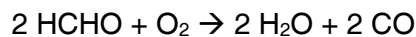


Figure 2: HCN formation on a SCR catalyst in methanol fuel operation, conditions as stated in previous Figure 1. Occupational HCN threshold limit value (TLV) of EU REACH for reference.

Besides the increased HCN formation, formaldehyde is formed from partial methanol oxidation on the SCR catalyst reaching a concentration of 700 ppm at 250°C (see Figure 3), clearly exceeding existing emission limits such as given by the 44. BImSchV for lean burn engines, which would typically be around or below 10 ppm (defined in regulation as 20 mg/Nm³ at 5% Oxygen reference). The emitted HCHO levels decrease strongly with increasing temperature, reaching less than 100 ppm at 500°C as the SCR catalyst's activity for formaldehyde oxidation increases with temperature [4]. The reaction product is mainly CO in accordance with [R3] which in turn is confirmed by increasingly high CO levels (see Figure 3) reaching 2'500 ppm at 500°C.



R3

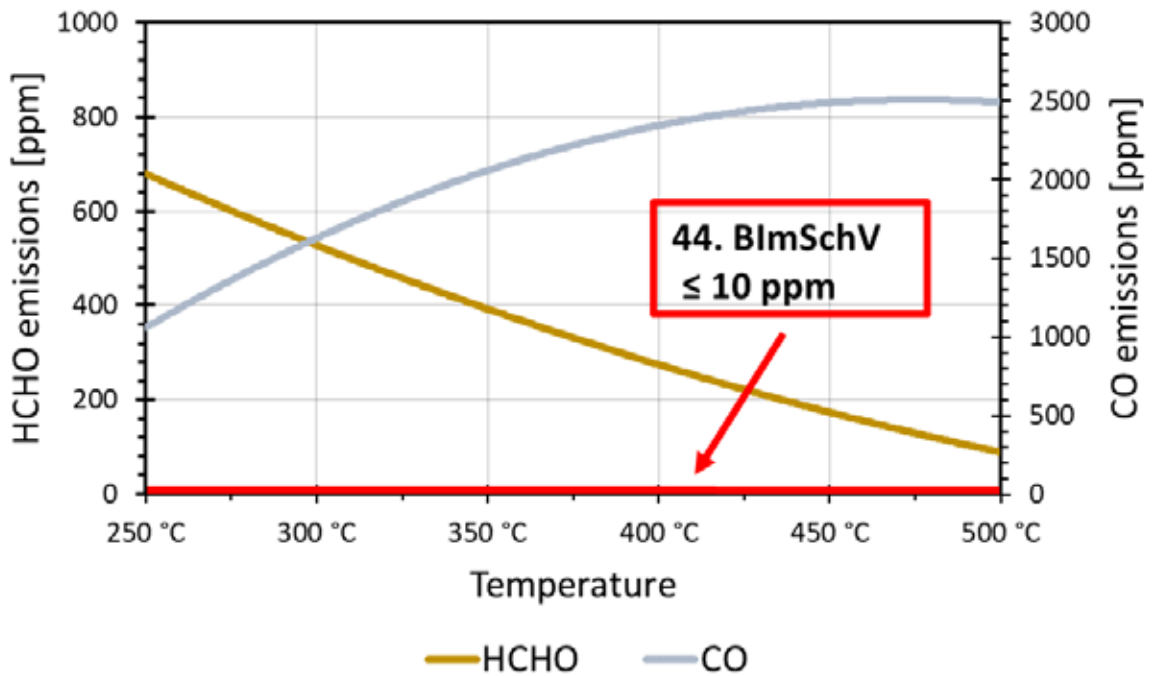
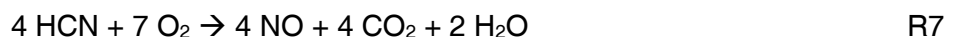


Figure 3: Formaldehyde and CO formation on a typical VWT honeycomb catalyst in methanol fuel operation. Conditions as stated in Figure 1. Approximate emission limit for HCHO of natural gas engines according to 44. BImSchV given as reference.

For systems which include a platinum group metal (PGM)-based oxidation catalyst after the SCR stage, CO and HCHO emissions can be avoided by oxidizing both to CO_2 [R4, R5] regardless of the fuel type. For systems operating on Diesel fuel the impact of oxidation stage on NO_x conversion downstream of the SCR catalyst is limited under the tested conditions to temperatures below 350°C due to oxidation of NH_3 slip to NO_x [R6].



However, in methanol operation, the impact is significantly higher, limiting the NO_x conversion to less than 20% at 350°C while under the same reaction conditions NO_x conversion of ca. 90% can be achieved in Diesel operation. As NH_3 is almost completely consumed in methanol operation due to the formation of HCN [R2], the impact of NH_3 oxidation towards NO_x on the PGM catalyst is of minor importance. However, the oxidation of HCN with a high selectivity towards NO_x [R7] strongly impacts the overall NO_x conversion.



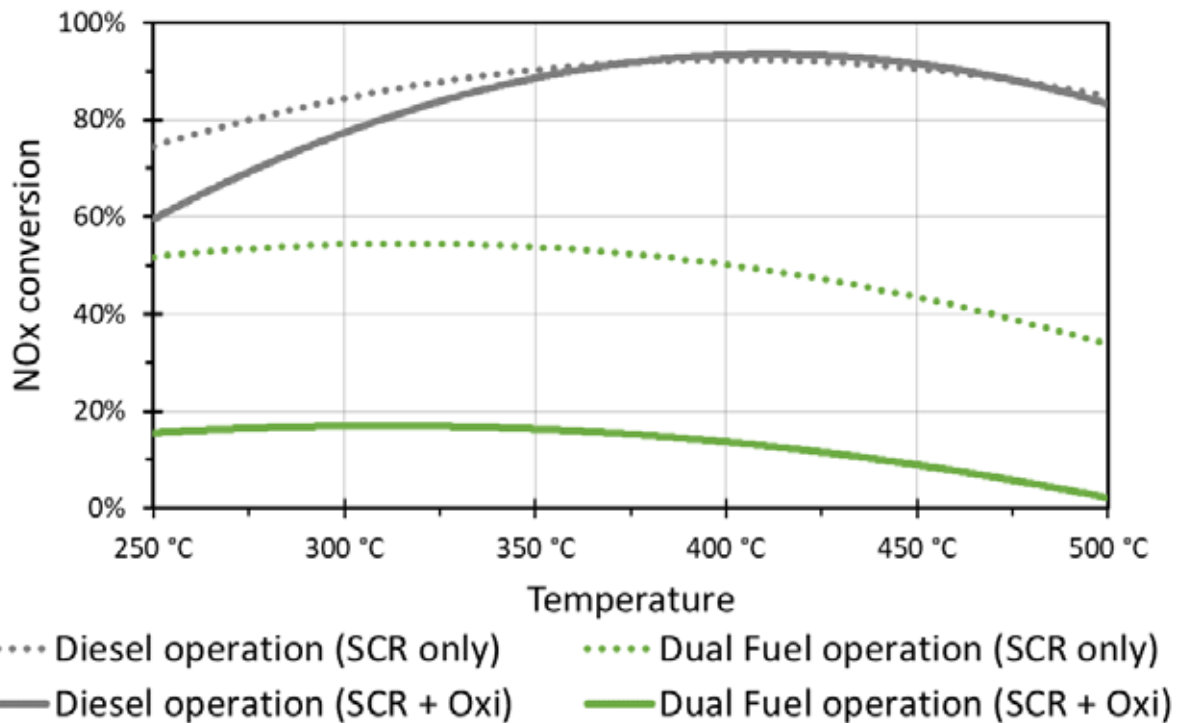


Figure 4: Overall NO_x conversion in Diesel and methanol operation on a typical VWT honeycomb catalyst and subsequent oxidation catalyst. SCR only performance repeated from previous Figure 1 as reference. Conditions as stated in Figure 1.

Even though after the oxidation catalyst HCN levels are well below acceptable levels, the NO_x conversion is strongly diminished, rendering existing systems as non-compliant under current legislations.

3. Solutions for high NO_x conversions in methanol operation

To counter the challenges in methanol operation posed by increased hydrocarbon contents, especially CH₃OH and HCHO, in the exhaust gas, several approaches are possible. For new systems without severe size restrictions, a dedicated methanol oxidation stage prior to urea injection is an option. Hereby, the pilot Diesel fuel quality determines the chemical composition of the methanol oxidation catalysts. While for EN590 grade Diesel a PGM-oxidation catalyst is feasible, lower fuel qualities require a PGM-free oxidation catalyst for extended endurance. For this reason, the performance of a robust and proven PGM-free catalyst in methanol oxidation is also presented in this paper as this type of catalyst has a high resistance towards typical catalyst poisons (e.g. S and P). A general concept of the setup described is shown in Figure 5.

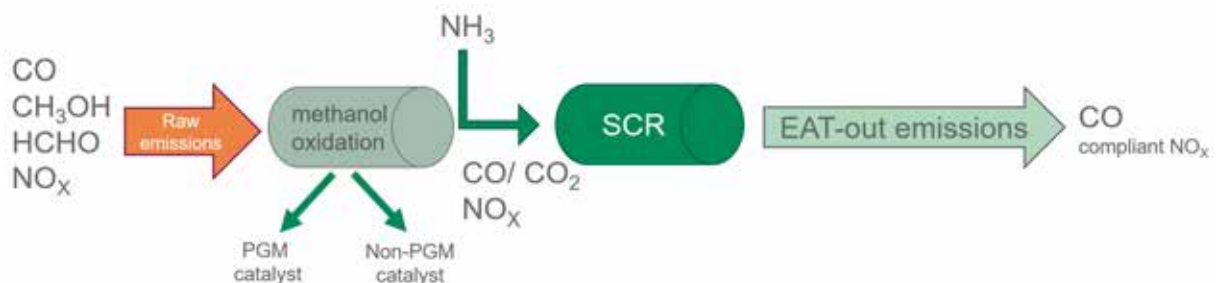
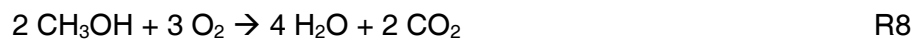


Figure 5: Concept of an exhaust gas aftertreatment system for methanol operation including a dedicated methanol oxidation stage prior to SCR requiring a separate reactor.

The performance of a PGM catalyst and a non-PGM oxidation catalyst is shown in Figure 6. In this diagram both catalysts are equally sized to enable a comparison under identical conditions. While for the PGM catalyst full conversion is achievable for all relevant temperatures, the non-PGM catalyst requires temperatures above 300°C to oxidize more than 80% of the incoming methanol. However, at temperatures above 400°C the PGM-free catalyst exhibits methanol conversion rates close to those of a PGM oxidation catalyst making it a realistic and cost-effective alternative. For temperatures below 300°C, a sizing factor between PGM and non-PGM catalyst of approx. 5 applies (depending on exact exhaust gas conditions and targeted downstream oxidation catalyst concentration) to achieve comparable conversions.

Independent of the reaction temperature, both catalysts depict a very different product selectivity with the PGM catalyst forming from methanol mostly CO₂ [R8] while the non-PGM oxidation catalyst forms mostly CO [R9]. Both compounds are chemically inert in a downstream SCR stage.



However, as the formation of CO₂ is strongly exothermic and releases approximately twice as much energy as the formation of CO, the respective temperature increase must be considered for the downstream SCR stage avoiding any exceedance of the SCR catalyst's temperature limit. The amount of unburnt methanol and HCHO contained in the engine raw exhaust gas is essential in assessing the maximum expected temperature increase due to the exothermic oxidation reactions which can increase exhaust gas temperatures significantly.

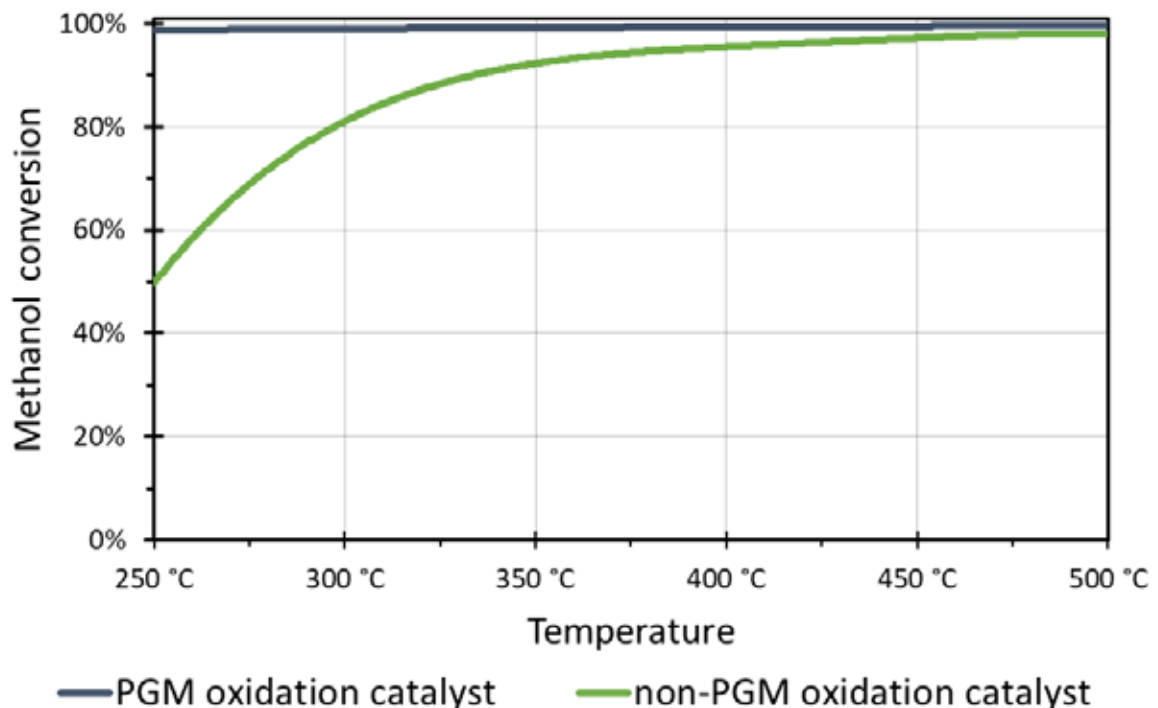
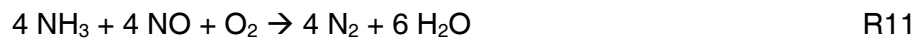


Figure 6: Methanol conversion in methanol operation on a PGM oxidation honeycomb catalyst and a non-PGM oxidation honeycomb catalyst of equal size. Conditions as stated in Figure 1 without NH₃ injection.

While the concept with upstream methanol oxidation (see Figure 5) is feasible for new systems, space restrictions are often limiting in retrofit methanol conversion projects to fit a dedicated upstream reactor. For these applications, the concept depicted in Figure 7 is preferable. Here, a secondary catalyst is placed inside an existing SCR reactor after the standard SCR catalyst partially replacing it. This new catalyst acts as an HCN-SCR catalyst using the HCN formed on the VWT catalyst to reduce NO_x . The relevant reaction is a two-step process of HCN hydrolysis forming NH_3 [R10] which in turn reacts with NO_x present in the exhaust gas according to standard SCR [R11] [5].



Hereby both pollutants, HCN and NO_x , are mutually eliminated forming CO and N_2 .

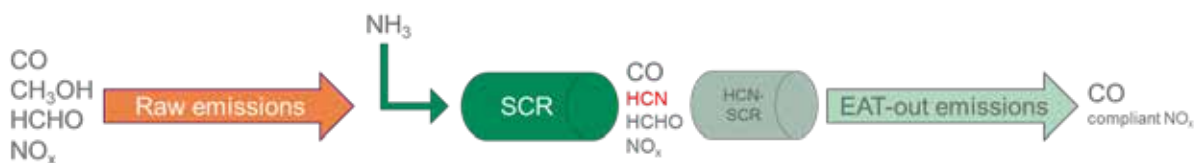


Figure 7: Concept of an exhaust gas aftertreatment system for methanol operation including an HCN-SCR stage after a typical VWT honeycomb catalyst fitting in an existing reactor.

When testing the described setup consisting of a common SCR and consecutive HCN-SCR catalysts (see Figure 7) under conditions previously used for SCR-only and SCR + oxidation catalyst, no penalty in NO_x conversion due to methanol operation in comparison to Diesel operation mode is visible (see

Figure 8). No effect of the increased HC in the exhaust gas consisting of 3'000 ppm unburnt methanol on De NO_x performance is apparent. When adding an oxidation catalyst downstream of the De NO_x stage to ensure compliance with e.g. CO and HCHO limits, a slight decrease in NO_x conversion at temperatures below 400°C due to the oxidation of HCN to NO_x [R7] becomes visible.

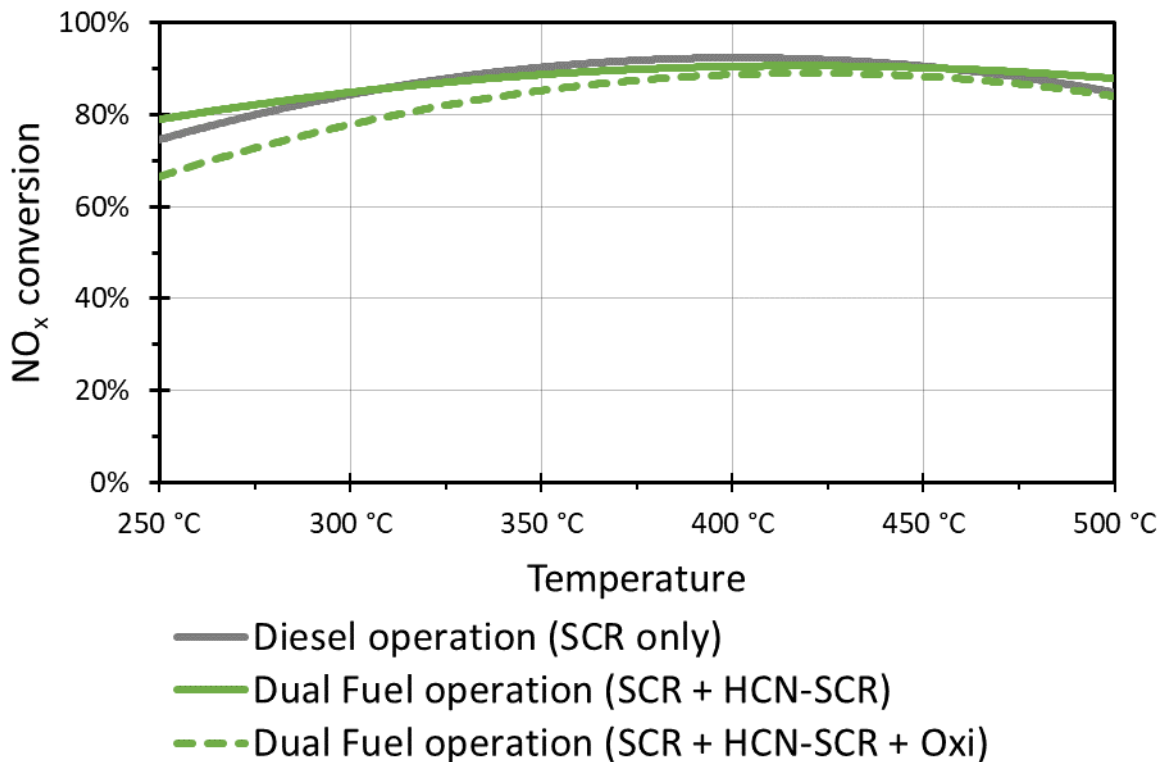


Figure 8: Overall NO_x conversion in Diesel operation on a typical VWT honeycomb catalyst as well as methanol operation on SCR + HCN-SCR catalysts and SCR + HCN-SCR + Oxi catalyst. Conditions as stated in Figure 1.

If operating without an oxidation catalyst after the DeNO_x stage in methanol mode, HCN emissions of the system SCR + HCN-SCR are lowered significantly in comparison to SCR only systems approaching single digit concentrations (see Figure 9). Also, HCHO emissions are more than halved by the HCN-SCR part of the SCR stage in comparison to SCR only systems while strongly increasing CO levels. If compliance with CO and HCHO limits is required, all remaining secondary emissions (CO, HCN, HCHO) can be eliminated by a standard PGM oxidation catalyst in the last position (see Figure 10).

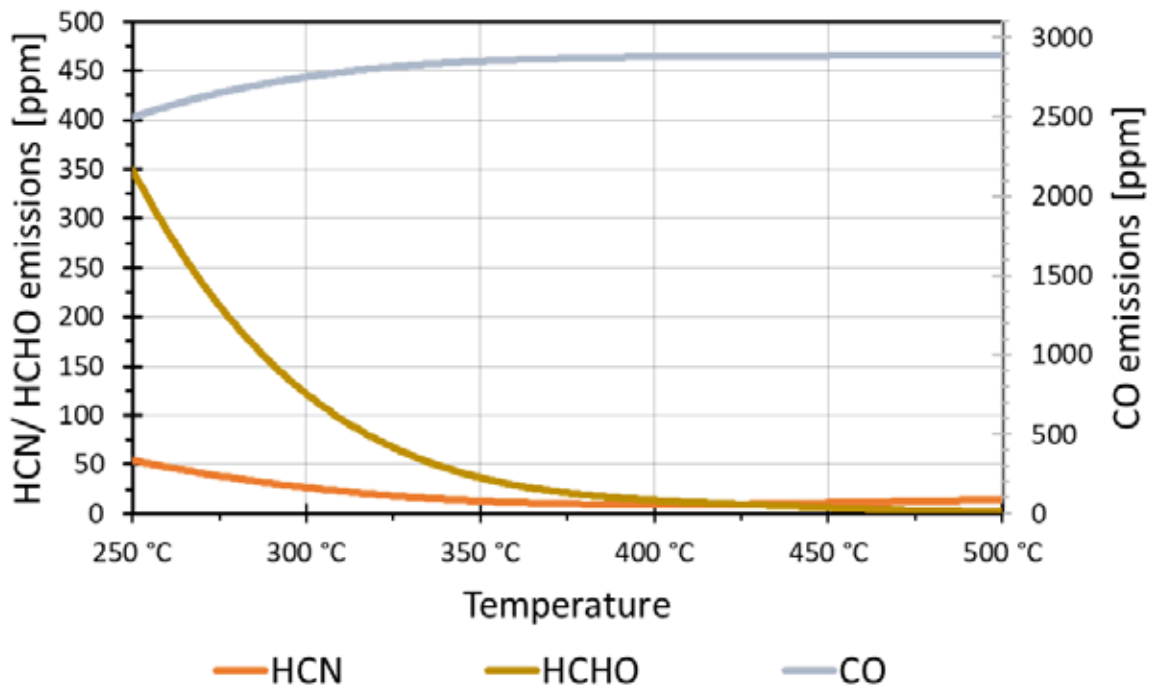


Figure 9: HCN, HCHO and CO formation in methanol operation for SCR + HCN-SCR systems. Conditions as stated in Figure 1.

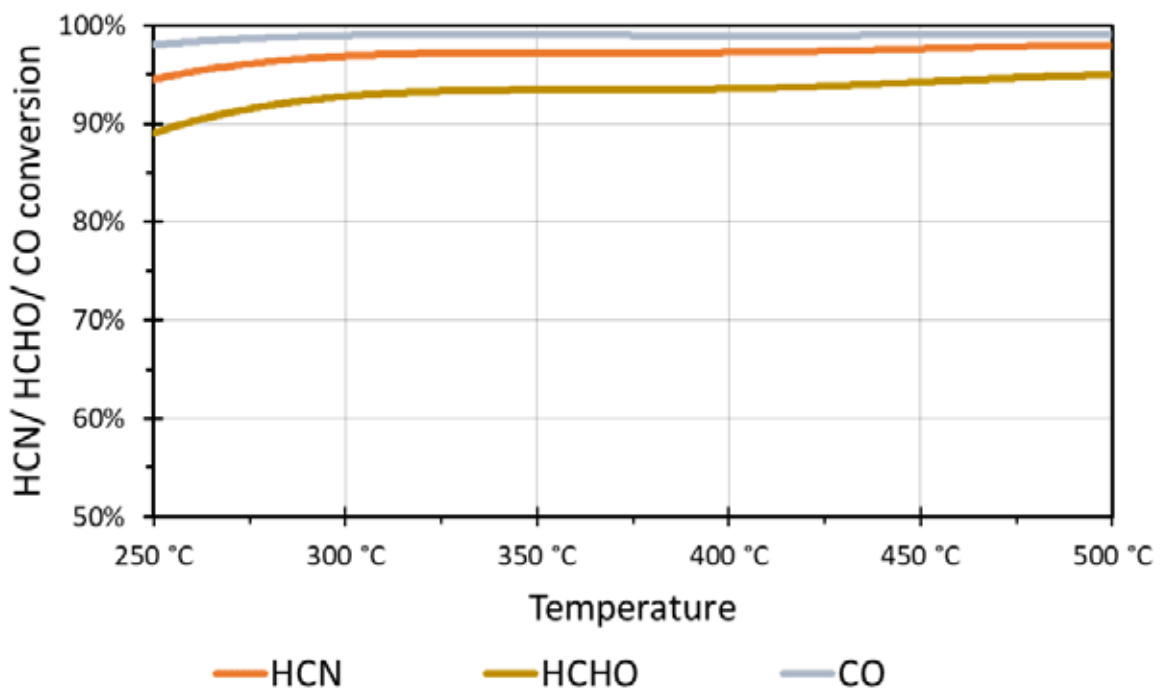


Figure 10: HCN, HCHO and CO conversion on a PGM oxidation catalyst of components formed on the SCR + HCN-SCR part of an exhaust gas aftertreatment system in methanol operation. SCR Inlet conditions as stated in Figure 1.

4. Summary

Methanol is considered a possible pathway for internal combustion engines to achieve low net CO₂ emissions – several combustion concepts are developed for various engine platforms in the industry. In terms of pollutants, the injection technology approach significantly impacts the concentrations of exhaust compounds. While possibly not considered at first sight, the amount of incompletely or unburnt hydrocarbon compounds significantly impacts NO_x conversion in SCR systems and may impact emission compliance when moving from Diesel to methanol operation. Furthermore, toxic side products (like HCN and HCHO) are formed during the SCR process due to the presence of methanol and ammonia.

An oxidation catalyst downstream of the SCR to remove side products can be even more detrimental to DeNO_x performance. However, two feasible pathways for avoiding any impact to NO_x compliance or the emission of toxic side products are presented. Both options come with specific advantages and restrictions, but both enable engine operation on methanol also for any combustion concepts chosen on the engine side. Exact dimensioning depends as usual on the exhaust conditions and compounds. The more exhaust characteristics in methanol operation resemble typical Diesel exhaust gas, the less additional modifications compared to a Diesel engine aftertreatment system are required. Close collaboration between engine and aftertreatment system design ensures optimized setups.

In contrast to methane slip issues still encountered for gas combustion and hard to abate with aftertreatment technology, methanol does not bring along unresolvable emission challenges in terms of greenhouse gas emissions or other pollutants. Hug Engineering has developed solutions to support engine builders and operators to enable their transition to low net CO₂ engine operation, for methanol and other future fuels.

References

- [1] M. Svenson, P. Molander, B. Ramne, M. Tunér and S. Verhelst, "The development and certification of a single fuel high speed marine CI engine on methanol," vol. 535, 2023.
- [2] D. Peitz, M. Hanschke and M. Kühnel, "Exhaust gas aftertreatment for stationary gas engines in times of energy transition and renewable fuels," no. 12th Dessau gas engine conference proceedings, 2022.
- [3] D. Peitz, D. Gschwend, K. Christianen and K. Lehtoranta, "Ultra-low emission medium speed engine of EU Stage V," vol. MTZ worldwide, no. 46, 2021.
- [4] L. Zheng, M. Casapu and M. Stehle, "Selective Catalytic Reduction of NO_x with Ammonia and Hydrocarbon Oxidation Over V₂O₅-MoO₃/TiO₂ and V₂O₅-WO₃/TiO₂ SCR Catalysts," *Top Catal*, pp. 129-139, 2019.
- [5] T. Nanba, A. Obuchi, S. Akaratiwa, S. Liu, J. Uchisawa and S. Kushiyama, "Catalytic hydrolysis of HCN over H-ferrierite," *Chem Lett*, pp. 986-987, 2000.

We invite you to the
Evening Event
Conference Dinner on
Wednesday May 15th, 2024 - 07:00 pm

The conference fee includes attendance at the evening event of the congress.



Technikmuseum „Hugo Junkers“

Kühnauer Str. 161a, 06846 Dessau-Roßlau

Photo © WTZ Roßlau

Keynote 2

**Analyse der globalen Wasserstoffversorgungsketten
- Transportmöglichkeiten, Kosten und Anwendungen
Global Hydrogen Supply Chain Analysis
- Transport options, Costs and Applications**

**Robert Szolak
Fraunhofer Institute for Solar Energy Systems ISE**

Global Hydrogen Supply Chain Analysis – Transport Options, Costs and Applications

Analyse der globalen Wasserstoffversorgungskette – Transportmöglichkeiten, Kosten und Anwendungen

R. Szolak, M. Holst, C. Thelen, C. Kost, A. Schaadt, T. Smolinka, C. Hank

Fraunhofer Institute for Solar Energy System ISE

Abstract

Green hydrogen and its derivatives – ammonia, methanol, and synthetic kerosene – store energy from the sun and wind to transfer it efficiently from distant regions to Europe. At the same time, many industries that cannot use electricity directly as an energy source will rely on these climate-neutral alternatives to fossil gas and oil, in addition to domestically produced hydrogen derivatives. On behalf of the H2Global Foundation, the Fraunhofer Institute for Solar Energy Systems ISE has examined 39 regions in 12 countries, preselected by H2Global, to determine where the production of such Power-to-X (PtX) products, in conjunction with transport to Germany, would be most cost-effective by 2030. The result: Brazil, Colombia, and Australia offer particularly good conditions for the import of green ammonia, methanol, and kerosene. If pipelines are available in time for transport, low-cost gaseous green hydrogen could be imported from southern Europe or North Africa.

Kurzfassung

Grüner Wasserstoff und seine Folgeprodukte Ammoniak, Methanol und synthetisches Kerosin speichern Strom aus Sonne und Wind, um diesen aus weiter entfernten Regionen energieeffizient nach Europa zu transportieren. Gleichzeitig sind viele Industrien, die nicht direkt Strom als Energieträger einsetzen können, zukünftig auf diese klimaneutralen Alternativen zu fossilem Gas und Öl angewiesen. Das Fraunhofer-Institut für Solare Energiesysteme ISE hat im Auftrag der Stiftung H2Global für 39 Regionen in von der Stiftung vorausgewählten 12 Ländern untersucht, wo die Herstellung solcher Power-to-X-Produkte bis zum Jahr 2030 in Verbindung mit dem Transport nach Deutschland am günstigsten umsetzbar wäre. Das Ergebnis: Für den Import grünen Ammoniaks, Methanols und Kerosins bieten Brasilien, Kolumbien und Australien besonders gute Bedingungen. Importe von gasförmigem grünem Wasserstoff könnten aus Südeuropa oder Nordafrika stammen, sofern dafür rechtzeitig Pipelines zum Transport zur Verfügung stehen.

1. Introduction

Climate protection and energy security are moving more and more into the center of societal awareness and behavior. The 'net-zero emissions' targets to be met by a vast number of countries by mid-century define a paradigm shift towards the strict limitation of the global temperature increase to 1.5°C. It becomes obvious that the regulatory framework and the financial backing as well as the trackable, tradeable, transparent, and trustworthy guarantees of origin for the sustainable energy carriers, are essential.

In addition to the demand for hydrogen of around 70 Mt H₂/a that already exists today, there will be also a large additional demand of Hydrogen across several sectors to achieve carbon neutrality, with an expected demand of approx. 600 million tons of hydrogen by 2050. Therefore, different trade flow patterns of hydrogen could emerge. Green molecules in the form of renewable hydrogen and hydrogen-based energy carriers will play a key role in the defossilisation of the global energy system. Green energy molecules complement the ongoing expansion of renewable electricity and provide solutions for applications that are hard to electrify, such as seasonal energy storage, global energy trading, aviation, ship, and industrial applications.

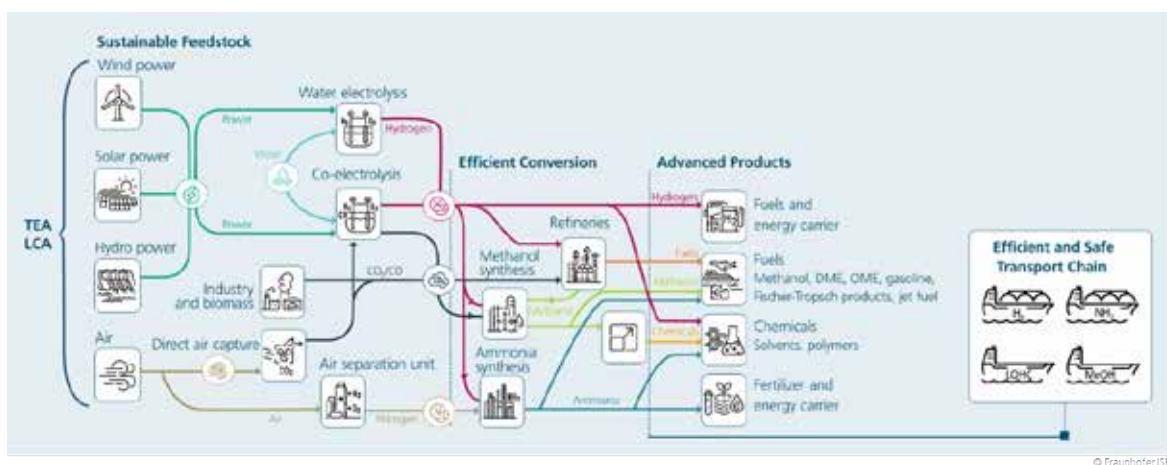


Fig. 1: The future energy system is dominated by green electricity and Power-to-X-Products (Hydrogen and Derivatives)

This research delves into an analysis of the production, transportation, and supply expenses associated with key Power-to-X commodities projected for the year 2030. A comprehensive examination was conducted across 39 diverse regions worldwide, primarily in developing and emerging nations, to evaluate their potential for renewables and Power-to-X production and supply cost efficiency. The results presented include a thorough techno-economic assessment derived from extensive country-level analyses, covering factors such as renewable energy generation potential, identification of promising regions, and comprehensive simulations and optimizations of Power-to-X production and supply pathways tailored to each region.

2. Where Germany's imports of hydrogen and Power-to-X products could come from

The study primarily centers on scrutinizing the costs of renewable electricity generation within these nations, followed by detailed design and simulation-based optimization of Power-to-X chains to produce green hydrogen, ammonia, methanol, and jet fuel. In scenarios involving imports, the study considers long-distance transportation of green energy carriers to Germany via ocean vessels or hydrogen pipelines. A fundamental prerequisite is the utilization of dedicated renewables solely to produce 100% green hydrogen. An electricity production system that relies on variable renewables requires a holistic approach to system design and operational strategies.

The methodologies used include site-specific Geographic Information System (GIS) analyses and hourly-resolved simulation and optimization of entire Power-to-X supply pathways. The study concludes by highlighting insights specific to each pathway, discussing key challenges, and addressing geopolitical interdependencies within global Power-to-X chains.

Key findings and conclusions drawn from this study:

- Site-specific analyses are crucial for accurately estimating Power-to-X production costs due to the intricate interplay of factors such as wind and photovoltaic production profiles, topographical and infrastructural conditions, and administrative considerations.
- Total product transport distance can significantly impact costs, but it is not necessarily a determining factor.
- The low levelized cost of renewable electricity generation and high full load hours greatly influence electrolysis capacity utilization and total Power-to-X product output.
- Favorable conditions for combined wind and PV power generation can be more advantageous than locations with exceptional conditions for only one renewable source. Hybrid renewable energy (RE) locations lead to higher utilization and lower requirements for intermediate hydrogen storage.
- A low weighted average cost of capital has a considerable impact on final production and supply costs.

Brazil and Australia emerge as particularly noteworthy countries in terms of achievable 2030 Power-to-X supply costs. The local production costs of gaseous green hydrogen in these nations range between 95-110 EUR/MWh (3.17-3.67 EUR/kg H₂) due to favorable wind and PV combinations, high plant utilization, and relatively low capital costs. When considering long-distance transport via ships, the final supply costs for liquid hydrogen range between 171-217 EUR/MWh (5.70-7.23 EUR/kg) and 171-172 EUR/MWh in the case of ammonia.

Additionally, the La Guajira region in northern Colombia stands out due to its excellent wind potential, resulting in comparatively low Power-to-X production and supply costs. However, the unique conditions in this region are nothing new and numerous renewable energy projects have already failed here due to a lack of coordination of the needs of the local population.

Dialogue and participation are key to the successful implementation of large-scale RE and PtX projects.

Furthermore, countries in the MENA region, such as Morocco, Algeria, and Tunisia, exhibit above-average conditions for wind and PV electricity generation and Power-to-X production. Algeria and Tunisia consistently demonstrate favorable green ammonia and methanol production and supply costs ranging from 190-250 EUR/MWh.

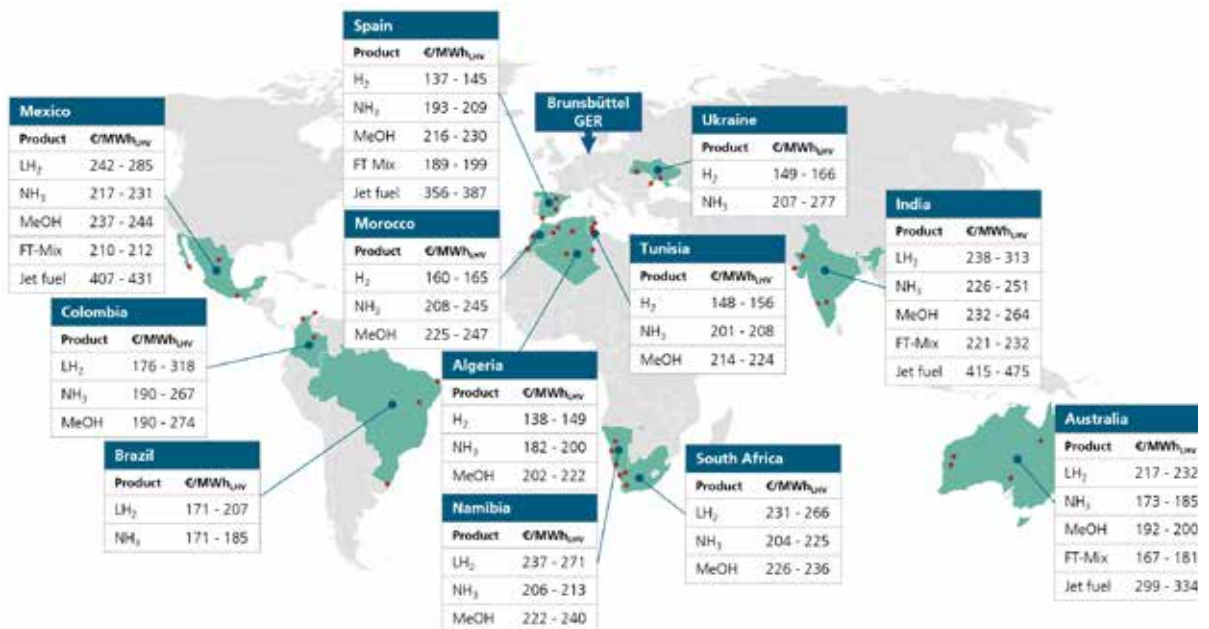


Figure 2: Overview of the countries analyzed regarding hydrogen and Power-to-X products and their provision costs, including transport to Germany. The calculation of the costs to produce liquid hydrogen (LH₂), ammonia (NH₃), and methanol (MeOH), as well as kerosene (jet fuel) and Fischer-Tropsch products (FT-Mix) is based exclusively on the assumption of additional renewable energy plants having been built in the respective export country. For the carbon-based energy sources, atmospherically captured CO₂ obtained using direct air capturing (DAC) technology is assumed.

Geographical Information System (GIS)-based infrastructure analysis shows that ports earmarked for export are generally sizable and have adequate draught for the vessels envisaged. However, some ports designed primarily for bulk cargo may require modifications to accommodate large-scale green energy exports. Alternatively, floating offshore terminals could be considered for larger Power-to-X projects. It is worth noting that certain regions with high solar irradiance and wind speeds were excluded from analyses due to inadequate road and grid capacities.

Addressing key challenges and geopolitical dependencies, the study emphasizes the importance of initiating large-scale Power-to-X projects promptly, given their long planning and construction phases. Additionally, there is a notable dependence on the Asian market for renewable energy technologies and associated components. To mitigate this dependence, there is a need to promote the development of manufacturing industries for water electrolysis and scale up production capacities. Furthermore, infrastructure bottlenecks must be addressed, not only in Power-to-X generation but also in downstream process chains necessary for import purposes.

In conclusion, this study underscores the potential of green hydrogen and its derivatives as viable alternatives amidst geopolitical uncertainties in the fossil fuel market. It suggests that long-term Power-to-X contracts facilitated by instruments like H2Global could reduce risks for investors and producers, thus fostering the growth of sustainable energy systems.

References

- [1] Christoph Hank, Marius Holst, Connor Thelen, Christoph Kost, Sven Längle Achim Schaadt, Tom Smolinka, *Site-specific, comparative analysis for suitable Power-to-X pathways and products in developing and emerging countries*, Fraunhofer ISE, 2023, commissioned by H2Global Foundation in cooperation with Gesellschaft für internationale Zusammenarbeit (GIZ). It was financed by the Federal Ministry for Economic Cooperation and Development (BMZ) → [Link](#)
- [2] Deloitte's 2023 global green hydrogen outlook

Handwriting practice area with horizontal lines.

Session 5

Nasserstoff - Mobile Anwendungen
Nydrrogen - Mobile applications

Moderation: Moderation: Prof. Hermann Rottengruber
Otto-von-Guericke-Universität Magdeburg

State-of-the-art H2 combustion at the MAN H4576

Moderne H2-Verbrennung am MAN H4576

P. Albrecht*, D. Hyna, M. Weidner, F. Lindner, T. Malischewski,
R. Zakrewski, Dr. A. Broda

MAN Truck & Bus, München und Nürnberg

Abstract

Facing the existing EU CO₂ limits for the heavy duty fleet and also their discussed decrease, the transition from diesel to CO₂-neutral propulsion is necessary. Beside the pure electric propulsion (BEV) for different reasons there are also hydrogen driven vehicles which have actual advantages especially when it comes to long-haul operation. For the ramp-up of the hydrogen chain in European transport business, market needs after all robust and economic solutions, offering high uptime and high equality in properties - compared to the diesel driven vehicles – to lower the inhibition threshold for an early usage at the customers. For that purpose the hydrogen combustion engine is the preferable solution. The MAN H4576 which was developed in an research project as direct-injecting hydrogen engine, certified as Zero-Emission for longhaul application. This paper is dealing with the further development steps leading the engine to market maturity.

Kurzfassung

Vor dem Hintergrund der bereits beschlossenen CO₂-Flottenziele für schwere Nutzfahrzeuge in der EU sowie deren diskutierter Verschärfung ist eine Abkehr vom Dieselmotor unabdingbar und der Übergang auf CO₂-neutrale Antriebskonzepte gefordert. Außer dem rein elektrischen Antrieb (BEV) bietet sich aus verschiedenen Gründen der Antrieb mit Wasserstoff an, der insbesondere im Bereich hoher geforderter Reichweiten derzeit Vorteile bietet. Für den Hochlauf der Wasserstoffkette im Transportwesen sind vor allem preiswerte und robuste Lösungen gefordert, die mit hoher Nutzungsverfügbarkeit und vergleichbaren Eigenschaften wie beim herkömmlichen Diesel-Nutzfahrzeug für gute Kundenakzeptanz sorgen und damit die Hemmschwelle für eine frühe Marktdurchdringung möglichst gering setzen. Hierfür ist der H₂-Verbrennungsmotor die geeignete Lösung. Der MAN H4576 ist im Rahmen eines Forschungsprojekts als direkteinspritzender H₂-Motor für den Fernverkehr entstanden, wobei er als Zero-Emission-Antrieb seinen Diesel-Pendants hinsichtlich der kundenrelevanten Eigenschaften sehr nahekommt. In diesem Beitrag werden die aktuellen Entwicklungsschritte zur Serienfähigkeit beschrieben.

* Speaker/Referent

1. Motivation H2-Antriebe

Die Nutzfahrzeugindustrie leistet schon seit jeher einen guten Beitrag zur CO₂-Reduzierung im Straßenverkehr. So wurden beispielsweise bei MAN Truck&Bus die CO₂-Emissionen im Zeitraum zwischen 1994 und 2019 um 40% gesenkt. Bis 2025 werden die CO₂-Emissionen um 55% abgesenkt sein. Dies kann aktuell überwiegend noch durch Wirkungsgradverbesserungen des Dieselmotors erreicht werden. Für die nach 2025 geforderten EU-CO₂-Flottenziele für schwere Nutzfahrzeuge ist es jedoch für jeden OEM unabdingbar, einen signifikanten Anteil seiner für die EU produzierten Fahrzeuge als ZEV (zero emission vehicle) anzubieten und diesen Anteil in den kommenden Jahren kontinuierlich zu steigern, bis in 2040 der Dieselantrieb nur noch eine Nischenanwendung sein wird.

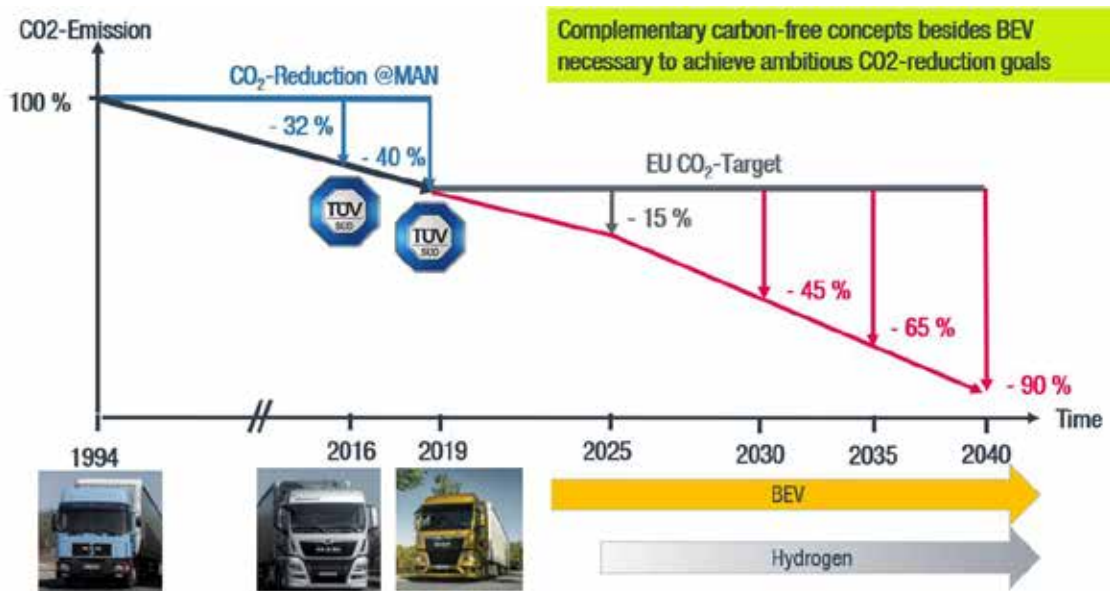


Bild 1: Entwicklung der CO₂-Emissionen

Das batterieelektrisch angetriebene Fahrzeug (BEV) ist hierbei bei praktisch allen OEMs die erste Wahl zur Darstellung eines ZEVs.

Der Antrieb von Fahrzeugen mit Wasserstoff als Energiespeicher bzw. Kraftstoff stellt hier eine zusätzliche, sinnvolle Ergänzung des Portfolios dar, wo es z. B. um hohe Reichweiten und Nutzlasten oder dünne Elektroinfrastruktur bzw. hohe Flexibilität in den Einsätzen geht.

2. Motivation H2-Verbrennungsmotor

Zu Beginn jeder neuen Entwicklung werden sich die Marktdurchdringung und damit die produzierten Stückzahlen zunächst nur langsam steigern. So auch beim Wasserstoff-Antrieb, dessen Hochlauf durch die Marktreife geeigneter Technologien, dem Vorhandensein von Infrastruktur und nicht zuletzt von der Kundennachfrage geprägt sein wird.

In dieser ersten Phase sind robuste, preiswerte Technologien mit kleineren Technologiesprüngen sinnvoll. Hierdurch können frühere Markteintritte mit hoher technischer Reife bei gleichzeitigem Aufbau auf bewährte Konzepte realisiert werden. Die Anpassungen in Produktion und dem für den Kunden extrem wichtigen Aftersales sind überschaubar und mit hoher Qualität darstellbar. Mit zunehmender Marktdurchdringung und höherem Stückzahlpotential können dann größere Technologiesprünge wirtschaftlich

und mit hoher Qualität und Reife - sowohl im Produkt wie auch im Service - realisiert werden.

Der als ZEV zertifizierte H2-Verbrennungsmotor stellt eine ideale Lösung zur Marktbereitung für den Kraftstoff Wasserstoff dar, da er mit hoher Gleichteilquote auf ausgereiften Lösungen basiert, im Vergleich zu einem Brennstoffzellenantrieb preiswert ist und keine übermäßigen Eingriffe in das Gesamtfahrzeugkonzept verlangt, wodurch z. B. auch viele kundenspezifische Lösungen vom Dieselfahrzeug einfach übernommen werden können (z.B. PTOs). Dies wird jedoch mit einem geringeren Gesamtwirkungsgrad erkauft, was zu gegebener Zeit den Markt auch für den Brennstoffzellenantrieb bereiten wird, der sich zukünftig auf das immer breiter werdende Portfolio elektrifizierter LKWs als Basisfahrzeug stützen kann.

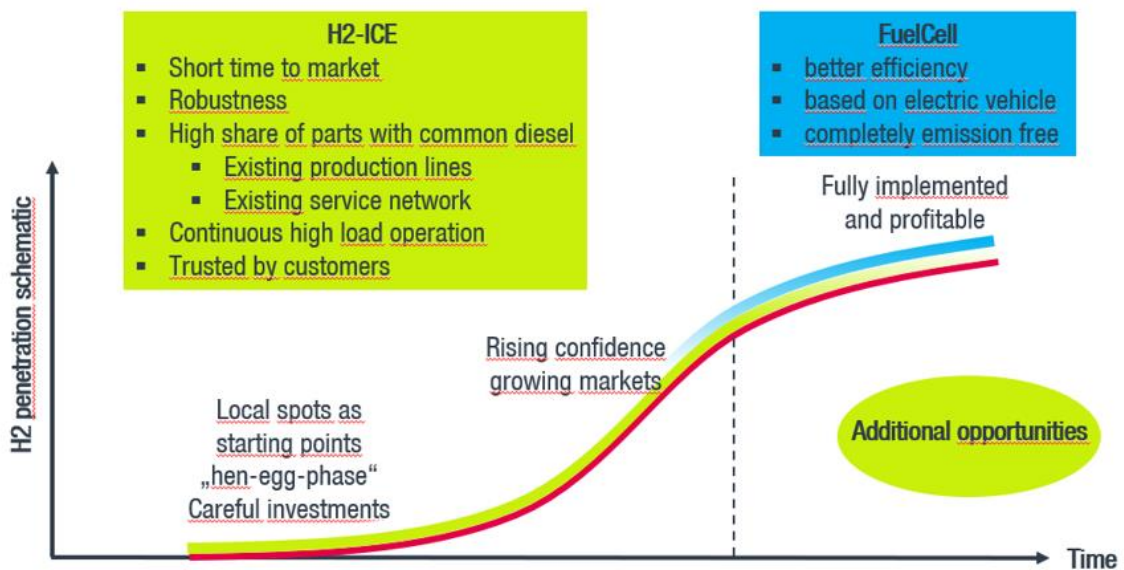


Bild 2: H2-Marktbereitung mit Verbrennungsmotor

Der H2-Verbrennungsmotor kann aber auch noch länger parallel zum Brennstoffzellenantrieb im Lkw oder anderen, davon abgeleiteten Anwendungen seine Berechtigung haben, wo es z. B. um höchste Dauerleistungen, Spezialanwendungen oder Toleranz gegen mindere H2-Qualitäten geht.

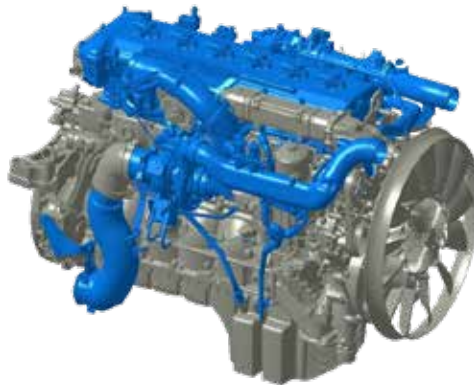


Bild 3: mögliche Anwendungen für H2-Verbrennungsmotoren

3. Der H4576LF01 als Teil der D38-Motorenfamilie

Die hier vorgestellte Variante des MAN H2-Verbrennungsmotors ist die Weiterentwicklung des in einem Forschungsprojekt entwickelten H4576. Beide Motoren basieren auf dem D3876, der als schwerer LKW-Dieselmotor bei 15,2l Hubraum bis zu 470kW und 3000Nm abgibt.

Das Ziel der Weiterentwicklung war, durch Vereinfachung im Aufbau, Integration bereits erprobter Komponenten aus dem MAN-Motorenbaukasten und Optimierungen im Detail, das Konzepts hinsichtlich Robustheit, Leistungsabgabe und Kosten zur Serienfähigkeit zu bringen. Eine zusätzliche Leistungs- und Drehmomentsteigerung gegenüber dem Forschungsmotor rundet die Optimierung ab.



H4576 LF 01

Cylinders	6 / inline
Bore / stroke	145mm / 170mm
Displacement	16.8 l
Compression ratio	1:12
Cylinder Peak Pressure	170 bar
Engine Power	382 kW @ 1800rpm
Engine torque	2500 Nm @ 930 ... 1350rpm
Fuel Injection	low pressure DI
Maximum fuel pressure	22 bar
Ignition	Central cold spark plug
Turbocharging	VTG
Charge air cooler	direct air-to-air
Cam Shaft	SOHC
Exhaust aftertreatment	SCR

Tabelle 1: Technische Daten des weiterentwickelten H4576LF01

4. Weiterentwicklungen am H45

Dem Ziel der Vereinfachung und Kosteneinsparung gegenüber dem Forschungsmotor wurde u. a. durch Umstellung des Ventiltriebs von DOHC auf SOHC genüge getan, wodurch gegenüber der Dieselvariante nur noch geringe Änderungen am Zylinderkopf für H₂-Injektor und Zündorgane notwendig werden.

Außerdem wurden Neuteile für die Ansaug- und Abgasanlage sowie Zylinderkopfhaube entwickelt. Kolben, Laufbuchse und Ringpaket wurden optimiert.

Insgesamt teilt sich der H45 ca. 90% der Bauteile mit der Dieselvariante.

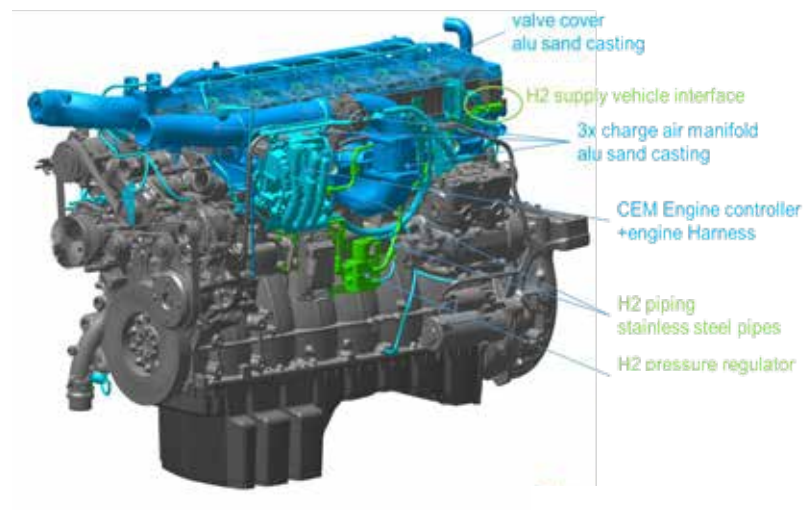


Bild 4: Ansicht der linken Motorseite mit neuen Komponenten

Unverändert blieb das Verbrennungskonzept als direkt einblasender Fremdzünder mit mittiger Zündkerze, das eine exzellente Gemischbildung und den Betrieb des Motors mit hohem Luftüberschuss ermöglicht und die Basis für niedrige Emissionen bei guten Wirkungsgraden darstellt.

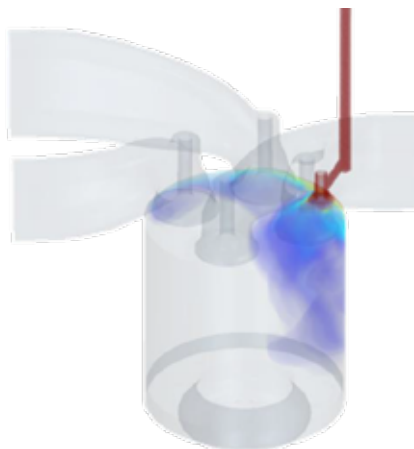


Bild 5: 3D-Simulation der Gemischbildung

Zusätzlich lassen sich durch dieses Konzept mit Einblasung nach Einlass schließt gutes Instationärverhalten durch bessere Füllung ohne die Gefahr von Rückzündungen realisieren.

Andererseits kann durch Einblasen bei geöffnetem Einlassventil eine Entdrosselung des Ladungswechsels und Steigerung des Wirkungsgrads bei höheren Drehzahlen erreicht werden.

Im folgenden Bild werden die Lage der verschiedenen Einblasstrategien illustriert und die positiven Effekte auf Instationärverhalten und Wirkungsgrad gezeigt.

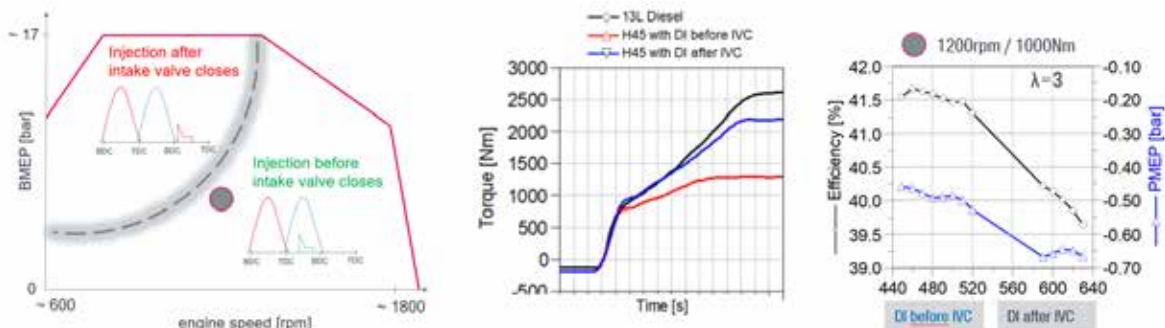


Bild 6: positive Effekte der Direkteinblasung

Eine thermodynamische bedeutende Änderung ist der Entfall der Abgasrückführung. Die entstehenden Nachteile in Gaswechsel und Verbrennung wurden durch Änderung der Aufladung von Wastegate-ATL zu VTG und Feintuning an der Gemischbildung in Verbindung mit einem neuen H2-Injektor kompensiert. Diese Änderungen bringen deutliche Kosteneinsparungen in der Entwicklung durch Einsatz eines bereits bei einem MAN Einbaumotor validierten VTG-Abgasturboladers sowie durch Entfall des Abgasrückführungssystems.

Zusätzlich verbessert die VTG wesentlich das Ansprechverhalten und das Dauerbremsmoment des Motors

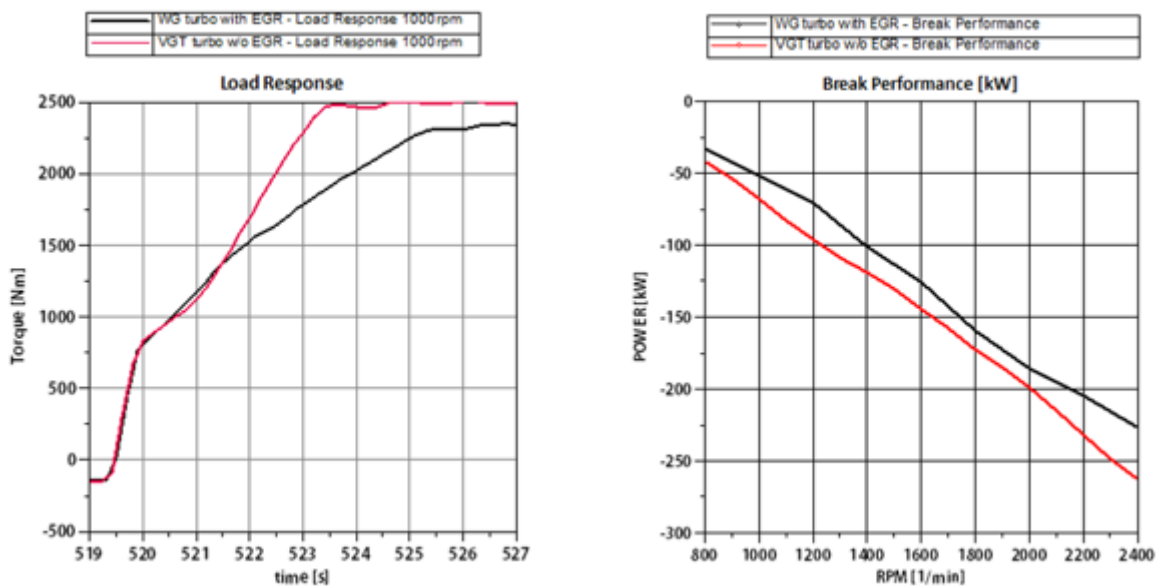


Bild 7: Einfluss der VTG auf Instationärverhalten und Dauerbremsmoment

Zusätzlich ist es gelungen, die Leistung des Motors bei unverändertem Wirkungsgrad noch etwas gegenüber dem Forschungsmotor zu steigern, so daß der H4576 nun 382kW / 520PS @ 1800/min und 2500Nm @ 930...1400/min leistet. Die Eckdrehzahlen der Vollastkurve entsprechen somit denen der MAN-Dieselmotoren in diesem Segment, was große Vorteile bei Antriebstrangauslegung und Fahrzeugintegration bietet.

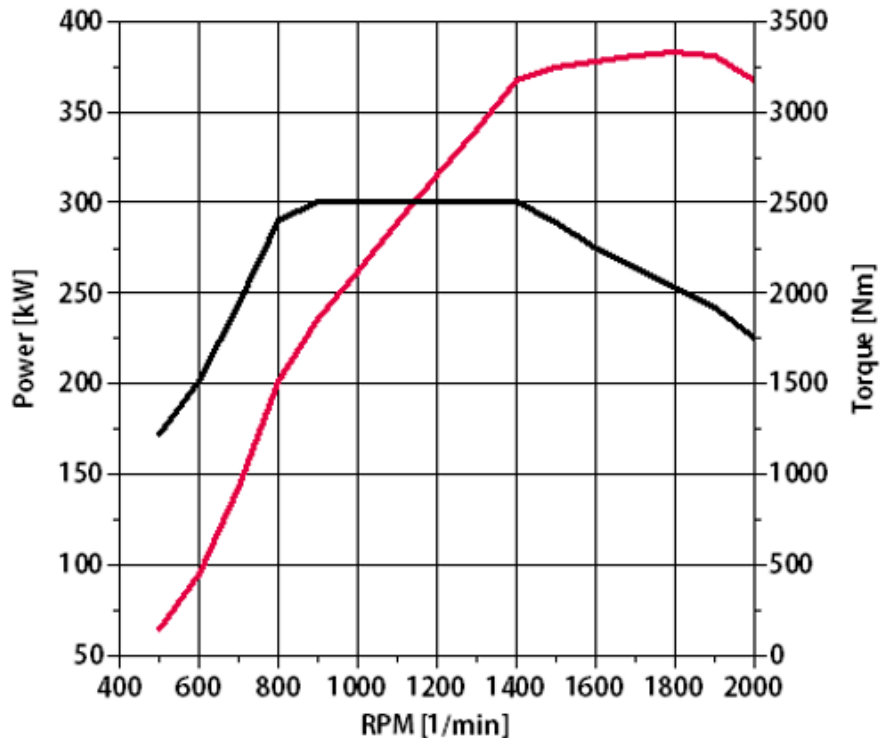


Bild 8: Leistung und Drehmomentkurve

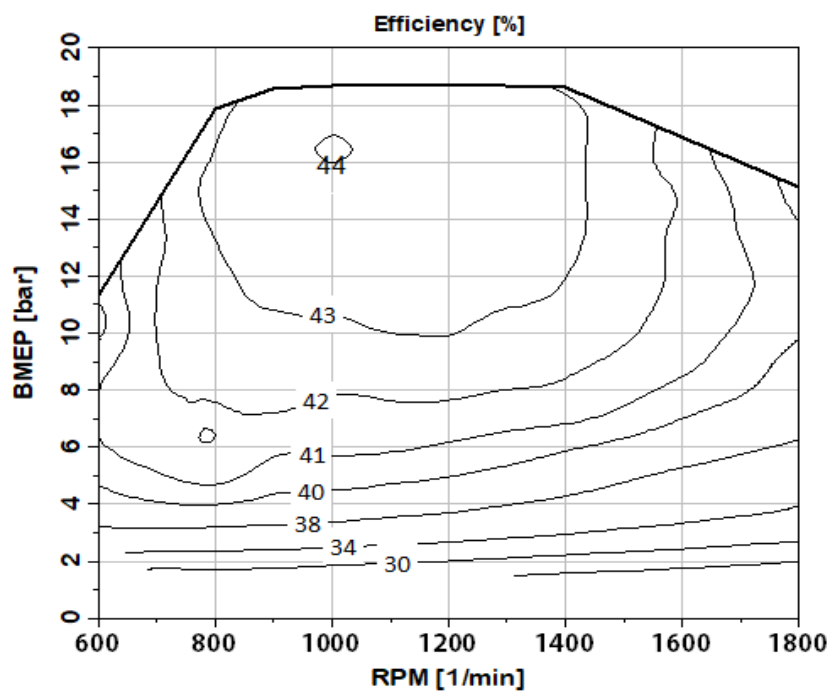


Bild 9: Wirkungsgradkennfeld

Da der Motor als Magermotor mit deutlichem Luftüberschuss betrieben wird, bewegen sich die Roh-NO_x-Emissionen auf sehr niedrigem Niveau. Es können die EU7 Grenzwerte in Verbindung mit einem SCR-System sicher und mit niedrigem AdBlue-Verbrauch unterschritten werden.

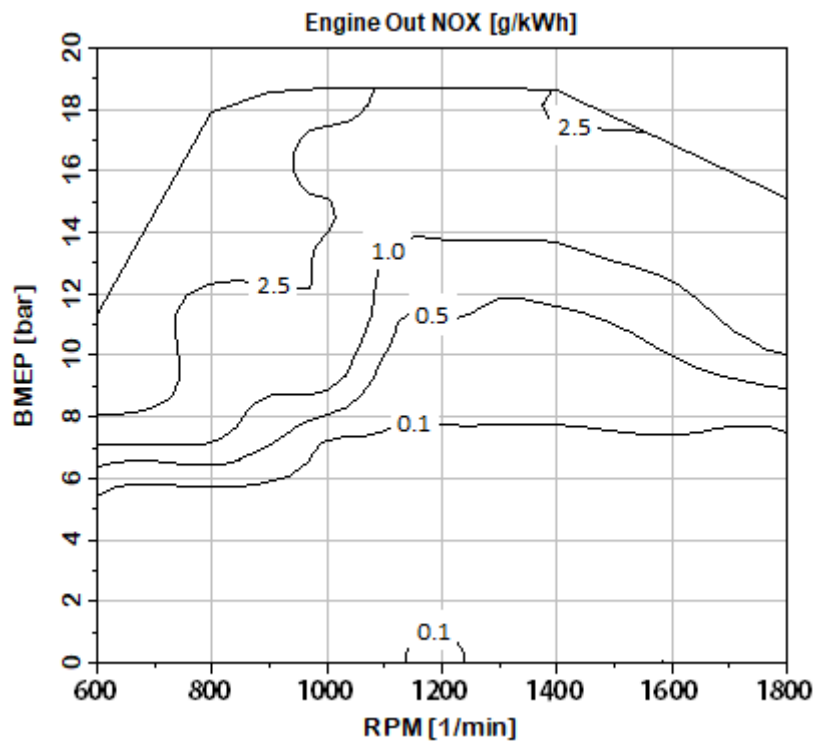


Bild 10: Roh-NO_x-Emission

5. PEMS-Messungen

Bei den nach den EUVle-Richtlinien durchgeführten PEMS-Messungen konnten aufgrund der niedrigen Roh-NO_x-Emissionen und des guten Abgastemperaturniveaus die EUVII-Grenzwerte in Verbindung mit einem SCR-System deutlich unterschritten werden. Der AdBlue-Verbrauch liegt dabei bei ca. 10% des AdBlue-Verbrauchs von Dieselmotoren.

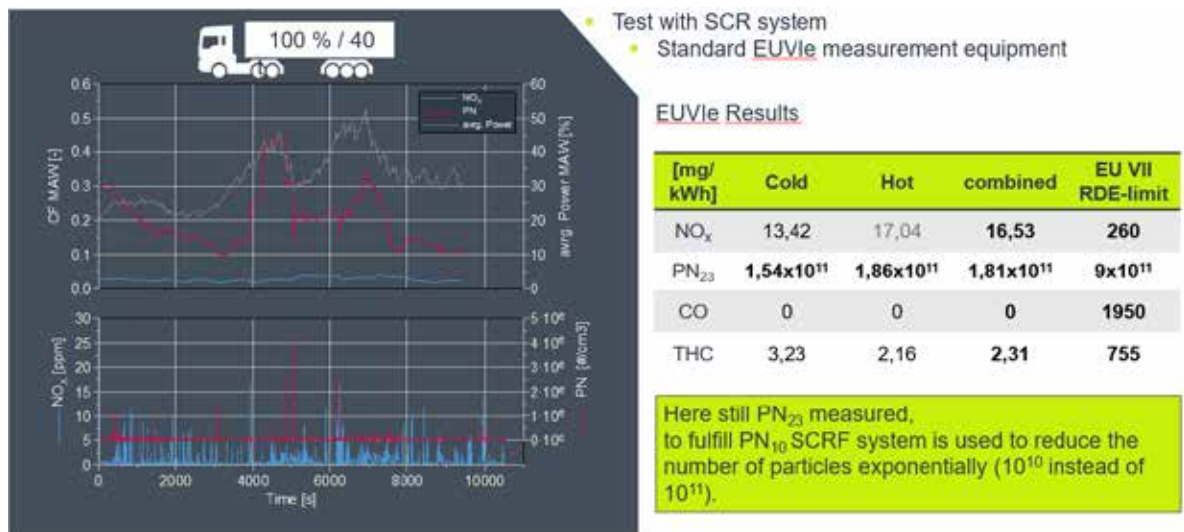


Bild 11: PEMS-Ergebnisse für 40t

6. Fahrzeugintegration

Generell bietet die Integration dieses Wasserstoffverbrennungsmotors den großen Vorteil, den Antriebstrang des Fahrzeugs in weiten Teilen unverändert lassen zu können. So sind Kupplung, Getriebe und Kühlanlage vom Dieselpendant übernommen. Aufgrund des gleichen Drehmomentverlaufs und Drehzahlniveaus sind auch Hinterachse und deren Übersetzung unverändert, was zusätzlich Synergien bei der Abstimmung des Triebstrangmanagements mit sich bringt.

Beim 700bar-Tanksystem kommt eine neu entwickelte Variante zum Einsatz, die nun 55kg H₂ fasst, womit sich im Longhaul-Betrieb mit 40t Zuggesamtmasse Reichweiten um 600km erzielen lassen.

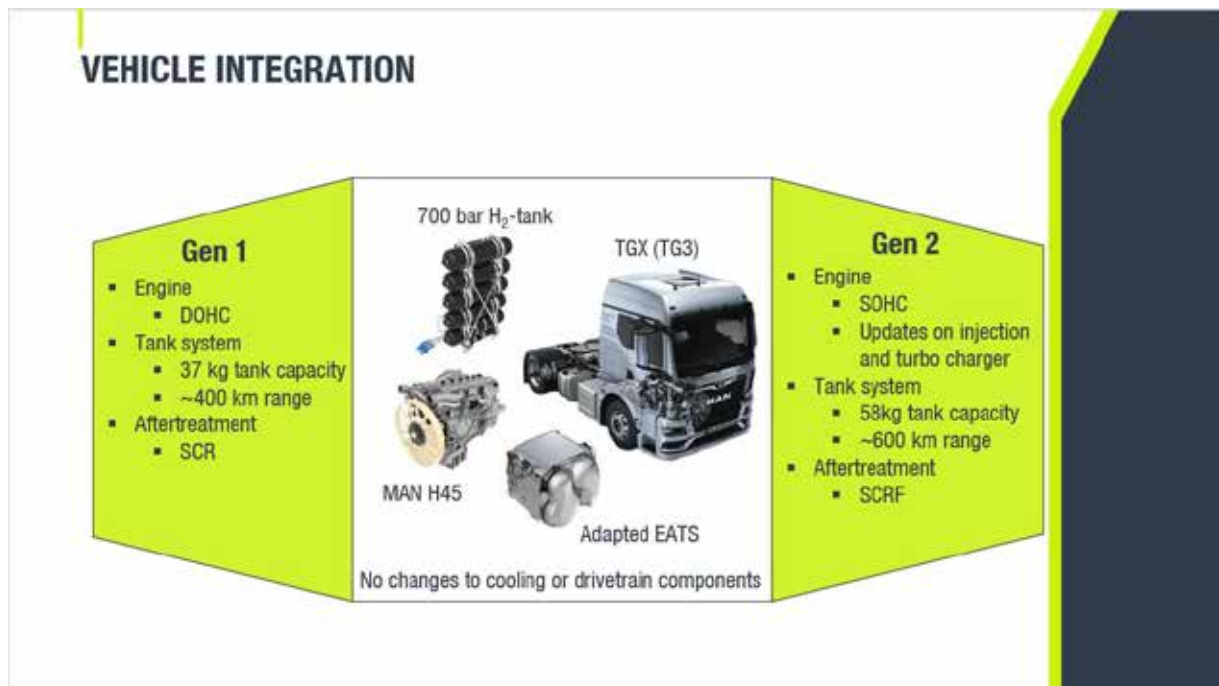


Bild 12: Fahrzeugseitige Modifikationen

6. Beispiel für erste Kundenanwendung

H₂-ICE TRUCK CHARACTERISTICS

89K TGX 28t 6x2-2 BL-SA

- 🔊 520hp / 2500Nm
- 📏 9kg/100km / ~600km range
- 🚛 Same payload as Diesel
- 🏠 Classified as ZEV within the EU
- 🚰 700bar H₂ tank system
- 🚰 56kg hydrogen
- ⏱ Short refueling time <15min
- 🔧 ~90% component share with Diesel
- 📋 Prepared for ADR regulation
- 📅 Market entry from 2025 possible

Bild 13: erste Kundenanwendung

Zusammenfassung

Der Wasserstoffverbrennungsmotor ist nicht nur in der aktuellen Phase des H2-Hochlaufs sondern auch darüber hinaus eine wirtschaftliche und robuste ZEV-Antriebsquelle im Nutzfahrzeugsbereich.

Bei MAN H4576LF01 ist es gelungen, einen Zero-Emission-Antrieb darzustellen, der

- im oberen Bereich der 13l-Dieselmotoren angesiedelt ist und die Kundenanforderungen an einen entsprechend performanten Antrieb vollumfänglich erfüllen kann.
- aufgrund des Magermotorkonzeptes mit ultraniedrigen Emissionen aufwartet
- bereits die EU7-Abgasnorm erfüllt und dazu 90% weniger AdBlue verbraucht als ein entsprechender Diesel
- aufgrund der gegenüber der Dieselvariante geringeren Bauteilbelastungen eine hohe Robustheit aufweist
- unempfindlich gegen mindere H2-Qualitäten ist
- mit den gleichen Intervallen wie das Dieselpendant gewartet werden kann
- geringe fahrzeugseitige Modifikationen erfordert und somit das Potential zu einem weiten Portfolio an kundengerechten ZEV-Transportlösungen auf Basis Wasserstoff bietet.

Der H4576 ist der richtige H2-Antrieb zur richtigen Zeit und erfreut sich bereits hoher Kundennachfrage.

References

- [1] Lindner, Weidner, Hyna, Malischewski, Dr. Broda, Teubner, Schmitt, Dr. Schraml, 4x2 tractor with a hydrogen combustion engine – highest performance with lowest emissions, 10. Internationaler Motorenkongress 2023
- [2] Lindner, Dr. Schraml, Weidner, Hyna, Teubner, Dr.-Ing. Broda, Strategy for heavy duty trucks with hydrogen combustion engine, 20. FAD-Konferenz, 08.11.-09.11.2023

Performance improvement of direct injection H₂-ICE with flat cylinder heads

Leistungssteigerung von direkteinspritzenden H₂-Motoren mit flachem Brennraumdach

Dr. A. Güdden*, **Dr. B. Franzke**, **A. Boberic**

FEV Europe GmbH, Aachen

P. Zimmer, **Prof. S. Pischinger**

Chair of Thermodynamics of Mobile Energy Conversion Systems, RWTH Aachen University

Abstract

Hydrogen internal combustion engines offer great potential for cost-effective decarbonization in combination with a short-term market entry, especially in the commercial vehicle and construction machinery sectors.

An important goal of hydrogen engine development is to increase power density to the level of equivalent diesel engines. However, premixed combustion systems are limited in their maximum load by combustion anomalies such as pre-ignition and knock. The occurrence of these undesirable combustion processes is favored by the properties of hydrogen. Hotspots, glowing oil residue, and local residual gas pockets are potential sources of uncontrolled combustion. Since the ignitability of the hydrogen-air mixture is significantly influenced by the local composition, the optimization of mixture formation is one goal of combustion system development.

In this paper, the influence of various parameters to mitigate abnormal combustion phenomena is discussed and the potential to enhance the performance is investigated. On the one hand, the investigations consist of a 3D-CFD simulation study of in-cylinder flow to analyze the influence of a tumble motion on mixture formation for an engine with a flat combustion chamber roof. On the other hand, extensive measurements on a heavy-duty single cylinder engine with varying hardware configurations have been conducted with focus on performance limits set by an acceptable frequency and intensity of abnormal combustion.

The results of the simulation study show that a tumble charge motion can improve the coefficient of variation of the equivalence ratio, which serves as a measure for the homogeneity of the mixture, by 28 %. This simulative result and the importance of mixture homogenization are confirmed by a reduction in the load-dependent frequency of combustion anomalies in the experimental investigations with the single-cylinder engine. Furthermore, a comprehensive testing campaign has revealed that the sealing of the valves as well as the oil management of the piston rings are essential parameters to mitigate the frequency of abnormal combustion.

Overall, the findings prove that a direct injection H₂-ICE with a flat combustion chamber roof can achieve indicated mean effective pressures levels similar to diesel engines of above 25 bar without special technology features such as cooled EGR or water injection.

* Speaker/Referent

Kurzfassung

Wasserstoffverbrennungsmotoren bieten vor allem im Nutzfahrzeug- und Baumaschinen-sektor großes Potential für eine kosteneffiziente Dekarbonisierung der Antriebe in Kombination mit einem zeitnahen Markteintritt.

Ein wichtiges Ziel der Wasserstoffmotorentwicklung ist die Steigerung der Leistungsdichte auf das Niveau äquivalenter Dieselmotoren. Vorgemischte Brennverfahren sind jedoch durch Verbrennungsanomalien wie Vorentflammungen und Klopfen in ihrer maximalen Last limitiert. Das Auftreten dieser unerwünschten Verbrennungsvorgänge wird durch die Stoffeigenschaften von Wasserstoff begünstigt. Heiße Oberflächen, glühende Ölrückstände und lokale Restgasnester sind als potenzielle Quellen für unkontrollierte Verbrennungen zu nennen. Da die Zündwilligkeit des Wasserstoff-Luft Gemischs maßgeblich von der lokalen Zusammensetzung beeinflusst wird, ist die Optimierung der Gemischbildung ein Ziel in der Brennverfahrensentwicklung.

In diesem Beitrag wird der Einfluss verschiedener Parameter zur Minderung abnormaler Verbrennungsphänomene diskutiert und das Potenzial zur Leistungssteigerung untersucht. Die Untersuchungen bestehen zum einen aus einer 3D-CFD-Simulationsstudie der Zylinderinnenströmung, um den Einfluss einer Tumble-Ladungsbewegung auf die Gemischbildung bei einem Motor mit flachem Brennraumdach zu analysieren. Des Weiteren wurden umfangreiche Messungen an einem Nutzfahrzeug-Einzyliermotor mit unterschiedlichen Hardware-Konfigurationen durchgeführt, wobei der Fokus auf den darstellbaren Leistungsgrenzen bei einer akzeptablen Häufigkeit und Intensität irregulärer Verbrennung liegt.

Die Ergebnisse der Simulationsstudie zeigen, dass eine Tumble-Strömung den Variationskoeffizienten des Verbrennungsluftverhältnisses, der als Maß für die Homogenität des Gemischs dient, um 28 % verbessern kann. Dieses Ergebnis und die Bedeutung der Gemischhomogenisierung werden durch die Verringerung der lastabhängigen Häufigkeit von Verbrennungsanomalien bei den experimentellen Untersuchungen mit dem Einzylindermotor bestätigt. Darüber hinaus hat eine umfangreiche Versuchskampagne gezeigt, dass die Dichtigkeit der Ventile sowie das Ölmanagement der Kolbenringe wesentliche Parameter sind, um die Häufigkeit von Verbrennungsanomalien zu reduzieren.

Die Ergebnisse belegen, dass direkt einblasende H₂-Verbrennungsmotoren mit einem flachen Brennraumdach auch ohne Technologien wie gekühlte Abgasrückführung oder Wassereinspritzung ähnliche indizierte Mitteldrücke wie Dieselmotoren von über 25 bar erreichen können.

1. Introduction

Hydrogen engines offer the possibility to combine a carbon free energy carrier with the reliability of a combustion engine, especially in the off-road medium- and heavy-duty segment. Since the first generation of H₂ ICEs is usually basing on existing Diesel engines, a flat cylinder head design is frequently a predefined boundary condition. The reason for this is that a high share of carry-over parts from existing ICEs enables a fast and cost-effective market entry. However, the fuel characteristics of hydrogen – especially the low ignition energy – require changes in the engine layout compared to conventional fuels. This characteristic makes hydrogen prone to pre-ignite. Two general approaches regarding the occurrence of abnormal combustion during engine operation and related countermeasures are depicted in figure 1.

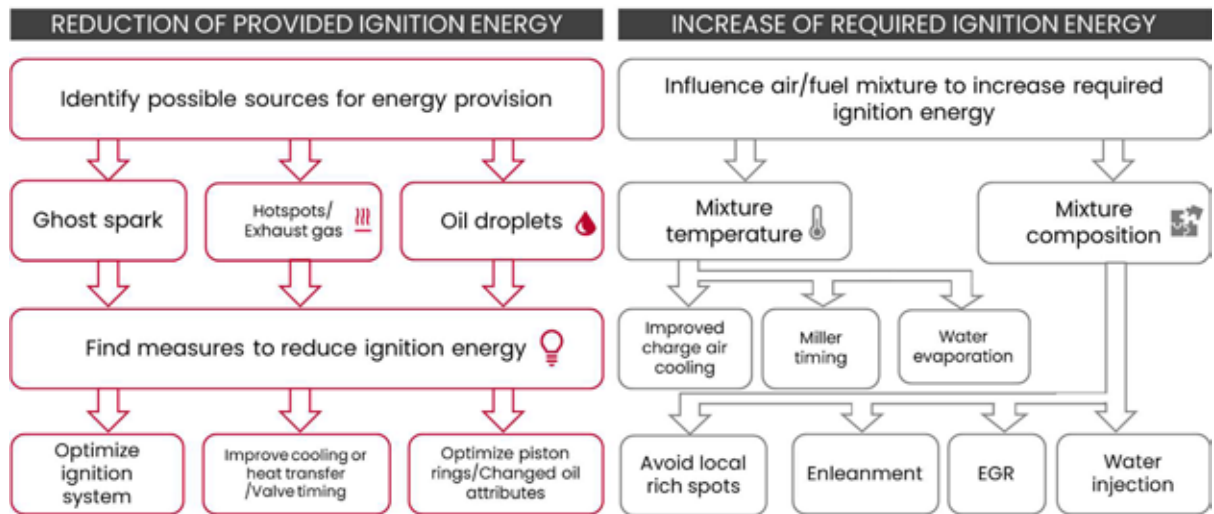


Figure 1: Overview of causes for abnormal combustion with H2 ICE [1]

Engine operation with a lean air-fuel-ratio in combination with direct H₂ injection and the use of thermally optimized hardware components such as piston, valves and spark plug have already proven to be keys to increase the specific power [1], [2]. However, the previous investigations have also revealed that further measures are required to run the engine at a specific load above IMEP = 20 bar without special technology features such as cooled EGR or water injection. In this context, it is obvious that the development target for a permissible pre-ignition frequency cannot be set to zero. Figure 2 shows various examples for abnormal combustion with different impacts on engine operation.

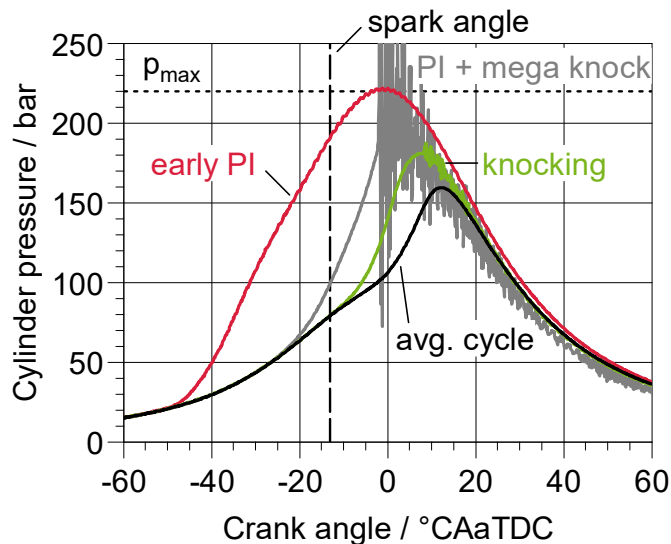


Figure 2: Examples for abnormal combustion cycles

Compared to the average combustion cycle, a fast-burning cycle with a short burn delay exhibits knocking (green curve). Since the combustion is initiated with the electrical spark, a retardation of the spark angle can mitigate this abnormal combustion phenomenon. Besides this typical spark knock, it is important to distinguish between different kinds of cycles with pre-ignition (PI). Very early pre-ignited cycles comprise the risk of violating the peak cylinder pressures limit since the combustion takes place during the compression stroke (red curve). However, cycles in which the pre-ignition leads to an auto-ignition in the end gas zone resulting in a heavy knocking event – the so called mega knock – are even more critical (grey curve). This extreme mechanical and thermal stress for the engine must be prevented. Still, a

certain frequency of pre-ignitions events without mega knock and critical peak pressure must evidently be accepted for high load operation.

By default, FEV uses multiple criterions to detect a pre-ignition event based on analyzing the heat release rate and the cylinder pressure trace in the time range of the spark angle. Therefore, a detailed PI assessment and statistical post-processing is applied for the following evaluations of the thermodynamic testing on FEV's H₂ HD single cylinder engine.

2. Test carrier

For the experimental investigations, a heavy-duty diesel single cylinder engine was modified to a pre-mixed hydrogen combustion system. The single cylinder engine as well as the combustion chamber layout are depicted in figure 3.

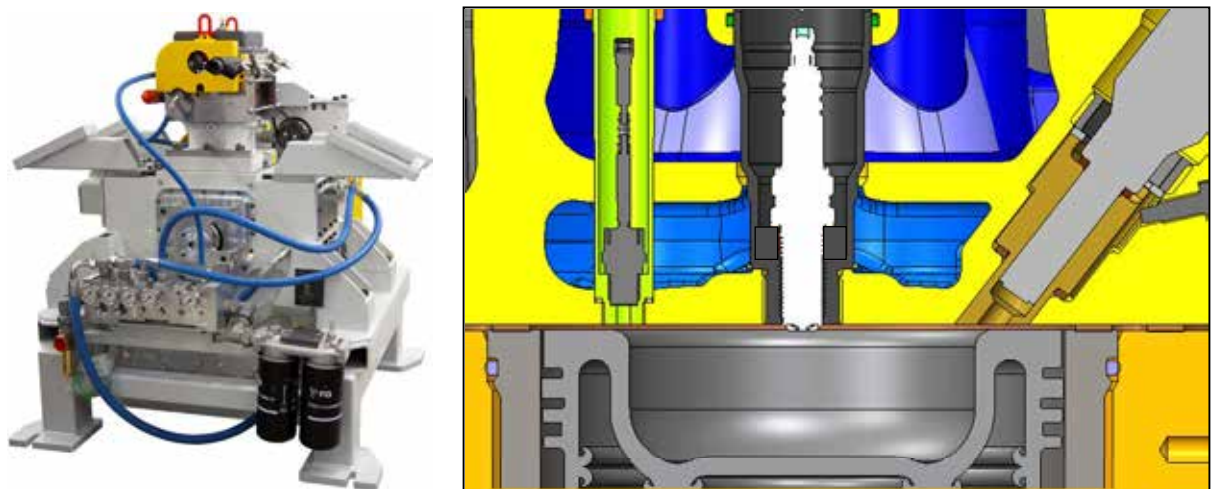


Figure 3: FEV HD hydrogen single cylinder engine and corresponding combustion chamber layout

A pot bowl design has been chosen to achieve a comparatively low compression ratio of 10.6:1 with the flat cylinder head design of the diesel base engine. The cylinder head was redesigned to implement the low-pressure direct injection of hydrogen in a lateral position. A common parts approach to the diesel base engine was applied manifesting in carrying over e.g. the valve position. The intake ports provide maximum cylinder filling with a very low level of charge motion.

During all measurements, the exhaust backpressure was controlled to be equal to the boost pressure. To avoid engine damage, the operating limits of this engine have been defined by the maximum pre-ignition frequency and knock peak-to-peak (KPP) parameter respectively. A summary of the engine specifications and further boundary conditions for operation can be found in Table 1.

Table 1: Engine characteristics and boundary conditions for operation

Description	Unit	Value
Bore x stroke	mm	132 x 156
Displacement	cm ³	2135
Compression ratio	-	10.6:1
Coolant / oil temperature	°C	90 / 90
Temperature after charge air cooler	°C	25
Injection pressure (DI)	bar	25
Spark Plug	-	Cold heat range
Charge motion	-	None / Tumble
Maximum pre-ignition frequency	%	3
Maximum KPP Value	bar	20

3. Measures for performance improvement

The following sections focus on the different measures to improve the performance of the DI H₂ ICE. Initially, the influence of the valve sealings is discussed, followed by charge motion and the oil droplet management.

3.1. Valve sealing

In hydrogen measurement campaign, suddenly a heavily increased pre-ignition frequency at IMEP = 16 bar was detected. However, there was no change in operating conditions. The change in engine behavior interpreted as an indication for a hot spot in the combustion chamber. An investigation with a fiber optical spark plug confirmed this theory and located the PI origin in the areas of the exhaust valves. During an endoscopy and disassembly of the engine, soot deposits and material discoloration as signs of a local thermal overload at the valve seat and at the top edge of the liner were found, see pictures in figure 4.

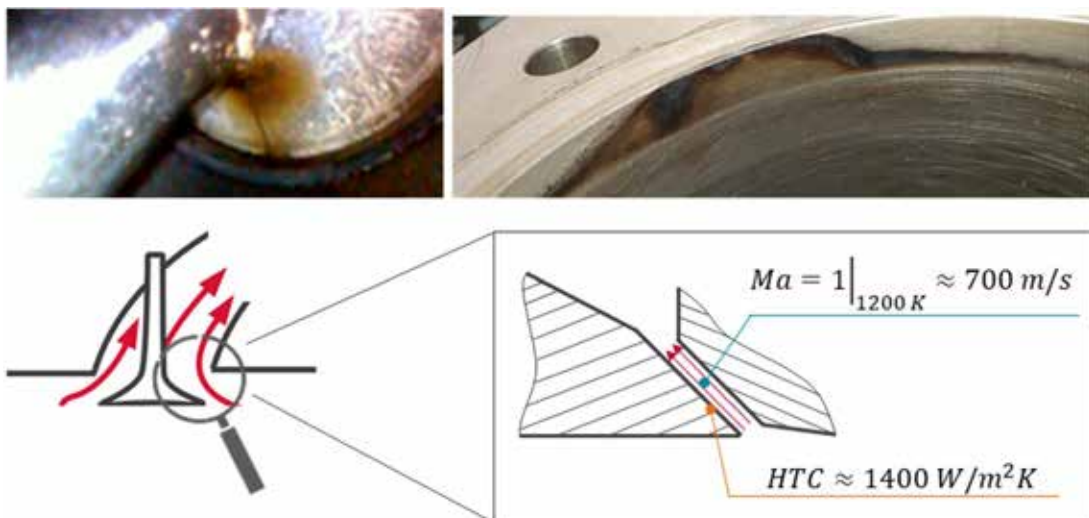


Figure 4: Soot deposits and material discoloration by valve leakage and sketch of flow conditions

The intensity of the gas leakage has such a low extent that no indications are found in the cylinder pressure trace. However, figure 4 illustrates that even a minimal level of leakage

leads to a jet flow with Mach number = 1 in the gap since there is a supercritical pressure ratio during the combustion and expansion. One consequence of the large flow velocity is a very high local heat transfer coefficient (HTC) estimated basing on a Nusselt number correlation for a local turbulent boundary layer [3] which is increasing the total heat transfer to the valve disk and seat ring. Furthermore, the missing contact between valve disk and seat ring hinders the essential heat dissipation during the phase in which the valve is closed. Overall, the leakage increases the local valve temperatures from the already elevated level. This hot spot serves as a trigger for pre-ignitions.

Figure 5 depicts a load sweep comparison between engine operation with and without exhaust valve leakage under identical boundary conditions. According to the behavior of pre-ignition and knocking, it is noticeable that the achievable IMEP level is more than 6 bar lower for the case with leakage. Thus, the hot spot resulting from valve leakage limits the engine performance considerably. The early pre-ignited combustion and partial auto-ignitions enhance the thermal load further which is evident by the increase in the NO_x emissions. Thereby, a self-amplifying effect is existing with a high risk for critical engine operation. Differences in the values of the indicated efficiency at the same load (e.g. IMEP = 16 bar) are influenced by the different intensity of pre-ignitions.

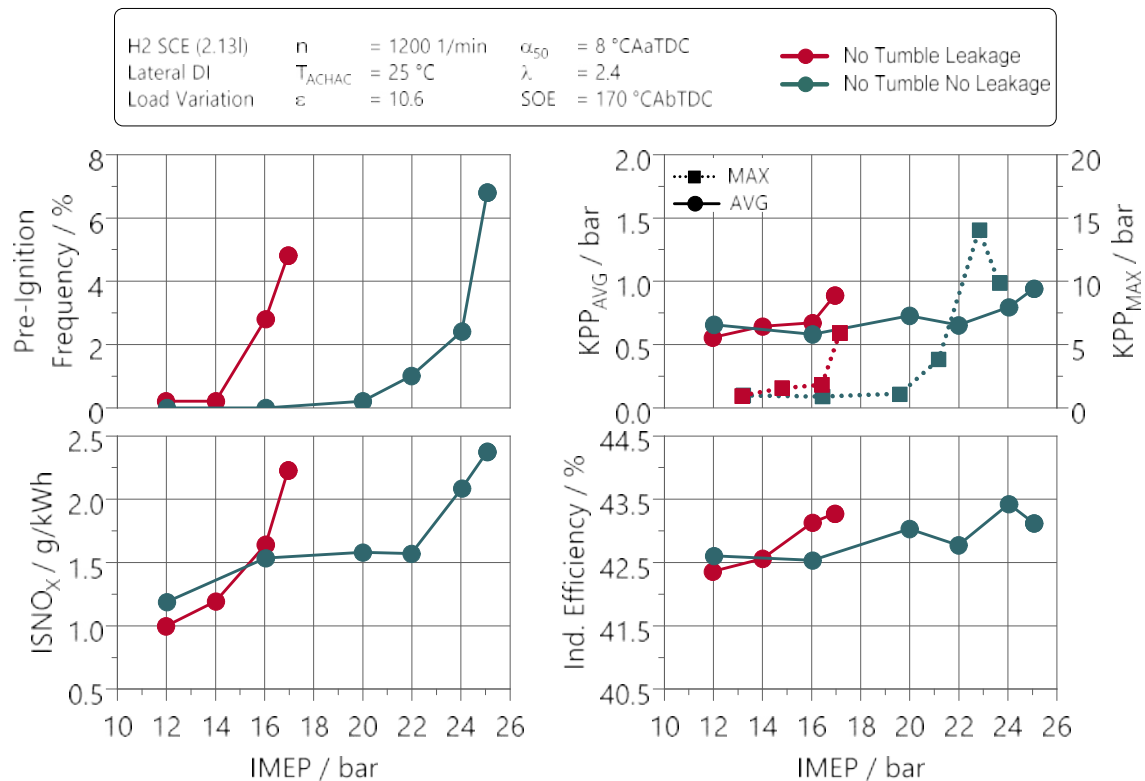


Figure 5: Influence of a hot spot caused by valve leakage on the specific load limit.

Finally, a more detailed combustion analysis by means of a comparison between a PI and a regular burning cycle is shown in figure 6. The interval between the ignition angle and the 5 % heat release point is clear evidence that the combustion of the red cycle is induced by a pre-ignition. The extreme short period of 3.7° CA compared to 9.5° CA for the regular combustion cycle is far below the statistical range of cycle-to-cycle fluctuations. In addition, the 10-90 % heat release duration is shortened by 33 % from 11.7° to 7.8° CA. The consequence is that approx. 80 % of the combustion occurs before the top dead center increasing the peak pressure and temperature significantly.

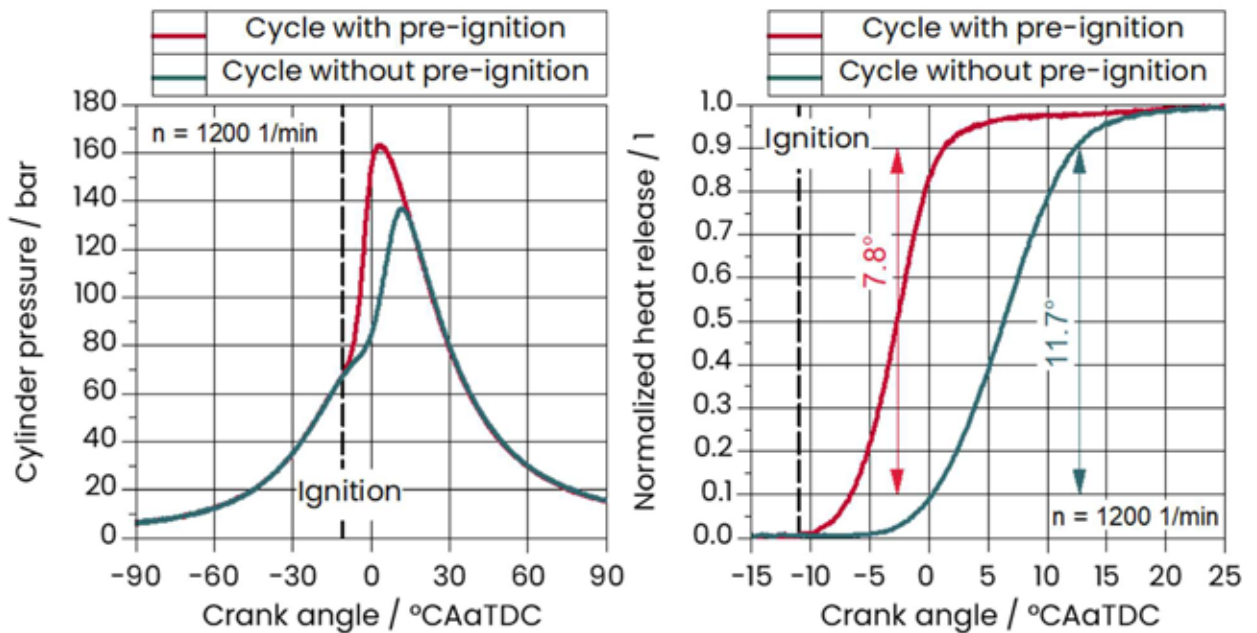


Figure 6: Pressure trace and heat release of a cycle with and without pre-ignition

In conclusion, the sealing effectiveness of the valves is a very sensitive item for a H₂ ICE, especially if a carry-over of valves originally designed for Diesel engines is considered. There is a demand for a high robustness against leakage by means of a precise interaction between valve disk and valve seat ring under a wide range of thermal conditions.

3.2. Charge motion

One approach to reduce abnormal combustion phenomena is to introduce charge motion. For this purpose, tumble blends are mounted together with the valve seat rings in the cylinder head as depicted in figure 7. The tumble blend is positioned with a pin in the cylinder head and mounted in combination with a modified seat ring. The intake flow is redirected towards the exhaust side, cooling the exhaust valves during the intake stroke and flushing residual gas pockets in the flame deck area with fresh air.



Figure 7: Cut through intake port with tumble blend.

A comprehensive 3D CFD RANS simulation study of the in-cylinder flow has shown, that the introduction of tumble blends leads to an increase in charge motion compared to the base setup with a filling port design as depicted in figure 8. A significant increase of the tumble motion around the Y-axis can be observed during the intake stroke between 360° and 540° CAaTDC. The difference in the tumble level between both configurations is reduced after the start of injection (SOI) at 180° CAaTDC in bottom dead center. From then on, the injection dominates the charge motion in the cylinder introducing a tumble motion around the X-axis.

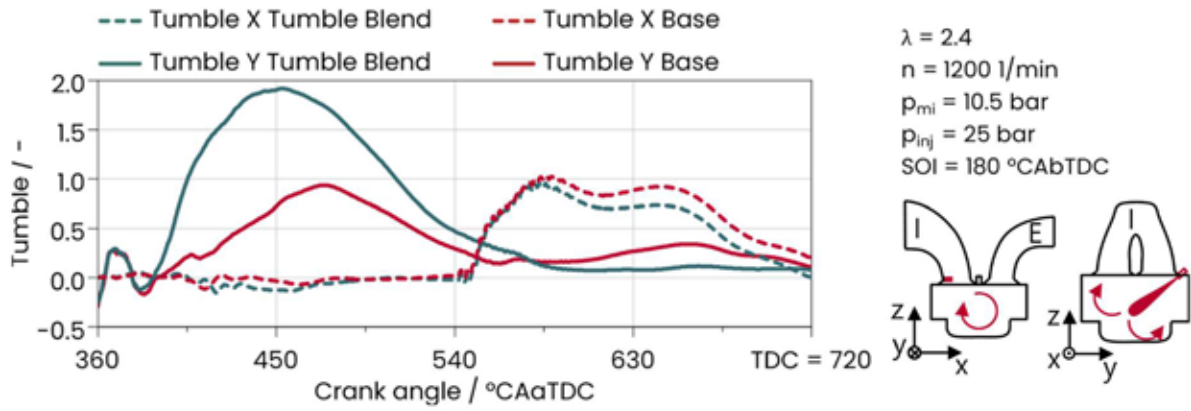


Figure 8: Tumble level around X and Y-axis, orientation and investigated part load point.

The turbulent kinetic energy (TKE) shows a similar course with an increase in TKE due to the intake flow, followed by the dominating influence of the injection, shown in figure 9. The TKE is slightly increased during and after injection for the tumble setup.

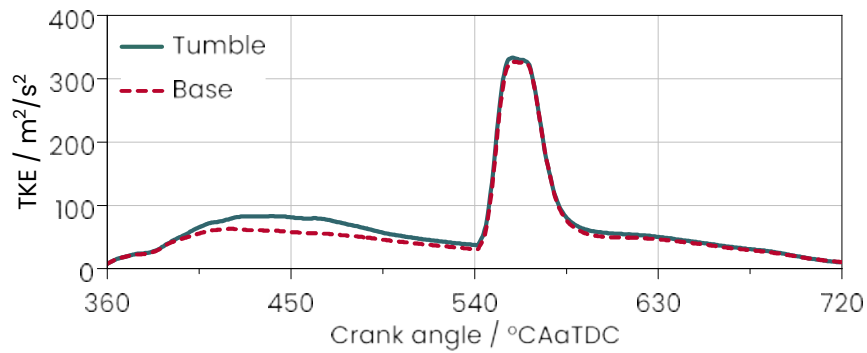


Figure 9: Turbulent Kinetic Energy Base vs Tumble setup at part load

An increase in large- and small-scale charge motion leads to an improvement in mixture formation as shown in figure 10. Especially the mass fraction of hydrogen in very rich zones is reduced and shifted towards the aspired rel. air-fuel ratio (λ) of 2.4. Lean mixtures are less prone to abnormal combustion due to the elevated minimum ignition energy and auto-ignition time. Furthermore, the occurrence of very lean zones is reduced compared to the base setup making the burn delay more reproducible.

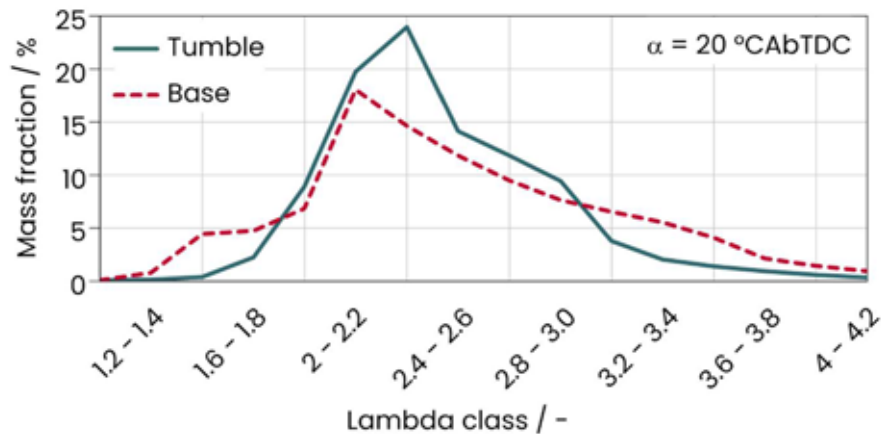


Figure 10: Distribution of hydrogen at 20 °CAbTDC at part load

In figure 11 the 3D λ distribution 20° CA before top dead center (TDC) is shown. Analogous to the λ class distribution significant differences can be identified. For the base configuration a rich zone with $\lambda \approx 1.2$ is present at the exhaust valves representing a potential source of abnormal combustion. With tumble charge motion this zone is significantly leaner but still not eliminated. Regardless of charge motion, the injector recess is not flushed properly indicating another area for optimization by reducing crevice volumes as much as possible. The coefficient of variation (CV) of the equivalence ratio $\Phi = 1/\lambda$ was reduced from 25 % to 18 %.

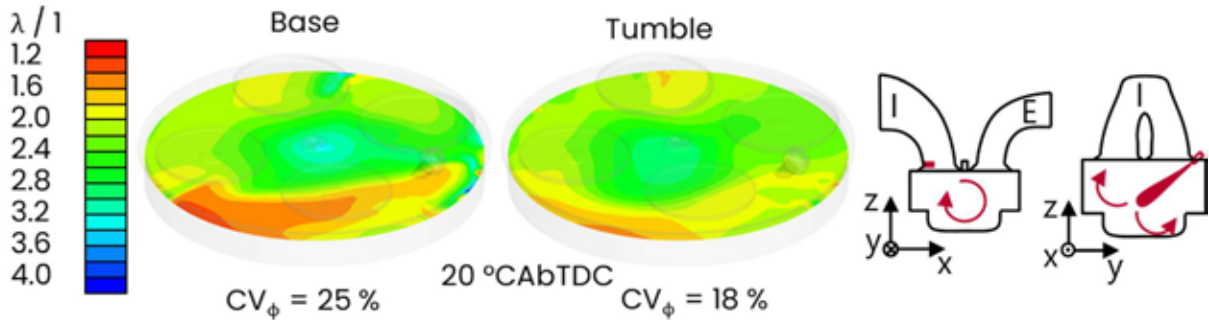


Figure 11: Simulations of charge motion and mixture formation at part load

Although the tumble level and mixture homogenization leave space for improvement, an enhancement in engine performance can be observed in figure 12.

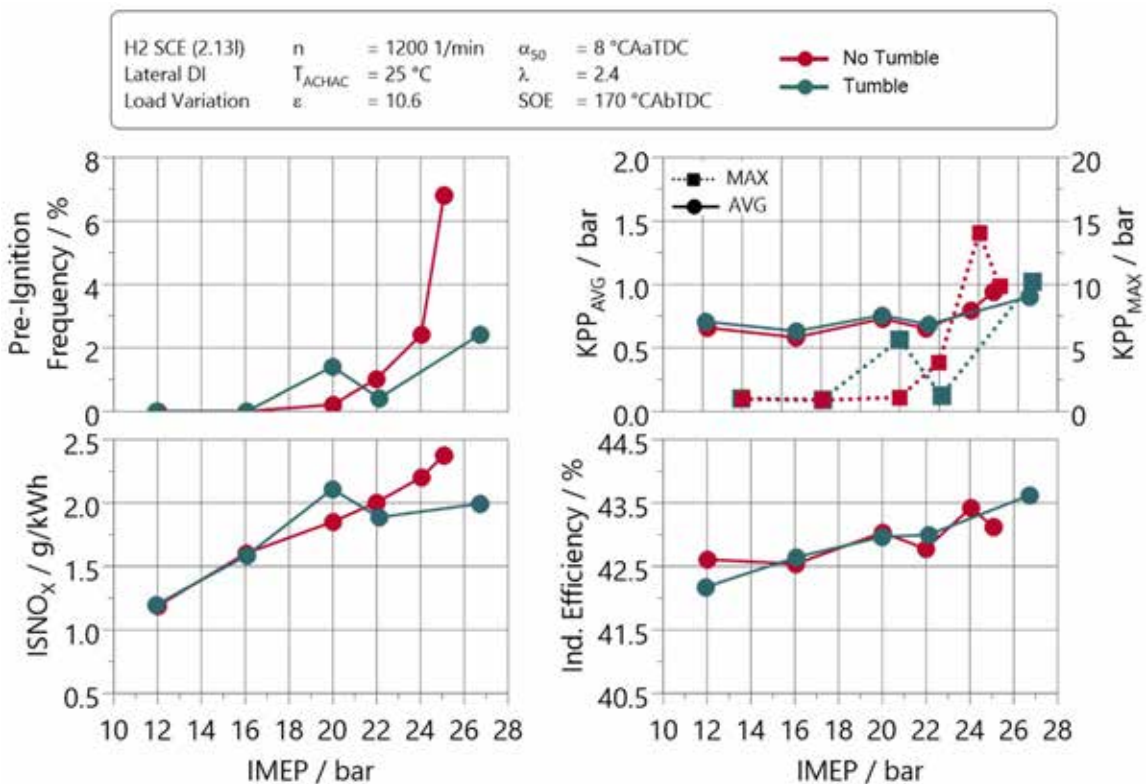


Figure 12: Load sweep Tumble vs No Tumble at 1200 1/min

The safely achievable IMEP was increased by approximately 3 bar from 24 to 27 bar. The pre-ignition frequency limit of 3 % was reached earlier without tumble as well as the knock limit of $KPP_{MAX} = 10$ bar. In terms of NO_x formation, no advantage can be observed. NO_x formation inhibited by better homogeneity might be compensated by higher temperatures due to higher combustion efficiency. Indicated efficiency is on par as the improved

combustion efficiency with tumble is compensated by increasing gas exchange losses due to the tumble blends.

The success of introducing tumble blends with moderate tumble charge motion opens opportunities for further increased tumble levels by means of port design adaptations. This is required to clarify the influence of tumble on the suppression of abnormal combustion but also to identify challenges associated with high charge motion like elevated gas exchange losses. The goal is to find the best compromise between a stable combustion system and efficiency for heavy duty H₂ ICEs.

3.3. Oil droplet management

As depicted in figure 1 oil droplets entering the combustion chamber can be a source of pre-ignition. Besides entry from external sources like the valve stem and turbocharger sealings, the piston rings are a main contributor to oil introduction into the combustion chamber. To test the influence of oil transportation via the piston rings, two piston ring packages have been investigated on the test engine. One ring package was modified to significantly increase the blow-by volume flow, thus leading to a reduction of oil entering the combustion chamber [4]. A comparison of the soot formation after engine operation of the two piston ring setups is depicted in figure 13.

The effect of those modifications is visualized by the soot formation on the piston. The reference ring package displays high residue formation on the piston top land, indicating that the hydrogen flame is not quenched by the gap and oil entering through the piston rings is burned. The elevated blow-by leads to a reduced oil transport into the combustion chamber, resulting in a significantly lower number of pre-ignitions and less soot formation.

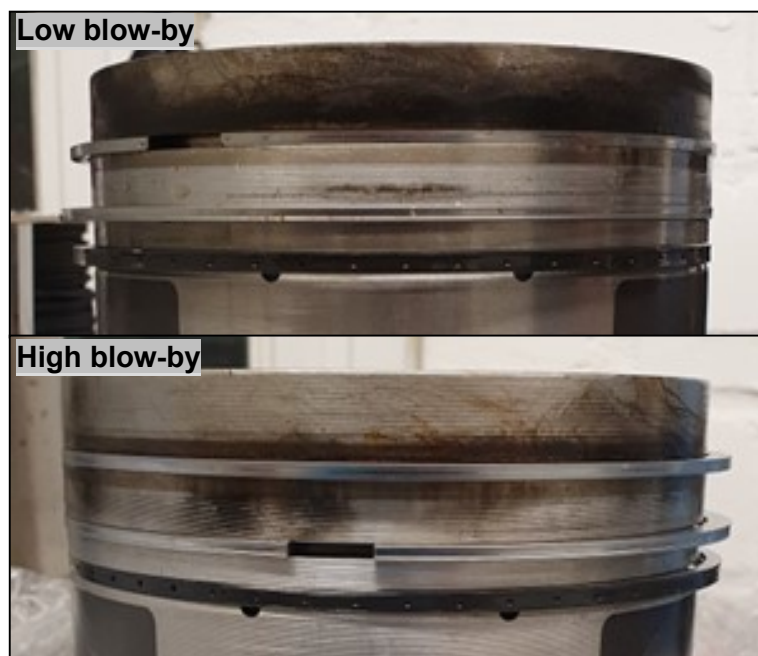


Figure 13: Oil residue on the investigated pistons after operation

To investigate the influence of the reduced oil introduction on the abnormal combustion phenomena, a load sweep was performed with both piston ring configurations. The measurement results are displayed in figure 14.

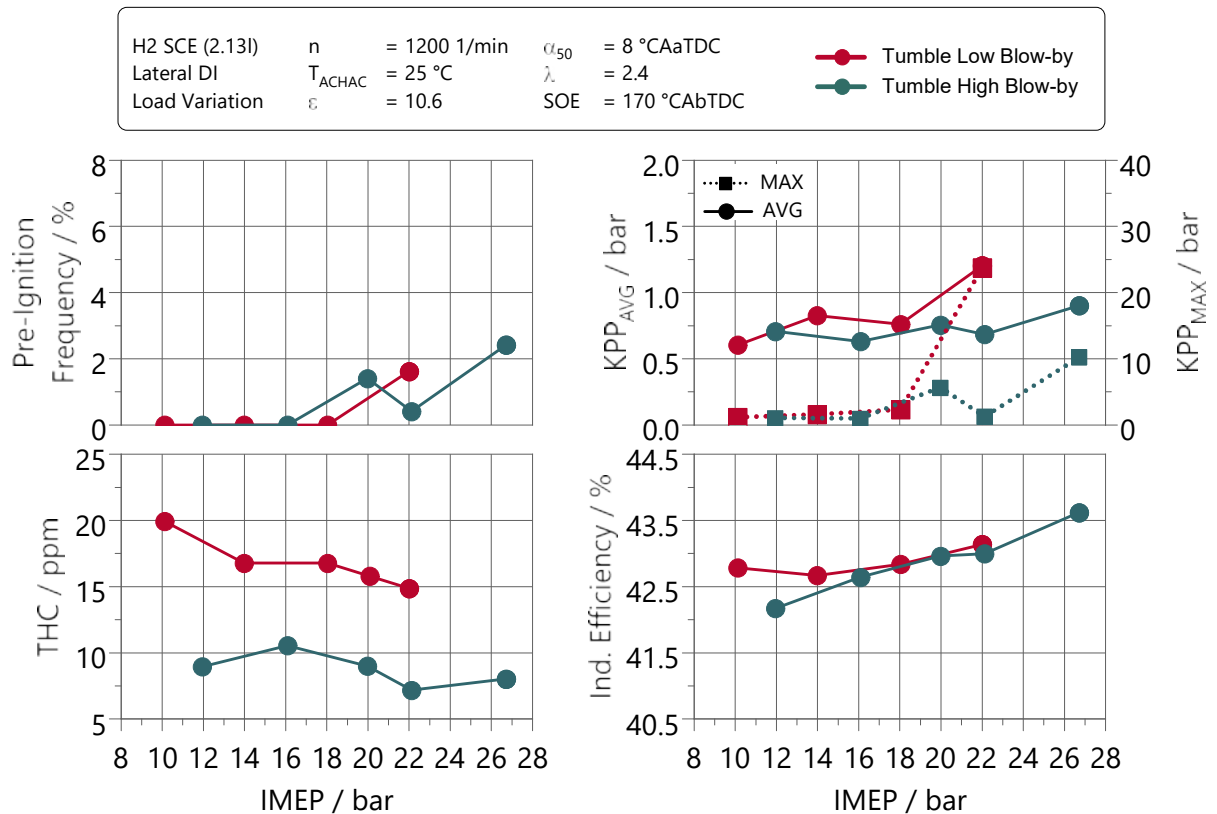


Figure 14: Influence of oil introduction on the IMEP limit

The reduced HC emissions of the high blow-by piston ring package suggest that the increased blow-by flow leads to less oil entering the combustion chamber. Both configurations demonstrate an increase in pre-ignition frequency at IMEP = 22 bar, though the value is significantly reduced with the modified piston rings, suggesting that oil is entering the combustion chamber less frequently. This behavior is reflected in the knock parameter KPP_{MAX} . Hence, the knock intensity is reduced and a higher maximum load can be achieved. The increased blow-by negatively affects the high-pressure cycle, but only slightly reducing the thermal efficiency of the engine.

In series production, increasing blow-by flow to reduce oil introduction into the combustion chamber is not feasible. Besides the efficiency diminution, unburned hydrogen entering the crank case via the piston rings during the compression and combustion phase poses a safety risk, as the concentrations easily exceed the lower flammability limit. Therefore, a much greater effort must be made to avoid hydrogen accumulation in the crank case. Consequently, piston rings must be optimized for hydrogen operation with regards to oil management and blow-by.

4. Summary

The conversion of an existing Diesel engine with its flat cylinder head to a hydrogen ICE with a similar IMEP level is a central challenge in the combustion process development. FEV has conducted numerical and experimental investigations on their 2.13 L HD SCE to determine further key parameters to increase the engine load limit considering frequency of occurrence and intensity of abnormal combustion within given thresholds.

Three pillars to improving the trade-off between high specific load and high efficiency were investigated:

- The valve sealing was identified as a significantly parameter of high importance. The onset of pre-ignitions was shifted by 6 bar of IMEP, while the pre-ignition frequency limit threshold of 3 % was reached at 8 bar higher IMEP when comparing leaking valves to properly sealing ones.
- Tumble charge motion improved the mixture homogeneity (CV_ϕ) by 28 %, effectively eliminating rich λ zones and yielding an improved specific load by approximately 3 bar IMEP on the test engine.
- Finally, oil droplet management was identified as a key parameter by means of a modified piston ring package. Oil droplets have proven to be another key aspect in pre-igniting hydrogen combustion. An improvement in the IMEP by 5 bar was measured.

5. Outlook

In addition to the presented results, FEV has a clear indication that residual gas pockets have a strong impact on the pre-ignition occurrence. Local accumulations of residual gas combine a high temperature with a shortened auto-ignition time and lowered ignition energy in an unfavorable manner. For instance, a switch from a relative air-fuel ratio of 2.5 to 1.0 reduces the ignition energy by 31 % and the H_2 auto-ignition time by 42 % for the same boundary conditions of 1000 K and 50 bar, see figure 15:

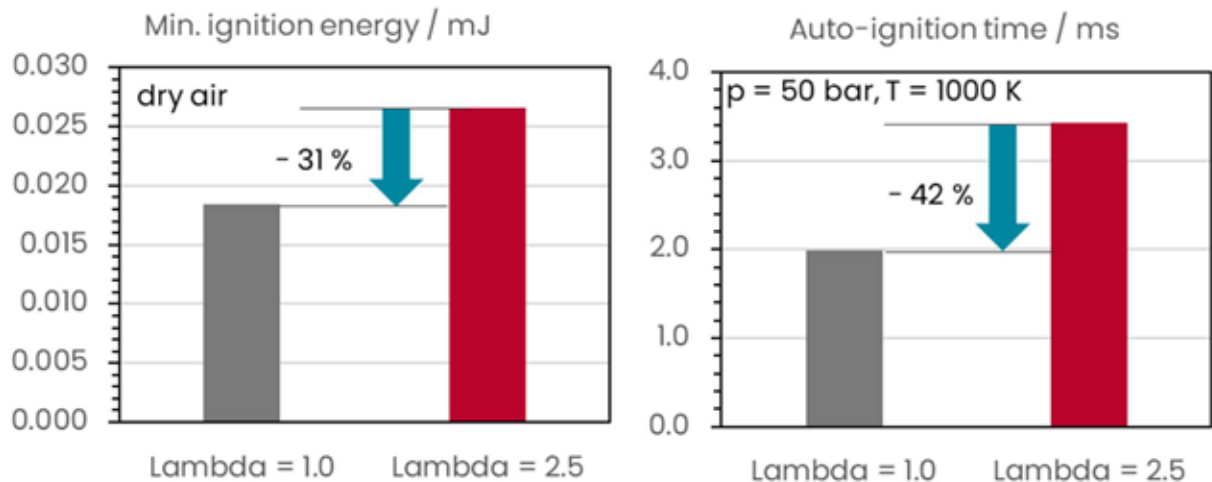


Figure 15: Minimal ignition energy in dry air [5] and the auto-ignition time basing on Zhang reaction kinetic mechanism [6] for two different rel. air-fuel ratios of H_2

According to this considerable sensitivity, the crevice volume around the injector tip and the flow cap is a design optimization parameter. FEV has found in the SCE investigations that an increased crevice volume at the injector correlates with a higher frequency of early pre-ignitions. However, different injector designs have always individual injection characteristics so that potential cross-effects from mixture formation must be analyzed in detail to verify this hypothesis. The overall target is to determine design specifications for the injector tip area as well as the flame deck as a contributor to an optimized combustion process.

Acknowledgments

FEV would like to thank TENNECO for the great cooperation and the provision of hardware components during the SCE investigations. Moreover, a special thanks goes to Jacob Weyer for his support in performing the 3D CFD simulations.

References

- [1] Boberic, A. et al.: Measures to achieve high specific power with a heavy-duty H₂ internal combustion engine: A numerical and experimental analysis, 31. Aachen Colloquium Sustainable Mobility, 2022
- [2] Franzke, B., Boberic, A., Virnich, L., Müller, V.: Leistungsstarke H₂ DI-Motoren für MD/HD-Anwendungen, ATZ heavy duty 1/23, 2023
- [3] Kestin, J., Maeder, P.F., Wang, H.E.: Influence of turbulence on the transfer of heat from plates with and without a pressure gradient, Int. J. Heat Mass Transfer 3, 133/154, 1961
- [4] Meske, R., Zimmer, P., Virnich, L., et al.: Component and Combustion Optimization of a Hydrogen Internal Combustion Engine to Reach High Specific Power for Heavy-Duty Applications, JSAE Kyoto, 2023
- [5] Ono, R: Minimum ignition energy of hydrogen–air mixture: Effects of humidity and spark duration, Journal of Electrostatics, 2007
- [6] Zhang, Y. et al.: Further insights into the core mechanism of H₂ /CO/NO_x reaction system, Combustion and Flame 245, 2022

Session 6

Methanol-Schiffsanwendung Methanol - Marine applications

**Moderation: Moderation: Prof. Peter Eilts
Technische Universität Braunschweig**

Methanol Retrofits for a fast net-CO₂ reduction in the Marine Market

Methanol Retrofits für eine schnelle Netto-CO₂-Emissionsreduzierung im maritimen Markt

Christian Kunkel*, Paul Hagl, Dr. Bhuvaneshwaran Manickam, Dr. Christopher Gross, Florian Eppler, MAN Energy Solutions

Abstract

In 2018 the IMO (International Maritime Organization) announced its initial GHG-reduction strategy with the aim to reduce the yearly GHG-emissions until 2050 by 50% compared to 2008. In July 2023 and with support from all IMO member states a new GHG-strategy was adopted and the targets were tightened with the aim to be climate neutral in the year 2050. However, while sectors such as electric power or commercial heating are relatively easy to decarbonize, others still rely heavily on energy-dense hydrocarbon fuels. Among those sectors are long-distance aviation and deep-sea shipping. Furthermore, ships and the installed engines are in operation for several decades. Thus, retrofit solutions are an attractive and economic way to achieve a very fast impact on the net-GHG-emissions of the maritime industry. In this paper, different retrofit solutions and different renewable fuels are discussed and assessed concerning their reduction potential from a general point of view and with respect to the "time to market"-aspect. Furthermore, the favored MAN-solution for methanol will be highlighted with focus on the combustion and thermodynamic principle. CFD-simulation results to determine the preliminary design of the engine and the testing results on the single cylinder engine regarding combustion and emission performance are included accordingly. The paper is concluded with an outlook to MAN Energy Solution's upcoming steps for market introduction of the described retrofit solutions for methanol.

Kurzfassung

2018 kündigte die IMO (International Maritime Organization) ihre initiale THG-Reduktionsstrategie mit dem Ziel an, die jährlichen THG-Emissionen bis 2050 im Vergleich zu 2008 um 50% zu reduzieren. Im Juli 2023 wurde mit Unterstützung aller IMO-Mitgliedstaaten eine neue THG-Reduktionsstrategie mit verschärften Zwischenzielen und dem Ziel im Jahr 2050 klimaneutral zu sein, verabschiedet. Während Sektoren wie der Strommarkt oder Wärmezeugung relativ einfach zu dekarbonisieren sind, sind andere Sektoren immer noch stark auf Kohlenwasserstoffe mit hoher Energiedichte als Energiequelle angewiesen. Dazu gehören Langstreckenflüge und die Hochseeschifffahrt. Darüber hinaus sind Schiffe und die verbauten Motoren mehrere Jahrzehnte in Betrieb. Daher sind Retrofitlösungen eine attraktive und ökonomische Möglichkeit einen schnellen Einfluss auf die Netto CO₂-Emissionen der maritimen Industrie zu nehmen. In diesem Paper werden verschiedene Retrofit-Lösungen und unterschiedliche erneuerbare Kraftstoffe diskutiert und hinsichtlich des Netto-THG-Reduktionspotenzials aus allgemeiner Sicht und unter Berücksichtigung des Aspekts "Time to Market" bewertet. Darauf aufbauend wird die favorisierte MAN-Lösung für Methanol unter Berücksichtigung des Verbrennungsprinzips und der Thermodynamik beschrieben. Die Beschreibung umfasst die CFD-Simulation zur Vorauslegung des Motors und die Untersuchungen am Einzylindermotor. Das Paper schließt mit einem Ausblick in die Zukunft bezüglich der nächsten Schritte von MAN Energy Solution hinsichtlich der Markteinführung der beschriebenen Methanol-Retrofits.

* Speaker/Referent

1 Introduction

1.1 The IMO strategy 2023

In 2018 the IMO (International Maritime Organization) announced its initial GHG-reduction strategy with the goal to reduce the yearly GHG-emissions until 2050 by 50% compared to 2008. In July 2023 and with support from all IMO member states a new GHG-strategy was adopted and the targets were tightened with the goal to be climate neutral in the year 2050. The following picture shows the adopted IMO strategy including the intermediate steps and targets.

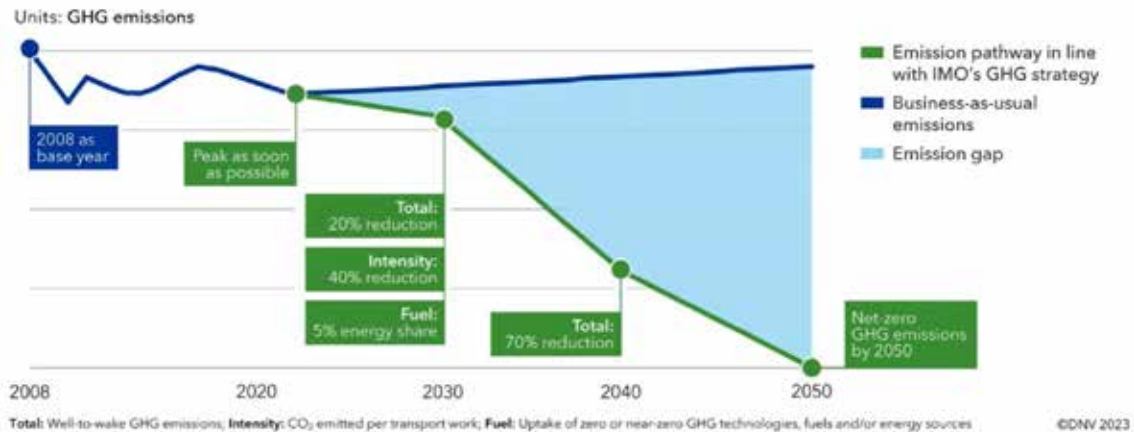


Figure 1: IMO GHG Strategy adopted 07.07.2023 [1]

The blue line shows the GHG-emissions for the “business as usual scenario”. The green line shows the new scenario adopted in 2023.

The intermediate targets are the following:

In 2030 the GHG-reduction shall at least be 20%, but striving for 30%, whereby the intensity (CO₂ per transport work) shall be reduced by 40%. In 2040 the goal is a minimum 70% GHG-reduction, striving for 80% and finally by 2050 Net-zero GHG-emissions shall be reached.

Regarding the calculation method for the GHG levels, a well-to-wake approach is to be taken into account, based on the IMO Life-Cycle-Assessment Guidelines.

The goals of this new strategy are very ambitious and will definitely not be achieved solely by building new green ships due to the long service life of ships and its engines installed. Retrofits of installed engines will therefore play a very decisive role in achieving these goals.

2 Assessment of different energy carriers for maritime applications

2.1 Storage on board

For all long-distance remote applications without the possibility of refueling, the energy density of the energy source is of crucial importance. In the following diagram (Figure 2) a comparison of different energy carriers with respect to their volumetric energy density and gravimetric energy density is given.

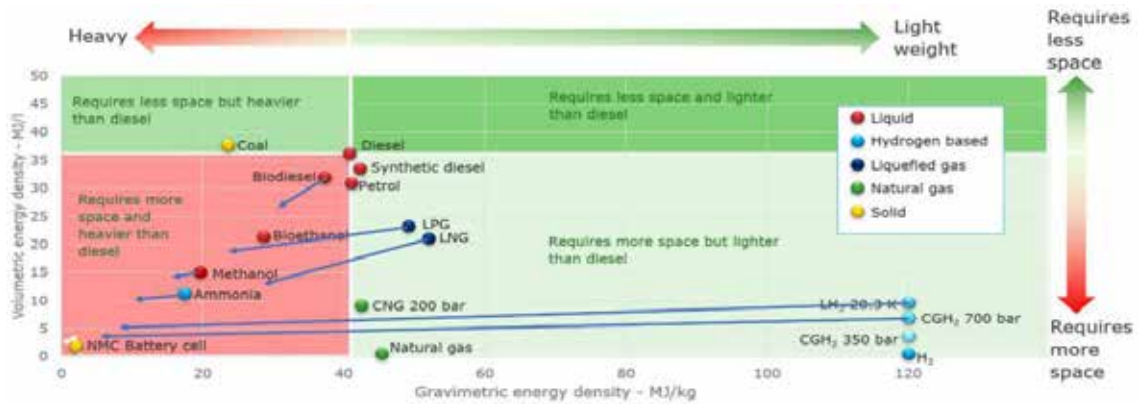


Figure 2: Comparison of gravimetric and volumetric energy density of different energy carriers [2]

The dots are based on the physical properties, while the blue arrows in the diagram indicate the energy density with the specific tank volume taken into account.

It is very obvious, that Diesel and Diesel-like fuels set the benchmark regarding volumetric and gravimetric energy density. In extreme contrast, batteries are very poor with regard to these criteria and simply not suitable for long-distance applications. Only liquid fuels and liquefied gases are within reach of the Diesel's energy density. In this context the added complexity for the use of hydrogen has to be mentioned.

2.2 Economical aspects

The following diagram gives an overview of the energy efficiency of the production processes for different e-fuels.

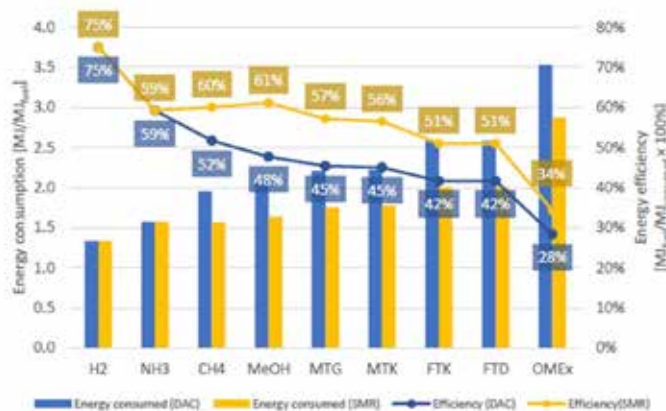


Figure 3: Comparison of needed energy during the production process of different e-fuels [3]

As hydrogen is the basis for all other e-fuels, it is not surprising that the production process for hydrogen has the highest efficiency. As a rule, the longer the atomic chains of the fuels become, the lower the production efficiency gets.

Even more important are the costs for the production of e-fuels. These are compared in the following diagram (Figure 4). As already mentioned, all e-fuels are produced with hydrogen on the basis of electrolysis. One could therefore conclude that hydrogen is the cheapest e-fuel. However, as other costs, such as construction of refueling stations and fuel distribution itself, also play a role, hydrogen is in the end not the cheapest e-fuel.

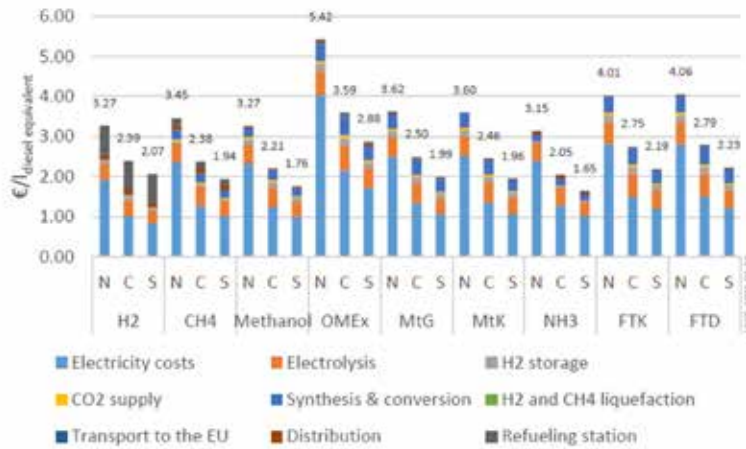


Figure 4: Production cost comparison for different e-fuels in 2020 [3]

The specific cost distribution of the complete production process for the different e-fuels is highlighted for three European regions (N=North, C=Central, S=South). The CO₂ feedstock is based on a concentrated CO₂ source (e.g. from the cement industry). Thereby showing that methanol is the second cheapest fuel only trailing ammonia.

Another important aspect is the price development over the upcoming years. This is illustrated for the southern European region in the following figure (Figure 5). It is assumed that by 2050 the cost- and energy-intensive technology of direct air capture is required. Thus, causing production prices in 2050 for C-based fuels to closely remain at the 2030-levels, whereas prices for non-carbon fuels, such as H₂ + NH₃ are expected to decrease towards 2050.

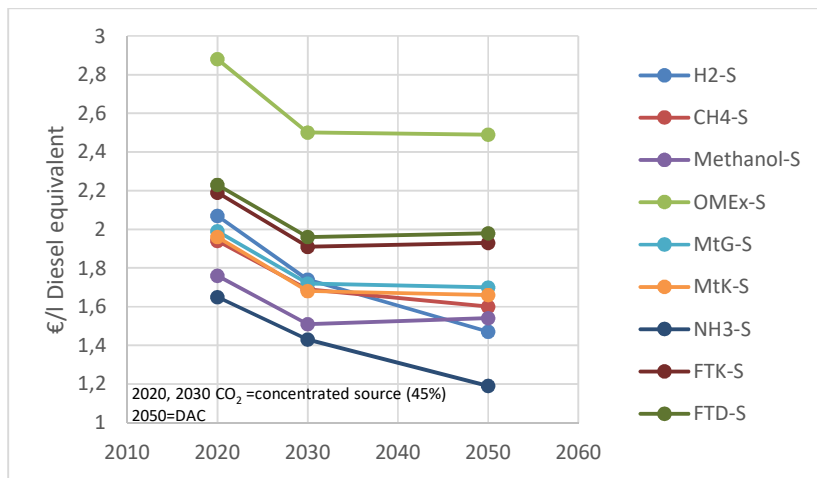


Figure 5: forecast production price development for e-fuels (based on [3])

The values and diagrams (Figure 2- Figure 5) are based on the assumption that the fuels are produced in Europe. In the global maritime shipping industry, the transport costs for the fuels are of great importance and play a decisive economic role in determining where the fuels will be produced. The following diagram (Figure 6) compares a selection of future marine fuels in terms of transport costs on a representative route from Oman to Japan, a distance of about 8000km.

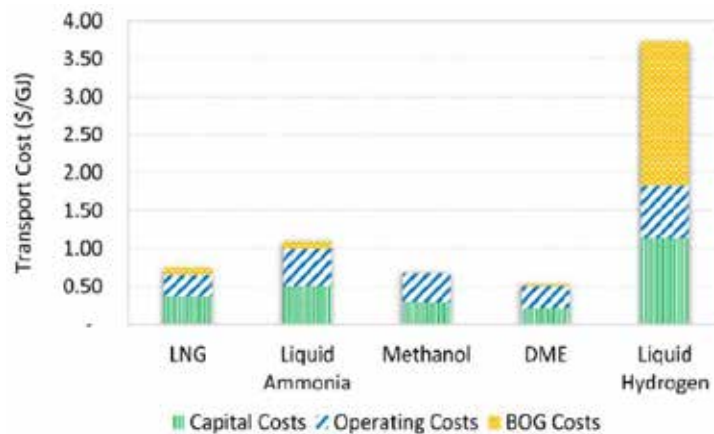


Figure 6: Transportation Costs for future fuels from Oman to Japan [4]

It is quite obvious that methanol is an attractive fuel in terms of transport costs, while hydrogen is not a first choice, at least for long-distance transport. Therefore, ammonia imports are generally being considered when it comes to hydrogen imports, as ammonia serves as a better energy carrier than hydrogen itself.

One of the drivers for transport prices are the costs for reliquefaction of the boil-of-gas (BOG-Costs). The following table shows the boiling point under atmospheric conditions. Due to its physical properties, methanol can be stored under atmospheric conditions without boil-off and thus expensive countermeasures.

	Diesel	Methanol	Ammonia	LNG	Hydrogen
Normal boiling point [°C]	>120	64	-33	-161	-253

Table 1: comparison boiling point for different fuels

These economic fuel cost assessments for various e-fuels show that methanol and ammonia are the most promising fuels for maritime applications in the future. Yet, hydrogen could also become attractive in the distant future. Thus, the following sections focus on these three fuels as well as e-LNG, also called synthetic Methane. The reason for including e-LNG is quite simple: As LNG-technology on ships is already state of the art and is becoming increasingly widespread, fossil LNG can fully be substituted by up to 100% CO₂-neutral e-LNG without having to make any changes to existing LNG-powered ships.

2.3 Retrofitability

Ships and engines are in operation for 20-40 years and longer. Installing new engines on existing ships is very time-consuming and often uneconomical. Retrofits of existing engines can be realized with significantly less effort and with significantly lower economic losses [5]. Retrofits therefore enable a very rapid and easy reduction in GHG-emissions.

For LNG, ammonia and hydrogen, special and expensive tanks are required in suitable locations on board. The toxicity of Ammonia and the associated additional safety requirements represent a further obstacle to the integration of ammonia tanks in many existing ship designs. In contrast, methanol tanks are inexpensive and can be installed comparatively easily in a wide variety of locations on board. Installations close to the outside of the ship walls are also possible, as methanol quickly dilutes with water in the event of an accident and is harmless in low concentrations. This is the reason why methanol is considered as one of the most promising fuels for retrofitting existing engines to green and carbon neutral engines.

2.4 Summary fuel assessment

The fuel assessment above is summarized by the following overview (Figure 7) for the e-fuels methanol, ammonia, hydrogen and natural gas:

e-fuel	H ₂	CH ₄	MeOH	NH ₃
energy density	-	+	++	+
production costs as e-fuel	0	0	+	++
transportation costs	--	++	++	+
storability	-	0	++	+
Risk of GHG (other than CO ₂)	+1	-2	++	-3
Retrofitability (shipping industry)	0	0	++	-4

1: H₂ incl. GHG w. GWP₁₀₀=11 (Warwick 2022)
 2: CH₄ slip GWP₁₀₀=28 (IPCC AR5)
 3: risk of N₂O-emissions GWP₁₀₀=265 (IPCC AR5)
 4: most studies show, that new ship design will be needed

Power application + short distance shipping
 CO₂-neutral → drop in fuel to NG

Fuel for new built ships
 CO₂-neutral → retrofit of Diesel-engines

Figure 7: Fuel assessment summary for maritime e-fuels

The summary for the evaluated categories paints a clear picture. Methanol, as an e-fuel, is the most promising fuel overall. It is followed by ammonia, which will certainly play a crucial role in the future for the application in new ships, where safety issues can be solved with reasonable effort, e.g. container ships and ammonia transport ships. Furthermore, retrofits for ammonia will be important, where the ship design is suitable. Thus, many ships are already being designed and delivered as “ammonia-ready”. Methane, on the other hand, as an e-fuel, is ideal for reducing the net CO₂-emissions of existing LNG-ships by blending it with fossil LNG, while hydrogen, as a e-fuel, will become relevant for power generation on land and probably for short-distance shipping.

2.5 Combustion concepts for methanol

The fuel properties determine whether a fuel is suitable for the Otto and/or Diesel combustion process. In this section, methanol is evaluated as a fuel for dual-fuel applications with a Diesel-fuel back-up mode. Note that in most marine applications, for safety and redundancy reasons, a back-up mode is required for engines that do not run exclusively on Diesel. Diesel, at least for the time being, as well as in the future, is most probably the best back-up fuel, as it is available in all harbors around the world.

The following table summarizes the most important properties of methanol regarding its combustion behaviors in an internal combustion engine.

	Methanol	Comparison (Otto-/Diesel-fuel)
CN [-]	<5	DMA>40
ROZ [-]	106	LNG<130
Auto ignition temp. [°C]	440	LNG: ~537 DMA: ~220
Latent heat of evaporation [kJ/kg]	1101	RON 91: ~420
Lower Calorific Value [MJ/l]	15,8	RON 91: ~35 DMA: ~36
Laminar flame speed [cm/s]	46	LNG: ~40
Boiling temperature [°C]	65	ROZ 91: 30-215
Viscosity [mm ² /s]@50°C	0,5	DMA: ~3,0

Table 2: properties of methanol as fuel

Without an additional ignition source, the low cetane number disqualifies methanol as a fuel for Diesel-like, diffusive combustion. To realize a Diesel cycle, additives or ignition sources

such as a Diesel pilot fuel are therefore necessary. The octane number and auto-ignition temperature, on the other hand, qualify methanol as an Otto-cycle fuel.

The cooling effect of injected liquid methanol in an internal combustion engine is comparatively high due to the latent heat of vaporization. In relation to the same calorific value, the cooling effect is around 5 times higher than with RON 91 Gasoline. Thus, in a Diesel-cycle, NOx emissions are reduced significantly by this cooling effect compared to Diesel [7]. For the Otto-cycle, where a pilot fuel-oil injection is used as an ignition source, the influence of the cooling effect on the ignition delay must be taken into account. The laminar flame speed and the boiling temperature are within the known range of common Otto-fuels. The viscosity of methanol and the lower calorific value are significantly lower than those of Diesel fuels. This has an impact on the injection system e.g. in terms of injection pressure, injector itself and nozzle design.

Furthermore, methanol as a molecule has only one C-atom. Therefore, extremely low soot emissions are to be expected in a Diesel-cycle. The main source for soot emissions is found in the pilot injection and lubricating oil used.

In conclusion, it can be said that methanol is suitable for both the Diesel- and the Otto-cycle. In the Otto-cycle, combustion is restricted by the elongated ignition delay of the Diesel pilot-fuel due to the high cooling effect, and by a low resistance to knock due to the low RON compared to LNG. On the other hand, the Diesel-cycle requires an injection system that can not only inject both Diesel and methanol, but also must be able to realize full load or at least close to full load in both methanol and Diesel mode. It must also be ensured that the Diesel and methanol spray cones are orientated in relation to each other so that the Diesel plume can ignite the methanol plume.

Furthermore, a distinction is made between port fuel injection (PFI) and low-pressure direct injection (LPDI) for the Otto-cycle (Figure 8). With LPDI, the cooling effect in the cylinder increases in comparison to port fuel injection and thus the challenge of ignition delay is higher. Another challenge using LPDI is to ensure a sufficient mixture homogeneity. In addition, the injection system becomes more complex due to the boundary conditions in the combustion chamber, i.e. pressure and temperature. The restrictive space conditions in the cylinder head increase the complexity even more. Due to this high complexity and the added challenges with the LPDI-concept, only the Diesel-cycle-concept of high-pressure direct injection (HPDI) and the Otto-cycle concept with PFI will be compared and evaluated in the following. The scope of the evaluation will be reduced to the following two, most important criteria – engine performance and retrofit efforts.

Engine performance: The following evaluation is based on fundamental considerations of fuel properties and combustion concepts. Regarding the engine performance criteria, i.e. power density, robustness of combustion and load-response behavior, it can be assumed that the HPDI concept is comparable to conventional Diesel engines. Due to the fuel properties, fewer challenges can be expected related to the smoke limits and as such a more favorable NOx behavior. Therefore, the methanol HPDI operation has the potential to be superior to known Diesel engines. Engine performance for large medium-speed engines in relation to the above listed criteria is generally worse for Otto-cycle engines in comparison to Diesel engines. In addition, the properties (octane number) of methanol do not suggest that methanol can improve the performance compared to LNG. The conclusion is that the HPDI concept is most likely superior to the PFI concept in the engine performance category.

Retrofit efforts: This is the category in which the PFI concept has its main advantages. To emphasize the most important advantages: The injection system is a relatively simple low-pressure system that is not exposed to the temperatures and pressures of the combustion chamber. The development and adaptation of the injection system to different bore sizes can therefore be realized much faster compared to the HPDI systems. In addition, the injection system is integrated into the intake port, so that no new cylinder head design is required. Furthermore, the complexity of the fuel supply system and the associated costs are

significantly lower compared to the high-pressure system required for the HPDI concept. Thus, the PFI concept is comparatively easy to retrofit, and the adaptation to different engine base concepts across different bore sizes can also be realized quickly, which significantly increases the potential number of retrofits.

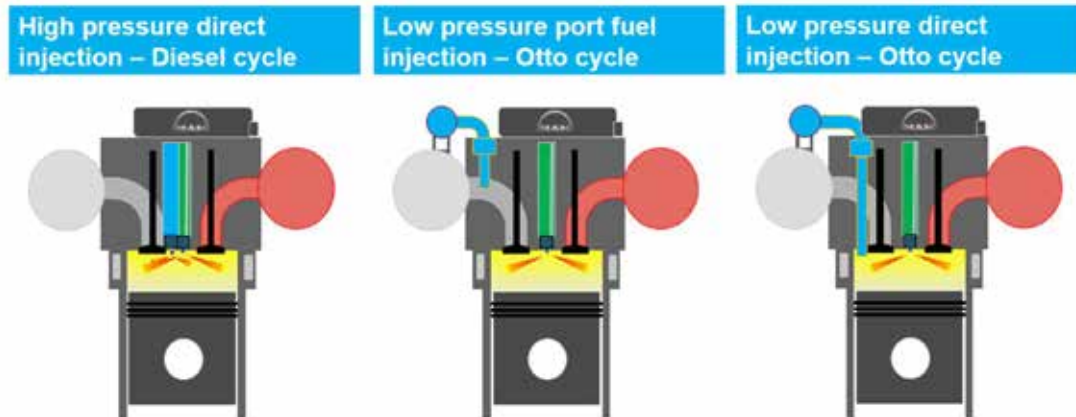


Figure 8: Illustration of combustion concepts for Methanol

To summarize the "Combustion concepts" chapter in one sentence: The PFI-Otto concept is applicable as a retrofit concept on a broad base of field engines, the HPDI concept is the suitable concept for new developments and for retrofitting engines with a suitable base for this purpose. Thus, in the following chapters the Otto-PFI concept will be highlighted in more detail.

3 Port Fuel Injection of Methanol: Mixture formation (CFD)

Mixture formation and evaporation plays a significant role for the emission and performance behavior of an Otto-cycle methanol engine. Thus, from the very start CFD-calculations were conducted to determine the injector position and define the necessary injector specification.

3.1 CFD simulation: Modelling of methanol injection and mixture formation

For the retrofit solutions, the low-pressure PFI methanol injector position plays a significant role in achieving a more complete combustion, and lower emissions. A suitable position for the injector is vital to create, not only a more homogenous methanol/air mixture in the cylinder, but also to reduce the methanol liquid film on the intake runner and the methanol pooling in the intake port, thereby lowering fuel slip during the valve overlap. For example, while on one hand, spraying methanol against the intake wall or intake valve could facilitate the liquid droplet breakup, on the other hand it creates a liquid film on the intake port and thus increases the fuel slip during intake and exhaust valve overlap. Note, a certain valve overlap is needed for the pure Diesel operation mode of the engine. Moreover, the wall-bounded gas and droplet flow alters the path of liquid fuel distribution in the cylinder, thus creating local high-concentration fuel clouds, which could cause knocking and locally increase the component temperature. Thus, CFD simulations have been carried out to determine the influence of the following injection parameters on mixture formation and its resulting effects:

1. Injector position: Position 1 / Position 2
2. Number of injectors: one per cylinder / two per cylinder
3. Injection spray cone angle: 25 / 45 / 70 degree

3.1.1 Numerical modelling: Flow and spray

The charge-cycle and combustion simulation have been carried out using the RANS approach implemented in the AVL FIRE CFD code [6]. For turbulence modelling a $k-\zeta-f$ model with

hybrid wall treatment methods has been selected. The numerical stability of the $k-\zeta-f$ model has been improved by solving a transport equation for the velocity scale ratio ($\zeta = v^2/f$) instead of velocity (v^2). The spray simulation involves multiphase flow phenomena and simultaneously requires solutions for conservation equations for the gas and liquid phase. The spray calculations are based on the Discrete Droplet Method (DDM) in which droplet trajectory, momentum, heat and mass transfer are solved. The droplets are tracked in a Lagrangian way through the computational grid used for solving the gas phase equation in the Eulerian framework. The atomization process of sprays is modelled using submodels such as TAB. For the droplet-gas momentum and mass exchange, the sub-models such as Schiller Naumann for drag and Abramzon for liquid evaporation are employed. A significant amount of the liquid fuel can be deposited on the walls as a thin liquid film due to incomplete evaporation and wall collisions of injected droplets. Depending on the local wall and film conditions, the film evaporates or is driven along the wall. Furthermore, some amount of liquid film is sheared off and entrained back into the airflow. Similar to the spray modelling, all relevant physical effects that influence the film formation and flow of film are regarded via sub-models. One of the sub-models used for modeling the droplet generation from the liquid film due to high-velocity air is Schadel-Hanratty. In addition, the generated droplet size from the film is modelled using the Kataoka model, and the spray-wall interaction using the Kuhnke sub-model.

3.1.2 Simulation model and boundary conditions

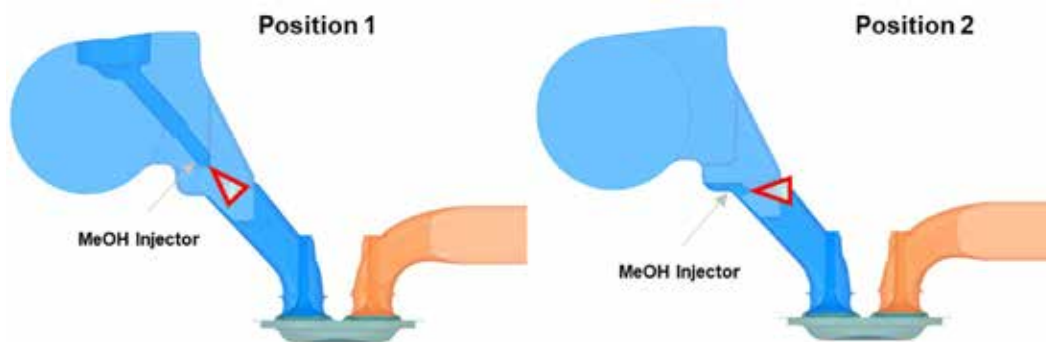


Figure 9: CFD simulation model with methanol injectors for position 1 and position 2

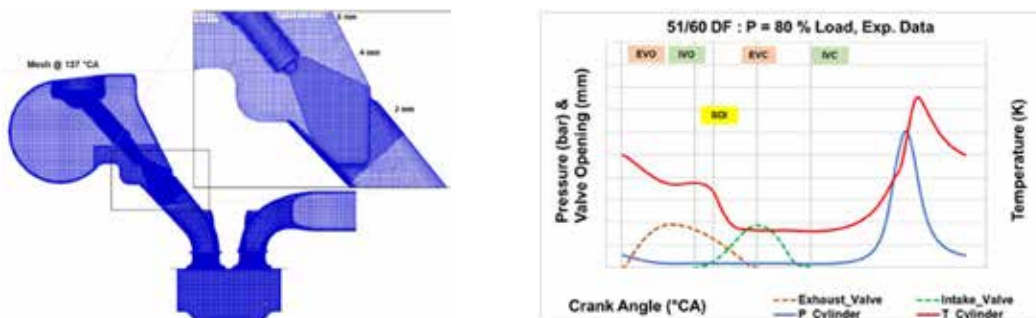


Figure 10: Simulation mesh with local refinement (left), measured cylinder pressure and temperature, valve opening and closing (right)

The simulation models that have been used for the CFD analysis, the cut section of the simulation mesh, and the boundary conditions used are shown in Figure 9 and Figure 10. At the inlet and outlet, measured pressures and temperatures are assigned. At the beginning of the simulation, the cylinder is initialized using the measurement data shown in Figure 10. The methanol injection starts immediately after the intake valve opening. The secondary

atomization and wall film formation are modelled by defining the droplet distribution using the Rosin-Rammler relation. The injected methanol mass corresponds to 90 % of the total energy. The injection profile has a trapezoidal shape with initial ramp-up and final ramp-down curves, along with a constant flat profile in the middle. The injection duration leaves enough time for most of the injected droplets to flow into the cylinder. For every condition, two complete cycles are simulated. The first cycle of the simulation is to determine the amount of methanol stored in the intake port in the form of liquid, vapor, and film. Where, the second cycle is to predict the methanol slip, the mass of the liquid film, and the homogeneity of fuel in the cylinder.

3.2 CFD Simulation Results

As mentioned, the first charging cycle prediction at the intake port was used as a starting point for the second cycle. Figure 11 shows the resulting spray droplet distribution and wall temperature for the second cycle. For injector position 1, the spray gets narrower, as the droplets move along with the air flow faster. Thus, the breakup occurs relatively late while the methanol enters the cylinder earlier. For position 2, due to the strong interaction between the injection droplets and the charge air, the droplets break up immediately after the injection. Note that the contours of the wall temperature clearly indicate that wall film formation depends highly on the injector position. For position 1, the liquid film mass is relatively high on the intake valve itself, whereas for position 2, it is highest on intake port. Furthermore, Figure 12 illustrates the increased concentration of methanol on the left-hand side around the intake valves for the two injector position. Overall, independent of minor deviations between position 1 and position 2, the fuel homogeneity in the cylinder at top-dead-center (TDC) reaches a nearly identical value.

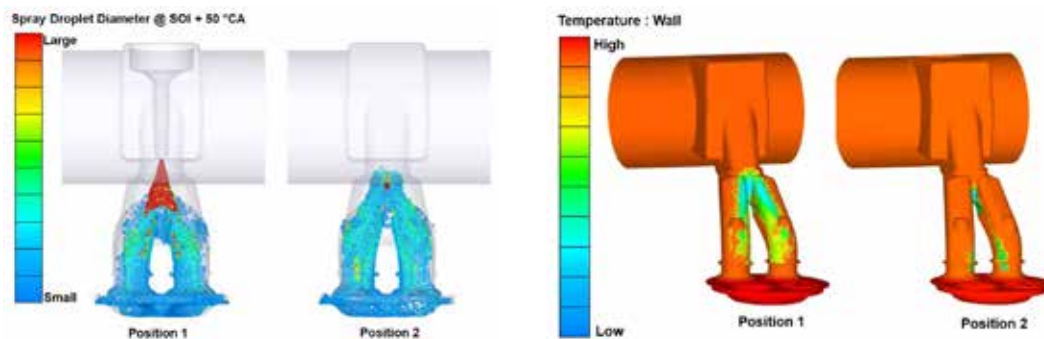


Figure 11: Spray distribution (left) and wall temperature (right) for position 1 and position 2

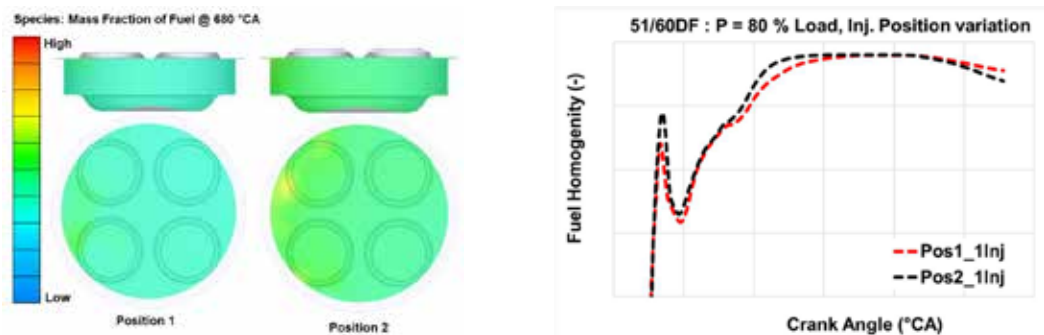


Figure 12: Contours of fuel concentration (left) and homogeneity (right) for position 1 and 2

Based on these results, a single injector and a double injector concept are compared. The goal was to compare the distribution of the liquid droplets and mixture formation for these two variants, as shown in Figure 13. The total injected methanol mass and the injection duration remained identical for both variants. The spray-wall interaction enhances droplets breakup and wall-film formation for the single injector variant. The droplets are injected in the middle of the

intake channel, so it takes slightly longer to break into smaller droplets. When using two injectors, the wall film mass was reduced, and more liquid mass flowed into the cylinder. Furthermore, the contours for fuel concentration indicate that high concentration methanol clouds exist around the intake valve. Therefore, the predicted methanol homogeneity in the cylinder is slightly lower for the two injectors variant compared to the single injector variant.

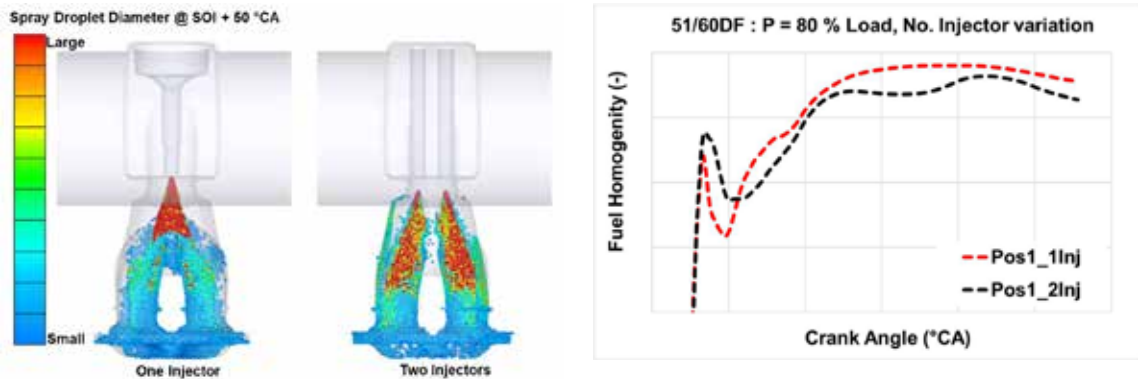


Figure 13: Spray distribution (left) and fuel homogeneity (right) for 1 and 2 Injector variants

As stated, the injection spray cone angle also has a considerable effect on mixture formation and liquid film mass. Those effects were evaluated for 25°, 45°, and 70° cone angle and the results are presented in this section. As shown in Figure 14, the droplet size drastically reduces when increasing the spray cone angle from 25° to 70°. High radial liquid penetration and high shear forces on the liquid droplet stemming from the air are causing a better breakup for larger spray cone angles. As a result, smaller droplets are formed, which evaporate faster than large ones, forming more fuel vapor in the intake port.

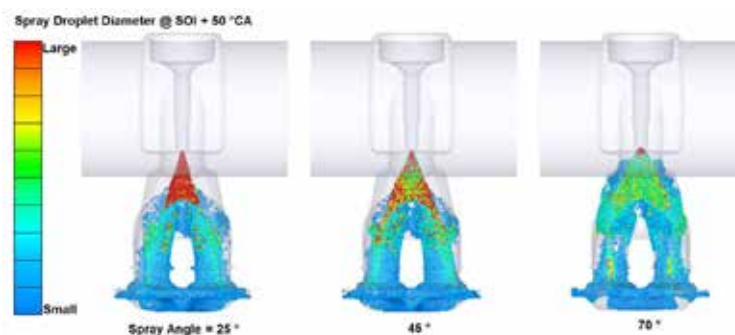


Figure 14: Spray distribution for position 1 and three spray cone angles – 25, 45, and 70 °

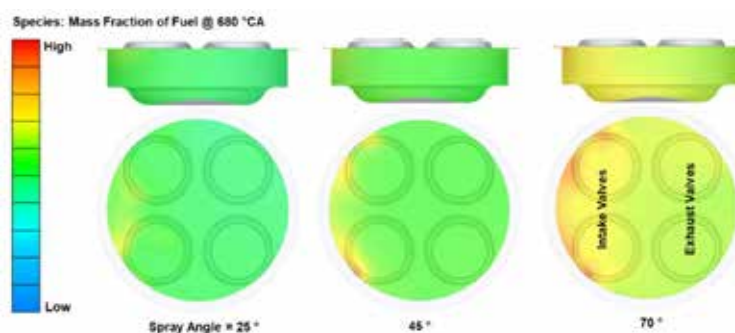


Figure 15: Contours of fuel concentration (left) for position 1 and spray angles 25, 45, 70 °

The contours of fuel concentration shown in Figure 15 also indicate that more fuel mass directly enters the cylinder when larger spray angles are used. For all spray angle variants higher fuel concentration around the intake valve is observed compared to the exhaust valve. The calculated fuel homogeneity in the cylinder is highest for the 70 ° spray angle with the beginning of injection due to better methanol-air entrainment in the intake port, thus enhancing breakup, evaporation and mixing. The wall film mass reduces by 10 % and 20 % when increasing the spray angle from 25 ° to 45 ° respectively, and even further at 70 °.

Ultimately, the CFD analysis shows that regardless of the position the single injector variant shows best fuel homogeneity while having a slightly higher liquid film mass. However, increasing the spray cone angle further reduces the wall film mass while maintaining the same level of mixture homogeneity. On the other hand, the two-injector variant increases the interaction between droplet-air and minimizes the liquid film mass, but it alters the air flow area in the intake channel and thus the air flow quality. After careful consideration, it was decided to select injector position 1 with a high spray cone angle for on-engine testing.

4 Combustion Development

The scope of the combustion development was to investigate and assess different engine technologies with the goal to derive fundamental retrofit concepts for MAN Diesel engines. These investigations take into account, that not all engine technologies are available for all MAN-engines. To give an example, MAN has small bore engines in the field, like the series 21/31 (bore/stroke in cm), that are equipped with a conventional Diesel injection system. Furthermore, the 21/31 is neither equipped with a variable valve timing (VVT), nor a cylinder pressure based advanced combustion control (ACC) unit, nor a charge air pressure control system, all important technologies for the realization of an Otto-cycle concept. In addition, the integration of a pilot injector in such an engine is challenging due to the limitations in cylinder head space and thus the increased costs for the retrofit. To summarize, one could say that the genes of an 21/31 for the optimized implementation of an Otto-cycle concept are limited. In contrast to the 21/31 engine, the MAN 48/60 Diesel engine when retrofitted to a 51/60DF engine that already operates in Otto-cycle during LNG-operation, is a very suitable base for an Otto-cycle combustion concept. The 51/60DF is equipped with an additional pilot injector capable of achieving small amounts of pilot fuel injection as well as multiple injection. Furthermore, charge air pressure control, a VVT and an ACC unit are applicable technologies. Between those technological extremes, the possible combinations were evaluated on a single cylinder engine and, with economic factors being taken into account as well, the most suitable retrofit-concepts were derived. The investigations took place on a single-cylinder engine series 32/44.

Number of cylinders [-]	1
Bore [mm]	320
stroke [mm]	440
Diesel-injection system	various
Methanol injection	into inlet port
Nominal engine speed (rpm)	720 / 750

Table 3: Engine Data of test engine

4.1 SCE testing results concept for 21/31

The following parameters were varied in order to find the optimum within the limits specified for this type of engine:

- charge air temperature
- air fuel ratio
- methanol share
- injection timing of methanol
- injection pressure of methanol
- position of methanol injection valve

For fuel oil injection, a mechanically controlled unit pump injection system, suitable to fulfil IMO Tier 2 emissions in Diesel operation, was used. During methanol-operation this injection system also provided the pilot fuel necessary to ignite the methanol-air mixture.

In the following figure the results for this engine concept are condensed in an engine operating map.

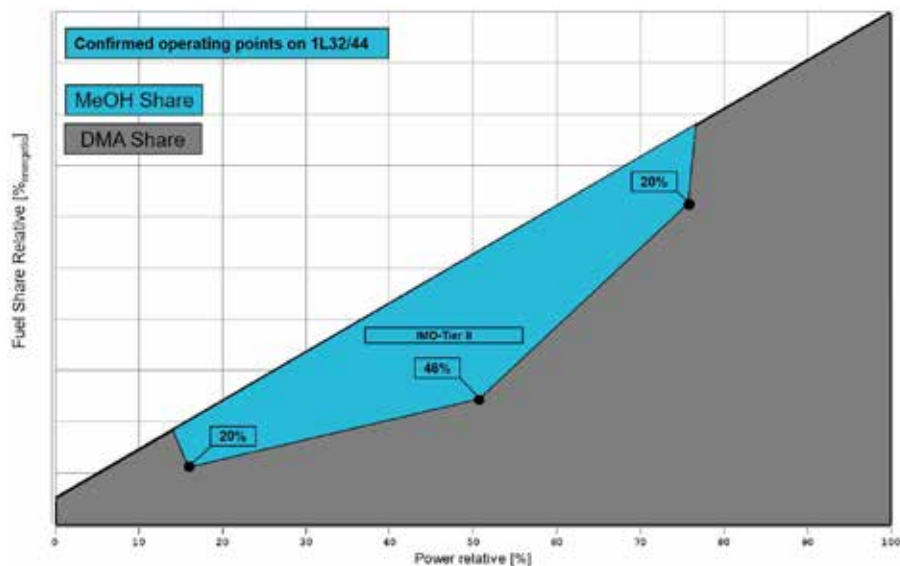


Figure 16: Operating map for Methanol PFI Combustion – Concept 21/31

The diagram shows the methanol-share as a function of the relative engine power. As the engine is an auxiliary genset, the engine speed is constant and 100% power corresponds with the MCR of the 8L21/31 Diesel-engine. The methanol share is calculated on an energy-basis and thus the net-CO₂-reduction can easily be estimated. The numbers of the energetic methanol share and the net-CO₂-reduction are the same if the engine efficiency remains identical between pure Diesel and methanol-operation mode and renewable methanol is used. On a volumetric base, the methanol share is significantly higher. Note that the share is optimized with regard to engine efficiency and completeness of combustion and thus is fixed and not variable in methanol-mode. All engine limits, i.e. mechanical limits and applicable emission limits (IMO Tier 2), are fulfilled in methanol-operation.

The maximum methanol share is primarily restricted by mechanical limits and misfiring of the engine. The injected liquid methanol has a high cooling effect on the cylinder charge and thus,

leads to longer ignition delays of the Diesel and therefore, to higher pressure gradients or even misfire.

With the given methanol shares the engine behavior is stable and determined by the diffusive Diesel combustion and not the Otto-like combustion of methanol, best described by the conceptual name “co-burning of methanol in a Diesel engine”. In comparison to the Diesel engine, only few additional technologies are necessary to realize this concept: the methanol injectors, methanol fuel supply system, the necessary ECU-functionalities to control these, the charge air pressure control and finally the charge air temperature control.

4.2 SCE testing results concept for 48/60

As mentioned previously, the 48/60 platform, respectively the series 51/60 can rely on the same technology as the 51/60DF LNG-engine, and thus is equipped with an additional CR-pilot injection system and can be adapted for a variable-valve timing (VVT). The pilot system is suitable for small amounts of pilot oil and can also be used for multiple injection.

As a consequence, the performed tests included the following additional parameters (compared to 4.1) for the optimization of the combustion:

- injection timing pilot fuel
- injection mass pilot fuel
- injection pressure pilot fuel
- variable valve timing of inlet valve (VVT)

Additionally, the engine is equipped with the proven cylinder pressure based Advaptive Combustion Control (ACC) unit which enables stable combustion under various conditions. In the following figure the results for this engine concept are again condensed in an engine map.

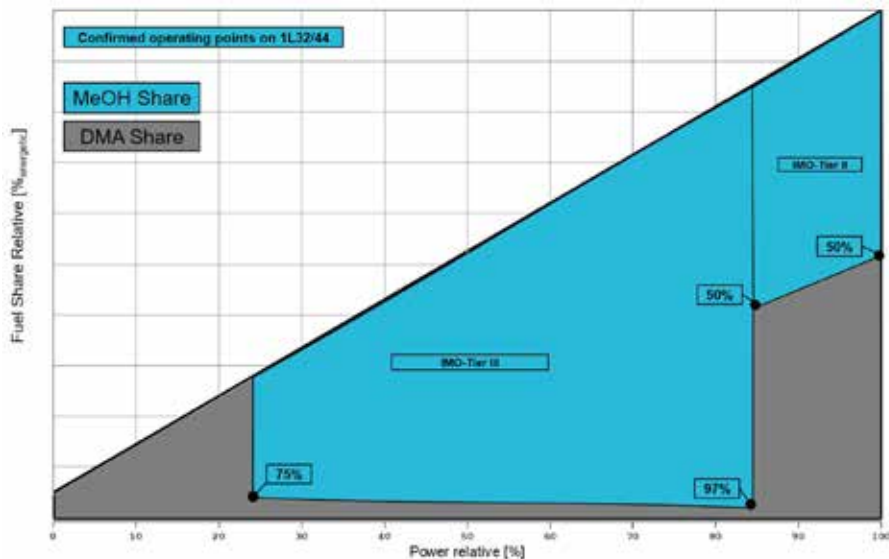


Figure 17: Operating map for Methanol PFI Combustion – Concept 51/60

Like in the upper diagram (Figure 16), this diagram shows the energetic methanol-share as a function of the relative power. Engine speed is constant and 100% power corresponds with the MCR of the 51/60DF LNG-engine. Once again, the methanol share is fixed and not variable in methanol-mode, as well as all mechanical limits and applicable emission limits (see Figure 17) are fulfilled in methanol-operation. In the power range between 25% and 85% the engine is

running in real Otto-cycle with the known but well-controllable sensitivities of a lean burn Otto-engine. In this operation range IMO Tier 3 emissions are fulfilled without exhaust gas after-treatment. In this wide power range realizing Otto-like combustion, the CR pilot injection system, VVT, and ACC are the key-enablers for this advanced DF concept. Load is limited to 85% due to knocking. For methanol-operation at higher loads, the single cylinder engine was operated via the co-burning principle as described in section 0. The drawback is, that only IMO Tier 2 emissions are fulfilled in this power range.

5 MAN's Methanol Retrofit concept

As highlighted in the previous chapter, methanol is an important addition to the carbon free fuel options giving an advantageous trade-off between energy density, combustibility and toxicity and as such stands in the center of the MAN ES company strategy and its ingenuity focus. By anticipating a continuously raising demand for sustainable methanol within the marine sector, driven by ambitious worldwide emissions targets and tax incentives for such a new alternative fuel, MAN ES is working not only on new build options, but also retrofit options for currently Diesel-fueled customer engines. The retrofitability of our engines is a pillar of our development efforts towards a Methanol-capable engine portfolio. As such, the 48/60CR (Diesel) but also the 51/60DF (LNG) engines are in the forefront of our retrofit development and thus will make use of the aforementioned PFI-concept.

Combining a simplified integration and a less complex fuel supply system, the PFI-system offers a fast market availability as well as low unit costs. Both crucial key performance indices for a successful introduction in today's fast-moving maritime market. At this point, it is worth mentioning once again that the engine will feature a dual-fuel combustion system, therefore giving the possibility to switch to Diesel operation at any time. This is a key element for engine availability and fuel independence, as sufficiently large and widespread methanol infrastructure has yet to be established throughout the years to come.

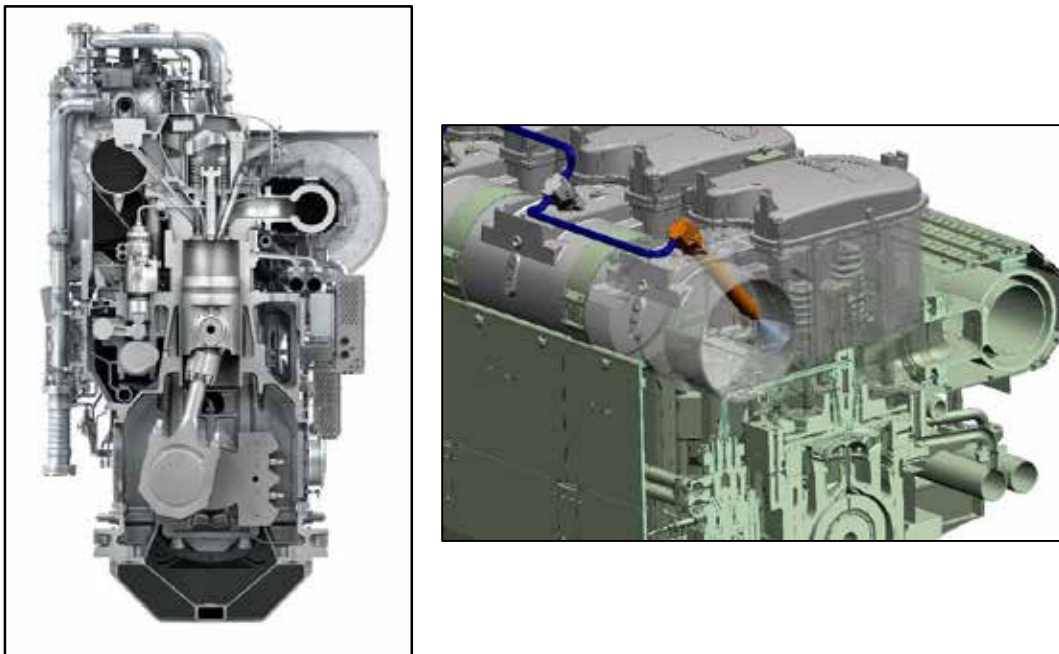


Figure 18: Rendering of the 48/60CR engine and 3D-PFI concept layout

The underlying Otto-like combustion that was introduced previously is achieved by injecting the Methanol directly into the intake air stream through the PFI injector, similar to our current injection system for LNG and DF engines. The injector is placed close to the intake valve. The injection begins when the inlet valve opens and thus ensures the same safety levels as our standard DF-engines operated with LNG. The Diesel fuel from a pilot injector serves to ignite the air-methanol mixture and the aforementioned ACC unit is used to optimize and monitor the combustion in each cylinder individually.

Furthermore, while simple in comparison to a HPDI-concept, there are yet significant changeovers needed in order to successfully implement this concept and achieve combustion characteristics at highest levels of efficiency and the observance of all underlying emission regulations. The complete retrofit kit for a 48/60CR engine consists of the following main components:

Automation

The automation components required for Methanol combustion will be based on the known automation system for the DF- and NG-systems, yet evolving to our latest SaCos5000 modular system in order to be able to handle all additional requirements. Fed by the I/O's stemming from the ACC (Adaptive Combustion Control) unit, the Methanol-specific P&ID components, and the emerging safety requirements these new functionalities are featured in this latest methanol automation system release.

Base Engine

The retrofit kit for the base engine consists of several different items. Thereby, the implementation of the methanol supply system, along with adaptations regarding cable routing and air ducting as well as heat shields, will be moderate due to the simplicity of the PFI-system. Meanwhile the engine power unit, i.e. piston, liner and ring package, will be undergoing a design upgrade, yielding a larger bore size (48 to 51cm) as well as an adjusted epsilon. Lastly, the integration of the PFI injector requires adaptations to the cylinder head's intake air manifold segment (Figure 18).

Injector

As mentioned above, the injection system consists of two separate fuel supply loops. The low-pressure PFI injector is a newly developed injector that is electronically controlled and optimized for Methanol operation. The injector itself is optimized regarding the spray pattern and orientation to reach high efficiency and power outputs through homogenous combustion, while managing methanol-slip and wall-wetting. It is operated with 30bar injection pressure and can supply a Methanol-share necessary to operate at full load with 95% energetic fuel-share. Safety aspects are considered as the injector is built up with Methanol-compatible materials and gaskets, a double walled interior and a separate flow limiting valve.

On the Diesel main side a well approved MAN high pressure common rail system is used in combination with a pilot injector, where both are controlled via the ACC unit. The use of a pilot injector enables small and precise pilot injections down to 1% energetic fuel-share during Methanol operation.

Safety-Concept

The Safety Concept (Figure 19) for the methanol supply system is closely related to the well-known, approved and validated dual fuel gas safety concept for existing DF engines, meeting the requirements of the IGF code. By taking into account the methanol specific fuel properties, new features have been added in order to fulfill the requirements of existing interim guidelines for methanol. The safety concept system is highlighted in the following figure.

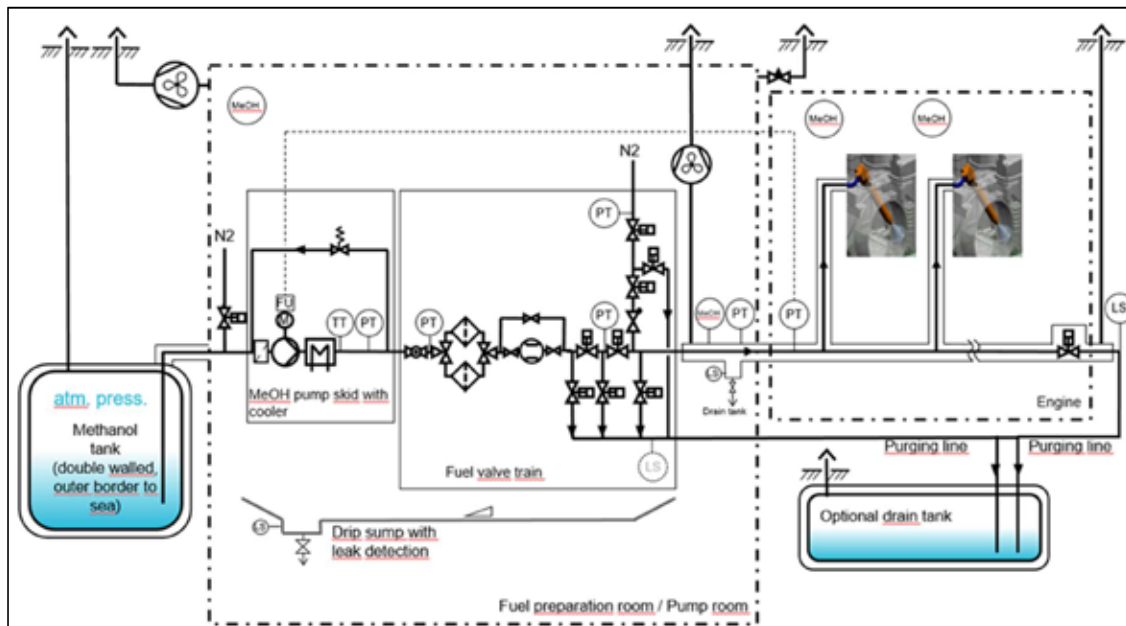


Figure 19: Safety/Plant concept for Methanol PFI concept

The system consists of the fuel supply system to the engine, i.e. the fuel supply skid with a frequency-controlled pump, the single-walled fuel valve train enclosed in the fuel preparation space, the double walled fuel piping system on the engine incl. ventilation, leakage detection for liquid and gaseous methanol, drainage ports, and a nitrogen-based purging system.

6 Summary and outlook

As highlighted in this paper, methanol is an important addition to the CO₂-neutral fuel landscape due to its advantageous trade-off between energy density, combustibility and toxicity, and as such is playing a major role achieving the aforementioned IMO GHG-reduction targets for marine applications. Simultaneously, as depicted in the paper, methanol stands in the center of the MAN ES company strategy and ingenuity focus, where it has set out to decarbonize its 4-stroke engine portfolio through roughly.

The introduction of new build options for methanol operation optimized engines is important and without alternative. As shown in Figure 20, methanol retrofit solutions will be introduced for already installed engines as well as engines sold today in order to reach a fast net-CO₂-emissions reduction, and ultimately the net-zero GHG-emission targets of the maritime industry. Thereby, as noted previously, the PFI technology will be first implemented as a retrofit solution for MAN's 48/60 and 51/60 engine platform as well as for the 21/31 genset engines, followed by PFI solutions for the 35/44 and the 175 engine platform.



Figure 20: Development Roadmap methanol engines with PFI

This methanol roadmap, from high-speed engines all the way to large bore engines, is benefiting from MAN Energy Solution's profound experience with dual-fuel natural gas engines and new on-going research. Research that is focused on technology, safety, plant, and aftertreatment concepts, that are needed for an efficient and reliable way of combusting methanol and where in addition each one of those engine platforms will build upon the knowledge gained throughout previous engine's single-cylinder and multi-cylinder testing and validation campaigns.

7 Acknowledgments

The investigations on the single cylinder engine, the CFD-simulation (partly) and evaluation of the combustion concepts were funded by the German Federal Ministry for Economic Affairs and Climate Action on the basis of a decision by the German Bundestag (project no. 03SX585A), which is gratefully acknowledged. In this context the authors would like to acknowledge the collaboration and support of the CliNeR-ECO project-partners WTZ Roßlau gGmbH and the University of Darmstadt.



References

- [1] DNV Maritime Forecast 2023
- [2] DNV GL – Report No. 2019-0567, Rev. 4
- [3] Alba Soler et al. - E-Fuels: A techno-economic assessment of European domestic production and imports towards 2050
- [4] Al Breiki et al. - Energy Reports Volume 6, November 2020, Pages 1897-1909
- [5] Bauer et al. - The Development of the MAN 58/64R-DF Retrofit Kit (12. Gasmotorenkonferenz Dessau 2022)
- [6] AVL List GmbH: AVL Fire Version 2021.2, User Manual, Flow- Spray & Wall Film
- [7] Auer et al.– CIMAC Paper 2023-049 MAN Energy Solutions – Four-stroke engine solutions for low-carbon and carbon-free fuels
- [8] Wilke et al. – CIMAC Paper 2023-146 MAN Energy Solutions 49/60DF - Maximum performance from the modular system

ABC's methanol future

ABCs Methanolzukunft

Ing. L. Mattheeuws*, **Ing. A. Van Gijzeghem**, **Ir. R. De Graeve**,
Dr. Ir. R. Verschaeren

Anglo Belgian Corporation, Ghent (Belgium)

Abstract

The development of methanol combustion engines at ABC started with a technology scouting exercise for our DZ engine family. Design was quickly followed by testing engine parts and finally full engine testing on our testbench, adapted for methanol. The first pilot project, a retrofit project, was identified early in the project, and development work was scaled-up. And as of today, serial production is running.

Along with this project came multiple challenges, with diverse aspects. Firstly, the technical aspect: how to inject, compress and combust methanol? Secondly: how to make a commercially competitive design with market conform efficiency and power density? Thirdly, the engine design needs to adhere to various rules and regulations: marine approval and emissions standards. This was especially a challenge, because at the start of the project there was little knowledge in the market about these aspects. Besides, methanol ready components were scarce.

A review of the current engine design and the installation of the engine on first vessels will be discussed. Challenges going even further will be highlighted as well: is the market methanol ready now? Do rules and regulation need further improvement for methanol as a fuel to be ready for the future? Is there a limit on the engine design on methanol? And finally: what are the challenges to run engines on pure methanol?

Research and development is an ongoing process and never stops, but we are proud to have a methanol engine platform commercially available in the market. And of course, we continue to work on further improvements with big potential.

Kurzfassung

Die Entwicklung von Methanol-Verbrennungsmotoren bei ABC begann mit einer Technologie-Bewertung für unsere DZ-Motorenfamilie. Auf die Entwurfsphase folgte schnell die Erprobung von Motorenteilen und schließlich Vollmotorenuntersuchungen auf unserem Prüfstand, der für Methanol angepasst wurde. Das erste Pilotprojekt, ein Nachrüstungsprojekt, wurde schon früh im Vorhaben identifiziert sowie die Entwicklungsarbeit ausgeweitet und inzwischen ist die Serienproduktion angelaufen.

Dieses Projekt war mit zahlreichen Herausforderungen verbunden, die verschiedene Aspekte umfassten. Erstens die technischen Gesichtspunkte: Wie kann man Methanol einspritzen, verdichten und verbrennen? Zweitens: Wie lässt sich ein kommerziell wettbewerbsfähiges Design mit marktkonformer Effizienz und Leistungsdichte entwickeln? Drittens muss die Motorkonstruktion verschiedene Regeln und Vorschriften einhalten: Schiffszulassung und Emissionsstandards. Dies war eine besondere Herausforderung, denn

* Speaker/Referent

zu Beginn des Projekts gab es auf dem Markt nur wenig Wissen zu diesen Fragestellungen. Außerdem waren methanolfähige Komponenten Mangelware.

In diesem Beitrag wird ein Überblick zur aktuellen Motorkonstruktion und zum Einbau des Motors in die ersten Schiffe gegeben. Darüber hinaus werden die Herausforderungen beleuchtet: Ist der Markt jetzt für Methanol bereit? Müssen die Regeln und Vorschriften für Methanol als Kraftstoff weiter verbessert werden, um für die Zukunft gerüstet zu sein? Gibt es Grenzen für die Motorenkonstruktion mit Methanol? Und nicht zuletzt: Welche Herausforderungen gibt es beim Betrieb von Motoren mit reinem Methanol?

Forschung und Entwicklung sind kontinuierliche Prozesse, die nie aufhören, aber wir sind stolz darauf, eine Methanol-Motorenplattform auf dem Markt anbieten zu können. Und natürlich arbeiten wir weiterhin an weiteren Verbesserungen mit großem Potenzial.

1. Introduction

At Anglo Belgian Corporation the methanol engine is now already some time under development and the market is responding well. The technology was firstly discovered at a single cylinder of the DZ-series. Further tested and developed to a multi-cylinder. This is already going under many projects. Even other engine families are under development for the moment for methanol.



Figure 1 - DZ engine on methanol

2. First experiences on methanol

At the beginning of the project, we needed to gain some theoretical and practical knowledge about the combustion of methanol. Therefore a single-cylinder engine was used. The project was very challenging because no knowledge on methanol combustion of an engine with our bore size and no injection equipment was available. At the start single-cylinder engine we used the diesel engine parameters as boost pressure, intake temperature and so on as a reference. Then we started a sweep of parameters like lambda, SOI and so on. The results are summarized in the following table.

Table 1: Parameters with the first effect on the efficiency and substitution ratio of a methanol engine

	Efficiency	MeOH Substitution
Lambda↓	↑↑	↓
Start of injection↓	↑	↑
Temperature inlet collector↑	↑	↑↑
MeOH spray angle↑	-	↑
MeOH spray duration↑	↑	↑↑
MeOH spray pressure↑	↑	↑
Diesel injection pressure↑	-	-
Compression ratio↑	↑	↑

Methanol has as following chemical and physical properties:

- The volumetric and mass energy density is almost half in comparison to gasoline or diesel.
- The vaporization heat is very high compared to gasoline; as it takes almost eight times more energy to vaporize the same amount of methanol compared to gasoline.
- A low flashpoint fuel needs special safety devices (e.g. double wall components, recirculating fan...), increasing complexity and costs of the technical solution.

This results in a difficult trail of engine modelling and testing and simulation to find a good solution. For example, the increase in lambda helps for the substitution ratio while the efficiency drops. The end goal is high substitution ratio and efficiency.

3. Multi-cylinder engine design and testing

The end goal for an engine builder is to have an engine ready and performing in a way to be ready for sales. ABC's multicylinder engine was ready on test bench in 2022 and tested for intensive period. This was the result of a dedicated team and intensive research together with partners. This is within the project of FASTWATER and others. See the Figure 2 taken during the FASTWATER meeting at ABC in the week 45 of 2021.

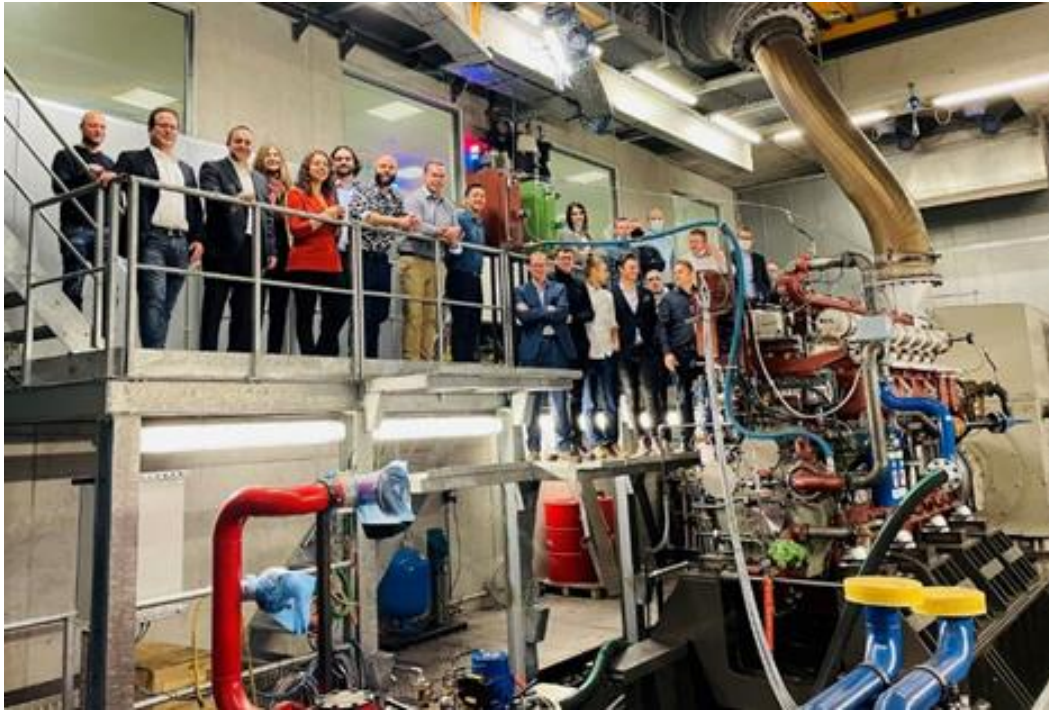


Figure 2 - FASTWATER General assembly at ABC

This engine design didn't come by itself. The deep knowledge came from combining the physical properties of methanol within the current engine design. The first investigations show that there was a great importance for the heat of evaporation in the engine. This was a challenge, mainly due to the time for one intake and compression stroke on a 1000 rpm engine that is 60ms, so the maximum should be obtained out of the evaporation process.

The first process is solved within the injector design. Small droplet sizes have to be achieved to get a great liquid surface to increase heat transfer from the air in the manifold to the methanol. For this we have developed a model, based on the dew point and latent heat for evaporation of methanol. Nevertheless, this resulted in a model for methanol evaporation but also the diesel needs evaporation energy. With this model we got the temperature layout for the air collector and compression ratio. This was one part of the puzzle.

Secondly, we need to get the peak firing pressure under the design limit of the engine while still supplying a sufficient amount of air for the combustion of diesel and methanol for a good efficiency. All of this needed to be accomplished without exceeding the IMO II NO_x limits engine internally such that the use for an expensive SCR (Selective Catalytic Reduction) system is avoided. Therefore, we used a GT-power model as shown in Figure 3.

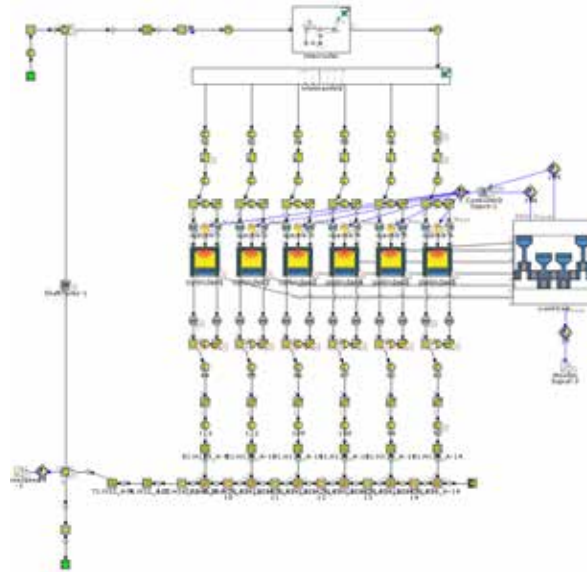


Figure 3 - GT Power model

The air flow through the engine at the temperature and pressure to achieve combustion with the requested efficiency and methanol substitution was done for multiple engine load and speed setpoints. The boost pressure and intake temperature are matched with an optimized turbocharger and a new compression ratio after several iterations. This still left two things open for a good engine design. The first is matching the theoretical charge cooler with the current charge air cooler and make an optimal mixing to reduce knocking and achieve a reasonable COV of IMEP and p_{max} .

For the charge air cooler, we want to have a one cooler for diesel mode and dual fuel mode. The difference is the cooling capacity for diesel needs to be more than for dual fuel to reduce the NO_x in diesel mode and in dual fuel operation we need heat for the methanol evaporation. This resulted in an optimization of the split cooling circuit with reduced air to water surface of the charge air cooler and an electronic thermostatic valve before the charge air cooler to control the water intake temperature of the charge air cooler. This thermostatic valve is at location Th2 (outlet thermostat 2) of Figure 4.

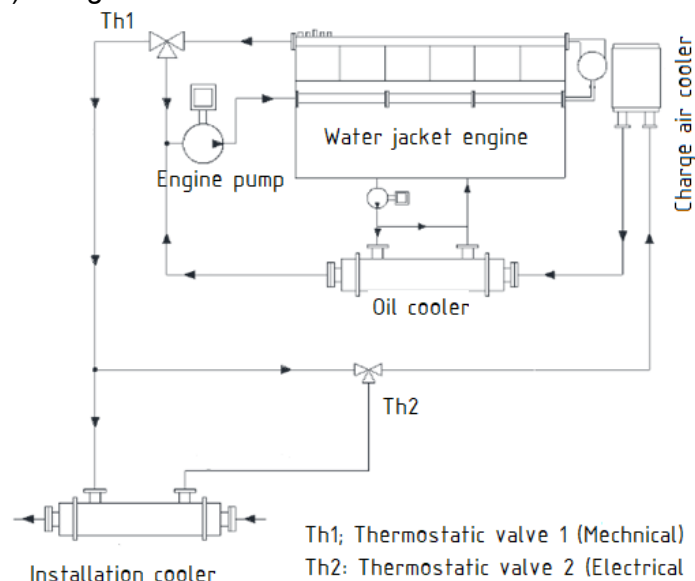


Figure 4 - Cooling water circuit of the methanol engine

Lastly, a mixing simulation was done to get an optimal mixture in the cylinder this to improve evaporation and combustion stability (Figure 5). The main difficulty is to get a stable mixture without wall film formation.

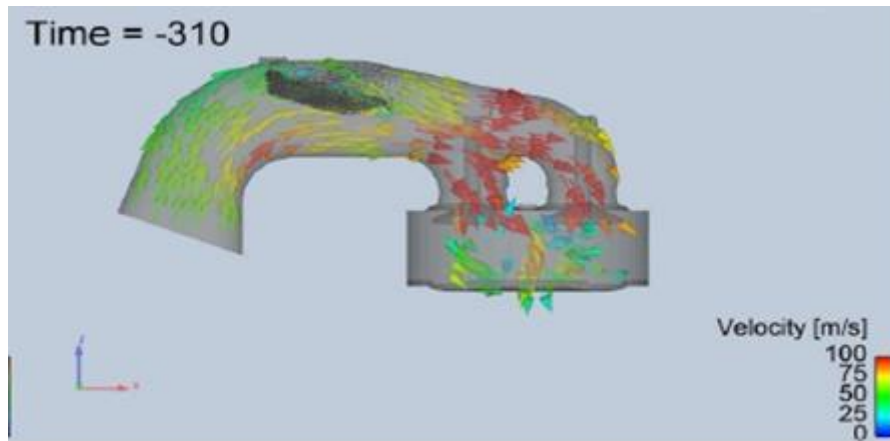


Figure 5 - Mixing simulation with methanol port fuel injection.

With all the iterations and testing we believe we have achieved the maximum potential out of the DZ-engine and have made it ready for market.

4. Current projects on the DZ-engine

The development of the ABC DZD methanol engine and demonstration project of Port of Antwerp-Bruges (PoAB) has gained attraction and has led to several engine orders for newbuild ships. At the moment, offshore supply vessels both for Esvagt and Acta Marine are under construction and will be powered by ABC methanol engines.

For the Methatug, the engines are type approved by BV class, for the offshore supply vessels, the engines will be DNV certified. All engines will be IMO Tier III compliant using an SCR system. Although not required by IMO, an oxidation catalyst is integrated in the SCR housing to reduce CO and HC emissions to diesel-like values.

With even more engines ordered, it is clear methanol has gained serious traction during the past years.



Figure 6 - Mockup of the Methatug tugboat from Port of Antwerp-Bruges (PoAB)



Figure 7 - Ship of Esvagt



Figure 8 - Ships of Acta Marine

5. Request for even bigger engine development

Guided by the success of the DZ methanol engine, ABC customers have come to expect alternative fuel capabilities across all engine series, reflecting the company's commitment to advancing a sustainable future. Responding on customer demand. Right now, our smaller engine, the DZ, enjoys a competitive advantage, by already having quite some experience running on methanol. The prevailing focus among competitors is on high-pressure direct injection.

ABC recognizes the urgency of establishing a competitive foothold in this segment and believes that adopting a port fuel injection strategy is a pragmatic approach. This strategy not only simplifies implementation but also facilitates cost-effective retrofitting on existing engines, offering a more economical alternative compared to the intricate direct injection technology embraced by our competitors.

6. Design of the future Port Fuel Injected MeOH-engine

The initial PFI-concept will draw inspiration from the state-of-the-art DZ PFI design, with a strong emphasis on continuous improvement. The development process is facilitated by two main drivers. First, the ABC Single Cylinder Engine (SCE) testbench, a powerful tool which is deployed very early in the development process. The SCE is strategically located in close proximity of the factory, enabling an incredibly short feedback loop among design, manufacturing, and testing, facilitating swift adaptations and course corrections throughout the development process.

In the initial phase as much hardware as possible is reused from the DZ engine on the SCE. Simultaneously, new hardware is developed and will be seamlessly integrated as soon as it becomes available. Manufacturing of these prototype parts will be done on site and in close cooperation with external suppliers.

The second driver in the development will be flow and combustion simulations, complementing the SCE testing. The SCE will be used to correlate the simulation models and the trends of the simulation models are tested against reality.

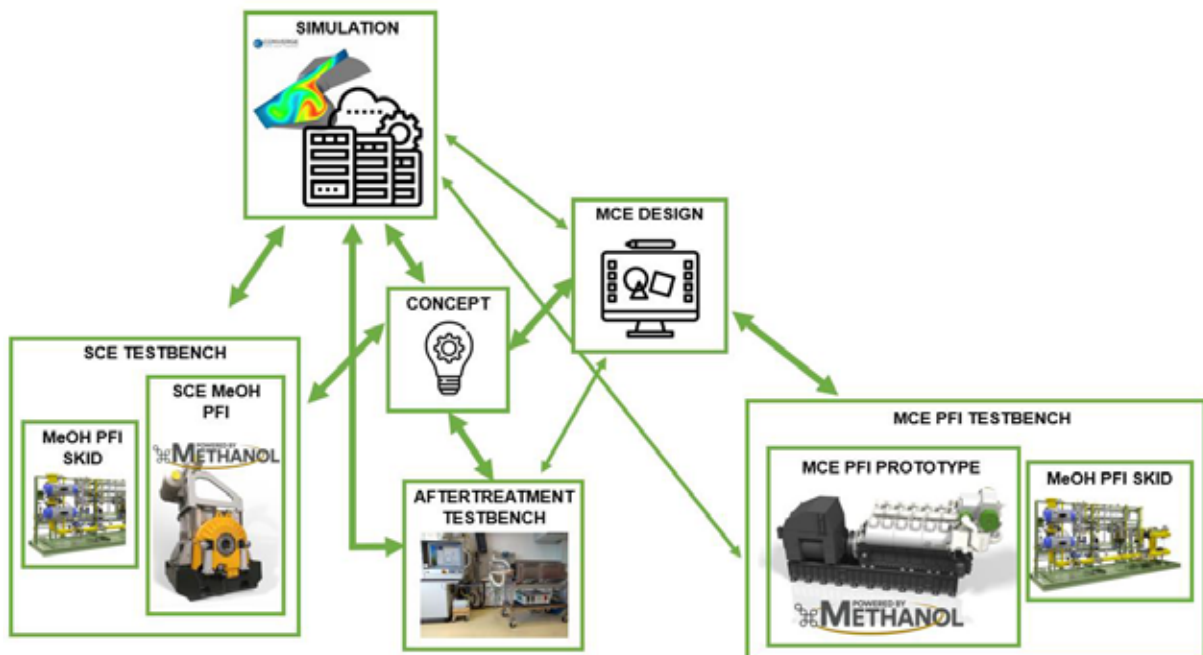


Figure 91 - Interaction diagram of PFI development

In the beginning of the development the emphasis lays on inlet temperature management and compression ratio. As these parameters are hard to change on a multicylinder engine. This makes thermal management of inlet temperatures hard to change on the MCE. The compression ratio is hard to change on an MCE but can be changed relatively quickly on a SCE and with simulation.

Results from SCE testing and simulations will directly implicate the MCE design. Modifications to the MCE will first be tested on the testbench, in cooperation with our clients and development partners, the modifications will be applied on existing engines.

7. Single cylinder test bench

For the development of the methanol combustion system on the DZ engine, the single cylinder experiments were essential for concept elimination selection and initial optimization.



Figure 10 - Single Cylinder Engine Testbench

The SCE is designed for flexibility and accurate measurements. In the air path it is equipped with two external variable speed compressors with different maximum capacities. This allows precise control of the air pressure over the whole operation range of the engine. Furthermore, both compressors are equipped with a mixing valve between the hot and cold air outlet to control the inlet temperature as well. The outlet pressure is controlled by a proportional back-pressure valve and orifice.

The pressure and temperature of the engine oil, coolant and fuel are also conditioned in a separate technical room to ensure a good repeatability of the experiments.

The engine is instrumented with several specific sensors; the following parameters are measured continuously: cylinder pressure, inlet-, and outlet pressure, injection pressure. The system is expanded with additional sensors for some measurement campaigns, e.g.: a vibration sensor for knock measurement, ...

The emissions are measured with an FTiR emissions analyzer. This has the advantage of detecting many different species with only a single analyzer. The components that are currently detected are CO; CO₂; O₂; H₂O; NO; N₂O; NO₂; NH₃; methanol; methane, ethane, propane; formaldehyde.

To get started with design evaluation on the single cylinder engine, it is important to evaluate the match of the performance to the multi-cylinder application. For the power unit there are measurement results available for diesel operation so the performance difference can be easily quantified. The first experiments on the single cylinder used boundary conditions that were measured in the multi-cylinder and resulted in a similar cylinder pressure trace, but after evaluating in more detail two issues were found: firstly, there is an offset in start of combustion and secondly the cylinder pressure after compression was higher than expected. This is shown

on the lefthand side in FigureFigure 11. The pressure at the beginning of the compression stroke is shown on the righthand side. This indicates clearly that the charge air pressure was set to a too high value during the single cylinder experiments and decreasing this setpoint resulted in an identical compression curve. The difference in this value can be explained by different pressure oscillations in the intake manifold, and the measurement location of the pressure sensor in the multicylinder engine.

After this correction, the cylinder pressure is still slightly higher than measured in multi-cylinder. This can be resolved by retarding the injection timing slightly. Looking at the signal quality, it seems that the multi-cylinder data has been filtered more strongly during the power stroke and this could have an effect on the peak pressure and start of combustion detection as well.

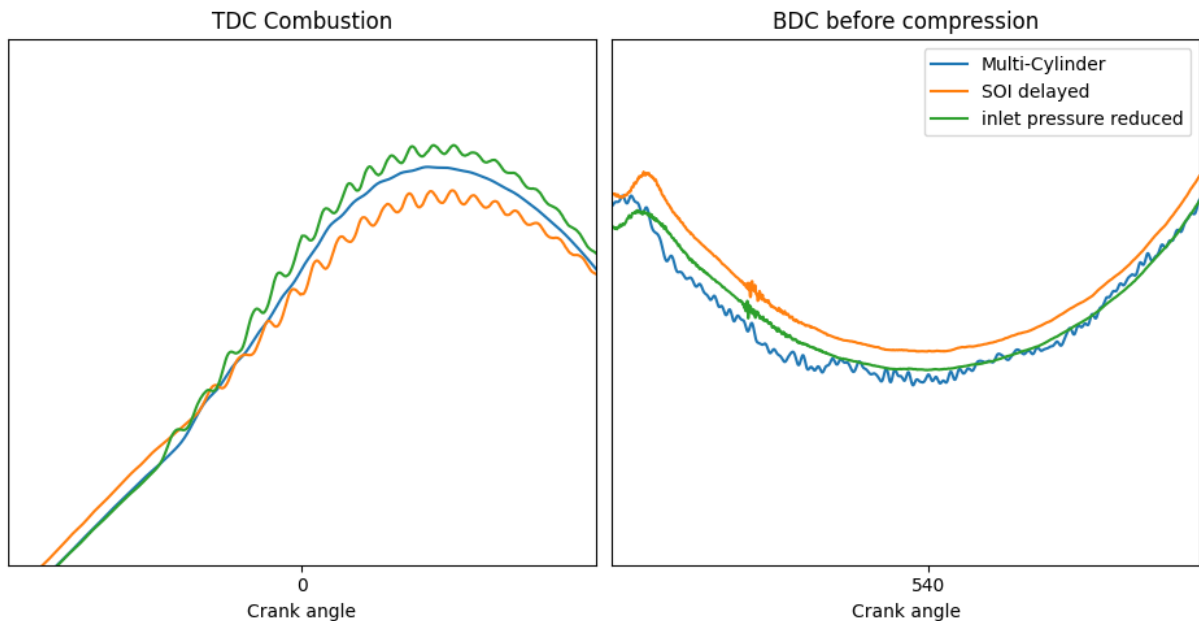


Figure 11: cylinder pressure comparison between multi-cylinder and single-cylinder

After conducting the reference measurements and hence making sure that the SCE accurately represents a MCE, the testing campaign started.

The testing plan employs a strategic approach to evaluate the performance for dual fuel operation. The plan focuses on three key factors: injection timing (for both fuels), compression ratio, and charge air temperature. By utilizing a balanced experimental design, the plan aims to maximize data acquisition while maintaining operational efficiency.

8. Projects for the D36-series

ABC signed a contract with Jan De Nul for methanol engines. The Belgian dredging company is building the *Fleeming Jenkin*, the largest cable laying vessel to date. It will be powered by five ABC engines fueled by methanol. The vessel will also be outfitted to comply with ULEv notation from Bureau Veritas. The Ultra-Low Emission Vessels notation goes beyond the existing MARPOL requirements. In this way, Jan De Nul will take a big step towards a more sustainable fleet.



Figure 12: *Fleeming Jenkin*

9. Conclusion

ABC is making significant investments in the research and development of internal combustion engine technology, aiming to ensure its sustainability and future resilience. As shown in previous publications at cimac 2023; “ABC completes the upgrade of its DZ engines into hydrogen dual fuel and spark ignition”, ABC has already successfully completed the development for both a hydrogen dual fuel engine and a hydrogen spark ignited engine which are based on the DZ engine platform. Now we are expanding the capability of the DZ and other engine families towards dual fuel methanol operation.

The research and development of the ABC DZD methanol engine was completed last year. And as the demand is high, series production has begun, of which the first engines have already left the factory.

References

- [1] Mattheeuws L., De Wilde E.: ABC completes the upgrade of its DZ engines into hydrogen dual fuel and spark ignition. In CIMAC Congress, Paper No. 203, Busan, Korea, (2023).
- [2] Sorrentino A, Leytes V., Mattheeuws L., De Wilde E.: Methanol port fuel injection for mediumspeed application: injector development and engine design. In CIMAC Congress, Paper No. 104, Busan, Korea, (2023).
- [3] Mattheeuws L.: ABC’s dual fuel engines running on renewable fuels like methanol and hydrogen. In: Dessau Gas Engine Conference, Dessau-Roßlau, Saxony-Anhalt, Germany, (2019).

Development of a high speed methanol marine engine within the project “MeOHmare”

Entwicklung eines schnelllaufenden Methanol-Marinemotors im Projekt „MeOHmare“

Dr. P. Moll, Dr. J. Kech, S. Theiß

Rolls-Royce Solutions GmbH, Friedrichshafen, Germany

Abstract

To achieve IMO targets to reduce emissions in global shipping, the industry has to switch to green fuels among which methanol is a promising solution. Therefore the Federal Ministry for Economics and Climate Action together with Rolls-Royce Solutions and partners Woodward L'Orange and WTZ Rosslau develops a CO₂ neutral single-fuel methanol high-speed marine engine on the basis of its successful series 4000 within the publicly funded project “meOHmare”. The aim is, to reduce the integral CO₂ emissions by 90 %. In this lecture the challenges are highlighted, and first results of the project are shown.

Within the scope of the project a spark-ignited methanol combustion process is investigated in a first step by simulation (CFD) and single-cylinder experiments. Different injector types and injection positions for port-fuel injection are tested and compared with the aim of optimizing spray targeting and avoidance of wall film. The results show a strong influence of port filling on the combustion quality, especially HC emissions. Furthermore, the air management with two single-stage turbochargers, fuel system (inclusive fuel pump) and engine management are being investigated. As a synthesis of this work a concept for a full engine with 16 cylinders in V-configuration with 76-liter displacement is conceived. In a second step this engine will be built up and tested in the ongoing project duration until 2026. The project began in January at Technology Readiness Level 3 (TRL 3) with testing injection components in the single-cylinder engine. The development activities are to be advanced until TRL 6 in 2025.

Kurzfassung

Zur Erreichung des Reduktionsziels der IMO die Emissionen der globalen Schifffahrt zu reduzieren, muss die Industrie zu grünen Kraftstoffen, unter welchen Methanol eine vielversprechende Lösung ist, wechseln. Hierfür hat das Bundesministerium für Wirtschaft und Klimaschutz zusammen mit der Rolls-Royce Solutions GmbH, der Woodward L'Orange GmbH und dem WTZ Rosslau das geförderte Projekt „meOHmare“ initiiert. Ziel ist es, einen fremdgezündeten schnelllaufenden Otto-Methanolmotor auf Basis der Baureihe 4000 für den maritimen Einsatz zu entwickeln, um so die bilanziellen verbrennungsmotorischen CO₂-Emissionen um mehr als 90 % zu reduzieren. Im folgenden Vortrag wird auf die Herausforderungen, die im Zusammenhang mit Methanol stehen, eingegangen und erste Ergebnisse des Projektes vorgestellt.

Im Rahmen des Projektes wird der fremdgezündete Verbrennungsprozess von Methanol im ersten Schritt durch Simulation (CFD) und Einzylinderexperimenten untersucht. Verschiedene Injektortypen und Einspritzpositionen für die Saugrohreinspritzung werden getestet und verglichen. Ziel ist es hier, die Strahlausrichtung zu optimieren und Wandbenetzung zu vermeiden. Die Ergebnisse zeigen einen starken Einfluss der Kanalfüllung auf die Verbrennungsqualität, insbesondere auf HC-Emissionen. Darüber hinaus werden das Luftmanagement mit zwei Turboladern, das Kraftstoffsystem inklusive Kraftstoffpumpe und das Motormanagement untersucht. Als Ergebnis dieser Themengebiete

* Speaker/Referent

wird ein Vollmotor mit 16 Zylindern in V-Anordnung und 76 Litern Hubraum konzipiert. Im zweiten Schritt wird dieser Motor in der kommenden Projektlaufzeit bis 2026 aufgebaut und getestet.

Das Projekt startete im Januar auf Technologie Readiness Level 3 (TRL 3) mit der Erprobung von Einspritzkomponenten am Einzylinderaggregat. Die Entwicklungsaktivitäten sollen bis TRL 6 im Jahr 2025 vorangetrieben werden.

1. Introduction

The International Maritime Organization (IMO) has adopted a new more ambitious strategy on the reduction of greenhouse gas emissions from ships in their MEPC session in July 2023 to reach net-zero emissions by or around 2050 [1]. With the intermediate goal to cut total annual greenhouse gas emissions from international shipping by at least 20%, striving for 30% by 2030 (compared to 2008) immediate action by all members of the marine industry is required. Among other possible technical and operational solutions, the use of hydrogen or other synthetic fuels for ship propulsion and onboard power generation has the biggest lever to reduce emissions [2].

One of the most promising alternative fuels for shipping is methanol. Compared to today's most common fuel HFO (heavy fuel oil), commercially available methanol can reduce emissions of NO_x by 80 %, SO_x by 99 % and particles by 95 % [3]. With a value of 16 GJ/m³ methanol has the best volumetric energy density among all other alternative fuels such as hydrogen or ammonia, taking only two times the bunker volume of diesel for a given range. As methanol is in liquid state at ambient temperature fuel handling and bunkering is easily possible without the need of cryogenic infrastructure or high pressures allowing fuel tanks with flexible geometry and easy integration near the ships outer hull. With methanol being traded as a commercial commodity for many years there are established regulations and safety measures for its handling. Additionally, methanol is available at more than 120 ports worldwide and shipped globally [3]. Current production of around 100 Mt methanol per year allows shipping companies ample procurement options and a fast transition of their fleets to emission reduction, although today's methanol is mostly produced from steam reformation of natural gas. With more than 80 renewable methanol projects already announced a clear path towards net zero operation with methanol is paved [4]. Thanks to the mentioned advantages major shipping companies are adopting methanol as a marine fuel for use in e.g. box ships, tankers and cruise ships [5]. This surge in methanol powered ships is creating the ecosystem for production, logistics and bunkering of methanol from which also other marine applications will profit.

First marine engines capable of running on methanol entered the market in the mid-2010s being 2-stroke dual-fuel engines. These engines were mainly used in ships carrying methanol as a cargo. With the order of a significant number of methanol fueled box ships beginning of the 2020s sales numbers for 2-stroke dual-fuel engines increased with different engine manufacturers serving the market. Regarding 4-stroke engines first experiences were made with the conversion of the Baltic Sea ferry Stena Germanica to methanol fueled operation with four medium-speed engines using diesel as a pilot fuel for methanol ignition. An alternative concept is pursued by the Swedish company Scandinaos with a modified Scania 8-cylinder diesel engine using a special additive to realize methanol combustion with compression ignition. Both technologies require either an additional additive or diesel as second fuel for ignition. Engines running purely on methanol in a spark-ignited otto process are only known from an academic environment with much lower mean effective pressures and smaller bore diameter for research purposes. Hence, for use in commercial marine applications no spark-ignited methanol engine is available.

Therefore, within the publicly funded project "meOHmare" Rolls-Royce Solutions and its project partners Woodward L'Orange and WTZ Rosslau develop an engine concept for a high-speed four-stroke marine engine running on green methanol. Based on the

requirements of commercial shipping demanding high power density the aim is to achieve more than 120 kW per cylinder which translates in a mean effective pressure of 17 bar. To validate the engine concept a 16-cylinder engine will be built and tested on a development test bench achieving technology readiness level TRL 6 until end of 2025.

In this paper we will show first results of the combustion development on the single cylinder engine testbench (SCE) with methanol port fuel injection. Based on this, the engine concept is presented outlining the general specification and features of the most relevant subsystems. Finally, the engine's behavior in a potential target marine application has been simulated in a 1D-simulation to validate the concept.

2. Methanol Combustion Development

Methanol is a globally traded chemical substance used in many industrial applications. It is also an energy carrier especially for green energy. In this case Methanol is a so-called e-fuel with suitable properties for spark ignited engines. The properties concerning engine development are the lower heating value compared to Diesel, high evaporation enthalpy, furthermore high octane number and low cetane number. The characteristics of methanol pose new challenges for engine development. In addition to the high octane number, which has a positive effect on the combustion, methanol has other properties that pose major challenges for combustion development. For example, the high enthalpy of vaporization, which requires the best possible mixture preparation from injector components. The lower heating value, which is only half of diesel, and the higher tendency to cavitation require new performance from all fuel preparation components in terms of pressure preparation, fuel delivery and injection. The materials of all components that are in contact with methanol must also be tested and reselected, considering the corrosive properties of the low flashpoint fuel. The aim of all these challenges is to develop a stable and efficient combustion process.

A multi-layered iteration cycle consisting of component tests, CFD analyses and single-cylinder tests will be used to develop the combustion process. The focus is on investigating the requirements for stable mixture preparation to make a targeted start on the development of a PFI system.

For mixture formation the injector is the central component in the focus of the investigations. A technology analysis is therefore carried out at the beginning of combustion development. The aim is to cover a wide range in terms of both pressure and jet geometry with as few components as possible. For this purpose, three different injectors have been compared in a test program on the single cylinder engine. Besides two automotive injectors, one low pressure and one high pressure injector, a medium pressure off-highway injector was included.

The injectors are tested for spray formation in chamber tests and the spray data is then used for CFD modeling. Various positions on the cylinder head and in the intake manifold are available for this purpose.

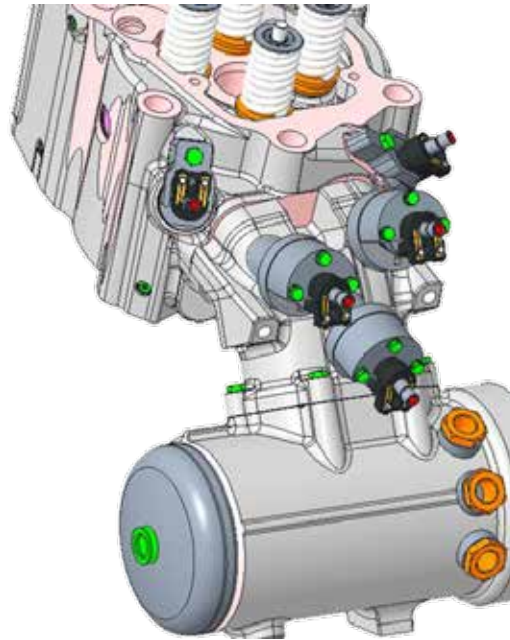


Figure 1: Single cylinder head with possible injector positions

As shown in Figure 1, five different positions and more combinations can be realized. There are two positions in the cylinder head itself for fuel injection close to the valves. Due to the close distance to the inlet valves an injection concept can be realized without high risk of wall film formation. By combining it with a suction-synchronous injection strategy most of the fuel can be injected directly into the combustion chamber via the inlet valves. Like in the first cylinder head position described, it is also possible to equip each port with injectors individually or simultaneously via the intake manifold. This allows to determine the influence of the respective port in terms of mixture formation in the combustion chamber. It is also possible to inject into both ports. This position with more distance to the inlet valves offers a larger volume for mixture preparation. Methanol can be enriched in the air before the valves are opened. An additional central positioning is provided further back centralized in the intake manifold. Experiments can take place here with an injector that can be used to inject into both inlet ports at the same time.

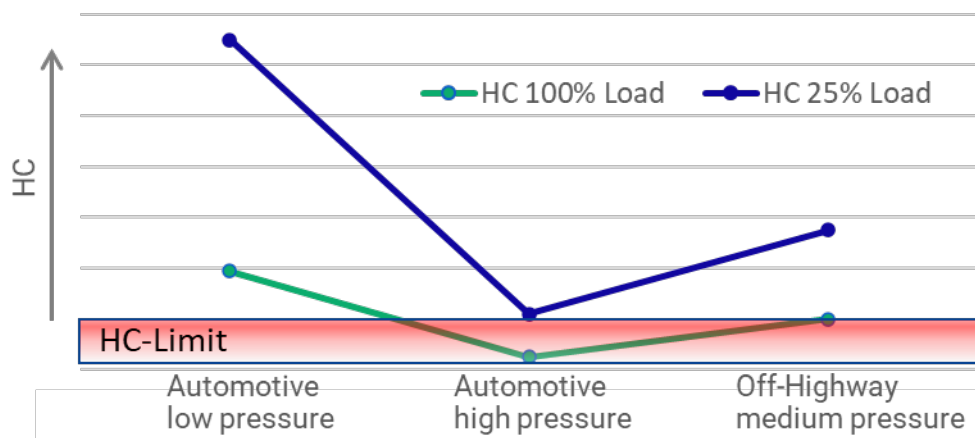


Figure 2: Comparison of different injectors

The injectors are evaluated for their respective fuel preparation based on the measured hydrocarbon (HC) emissions. This is an opportunity to use the SCE results to provide a first and simple comparison option. The results show that both the position and the injection pressure have an influence on these emissions in combination with the given injectors (see Figure 2). A clear tendency of the injection pressure can be seen, with higher injection

pressures leading to better fuel preparation, based on the S4000 intake port design. At this point, further investigations are needed to understand the spray and fuel preparation behavior within the intake ports.

To be able to make well-founded statements about the respective injection concepts, CFD studies are carried out. For this purpose, the injectors are first measured on component test stands and the spray characteristics are then examined in injection chambers. The results of the physical tests become input variables for the CFD simulation. The focus of the investigations is on the wall film formation of methanol within the intake port. In Figure 3 is shown that the wall film thickness is highest directly after the injector and in the curves of the intake port. This is happening in both ports.

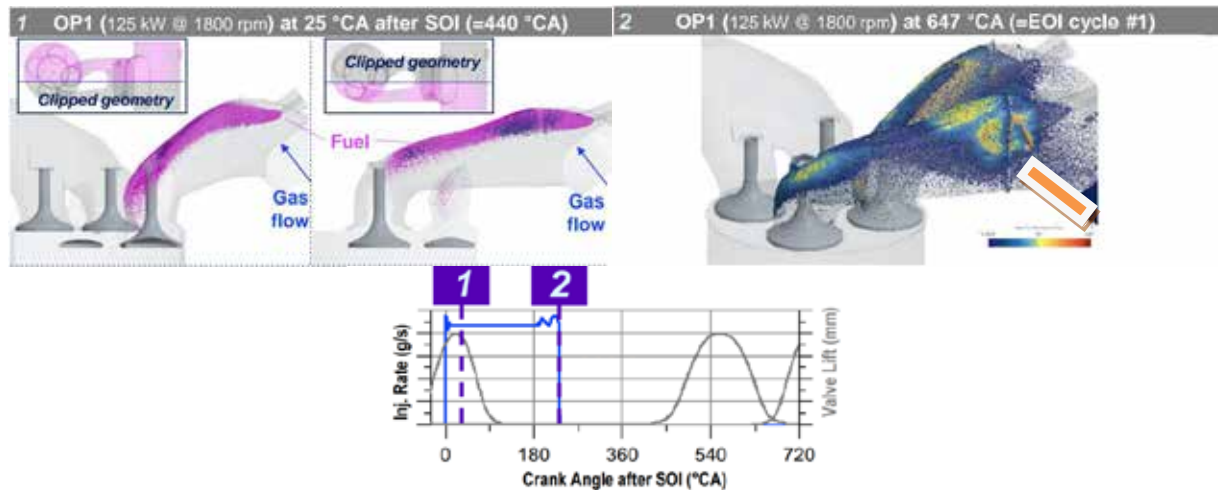


Figure 3: Wall film simulation of inlet ports at different CA

The wall deposits are particularly interesting for evaluating an injection concept in terms of combustion stability. Tests on the SCE revealed that individual cycles exhibit knock-like behavior at load points with a high tendency for wall film formation and low combustion stability. In Figure 4 two cycles can be seen, which are recorded one after the other and reflect such behavior.

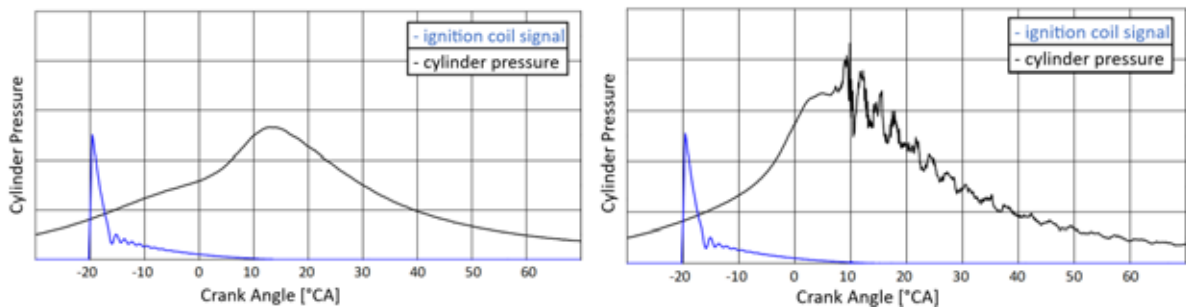


Figure 4: Normal cylinder pressure curve vs. knocking-like combustion

These cycles with a knock-like pressure curve usually only occur once and therefore remain individual events. One explanation for this can be based in the forming of wall films. If a high wall film rips off, a significantly higher injection quantity spontaneously occurs and at the same time a richer mixture is created. In the area shortly after the ignition signal there is a steeper pressure increase, which indicates a faster combustion even before top dead center (TDC). Since combustion begins during compression, additional ignition sources arise due to higher temperatures and pressure in the combustion chamber at TDC. Classic knocking can be ruled out here because there is no significant increase in pressure before the ignition signal.

To look closer through the combustion behavior, a variation of the Start of Injection (SOI) is made. Therefore, it is possible to set injection timings in such a way that either a preliminary storage of methanol or a subsequent storage within the intake port can take place. Furthermore, suction-synchronous injection can be realized in the section between. The results of parameter variation shown in Figure 5 are recorded simultaneously within one experiment. In the experiment, a Miller-principle is used with an intake close (IC) at -200 °CA.

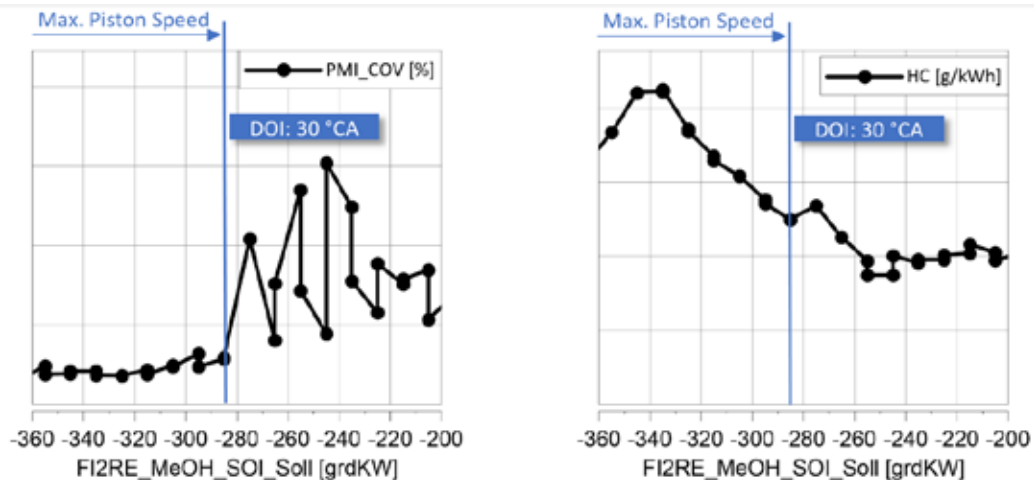


Figure 5: Combustion stability and HC-emission over start of injection

When comparing the two series of measurements, a trade-off becomes apparent. If HC-emissions fall, combustion stability decreases and vice versa. Especially at the beginning of the intake stroke up to the highest piston speed, a better combustion stability exists, but with high HC-emissions. The HC-emissions decrease till -230 °CA where the pre-storage begins. It is assumed that the piston speed is approximately proportional to the air velocity in the intake port. It is at its highest point at -284 °CA and from there HC-emissions increases again till IC at -200 °CA. At the same time, combustion stability decreases, which can be an indication of uneven mixture preparation due to the high relative velocities in the intake port. With late injection and pre storage of methanol from -230 °CA, it is noticeable that the methanol staying within the intake port has no negative effects on HC-emissions. Combustion stability also increases. The additional time that is given to evaporate until the valve opens again can be an explanation for this effect.

When developing a combustion process for a methanol spark ignited engine with high demands on power density, it is important to know the limits of the respective combustion process. The knock limit can be used as a limit for this. Using a lambda variation, different compression ratios (CR) are achieved up to the knock limit. As the compression ratio increases, the possible mean effective pressure (BMEP) decreases, as shown in Figure 6. Lambda must also be reduced to remain below the knock limit. If the compression ratio decreases, higher mean effective pressure can also be reached. Both the decreasing efficiency and the expected deterioration in cold start behavior must be considered. In the case of the meOHmare-engine, a CR of 15 is chosen.

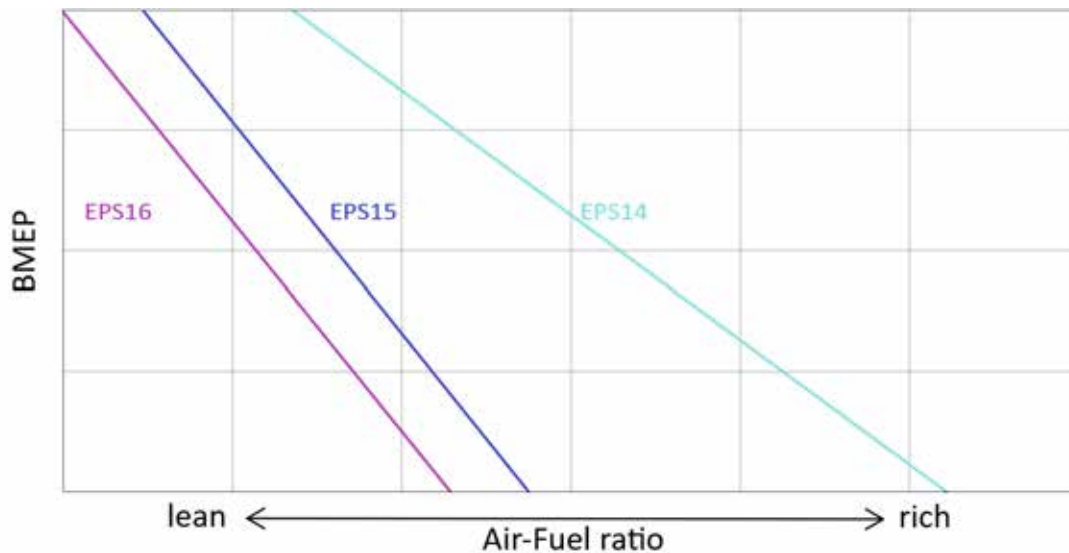


Figure 6: Combustion limits based on compression ratio.

With the variation of compression ratio shown above, the combustion air consumption can be simulated via the air-fuel ratio by setting the CR to a fix value. In further steps, further subsystems can be initially designed, such as the crank drive and the turbocharging system. Together with the given test and simulation results from the injector and wall film investigation, an initial high pressure PFI concept can be designed. All things considered, it is now possible to draw up a first meOHmare engine concept using the subsystems mentioned above.

3. Engine Concept

Based on the results of the presented methanol combustion development an engine concept for a 16-cylinder engine has been derived. Within the scope of project “meOHmare” the aim is to validate this engine concept on a test bench only, nevertheless requirements from a real use case of the engine in a tugboat have been considered. This includes operational requirements as well as fulfillment of regulatory aspects relevant for use of low flashpoint fuels onboard a vessel. The basis for the engine concept, which is also outlined in Figure 7, is the latest version of the well-proven series 4000 *mtu* marine engine 16V4000M65. Additionally, a lot of knowledge from the development of the *mtu* mobile gas marine engine particularly concerning safety systems and controls was transferred into this engine concept.

To fulfill the requirements the engine will generate a power of 2,000 kW at 1,800 rpm out of 16 cylinders in V-configuration with 125 kW each. The engine base is taken from the existing S4000Mx5 engine platform with slight modifications with respect to the characteristics of a spark-ignited combustion. Hence, the compression ratio is reduced compared to the usual ratio which is used in diesel fueled engines and consequently the piston geometry is adapted. A potential power increase with 2,000 rpm has already been considered in the dimensioning and design of the crank drive components. The engine air supply will be realized with a single stage using one inhouse-built ZR3 turbocharger for each cylinder bank. The air flow can be controlled with a wastegate, throttle flaps and a compressor bypass valve.

An entire new design is required for the methanol fuel system to comply with the rules given by the IGF code and class societies for low flashpoint fuels as is methanol. The liquid methanol will be piped to the injectors inside a double-walled pipe with ventilation of the space between the two walls. The injectors developed by the project partner Woodward L'Orange inject the methanol into the intake manifold (port-fuel injection), where the mixture is formed (cf. the results shown in chapter 2).

A lot of importance comes to the engine management concept to control the combustion. The engine power is governed as is typical for Otto-engines by controlling the air flow via throttle flaps. To ensure a stable combustion the fuel mass for each cylinder is calculated individually. This results in an overall lambda that ensures adherence of desired emissions. The fuel pressure is optimized for each load to ensure a stable combustion. Emphasis was given to the detection of unstable combustion cycles which is achieved via knock sensors. Those sensors are connected to an in house developed knock detection module. The knock detection algorithm takes methanol specific burn characteristics into account. Knock information is transmitted to the engine controller which reacts to single or continuous knocking.

Regarding emissions the project goal is to achieve IMO-III without the need for an SCR catalyst following the engine. Single cylinder engine results have shown that emissions can be kept well below the limit of 1.8 g/kWh, so indeed no SCR will be required, saving valuable space in the engine room. Nevertheless, the hydrocarbon (HC) emissions do require an additional oxidation catalyst (cf. Figure 2). Based on the emission composition detected during combustion development on the single cylinder engine a ceramic base catalyst will be used.

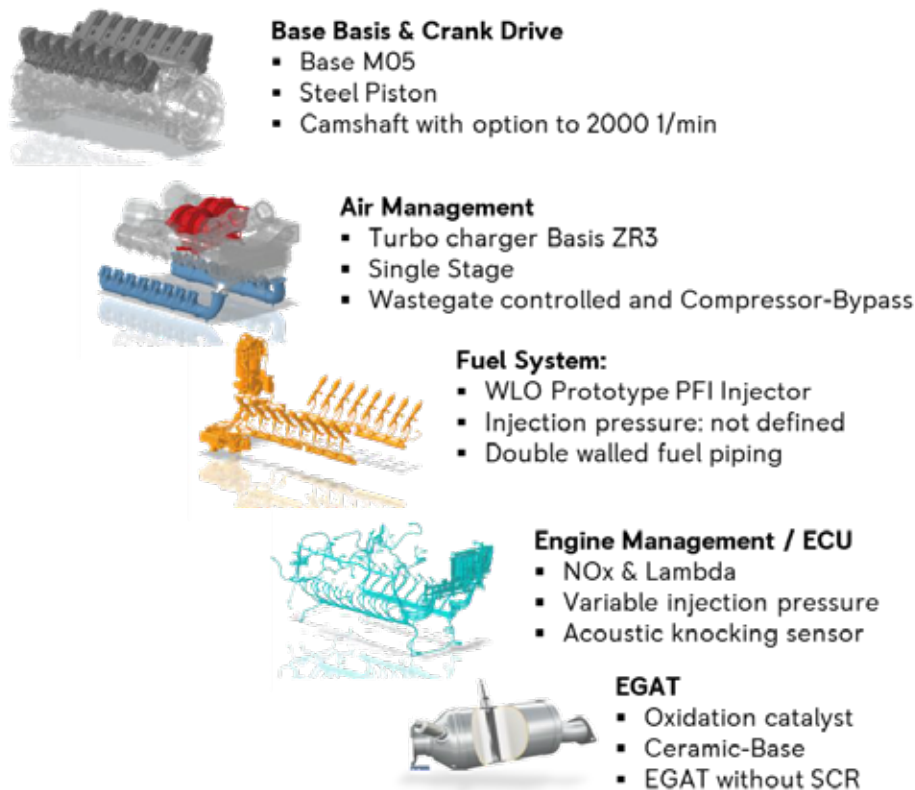


Figure 7: Main specifications for “meOHmare” high speed methanol marine engine concept

4. Application Simulation

To check if the described engine concept is suitable for use in a real marine application it has been validated using simulation. Within the context of project “meOHmare” the commercial application of the engine in a tugboat has been chosen as use-case. For this investigation a 1-D simulation model of the methanol engine concept has been created in the engine simulation software GT-Power. The model allows to simulate how the engine behaves in different drive scenarios. For this purpose, three drive scenarios were selected which represent particularly demanding situations in the operation of a tugboat. The data for the simulation originates from load profiles of existing series 4000 marine diesel engines running on a tugboat in the field.

The first simulated drive scenario is the so-called transverse reverse arrest to slow down a towed ship with a tugboat. This describes a braking scenario, where the thrusters turn in the opposite direction of movement with the goal to generate a braking force that act in the opposite direction. The thrusters are rotated from their initial position along the tugboat's direction of movement (0°), to 90° which is transverse to the direction of movement. After this quarter turn the thruster is turned another 90° towards 180° against the flow.

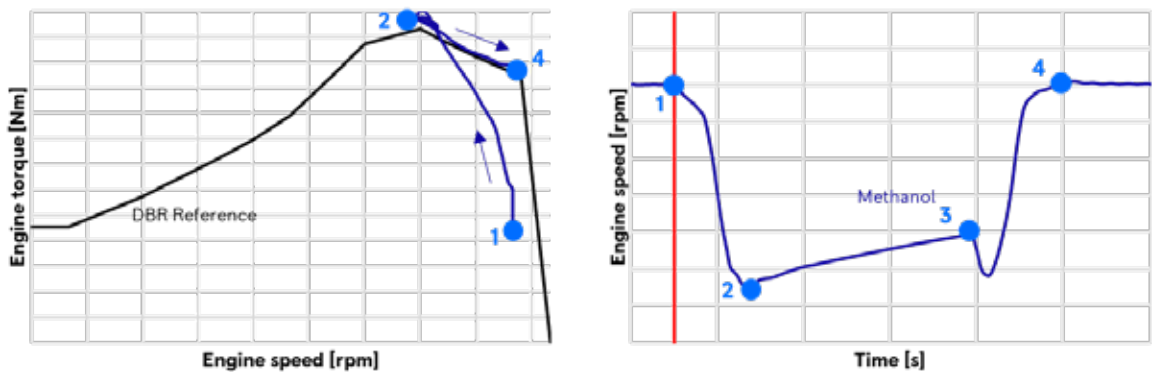


Figure 8: Engine speed and torque during the transverse reverse arrest maneuver with (1) start of rotation from 0° to 90° , (2) thruster reaches 90° , (3) thruster starts to rotate from 90° to 180° and (4) thruster reaching 180°

In Figure 8 showing engine speed and torque during the maneuver it is noticeable that turning the thruster transversely to the direction of movement requires the most drive torque. The simulation shows that the engine control must go into overload while turning thrusters from point (1) to (2) in order to maintain this load. In this case, the requested torque is too high for the referenced torque curve. In further investigations a higher maximum torque setup must be checked.

In the second simulated drive scenario which is called reverse arrest, the thruster is turned directly from the direction of movement 180° against the flow. From this point the engine must adjust back to the initial 1000 rpm. This maneuver is used to prove the load capacity of the engine concept in the lower speed range.

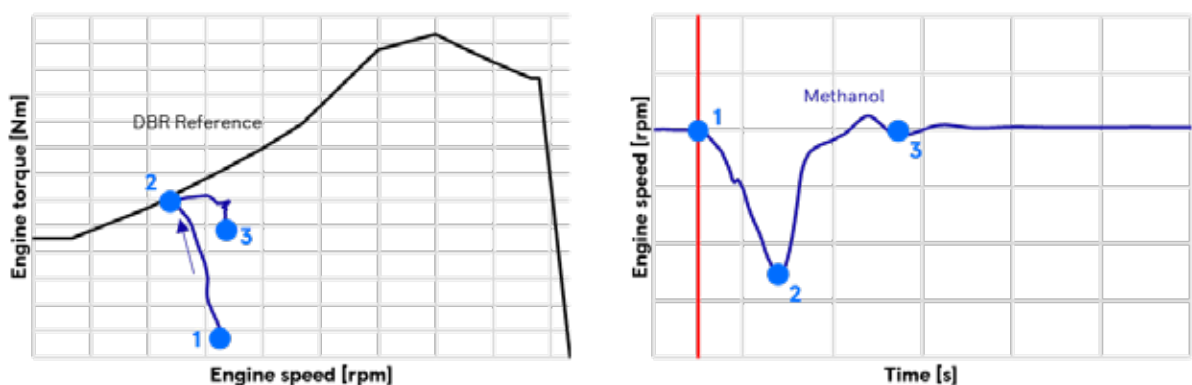


Figure 9: Engine speed and torque during the reverse arrest maneuver with (1) start of rotation from 0° to 180° , (2) thruster reaching 180° and (3) engine speed recovering to initial value

As can be seen in Figure 9 the methanol engine is pushed down to 870 rpm from point (1) to (2) as a result of the thruster rotating against the flow. At point (2) the full load curve is reached and the engine recovers from point (2) to (3). In this case the engine proves to be

well suited for tugboat applications. Particularly in the lower load range, a high level of agility is required when maneuvering to ensure stable running.

In a final validation case, the acceleration along the propeller curve describing the acceleration behavior of the methanol engine is validated. The requested time for speed up from idle to nominal speed is 15 seconds.

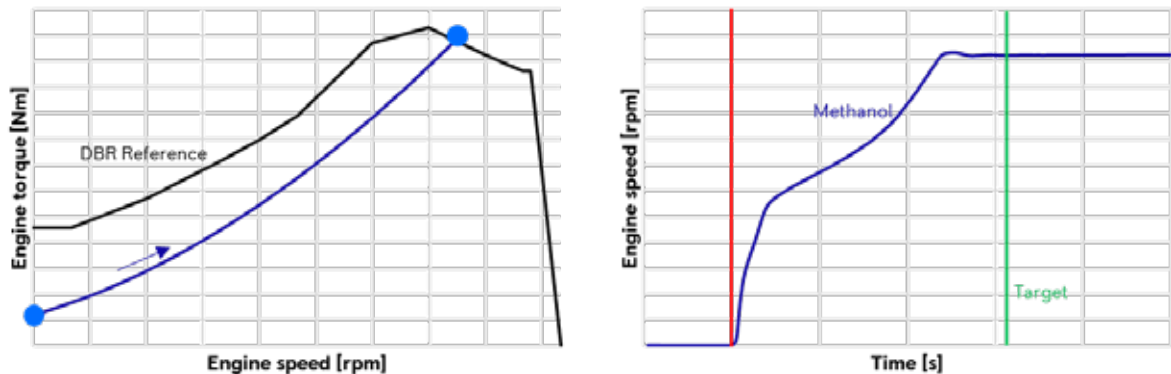


Figure 10: Engine acceleration along propeller curve (left) and time for acceleration (right)

The simulation results outlined in Figure 10 show that the methanol engine can speed up from the red line till the green line within less than the requested 15 seconds. This maneuver is representative for the acceleration behavior of the boat proving that the engine behaves sufficiently compared to the state of the art in terms of maneuverability and agility.

The meOHmare engine concept can perform two maneuvers, the reverse arrest and the propeller curve speed up, out of three directly. In the case of the third, the transverse reverse arrest, a further iteration loop must be taken via the map design. In future multi-cylinder tests, the results simulated here will be used as a basis and replicated on the test bench. In these tests, the transient requirements can be demonstrated physically.

5. Summary and Outlook

In this paper the first development results for a high-speed methanol marine engine generated in the publicly funded project “meOHmare” have been shown. Intensive combustion development for methanol has been conducted with a single cylinder engine with a focus on port-fuel injection and spark-ignition determining injector positioning in the injection manifold, start of injection (SOI) and compression ratio (CR). To support experimental development CFD analysis have been carried out to investigate mixture formation in detail showing a big influence of wand film formation on combustion quality. Based on the combustion development results a concept for a 16-cylinder methanol engine has been conceived with particular focus on the fuel system and engine management. Simulation has shown that this engine concept is well suited for the demanding operational requirements in a tugboat.

In the following months of project “meOHmare” the engine concept shown in this paper shall be validated using a 16-cylinder engine on a company-owned development testbench. Currently all components for the engine are procured and manufactured with assembly planned in late 2024. In parallel the test bench infrastructure is prepared for engine operation with methanol, including fuel supply from a central storage, safety systems (ventilation, sensors, fire detection) and additional measurement equipment. First test runs are planned for early 2025.

Acknowledgement

The results showed in this paper have been gathered in the publicly funded project “meOHmare”. This Project is supported by the Federal Ministry for Economic Affairs and Climate Action (BMWK) on the basis of a decision by the German Bundestag.

References

- [1] International Maritime Organization. “2023 IMO Strategy on Reduction of GHG Emissions from Ships”, July 2023.
<https://wwwcdn.imo.org/localresources/en/OurWork/Environment/Documents/annex/MEPC%2080/Annex%2015.pdf>. Accessed 13 February 2024.
- [2] DNV. “Energy Transition Outlook”, 2021.
- [3] Methanol Institute. “Marine Methanol: Future-Proof Shipping Fuel”, May 2023.
https://www.methanol.org/wp-content/uploads/2023/05/Marine_Methanol_Report_Methanol_Institute_May_2023.pdf.
Accessed 13 February 2024
- [4] John Snyder, Riviera AMM. „Green methanol needed to quench thirst for newbuilds”.
<https://www.rivieramm.com/news-content-hub/news-content-hub/green-methanol-needed-to-quench-thirst-for-newbuilds-75090>. Accessed 13 February 2024.
- [5] DNV Alternative Fuels Insight platform, 2024. Accessed 14 February 2024.

Session 7

Gemischbildungskomponenten Injection components

**Moderation: Karsten Stenzel
WTZ Roßlau gGmbH**

Hydrogen combustion results with low-pressure direct injection for 130 mm bore size engines

Wasserstoff-Verbrennungsergebnisse unter Niederdruck-Direkteinspritzung für Motoren mit 130 mm Bohrungsdurchmesser

Patrick Send*, Dr. János Csató, Richard Pirkl, Günther Neuhaus;
Liebherr-Components Deggendorf GmbH;

Francois Masson;
Liebherr Machines Bulle SA

Abstract

The hydrogen engine will also make its contribution in reducing greenhouse gases in the future. One of the key technologies in this type of engine is the injection system with its core component, the injector. Liebherr-Components Deggendorf GmbH has expanded its diesel product portfolio with a new direct-actuating concept to ensure hydrogen injection both in the intake manifold and under low pressure directly into the cylinder. This article focuses on individual combustion studies with hydrogen and direct injection up to pressures of 30 bar for heavy-duty engine sizes.

Kurzfassung

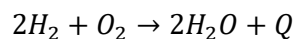
Zur Reduktion der Treibhausgase wird zukünftig auch der Wasserstoffmotor seinen Beitrag leisten. Eine der Schlüssel-Technologien bei dieser Art von Motor ist das Einspritzsystem mit seiner Kernkomponente Injektor. Liebherr-Components Deggendorf GmbH hat sein Diesel-Produktportfolio hierzu mit einem neuem direkt-angesteuerten Konzept erweitert, um die Wasserstoff-Einblasung sowohl im Saugrohr, als auch unter Niederdruck direkt in den Zylinder zu gewährleisten. Dieser Beitrag fokussiert sich hierbei auf einzelne Verbrennungsuntersuchungen mit Wasserstoff und der Direkteinblasung bis zu Drücken von 30 bar für Heavy-Duty-Motorengrößen.

* Speaker/Referent

1. Introduction

There are two types of propulsion technologies that can be powered by hydrogen: hydrogen combustion engines and hydrogen fuel cells. The choice between these drive options depends on several factors, such as efficiency, performance, cost, availability, cooling possibilities or application conditions, but also offers complementary applications. While the fuel cell generates electricity from the “slow” reaction with hydrogen and oxygen or air, a mixture of hydrogen and oxygen/air is burned in a chamber in the combustion engine to generate mechanical work. If the hydrogen used comes from sustainable, renewable sources, both drive technologies stand for emission-free mobility (Zero Emission Vehicle) and can significantly reduce the use of fossil fuels such as gasoline or diesel, especially in the combustion engine. Thus, hydrogen has the potential to be an environmentally friendly fuel with a remarkably high calorific value (about 120 MJ/kg) and therefore legitimizes the development of a global hydrogen economy. The advantages of using hydrogen are therefore the high mass related energy density that allows for high performance and efficiency, the low environmental impact as the combustion products consist only of water and nitrogen oxides, and the possibility of producing hydrogen from renewable energy sources. However, there are also challenges like storing and transporting hydrogen or fuel infrastructure, which require high safety requirements, adapting existing engines, and the costs and availability of renewable hydrogen compared to other fuels.

The following chapter focuses on the theoretical foundations of the injection technology of a hydrogen combustion engine, which is based on the principles of thermodynamics, chemistry, and fluid mechanics. The combustion of hydrogen (H_2) and oxygen (O_2) is an exothermic reaction that produces water (H_2O) and heat (Q). The reaction equation is:



This reaction takes place in the engine cylinder. The piston inside converts the heat energy generated into mechanical energy and the remaining combustion products are directed into the atmosphere via the exhaust valves. Combustion depends on various parameters, such as the air-fuel ratio (AFR), compression ratio (CR), ignition time, flame velocity, knock resistance or heat transfer to the cylinder wall. Hydrogen as a fuel also has different combustion properties than conventional fuels such as diesel or natural gas. Table 1 shows some of the properties of hydrogen relevant to an internal combustion engine compared to the values for a typical CNG composition and to gasoline and diesel.

Table 1 Hydrogen properties compared with compressed natural gas (CNG), gasoline and diesel [1]

Property	Hydrogen	CNG	Gasoline	Diesel
Carbon content (mass%)	0	75 ^e	84	86
Lower heating value (MJ/kg)	119.7	45.8	44.8	42.5
Density ^{a,b} (kg/m ³)	0.089	0.72	730–780	830
Volumetric energy content ^{a,b} (MJ/m ³)	10.7	33.0	33 × 10 ³	35 × 10 ³
Molecular weight	2.016	16.043 ^e	~110	~170
Boiling point ^a (K)	20	111 ^e	298–488	453–633
Auto-ignition temperature (K)	858	813 ^e	~623	~523
Minimum ignition energy in air ^{a,d} (mJ)	0.02	0.29	0.24	0.24
Stoichiometric air/fuel mass ratio	34.5	17.2 ^e	14.7	14.5
Stoichiometric volume fraction in air (%)	29.53	9.48	~2 ^f	-
Quenching distance ^{a,c,d} (mm)	0.64	2.1 ^e	~2	-
Laminar flame speed in air ^{a,c,d} (m/s)	1.85	0.38	0.37–0.43	0.37–0.43 ^g
Diffusion coefficient in air ^{a,b} (m ² /s)	8.5 × 10 ⁻⁶	1.9 × 10 ⁻⁶	-	-
Flammability limits in air (vol%)	4–76	5.3–15	1–7.6	0.6–5.5
Adiabatic flame temperature ^{a,c,d} (K)	2480	2214	2580	~2300

^a at 1 bar, ^b at 273 K, ^c at 298 K, ^d at stoichiometry, ^e methane, ^f vapor and ^g n-heptane.

- Stoichiometric combustion of hydrogen occurs at an **air-fuel ratio** of approximately 34. However, hydrogen can also be burned in a wide range of AFR ratios, from (“ultra”) lean to rich, depending on the requirements of the engine [2].
- The **compression ratio** is a key factor in the performance and efficiency of an internal combustion engine. A higher CR increases the thermodynamic efficiency and specific power of the engine, but it also increases the risk of irregular combustions, like pre-ignition or knocking, which can lead to engine damage [2]. Knocking is an uncontrolled combustion caused by spontaneous ignition of the fuel-air mixture before being reached by the flame front initiated by the spark plug [2].
- **Ignition timing** is when the spark plug produces a spark to initiate combustion. The optimal ignition timing depends on numerous factors, such as AFR ratio, CR, engine speed, load, and mixture conditions (pressure, temperature) [2]. Ignition too early or too late can lead to a loss of power, increased fuel consumption and higher pollutant emissions [2].
- **Flame velocity** is the speed at which the flame front moves through the fuel-air mixture. The flame velocity of hydrogen is much higher than that of gasoline, resulting in faster and more complete combustion [2].
- **Knock resistance** is the ability of a fuel to resist spontaneous ignition. The knock resistance of hydrogen is lower than that of gasoline, which means that hydrogen is more susceptible to knocking [2] and ignition is more difficult to control [3].
- **Heat transfer to the cylinder wall** is the process by which heat is transferred from the combustion gases to the cylinder wall. Heat transfer to the cylinder wall reduces thermal efficiency, increases heat load of the components, and increases the engine's cooling needs [2].

The introduction of hydrogen by means of injection systems varies depending on the combustion process, injection pressure and mixture formation and thus has different effects on the combustion parameters mentioned above. Some examples are:

- **Diesel process (dual fuel):** In this process, the hydrogen is injected into the combustion chamber as a gas or liquid, where it is ignited with a diesel pilot jet. This system takes advantage of the advantages of the diesel cycle, such as high compression ratio, good mixture formation and low nitrogen oxide formation [4].

- **Active pre-chamber injection:** In this process, the hydrogen is injected into a small pre-chamber connected to the main combustion chamber of the diesel engine. The pre-chamber serves as an amplifier of the ignition energy for the fuel, thus enabling faster combustion. This system allows a better mixing of fuel and air, higher flame propagation speed, higher compression ratio, reduced knocking tendency, reduced cycle-to-cycle variations [5].
- **Intake manifold injection / port fuel injection:** In this process, hydrogen is injected into the intake manifold in front of the intake valve and mixed with air. This system is simple and inexpensive. It gives the best mixture homogeneity, but reduces volumetric efficiency, which reduces power density and/or requires higher boost pressure and has a higher risk of backfiring [4].
- **Direct injection:** In this process, hydrogen is injected directly into the combustion chamber. This system allows for better control over the air-fuel ratio, reduces backfiring hazard and principally allows higher power density due to high volumetric efficiency. Injection timing can be selected early, so that the fuel is injected during the intake stroke or earlier in the compression stroke (low-pressure direct injection (LPDI)), but also late, that the injection takes place late in the compression stroke (high-pressure direct injection (HPDI)) with the intake valve closed. There is no clear boundary between the two concepts, and the later the injection event occurs the higher the pressure must be. LPDI results close to a homogeneous mixture composition, while HPDI results in stratified charge composition due to the insufficient time for complete mixture homogenization. However, there can be no back-ignitions or early pre-ignitions with HPDI, as no hydrogen enters the intake tract through the closed intake valve and there is no fuel in the combustion chamber during the early compression phase [4].

The following chapters refer to various investigations on single-cylinder engine (SCE) test benches with a hydrogen injector from Liebherr, which injects at a maximum of 30 bar (LPDI).

2. Liebherr H₂ system layout and test bench layouts of SCE

The usage of hydrogen in comparison to diesel significantly influences the design and functionality of the components, system- and control strategies. As illustrated in Fig. 1 the actuators demand high magnetic forces due to the high cross section necessary to ensure the hydrogen flow and limit the pressure drop through the system. The gas-metering valve (GMV) and injector used in Liebherr H₂ system are directly actuated valves.



	Diesel System	Hydrogen System
		
Material	Martensitic & Bainitic Steels high pressure resistance, low sulfur, high purity class, high strength	Austenitic Steels resistance against hydrogen embrittlement weldable, low carbon content
Sealing	Metal to Metal + DLC coating, +cone seat	Elastomer to Metal + flat seat
Guidance	Metal to Metal + Fuel/Oil lubrication + DLC coating	PTFE to Metal + Dry friction + DLC coating
Fuel density & heat value	Small Cross Section hydraulic actuated valve (servo)	High Cross Section → High Power Magnet direct actuated valve
Solenoid	Wet operating in oil	Dry hermetical separated from oil

Figure 1: Comparison between diesel and hydrogen injection system

The system tightness requires the usage of specific material such as elastomer leading to potential sensitivity in terms of control of low quantity, part to part and ageing. This requires the development of specific control structures and strategies. First, this Liebherr hydrogen injection system will be explained in more detail and afterwards excerpts of the test bench results will be highlighted.

2.1. Liebherr H₂ fuel injection system

The H₂ system guarantees a precise delivery of hydrogen to the engine within a specified period, typically related to the intake valve opening, and at a given pressure. Pressurized H₂ is stored in a tank with a maximum pressure of 700 bar. Prior to entering the Liebherr H₂ system, a coalescing filter eliminates any potential liquid residuals like water and the pressure is reduced to an acceptable level via a mechanical pressure regulator.

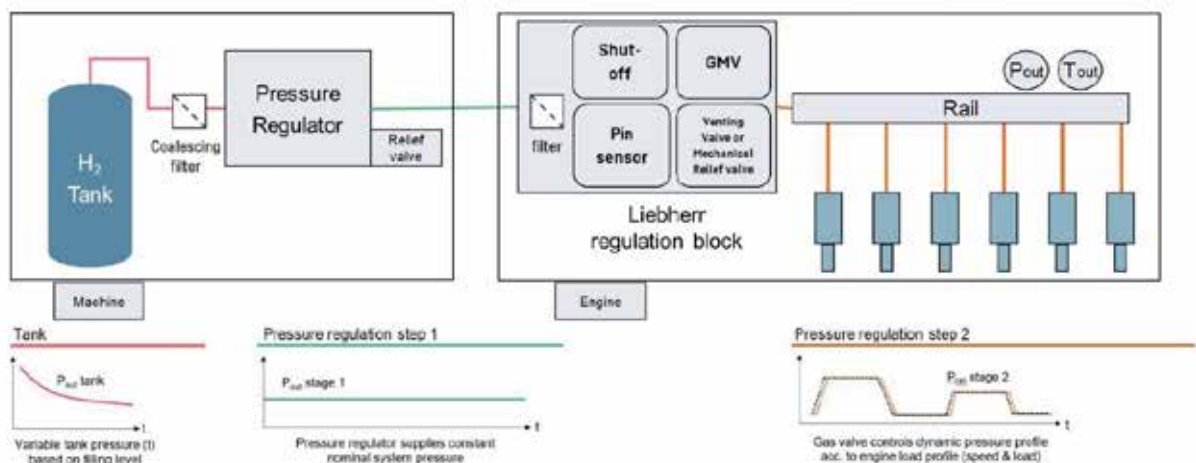


Figure 2: H₂ system schematic view – machine and engine related part

The Liebherr system is easy to adapt for engine integration and can be conveniently packaged. Its modular design offers the advantage of requiring minimal adjustments to be mounted in any kind of customer engine [4]. It consists of the following individual components:

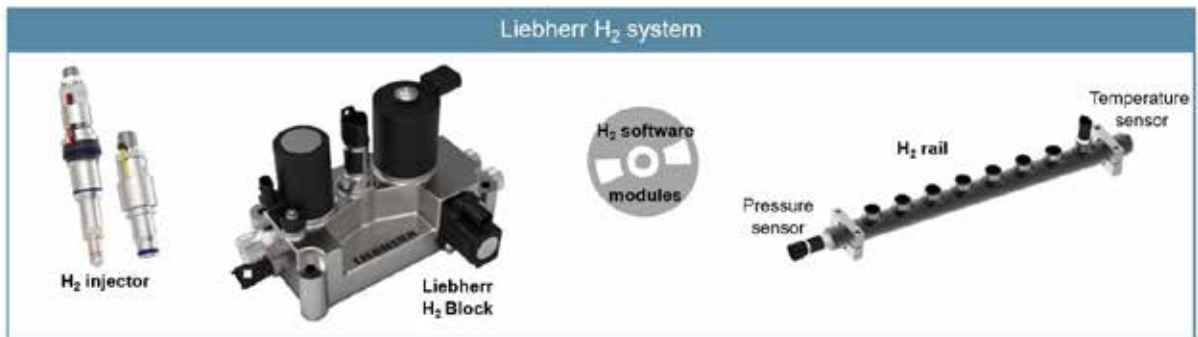


Figure 3: Individual components of Liebherr's hydrogen injection system

The regulator block ensures the system pressure control and safety functionality. It includes a proportional valve, so called gas-metering valve (GMV), which allows the control of flow entering in the system and consequently the regulation of the fuel pressure from atmospheric to max pressure. The pressure upstream the GMV is also measured in the block so that the pressure control can be fine-tuned. There are two naturally closed valves at the inlet and outlet of the block, which allow the filling line to be closed and the remaining hydrogen to be removed from the system when the engine is stopped. Specific control sequences are defined to ensure a safe engine start and engine stop and to monitor the system and component functionality.

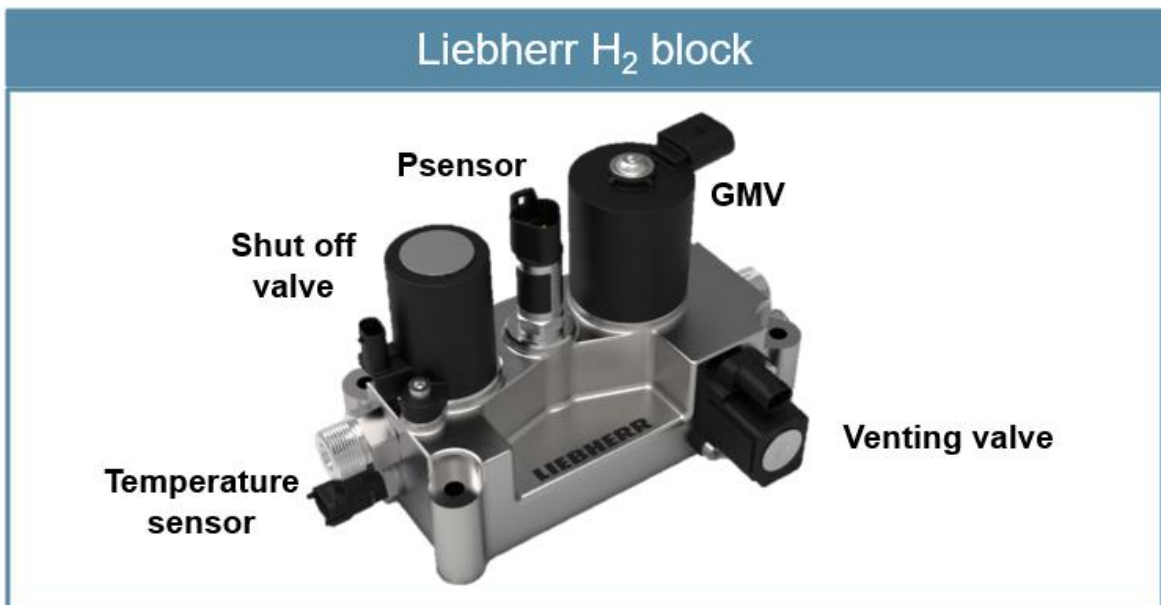


Figure 4: Individual components on Liebherr's hydrogen regulation block

Like most hydrogen (and other gas) injector concepts, the Liebherr hydrogen low-pressure direct injector (product specification LDI) is directly actuated and is designed to meet the necessary flow rate requirements of heavy-duty engines. The outer dimensions of the LDI are close to those of corresponding diesel injectors, particularly regarding the critical maximum outer diameter. Maintaining the existing packaging dimensions is advantageous in the case of a central injector position and certainly, the maximum injector dimensions are limited even in the case of a lateral injector position. Over the last few months, various combustion tests have been conducted on single-cylinder engines and on customer engines using the LDI, which represented different engine configurations and provided a lot of knowledge for the next development activities. The engine configurations on which the knowledge is based are presented below.

2.2. Test bench layouts of SCE

A single-cylinder engine (SCE) test is a method of evaluating the performance, fuel consumption, emissions, and other parameters of an internal combustion engine. It involves isolating a single cylinder from a multi-cylinder engine and testing it under various conditions. The advantages are:

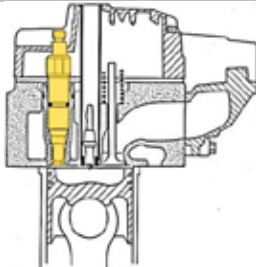
- It is more cost-effective and easier than an examination of the entire engine, as fewer components and measuring devices are required.
- It allows a more precise analysis of cylinder dynamics, combustion processes and heat transfer, as the interference of the other cylinders is eliminated.
- It allows a faster and more flexible modification of the engine hardware, such as compression ratio, injection components, allows higher degree of freedom in the charging system behavior or exhaust gas recirculation, without having to rebuild the entire engine.

Whereas the disadvantages are:

- It cannot map the interactions between the cylinders and the overall system, such as vibrations, gas exchange losses or thermal stress on the engine.
- It cannot mimic the real operating behavior of the engine, such as transient operation, or the effect of operational conditions.
- It cannot measure relevant tailpipe emissions, such as particulate matter or nitrogen oxides, as these depend on the exhaust gas after treatment, which is missing in a single-cylinder engine.

The installation situation of the injection system is influenced by the engine design, with the cylinder head design and possible injection position being particularly relevant to combustion behavior. For any injector position several operating characteristics of the injection system and calibration parameters influence the combustion. These factors must be balanced to achieve optimum performance, low fuel consumption and low pollutant emissions. In the results considered here, existing SCEs were converted and the Liebherr LDI was installed without analyzing the interaction between fuel spray and air flow, namely the mixture preparation. Thus, there was no optimization between injector and engine to achieve the best possible engine results. Initially, the primary objective was to examine the injector, i.e. a part of the Liebherr hydrogen injection system in an environment like that of an application, to determine future development priorities.

Table 2: Overview of H₂-SCEs with Liebherr LDI for this report.

SCE No.	1	2	3
Injector installation (scheme)			
Injector position	inclined	vertical	vertical
Engine model	Platform engine A	Platform engine B	Liebherr D946
Bore- \varnothing [mm]	132	131	130
Stroke [mm]	156	158	150
Compression ratio [-]	10,5:1	9,5:1	13:1
Max. running time for LDI [h]	7	100	32,8

3. Results of SCE

In the following part some results are depicted from SCE testing. In this frame only some insights and not the complete picture can be shown. Depending on the tasks for the given engine and on the possibilities and limitations, different operating points were run and measured. Figure 5 gives an overview of the operating points on the SCE variants.

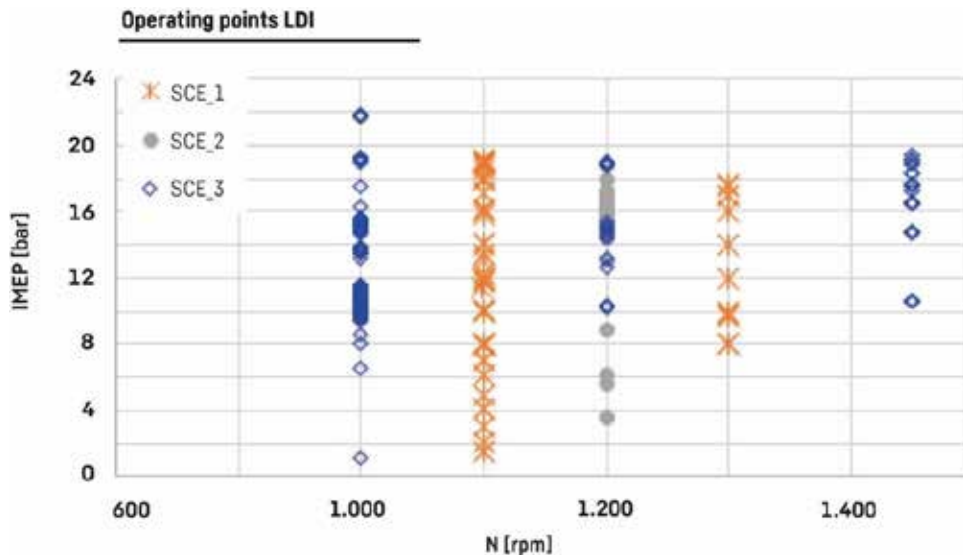


Figure 5: Operating points on the SCE variants

On one of the SCE engines, injector durability was the main aspect. After initially finding a higher load point with acceptable stability and frequency with irregular combustions the engine was run for over 100 hours. Figure 6 summarizes some relevant values of this “endurance” run.

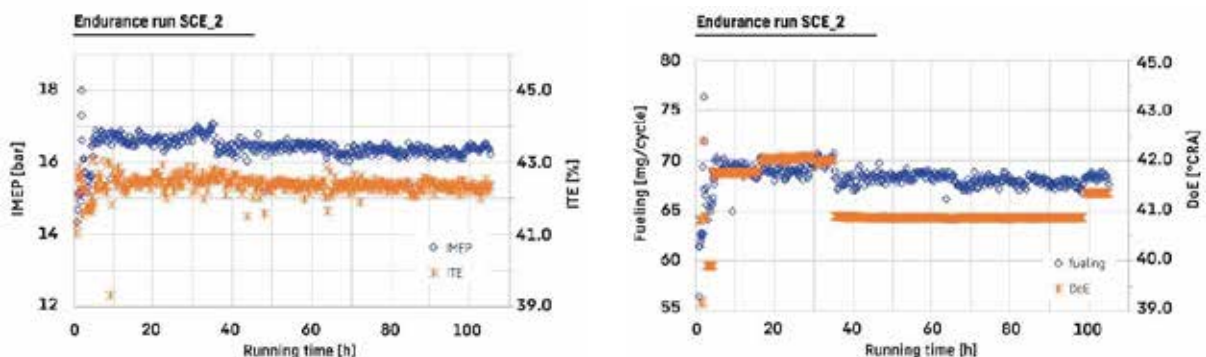


Figure 6: Operating points on the SCE variants

On the other SCE engines simple parameter variations were accomplished to see the behaviour. Figures 7 and 8 clearly show that the achievable results, trade-offs are depending on the engine configurations using the same injector. The engine results using the same injector depend on several factors, like

- injector installation
- injector location and spray direction relative to the intake ports and intake flow, relative to the spark plug
- intake port shape, charge motion and
- calibration parameters, etc.

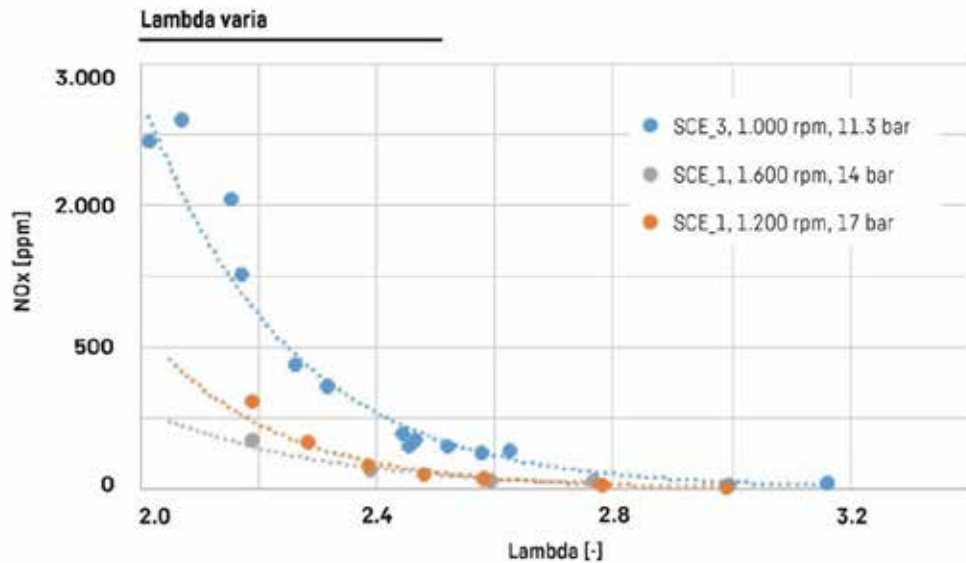


Figure 7: NOx emission over air-fuel ratio

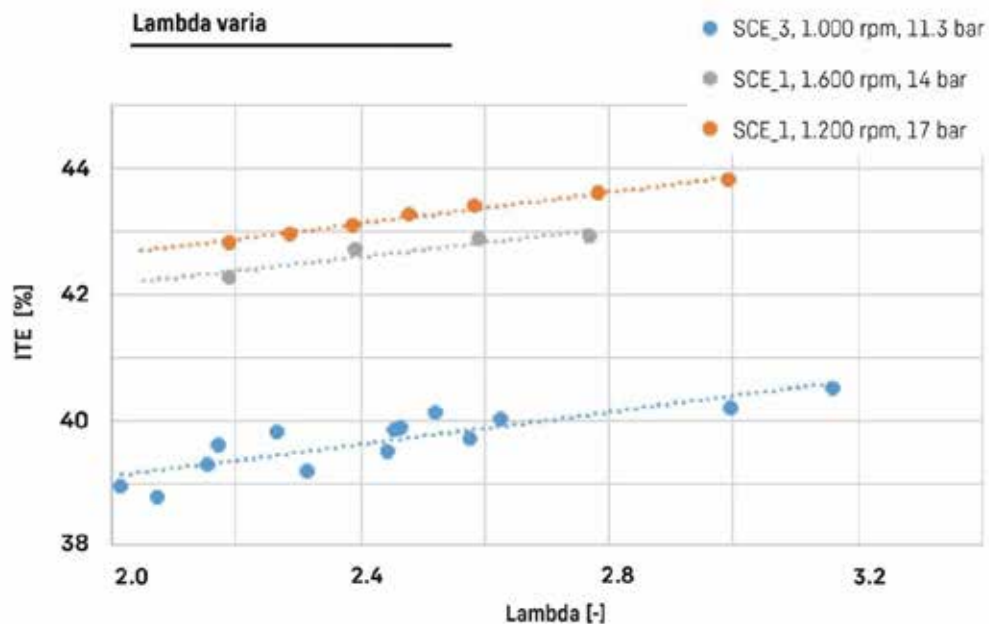


Figure 8: Indicated thermal efficiency over air-fuel ratio

As shown in Figure 7, the NOx emissions measured on the different engines varied widely. Most probable and realistic explanation of this can be more inhomogeneity resulting in local less lean spots with higher local temperatures during combustion for the engine with higher NOx emissions.

Similarly, not only the performance results, but the tendency for irregular combustions depend both on the injector performance and on other factors, like on the engine design, on the engines thermal situation, on the charge motion, on the ignition system capabilities. Thus, the frequency of irregular combustion and high load behaviour was strongly different, depending on the engine. Figures 9-10 show for 2 SCE engine variants the cylinder pressure trace for several cycles. While on one of the SCE variants showed stronger tendencies to pre-ignition and limited the IMEP level, the other engine still showed less severe pre-ignition at higher IMEP levels and with lower frequency. The frequency and strength of the irregular combustions is influenced not only by technical aspects and factual thermodynamic properties, but also by the operating style, how hard vs. cautious the borders were approached.

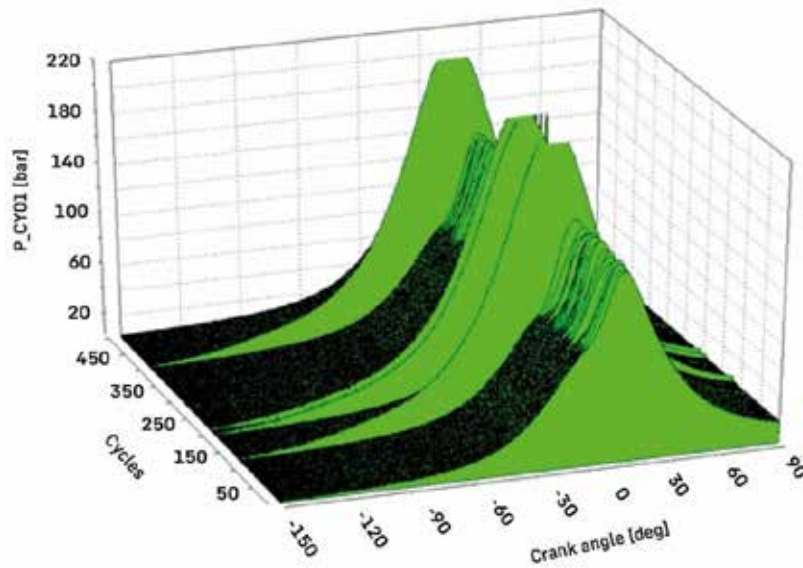


Figure 9: IMEP=19.2 with heavy and more frequent pre-ignition on SCE_1

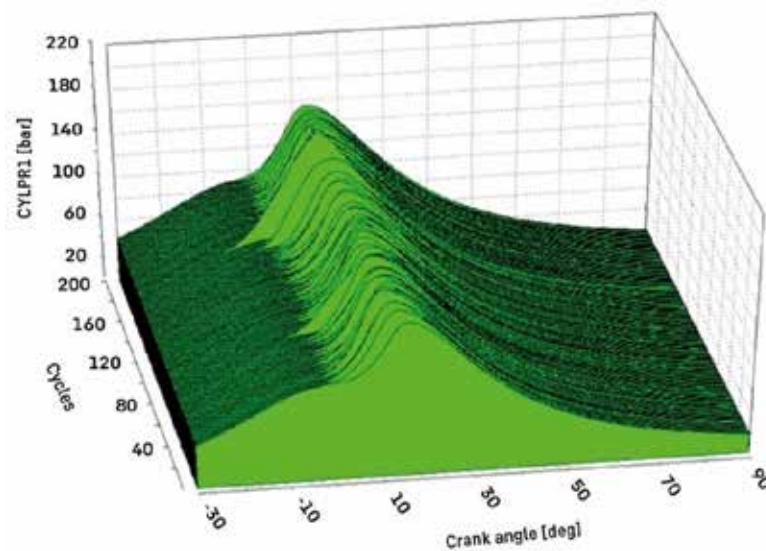


Figure 10: IMEP=21.9bar with mild and rare pre-ignition on SCE_3

Cycle to cycle stability without irregular combustions was particularly good, mostly < 2.5%. Typically, it is more challenging to reach low cycle to cycle variability at lowest engine loads. The baseline for high stability at lower loads gives the injector by its stable behaviour and low variability of the injected mass. Figure 11 shows in a low part load investigation the measured stability by coefficient of variation for IMEP and the corresponding energizing durations of the injector. Figure 12 represents at 3 selected lower load levels the distribution of apparent released heat in 500 cycles and Figure 13 shows the cylinder pressure at the corresponding operating points at 7.0, 4.1 and 1.6bar of IMEP.

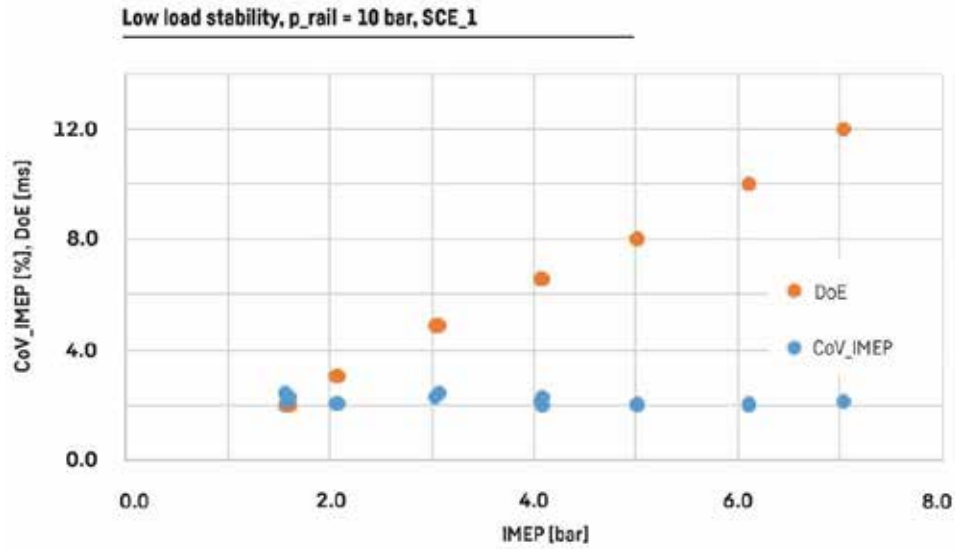


Figure 11: Low load stability and duration of energizing for the injector on SCE_1

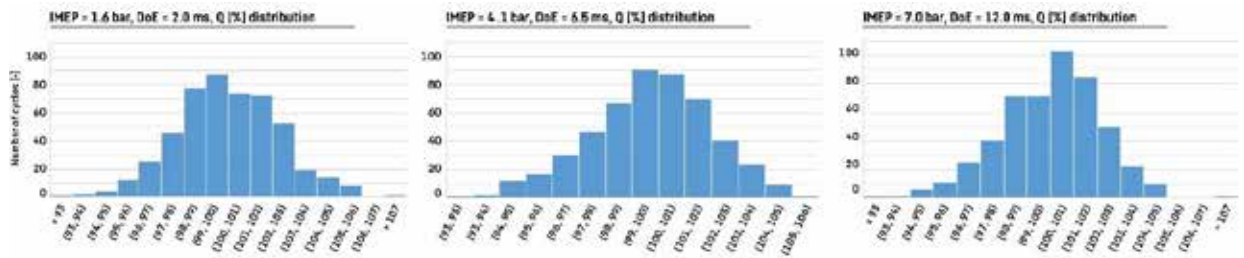
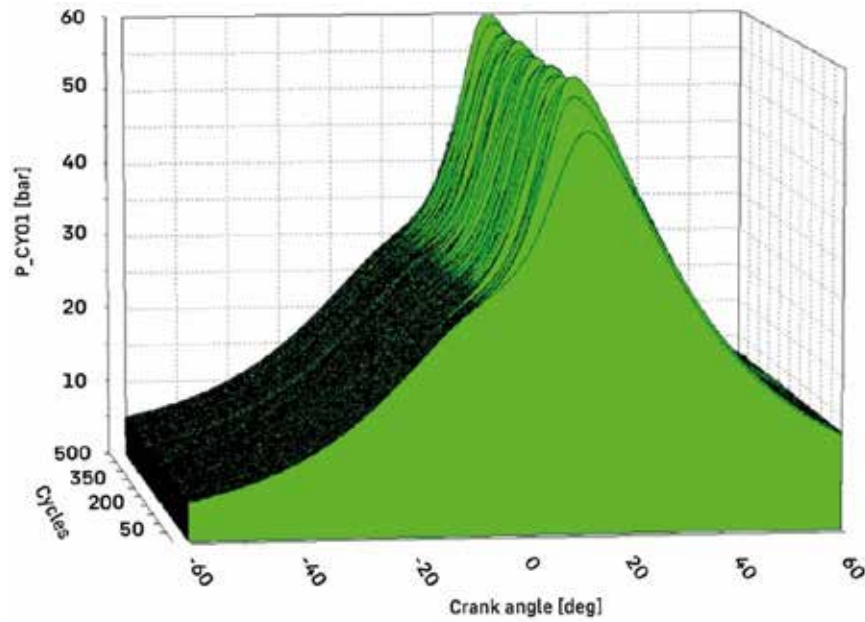


Figure 12: Scatter width and distribution of normalized released heat amount at three load and quantity levels, each for 500 cycles on SCE_1



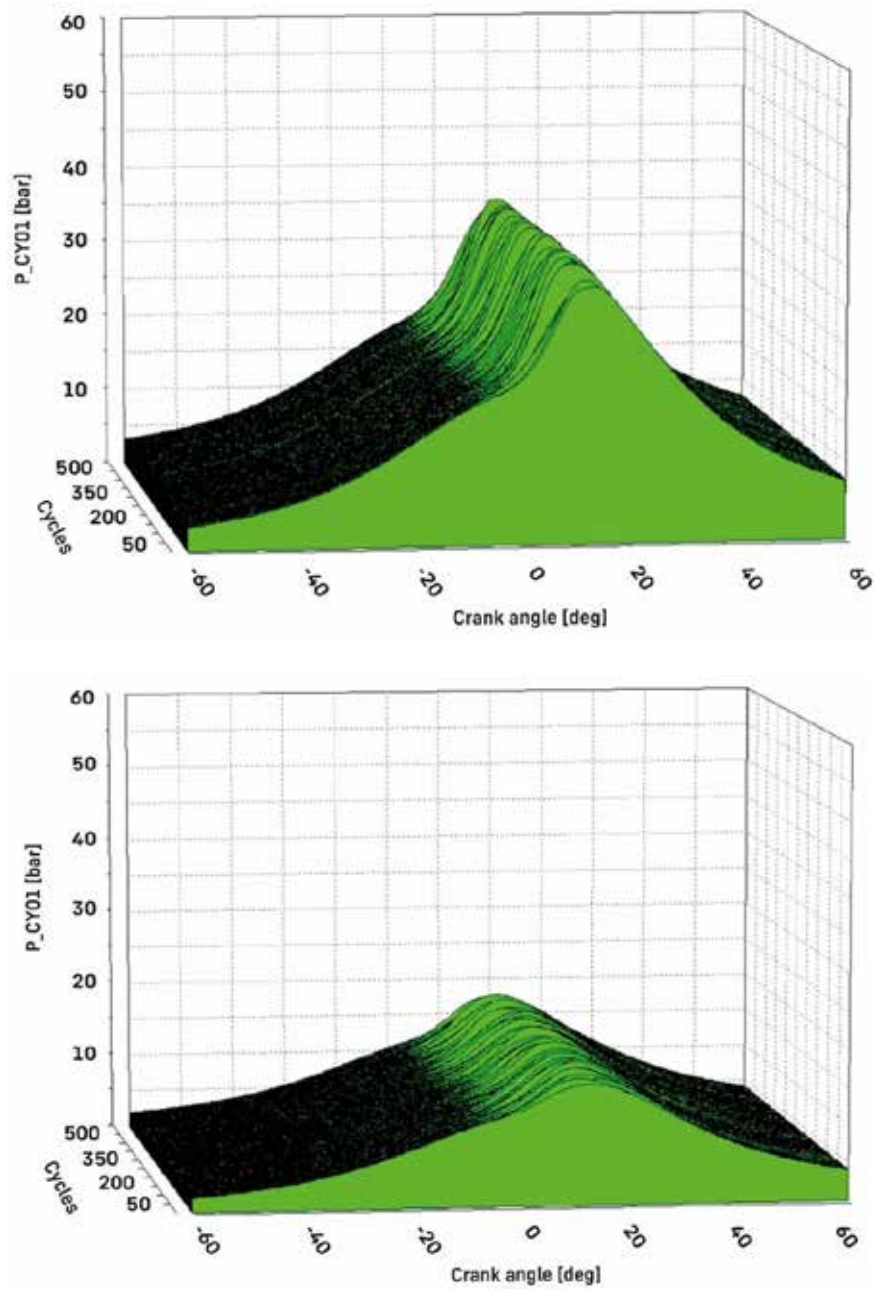


Figure 13: Cylinder pressure traces at the above three load levels on SCE_1

4. Summary and Outlook

SCE test results show a wide range of speed and load achieved with Liebherr LDI. Summarizing some key facts:

- The service life of the injectors depends on several factors. These include the working environment, the thermal as well as mechanical loads caused by the installation position and the operating mode of the engine, plus the frequency and intensity of irregular combustion.
- Achieved engine results depend on the injection system and on several engine design element.
- The Liebherr LDI system allows reaching stable operation in wide speed and load or, in injection terms, in wide energizing duration range, including low load, short injection durations.

Comparing results on the different engine platforms it can be stated that on SCE_3 higher load level and at higher load level more stable combustion but with higher NO_x emission was reached. A generally higher indicated efficiency was measured for SCE_1. Depending on the case, on the application various aspects have different weightings. How far these differences in the results can be contributed to intrinsic features of the individual SCE variants and to the matching of the individual components was not considered in these investigations. For an H₂ ICE product not only the individual components by themselves but their matching, their fit to each other, their interaction must be optimised (first injector + charge air motion + spark plug).

All these results were reached without EGR or without water injection. Both offer the possibility of reducing the tendency to irregular combustions thus for load increase. On the other hand, both, and especially water injection, presented another challenge: the increased corrosion load on the injector. However, the investigations carried out so far have provided further insights for the future development work of the LDI. To install the product in different cylinder heads, it is necessary to reduce the outer contour to obtain a more compact design. During these geometrical adjustments, a minimum dead volume is also achieved between the combustion chamber and the fuel outlet of the injector. The main platform of our current development for hydrogen injection is the port fuel injection system and the associated injector called LPI. The basic design goal is to ensure a modular platform so that findings, such as corrosion resistant and hydrogen compatible materials, wear prevention measures due to dry friction or developed assembly processes can be transferred to the LDI platform to maximise the use of common parts. However, more specific problems due to direct injection, such as sealing against hot combustion gases, the effects of the installation situation on thermal management (cooling and/or heating) and lean angle, as well as the effects of engine geometry, such as the compression ratio, are being further investigated and analysed and are incorporated directly into Liebherr's development work.

For this reason, Liebherr is planning further investigations with the LDI in parallel to the development of the Liebherr hydrogen engine with its own port fuel injection system. On the one hand, the SCE investigations of number 3 have not yet been completed (planned end of Q2/2024), and on the other hand, further investigations are pending on another SCE (planned start Q2/2024), which is based on a different engine platform (thus SCE number 4). In addition, we would like to commission another test campaign on the SCE 1 with an already optimised LDI during this year.

References

- [1] Ho Lung Yip et al. (2019/11/19): A Review of Hydrogen Direct Injection for Internal Combustion Engines: Towards Carbon-Free Combustion, [online] [Applied Sciences | Free Full-Text | A Review of Hydrogen Direct Injection for Internal Combustion Engines: Towards Carbon-Free Combustion \(mdpi.com\)](#) [accessed on Feb. 1, 2024]
- [2] Stefano Beccari et al. (2023/03/01): Analysis of the Combustion Process in a Hydrogen-Fueled CFR Engine, [online] [Energies | Free Full-Text | Analysis of the Combustion Process in a Hydrogen-Fueled CFR Engine \(mdpi.com\)](#) [accessed on Feb. 1, 2024]
- [3] Pirelli & C. S.p.A.: HYDROGEN AS A FUEL: THE PROS AND CONS, [online] [Hydrogen as a fuel: the pros and cons | Pirelli](#) [accessed on Feb. 1, 2024].
- [4] Helmut Eichseder et al.: Wasserstoff in der Fahrzeugtechnik – Erzeugung, Speicherung, Anwendung. 4. Auflage. Springer, Wiesbaden 2018, ISBN 978-3-658-20446-4.
- [5] Liebherr press release (2021/10/14): MAHLE Powertrain collaborates with Liebherr to co-develop active pre-chamber technology for heavy-duty hydrogen-fueled engines, [online] [MAHLE Powertrain collaborates with Liebherr to co-develop active pre-chamber technology for heavy-duty hydrogen-fueled engines | Liebherr](#) [accessed on Feb. 1, 2024].
- [6] Richard Pirkl et al. (2022) Liebherr's approach to hydrogen fuel injection systems. 17th International MTZ Conference on Heavy-Duty Engines, Donaueschingen.

New Mixture Formation Processes in H₂ Engines

Neue Aspekte zur Gemischaufbereitung bei direkteinspritzenden Wasserstoffverbrennungsmotoren

Dr.-Ing. Olaf Weber*, **Dipl.-Ing. Jan Leberwurst**, **Dr. rer. nat. Jochen Broz**, **Dipl.-Ing. Sebastian Sulzer**, **Dr. rer. nat. Oliver Hahn**

Schaeffler Technologies AG & Co. KG, Herzogenaurach, Germany

Abstract

First hydrogen combustion engines will go into production with port-fuel injection, based on Diesel engine hardware. It is already clear that direct injection concepts will represent the second generation of mixture formation systems. Challenges like injection nozzle design and mixture formation for highest levels of homogeneity are already well known. Market participants are improving these kind of product properties. The presentation will discuss several opportunities to increase the homogeneity index of direction direct injection concepts with a consequence of lower NO_x and/or higher torque output at the borderline air/fuel/ratio of app. 2.4.

Kurzfassung

Erste Wasserstoffverbrennungsmotoren werden mit einer Saugrohreinspritzung in Serie gehen. Es ist bereits jedoch heute absehbar, dass weitere Verbesserungen sich mit der Gemischbildung bei direkteinspritzenden Wasserstoffmotoren beschäftigen werden. Dabei kommt es auf Druckverhältnisse, Strömungsformen und Gemischgleichverteilungen an.

Diese sind entscheidend für die Stickoxyd Emission. Es ist denkbar, dass bei deutlich weniger heterogenen Gemischen bei gleichem globalen Luftverhältnis wesentlich geringere NO_x-Emissionen entstehen. Das Papier zeigt Möglichkeiten auf, diesem Prozess zu folgen.

1. Introduction

1.1 Regulation

The European Union has recently published an updated road map for CO₂ reduction for commercial vehicles targeting CO₂ neutrality in 2050. Originally, only battery electric vehicles or fuel cell powered vehicles were considered to be zero emission vehicles. The new proposal also considers commercial vehicles, driven by an Internal Combustion Engine, emitting less than 1g of CO₂/t-kilometer, as zero emission vehicles.

The EPA also has proposed an update for the nationwide greenhouse gas regulation on commercial vehicles in 2023. Tailpipe CO₂ emissions from battery electric vehicles, fuel cell electric vehicles and vehicles with engines, fueled with neat hydrogen, are defined to be zero emission vehicles. No CO₂ related testing is required for these vehicles /8/.

* Speaker/Referent

China already has introduced a numerous fleet of hydrogen powered vehicles using fuel cells. It is expected, due to the technology open environment, that internal combustion engines will also be used to decrease the amount of CO₂ emitted by burning green hydrogen.

1.2 Markets

As the regulators step by step allow a high variety of machines converting hydrogen into motion, battery electric vehicles and fuel cells remain in the discussion. In addition, internal combustion engines using hydrogen are gaining share. Remote regions and locations, difficult applications requiring robust, low cost and low risk solutions provoke new approaches with internal combustion engines.

The market seems to be starting on the mid duty and heavy-duty engine side with displacements up to 16 liters. But also light commercial vehicle applications are subject to hydrogen combustion engines as refueling and service are easy compared to the huge advantage being counted as a zero emission vehicle. Even passenger vehicles are not the exception. Numerous manufacturers are testing 4-cylinder passenger car engines and their ability to get converted into hydrogen engines competing with fuel cell powered vehicles.

1.3 Technologies

Hydrogen and its properties regarding combustion initiate some changes in the internal combustion engine [1]. Ignition systems and piston ring packages have to be adjusted to the ignitability and fast combustion characteristics. The blow-by, covering unburnt hydrogen as well as burnt hydrogen in form of water, increases the partial pressure of water vapor in the crankcase significantly. Investigations are ongoing in how far the higher amount of water in the crankcase ventilation and/or lubricating oil causes different design efforts to keep the combustion engine as reliable as before.

The introduction of hydrogen into the engine and its mixture formation is a subject of a huge amount of investigations. As the markets are demanding clean solutions in a short amount of time, engine manufacturers are looking for practical solutions. The port fuel injection of hydrogen might be the first mixture formation system introduced to the marketplace. Replacing the Diesel injector by a spark plug, adjusting the compression ratio by a CNG based piston and applying CNG like injectors into the induction port seems to be realistic to face a soon SOP. Disadvantages like limited torque output and the potential of back firing during the gas exchange process are well known and taken into consideration. The homogeneous mixture between hydrogen and air guarantees NO_x free combustion beyond the air fuel ratio of 2.4.

2. Hydrogen Direct Injection

Hydrogen, directly applied into the intake port causes naturally a higher compressor pumping work. The air and the supplied hydrogen have both to be pushed into the combustion chamber. This leads to higher boost pressures or and smaller amounts of air facing the same air fuel ratio ending up in a lower engine torque. In addition, the high energy level of the hydrogen applied due to a pressure between 20 and 60 bar is not being used at all.

As the hydrogen combustion engine compared i.e. to its brother the Diesel engine is facing an air fuel ratio limit due to the homogeneous combustion avoiding NO_x emission, lean operation will be preferable in the entire engine map. This limits the boost pressure in addition under steady state conditions. Replacing a reliable port fuel injection system by a new direct injection system is therefore necessary to keep the hydrogen engine in a

reasonable torque range. On the other side, also seen in Figure 1, the mixture formation in the combustion chamber might not lead to a perfect homogenization.

We do then need a higher average air fuel ratio to avoid the creation of NO_x emission in the engine map leading again to a lower available torque. The capability of a direct injection system in terms of homogenization is therefore crucial for the performance of a hydrogen combustion engine.

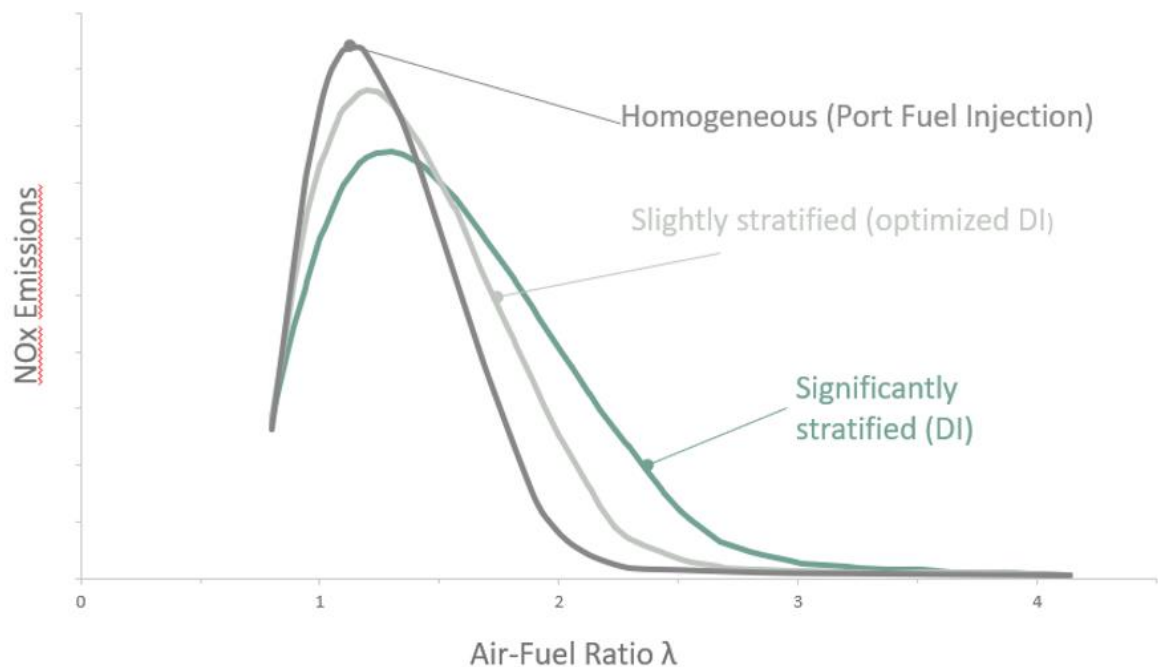


Fig. 1. Lean Running Combustion Engines targeting homogenous Mixture Formation /9,10/

Published Solutions

Based on these challenges a lot of investigations have been already done. The usage of the Schlieren method as a visualization tool for hydrogen flow is also understood as a tool to calibrate and understand CFD based methods. Figure 2 shows some investigation examples/3,4/. The injector nozzle is applied to different vertical positions on the cylinder axis. Different positions cause different kind of flow patterns. In some cases like on the left hand side, with a nozzle already penetrating the combustion chamber, the flow pattern is flat and horizontal, towards the right hand side, where the position of the nozzle is more in a recess, the flow pattern goes straight in parallel to the cylinder axis towards the surface of the piston. The back pressure in the combustion chamber is also influencing the flow pattern but seems to be a minor factor compared to the injector position.

To create a more directed flow /5,11/ into the combustion chamber, flow caps, spray caps or deflector caps are being used. Those caps take the out of nozzle flow and direct it into a certain position in the combustion chamber, Figure 3. A lot of investigations have been made to determine the best orientation and position of those caps with different hole configurations. Tremendous improvements can be made by varying these positions for certain operating points. Figure 4 shows the reliable CFD simulation when compared with the Schlieren method using different kinds of caps for different purpose. However, the mixture formation process is still uncomplete and the design parameters of the injection equipment is not totally understood.

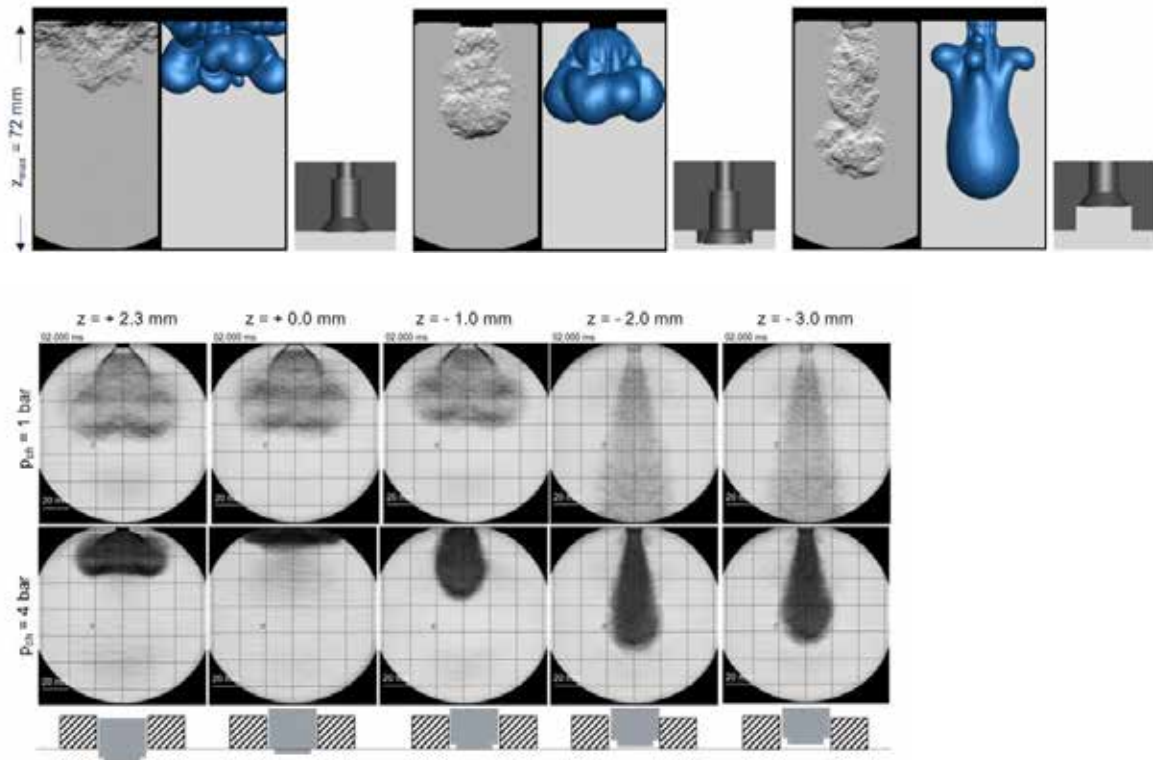


Fig. 2. Schlieren and CFD Images for Injector Mounting Positions at different Backpressures /4,11/

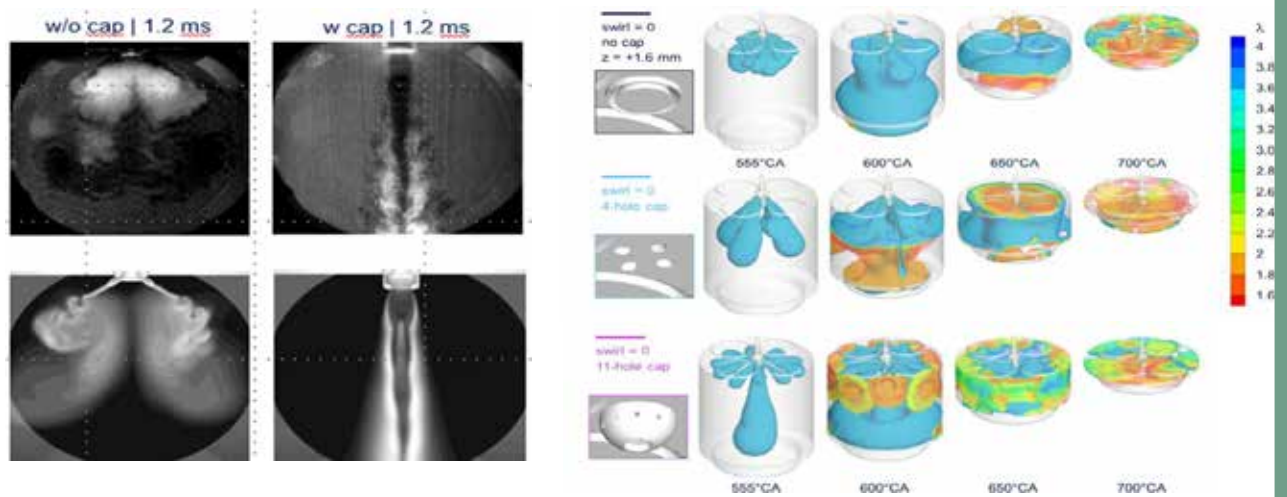


Fig. 3. Comparison of Turbulence Distribution with and without Spray Caps /5,11/

Flush mounted injectors can also generate the so-called Coandă effect /5,11/. Other effects lead to a close to the surface flow which inhibits the penetration of the combustion chamber by the H₂ spray. The majority of the investigations try to avoid this Coandă effect as it seems to be a more unpredictable phenomena disturbing any directed development of a new product. The occurring Coandă flow patterns are understood as they are accepted.

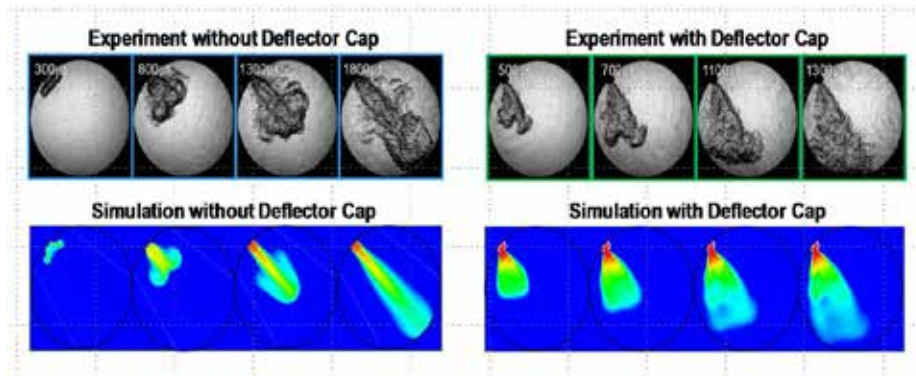


Fig. 4. Correlation between Schlieren Spray Images and simulation Results /5/

Macroscopic effects for H_2 LP-DI mixture formation

1. H_2 spray shapes vary with nozzle mounting position. Flush mounted nozzles can lead to Coandă effect with wide and low penetrating spray.
2. Spray caps show potential for improved air entrainment (cylindrical spray \rightarrow conical spray) and high flexibility in spatial fuel distribution.
3. Significant swirl motion applied to a non-homogeneous mixture with H_2 fluid zones leads to agglomeration of H_2 in center regions (low density and inertia of H_2).

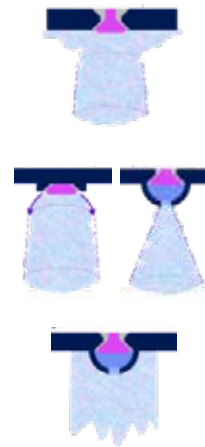


Fig. 5. Coandă Effect and how to avoid it /5/

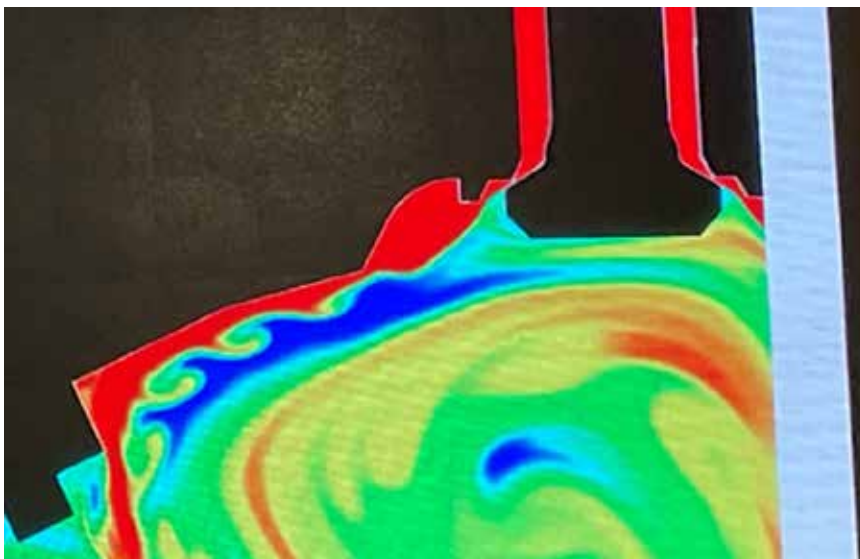


Fig. 6. Coandă Effect according to /7/ on overexpanding nozzles: Hydrogen (red) flows on the cylinder head surface reaching the spark plug on the left hand side

But the Coandă effect is also used to create stratified mixture formation processes like in /7/, Figure 6, due to the pressure conditions around an overexpanded flow caused by a supersonic nozzle. The Coandă effect ensures a strict stratified mixture formation process where the hydrogen is flowing on top of the combustion chamber surface straight to the spark plug and ensures a proper ignition and later on stratified combustion leading to overall low NO_x and reliable combustion /7/.

As a summary, the position of an injector and the upcoming Coandă effect are influencing the flow patterns significantly. A viable solution for an injector should comprise these two parameters.

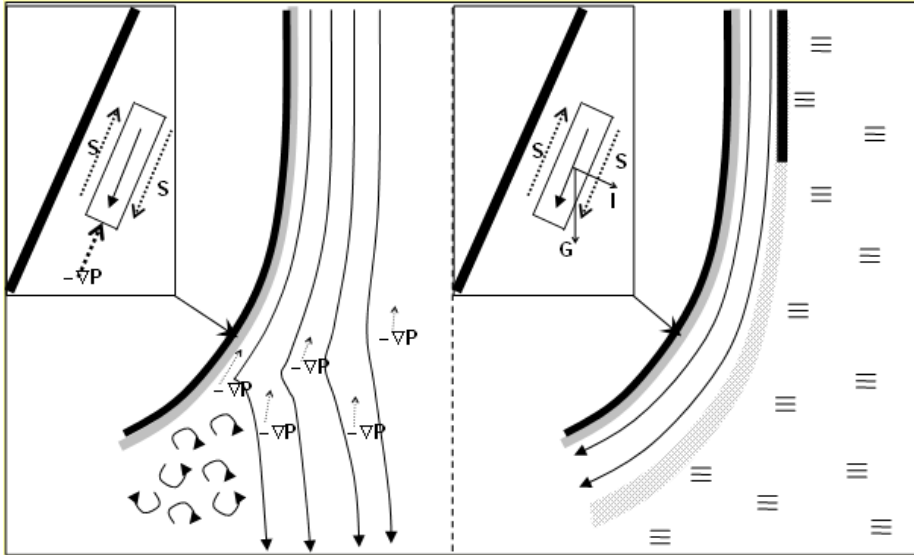


Fig. 7. Coandă Effect according to /6/

A new Approach to improve the Mixture Formation Process

Intensive development work led to a variable supersonic nozzle which controls the amount of hydrogen and the flow pattern at the same time. In addition, the pressure ratio across the injector is also decisive to direct the H_2 flow into the combustion chamber, Figure 8.

On top of Figure 8 the nozzle is shown with two different operation conditions. The left-hand side shows the jet flow where all the hydrogen flows parallel to the cylinder axis into the depth of the cylinder. On the right hand-side we can see the hydrogen flowing as a Coandă. The hydrogen is flowing parallel to the surface of the flat cylinder head. Figure 8 is showing two different flow patterns at the same time although the nozzle will of course create a rotational symmetrical flow pattern. The lower part of Figure 8 explains the conditions leading to the different flow patterns: the H_2 pressure in the injector is plotted against the cylinder pressure. The drawn angle bisector divides the figure into two main parts: on the top left side we have an ordinary jet flow into the cylinder. On the righthand side of the angle bisector the flow is just reversed, hydrogen flow from the cylinder into the injector occurs.

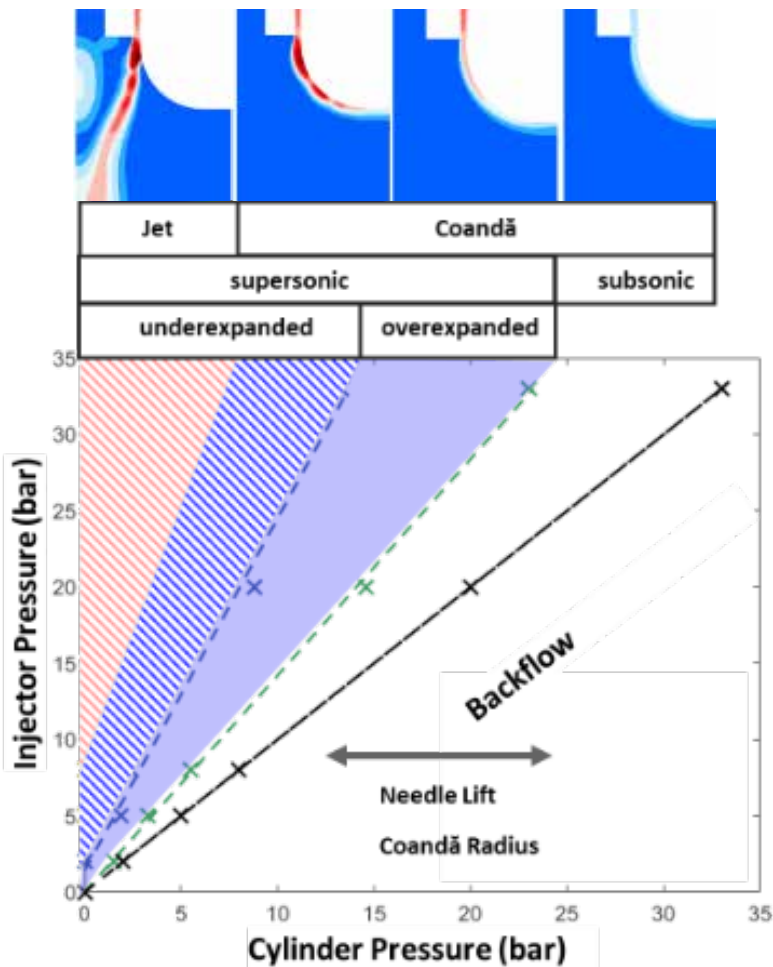


Fig. 8: Schaeffler Coandă Control of a supersonic injector

The dividing line between Coandă and jet flow is located on the very lefthand side. The Coandă and the jet are both flowing under supersonic, underexpanded conditions. The hydrogen, arriving at the nozzle exit, can still expand into the gaseous environment in the combustion chamber beyond the pressure at the nozzle exit.

The area of the over expanded Coandă flow is reached when the pressure in the combustion chamber reaches the pressure at the nozzle exit. The Coandă flow remains, even when the hydrogen flow changes to subsonic conditions.

The switching between the Coandă flow and the jet flow can now be controlled by all these parameters plotted in Figure 8. Increasing combustion chamber pressures will create a Coandă flow and decreasing combustion chamber pressures at one point of time a jet flow. The reverse effect can be seen for example at constant combustion chamber pressure by raising the injector pressure. This will cause a change from Coandă to jet flow. The method to combine all these engine parameters like cylinder pressure, injector pressure and needle lift leads to a wide field of opportunities to control the flow into the combustion chamber.

The Coandă radius of the injector is constant and can be seen with the same rigor as the design, orientation and position of a spray cap. The injector needle lift can be seen as the above-mentioned vertical position of the injector, flush or in recession mounted. The before mentioned in engine operation fixed parameters of spray caps and injector position and orientation can now be controlled by the new injector.

An example, how jet flow and Coandă flow can fill up a combustion chamber with hydrogen is plotted in Figure 9. The Coandă flow towards the end of compression fills up the “lean” combustion chamber area.

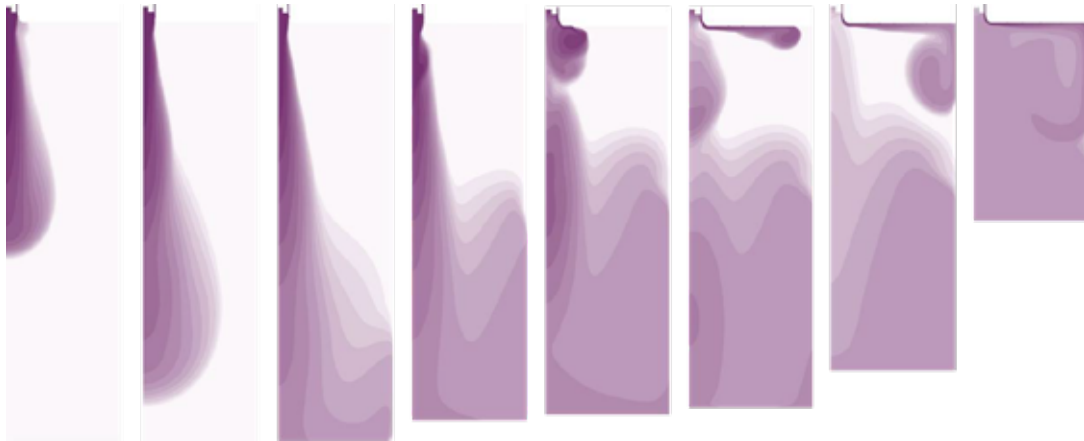


Fig. 9: Jet and Coandă flow share versus crank angle during the compression stroke. The compressing piston cuts the lengths of the snapshots from the bottom.

This concept can now be applied to a combustion engine, at first with a simulation tool. We applied tools like Fluent and Converge depending on the task and its complexity. Figure 10 shows the Lambda distribution in a combustion chamber at FTDC. The plots show a cross section of half of a combustion chamber, the piston bowl can be recognized, the central injector is placed on the righthand side of the plots, the cylinder wall is, consequently, located on the lefthand side. Data for the start of injection, SOI, the homogeneity index HI, and the injected mass distribution between jet and Coandă is being varied and caused by the start of injection.

The nine visible flow patterns start with a comparatively early start of injection (638 deg Crank) and end up with a late start of injection (668 deg crank). Parallel to the later SOI, the cylinder pressure is higher at later injection windows. This creates different shares of jet and Coandă, causing very different flows and Lambda distributions. The best HI can be detected using the SOI of 658 deg crank, with a HI of 0,74 and a jet/Coandă mass ratio of 31/69. Later SOIs than 658 deg crank eliminate the jet flow totally, the differences in Lambda distribution are just due to the different time difference between SOI and FTDC.

The calculations were made without any air charge motion induced into the combustion chamber. All kinetic energy (TKE) has been induced by the flow of the hydrogen. These figures just show a very first example of the investigations made. Further steps will be the optimization of the start of injection (SOI) considering the air intake flow and different engine conditions like rail pressure and boost pressure. In addition, combustion simulations will be done to understand the link between mixture formation and related knock sensitivity. It is expected that less inhomogeneous mixtures will reduce NO_x emissions.

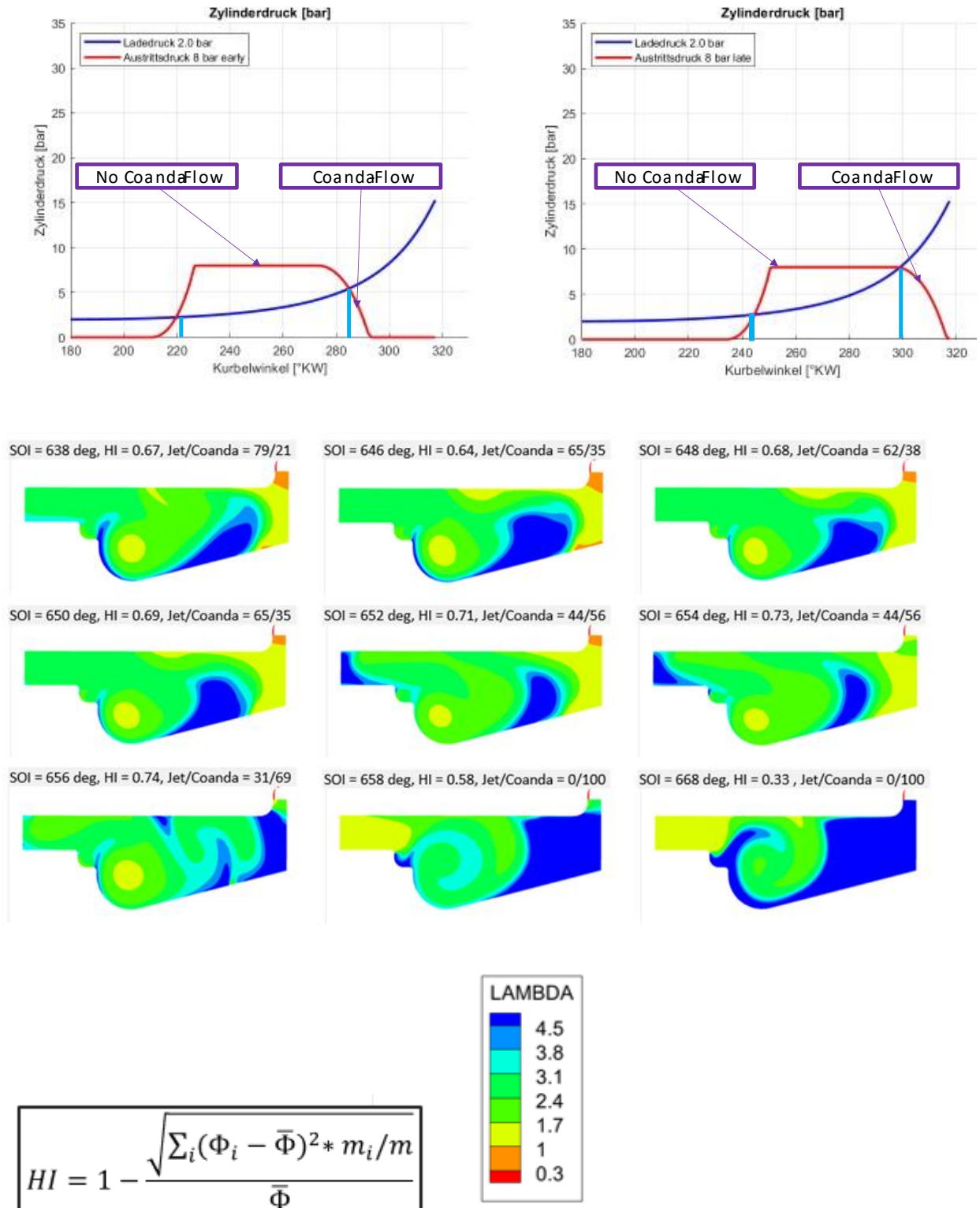


Fig. 10: Mixture Formation influenced by 2 different Injection Timings, upper part. The lower part represents an omega piston left-hand-side cross section of a combustion chamber and the Lambda distribution.

The flow patterns change based on pressure ratios and injector needle lift. These different flow patterns can now be applied by different crank angles during the mixture formation process and it is therefore possible to reach out to extreme regions in the combustion chamber which cannot be reached by rigid elements like flow caps or fixed positions of injectors. This new approach combines variable injector positions and a controlled Coandă effect to improve the mixture formation process.

3. Durability

Due to the missing lubrication, the H₂ injectors are tremendously exposed to very difficult conditions regarding wear, both at the needle guide as well as the needle seat. The issue is even worse compared to natural gas injectors where in some cases residuals of lubricating oil are still existing. Fuel cells require a high purity of hydrogen used to avoid poisoning of the catalytic surfaces. As the combustion engine has to use the same purity of hydrogen by regulation, the challenge for a highly reliable injector is even more difficult.

In the past, Schaeffler has understood a lot of different wear processes under very difficult and different conditions (Figure 11). The result is a set of methods to analyze and understand the wear process faced by different surfaces. In addition, coating recipes with the focus on wear, corrosion, friction as well as the assigned production recipes need to meet the necessary requirements (Figure 12).

The development priority of durable injectors is at least as high as a good mixture formation process under all perceived engine conditions.

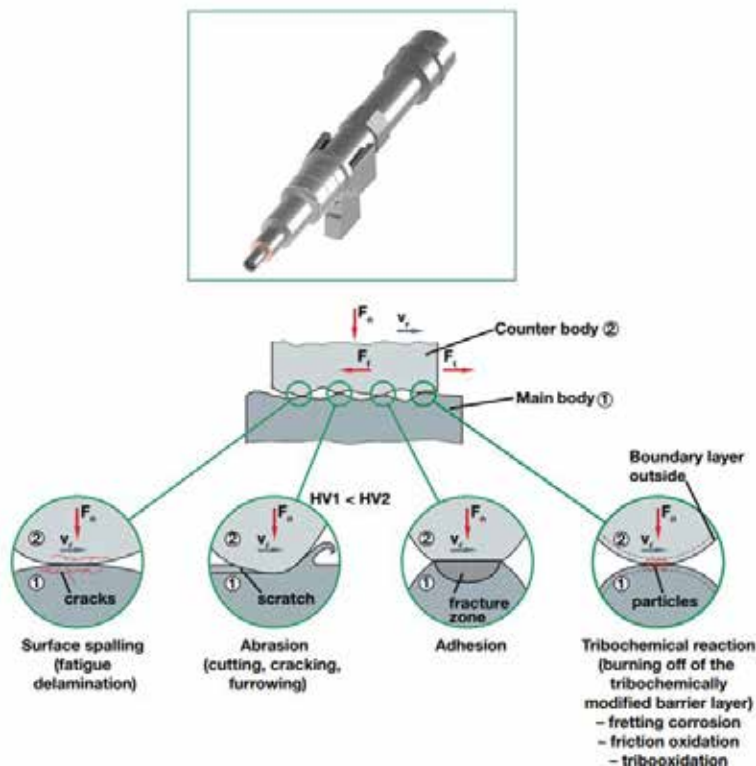


Fig. 11: Structure and mechanisms leading to wear

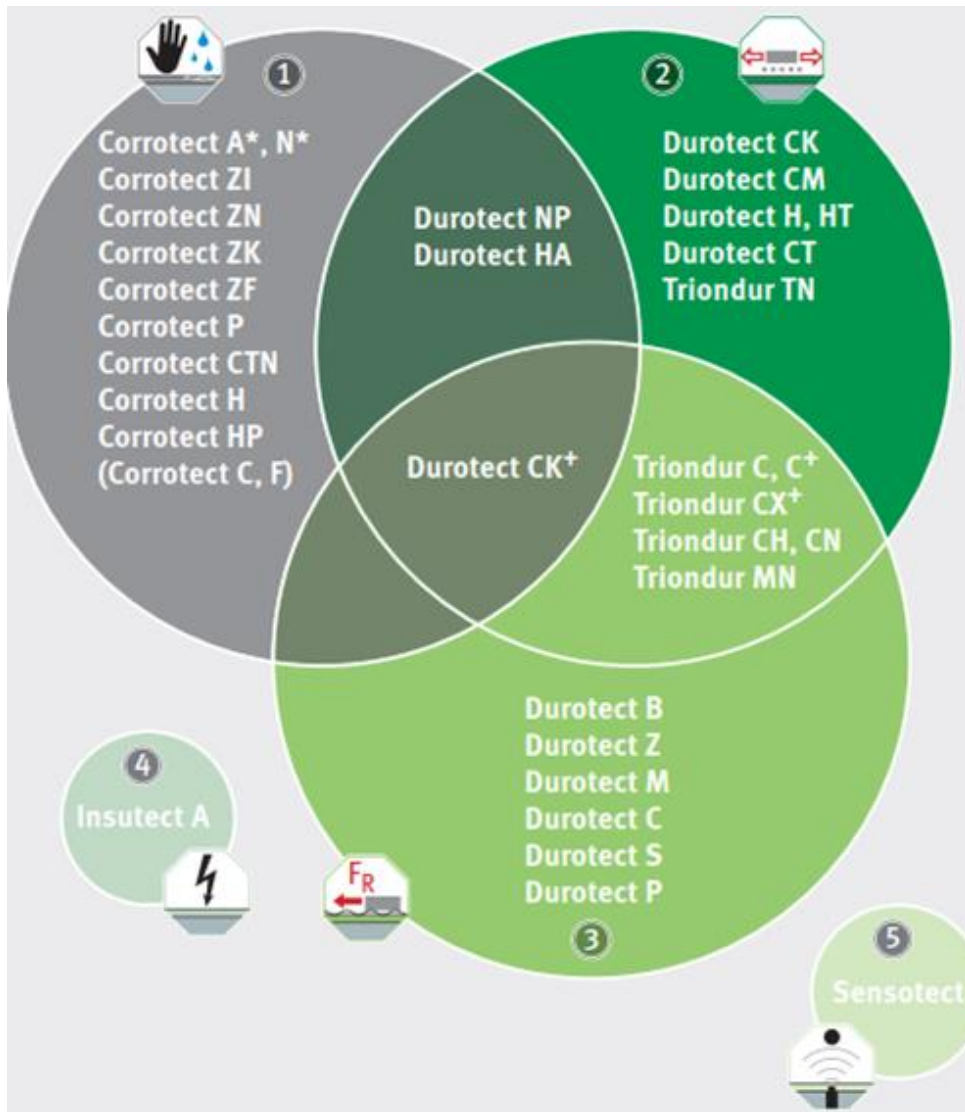


Fig. 12: Excerpt of Schaeffler durability concepts for corrosion, wear, friction and insulation

References

1. Heinz Stutzenberger, Untersuchung des Betriebsverhaltens eines Wasserstoff-Wankelmotors, Dissertation RWTH Aachen, 1983
2. David Lejsek, Philippe Leick, Paul Jochmann, Peter Grabner, Eberhard Schutting: Analysis of Mixture Formation and Combustion in H₂ Engines for Passenger Cars and Light Commercial Vehicles. 9th International Engine Congress, BadenBaden, 2022.
3. Dr.-Ing. Niklas Geiler, Dipl.-Ing. Klaus Moritz Springer, Dipl.-Ing. Thomas Lorenz, M.Sc. Michele Blomberg, M.Sc. Jens Achenbach, Dr.-Ing. Peter Bloch: H₂ engine Hybrid Powertrain for future Light Commercial Vehicles, 10th International Engine Congress, BadenBaden, 2023.
4. David Lejsek, Dimitri Seboldt, Jan Niklas Geiler, Philippe Leick, Michael Frank, Karl Georg Stapf: Mixture formation and Combustion in a Passenger Car engine with Low Pressure H₂ Direct Injection, 19th Symposium "sustainable Mobility, Transport and Power Generation, Graz, September 28-29, 2023
5. Dr. Maximilian Brauer, Lorenz von Römer, Michael Riess, Dr. Jochen Maaß, Anja Fink, Oliver Nett: Hydrogen DI Combustion System Development on a Retrofitted Medium Duty Diesel Engine, 19th Symposium for Sustainable Mobility, Transport and Power Generation, Graz, September 29th, 2023
6. <https://de.wikipedia.org/wiki/Coand%C4%83-Effekt#/media/Datei:CoandaEffect3.png>
7. Hans-Jürgen Berner, The investigation of hydrogen based vehicle propulsion systems at FKFS and IFS, The 7th Shanghai-Stuttgart-Symposium on Automotive and Powertrain Technology, Shanghai, December 2023
8. Anton Arnberger, Martin Wieser, AVL List GmbH, Andre Ferranese, Tupy S.A. Joinville, Paul Christoffette, Peter Grabner, Helmut Eichelseder, TU Graz: Hydrogen Engine with 50% BTE – Benefits of High Pressure Direct Injection – ITNA, September 29th 2023
9. M.Schumacher, P. Renninger, C.Barba, J.Lehmann: Hydrogen Engine – Robust Low Emission Powertrain for Heavy Duty Trucks, Wasserstoffmotorkonferenz 2023, September 12th.
10. Gavin Dober, Guy Hoffmann, Walter Piock, BorgWarner, Luxemburg; Laurent Doradoux, Guillaume Meissonnier, Emmanuel Quali, Borgwarner, France; James Kewley, Christophe Cardon, Simon Coster, Jonathan Wray, BorgWarner, U.K.; Stefan Münz, Sascha Weiske, BorgWarner, Germany: Application of H₂ICE Technology on Commercial Vehicles, 31st Colloquium for sustainable Mobility, Aachen, October 2022
11. Dr. Maximilian Brauer, Dr. Jochen Maaß, Lorenz von Römer, Michael Riess, Marc Sens, Wolfgang Tschiggfrei, all Ingenieursgesellschaft Auto und Verkehr (IAV) GmbH, Berlin, Germany; Anja Fink, Oliver Nett, Technische Universität Berlin, Germany; Optimization of the mixture formation in DI hydrogen combustion engines by modified injector nozzle design: 31st Aachen Colloquium Sustainable Mobility 2022, Aachen, October 10th to 12th, 2022, Paper No. 62 ISBN 976-3 -00-072524-1

Challenges for the transition to renewable fuels from component perspective with focus on MPI valves for Large Engines

Herausforderungen für den Umstieg auf erneuerbare Energieträger aus Komponentensicht mit Fokus auf MPI-Ventile für das LE-Motoren Segment

C. Hengstberger*, Dr. P. Christiner, M. Köhler, M. Schmitzberger, Dr. J. Stein

Robert Bosch AG, Hallein

Abstract

During the last decades, gas engines have gained additional share on the global industrial engine market. As the demand for efficient and robust engine solutions is growing, gas engines have become increasingly important to provide reliable solutions for decentral power supply as well as for mobile applications in the marine, commercial and industrial market segment. The recent trend towards zero-impact fuels poses challenges for the development of gas engines.

Different factors must be considered during the development of ported fuel injection valves. Customer specifications as well as legal requirements and economical goals pose a challenge during the development process. In addition, due to the increasing demand for usage of non-carbon fuels additional key requirements must be taken in consideration in order to achieve robust components, that are capable to meet the market requirements.

In this paper the authors present aspects of an integrated approach for the optimization of ported fuel injection valves for large bore engines to meet those requirements with special focus given on current challenges from the market and the achieved benefits for engine operation.

Special focus is given on the experience with alternative fuels and the resulting challenges during development. Used testing facilities and derived results are explained and an outlook of upcoming challenges is given.

Some of the challenges occurring during operation of MPI valves are important to be considered early during development and validation process of the valve concept but are difficult to be covered by pure component testing. Changing gas qualities and composition (Methane, Hydrogen, Ammonia), different gas-accompanying materials as well as abrasive particles lead to impairment and abrasive wear, difficult to consider in early development phases. Those challenges and measures to achieve the development targets are outlined in the paper.

Kurzfassung

Während der vergangenen Jahrzehnte konnte der Gasmotor seinen Anteil im globalen Industriemotorensegment deutlich steigern. Der ständig steigende Bedarf an robusten und effizienten Motorkonzepten für die dezentrale Energieversorgung und mobile Anwendungen

* Speaker/Referent

führt zu einer zunehmenden Bedeutung von Gasmotoren im Marinen Bereich ebenso wie im kommerziellen und industriellen Anwendungsbereich. Zusätzlich führt der klare Markt-Trend zu CO₂ neutralen oder CO₂ freien Kraftstoffen zu weiteren Herausforderungen für die Entwicklung von Gasmotoren.

Während der Entwicklungsphase von Gaseinblaseventilen müssen verschiedene Einflussfaktoren berücksichtigt werden. Kundenanforderungen, gesetzliche Anforderungen und wirtschaftliche Zielsetzungen stellen eine Herausforderung dar. Darüber hinaus führt der Wandel im Kraftstoff-Mix zu CO₂ freien Kraftstoffen zu weiteren Schlüssel Anforderungen, die während der Entwicklungsphase des Produkts Eingang finden müssen, um das Ziel eines robusten Produkts mit guten Marktaussichten erreichen zu können.

Im vorliegenden Paper zeigen die Autoren wie durch die Anwendung eines integrierten Entwicklungsprozesses für die Optimierung von PFI-Ventilen für großmotorische Anwendung die unterschiedlichen Anforderungen erreicht werden können. Dabei wird insbesondere auf die aktuellen Anforderungen vom Markt und die erreichten Produktvorteile für den motorischen Betrieb eingegangen. Besonderes Augenmerk wird dabei auf Erfahrungen mit alternativen Kraftstoffen wie Wasserstoff und Ammoniak gelegt. Besondere Herausforderungen in der Entwicklung werden ebenso vorgestellt wie verwendete Prüf-Infrastruktur zur Erreichung der Entwicklungsziele. Die erreichten Ergebnisse werden im Detail beschrieben und ein Ausblick auf weitere Entwicklungsschritte und den damit verbunden Herausforderungen wird beschrieben.

Einige der jüngsten Herausforderungen für den Betrieb von MPI-Ventilen sollten schon in einer frühen Entwicklungs- und Validierungsphase Berücksichtigung finden. Ansätze für eine Berücksichtigung zu Erreichung der Entwicklungsziele werden im Paper beschrieben.

1. Introduction

Robert Bosch is supporting various technologies to fulfill the climate goals of the Paris Agreement. All these technologies aim for reduced CO₂ and GHG emissions; battery-electric vehicles, PEM fuel cells for on-highway vehicles, sulfur-oxide fuel cells for electricity production and the usage of climate-friendly fuels like hydrogen, PtX and bio-fuels in combustion engines [1].

With an initial focus on the potential of the fuels, a first option is to introduce bio-fuels or e-fuels which can replace the fossil-based diesel at least partially (drop-in). For backward-compatibility and a fast implementation, conformity with the diesel specifications is mandatory.

Alternative fuels represent another option that requires new engine and FIE technologies and an appropriate infrastructure including production capacities. The alternative fuels with the biggest potential are methane (CH₄), hydrogen (H₂), methanol (CH₃OH) and ammonia (NH₃). As regards certain combustion and emission challenges, the use of ammonia requires further analysis [2,3]. Natural gas (NG) containing methane as its main component has already been introduced successfully in the market; hence the use of methane as a fuel is comparable to the burning of natural gas (e.g. LNG).

The four sub-segments (marine, genset, railways, mining) and the related use cases can be clustered specifically according to the typical duration of operation (mileage/utilization time) and the infrastructure (fuel supply/storage), see Figure 1.

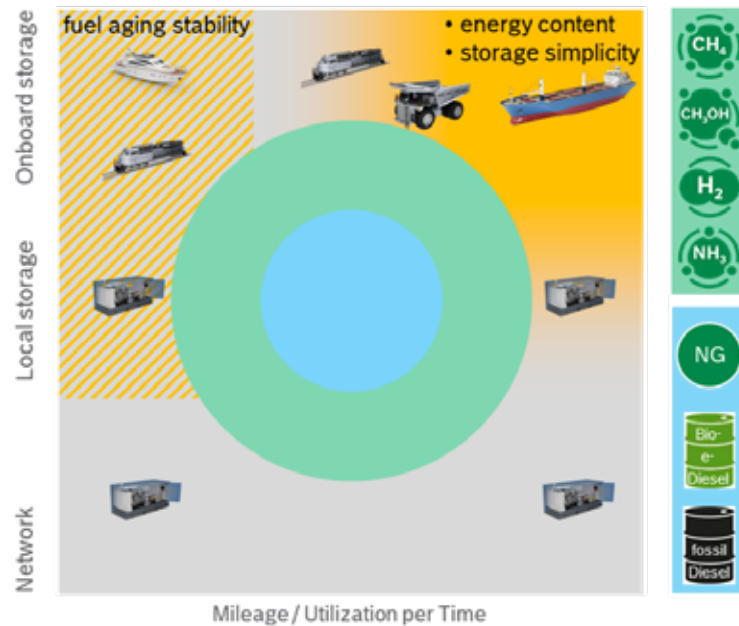


Figure 1: Infrastructure and operating conditions

2. Alternative fuels

The most promising CO₂-free e-fuels for large engines are hydrogen and ammonia, and the most promising CO₂-neutral e-fuel and bio-fuel is methanol and in some regions ethanol. A blend of lignin and ethanol could also become an interesting option in future. All these fuels require significant adaptations in the combustion and mixture preparation systems to enable best fuel consumption and lowest emissions.

The physical and chemical parameters of these fuels differ a lot from diesel and natural gas. Differences in viscosity, lubricity, density, energy density, vapor pressure, evaporation energy, flash point, flammability, ignition energy, cetane number, octane number and flame propagation require significant adaptations at the fuel injection/admission system as well as the combustion system.

Hydrogen has an extremely low density of 0.09 g/m³ in combination with very low ignition energy of 0.017 mJ, a very wide ignitable air-fuel ratio from 0.13 to 10, and a very high flame propagation rate of 230 cm/s.

Methanol and ethanol have a very high octane number (107) and, compared to diesel, a very low viscosity (< 1,2 cSt). At 50% and 30%, respectively, the energy density of methanol (20 MJ/kg) and of ethanol (27 MJ/kg) is below the energy density of diesel. The evaporation energy of ethanol (841 kJ/kg) and methanol (1089 kJ/kg) is very high compared to diesel (250 kJ/kg). Formaldehyde emissions also have to be considered.

Ammonia is very toxic and requires specific safety procedures. It has an energy density slightly below methanol (18,6 MJ/kg), a low flammability and very low flame propagation rate (6.7 cm/s). Furthermore, N₂O and NO_x emissions have to be considered. In terms of production costs, H₂ and NH₃ seem to be the most promising fuels.

With respect to the combustion systems, Figure 2 gives an overview of the relevant parameters and the respective categorisation. In contrast to diesel, the alternative fuels have a very low ignition quality (CN < 5) but an excellent knock resistance (RON > 110). Therefore, they do not

self-ignite and require appropriate measures (e.g. spark plug, pre-chamber, pilot injection, ignition improver) to start the combustion [4].

		air/fuel mix. formation		alternate fuels		combustion	ignition	cycle
		outer	inner	liquid	gas			
future	outer	PFI		CH ₃ OH, NH ₃ , CH ₄ , H ₂		pre-mixed	spark-plug pre-chamber pilot injection	Otto
	inner	LPDI/MPDI		CH ₃ OH, NH ₃ , CH ₄ , H ₂		pre-mixed	spark-plug pre-chamber pilot injection	Otto
		HPDI		CH ₃ OH, NH ₃		diffusive	pilot injection	Diesel
today	outer	PFI		NG		pre-mixed	spark-plug pre-chamber	Otto
	inner	HPDI				diffusive	self	Diesel

■ fossil ■ bio- / e- Diesel

Figure 2: Categories and combustion parameters

Figure 3 shows the injection pressure levels for different combustion systems and injection approaches (PFI, LPDI, HPDI). Being a simple system, the PFI technology is comparatively easy to install and represents the preferred solution for retrofit and dual-fuel applications as it does not require the integration of the alternative fuel injector (AFI) into the combustion chamber. Additionally, reduced calibration efforts are required compared to the direct-injection approach.

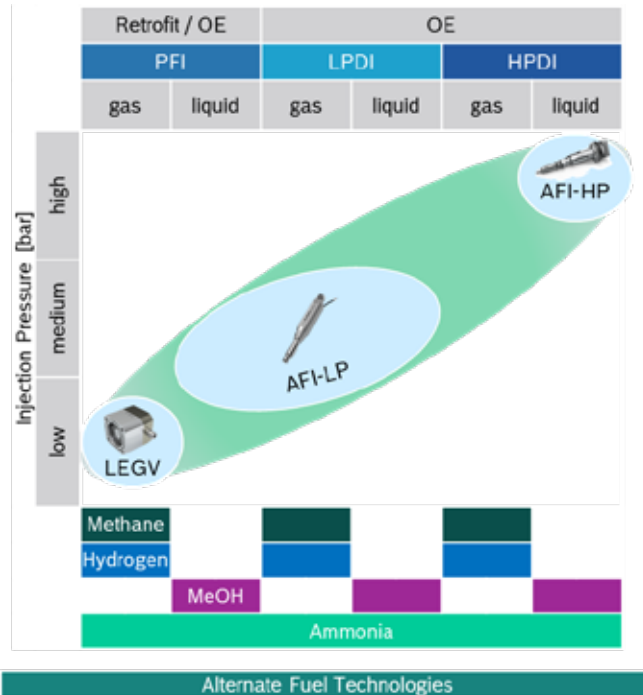


Figure 3: Injection pressure range for alternative fuels and different combustion systems

In Figure 4 the portfolio for the alternative fuels is shown. It covers the entire alternative fuel variety and combustion technologies. The LEGV for the admission of gaseous fuels into the manifold (PFI), the modularity of the Alternative Fuel Injector – Low-Pressure (AFI-LP) for LPDI of liquid and gaseous fuels including PFI for liquid fuels. For HPDI of liquid fuels the Alternative Fuel Injector – High-Pressure (AFI-HP). Finally, it includes the ECU with a sophisticated software to control the FIE and engine functionalities. Robustness of new injection systems must fulfill the same requirements as existing FIE. With our alternative fuel product portfolio Bosch is supporting these requirements.

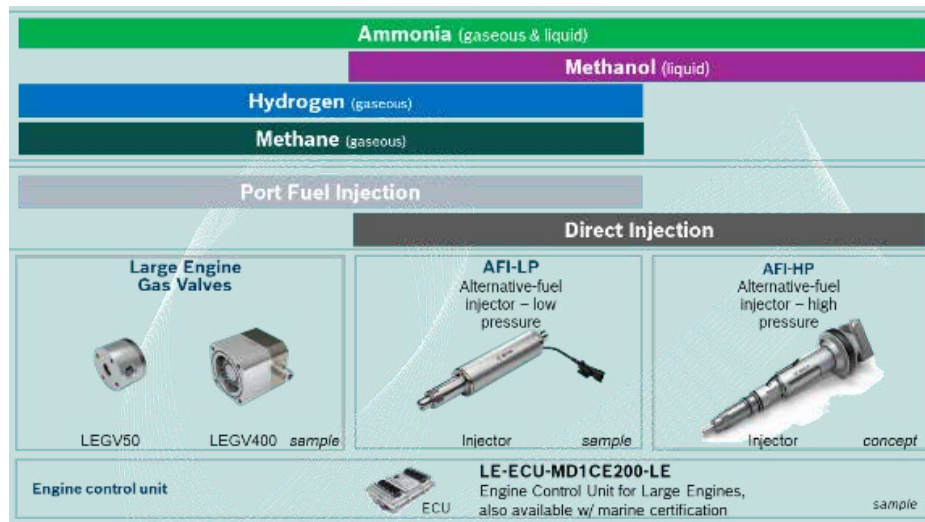


Figure 4: Product Portfolio Alternative Fuel

3. Challenges for testing MPI gas valves

The transition of the existing MPI gas valves to renewable fuels leads to a new test and validation program, for both the functional assessment and the proof of reliability. The original large engine gas valves for natural gas applications were validated through various tests, using methane as well as oil-free dry compressed air.

The utilization of oil-free dry compressed air as test medium allowed a faster, easier, and most notably, a more extensive testing compared to a validation exclusively with methane. To prove the correctness of this approach, a detailed investigation was performed before starting the actual validation program. This investigation included a theoretical assessment about the tribology contacts and the occurring wear mechanisms as well as endurance runs with different test media under the same testing conditions. MPI gas valves, that run on the component test bench with oil-free dry compressed air were compared to valves, operated with natural gas. And furthermore, at a later point, also to valves that were on an actual engine. Ultimately, the goal is to have transferable results on test benches to results from field engines.

The focus of the evaluation for a confirmation of oil-free dry compressed air as substitute media were the change of valve performance as well as the occurring wear on moving parts. The valve performance is mainly described through the mass flow, the opening and closing times, and the seat leakage. Since both the functional changes and the wear comparison showed similar results between the used fuels, the conclusion was to use oil-free dry compressed air as a substitute media for methane at the component test bench.

Figure 5 shows one of the endurance run test benches operated with oil-free dry compressed air, located at the Bosch site in Linz, Austria. These test benches were built based on all theoretical considerations and pre-tests described above.

For designing and building these test benches, also research and analyses regarding the requirements and quality of the compressed air used for testing was done. The quality focused especially on particles, water and oil contamination of the gas. Purity classes according to ISO

8573 were defined. Additionally, a suitable gas quality monitoring concept was derived, to ensure the necessary quality throughout the whole endurance run.

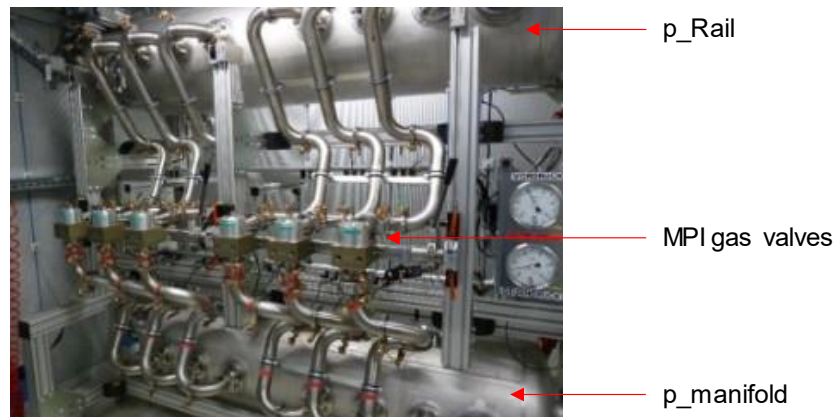


Figure 5: MPI gas valve test bench for endurance runs at Bosch Linz

Most endurance runs for the release of the MPI gas valve for methane were performed on these component test benches. However, for a final validation, also additional engine tests were done. Engine testing with the actual fuel and under actual operating conditions is crucial. On a component test bench, it will never be possible to simulate a running engine, where in addition to the used fuel, temperature and vibrations have considerable influences on the functional behavior and the lifetime of single parts. This, of course, applies to all possible fuels.

To validate and release MPI gas valves for alternative fuels, a similar testing strategy as for the MPI gas valves for methane has to be developed. All previous knowledge gained and especially the performed theoretical assessments are used for this evaluation. Additional tests with hydrogen and ammonia are performed as new input.

The theoretical evaluation of hydrogen testing already leads to the conclusion that using a substitute test medium is only possible with limitations. There are two main reasons for this limitation, hydrogen embrittlement and the chemical reactions of coatings used in the MPI gas valve with hydrogen.

Hydrogen embrittlement is, of course, considered during the design phase, by the choice of materials and by using accordingly lower safety factors in strength calculations, as stated at another point of this paper. However, hydrogen embrittlement also has to be considered in the validation plan. Only when actually testing with hydrogen or gas mixtures with a certain amount of hydrogen, this effect can be tested and the valve concept can be validated.

The same applies for coatings or layers. Coatings in MPI gas valves are used to protect metals from direct contact with hydrogen fuel and thus hydrogen embrittlement. Furthermore, wear protecting coatings are used. These coatings usually need hydrogen molecules for a chemical reaction to work correctly and to reduce friction between contact partners. That means both types of coatings used, need hydrogen fuel for correct function and for a correct assessment. With different fuels, the results about lifetime are not correct, and the MPI gas valves cannot be released for hydrogen fuels.

A comparison of endurance runs with oil-free dry compressed air and hydrogen confirms different results in the wear behavior, even at parts without any coating. The occurring wear in hydrogen endurance runs usually is higher compared to ones with natural gas and oil-free dry compressed air. The main reason is the lower viscosity of hydrogen compared to other gases. Nevertheless, some endurance runs during the MPI gas valve development for hydrogen are still performed with a substitute medium. However, these endurance runs are not primarily used for wear testing, but to test other aspects.

For releasing ammonia as fuel for MPI gas valves, again, a theoretical analysis is done first. This analysis results in one main focus point, corrosion resistance of the used materials against ammonia. To validate the chosen materials, exposure tests are conducted. The results are described at a different point of this paper.

Endurance runs with ammonia are challenging, because also for testing possible corrosion must be considered. All test bench materials have to be compatible with ammonia. This especially applies to sealing elements, since elastomers are usually quite sensitive against ammonia. Another challenge is the high toxicity of ammonia. This makes extensive safety measures necessary.

Considering the results of the theoretical assessment, all available wear and endurance run results with all different fuels, the testing program for the release of ammonia as fuel, mainly consists of exposure tests and engine tests with ammonia.

As described above, not only the fuel used as test medium itself is essential, also the quality. There are international standards concerning the purity and quality of hydrogen and ammonia, however not directly analogous to the widespread standards used for compressed air. There, ISO 8573 describes purity classes for the allowed contamination with particles, water and oil. Looking at hydrogen, the low viscosity leads to challenges especially regarding oil contamination. Even very small amounts of oil in the fuel can change test results significantly, due to a change in friction. This would lead to false positive test results and needs to be considered in the design of test benches. Using test benches with recirculation for endurance runs seems reasonable to save fuel and thus costs. However, using compressors to recirculate the fuel can lead to contamination, influencing the test results regarding wear.

Looking at ammonia, water in the test medium is most crucial. Certain water content can accelerate corrosion significantly and an adequate quality of the test medium has to be ensured.

All these points must be considered when choosing a test medium, or even a substitute medium and for defining the quality of this test medium.

For testing the function of MPI gas valves, the used fuel is not as essential as for the validation of the lifetime. The function of gas valves is mainly described by the mass flow through the valve under certain conditions, such as pressure and energizing time. Usually, also opening and closing times are measured during a functional assessment.

Figure 6 shows a functional test bench at Bosch Linz, used for the development of MPI gas valves. This test bench can be operated with oil-free dry compress air (like the endurance test bench shown in Figure 5) as well as nitrogen. The mass flow measured with the test medium can be converted to any other fuel.

Similar to the endurance run test bench, also the functional test bench is designed without recirculation of the gas, to ensure a high and stable quality of the test medium.



Figure 6: MPI gas valve functional test bench at Bosch Linz

4. Methodical approach for robustness improvement for using alternative fuels.

To start the transformation to new renewable fuels with focus on MPI valve technology a detailed analysis about main impacting factors on functional behavior and valve lifetime have to be performed.

In this chapter the impacting factors regarding useful lifetime related to hydrogen are analyzed. During development of your PFI valves for natural gas a methodical approach was used. Therefore a deep understanding of key topics related lifetime and functional behavior is needed and derived by the mentioned approach.

During the development phase for the CH₄ applications, some components turned out to be critical in terms of durability. These components are marked in Figure 7 : 1: Valve Seat 2: Valve Plate, 3: Lift Stop.

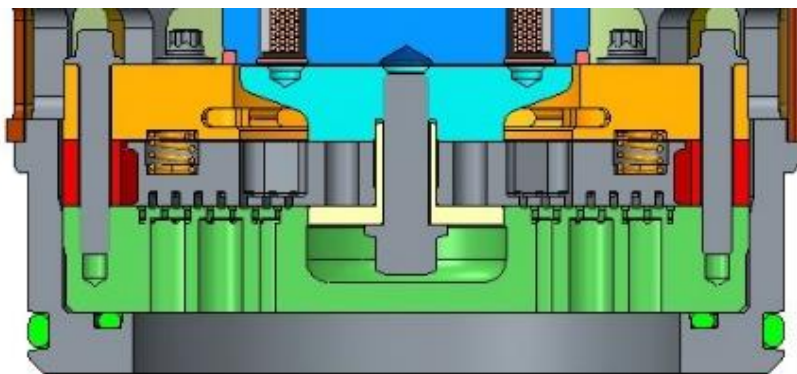


Figure 7: Cross Section of MPI valve

To cope with the changes in operational behavior linked to the usage of hydrogen a detailed assessment strategy based on the combination of measured input values and detailed FEM simulations was used.

As shown in Figure 8 so-called load cases are shown representing different operation conditions during valve operation. These cases were statistically derived from high numbers of test results and represent a nominal load and a worst-case scenario. Each load case is determined by an impact speed and an inclination of the valve disk.

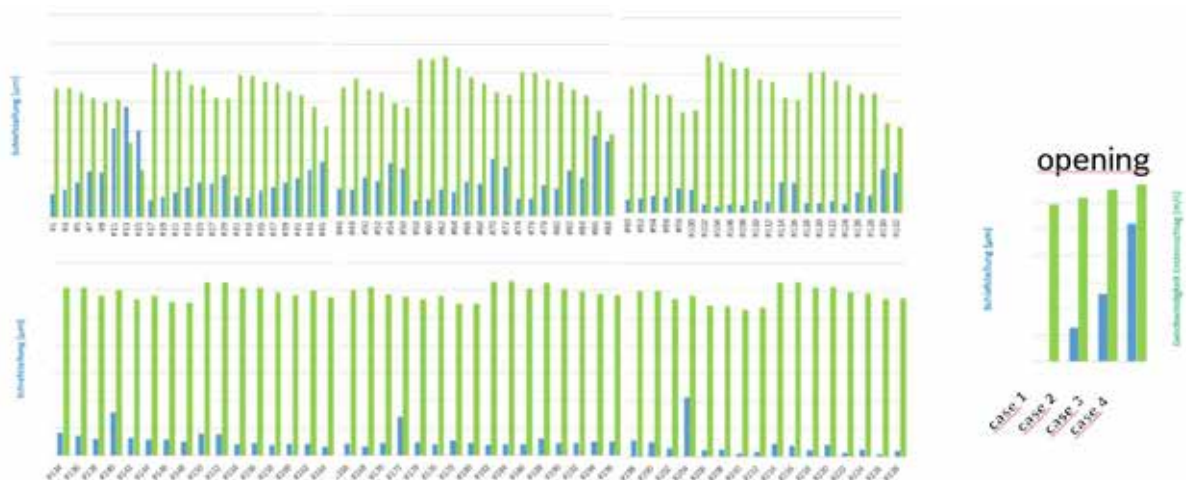


Figure 8: Assessment of different load cases by simulation and measurement

Based on the derived assessment it was proven, that the valve plate does not hit the lift stop or valve seat in a plane-parallel manner. In most cases it will hit tilted (misalignment). This leads to a first impact impulse at the location of the first contact followed by a second one 180

degrees offset from it. This second contact has typically an increase in load due to the rotational movement. In Figure 9 the used kinematic model is depicted.

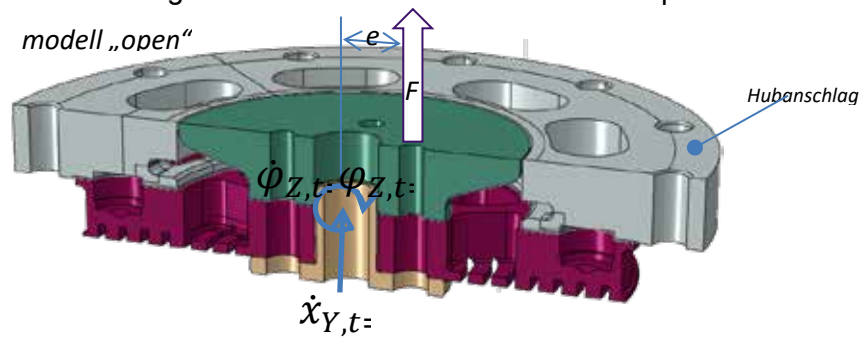


Figure 9: Derived kinematic model of valve operation

From the previous CH4 development, the critical, high-stress points on the individual components were identified and are verified for the usage with alternative fuels. In Figure 10 the results derive for the usage of NG are shown. Each of the three shown components has specific areas of increased stress levels.

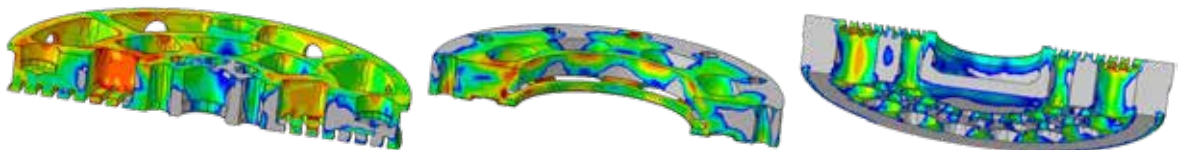


Figure 10: FEM result of operational stress loading

Based on the evaluated results in the next step the link to the usage with hydrogen is performed. As an example the approach for the valve plate component is shown in more detail and the release process for H2 is described.

The "open" valve phase is considered by determining the maximum load for this component when it hits the upper lift stop.

The FEM simulations were performed covering all significant load cases. To reduce the complexity when evaluating the results 4 exemplary load cases were defined. In Figure 12 the evaluation of the load cases is shown.

The evaluation indicates a lower safety margin for load case 3 and 4. The second influence parameter are the material parameters, also considered in the used methodology.

For CH4 application different materials are considered in the simulations. The evaluated materials are capable for renewable fuels, for example hydrogen as shown in Figure 12.

A reduced safety margin for hydrogen as operational fuel in comparison to CH4 application must be considered for all 4 load cases.

Thus, a specific safety factor was determined for these three valve components depending on the valve size and application parameters such as current profile and differential pressure.

Based on used measurement data a statistical evaluation potential use cases (operation conditions) were performed.

In Figure 11 the derived measurement data is plotted and a border line is derived. The border line separates used cases, that can occur during operation from theoretical use cases.

As shown in Figure 11 the use-case 3 and case 4 are unlikely to happen and overall the realistic case of inclination and velocity (opening speed) is roughly at case 2.

Below line poly.(P) all relevant and possible application variants of BOSCH LEGV are included.

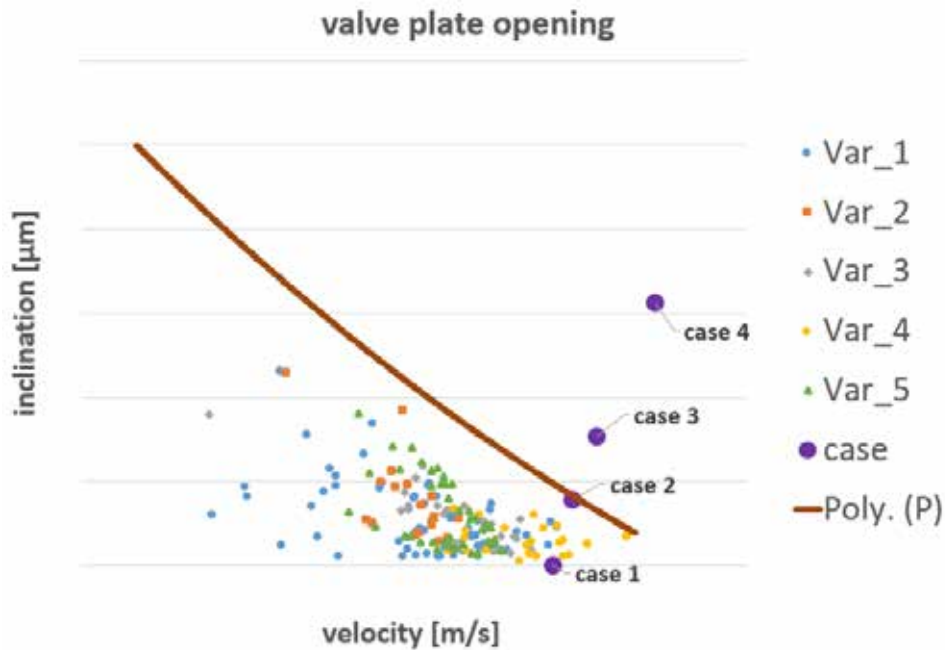


Figure 11: Statistical evaluation of operational conditions

With the derived assessment result of Figure 11 the next step in the evaluation process was taken. Exemplary for the valve plate the evaluation is shown in Figure 12.

A material safety margin for different materials for the valve plate and the impact of Hydrogen on robustness are evaluated separately. As can be seen, hydrogen has a negative impact regarding of corrosion and material behavior overall.

In Figure 12 all 4 cases are investigated regarding safety margin at CH₄ and H₂. As can be seen case 4 would lead to a decrease in safety margin below the given limit. As explained above in Figure 11 Case 3 and Case 4 are not relevant for normal valve operation. As result of the derived simulations the chosen material 1 and material 2 both fit all evaluated fuel types. Using those material, the valves can be applied for the operation in hydrogen an ammonia engine.

Because of the higher safety requirement of material 3 the material is not usable for usage with CH₄ or H₂.

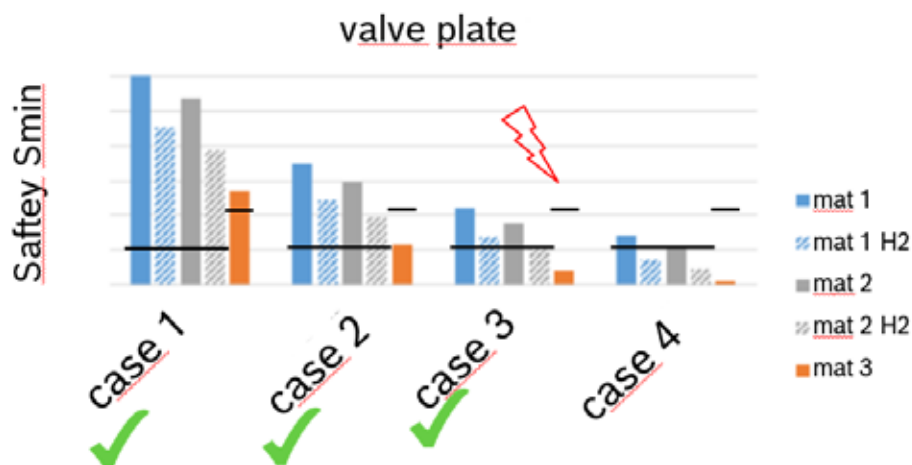


Figure 12: Evaluation of different load cases

As mentioned above there are not only one part of interest, so the same development approach was performed for all 3 parts (lift stop, valve plate and vale seat). This leads to

an overall conclusion that the out BOSCH valves are fully capable for renewable fuels like hydrogen and ammonia.

.....

5. Experience with alternative fuels Hydrogen and Ammonia

Robert Bosch LEGV was initially developed focusing on the usage of natural gas as fuel in Large Engine Gas Systems. Already during the industrialization phase of the base product, the first requests regarding its compatibility with alternative fuels (primary Hydrogen and Ammonia) arose from the market. Therefore, the need to qualify the LEGV for these fuels became inevitable and an additional target for the LEGV development. Due to the high mass flow demand of the LEGV, component testing with Hydrogen and Ammonia is difficult to realize and results in high efforts for the necessary testing infrastructure. Consequently, Robert Bosch indicated already in an early development phase to support the market requests by providing samples for various SCE and MCE Tests and agreed to use them with Hydrogen and Ammonia for combustion process development. After the successful completion of the tests, investigation of these ran-parts serves as input for the development team to identify valve features with potential needs for further improvement.

5.1. Hydrogen

Majority of the testing was performed for engine target power range's between of 40 – 80 kW/cyl. For natural gas this is the power range for LEGV Size – type.

The tryouts typically start with SCE testing, for basic investigation of e.g. combustion stability, necessary Injection timing, gas pressure demand or characteristic control parameters of the valve. Since the Gas admission valve is a crucial component for these investigations, the Robert Bosch development team is eager to supply all necessary information for successful engine setup. After positive testing, the applied parameters are confirmed on a multicylinder engine. Figure 13 shows the approach and gives an exemplary overview about approximately achieved engine run hours before successfully completing the tests.

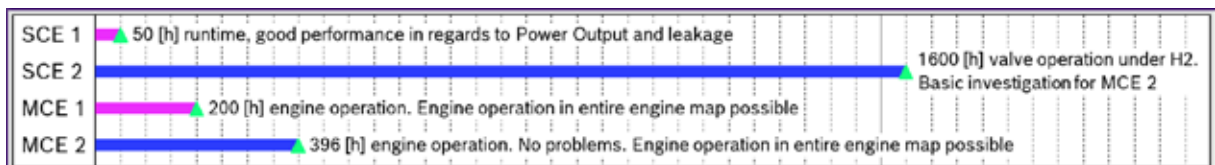


Figure 13: Overview of performed Hydrogen Testing

All performed activities were successful.

Target cylinder powers were reached in all investigations and the transfer from SCE to MCE went smoothly with LEGV as main gas admission valve. After testing, parts were returned to Robert Bosch for detailed investigation to rate the compatibility of the LEGV with Hydrogen. Regarding functionality no major differences to already known performance compared to natural gas were found (Figure 14).

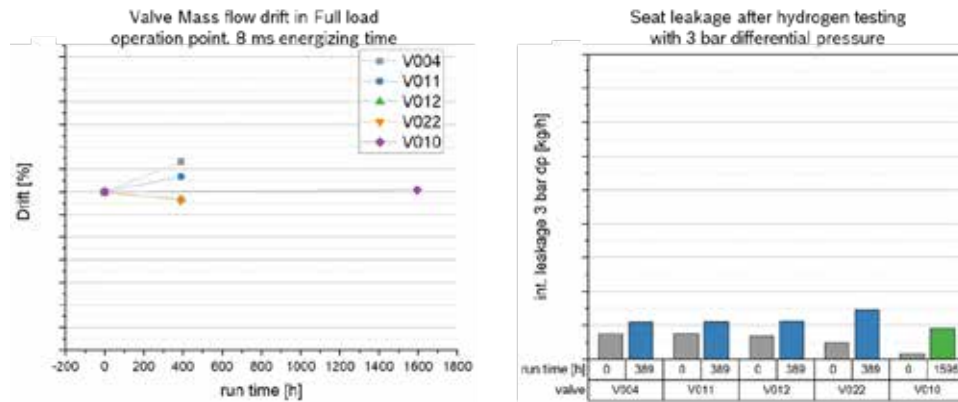


Figure 14: Mass flow drift (l.); Seat leakage (r.)

The valve mass flow slightly changed within the first 100 hours compared to the 0 [h] measurement, which is a common behavior for the LEGV and stabilization over longer operation time is seen (see Valve010). Although the internal seat leakage slightly increased, it lies within expected range, and no indication is available, that the tightness of the valve is affected by exposition to hydrogen.

While functional, no differences were detected, part analysis showed minimal increased wear when operating under hydrogen. While in natural gas, the wear over End Stop – Valve Plate – Valve Seat is completely evenly distributed on very low level, under Hydrogen a minimal increased wear was detected in the lift stop region (Figure 15).

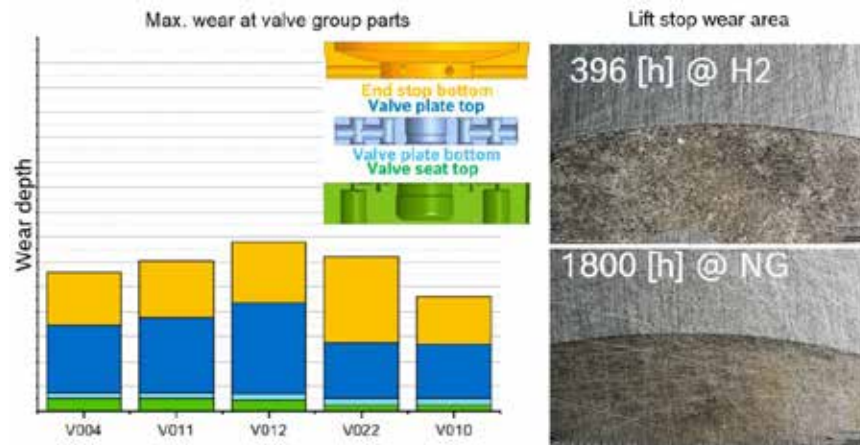


Figure 15: wear distribution (l.) ; Detail of microscopic lift stop investigation (r.)

Microscopic investigations revealed different wear pattern in the contact area between valve plate and valve seat, that can be linked to the usage with hydrogen. Further investigation will be performed in Q1/2024. Since, as mentioned before, functionality and useful lifetime were not negatively affected, the result is currently evaluated in more detail..

As Prospect, in 2024 several engines will start their operation in Field, equipped with Robert Bosch LEGV as PFI valve for admission of pure Hydrogen into the air manifold.

5.2. Ammonia

For Ammonia try outs the same approach is followed as for Hydrogen. Unfortunately, the opportunities to gather long valve operation time were very limited in passed time, see Figure

16. Main reason is here the novelty level of the concept, supply of NH₃ via PFI valve, and the contest with other technologies as e.g. low pressure direct Injection.

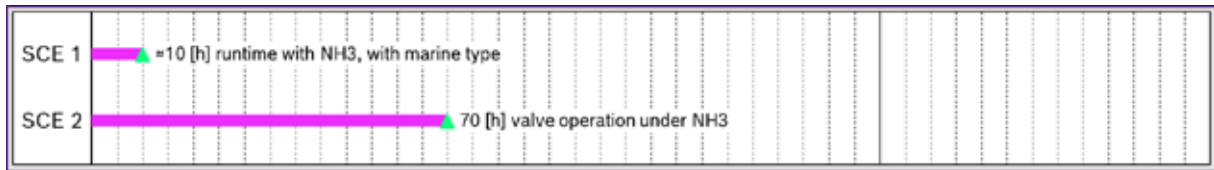


Figure 16: Overview of performed Ammonia Testing

Functional investigation of the valves indicated that exposure to Ammonia did not impact the valve functionality, similar to the observed behavior under Hydrogen operation. Change of injected gas mass, as well as internal seat leakage are negligible and 100% comparable to result with natural gas operation (Figure 17).

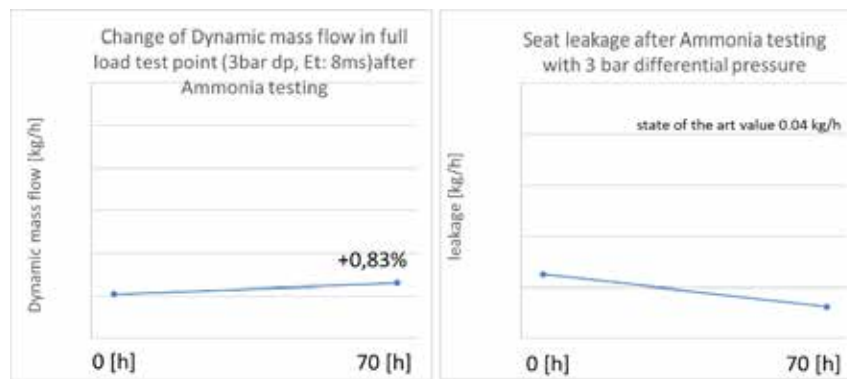


Figure 17: Change of dynamic mass flow and internal leakage after Ammonia testing

Investigation of single parts showed clearly visible deposits on the functional parts. These deposits were removed within an ultrasonic bath without problems, revealing the origin surface without any damages caused by Ammonia exposure.

In Figure 18 the contact counter parts, responsible for internal sealing function, are shown. The good condition fits to the positive leakage measurement results.

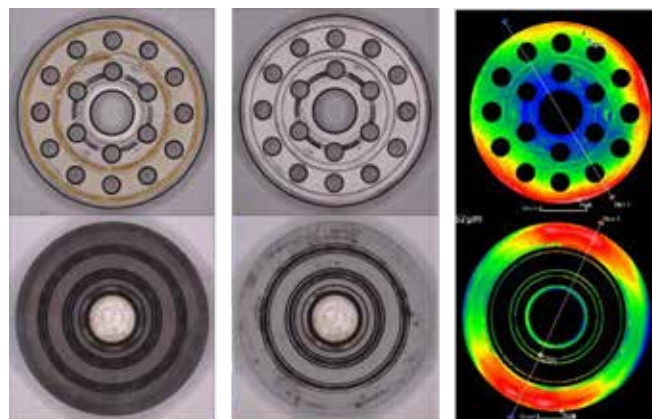


Figure 18: Deposits on Valve Plate and seat (l.); cleaned parts (m.); WLI (r.)

Additionally, to performed SCE testing, material compatibility test with Ammonia were performed for all materials within the LEGV.



Figure 19: Parts in Ammonia solution

For this test, material samples as well as series parts of the LEGV were exposed to an 25% Ammonia solution for 1000 [h] (Figure 19).

The following analysis of the exposed parts has resulted in no indication of negative Ammonia impact on the materials used within the LEGV. Despite of the short try out time, it can be stated that the usage of the LEGV with Ammonia was successful and no problems occurred, proving that the LEGV design is fully capable to operate with this alternative fuel.

As Prospect, in 2024 several different designs of LEGV will be tested with Ammonia in SCE testing, as well as in first MCE-test for marine application.

6. Impact of fuels on Gas valve dimensioning and Valve lineup

Robert Bosch LEGV Platform is available in different designs (fitting to industry standard engine interfaces) and valve size's, capable to cover a wide range of engine applications (Figure 20). Nevertheless, since the initial use case for the definition of the Platform was natural gas, an evaluation for the extension to Hydrogen and Ammonia was necessary.

Land based application		Marine Application		
LEGV Platform Design	LEGV Block Design	LEGV Integrated Design	LEGV Platform Design	LEGV Marine Design
Drop in replacement		Drop in replacement		
Continuous adjustment of valve size between LEGV240-LEGV400 max. nominal differential pressure during operation $\Delta p = 2$ [bar]			Continuous adjustment of valve size between LEGV40-LEGV65 max. nominal differential pressure during operation $\Delta p = 3$ [bar]	

Figure 20: Overview of available LEGV design, M-size (r.) and S-Size (l.)

Bosch noticed that OEM's often set up their new engine developments on already existing natural gas engines (usage of available interface, gas supply routing etc.). For comparison of the gas valve requirements, a generic engine use case can be considered (Table 1).

Table 1: Generic engine use case

Generic Use Case (full load)	
RPM (S-size)	1500 1/min
RPM (M-size)	750 1/min
Efficiency	0.4
max. Injection time	80 DegCA
Charge air-level p2	3 barA
Δp_{max} (S-size)	3 bar
Δp_{max} (M-size)	2 bar

Based on previous experience, engines with smaller power output per cylinder, run with higher rpm and normally aim for a LEGV S-size, while bigger engines turn slower and use LEGV M-size type. The Charge air level as well as the max. available crank angle for full load are engine specific and exemplary chosen. It is assumed that max. possible gas rail pressure is applied, and the injection window is fully exploited.

With these assumptions, in Figure 21 the max. achievable cylinder power in dependence of the used fuel is mapped. The spanned range for a specific fuel is based on the difference of the injected fuel mass between min and max. available valve size of this type (LEGV 40 – LEGV 65, LEGV 240 – 400).

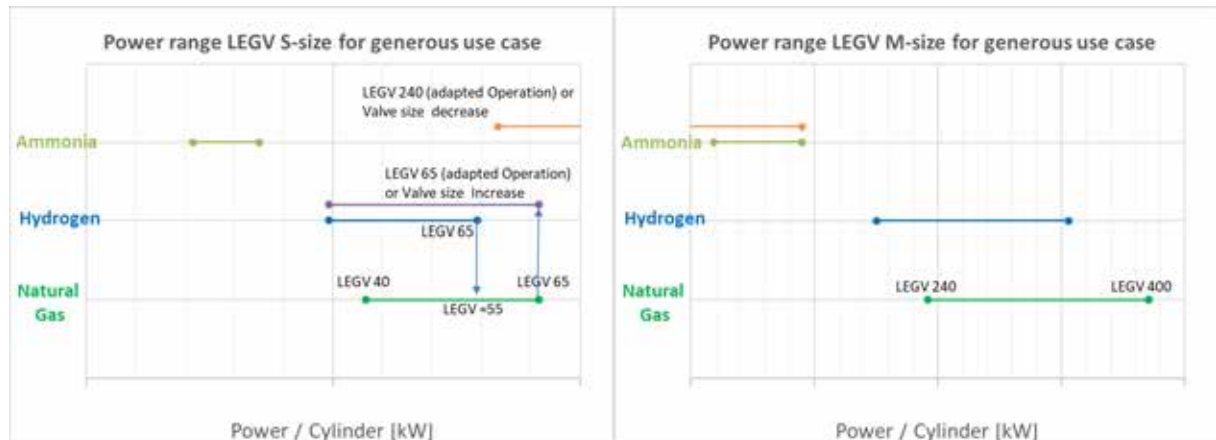


Figure 21: Power range¹ map for generic use case

¹The minimum values could be lowered, by applying gas supply pressures smaller than then $p_2 + \Delta p_{\text{max}}$ or by reduction of the used injection time. The map will be shifted to higher/smaller Power levels, if the charge air level is raised/decreased.

Hydrogen:

It is clear to see, that a valve originally chosen for operation with natural gas, cannot be transferred to a Hydrogen use case and achieve the same cylinder output under same operation conditions. The available maximum power output using Hydrogen (with LEGV 65) is a little bit smaller compared to natural gas case (comparable with LEGV 55). This means, to reach the original output level under same operation conditions, a slightly bigger gas admission valve will be necessary. Should the gas valve be kept, adaption of the operation

conditions need to be applied, but limitations need to be considered. Table 2 summarizes the possibilities.

Table 2: Overview valve adaption for Hydrogen fit

Adaption	Effect	Limitation
Increase of valve size	more injected mass with constant operation conditions. Injection time + Supply pressure stays constant.	Functionality outside available Platform solution
Increase of gas supply pressure $p_1=(p_2 + \Delta p)$	more injected mass with constant valve size. Supply pressure increased; injection time stays constant	max. delta pressure over PFI valve max. charge air level from engine side
Increase of injection time window (DegCA)	more injected mass for constant valve size. Supply pressure constant, injection time increased.	max. injection time window from engine side

Especially for Hydrogen and its higher backfire tendency, the targeted injection time windows will be smaller compared to natural gas, acting contrary in this situation, leading for an even higher mass flow demand (larger valve, higher Δp abilities). The charge air pressure cannot be arbitrary changed, due to its dependency on the overall engine setup. The most important variable remains the therefore the functional capability of the gas admission valve.

Therefore, from LEGV point of view, following steps were identified as being beneficial for future engine projects with focus on Hydrogen:

- Enlarge the available Platform to valve sizes > LEGV 65
- Enable available Platform to operate with $\Delta p > 3$ bar

Both paths are currently under investigation at Robert Bosch and might be exploit depending on sufficient market needs.

The same evaluation could be performed for the LEGV M-size, leading to equal findings.

Ammonia:

As can be seen in Figure 21, for Ammonia another situation is faced. Due to the much lower heat value (17.2 MJ/kg), while reaching similar density (0,7718 kg/Nm³) compared to natural gas (50 MJ/kg ; 0.715 kg/Nm³) the energy input per shot for same boundary conditions is much smaller. This results in a smaller possible power range covered by the same gas admission valve type. This statement is valid for LEGV S as well as LEGV M size applications. For compensation the same principles as for Hydrogen (Table 2) could be used. In regards of operating conditions, the spread between the two fuels would demand an an extension of injection time window, roughly by factor 3. Increasing the Gas supply pressure is just limited possible, due the change to the liquid state at roughly 9 barA. In the end, 100% compensation will not be possible, so other solution need to be found. Partly substitution with NH₃ might be one possibility, were e.g. 1/3 of the power demand is delivered by NH₃ injected by an PFI Valve, while the remaining power comes from central gas mixer, or from diesel within a dual fuel engine. For pure Ammonia engines, at least for small cylinder powers, one possibility is the integration of an LEGV M-Size instead of LEGV S-size. As can

be seen in Figure 21, the lower limit of the M-size power output with Ammonia, can nearly reach the upper Power Output of LEGV S-size with natural gas. By decreasing the Valve size further, or not exploiting the maximum injection time window, the prior power achieved with natural gas can be recovered. Prerequisite for this approach is the available space at the engine, what might be a hard limitation factor for the implementation of such a solution.

Therefore from LEGV point of view, following steps were identified as being beneficial for future engine projects with focus on ammonia:

- Cylinder Power range apart of classic range can be realized with LEGV
- Arrange LEGV as PFI valve for partly substitution of other main fuel with NH₃
- For common power range with 1500rpm, adaption of M-size valve should be taken into account

For path 2 and 3 Bosch already started first cooperation and tests. Further investigations might be exploit depending on sufficient market needs.

7. Results of first extension paths

As stated before, the investigation of platform extension already started with first tryout on Robert Bosch valve test benches. A comparison of the current available max. S-size valve (LEGV 65) under platform operation condition ($\Delta p = 3$ bar), was performed with an valve operating under extended operation conditions ($\Delta p = 5$ bar) and extended valve size (LEGV 80).

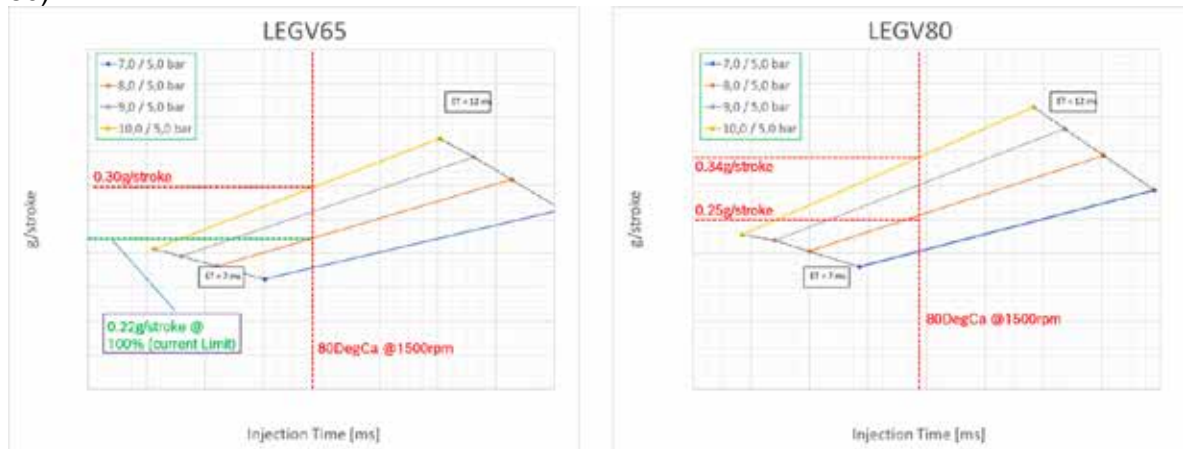


Figure 22: Comparison LEGV65 vs LEGV80

For constant injection angle, the increase of the operating pressure range for LEGV 65 led to an additional injected mass of 36%. The increase of the valve size, while operating within Platform conditions, led to 13% while the combination of both, results in 54% more mass per injection. This would mean a Cylinder Power output increase from 135¹ kW/Cyl to 205 kW/Cyl. In total, the functional testing was successful and no problem in form of overall valve functionality occurred. 1st Testing on SCE with this extension will be performed until Q2/2024, to rate the impact on combustion stability.

The attentive reader will already have noticed, that in the generic use case, for a given fuel, a power gap exists for the existing LEGV Platform. Additionally, to the described extension of the LEGV S-size, an introduction of an intermediate valve size is in evaluation. First Prototypes were already built and tested at Robert Bosch valve testbenches (**Fehler! Verweisquelle konnte nicht gefunden werden.**). Advantage of this design is the necessity of a smaller assembly space, compared to LEGV M-size, and a significant higher mass flow compared to LEGV S-size.



Figure 23: Prototype of intermediate valve design

In Figure 24 the impact of the power range for the generic use case is shown. The gap can be fully closed, leading to greater freedom for possible engine applications.

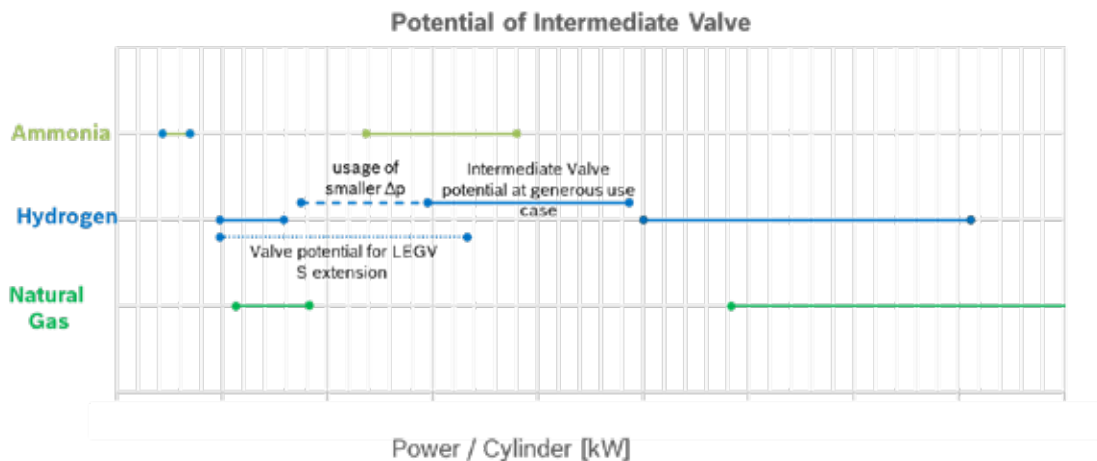


Figure 24: Potential of Portfolio extension of LEGV

Both paths are currently under investigation at Robert Bosch and might be exploited depending on sufficient market needs.

8. Summary

In the paper the specific challenges regarding MPI valve technology are described during the transition from conventional to renewable fuels.

The specific requirements for testing and validation of fuel injection equipment for the usage with alternative fuels were described in detail. Depending on the fuel type different aspects must be taken in consideration to fully describe the needed impacting factors. The focus in the paper is placed on development for Hydrogen and ammonia. In this case key requirements as functional testing, testing of leakages and wear are in the focus of development. The taken approach in case of the LEGV is pointed out.

The second part of the paper described the taken approach for the robustness improvement when using alternative fuels. A hybrid approach of testing results and comprehensive simulations is outlined, and the results and the interpretation were discussed in detail.

In the third part details of the experience in operation with hydrogen and ammonia are described. A good suitability for the operation with alternative fuels can be confirmed.

In the last part of the paper the impact of the physical properties of different fuels on the MPI valve dimensioning is explained. Key factors for the sufficient layout are explained. In the last part a new valve size to cope with the changed market needs is described.

References

- [1] Kendlbacher, Schratlbauer, Schimon; Robert Bosch AG – Business Unit Large Engines Institute of Internal Combustion Engines and Thermodynamics, Graz University of Technology: 18th Symposium "Sustainable Mobility, Transport and Power Generation", Graz, 2021
- [2] Peitz; Marberger; Gschwend; HUG Engineering AG; Germany: Exhaust gas aftertreatment for future large engine fuels, 7th Large Engine Symposium, Rostock, 2022
- [3] Brandmair, Alcove Clave, Georgieva, Fedeyko, McCarney; Johnson Matthey; UK: Ammonia as a Fuel – the role for catalytic components, 7th Large Engine Symposium, Rostock, 2022
- [4] Kendlbacher, Schratlbauer, Schimon; Stein Robert Bosch AG – Business Unit Large Engines CIMAC Congress, Busan, 2023
- [5] Christiner, Gasselsdorfer, Schmitzberger, et al. „Development Methodology for the new Large Engine Gas Admission Valves by Robert Bosch“ 28th CIMAC World Congress, Helsinki, 2016
- [6] Fontaine, Donnet, Grill, LeMogne, "Tribochemistry between hydrogen and diamond-like carbon films", Surface and Coatings Technology Vol. 146-147 (2001)
- [7] Christiner, Gasselsdorfer, Kendlbacher, et al. „Current challenges in operation of MPI valves for Large Engines – Derived benefits for engine application by usage of an integrated development approach “ 29th CIMAC World Congress, Vancouver, 2019
- [8] Christiner, Gasselsdorfer, Schmitzberger, Köhler „ MPI-Valves for the use in Large Engine Applications – Challenges in the development and derived benefits for operation“, 7th International Engine Congress, Baden-Baden, 2020

Session 8

Zündtechnologien Ignition technologies

**Moderation: Moderation: Prof. Bert Buchholz
Universität Rostock**

Smart Ignition Coil Development for H₂ ICE Application

Entwicklung intelligenter Zündspulen für Wasserstoff-Verbrennungsmotoren (H₂ ICE-Anwendung)

Stefano Papi^{1*}, Federico Ricci², Massimo Dal Re¹, John Burrows¹, Simone Daniele¹, and Carlo Nazareno Grimaldi²

* Corresponding Author: stefano.papi@tenneco.com

¹ Tenneco Powertrain

² University of Perugia, Department of Engineering

Abstract

Currently, considering the rapid advancement of alternative fuels for internal combustion engines to achieve decarbonization targets, hydrogen and hydrogen blends have garnered fresh attention, particularly within the heavy-duty internal combustion engine field. The evolution of internal combustion engines to work with hydrogen as an alternative fuel source is facing a multitude of challenges. Several components need adaptation and evolution to overcome current issues and meet the ambitious benchmarks. Within these components, ignition systems must also undergo adaptation to effectively address these progressively demanding thermal, mechanical, and electrical challenges. This paper describes the necessary evolution of the ignition systems to achieve the combustion challenges associated with H₂ICE. A typical "backfire" issue associated with port-fuel injection H₂ engines, known as the "ghost spark," has been investigated. A technical solution through coil features has been realized using analytical and experimental results from pressure bomb air bench tests and engine tests. A new strategy for diagnostic coil features has been reviewed, with a particular focus on "water bridge," "oil bridge," and main coil failures detection. Analytical models, experimental bench test data and H₂ engine tests data have been analyzed to correlate phenomena with diagnostic signal characteristics. A pressure bomb calorimeter with air has been used to analyze the influence of in-cylinder pressure on diagnostic signal characteristics. Additionally, in this work, the strategy of using a diagnostic signal has been analyzed on a single-cylinder optical engine fueled with H₂. The impact of combustion quality on diagnostic signal characteristics has been investigated, with a focus on stability at lean conditions. Preliminary results have been reviewed in combination with specific spark plug designs to demonstrate a positive impact on H₂ ICE issues, resulting in significant improvements in combustion stability and control.

Kurzfassung

Angesichts des raschen Fortschritts alternativer Kraftstoffe für Verbrennungsmotoren zur Erreichung von Dekarbonisierungszielen hat Wasserstoff und Wasserstoffgemische große Aufmerksamkeit erregt, insbesondere im Bereich der Industrie Motoren. Die Entwicklung von Verbrennungsmotoren, die mit Wasserstoff als alternativem Kraftstoff arbeiten, steht vor zahlreichen Herausforderungen. Mehrere Komponenten müssen angepasst und weiterentwickelt werden, um aktuelle Probleme zu überwinden und ehrgeizige Maßstäbe zu erfüllen. Um die anspruchsvollen thermischen, mechnischen und elektrischen Herausforderungen zu erfüllen müssen auch Zündsysteme angepasst werden. Dieser Artikel beschreibt die notwendige Evolution der Zündsysteme, um die

* Speaker/Referent

Verbrennungsprobleme im Zusammenhang mit H₂ICE zu lösen. Ein typisches "Backfire"-Problem, das mit H₂-Saugrohr Einspritzung verbunden ist, das als "Ghost Spark" bekannt ist, wurde untersucht. Eine technische Lösung durch Weiterentwicklung der Zündspule wurde mithilfe analytischer und experimenteller Ergebnisse aus Prüfstands- und Motorentests realisiert. Eine neue Strategie für diagnostische Funktion der Zündspule wurde überprüft, wobei ein besonderer Fokus auf der Erkennung von "Water Bridge", "Oil Bridge" und Funktionsfehlern lag. Analytische Modelle, experimentellen Prüfstands und H₂-Motortestdaten wurden analysiert, um Phänomene mit diagnostischen Signalcharakteristika zu korrelieren. Ein Druckkammerkalorimeter mit Luft wurde verwendet, um den Einfluss des Zylinderdrucks auf diagnostische Signalcharakteristika zu analysieren. Darüber hinaus wurde in dieser Arbeit die Strategie der Verwendung eines diagnostischen Signals an einem Einzylinderoptikmotor, der mit H₂ betrieben wird, analysiert. Der Einfluss der Verbrennungsqualität auf diagnostische Signalcharakteristika wurde untersucht, wobei der Schwerpunkt auf der Stabilität unter mageren Bedingungen lag. Vorläufige Ergebnisse wurden in Kombination mit spezifischen Zündkerzendesigns überprüft, um eine positive Auswirkung auf H₂-ICE-Probleme zu zeigen, was zu signifikanten Verbesserungen bei Verbrennungsstabilität und -kontrolle führt.

1. Introduction

In light of the swift progress in developing alternative fuels for internal combustion engines (ICE) in order to meet decarbonization targets, hydrogen and hydrogen blends have recently become the focal point of renewed interest, especially within the field of heavy-duty internal combustion engines [1]. However, this approach presents advantages and disadvantages.

The transformation of internal combustion engines (ICEs) to operate with hydrogen as an alternative fuel is encountering a myriad of challenges. Numerous components necessitate adaptation and evolution to surmount existing issues and fulfill ambitious benchmarks [2]. Among these components, ignition systems must also undergo adaptation to tackle the increasingly demanding thermal, mechanical, and electrical challenges associated with this transition [3]. Hydrogen stands out as the only fuel that holds the potential to generate minimal carbon, carbon monoxide, and carbon dioxide emissions. It offers the advantages of high engine efficiency. The wide flammability limits and rapid flame propagation rate of hydrogen contribute to a stable combustion process, particularly for lean mixtures [4]. Despite these benefits, the use of hydrogen in ICEs presents challenges, particularly in addressing abnormal combustion issues such as backfire in port fuel injection (PFI) engines [5]. The limitations arise from the low ignition energy and high flame propagation velocity of hydrogen fuel. Backfire can lead to a significant drop in volumetric efficiency, causing damage to intake and fuel injection systems. Factors such as high temperature residual exhaust gas, hot spots, and abnormal spark plug discharge contribute to pre-ignition of the hydrogen-air mixture, promoting backfire occurrences [5]. Numerous studies have been conducted to promote the use of hydrogen fuel in internal combustion engines [6], whether as a sole fuel or by adding it to fossil fuels to enhance engine brake thermal efficiency and reduce exhaust emissions [7]. However, the occurrence of backfire, an abnormal combustion in port fuel injection (PFI) engines, hinders further advancements in engine performance. This is due to factors such as low ignition energy, high flame propagation velocity, and the limited lean-burn capabilities of hydrogen fuel [8]. When backfire happens, the volumetric efficiency of port fuel injection engines significantly decreases, leading to power loss [9]. Backfire can also trigger engine knock [10], causing damage to cylinders and pistons [11]. Moreover, the intake systems and hydrogen injectors may suffer damage from high temperatures resulting from hydrogen combustion in the intake manifold [12]. Consequently, less hydrogen is delivered into the cylinders. Backfire in port fuel injection engines is typically caused by high residual exhaust gas temperature, hot spots, and abnormal ignition [13], all of which heavily depend on the engine's operating conditions. To mitigate these challenges, preventing pre-ignition due to ghost spark or hot spots around the spark plug is crucial. This can be achieved through the adoption of a cooled ignition

system or unconventional ignition methods which not only prevents pre-ignition but also facilitates the ignition of highly diluted hydrogen-air mixtures [5]. Within this context, the aim of this work is to review preliminary results obtained with an innovative ignition system called Hy2Fire®. This system is able to mitigate backfire phenomena in PFI H₂ engine with a fast discharge of residual energy trapped inside the coil at the end of the spark. In addition, a diagnostic feature has been analyzed to analyze spark plug status and detect brand new plug, water bridge and oil bridge short-circuit into plug gap. H₂ mono-cylinder engine has been used to demonstrate ghost spark backfire event elimination and preliminary correlation between voltage output, in cylinder pressure and coil diagnostic signal in motoring and idling condition. The results show that with this ignition system configuration, coil backfire can be managed, and water bridge and oil bridge can be detected thanks to a diagnostic signal length variation. Correlation between in cylinder pressure, voltage output and diagnostic feedback can be noted too even if additional investigation in different engine condition need to be done.

2. Materials and methods

2.1 Igniter

All tests reported in this manuscript have been executed with inductive spark ignition coil supplied by Tenneco defined as Hy2Fire® ignition system. This coil is provided with a power circuit formed by a high voltage transformer (14V to 40kV), charged by an ignition insulated gate bipolar transistor (IGBT) placed in cascade on the primary side circuit. At the secondary side a diode prevents the preignition avoiding positive current during the transformer charging phase, and a suppressor as EMI limiter. Internal magnetic core could store a maximum output energy manageable of 90mJ (Fig.1). In addition, this device has features suitable for Hydrogen application. It can discharge the residual energy stored in the secondary side of the transformer and makes measurement relative to the primary and the secondary current that flows on the transformer windings. The first feature is a protection called 'energy dumper', useful to avoid a pre-ignition event, while the last one is called 'diagnostic' because it generates a signal to understand abnormal behavior. The diagnostic circuit generates a signal that becomes active when the current at the primary side goes higher than a certain threshold, and it comes back in the inactive condition when the secondary side current (the spark current) is closed to zero ampere (Fig.2). The ECU can acquire this signal and calculates the time lapse between the trigger rise edge and the trigger falling edge of the diagnostic. It provides a precious information to understand if the charging time of the coil is aligned with the coils specification or could be a fault as open circuit or short circuit, or it could be useful to charge the core just enough to provide a good combustion without wear the spark plug more than needed. While the time lapse between the falling edge of the trigger and the rising edge of the diagnostic informs the ECU about the duration of the spark discharge than it could be correlated with secondary short circuit, open circuit, spark wear out, liquid inside the gap, and also the quality of the combustion. Moreover, is used to check the presence of backfire due to an unwanted spark.

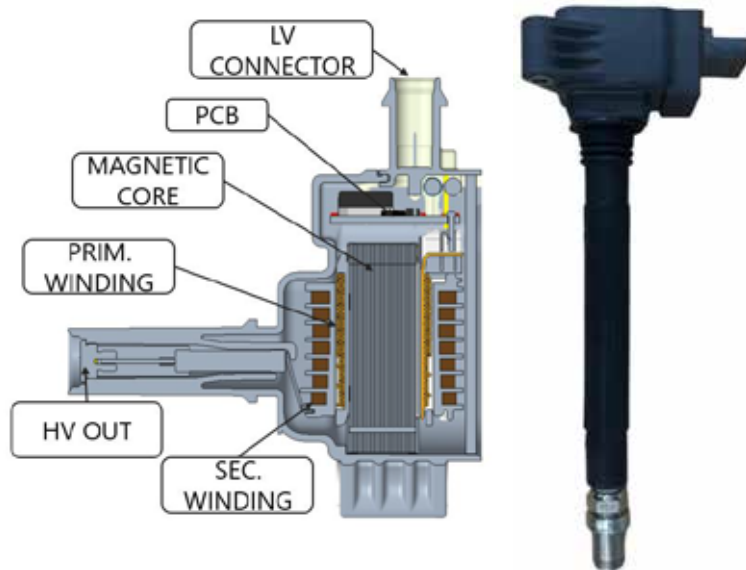


Figure 1: Hy2Fire® Design

The ignition coil requires a suitable sparkplug for engine operation. Normally, Tenneco would recommend a design with small gap and ring electrode such as those shown in Figure 2a below. These designs are implemented in m14 or m18 thread sizes in order to provide adequate lifetime at the high voltages of hydrogen combustion engines.



Figure 2a: H2 spark plugs design for industrial application.

However, in order to be compatible with the needs of the optical test engine, in this case, a Tenneco prototype M12 spark plug is used (designation REA23065D-WB), shown in Figure 2b. The plug has a 0.5mm gap between the central electrode and 2 radial ground electrodes (Figure 2b). This design is chosen for this work for several reasons:

- Low temperature of the electrodes and insulator allows the engine to operate without the risk of preignition or abnormal combustion as a result of hot-spot ignition of hydrogen.
- Modest spark gap (0.5mm compared to 0.8mm normally used for this engine type with conventional fuel) mitigates the high ignition voltage which may otherwise be required.
- Spark gap is directly visible from below the plug, making it suitable for optical investigation of the spark and early flame development.

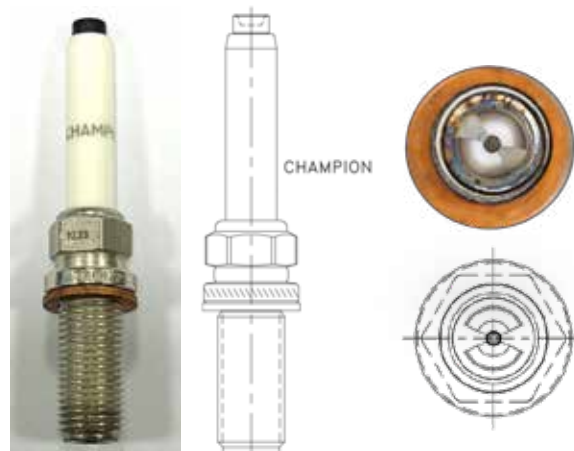


Figure 2b: REA23065D-Wb H2 spark plug.

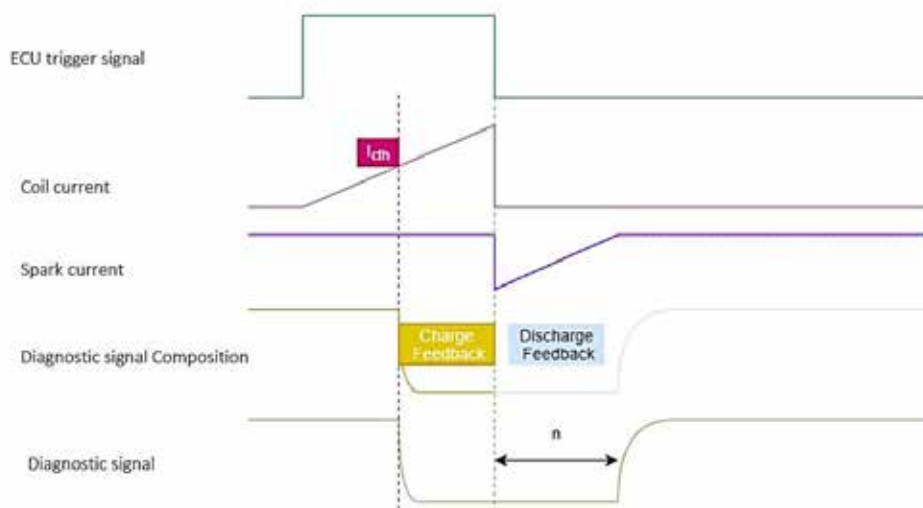


Figure 3: Hy2Fire® signals

2.2 Pressure Vessel

With the aim of analyzing the system's behavior under different gas pressures, a closed vessel has been designed with wide optical access, capable of operating up to 20 bars. Pressure vessel has a 30 cm³ volume with a M12x1.25 threaded insert for plug positioning on the top. Pressure of the medium inside the chamber is controlled by a pressure sensor (SPAN-P10R-G18M) and is regulated by means of a pneumatic system (precision pressor reduced Festo LRP, one way flow valves). Each signal event is triggered with a TTL signal generator Tektronix AFG1062. Main current is supplied to coil with a power supplier EA-PS9040-120. Additional power supplier Keithley 2230-30-1 is used to power up diagnostic signal. Oscilloscope Tektronix MS058B is used to monitor main coil ignition coil parameters, V_{in} , I_{in} , V_{out} . V_{out} is recorded using a high voltage probe P6015A connected to Hy2Fire® coil plug boot using a customized high voltage adapter. Pressure (P_{cyl}), Voltage output (V_{out}), diagnostic signal (Diag) has been recorded using logger HIOKI MR6000 datalogger. Pressure vessel overall configuration is described in Figure 4

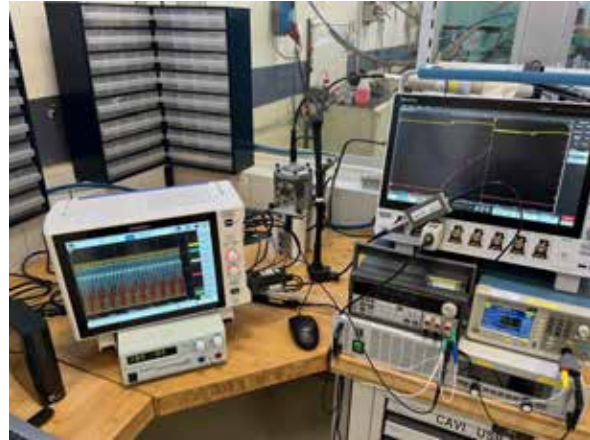
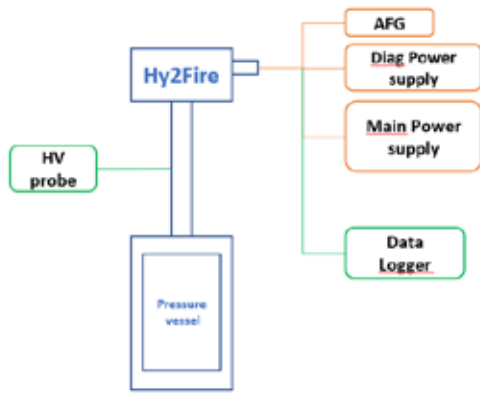


Figure 4: Pressure vessel set-up

Output voltage and diagnostic signals of 100 consecutive cycles have been analyzed as displayed in Figure 5 in order to obtain average value and standard deviation of the signals in the analyzed operating point. V_{out} has been analyzed as the voltage average during the spark including the initial voltage breakdown.

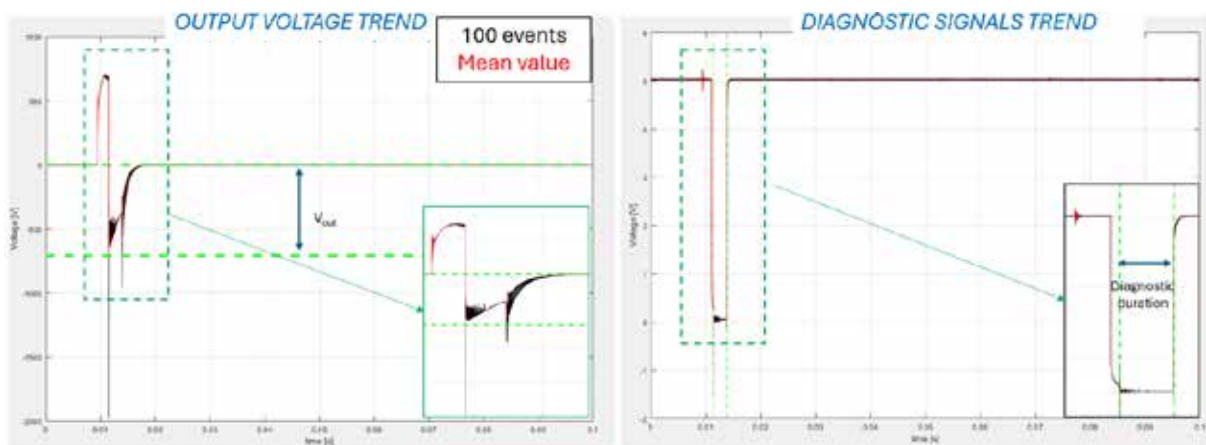


Figure 5: Voltage and diagnostic signal

2.3 Single-Cylinder Research Engine

Measurements were carried out on a 500-cc single-cylinder engine (Figure 6a) with four valves, pent-roof combustion chamber, and a reverse tumble intake port system which is designed to operate in Direct Injection (DI) or Port Fuel Injection (PFI) (Table 1). Further details are reported in Table 1. The tests were conducted at 1000 rpm in PFI mode with the igniters centrally located (Figure 6b). The engine can be also configured to allow optical access, however, in this work the quartz piston crown was replaced by a metal one (Figure 6c) to minimize leakage caused by potential un-combusted fuel, for instance. The optical configuration requires dry contact [14] between cylinder liner and piston rings, so that the latter are realized in a Teflon-graphite mix. For all the other moving parts of the engine, a conventional mineral lubricant was used: its temperature, together with the coolant one, was set at 343.0 ± 0.2 K. This value was chosen to guarantee longer engine durability and a reduced blow-by [15]. Piston thermal expansion was close to the tolerance limit and piston crown temperature was in the expected range of SI applications, even if coolant is about 20 K lower than commercial power units [17].

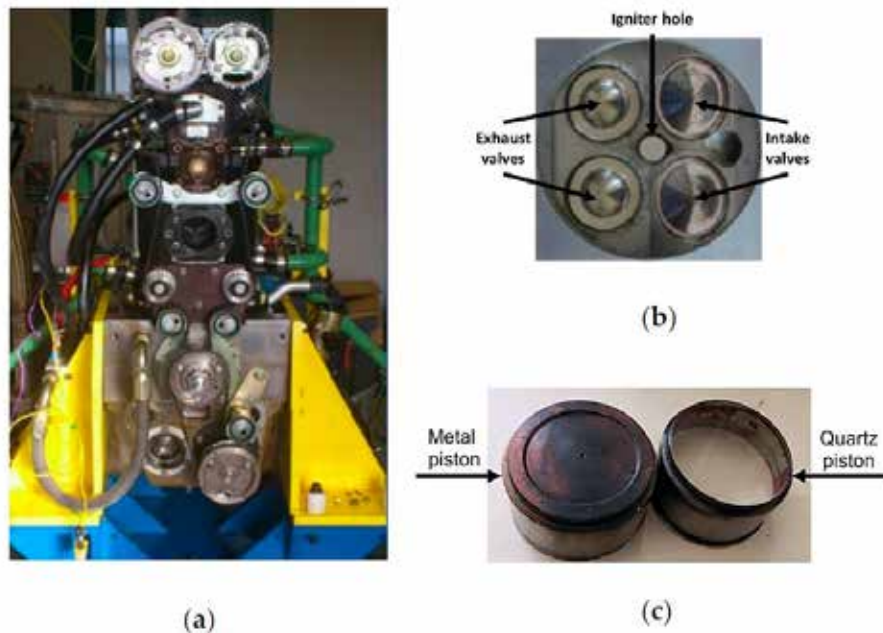


Figure 6: (a) Test engine, (b) details of engine head, (c) metal piston (left) and quartz one (right).

Table 1: Engine data

Feature, Value and Unit
Displaced volume 500 cc
Stroke 88 mm
Bore 85 mm
Connecting rod length 139 mm
Compression ratio 8.8:1
Number of valves 4
Exhaust valve open 13 CAD bBDC
Exhaust valve close 25 CAD aBDC
Intake valve open 20 CAD bBDC
Intake valve close 24 CAD aBDC

Airflow rate was regulated by means of a throttle valve upstream of the intake manifold; its position was maintained fixed for all the test points, so that the airflow inside the combustion chamber, as well as the in-cylinder charge motion, did not change. The air-fuel ratio was controlled only by increasing or decreasing the hydrogen fuel injected quantity, which had a fixed pressure of 4 bar absolute. A research ECU (Athena GET HPUH4) controlled the energizing time of the injector and the ignition timing by sending a trigger signal to the igniter control unit. A piezoresistive transducer (Kistler 4075A5) on the intake measured the intake port pressure and a piezoelectric transducer (Kistler 6061 B) on the side of the chamber measured the in-cylinder pressure. A Kistler Kibox (Figure 7 (a)) combustion analysis system (temporal resolution of 0.1 CAD) acquired the pressure signals, the absolute crank angular position measured by an optical encoder (AVL 365C), the $O_2\%$ measured by a fast probe at the exhaust (Horiba MEXA-720, accuracy of $\pm 2.5\%$), the ignition signal from the ECU. Trigger and diagnostic signals of the igniters, as described in section 2.1, are also acquired by the indicating analysis system (Figure 7 (b)). A total of 103 consecutive combustion events were recorded for each operating point tested.

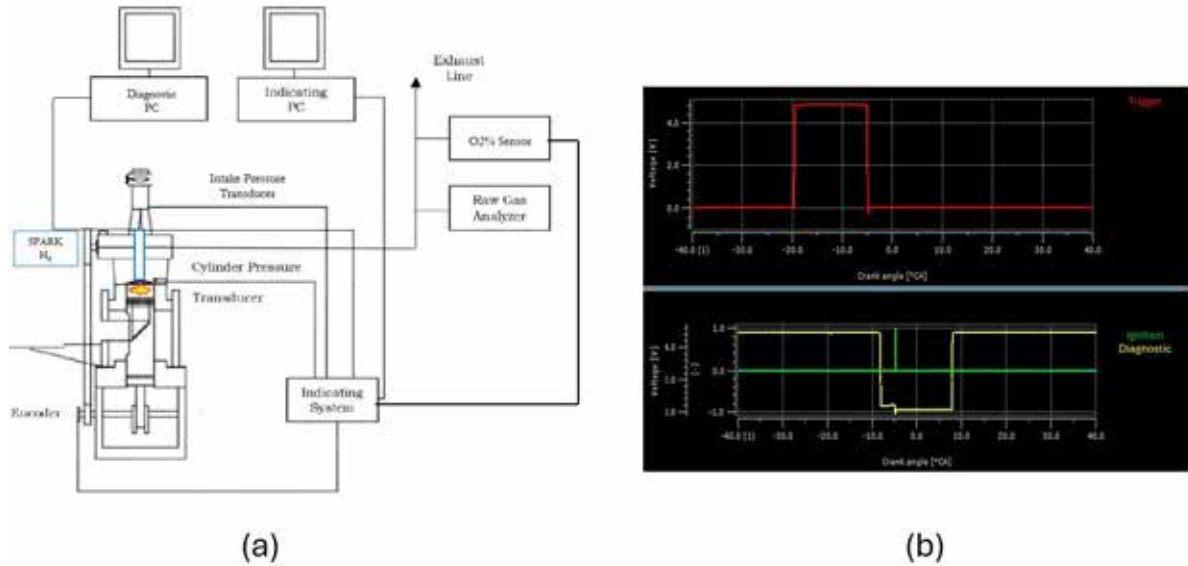


Figure 7: (a) Test engine setup, (b) details of the signals inhering the igniter control.

During operation, the λ value is adjusted in real-time based on the $O_2\%$ concentration, using the formula proposed by Azeem et al. [18] (equation 1):

$$\lambda = \frac{(1 + x_{O_2})}{\left(1 - \frac{x_{O_2}}{y_{O_2}}\right)} \quad (1)$$

where x_{O_2} and y_{O_2} are the wet concentrations of oxygen in the exhaust gas and intake air respectively.

3. Test Campaign

3.1 Vessel

Hy2Fire® ignition coil has been used coupled with M12 H_2 spark plug for the test campaign, (from now on spark $_{H_2}$). Pressure Vessel has been filled with air at 1 bar relative pressure. Hy2Fire® has been driven at 10Hz with a 2.5ms dwell time at voltage input of 13.5V stabilized with power supply EA –PS9040-20.

Output voltage and diagnostic signals of 100 consecutive cycles have been analyzed to obtain average value and standard deviation of the signals in the analyzed operating point. Sampling rate in the hioki logger have been set up to 500ks/s (Table 2).

Table 2: pressure vessel testing input parameter.

Test	Gas Type	Plug condition	Pressure(bar)	Dwell(ms)	F(Hz)	Vin(V)
A	air	new	1	2,5	10	13,5
G	air	waterbridge	1	2,5	10	13,5
I	air	oil-bridge	1	2,5	10	13,5

3.2 Single-Cylinder Research Engine

Test were carried out with the engine operating at 1000 rpm in idle mode and with a 1.6 λ operating condition. The performance of the proposed innovative spark for H_2 applications

was compared to the one obtained with traditional spark ignition system. ITs from -15 to -3 CAD aTDC have been tested with the aim of identifying the Maximum Brake Torque (MBT) area for this kind of application. It is worth noticing that the choice of the same IT regardless of the igniter allows us to compare kernel formation mechanism and flame development starting from the same in-cylinder conditions. As a result, the methodology herein adopted is meant to emphasize the differences, in terms of combustion stability and early flame behavior, among the tested combinations.

4. Results and Discussions

4.1 Pressure Vessels results.

The results concerning the activity conducted on the spark_{H2} in the pressure vessel (Figure 8) are presented and discussed below (Table 3).

Table 3 – resume of the main characteristics concerning the test of the pressure vessel.

Test	gas type	plug type	Pressure bar	Vout_avg kV	Vout_std kV	Diag_avg ms	Diag_std ms
A	O ₂	new	1	1.21	0.37	2.49	0.033
F	O ₂	water bridge	1	0.46	0.0035	5.68	0.03
H	O ₂	oil bridge	1	1.12	0.31	2.79	0.075

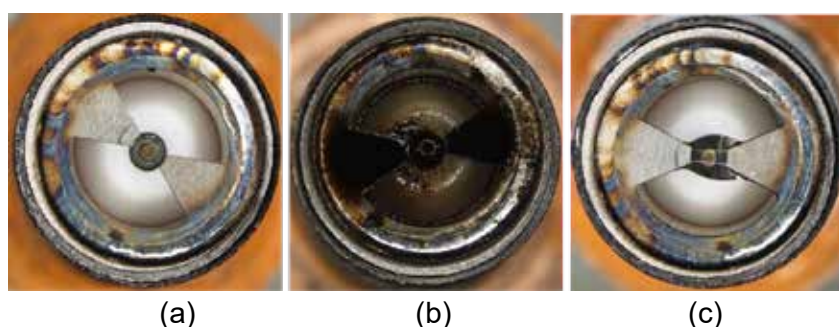


Figure 8: highlights of water-bridge(c), oil-bridge(b) on the igniter firing-end.

The findings obtained from the use of O₂ (test A, F, H in Table 3) indicate that:

- With respect to the reference *new*, water bridge and oil-bridge reduce the peak of output voltage (Figure 9, a). In particular, water bridge results in the most significant reduction in Vout over 60%.
- With respect to the reference *new*, the water bridge increases the diagnostic duration up to 5.68 ms, while the oil bridge tends to prolong the signal length but not with the same extension.

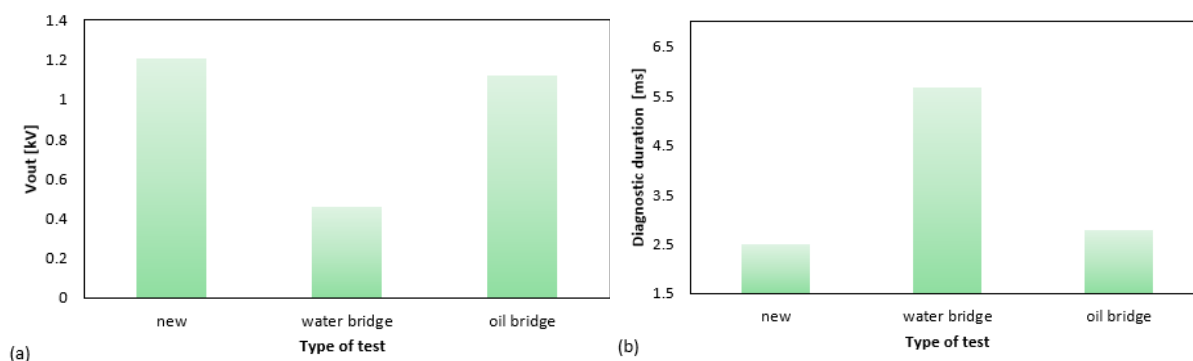


Figure 9: Vout and diag signal with plug condition listed in Table 3.

4.2 Single cylinder research engine results

The results concerning the activity conducted in the single cylinder research engine are presented and discussed below.

- Backfire analysis

By using the same input conditions, i.e. same IT equals to -11 CAD aTDC, the in-cylinder pressure traces together with the pressure traces at the intake port have been analyzed for both spark_{H2} (blue curves in Figure 10) and traditional spark ignition system (green curves in Figure 10). At the low engine speed and load conditions, characterizing the experimental test, together with the operational λ , and the short duration of the tests, prevent the attainment of high temperatures. Consequently, the backfire remains low and may go undetected by the cylinder pressure sensor. However, it is evident in the intake pressure as displayed by the conventional spark ignition system exhibits events marked by spikes in the intake sensor, a pattern not observed in the cases of spark_{H2}.

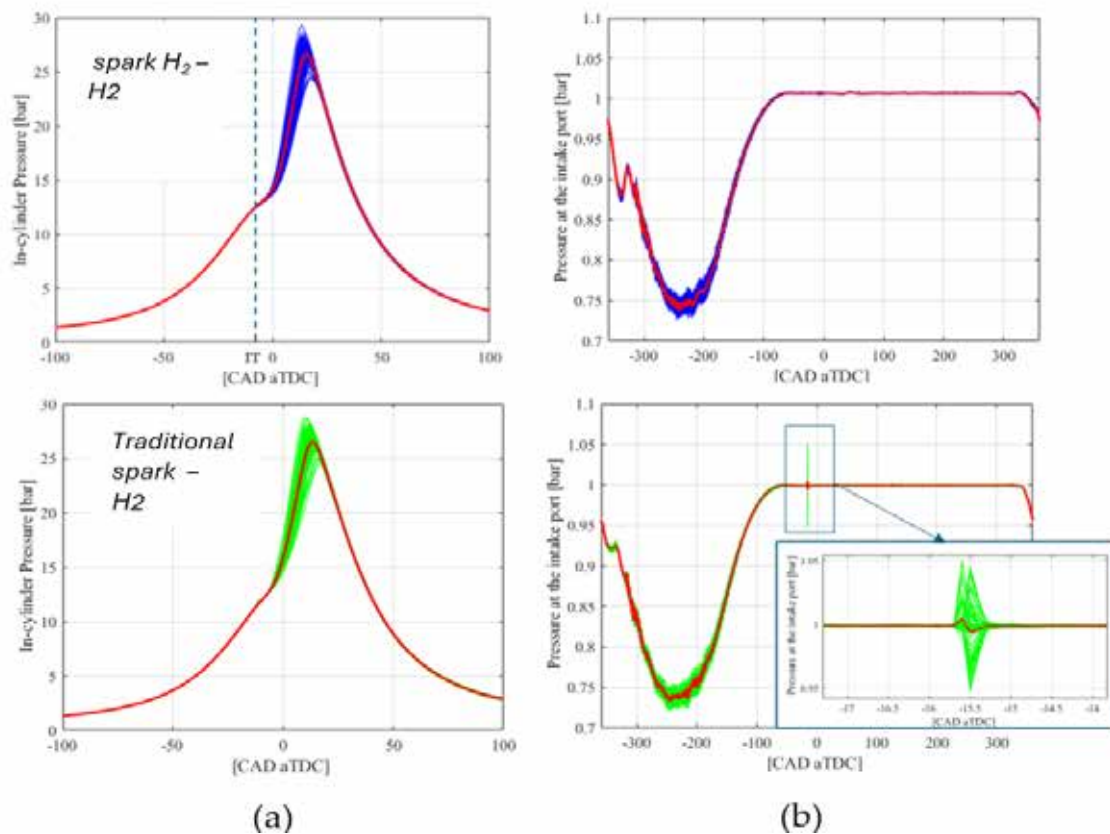


Figure10: Backfire event presence with and without Hy2Fire® coil.

- Analysis of the diagnostic signals

Figure 11 reports the trends of output voltage and diagnostic duration, both in motored and firing condition at different IT, i.e. at different levels of in-cylinder pressure. The results show that:

- Reducing the charge timing results in a shorter diagnostic duration.
- When the charge timing is held constant at 2.5 ms, the diagnostic signal duration tends to increase during motored conditions.

- The diagnostic duration exhibits a declining pattern as in-cylinder pressure rises towards the top dead center (TDC).
- The secondary voltage displays a characteristic 'umbrella' trend across the analyzed range, reaching its peak near the TDC.

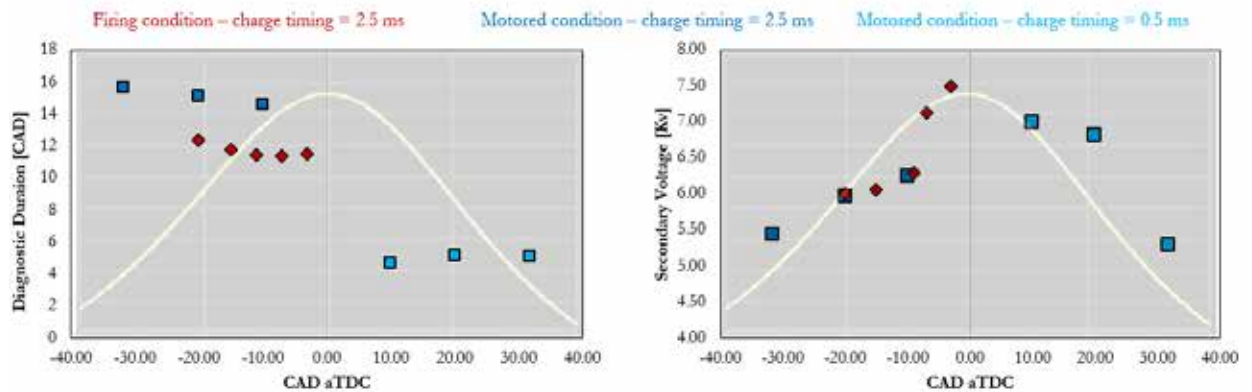


Figure 11: diagnostic and voltage output comparison in motoring conditions.

Concerning the firing condition, Figure 12 shows a noticeable bell-shaped trend is apparent, with the shortest duration observed in the central IT area and the longest duration at the extremes of this bell curve. Specifically, this aligns with Figure 12 b. The overlaid values show the average diagnostic duration of each operating point tested. Essentially, in this application, there is a correlation between the mean duration of diagnostic signals and reaching the MBT area, allowing the association of this value with the IMEP values characterizing the tested engine.

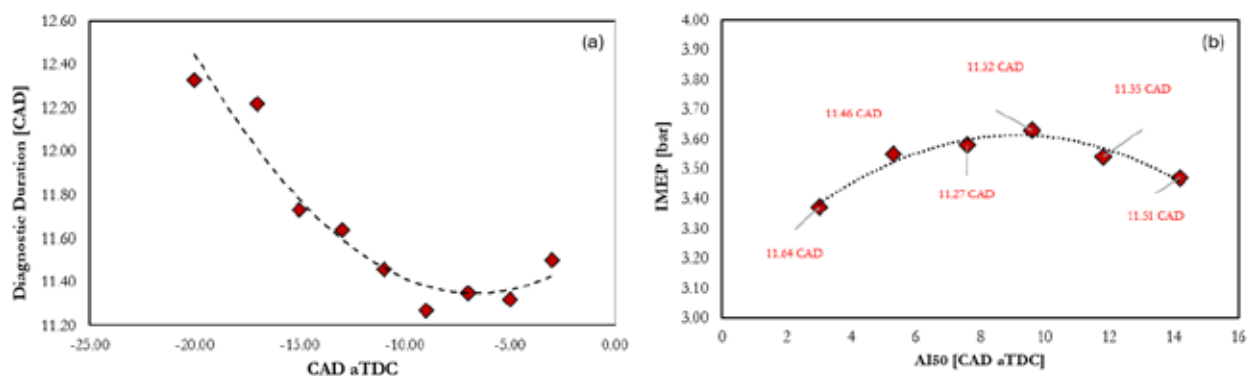


Figure 12: (a) Average value of the diagnostic duration plotted against the IT for each operating point tested at $\lambda=1.6$. (b) IMEP plotted against the CA50 with overlapped the diagnostic duration, in red.

- *Indicating Analysis Hydrogen H₂*

Combustion stability (Figure 13) was evaluated by means of the Coefficient of Variance (CoV) of the Indicated Mean Effective Pressure (IMEP), namely, the ratio between IMEP standard deviation and IMEP mean value. Figure 13 (a) depicts the CoV values found for each case studied plotted against the AI50 which has been used to identify the MBT area. AI50 is defined as the crank angle degree after the Top Dead Center (TDC) for which 50% of the mass is burned. It is determined through the indicating analysis system, starting from the in-cylinder pressure signals, as outlined in Section 2.3. The overlaid values show the IT of each operating point tested. Engine operating points are defined as fully stable if the

CoV_{IMEP} is lower than the 4% threshold [17]. Each condition tested shows CoV_{IMEP} lower than 2.5%, and in particular, the working area between $AI_{50}=6:10$ CAD aTDC has been identified as providing, on average, the best stability. As reported from the IMEP value, such an interval is also characterized by the highest delivered power and, therefore, defines the MBT area. At each condition tested, spark_{H₂} is capable of guaranteeing, at the same IT and in the MBT Area, faster flame development and a higher IMEP with gains up to 5%.

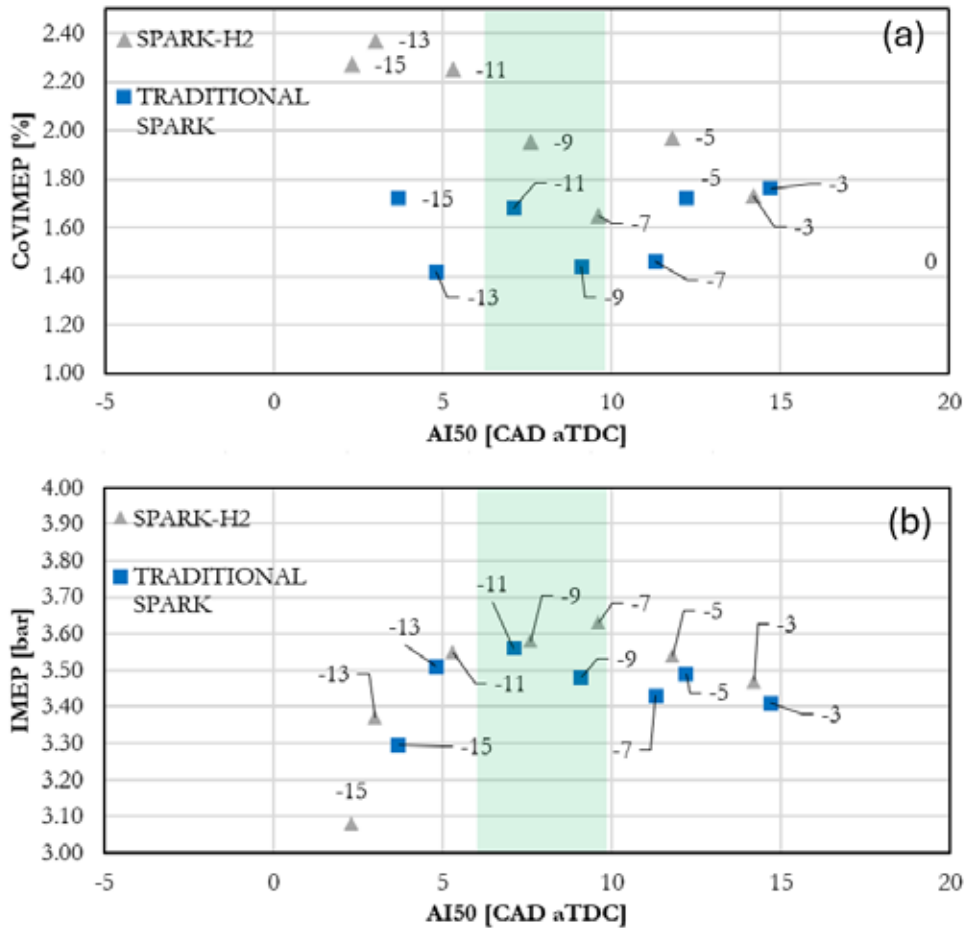


Figure 13: (a) CoV_{IMEP} and (b) IMEP plotted against the AI_{50} .

- Comparison between hydrogen H₂ and gasoline E5

As an example, the operating point with spark_{H₂} characterized by IT = -7 CAD aTDC can deliver approximately 3.6 bar and it is featured by the higher stability, i.e. CoV_{IMEP} = 1.6%. When compared to a Spark-Gasoline (E5) application at the same λ value, this value is about 0.8 bar lower than the one achieved through gasoline fuel, which was found to be equal to 4.37 bar [17]. For the sake of completeness, Figure 14 reports, at optimized $\lambda=1.6$, the in-cylinder pressure patterns of spark_{H₂}-H₂ combinations alongside those of traditional spark-E5 (depicted as black curves). In comparison to H₂, E5 displays pressure patterns marked by a higher CoV_{IMEP} (2.8%), affirming a tendency towards unstable operating conditions. Given the optimized IT for both scenarios, it's important to note that hydrogen demands lower IT values compared to gasoline. The need for reduced ignition timing with H₂ compared to E5 is related to the combustion characteristics and properties of the respective fuels [2]. For example, the elevated flame speed of hydrogen results in quicker ignition and flame spread [5]. Additionally, the broader flammability range, combined with

low ignition energy, facilitates the easy ignition of H_2 across a wide spectrum of air-fuel ratios [5]. These factors collectively impact the flame speed of hydrogen H_2 and the achievable delivered power. The higher levels of pressure recorded with H_2 are related to the faster first combustion stage (AI05) while the lower IMEP value is related to the lower energy content per unit volume compared to gasoline. Despite its higher energy content per unit mass, the lower density of hydrogen can result in a reduced total energy per unit volume (see the Integral of Heat Release Rate), impacting the overall power output [19].

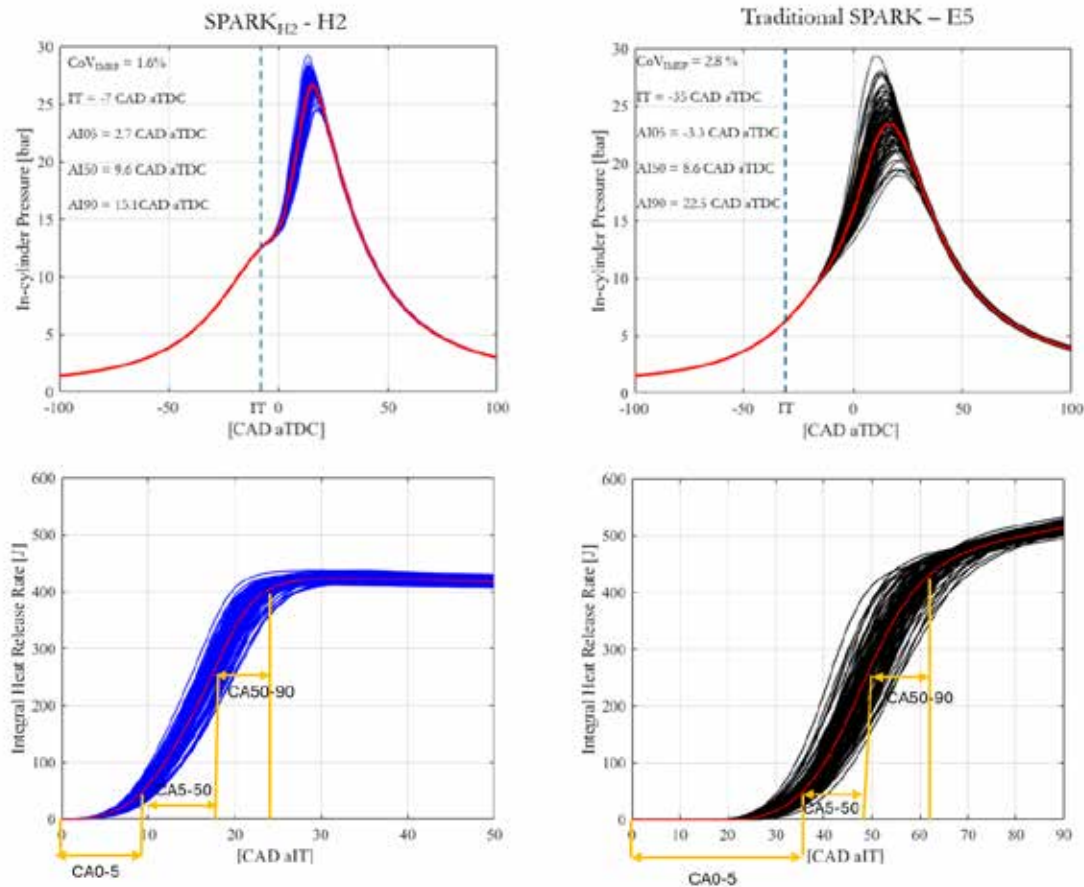


Figure 14: in-cylinder pressure traces and IHRR for both H_2 (blue curve) and E5 (black curve). The red curve of each graph indicates the average value of the 103 combustion cycles.

5. Conclusions

Preliminary investigation on new ignition system configuration called Hy2Fire® has been completed in pressure vessel configuration and H_2 Mono-cylinder engine in motoring and idle condition. The observations concerning the activity conducted are presented and discussed below:

- Hy2Fire® internal configuration can prevent Backfire event related to coil's Ghost Spark in PFI H_2 mono cylinder engine
- Hy2Fire® diagnostic feature can detect plug status and particularly detect phenomena of gap water short-circuit (water bridge) and oil gap short-circuit (oil bridge)
- Tested engine points showed a potential correlation between V_{out} , In cylinder pressure and diagnostic signal registered especially in motoring and firing condition.
- Bell curve distribution on V_{out} and diagnostic signal can be observed in engine condition at IT variations, potentially correlating this trend with analyzed signals.

References

- [1] Purayil, S. T. P., et al. "Review of hydrogen–gasoline SI dual fuel engines: Engine performance and emission." *Energy Reports* 9 (2023): 4547-4573.
- [2] Wang, Lijun, et al. "The effect of hydrogen injection parameters on the quality of hydrogen–air mixture formation for a PFI hydrogen internal combustion engine." *International Journal of Hydrogen Energy* 42.37 (2017): 23832-23845.
- [3] Catapano, F., et al. "Analysis of energy efficiency of methane and hydrogen-methane blends in a PFI/DI SI research engine." *Energy* 117 (2016): 378-387.
- [4] Sementa, Paolo, et al. "Exploring the potentials of lean-burn hydrogen SI engine compared to methane operation." *International Journal of Hydrogen Energy* 47.59 (2022): 25044-25056.
- [5] Gao, Jianbing, et al. "Review of the backfire occurrences and control strategies for port hydrogen injection internal combustion engines." *Fuel* 307 (2022): 121553.
- [6] Luo Q-h, Sun B-g. Inducing factors and frequency of combustion knock in hydrogen internal combustion engines. *IJHE* 2016;41(36):16296–305.
- [7] Aydin K, Kutanoglu R. Effects of hydrogenation of fossil fuels with hydrogen and hydroxy gas on performance and emissions of internal combustion engines. *IJHE* 2018;43(30):14047–58.
- [8] Huynh T, Kang J, Noh K, Lee JT, Caton J. Controlling backfire using changes of the valve overlap period for a hydrogen-fueled engine using an external mixture. *Internal Combustion Engine Division Fall Technical Conference*. 48116. 2007: 243–51.
- [9] Garmsiri S. Study of an internal combustion engine to burn hydrogen fuel and backfire elimination using a carburetor fuel delivery method. *UOIT* 2010.
- [10] Ye Y, Gao W, Li Y, Zhang P, Cao X. Numerical study of the effect of injection timing on the knock combustion in a direct-injection hydrogen engine. *IJHE* 2020;45(51):27904–19.
- [11] Ceschini L, Morri A, Balducci E, Cavina N, Rojo N, Calogero L, et al. Experimental observations of engine piston damage induced by knocking combustion. *Materials Design* 2017; 114:312–25.
- [12] Dieguez P, Urroz J, Sainz D, Machin J, Arana M, Gandía L. Characterization of combustion anomalies in a hydrogen-fueled 1.4 L commercial spark-ignition engine by means of in-cylinder pressure, block-engine vibration, and acoustic measurements. *Energy Convers Manage* 2018;172:67–80.
- [13] Tsujimura T, Suzuki Y. The utilization of hydrogen in hydrogen/diesel dual fuel engine. *IJHE* 2017;42(19):14019–29.
- [14] Petrucci, Luca, et al. "Detecting the Flame Front Evolution in Spark-Ignition Engine under Lean Condition Using the Mask R-CNN Approach." *Vehicles* 4.4 (2022): 978-995.
- [15] Ricci, Federico, et al. "Comparative analysis of thermal and non-thermal discharge modes on ultra-lean mixtures in an optically accessible engine equipped with a corona ignition system." *Combustion and Flame* 259 (2024): 113123.
- [16] Ricci, Federico, et al. "Investigation of a Hybrid LSTM+ 1DCNN Approach to Predict In-Cylinder Pressure of Internal Combustion Engines." *Information* 14.9 (2023): 507.
- [17] Martinelli, Roberto, et al. Lean Combustion Analysis of a Plasma-Assisted Ignition System in a Single Cylinder Engine fueled with E85. No. 2022-24-0034. *SAE Technical Paper*, 2022.
- [18] Azeem Naqash, et al. Comparative Analysis of Different Methodologies to Calculate Lambda (λ) Based on Extensive And systemic Experimentation on a Hydrogen Internal Combustion Engine. No. 2023-01-0340. *SAE Technical Paper*, 2023.
- [19] Shinde, Balu Jalindar, and K. Karunamurthy. "Recent progress in hydrogen fuelled internal combustion engine (H2ICE)–A comprehensive outlook." *Materials Today: Proceedings* 51 (2022): 1568-1579.

Same-Cycle Spark Control: The Future of Hydrogen Engines

Emmanuella Sotiropoulou*, **Luigi Tozzi**, **Supreeth Narasimhamurthy**

Prometheus Applied Technologies, LLC

Luc Mattheeuws, **Rik De Graeve**

Anglo Belgian Corporation NV

David Lepley

Altronic LLC

Bernhard Zemann

Hoerbiger Wien GmbH

Abstract

Global decarbonization necessitates the use of sophisticated technologies to take the current internal combustion engine (ICE) to the next level. One approach is burning green hydrogen (H_2) and having engine power density and efficiency comparable to those of advanced Diesel engines (i.e., “Diesel like performance”) but with zero emissions. Achieving this objective requires burning H_2 at ultra-lean conditions to prevent high thermal load on in-cylinder components and to enable reliable, durable, and cost-effective solutions. These considerations have created the motivation to develop new technologies in the areas of hydrogen prechamber combustion, ignition and fuel injection defining a holistic solution. In particular, the prechamber must operate with very lean lambda to prevent preignition and the ignition system must be able to deliver an adaptive spark energy rate that assures proper ignition of the ultra-lean hydrogen mixture while preventing the formation of hot spots on the electrodes leading to combustion instabilities like backfire, knock and preignition. Similarly, the hydrogen injection & mixing system must prevent the formation of rich pockets resulting in combustion abnormalities caused by lube oil preignition (LOP). This paper dives deeper, than previous publications by the authors, and illustrates in detail the performance potential of hydrogen engine combustion enabled by a holistic combustion solution. An understanding of the fundamentals that is applied to advanced state-of-the-art technologies is confirmed with engine test results. Moreover, the need for a targeted turbocharger system solution together with a staged development approach are discussed for mitigating the technical and commercial risks associated with the introduction of competitive hydrogen engine technology in the market.

1. Introduction

The growth in renewable energy sources like wind and solar is making carbon-free/neutral fuels increasingly more available creating the opportunity for engine OEMs to focus on further developing engine systems that can fully exploit the potential for net-zero emissions while being competitive on cost, power density, efficiency, and durability.

Currently, spark ignited hydrogen internal combustion engines (H_2 -ICEs) are not as competitive as they need to be, due to the challenges associated with combustion instabilities limiting the power density achievable with these engines.

Shown in Figure 1 is a typical sequence of events of consecutive engine combustion cycles leading to backfire in the intake (i.e., frontfire), thereby preventing reliable operation at higher power densities. It can be seen that, as a result of insufficient in-cylinder thermal management (e.g., high energy ignition), an initial high cycle can create hot spots on in-cylinder components (e.g., valve, piston crown, electrodes) and cause frontfire.

As a result of combustion instabilities, the power density of a H_2 -ICE is less than 64% of its Diesel counterpart. For example, if the base Diesel engine operates at 25bar BMEP, the H_2 -ICE version would operate at less than 16bar BMEP before the combustion becomes unstable.

* Speaker/Referent

As a result, the H₂-ICE efficiency would be less than 84% of the Diesel version. Thus, if the Diesel operates at 50% efficiency BTE, the hydrogen version would achieve less than 42%. To mitigate the combustion instabilities and allow for the H₂-ICE to approach the Diesel-like performance, the authors outline a holistic approach that is backed by engine test results.

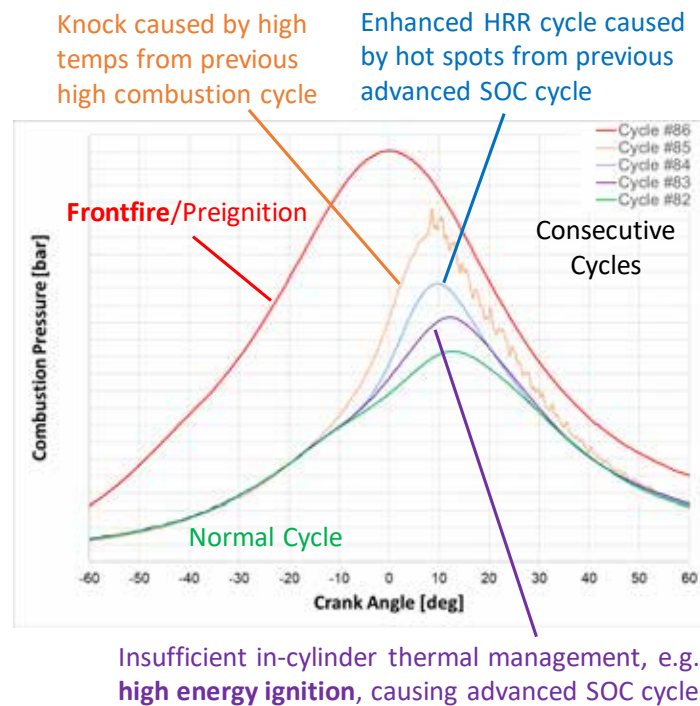


Figure 1. Typical sequence of events of consecutive engine combustion cycles leading to backfire in the intake (i.e., frontfire) or preignition.

2. Technical Approach

The approach used to achieve Diesel-like performance is leveraging recent advancements in technologies like lean-burn prechamber combustion, same-cycle adaptive spark control, and H₂ port fuel injection (PFI) homogeneous mixing to remarkably enhance the state-of-the-art of hydrogen engine power density (BMEP), efficiency (BTE) and NO_x emissions to approach “Diesel-like” performance with virtually zero emissions.



Figure 2. Holistic approach to H₂-ICE targeting “Diesel-like” performance & zero emissions

These technologies are combined and optimized as a holistic combustion system solution, depicted in Figure 2. Here, the lean burn prechamber (LBP) [1] uses an advanced H₂-ePCC fuel injector to accurately dispense small quantities of H₂ in a way to achieve the fuel stratification necessary to mitigate the H₂ propensity to preignition in prechamber. Then, the latest innovation in ignition system technology uses the same-cycle adaptive spark control (a.k.a., Predictive Model-Based Spark Control or Predictive Model-Based Spark Control Prechamber Ignition System) [2] to minimize the variations in the start of combustion (SOC) resulting from the hot spots that can be formed on the electrode surface by the high energy sparks needed with ultra-lean hydrogen mixtures [3]. Lastly, the PFI custom injector, injection strategy and mixing devices (e.g., intake turbulence inducer and port deflector) are typically necessary to achieve the in-cylinder mixture homogeneity needed to mitigate the propensity to lube oil preignition (LOP) and reduce cycle-to-cycle combustion variability [4-8].

The potential benefits of this approach are confirmed by testing a large bore hydrogen engine with an adaptive spark control prechamber ignition system and by comparing the results to those obtained with a state-of-the-art capacitive discharge spark plug ignition system. The hydrogen engine platform selected for this study is the ABC 6DZ used in marine propulsion shown in Figure 3.



Figure 3. ABC 6DZ hydrogen engine selected for this study and used in marine propulsion

The test version of the 6DZ is equipped with cylinder pressure transducers, high speed data acquisition system, NO_x exhaust gas analyzer as well as an electric generator.

2.1 Homogeneous H₂ Mixing

Discussed in a recent publication [4], are the main combustion anomalies limiting the H₂-ICE power density and efficiency. These are misfire, frontfire, knock and preignition. These abnormal combustion cycles result mostly from ignition induced variations in the SOC, as well as from mixture inhomogeneities causing LOP or end-gas knock at engine power densities in the range of 13-16bar BMEP.

Sufficient mixture homogeneity may be achieved with the combination of the following:

- a. High diffusion H₂ injector nozzle
- b. High turbulence kinetic energy (TKE) flow in port & in cylinder
- c. Optimal injection strategy

Regarding the injector nozzle, it must be designed in a way to assure sufficient H₂ diffusion in the port under relatively low injection pressure differential, approx. 1-7bar, as dictated by application safety regulations and overall system cost considerations. This goal can be achieved by customization of the injector nozzle design so that it can disperse the flow of H₂ over a large volume even under very low injection pressure differential. An example of a customized injector nozzle used with H₂ engines is provided in Figure 4 [6]. It can be seen that the lambda distribution of the H₂ mixture is already quite uniform in the intake valve region.

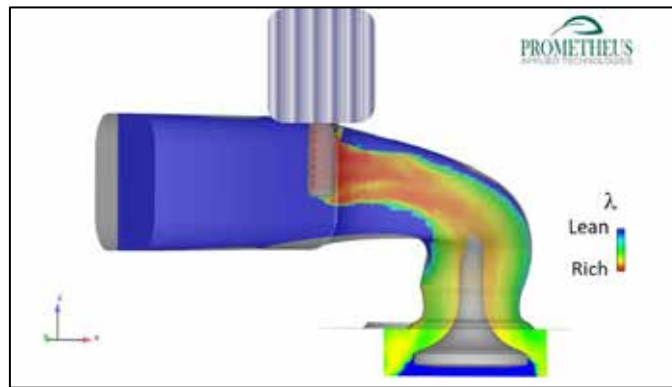


Figure 4. Example of customized injector nozzle used with H₂ engines

To assure the proper TKE in the port and cylinder, necessary to homogenize the fuel-air mixture, special devices suitable to create turbulence in the port (e.g., intake turbulence inducer) and an organized swirling flow in the cylinder (e.g., port deflector) are used during the development stage to define the target flow characteristics required for the proper design of the intake and the piston crown that will be used for the serial production. An example of the general effects of such devices is simulated in CFD and provided in Figure 5.

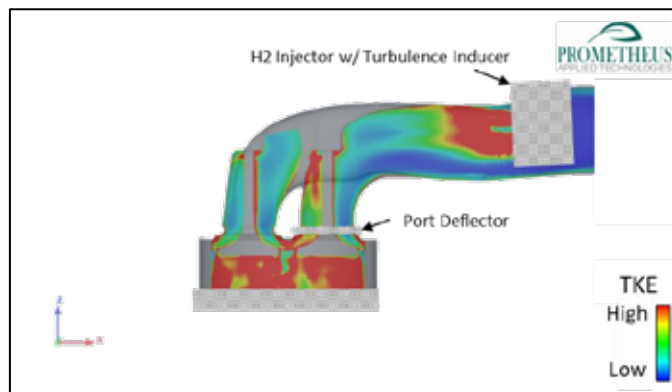


Figure 5. Example of the general effect of intake turbulence inducer and port deflector on port and in-cylinder turbulence.

Lastly, the injection strategy, defined as the start of injection (SOI) and injection duration, must be thoroughly considered to assure proper mixing and minimal H₂ slippage to the exhaust. Depicted in Figure 6 is an example of in-cylinder λ distribution simulated in CFD. It can be seen that the in-cylinder λ homogeneity achieved with a conventional mixing system is much worse compared to the advanced H₂ fuel injection and mixing system.

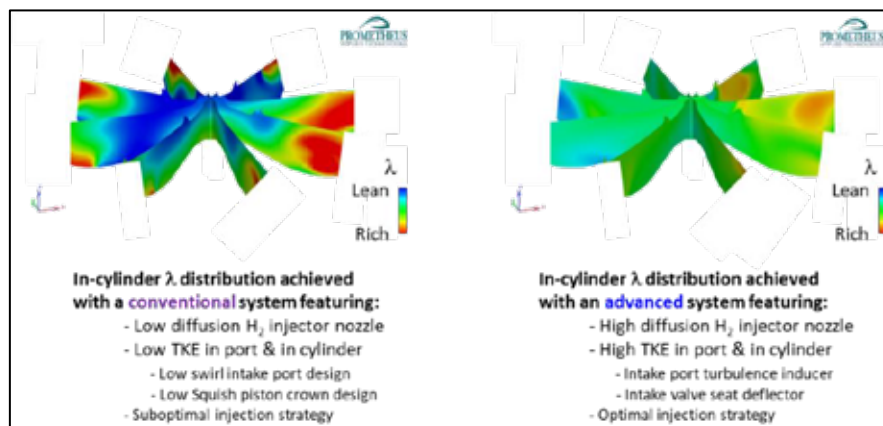


Figure 6. Example of a CFD comparison of the in-cylinder λ distribution achieved with conventional vs. advanced H₂ fuel injection and mixing system.

The improvement in λ distribution, and its repeatability from cycle to cycle, is the first step needed to mitigate the occurrence of combustion instabilities in H₂-ICEs and must be carefully considered during engine development.

2.2 Ultra-Lean H₂ Mixtures & High Energy Sparks

Ultra-lean H₂ mixtures, defined as λ greater than 3.0, are necessary to mitigate the high flame speed and propensity to autoignition experienced at the higher BMEP operations (greater than 12bar). With ultra-lean H₂ mixtures, the required ignition energy is considerably higher than that required by, for example, natural gas mixtures approaching a λ of 2.0. However, the high ignition energy can result in the formation of hot spots on the electrodes which can increase the initial flame growth rate causing an advancement in the SOC and resulting in frontfire, knock and preignition. This issue can be prevented by adapting the rate of spark energy delivered to the electrodes, during the spark event. This is done according to the location where the spark takes place on the electrode surface and how it travels across the gap [2, 4].

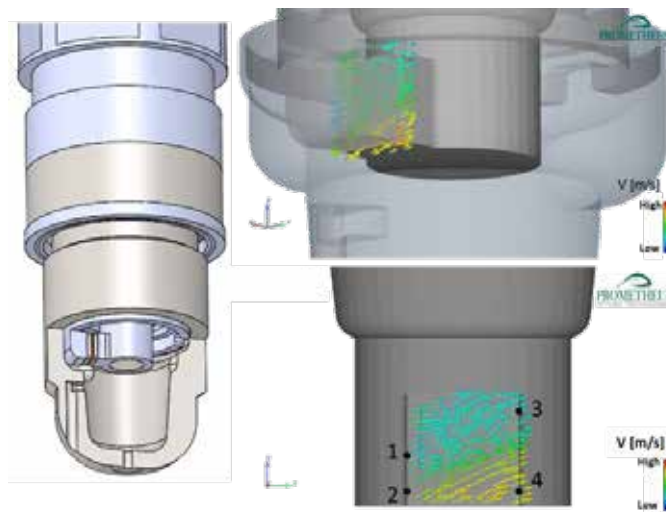


Figure 7. The radial gap of a prechamber spark plug with four typical spark locations

Depicted in Figure 7 is the flow velocity in the gap between the electrodes of a uniquely designed radial gap prechamber plug [9]. These electrodes are characterized by a large sparking surface and a small gap which is necessary to achieve a long-life spark plug at high engine BMEP. Moreover, this particular combination of electrode gap configuration and prechamber design is such to ensure an organized and consistent flow within the electrode gap. This condition is key for enabling the same-cycle adaptive spark control to properly operate. For this design, four distinct spark locations are denoted on the edge of the electrode surface. The direction of the arrows indicates that the flow moves from the left to the right. This flow direction defines locations 1 and 2 as being on the leading edge and locations 3 and 4 as being on the trailing edge of the electrode surface.

As a result of the flow direction, the flame kernel generated by the spark will traverse the electrode gap if the spark takes place on the leading edge (locations 1 and 2) with two different velocities (slower for location 1 and faster for location 2). When the spark takes place on the trailing edge (locations 3 and 4), the flame kernel will stay anchored to the edge for the entire duration of the spark and the flame kernel growth rate will be at two different rates (slower for location 3 and faster for location 4). Under these conditions, a leading-edge spark will be allowed to travel along the electrode surface, thereby distributing the spark energy onto a larger surface whereas in the case of a trailing edge spark the entire energy will be deposited in a single point location. Moreover, a leading-edge spark requires much more energy to offset the quenching effects taking place within the large electrode surface and a small electrode gap. In contrast, a trailing edge spark requires much less energy due to the absence of quenching

surfaces. It follows that for the same spark waveform (i.e., same rate of spark energy delivered) in both leading and trailing edge locations, the SOC will be very different and the resulting combustion pressure cycles will have very dissimilar magnitude and phasing. To minimize these variations, the same-cycle adaptive spark energy control is necessary to ensure a consistent SOC while preventing the formation of hot spots on the electrodes. It is important to note that the predictions of the SOC and the target SOC, are a central part of the algorithm and are determined via the use of the Prometheus Ignition and Combustion Model (ICM) which has been explained in a previous publication [4].

Shown in Figure 8 are the spark waveforms resulting from the same-cycle adaptive spark control for trailing spark location (left picture) compared to a leading spark location (right picture). Based on the spark voltage signal detected in the first part of the spark discharge, defined as the “control window”, a determination is made on the spark location and the magnitude of the flow field acting on that spark. According to this information, the ICM algorithm predicts the SOC and then, if necessary, adjusts the spark energy in the “adjustment window” during the same spark event to achieve a predetermined target SOC and minimize any hot spot formation on the surface of the electrode.

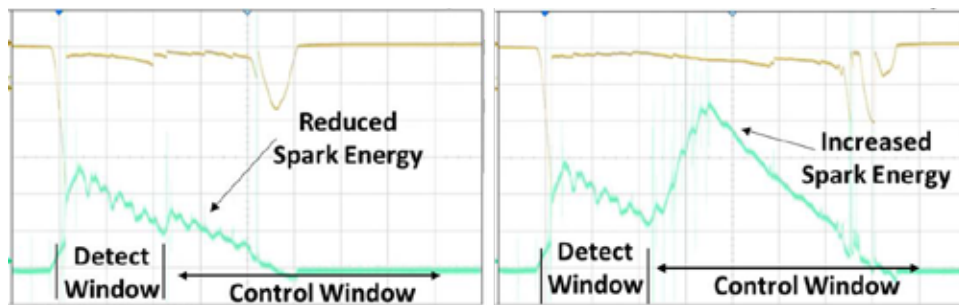


Figure 8. Example of spark waveforms during closed-loop operation for a trailing edge spark (top) and leading-edge spark (bottom)

The effect of the same-cycle adaptive spark control on the electrode surface temperature is described by transient FEA performed on the electrode surface and shown in Figure 9.

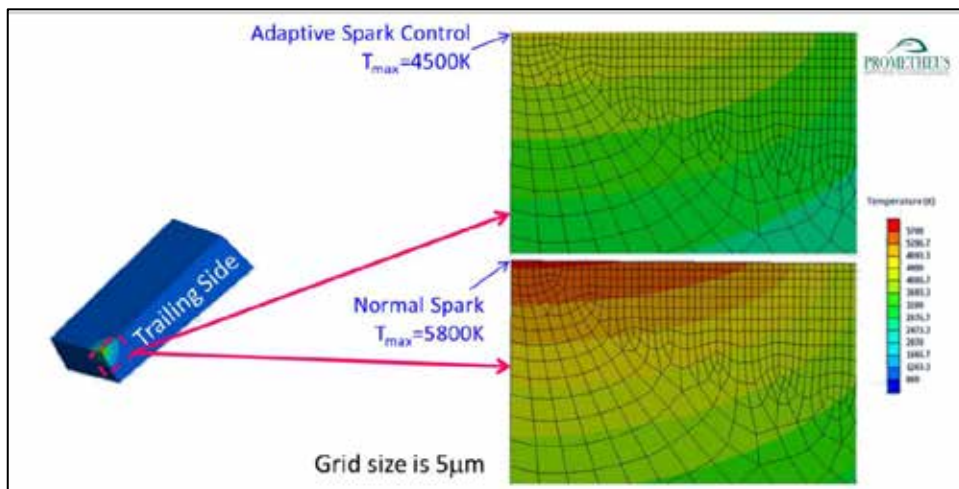


Figure 9. Example of electrode temperature difference from the use of the same-cycle adaptive spark control compared to a normal spark.

It can be seen that the difference in local electrode temperature between adaptive spark control compared to a conventional high energy ignition system (i.e., “normal spark”) can be in the order of 1300 K. This difference is sufficient to prevent hot spots causing large variation in SOC and fast electrode erosion rates.

2.3 Power Cylinder Thermal Management

Due to the very wide flammability range, H_2 mixtures exhibit very high propensity to autoignition. As a result, local surface temperatures and residual gas temperatures in crevices and anywhere else in the power cylinder must be kept below a certain limit throughout the intake process to avoid autoignition of H_2 streams while entering the cylinder causing frontfire. For an engine λ lower than about 3.0 and an BMEP greater than about 12bar, the temperature limit validated by the authors is approx. 800K.

Detailed combustion CFD and transient thermal FEA are necessary to determine the proper rate and phasing of combustion, the design and materials of the power cylinder combustion surfaces including spark plug and prechamber, the gas exchange process, and the PFI injection strategy.

Depicted in Figure 10 is an example of surface and residual gas temperatures determined by detailed CFD and FEA simulations and comparing the case of a properly designed prechamber plug to the case of conventional spark plug. It can be seen that, in the case of the prechamber plug (bottom) all surface and gas temperatures are well below 800K. This is due to the particular flow achieved by the design of the prechamber enabling a complete mixing and scavenging of the residual gases, together with an effective cooling of the prechamber internal surfaces. Conversely, in the case of a regular spark plug, the absence of a proper flow around the electrodes causes the formation of hot spots and hot pockets of residual gases having temperature levels in excess of 800K. This condition has been found to cause frontfire even at lower engine BMEP conditions.

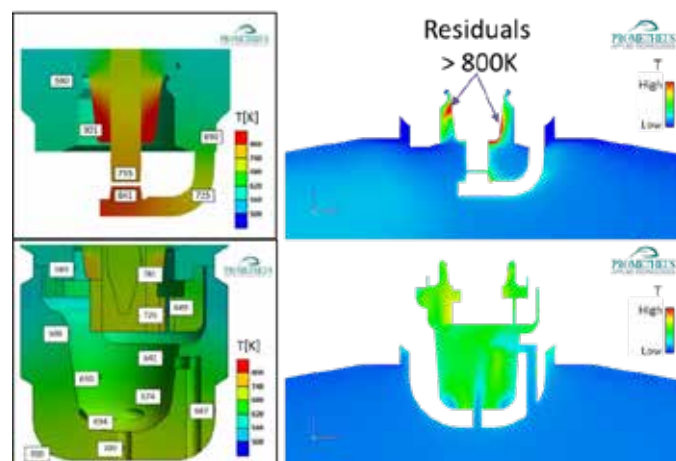


Figure 10. Example of surface (left) and residual gas (right) temperatures determined by detailed CFD simulations for a standard spark plug (top) and the Prometheus active scavenge prechamber (bottom).

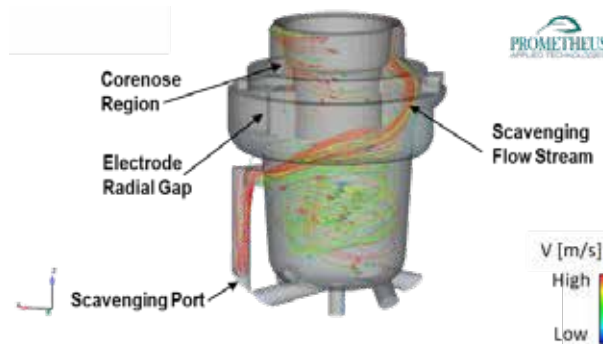


Figure 11. CFD simulation of the Prometheus active scavenge prechamber flow

The specific prechamber flow pattern needed to prevent pockets of hot gas and surface hot spots is depicted in Figure 11. Here a CFD simulation of the Prometheus active scavenge

prechamber shows how the flow is channeled through the scavenging port during compression in the corenose region (crevices) of the prechamber where hot residuals tend to be trapped [6].

2.4 Lube Oil Preignition

While the use of same-cycle adaptive spark control mitigates the variation in the SOC, it is of paramount importance to ensure ultra-lean and homogeneous mixtures to prevent the occurrence of LOP at BMEP levels typically higher than 12bar. Portrayed in Figure 12 is an example of a stratified in-cylinder condition (predicted by CFD) that leads to preignition of the lube oil present in the combustion chamber [8]. Such phenomenon has been studied for many years and is one of the factors limiting the higher BMEP operation with hydrogen [8].

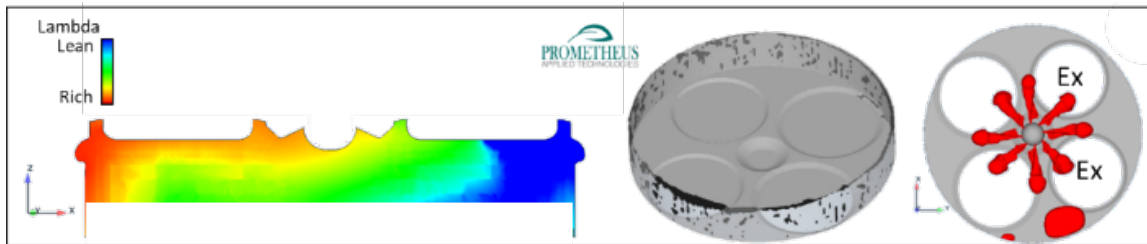


Figure 12. An example of a stratified λ distribution leading to LOP [8]

However, if the local lambda is sufficiently lean, the rate at which the flame propagates from the autoignition of the lube oil mist, will not be fast enough to cause a significant effect on the overall rate of combustion. Figure 13 shows the type of λ homogeneity and TKE distribution required for high BMEP H₂-ICE operation.

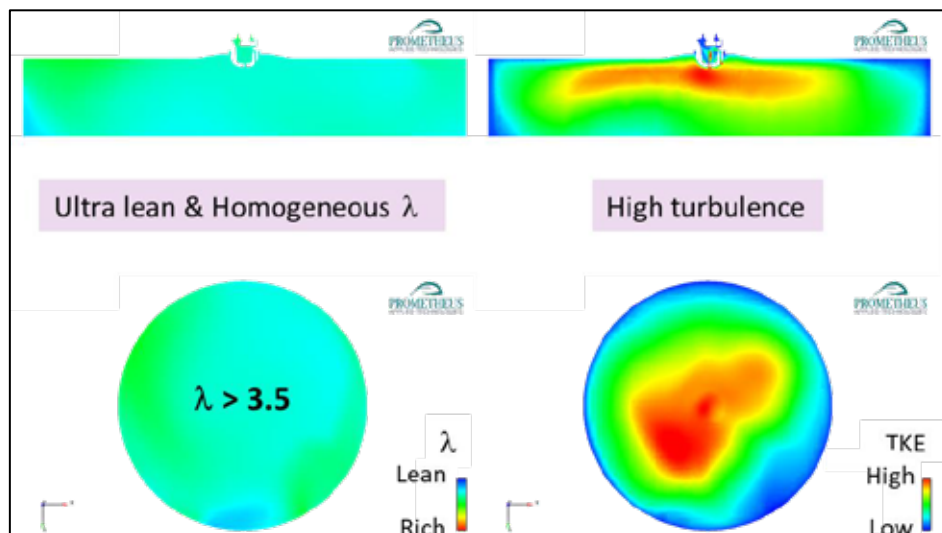


Figure 13. Example of the desired level of in-cylinder homogeneity and turbulence (TKE) distribution that can prevent the propagation of flame fronts from lube oil autoignition.

The objective is to achieve high global lambda ($\lambda > 3.5$) with homogenous distribution and high TKE to diffuse and dilute the oil mist preventing the propagation of flame fronts causing high pressure cycles, even in the presence of oil mist autoignition. By inhibiting the LOP and by means of the same-cycle adaptive spark control prechamber ignition, the “Diesel-like” performance targets could be achieved.

3. Engine Test Results

As previously mentioned, the engine testing is performed on an ABC 6DZ H₂ engine to further confirm and quantify the advantages of the holistic approach of the same-cycle adaptive spark

control. The comparison of the engine test results is between the “Baseline Configuration” which consists of an open J-gap type spark plug, a conventional capacitive discharge (CD) ignition system with a spark current waveform similar to that of Figure 14, and the “AdaptH₂ Configuration” which consists of a special prechamber spark plug, and the same-cycle adaptive spark control ignition system.

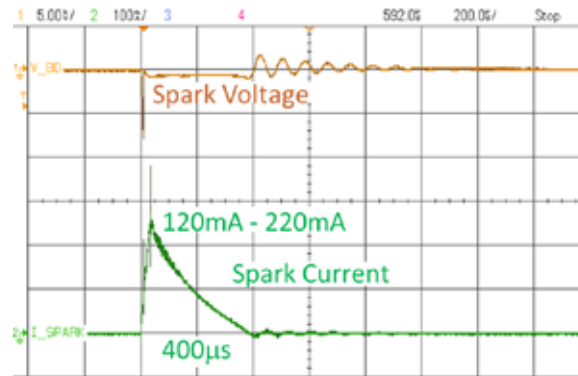


Figure 14. Conventional CD spark waveform with adjustable spark energy setting.

The conventional CD system needed to be set at a low spark energy setting to avoid creating hot spots on the electrode surface which led to frontfire. It is important to note that improvements in the homogeneity and the cycle-to-cycle mixing consistency, by the use of a port deflector, are present for both configurations. The improvements are depicted in Figure 15. It is also important to note that no flame arrestors were installed in the intake ports during this test.

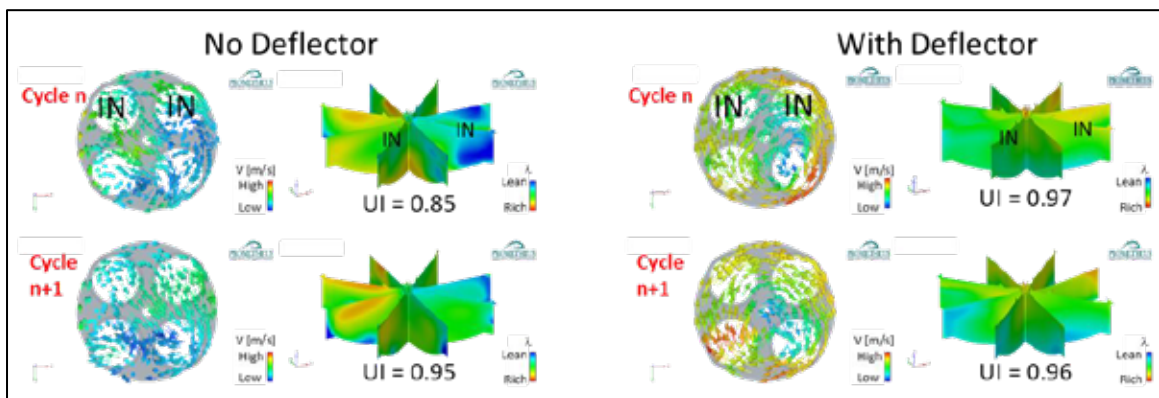


Figure 15. The use of deflector to improve in-cylinder homogeneity and the cycle-to-cycle mixing consistency (UI is the uniformity index).

Shown in Figure 16 [6] is the unfueled prechamber spark plug (PCP) using the “Active Scavenge” Prechamber technology [9] for operation with H₂-ICE [10]. This design has electrodes arranged radially, having a large surface and a small gap.

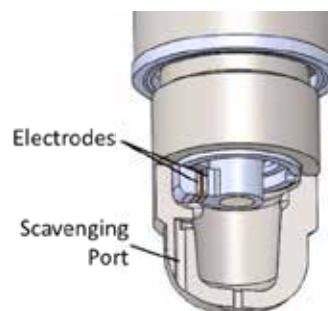


Figure 16. Prometheus unfueled prechamber spark plug, featuring the radial electrode gap and the Active Scavenge technology [9].

A picture of the alfa prototype, Adapth₂ ignition control unit used for this hydrogen engine test is shown in Figure 17. This is an alpha level prototype that is being rapidly developed into serial production in cooperation with engine OEMs.



Figure 17. Adapth₂ alpha prototype used for the same-cycle adaptive spark control

Throughout the engine test, and while trying to fine tune the injection strategy, various shutdowns took place due to frontfire. No LOP events were observed. This may be due to a combination of factors such as the improved homogeneity, sufficiently lean operation, engine LO consumption and LO composition. The key engine performance parameters monitored throughout the test are the combustion pressure over 300 consecutive cycles, the COV of IMEP, the COV of Pmax and the engine efficiency.

Shown in Figure 18 is the engine efficiency trend, and corresponding NOx emissions, at the different power levels for the two different configurations. The maximum load level achieved with the Baseline configuration is 100% which is not sufficient per the requirements of the marine engine regulations. On the other hand, the Adapth₂ configuration is able to reach the required operating point of 110% load. It is also important to note that it is not possible for the Baseline configuration to operate at 100% load for more than a few minutes without an incident of frontfire taking place. However, it can operate at 90% load indefinitely. Both configurations are measuring nearly zero NOx emissions.

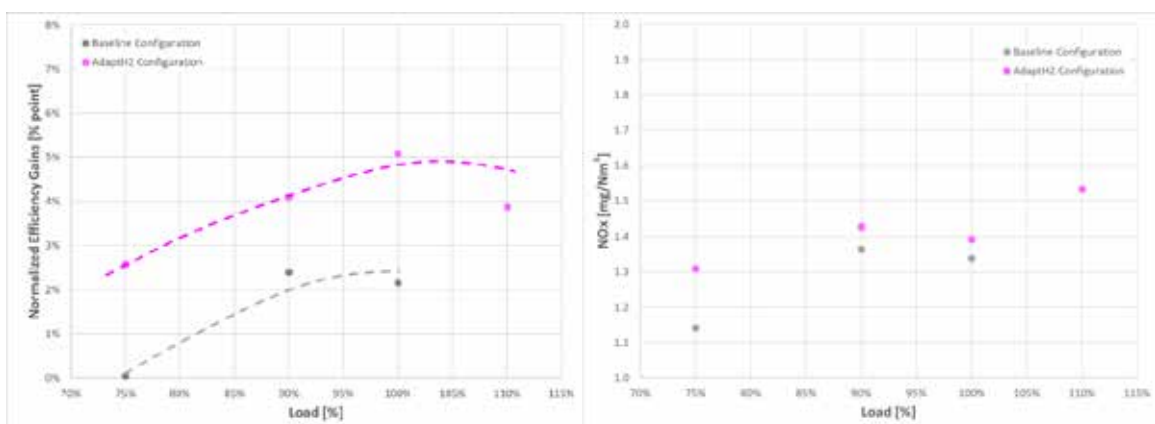


Figure 18. Baseline vs Adapth₂ Configuration - Efficiency trend and corresponding NOx emissions.

Diving a little deeper in the engine test results, allows us to understand why it was possible to achieve such an increase in load. Figure 19 indicates the combustion stability via the COV of IMEP. The comparison is stark with the Adapth₂ configuration operating at an acceptable COV of IMEP well below 2%. On the other hand, the baseline configuration exhibits a COV of IMEP that is random and unpredictable, indicating that the combustion process is not under control.

Typically, the COV of IMEP should decrease as the load increases which is exhibited by the AdaptH₂ configuration.

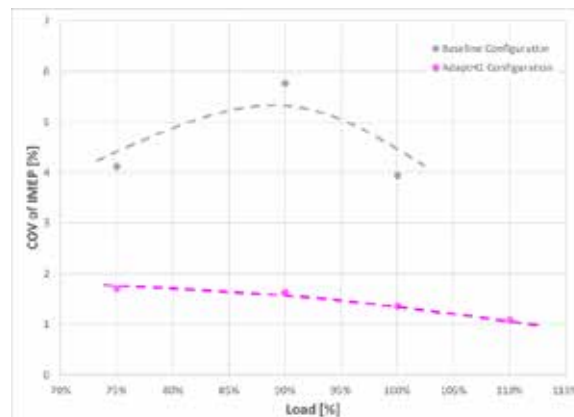


Figure 19. Baseline vs AdaptH₂ Configuration – COV of IMEP trend

In terms of combustion peak pressure variations, depicted in Figure 20 are the representative ranges of maximum combustion pressure (P_{max}) obtained with each configuration at their respective maximum operating load. The range of variations of the AdaptH₂ configuration are less than half of those obtained with the Baseline configuration. Furthermore, it can be easily seen that the increased stability provided by the AdaptH₂ configuration, allows the reliable operation at higher loads by reducing the propensity of frontfires.

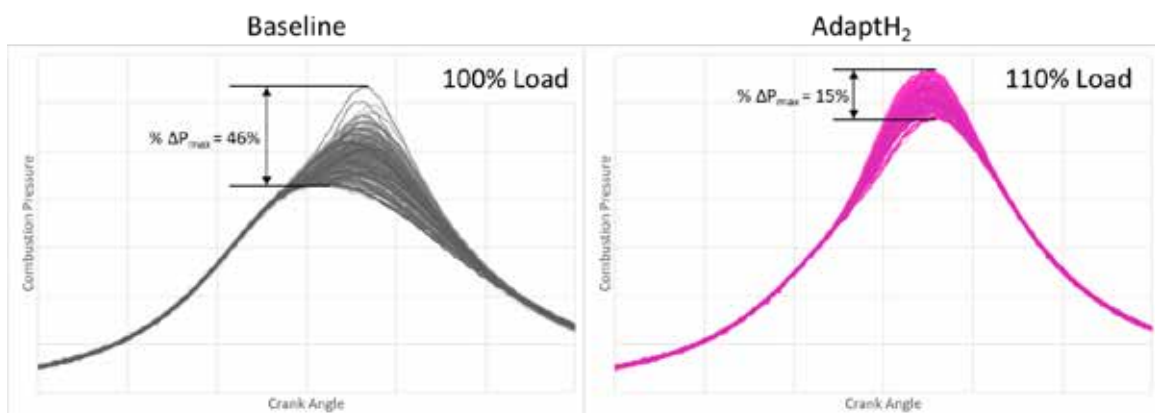


Figure 20. Baseline vs AdaptH₂ Configuration – Combustion Pressure Variations at maximum load for each configuration

4. Turbocharging System

Discussed by the authors in a previous publication [6] are the options for the H₂-ICE to be operated at ultra-lean/diluted conditions needed for the high BMEP operation of H₂-ICE to achieve the “Diesel-like” efficiency target. This is mostly for engine conversions from Natural gas where the turbocharger is sized for an approximate lambda 1.8. Shown in Figure 21 (left) is the conventional solution of the dual stage turbocharger. In this case high pressure ratios of $\pi > 7$ can be achieved and can yield lambdas of $\lambda > 4$. The cost of this approach can be justifiable for large engines, but it can seriously handicap the marketability of smaller engines. For smaller engines, the use of a single stage turbocharger in combination with a cooled EGR system, as shown in Figure 21 (right) can be a solution, but can also lead to issues with increased frontfire events and increased propensity to LOP, if not properly managed. In the case of the ABC 6DZ H₂ engine, which is converted from a diesel with a turbocharger sized for an approximate lambda of 2, a single stage turbocharger is sufficient for the target H₂ lambda required to avoid LOP at 110% load.

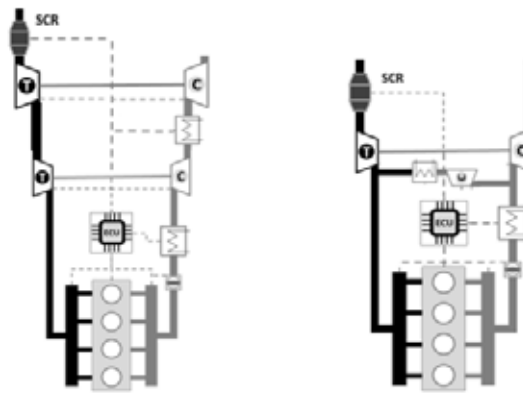


Figure 21. Engine system featuring a two-stage turbocharger (left) and a single stage turbocharger with a cooled EGR blower (right).

5. Mitigating the Development Risks of H₂-ICE

Achieving the “Diesel-like” performance out of an H₂-ICE has many challenges but the authors have gained enough experience to propose an approach, separated into two stages, that mitigates the risks of all the necessary modifications and changes to existing engine platforms.

In the **first stage**, the system designer needs to identify a state-of-the-art H₂ PFI system and design a custom nozzle to enhance the diffusion of hydrogen in the port. This system is typically coupled to an intake turbulence inducer and port deflector to enable the in-cylinder mixture homogeneity necessary to mitigate the propensity to LOP at the higher levels of BMEP. Both the intake turbulence inducer and valve deflector are designed by means of an advanced CFD to achieve the desired homogeneity while minimizing the pressure losses in the intake port. This first stage also includes the same-cycle adaptive spark control with a properly designed passive (unfueled) prechamber. This system is predicted to operate at a lambda of 2.8-3.0 and target BMEP levels of about 18bar with efficiency of 44% at 50mg/Nm³ NO_x.

In the **second stage**, the same H₂ PFI system with a custom nozzle design is used, as the first stage. However, the functionality of the intake turbulence inducer and port deflector are achieved by means of a CFD designed intake port and piston crown geometries generating a similar flow dynamic but with lower pressure losses (ΔP). Then, the same-cycle adaptive spark control prechamber ignition system is used but with a fueled H₂ lean-burn prechamber [1]. This type of prechamber generates the high momentum flame jets needed to stabilize combustion at higher BMEP levels of ≥ 22 bar. The predicted engine efficiency is of BTE $\geq 48\%$ at a λ of ~ 3.8 producing virtually zero NO_x emissions.

Through the AdaptH₂ cooperation, Prometheus, Altronic and Hoerbiger are currently pursuing both stages of development with selected engine OEMs.

6. Conclusion

The *Same-Cycle Adaptive Spark Control Prechamber Ignition System* concept embodied in the AdaptH₂ system has been further evaluated in an ABC 6DZ H₂ engine. The test results confirmed the potential for this system to enhance combustion stability and thus improve power output and efficiency while maintaining virtually zero emissions. In particular, a net gain of about 20% in power output was achieved and demonstrated that reducing the cycle-to-cycle combustion variabilities during ignition is a major key for achieving higher engine BMEP levels and, hence, it is central to the future of H₂-ICEs. On the other hand, the frontfire (intake backfire) has been the major limitation impeding reliable operation at the higher power outputs. To address this issue, detailed combustion modeling and simulations are needed to determine the optimum design solution for improving the mixture homogeneity, and the thermal management of the power cylinder to prevent the formation of hot spots as well as hot residuals gases causing the autoignition of H₂ streams during the intake process.

Finally, a staged development approach has been proposed for mitigating the technical and commercial risks associated with the introduction of sophisticated hydrogen engine technology in the market.

Through the AdaptH₂ cooperation, Prometheus, Altronic and Hoerbiger are currently pursuing both stages of development with selected engine OEMs [11].

7. Definitions, Acronyms, Abbreviations

BMEP: Brake Mean Effective Pressure	ITE: Indicated Thermal Efficiency
BTE: Brake Thermal Efficiency	ICM: Ignition-Combustion Model
CAD: Crank Angle Degrees	LBP: Lean Burn Prechamber
CFD: Computational Fluid Dynamics	LOP: Lube Oil Preignition
CHP: Combined Heat and Power	PFI: Port Fuel Injection
COV: Coefficient of Variation	SOC: Start of Combustion
FEA: Finite Element Analysis	TKE: Turbulent Kinetic Energy
ICE: Internal Combustion Engine	λ : Air-fuel equivalence ratio, lambda
IMEP: Indicated Mean Effective Pressure	

8. Acknowledgments

The authors would like to recognize AVL List GmbH for the continued support and assistance provided with the AVL FIRE-M software. The high-fidelity of the simulations are unmatched and are crucial in the implementation of the Homogeneous H₂ Mixing system, Predictive Model-Based Spark Control algorithm, and Prechamber Combustion system for the H₂-ICE.

The authors look forward to the continued cooperation with AVL and other engine OEMs who are genuinely interested in taking the hydrogen engine combustion technology to the next level of highly improved competitiveness.

References

- [1] Tozzi, L., et al: Improving the Efficiency/Emissions Trade-off with a Novel Lean-Burn Precombustion Chamber. 10th Dessau Gas Engine Conference, Dessau, Germany(2017).
- [2] Tozzi L., Sotiropoulou E.: Predictive Model-Based Spark Control. U.S. Patent Application number: 18/219,692; International Application Number: PCT/US23/27192.
- [3] Lepley, D.T., et al: Optimizing High-Energy Tunable Ignition Technology: Preventing Electrode Damage while Extending the Lean Flammability Limit of Gas Engines. In: GMRC Gas Machinery Conference, Nashville, TN, USA, (2014).
- [4] Sotiropoulou, E., et al: Holistic Solution Enabling High Power Density & Efficiency H₂-ICE, ATZ live Heavy Duty Engines 2023 – MTZ Conference (2023).
- [5] Sotiropoulou, E., et al: Prechamber Combustion: Enabling the Competitive Carbon-Neutral ICE. In CIMAC Congress, Paper No. 291, Busan, S. Korea, (2023).
- [6] Sotiropoulou, E., Tozzi, L., Trapp, C.: Breakthrough in Hydrogen Engine Combustion Enabling Zero Emissions and High Efficiency with Passive Prechamber Technology. In 12th Dessau Gas Engine Conference, Dessau, Germany (2022).
- [7] Sotiropoulou, E., et al: Improving Efficiency of the Premixed Combustion by Reducing Cyclic Variability. In CIMAC Congress, Paper No. 257, Helsinki, Finland, (2016).
- [8] Yasueda, S., Sotiropoulou E., Tozzi, L.: Predicting Autoignition caused by Lubricating Oil in Gas Engines. In CIMAC Congress, Paper No. 37, Shanghai, China, (2013).
- [9] Tozzi L., Sotiropoulou E.: Active Scavenge Prechamber. US Patent No. 9,850,806
- [10] Sotiropoulou, E., Knepper, S., Deeken, S., Grewe, F.: Prechamber Spark Plugs: The Evolution from Low Emission Natural Gas to Zero Emission H₂ Operation. MTZ Worldwide, vol. 2020-6, pp. 46-50, (2020).
- [11] Altronic Homepage, <https://www.altronic-llc.com/>, Altronic Partners with Prometheus Applied Technologies to Make Hydrogen Viable

Vorname/First Name	Name/Name	Firma/Company
Koki	Aiba	IHI Corporation
Peter	Albrecht	MAN Truck & Bus SE
Dr.-Ing. Sven	Annas	2G Energietechnik GmbH
Emil-Sándor	Bakk	Miba Gleitlager Austria GmbH
Michael	Baldermann	MAN Energy Solutions SE
Torsten	Baufeld	Liebherr Machines Bulle SA
Dr.-Ing. Sören	Bernhardt	Karlsruher Institut für Technologie
Dr. Stefan	Blodig	MAN Energy Solutions SE
Aleksandar	Boberic	FEV Europe GmbH
Robert	Böwing	INNIO Jenbacher GmbH & Co. OG
Annalena	Braun	Karlsruher Institut für Technologie
Dr. Samuel	Braun	Karlsruher Institut für Technologie
Dr. Andreas	Broda	MAN Truck & Bus SE
Dr. rer. nat. Jochen	Broz	Schaeffler Technologies AG & Co. KG
Prof. Dr.-Ing. Bert	Buchholz	Universität Rostock
Dr. John	Burrows	Tenneco Powertrain
Manuel	Cech	WTZ Roßlau gGmbH
Dr. Peter	Christiner	Robert Bosch AG
Dr. János	Csató	Liebherr-Components Deggendorf GmbH
Dr. Massimo	Dal Re	Tenneco Powertrain
Simone	Daniele	Tenneco Powertrain
Rik	De Graeve	Anglo Belgian Corporation
Dr. Lena	Engelmeier	The hydrogen and fuel cell Center ZBT GmbH
Forian	Eppler	MAN Energy Solutions SE
Dr.-Ing.	Enno Eßer	HUG Engineering AG
Lukas	Fehlemann	The hydrogen and fuel cell center ZBT GmbH
Dr.-Ing. Björn	Franzke	EV Europe GmbH
Mario	Frischmann	INNIO Jenbacher GmbH & Co. OG
Dr. Thomas	Gallinger	TÜV SÜD Industrie Service GmbH
Niklas	Gierenz	Universität Rostock
Frank	Grewe	2G Energy AG
Carlo Nazareno	Grimaldi	University of Perugia
Dr. Christopher	Gross	MAN Energy Solutions SE
Dr.-Ing. Arne	Güdden	FEV Europe GmbH
Dr. Paul	Hagl	MAN Energy Solutions SE
Dr. rer. nat. Oliver	Hahn	Schaeffler Technologies AG & Co. KG
Dr.-Ing. Christoph	Hank	Fraunhofer Institute for Solar Energy System ISE
Claudia	Hengstberger	Robert Bosch AG
Takayuki	Hirose	IHI Corporation
Marius	Holst	Fraunhofer Institute for Solar Energy System ISE
Antje	Hoppe	FVTR GmbH
Rudolf	Höb	Ostbayerische Technische Hochschule Amberg-Weiden
Pierre	Huck	TÜV SÜD Industrie Service GmbH
Dominik	Hyna	MAN Truck & Bus
Dr. Gernot	Kammel	LEC Graz
Shunsuke	Kazama	IHI Power Systems Co., Ltd.
Dr. Johannes	Kech	Rolls-Royce Solutions GmbH
Sebastian	Kirchhammer	Miba Gleitlager Austria GmbH
Dr. Christoph	Kost	Fraunhofer Institute for Solar Energy System ISE
Michael	Köhler	Robert Bosch AG
Tom	Krüger	WTZ Roßlau gGmbH
Dr.-Ing. Heiko	Kubach	Karlsruher Institut für Technologie
Christian	Kunkel	MAN Energy Solutions SE
Dr.-Ing. Marcel	Lackner	LEC Graz
Jan	Leberwurst	Schaeffler Technologies AG & Co. KG
David	Lepley	Altronic LLC
Florian	Lindner	MAN Truck & Bus SE
Dr. Maximilian	Malin	LEC Graz

Vorname/First Name	Name/Name	Firma/Company
Thomas	Malischewski	MAN Truck & Bus SE
Dr. Bhuvaneswaran	Manickam	MAN Energy Solutions SE
Till	Mante	Universität Rostock
Yutaka	Mashima	IHI Power Systems Co., Ltd.
Yutaka	Masuda	IHI Power Systems Co., Ltd.
Francois	Masson	Liebherr Machines Bulle SA
Luc	Mattheeuws	Anglo Belgian Corporation
Kenta	Miyauchi	IHI Corporation
Prof. Dr.-Ing. Hinrich	Mohr	GasKraft Engineering
Dr. Patrick	Moll	Rolls-Royce Solutions GmbH
Gitau	Mwathi	LOGE Deutschland GmbH
Sadao	Nakayama	IHI Power Systems Co., Ltd.
Supreeth	Narasimhamurthy	Prometheus Applied Technologies, LLC
Hiroki	Naruse	IHI Power Systems Co., Ltd.
Günther	Neuhaus	Liebherr-Components Deggendorf GmbH
Dr. Sebastian	Ohler	Caterpillar Energy Solutions GmbH
Dr. Stefano	Papi	Tenneco Powertrain
Dr. Daniel	Peitz	HUG Engineering AG
Richard	Pirkel	Liebherr-Components Deggendorf GmbH
Prof. Dr. Stefan	Pischinger	RWTH Aachen University
Jannik	Plass	The hydrogen and fuel cell center ZBT GmbH
Dr.-Ing. Sascha	Prehn	Universität Rostock
Marcel	Reinbold	Karlsruher Institut für Technologie
Federico	Ricci	University of Perugia
Dr.-Ing. Achim	Schaadt	Fraunhofer Institute for Solar Energy ISE
Stefan	Schiestl	INNIO Jenbacher GmbH & Co. OG
Markus	Schmitzberger	Robert Bosch AG
Dr. Marco	Schultze	Caterpillar Energy Solutions GmbH
Dr.-Ing. Lars	Seidel	LOGE Deutschland GmbH
Patrick	Send	Liebherr-Components Deggendorf GmbH
Darshit	Shah	Caterpillar Energy Solutions GmbH
Dr. Tom	Smolinka	Fraunhofer Institute for Solar Energy System ISE
Emmanuella	Sotiropoulou	Prometheus Applied Technologies, LLC
Dr. Nikolaus	Spyra	INNIO Jenbacher GmbH & Co. OG
Michael	Steffen	The hydrogen and fuel cell center ZBT GmbH
Dr. Jens Olaf	Stein	Robert Bosch AG
Sebastian	Sulzer	Schaeffler Technologies AG & Co. KG
Robert	Szolak	Fraunhofer Institute for Solar Energy System ISE
Stefan	Terbeck	MAN Energy Solutions SE
Connor	Thelen	Fraunhofer Institute for Solar Energy System ISE
Dr.-Ing. Martin	Theile	FVTR GmbH
Steffen	Theiß	Rolls-Royce Solutions GmbH
Carsten	Tietze	WTZ Roßlau gGmbH
Luigi	Tozzi	Prometheus Applied Technologies, LLC
Dr. Michael	Url	INNIO Jenbacher GmbH & Co. OG
Andreas	Van Gijzeghem	Anglo Belgian Corporation
Dr. Roel	Verschaeren	Anglo Belgian Corporation
Dominik	Voggenreiter	TÜV SÜD Industrie Service GmbH
Dr.-Ing. Olaf	Weber	Schaeffler Technologies AG & Co. KG
Maximilian	Weidner	MAN Truck & Bus
Michael	Werner	MAN Energy Solutions SE
Dr.-Ing. Nicole	Wermuth	LEC Graz/Technische Universität Graz
Prof. Dr. Andreas	Wimmer	LEC Graz/Technische Universität Graz
Roy	Zakrzewski	MAN Truck & Bus SE
Bernhard	Zemann	Hoerbiger Wien GmbH
Pascal	Zimmer	RWTH Aachen University
Andreas	Zunghammer	Miba Gleitlager Austria GmbH

Herausgeber/Editor

WTZ Roßlau GmbH
Mühlenreihe 2a
06862 Dessau-Roßlau
Deutschland/Germany
+49 34901 883-0
info@wtz.de
www.wtz.de

Verlag/Publisher

Forschungszentrum für Verbrennungsmotoren und Thermodynamik Rostock GmbH
Joachim-Jungius-Straße 9
18059 Rostock
www.fvtr-gmbh.de

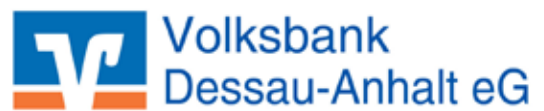
ISBN-Nummer/ISBN number

978-3-941554-27-6

Veröffentlichungsdatum/Release Date

Mai 2024/May 2024

Redaktionsschluss: 31. März 2024/Editorial deadline: March 31, 2024



WTZ Roßlau
Mühlenreihe 2a
06862 Dessau-Roßlau
Germany
www.wtz.de

Technikmuseum „Hugo Junkers“, Dessau-Roßlau, Foto: WTZ Roßlau / Technik Museum „Hugo Junkers“, Dessau-Roßlau, Photo: WTZ Roßlau

